



Natural Science in Archaeology

Ervan Garrison

Techniques in Archaeological Geology

Second Edition

Natural Science in Archaeology

Series editors

Günther A. Wagner
Christopher E. Miller
Holger Schutkowski

More information about this series at <http://www.springer.com/series/3703>

Ervan Garrison

Techniques in Archaeological Geology

Second Edition

 Springer

Ervan Garrison
Department of Geology, University of Georgia
Athens, Georgia, USA

ISSN 1613-9712
Natural Science in Archaeology
ISBN 978-3-319-30230-0 ISBN 978-3-319-30232-4 (eBook)
DOI 10.1007/978-3-319-30232-4

Library of Congress Control Number: 2016933149

© Springer-Verlag Berlin Heidelberg 2016
This work is subject to copyright. All rights are reserved by the Publisher, whether the whole or part of the material is concerned, specifically the rights of translation, reprinting, reuse of illustrations, recitation, broadcasting, reproduction on microfilms or in any other physical way, and transmission or information storage and retrieval, electronic adaptation, computer software, or by similar or dissimilar methodology now known or hereafter developed.

The use of general descriptive names, registered names, trademarks, service marks, etc. in this publication does not imply, even in the absence of a specific statement, that such names are exempt from the relevant protective laws and regulations and therefore free for general use.

The publisher, the authors and the editors are safe to assume that the advice and information in this book are believed to be true and accurate at the date of publication. Neither the publisher nor the authors or the editors give a warranty, express or implied, with respect to the material contained herein or for any errors or omissions that may have been made.

Printed on acid-free paper

This Springer imprint is published by Springer Nature
The registered company is Springer Verlag GmbH Berlin Heidelberg

This book is dedicated to my grandchildren, Kelsey and Hunter.

Contents

| | | |
|----------|---|----|
| 1 | Introduction | 1 |
| 1.1 | Organization of This Book | 6 |
| 2 | The Geomorphological and Geological Context | 11 |
| 2.1 | Introduction | 11 |
| 2.2 | Landscapes and People | 11 |
| 2.3 | Geomorphic Concepts | 13 |
| 2.4 | Geomorphic Setting | 14 |
| 2.4.1 | Fluvial Landforms | 15 |
| 2.4.2 | Coastal Landforms | 17 |
| 2.4.3 | Submerged Landforms | 19 |
| 2.4.4 | Mountain and Glacial Landforms | 22 |
| 2.4.5 | Ice Patches | 25 |
| 2.4.6 | Lacustrine Landforms | 28 |
| 2.4.7 | Loessic and Glacial Landscapes: Midwestern United States | 30 |
| 2.4.8 | Desert/Arid Landforms | 33 |
| 2.4.9 | The Sahara: Geoarchaeology of Paleolakes and Paleoclimate | 33 |
| 2.4.10 | Karst/Cave Landforms | 36 |
| 2.4.11 | Combe Grenal | 37 |
| 2.4.12 | Volcanic Landforms | 40 |
| 2.5 | Earthquakes: Volcanic or Otherwise | 42 |
| 2.6 | Mapping | 43 |
| 2.7 | Map Scale | 45 |
| 2.8 | Data Sources for Mapping | 46 |
| 2.9 | LiDAR | 48 |
| 2.10 | Structure from Motion (SfM) | 48 |
| 2.11 | Drones | 49 |
| 2.12 | Making the Map: ArcGIS to Google Earth | 50 |
| 2.13 | Other Types of Maps | 52 |
| 3 | Sediments, Soils, and Stratigraphy in Archaeological Geology | 55 |
| 3.1 | Introduction | 55 |
| 3.2 | A Brief Review of Sediments and Soils | 56 |

| | | |
|----------|--|------------|
| 3.3 | The Soil Catena | 63 |
| 3.4 | The Soil Chronosequence | 63 |
| 3.5 | Describing Archaeological Sediments and Soils in Profile | 64 |
| 3.6 | The Geological Stratigraphic Section | 72 |
| 3.7 | Nomenclature | 72 |
| 3.7.1 | Allostratigraphy | 74 |
| 3.7.2 | Sequence Stratigraphy | 75 |
| 4 | Techniques for Archaeological Sediments and Soils | 77 |
| 4.1 | Sampling Sediments and Soils: Monoliths to Sediment Grabs | 77 |
| 4.2 | One Method for Constructing a Soil Monolith | 79 |
| 4.3 | Handling and Description of Cores: Some General Considerations | 84 |
| 4.4 | Standard Operating Procedure for Collection of Sediment Samples | 85 |
| 4.5 | “1700 Sondages”: Geological Testing of the Plateau of Bevaix, Neuchâtel (Switzerland) | 89 |
| 4.6 | Analytical Procedures for Sediments and Soils | 90 |
| 4.7 | Particle Size Analysis | 92 |
| 4.7.1 | Hydrometer Method | 94 |
| 4.7.2 | The Pipette Method | 94 |
| 4.7.3 | The Modified Pipette or “Fleaker” Method | 95 |
| 4.7.4 | The Imhoff Cone Method | 95 |
| 4.7.5 | Organic Content Determination Methods | 98 |
| 4.8 | Determination of Total Phosphorus by Perchloric Digestion | 100 |
| 4.9 | Absolute Phosphate Analysis Versus Qualitative Color Tests | 101 |
| 4.10 | Colorimetry and Spectrophotometry | 102 |
| 4.11 | Micromorphology: Describing Archaeological Sediments and Soils with the Microscope | 103 |
| 4.12 | Palynology: A Micromorphological Study of Archaeological Pollen | 104 |
| 4.13 | Phytoliths for Archaeology | 109 |
| 4.14 | Phytolith Identification and Morphology | 110 |
| 4.15 | Phytolith Extraction and Counting | 111 |
| 5 | Geophysical Techniques for Archaeology | 115 |
| 5.1 | Introduction | 115 |
| 5.2 | The International Society for Archaeological Prospection (ISAP) | 117 |
| 5.3 | Electrical Methods: Resistivity | 117 |
| 5.3.1 | Resistivity Arrays | 119 |
| 5.4 | Vertical Sounding Methods in Archaeology | 122 |
| 5.5 | Electrical Methods: Electromagnetic/Conductivity | 123 |
| 5.5.1 | Application of EM Methods | 124 |

| | | |
|----------|---|------------|
| 5.6 | Conductivity (EM) Survey of a Burned and Buried Cherokee Seminary Building, Tahlequah, Oklahoma, Cherokee Nation, USA | 124 |
| 5.6.1 | Magnetic Methods | 124 |
| 5.6.2 | Magnetometers | 127 |
| 5.6.3 | Gradiometers | 129 |
| 5.6.4 | Magnetic Anomaly Interpretation: Basic Principles | 129 |
| 5.6.5 | Magnetic Prospection: Practice | 130 |
| 5.6.6 | Date Acquisition and Display | 131 |
| 5.6.7 | Advantages and Disadvantages | 131 |
| 5.7 | An Abandoned Nineteenth-Century Cherokee Cemetery, Park Hill, Oklahoma, Cherokee Nation, USA | 132 |
| 5.7.1 | Ground-Penetrating Radar: GPR | 132 |
| 5.7.2 | Field Survey Methods | 137 |
| 5.7.3 | Digital Post-Processing of GPR Data | 137 |
| 5.7.4 | Multiple Geophysical Techniques | 139 |
| 5.7.5 | Underwater Geophysical Survey Techniques in Archaeology | 139 |
| 5.8 | The Sabine River Paleovalley, Northern Gulf of Mexico, USA | 140 |
| 5.9 | Doggerland: Mesolithic Landscapes of the Southern North Sea | 141 |
| 6 | Petrography for Archaeological Geology | 145 |
| 6.1 | Introduction | 145 |
| 6.2 | Major Rock Types and Archaeology | 146 |
| 6.3 | Sedimentary Rocks | 146 |
| 6.3.1 | Arenite or Arenitic Sandstone | 148 |
| 6.3.2 | Arkose or Arkosic Sandstone | 149 |
| 6.3.3 | Graywackes or Clay-Rich Sandstone (“Lutitic”) | 150 |
| 6.4 | A Roman Quern Production and Smithy Works | 154 |
| 6.4.1 | Clastic or Calcarenite Limestones | 154 |
| 6.4.2 | Aphanitic Limestones | 155 |
| 6.4.3 | Dolomite and Dolomitic Limestones | 156 |
| 6.4.4 | Cherts, Gypsum, and Ironstones | 157 |
| 6.5 | Igneous Rocks | 159 |
| 6.5.1 | Granite | 160 |
| 6.5.2 | Diorite | 161 |
| 6.5.3 | Andesite | 161 |
| 6.5.4 | Basalt | 161 |
| 6.5.5 | Rhyolite and Obsidian | 162 |
| 6.5.6 | Gabbro/Diabase | 163 |
| 6.5.7 | Tuff | 164 |
| 6.6 | Metamorphic Rocks | 164 |
| 6.6.1 | Metamorphic Rocks: Foliated | 165 |
| 6.6.2 | Metamorphic Rocks: Non-foliated | 166 |

| | | |
|-------|--|-----|
| 6.6.3 | Metamorphic Rocks of Archaeological Interest | 166 |
| 6.6.4 | “Greenstone” | 170 |
| 6.7 | Techniques: Optical and Otherwise | 173 |
| 6.7.1 | Hand-Specimen Macroscopic Analysis of Rocks and Minerals | 174 |
| 6.7.2 | Optical Properties of Minerals | 175 |
| 6.7.3 | Quantifying Minerals in Thin Sections | 177 |
| 7 | Clay Minerals and Ceramics | 179 |
| 7.1 | Introduction | 179 |
| 7.2 | Clays | 180 |
| 7.2.1 | Clays in Paleosols | 181 |
| 7.2.2 | Clay Deposits | 183 |
| 7.3 | Ceramics and “Ceramics” | 185 |
| 7.3.1 | Ceramic Properties of Clay | 187 |
| 7.3.2 | Ceramic Ethnotechnological Study: Making Navaho/Diné Pottery | 193 |
| 7.3.3 | Geoarchaeological Study of Ceramics | 195 |
| 7.4 | Provenance | 198 |
| 7.5 | Methods | 199 |
| 7.6 | Optical Petrography | 199 |
| 7.7 | X-Ray Radiography | 201 |
| 7.8 | Chemical Analysis | 201 |
| 7.8.1 | An Example of Chemical Analysis Using X-Ray Diffraction (XRD) | 202 |
| 7.8.2 | Diagenetic Changes | 204 |
| 7.8.3 | Analysis of Residues | 205 |
| 8 | Instrumental Analytical Techniques for Archaeological Geology | 209 |
| 8.1 | Introduction | 209 |
| 8.2 | Analytical Techniques and Their Pluses (and Minuses) for Archaeology | 210 |
| 8.3 | X-ray Diffraction (XRD) | 213 |
| 8.4 | X-ray Fluorescence (XRF) | 215 |
| 8.5 | Is pXRF a Revolution or Just the Latest Development in XRF? | 217 |
| 8.6 | Electron Microprobe Analysis and Proton-Induced X-ray Emission (EMPA and PIXE; SEM) | 218 |
| 8.7 | Examples of Chemical Analysis of Nineteenth Century Transfer Printed Whitewares Using EMPA | 222 |
| 8.8 | Atomic Absorption, Inductively Coupled Plasma/Atomic Emission Spectroscopy (AAS, ICP/AES) | 224 |
| 8.9 | Mass Spectroscopy | 225 |
| 8.10 | Aphrodite? An Example of Isotopic Analysis Using Mass Spectroscopy | 228 |

| | | |
|-----------|---|------------|
| 8.11 | Inductively Coupled Plasma: Mass Spectroscopy (ICP-MS; LA-ICP-MS) | 230 |
| 8.12 | Neutron Activation Analysis (NAA/INAA) | 232 |
| 8.12.1 | Provenance Determination | 234 |
| 8.13 | An Example of Neutron Activation Analysis: Coinage and a Celtic Mint: The Titelberg, Luxembourg | 234 |
| 8.14 | Electron Spin Resonance (ESR) | 237 |
| 8.15 | Magnetic Susceptibility | 239 |
| 8.16 | Cathodoluminescence Microscopy (CL) | 240 |
| 8.17 | Infrared and Raman Spectroscopy | 241 |
| 8.18 | Instrumental Geochemical Techniques and Their Availability to Archaeology | 243 |
| 8.19 | A Closing Quote or Quotes | 245 |
| 9 | Metallic Minerals, Ores, and Metals | 247 |
| 9.1 | Overview | 247 |
| 9.2 | Early Metallurgy: Copper | 247 |
| 9.3 | Metallurgy: Copper to Bronze | 249 |
| 9.4 | Iron Metallurgy | 254 |
| 9.5 | A Metallurgy for the Common Man: African Iron | 257 |
| 9.6 | Metallic Minerals and Ore Genesis | 260 |
| 9.7 | Model Studies for the Analysis of Metal in Archaeological Geology | 265 |
| 9.7.1 | Slag: “The Archaeometallurgist’s Friend” | 265 |
| 9.7.2 | Example | 268 |
| 9.8 | Artifacts: “When Fortune Smiles” | 268 |
| 9.8.1 | Example | 268 |
| 10 | Statistics in Archaeological Geology | 271 |
| 10.1 | Introduction | 271 |
| 10.2 | Descriptive Statistics | 272 |
| 10.2.1 | Variables | 272 |
| 10.2.2 | Frequency Distributions, the Normal Distribution, and Dispersion | 273 |
| 10.2.3 | The Normal Distribution | 273 |
| 10.2.4 | Central Tendency | 275 |
| 10.2.5 | Arithmetic Mean and Its Standard Deviation | 275 |
| 10.3 | Inference: Hypothesis Testing, Types of Error, and Sample Size | 276 |
| 10.3.1 | Hypotheses and Testing | 276 |
| 10.3.2 | Probability | 276 |
| 10.3.3 | Types of Error | 277 |
| 10.3.4 | Confidence Interval and the Z-Score | 277 |
| 10.3.5 | Sample Size | 278 |
| 10.3.6 | Example 1: Cranial Capacity in <i>H. Erectus</i> | 278 |
| 10.3.7 | Scale and Size: Adequacy of the Sample in Geomorphology and Pedology | 280 |
| 10.4 | Data Analysis | 281 |

| | | |
|-----------------------------|--|------------|
| 10.4.1 | Example 2: Single Variable Data-Phosphorus in Soils | 281 |
| 10.4.2 | Data Analysis of More than One Variable | 281 |
| 10.4.3 | Covariation-Correlation, Causality or “Not” | 281 |
| 10.4.4 | Least-Squares Analysis and Linear Regression | 282 |
| 10.4.5 | Example 3: Alloys in Iron Age Metallurgy | 284 |
| 10.4.6 | “SHE” Measures of Variability of Assemblages | 285 |
| 10.4.7 | Paired Comparisons or Paired Difference Experiments | 286 |
| 10.5 | Exploration: Multivariate Approaches to Large Data Sets | 287 |
| 10.5.1 | Exploring Correlation Among n Greater than 2 Variables: Some Multivariate Statistical Techniques | 287 |
| 10.5.2 | Discriminant Function Analysis (DA) and Principal Components Analysis (PCA) | 288 |
| 10.5.3 | Cluster Analysis | 291 |
| 10.5.4 | Chi-Square: “Nonparametric” Calculation of Association | 292 |
| 10.5.5 | The Next “New” Thing?: Bayesian Analysis and Archaeological Age Determination | 293 |
| 11 | Theory and Practice in Geoarchaeology: A Brief Discussion with Examples | 297 |
| 11.1 | Introduction | 297 |
| 11.2 | Geoarchaeology and Landscapes | 298 |
| 11.3 | Geoarchaeology at the Scale of Sites and Artifacts | 299 |
| 11.4 | Geoarchaeology and the Origins of the Deliberate Human Use of Fire | 300 |
| 11.5 | Geoarchaeology and the Study of Natural Disaster | 301 |
| 11.6 | Geoarchaeology and a Brief History of Archaeological Theory | 301 |
| 11.7 | Enter Probability | 304 |
| 11.8 | Geoarchaeology, Theory, and Practice: Examples | 305 |
| 11.8.1 | The Medieval Norse Colonies of Greenland: What Were They Thinking? | 305 |
| 11.8.2 | Medieval Iceland to AD 1783–1784: Tephra and Time | 306 |
| 11.9 | Example 2: The Scull Shoals Mill Village Site, Oconee River, Georgia, USA | 307 |
| 11.10 | Concluding Thoughts | 309 |
| References | 311 | |

List of Figures

Fig. 2.1 Map of nearly 200 springs around Menngen Station (in *red*), Northern Territory, Australia (Map drawn by Senior Elder Yidumdua Bill Harney in 2010)

Fig. 2.2 Variety of fluvial terraces, paired and unpaired, created by erosional and depositional cycles

Fig. 2.3 The Hjulstrom diagram. Flow velocity is juxtaposed to sediment size to indicate “transport” (suspension) versus “sedimentation” (deposition) for various sediment grain sizes

Fig. 2.4 Jekyll Island, Georgia, with overlay of a paleochannel or “Old Channel” of the Brunswick River, occupied, in part, by Jekyll Creek, today (Chowns et al. 2008, Fig. 9)

Fig. 2.5 Present-day view of Jekyll Creek looking eastward from the “Old Channel” or “paleochannel” of the Brunswick River toward the “Pleistocene core” per Chowns et al. (2008) (cf. Fig. 2.4). Modern oyster reefs line the shoreline (Photograph by the author)

Fig. 2.6 (L) Illustration of the English Channel River (Redrawn from Osburn 1916, Fig. 26); (R) early Holocene Doggerland (Redrawn from Coles 1998)

Fig. 2.7 *Lower*. Maxilla of adult male mammoth dredged from the North Sea off the Netherlands (Photograph by author)

Fig. 2.8 Paleochannels of the “Transect River,” Georgia Bight, Atlantic Ocean, offshore South Carolina (see *inset, lower left*), as imaged using multibeam sonar data (Stubbs et al. 2007; Harris et al. 2013). *Inset, upper right*, shows incision of the paleochannel into Pliocene lithology

Fig. 2.9 (a) Shaded map showing the AD 563 turbidite deposits (“déplacements des sediments,” in *red*) and the supposed propagation of the tsunami (“raz-de-marée,” *blue arcs*) (Source. 24 Heures, Lausanne, March 8, 2011). (b) Shaded relief map (DEM) (Swiss Federal Office of Topography) of the Lake Geneva. Water depths are indicated by bathymetric contour *lines* (meters). The 563 AD turbidite is color shaded (*orange-blue*) as to extent and sediment thickness (meters). Vessel tracks for seismic lines are indicated. Sediment core locations are indicated by *black*

squares. The *inset* bathymetric profile, X-Y, shows the gradient of sediment thickness

Fig. 2.10 Schnidejoch (*site circled*) in the Bernese Alps of Switzerland (Fig. 2, Hafner 2012)

Fig. 2.11 The first underwater archaeology dive—August 24, 1854, Lac Léman (Lake Geneva). François Marie Etienne Forel, father of a then 13-year-old François Alphonse Forel, is seated in the boat with his back turned, presumably operating the air pump for the diver (Adolphe Morot), while Frédéric Troyon holds a safety line (Water color by Adolphe von Morot)

Fig. 2.12 Water color portrait of François Alphonse Forel in the room he used as his study and laboratory, at his home in Morges on the shores of Lake Geneva (Lac Léman), Switzerland (Watercolor by Ernest Bieler, no date, private collection)

Fig. 2.13 Map by Bettis et al. (2003) showing loess distribution and thickness in the Great Plains of the United States

Fig. 2.14 The Brady paleosol (Photograph courtesy of Charles Trautmann)

Fig. 2.15 The area of the Sahara Lakes (Adapted from: *Saudi Aramco World*, vol. 65 (3), 2014)

Fig. 2.16 The Rift Paleolakes: *NA* Northern Awash, *CB* Chew Bahir, *WT* West Turkhana, *TH* Tugen Hills, and *LM* Lake Magadi

Fig. 2.17 Combe-Grenal stratigraphy—Mousterian levels 24–54 are shown in photo and inset. The rear portion of the inset fence diagram (*B*) is correlated with the photograph, from Bordes (1968), above. Levels 56–64 are shown in the elevation section, below, which corresponds to the far left of the fence diagram (Bordes 1972)

Fig. 2.18 West profile at Pech de l’Aze’ IV. This profile typifies the deposits in this region. It consists of variously sized blocks of limestone *éboulis* fallen from the roof and walls of the cave within a sandy, iron-stained matrix. The sand is derived ultimately from breakdown of the limestone and accumulated via different sources from outside and mainly within the cave, including slope wash, creep, and solifluction (Photograph by Philippe Jugie)

Fig. 2.19 Tsunamigenic deposits for the Santorini eruption or eruptions, 17th c. BC, at East Beach cliff, Crete. The *white line* indicates the erosional contact, termed the basal unconformity, between the chaotic archaeological debris layer and the underlying geological strata. Wall remains and dislocated building stones are present as reworked material in the lower part of the archaeological layer

Fig. 2.20 Block diagram, with strata and folding illustrated (**a**) and geological map (**b**) further illustrating synclinal, anticlinal folding, strike-dip directions (From Allard and Whitney, Environmental Geology Lab Manual, Wm. C. Brown, Fig. 4 (1994))

Fig. 2.21 The first Landsat 8 image. Fort Collins, Colorado (Courtesy NASA/USGS)

Fig. 2.22 Three views of a historic slave cabin, Wormsloe Plantation, Savannah, Georgia, USA. The *upper* two views illustrate LiDAR views, and the lower view is a photograph of the cabin with the LiDAR unit shown (LiDAR and photo images courtesy Geospatial Mapping Center, the University of Georgia)

Fig. 2.23 Illustrating SfM. The *upper* view of an excavation was produced using the program 123D Catch. The *lower* view is a digital-surface view of the same unit using another program, Smart3D. Both views are scalable and rotatable (Images courtesy Geospatial Mapping Center, the University of Georgia)

Fig. 2.24 A small, commercial drone (eBee by SenseFly) being preflight programmed for a photographic survey. The photomosaic shown on the *right* is the result of this particular flight (Photographs courtesy of Chet Walker, shown programming the eBee drone)

Fig. 2.25 A Geo.pdf with the capability for embedding geographic coordinate information. The *red circles* are location of selected test locations across the survey area (Image courtesy of ARI, Tallahassee, Florida)

Fig. 2.26 Linear band ceramic (LBK) sites (*black dots*) plotted relative to loess soils (*gray*) in northwestern Germany (Adapted from Kuper et al. 1977)

Fig. 3.1 Soil profile with commonly found horizons

Fig. 3.2 The Munsell color system. Using this diagram, an example soil color such as “2.5YR5/4” can be understood as 2.5 *yellow-red* on the *hue circle*, 5 on the *vertical scale* for value, and 4 on the *horizontal section* for chroma

Fig. 3.3 Above, sand grains, roundness, and sphericity (Modified from Powers 1953), below, sorting of sand grains (Modified from Compton 1962, *Manual of Field Geology*)

Fig. 3.4 Example ternary diagram plots for, *left*, the United States and, *right*, Great Britain and Wales

Fig. 3.5 Bounding in a spodosol. The A horizon is bounded as “clear to abrupt”; that between the “A” and “E” is “gradual to diffuse” (Photograph by the author)

Fig. 3.6 Disconformable (allo)contact between the Central Builders member of the Wyoming Formation and the coarse gravel in the cutbank of Cayuta Creek in Sayre, Pennsylvania, at river km 452 (Thieme 2003)

Fig. 3.7 Olduvai Gorge, Tanzania. *Upper*, the *red* sandstone of Bed III is clearly visible as well as the *top* of Bed II, lower, stratigraphy of Olduvai (Photograph courtesy of Dr. Sandra Whitney)

Fig. 4.1 Cutting out a soil monolith

Fig. 4.2 Rotary corer. Shown deployed in the excavation of a Roman era cemetery in urban Tunis, Tunisia, the auger rapidly bores through the clastic sediments. Photograph by Nina Šerman

Fig. 4.3 A Giddings hydraulic coring system. The operators are exchanging a “Kelly (extension) bar” from the adjacent rack, to increase the depth of the core. The vertical “mast” contains a hydraulic

“ram” powered by a small engine (not shown) to push and pull, utilizing the lever controls (*red*), the core barrels used to collect sediments. The system is easily deployed using a vehicle as shown. A typical core takes less than 30 min to collect

Fig. 4.4 Ewing piston corer

Fig. 4.5 Sediment sampling log

Fig. 4.6 Sediment box corer

Fig. 4.7 The sediment grab sampler

Fig. 4.8 (a) Above, shallow sediment corer; (b) right, a sediment grab deployed at Jekyll Creek, Atlantic Intracoastal Waterway (AIWW), Georgia, USA

Fig. 4.9 Sediment grab sample on a screen box

Fig. 4.10 Typical sequence of sondages used to systematically characterize the landscape of the Plateau of Bevaix (Courtesy of the Archaeological Service, Canton of Neuchâtel)

Fig. 4.11 Typical stratigraphic sequence seen in the profile for a test unit. The “complexes” listed represent sediment deposits of colluvium and soils formed thereon

Fig. 4.12 The Hjulstrom diagram relating particle movement to size and stream velocity

Fig. 4.13 Imhoff cone and soil auger sample. Suspected B horizon shown separating in Imhoff cone

Fig. 4.14 Phosphate intensity plot for Great Zimbabwe using the colorimetric method (Courtesy of Paul Sinclair)

Fig. 4.15 The Neolithic site of Arbon-Bleiche 3 demonstrating the use of micromorphology; (a) site map with the ground floors of the houses and with the eight phases of the village. The pilings of the houses are marked as *black dots*. The position of the profile section B and the profile photograph (c) are marked with *white arrows* and highlighted in *red*. (b) The west profile through house A showing the typical sequence with two main organic cultural layers divided by a sandy layer. (c) The Arbon-Bleiche 3 thin sections of the column M 1030 (profile B) with the micromorphologically identified phases of installation, organic accumulations beneath the house’s floor and inwash of sand from the hinterland surrounding the village (Fig. 4.2 in Ismail-Meyer et al. 2013, used with permission)

Fig. 4.16 Typical triporate pollen grains: *left*, beech; *right*, oak

Fig. 4.17 Various phytolith types. *Arrows* indicate “cross-body” chlorodoid types, whereas a festicoid type may be present, center of the photomicrograph. The photomicrograph courtesy Dr. Liovando Marciano da Costa. The two close-ups of chlorodoids and festicoid types are from Ball et al. (1996)

Fig. 5.1 General multielectrode resistivity system. This system can be programmed for both Wenner and Schlumberger array configurations

Fig. 5.2 Resistivity pseudosection of Mound A, Etowah Mounds State Park, Cartersville, Georgia, USA. This 20 m-high Mississippian period temple mound was built sometime prior to 1250 AD. It has been the subject of several geophysical studies beginning in 1993 with the author's initial radar studies of this and adjacent mounds B (Garrison 1998). This figure is the result of a later electrical study (Garrison et al. 2005). The near-surface features in red are well-documented "robber trenches" but the deeper anomalies, in green, are prehistoric structural features

Fig. 5.3 The Cherokee female seminary, ca. 1,848. Courtesy of the Oklahoma Historical Society

Fig. 5.4 Three plots of geophysical data from surveys of the site of the Cherokee Female Seminary, Tahlequah, Oklahoma. The upper plots are, respectively, a plan view of quadrature phase data (330 Hz) and the isometric view of the same data. The lower image is a GPR "time slice" of the same area showing good correlation between the two sensors. Architectural interpretation has been added to the radar plot. The area outlined in red is buried ruin of the building

Fig. 5.5 Rose Cottage, from a painting of the house done from memory. Oklahoma Historical Society

Fig. 5.6 A GeoPDF showing the location of UGA survey grids and other landmarks at the Rose Cottage site

Fig. 5.7 Multisensor representations—left and above, magnetic; right, ground radar—of an abandoned Native American cemetery, Park Hill, Oklahoma, Cherokee Nation, USA. The magnetic anomalies correspond to rows of grave pits while the radargram indicates three sides of a buried stone wall. The latter view is 1.74 m depth and clearly shows the rectangular subsurface feature interpreted as a remnant of a stone or masonry wall. The magnetic features (*orange red*) in the plots show linear patterns. The separation between the anomalies indicate individual graves

Fig. 5.8 A profile view of radar data. The image is of a Chumash pit dwelling, roughly 2 m in width, as illustrated in the artist conception adjacent. This is an idealized view of an actual archaeological site on the island of Santa Cruz, California, USA, where the author conducted research on the late twentieth century

Fig. 5.9 The effects of refraction on the radar wave as the dielectric increases (*upper*) or decreases with depth (*lower*) (Adapted from Goodman 1994, Fig. 5.6)

Fig. 5.10 A typical survey grid and GPR units; foreground, a control unit and antenna using a survey wheel; background, another control unit mounted, along with an antenna, on a survey cart. Tapes indicate *transect lines* (Photograph by the author)

Fig. 5.11 Examples of post-processed radar data. Both represent a 2004 radar survey of a Roman villa site in western Switzerland. The plot on the left shows the burial depth at almost a meter, while the plot on the right highlights architectural details of the villa's principal building, the *pars urbana*

Fig. 5.12 Study area, in *red*, for the Sabine River paleovalley study, northern Gulf of Mexico, USA

Fig. 5.13 Acoustical profile and schematic view of sonar images produced by an acoustic sub-bottom profiler of a drowned paleochannel in 15 m water depth in the Gulf of Mexico. Sediment vibracore locations (Fig. 9.14) are indicated. This ancient estuary is illustrated its drowning at transgression ca. 6000 BC (Pearson et al. 2008)

Fig. 5.14 *Left*, sampling the drowned Sabine estuary shown in Fig. 9.13 with a vibracore; *right*, analyzing the sediments in a vibracore taken from the estuary (Pearson et al. 2008)

Fig. 6.1 Ancient and historic jewelry (Source: *National Geographic Magazine*). 1 Pendant of perforated *shell* ca.1000 BC; Syria. 2 Seal, *shell*, 7000–4000 BC; Syria. 3 Tubular bead, *bone*, 3000 BC; Syria. 4 Eye pendant, *glass*, 2000 BC; Egypt. 5 Pendant, *glass*, at least exterior; 600 BC; Punic-Phoenician? 6 Object made of *carnelian*, 600 AD; Central Asia. 7 “Bat wing” object—“parietal”? *Jasper*; Mesoamerica. 8 Bead, *lapis lazuli*, 1000 AD; West Asia. 9 Object fashioned from *fossilized shell*, 1000 AD; West Asia. 10 Incised disk, *shell*, 1900 AD; Mauritania. 11 *Kiffa* bead, *powdered glass*, 1930 AD; Mauritania. 12 Glass art depicting Marilyn Monroe, 2004; USA

Fig. 6.2 Dimension stone. Middle Jurassic sandstones. Dun Beag Broch, west coast of the Isle of Skye, Scotland. Historic Scotland

Fig. 6.3 The rock cycle

Fig. 6.4 Ternary diagram using Folk’s sandstone classification (1948, 1980) (Reproduced from Zahid and Barbeau (2011)). Arenitic, arkosic, and lithic categories are subdivided according to the percentage of each within the diagram. Subcategories, such as lithic arkose and feldspathic litharenite, are illustrated following a 75–50–25 % breakdown

Fig. 6.5 Sandstone Pictish standing stone. Perthshire, Scotland. So-called Class 1 Stone by virtue of only “pagan” Pictish symbols used in its decoration (Photograph by author)

Fig. 6.6 Two thin-section views of arenitic sandstones. *Left*, XPL showing undulatory extinction of the quartz grains (*black* grains). Crystals of sparite cement are clearly seen along the edges of holes (*blue* voids) in the thin section. The quartz grains show shattering due to sawing. *Right*, XPL image showing “twinning” of feldspar grains (*Left* image by author, *right* image courtesy the University of North Carolina-Chapel Hill)

Fig. 6.7 Neolithic Period stelae carved from sandstone, from the megalithic site of Petit-Chasseur, Sion, Valais, Switzerland (Musée d’histoire du Valais, Sion, photograph by R. Hofer)

Fig. 6.8 Rear, a siltstone, green “molasse” dimension stone; foreground, a “grès coquille” or bioclastic limestone (Photograph by the author)

Fig. 6.9 Thin-section views of Grès coquille bioclastic limestone, western Switzerland. The high density and lamination of shell and quartz are clearly visible (Image courtesy of the Archaeological Service, Canton of Fribourg, Switzerland)

Fig. 6.10 The Roman millstone quarry at Châbles-les-Saux, Switzerland (Photograph courtesy of Dr. Timothy A. Anderson (shown in *lower left*))

Fig. 6.11 Backscatter electron (BEI) image showing dolomite rhombs in thin section. A large rotaliid foraminifera (*center*) is surrounded by dolomite rhombs; large apatite grain appears in the *upper, center* portion of the image (SEM image by author)

Fig. 6.12 Novaculite. *Left*, in thin section; *right*, projectile points (Flenniken and Garrison 1975; Used with permission of Maney Publishing)

Fig. 6.13 Pillow lava basalts in road cut, Curaçao, the Netherlands Antilles. Clipboard for scale (Photograph by author)

Fig. 6.14 Bluestone rhyolite quarries, Fishguard Volcanic Group at Pont Saeson, North Pembrokeshire (Map modified from Fig. 1, Bevins et al. 2011)

Fig. 6.15 (a) Thin-section views of strongly foliated rhyolite with small, dark (1 mm) lenses elongated in the plane of foliation. Sample 142/1947.22 from Wilsford, described originally by Stone (1948) and subsequently by Ixer and Bevins (2010) (Courtesy of Professor Michael Parker Pearson). (b) Photomicrograph of strongly foliated rhyolite with small, dark (2 mm) lenses elongated in the plane of foliation. Sample SH08/265 from the 2008 Stonehenge excavations (Courtesy of Professors Tim Darvill and Geoffrey Wainright). (c) Photomicrograph of strongly foliated rhyolite with small, dark (0.5–1.5 mm) lenses elongated in the plane of foliation. Sample PS8 from the Fishguard Volcanic Group at Pont Saeson, North Pembrokeshire (cf. Fig. 6.14) (Photomicrographs per Richard E. Bevins; the National Museum of Wales and Wiltshire Studies)

Fig. 6.16 Metamorphic facies by pressure and temperature. “Low” temperature or “blueschist” facies are typified by steatite (talc); marbles are more “greenschist” facies

Fig. 6.17 The “almond-eyed korai” at the Acropolis Museum, Athens (Photograph by the author)

Fig. 6.18 Livia. Marble portrait (Courtesy the Estate of Dr. Norman Herz)

Fig. 6.19 *Left*, Botticino Agglomerate limestone (Italy); *right*, Rojo Alicante limestone (Spain)

Fig. 6.20 Limestone used for sculptural relief of a Roman tower tomb, *Aventicum, Germania Superior* (modern-day Switzerland). The subject is that of Greek mythology, Triton abducting a sea nymph or Nereide. Roman Museum of Avenches (Photograph by the author)

Fig. 6.21 Soapstone Ridge, Georgia, USA. *Upper*, bowl “blank” in situ; *left*, thin section showing high birefringence of talc; *right*, bowl

Fig. 6.22 Petroglyphic boulder. Granitic gneiss

Fig. 6.23 Menhir carved from schist discovered in the Canton of Neuchâtel, in 1997, during excavations along the then proposed autoroute A5, in the vicinity of the village of Bevaix. The stone is clearly carved as *stelae* and is dated to the Neolithic Period, ca. 5000 BP. The height is 3.2 m and the weight is 2,800 kg. On exhibit, Laténium Museum, Neuchâtel, Switzerland (Photograph by the author)

Fig. 7.1 Weathering of silicate minerals (After Horger 2000). Granites gneisses of the Appalachians produce kaolinite with gabbros yielding smectite and olivine-rich rocks yielding montmorillonite via the mechanisms illustrated below

Fig. 7.2 The silica and alumina tetrahedral/octahedral units

Fig. 7.3 Closed kiln

Fig. 7.4 Phase changes in pottery

Fig. 7.5 Forming the “wet” pot. Note appliqué

Fig. 7.6 Modern Navaho pottery (Photograph by Robert Hill)

Fig. 7.7 Two thin sections of late prehistoric earthenwares, Georgia, USA. In the *left*, firing differences—*black* indicating reducing conditions and *red-brown*, oxidizing. Such differences are not unusual for pit kiln-fired wares. The thin section on the *right* illustrates more uniform firing conditions as well as a more uniform grain-temper sizes. The temper in both is primarily quartz-dominated medium sand. Both photomicrographs were in PPL (Courtesy of Mark Williams)

Fig. 7.8 Sandhills regions, North Carolina. Clay sample locations are marked (Fig. 7.3, p. 34, Herbert and McReynolds 2008)

Fig. 7.9 Various pottery shards from the Sandhills regions. Pottery samples from the Kolb site (38 Da75): (a) JMH051, Yadkin Fabric Impressed; (b) JMH052, Yadkin/Hanover Fabric Impressed; (c) JMH053, Yadkin/Hanover Cord Marked; (d) JMH054, New River Cord Marked; (e) JMH055, Yadkin Cord Marked; (f) JMH056, New River Fabric Impressed (flex warp); (g) JMH057, New River Cord Marked; (h) JMH058, Cape Fear Fabric Impressed; (i) JMH059, Cape Fear Fabric Impressed; (j) JMH060, Hanover I Fabric Impressed (Fig. 7.8, p. 28, Herbert and McReynolds 2008)

Fig. 7.10 Ternary plots of Sandhills’ clay groups (Fig. 7.2, p. 117, Herbert and McReynolds 2008)

Fig. 7.11 The total ion chromatogram (*TIC*) of maize lipids. This shows primarily the plant and/or fish fatty acid ratio (more unsaturated C18:1 than saturated C16:0), plant biomarkers (sitosterol), and acylglycerols. Triacylglycerols are referred to as TAGs, diacylglycerols as DAGs, and monoacylglycerols as MAGs (Reproduced from Reber and Evershed 2004, Fig. 7.1)

Fig. 8.1 Schematic of X-ray diffraction. The diffractometer measures the “d-spacing” between the crystal planes following Bragg’s Law, $n\lambda = 2d \sin \varphi$, where n is the integer representing the peak of interest, d is the lattice spacing of the specific crystallized mineral or element, φ is the angle between the scattered X-ray and the incident radiation, and λ is the wavelength of the incident light

Fig. 8.2 Micro-X-ray fluorescence spectrometer examining painted and unpainted areas on the Orpheus Relief (Photograph by Jeff Speakman)

Fig. 8.3 Typical handheld pXRF instrument. Bruker Tracer pXRF model

Fig. 8.4 Electron and X-ray emission for EMPA showing the relationship between penetration depth, energy, and the sample's atomic number (Z)

Fig. 8.5 *Left*, green transfer printed whiteware shards; *right*, flow-blue transfer printed whiteware shard (scale bars = 1 cm)

Fig. 8.6 Schematic of atomic absorption spectrometer

Fig. 8.7 Schematic for a modern thermal ionization mass spectrometer (TIMS)

Fig. 8.8 Lead isotope ratios of lead curse tables and those of potential ore sources in Greece, England, Spain, Tunisia, and Wales (figure 5, Skaggs et al. 2012, p. 980)

Fig. 8.9 National Gallery of Art, Aphrodite

Fig. 8.10 Distribution of isotopes for various Aphrodites relative to known isotopic fields for ancient Mediterranean marble quarries (Herz and Pike 2005)

Fig. 8.11 Schematic of an inductively coupled plasma (ICP) spectrometer

Fig. 8.12 Schematic of a laser ablation inductively coupled mass spectrometer (LA-ICP-MS) system

Fig. 8.13 *Upper*, plan of Dalles Floor (*green*); *lower*, Dalles Floor (*green*) in stratigraphic section

Fig. 8.14 Coin mold fragments and coin flans from the Dalles Floor, Titelberg

Fig. 8.15 ESR spectra of marble showing typical hyperfine splitting of manganese (Mn)

Fig. 9.1 Central Vinča culture area (*left*); detail showing early Balkan mines (*right*)

Fig. 9.2 Chalcopyrite ore with a replica of Neolithic copper axe shown (Photograph by the author)

Fig. 9.3 Early metal site of Vučedol, located overlooking the Danube River, in eastern Croatia (Photograph by author)

Fig. 9.4 Experimental archaeology. Melting bronze ingots for casting in the stone mold shown in the foreground (Courtesy Latenium, Hauterive, Switzerland)

Fig. 9.5 Experimental archaeology. Cast duplicate of a bronze spear (Courtesy Latenium, Hauterive, Switzerland)

Fig. 9.6 Experimental iron metallurgy. A pit forge, stone hammer, and anvil (Photograph by author)

Fig. 9.7 A hypothesized crucible steel—"wootz"—process

Fig. 9.8 The Ncherenje mine on the Malawian Nyika Plateau (Photograph by David Wenner)

Fig. 9.9 One of the deep pits used to extract ore from the Mbiri iron mines, northern Malawi (Wenner and van der Merwe 1987) (Photograph by David Wenner)

Fig. 9.10 Malawian iron manufacturing, 1982, Chulu, Malawi; above, *left*, furnaces prior to firing; *above*, in operation; *above, right*, micrograph (1000 \times) showing iron (bright spheres) in bloom matrix; *right*, bloom showing large (macroscopic) iron inclusions produced by the smaller, forced-draft furnace (Photographs by Nicholas van der Merve)

Fig. 9.11 Characteristics of an ophiolite complex: axial magma chamber; pillow lava basalts; sheeted basaltic dikes; layered gabbro; dunite/peridotite

Fig. 9.12 European metal deposits with central European mines highlighted

Fig. 9.13 Copper ore, azurite (*left*); native copper (*right*)

Fig. 9.14 Schematic of Laurion's geology of alternating schist and limestone with metal bearing contacts (1–3) between them. The ore contacts, 1 and 3, the richest. Argentite: “silver ore” is associated with the lead ore, cerussite ($PbCO_3$). The principal silver ore mineral is silver chloride, cerargyrite ($AgCl$), and silver sulfide (Ag_2S). The latter is mixed with galena, PbS

Fig. 9.15 Back-scattered electron image of iron slag

Fig. 10.1 The normal distribution. **(a)** The area under the curve is, by definition, 1; **(b)** the measure of central tendency is the mean, which is, again, by definition, zero; **(c)** the curve is perfectly symmetrical about the mean; **(d)** the standard deviation, along with mean, completely defines the normal curve; **(e)** the mean, mode, and the median *all* have the *same* value. The probability $p(x)$ of occurrence of any observed values from 1 to 2 and 8 to 9 (a two-tailed σ is shown in shaded areas). The range of values in this example is 0–10 with the mean (x) = 5.2; 1.5σ indicates the standard deviations from the mean (Adapted from Waltham 1994, fig. 7.7, p. 119)

Fig. 10.2 Linear regression. Two correlations between the observed alpha-recoil track (ART) density in mica inclusions used as a tempering agent for prehistoric Hohokam pottery (“Sacaton Red,” “Vahki Plain,” etc.) versus age in years before the present (BP). The line width for each pottery type track density value is the standard deviation (Garrison 1973; Garrison et al. 1978)

Fig. 10.3 Pair-wise comparison of mtDNA sequences of observed differences in human-Neanderthal sequences and human-chimpanzee sequences

Fig. 10.4 Bivariate plot of elements within Pentelic marble. Two ellipses denote specific marble groups based on discriminating elements (Courtesy Scott Pike)

Fig. 10.5 *Left:* Spode blue printed design. *Right:* back-scattered electron (BSE) image of dye, with brighter areas those of high cobalt content

Fig. 10.6 Binary diagram of PbO and SiO_2 data for all Spode samples. Clusters of “open” samples manufactured before and after 1833, correlating with a change in ownership at the Spode factory

(cf. Table 10.3); the “unknown” (closed) samples are highlighted in gray and occur in their respective manufacturing group

Fig. 10.7 Three chi-square distribution curves. Note the higher degrees of freedom ($df = 19$) approximate the normal distribution

Fig. 10.8 For an assumed set of 6 samples #1 to #6 from the Hallstatt period (750–400 BC) with ages of 750 BC (#1), 745 BC (#2), 740 BC (#3), 735 BC (#4), 730 BC (#5), and 725 BC (#6) indicated by vertical thin lines, the corresponding ^{14}C ages were looked up in the calibration curve. Due to the flatness of the calibration curve, we get the same ^{14}C age of 2455 BP for all six samples. After adding a random scatter of ± 40 year, we obtain the following ^{14}C ages: 2546 BP, 2490 BP, 2402 BP, 2446 BP, 2386 BP, and 2491 BP. By individual calibration, the samples can no more be assigned to distinct regions. The resulting probability distributions (*gray curves*) rather cover the whole Hallstatt period. These probability distributions correspond to our simulated ^{14}C measurement data. After the Bayesian sequence algorithm is applied, one can see its tendency to divide the period into six parts of equal size (*black curves*). Due to the flatness of the calibration curve, the general shape of the individually calibrated and of the “sequenced” probability distributions is the same which true ages ever are assumed. In our example, the posterior 95 % confidence intervals of samples #4, #5, and #6 are not in agreement with their assumed true ages. All the calculations (single calibration and sequencing) were performed with OxCal v2.18 (Ramsey 1995) using the INTCAL98 ^{14}C calibration curve (Stuiver et al. 1998). The program normalizes the individual and the “sequenced” probability distributions to the same maximum (*probability*) value (Italics added for emphasis)

Fig. 11.1 Painting of the Scull Shoals mill, in the nineteenth century; at its peak

Fig. 11.2 A 1.5 m sediment core, using a cryoprobe at the Scull Shoals site, *right* (Photographs by the author)

List of Tables

Table 3.1 Designations of master soil horizons and subordinate symbols for soils (Adapted from Olson 1981)

Table 4.1 The standard grain-size scale for clastic sediments

Table 4.2 Sample preparation for pollen analysis

Table 4.3 Palynological composition of samples from Gray's Reef

Table 4.4 Process of phytolith extraction

Table 5.1 Resistivity of common materials

Table 5.2 Magnetic susceptibilities of common rocks and minerals (cgs units)

Table 5.3 Magnetic properties of soil minerals

Table 5.4 Typical values of radar parameters of common materials

Table 6.1 Classification of sedimentary rocks

Table 6.2 Common igneous rocks

Table 7.1 Climate and weathering of silicate precursor minerals

Table 7.2 Consistency water %

Table 7.3 Characteristics of ceramic bodies

Table 8.1 a: Green sherd, WDS data. b. Blue sherd, WDS data

Table 8.2 Isotopes utilized in NAA analysis of coins and molds from the Titelberg

Table 8.3 CL and other characteristics of selected white marbles

Table 8.4 Instrumental techniques and their detection limits

Table 9.1 Major mineral processes and deposits by origin (Carr and Herz 1989)

Table 9.2 a: Whole-rock chemical analyses of samples from the Mbiri mine. b. Whole-rock chemical analyses of samples from the Ncherenie mine

Table 9.3 Principal metallic ores

Table 10.1 Scales and statistical measures

Table 10.2 Compositional data (in %) for Iron Age artifact

Table 10.3 Spode pottery statistical analysis (Douglas 2000)

Table 10.4 Contingency table for winged versus socketed axes

This book is a survey of techniques used in archaeological geology or as it is more widely known, today—geoarchaeology. It is less a discussion of theory or methodology with regard to the various geological techniques that are presented. It is not an exhaustive presentation of the diversity of earth science methods that can be utilized in the service of archaeology. Earth science can be used in many ways in archaeology. Certainly there are other ways to approach the multiplicity of archaeological questions that confront the student of the past, and this book does not presume to suggest that the techniques presented herein are the only ones appropriate for addressing the many facets of archaeological inquiry.

The Penrose Conference, in 1987, sponsored by the Geological Society of America (GSA), archaeological geology was a rapidly growing interdisciplinary field in which archaeologists and geologists attempt to use the tenets of both their sciences to solve problems of mutual interest. This involves the application of the principles of geomorphology, sedimentation, isotope geochemistry, and petrology in the solution of problems of interest to both. As examples, the following may be cited: the effect of climate on sites and site selection; the extent to which archaeological sites may subsequently be modified by erosion, sedimentation, and tectonic activity; the application of geophysics in the search for and dating of sites; the application of dating techniques especially as related to the

Pleistocene and Holocene; the interrelation of diet, culture, and environment; and the relation of artifact raw material to site selection, trade route development, and ancient technology.

The acceptance of earth science techniques into archaeological study has been gradual but has grown to a point that we now have university-level programs in archaeological science, geoarchaeology, and/or archaeological geology. As Norman Herz, in *Geological Methods for Archaeology* (1998), stressed, it is less what one calls the use of earth science techniques in archaeology than what one realizes from their application. The practice of modern archaeology demands an understanding of earth science. One does not have to look any further than that of the importance of, first, Sir John Evans and Joseph Prestwich's and then Sir Charles Lyell's 1859 visits to the gravel beds of the Somme River. In the Somme gravels, Boucher de Crève Coeur de Perthes, in 1837, and, later, Jérôme Rigolot had painstakingly demonstrated the contemporaneity of ancient stone artifacts and extinct paleontology. Their visits brought the newly developed insights of the science of geology to the interpretation of the Somme deposits by which greater scientific validity was a result. This interplay of archaeology and geology has resulted in similar advances in our understanding of our human past.

Charles Robert Darwin, himself, wrote three separate treatises on the nature of archaeological

materials in the soil (1837, 1844, and 1881). Charles Darwin's so-called worm book influenced many early researchers who, following his lead, demonstrated how soil biota mechanically generate new strata and soil horizons, as well as blur or destroy them (Leigh 2001; Johnson 2002). The title of the first was *On the Formation of the Vegetable Mould* and that of the last was *The Formation of Vegetable Mould*, which is misleading to the modern reader unless they understand that "vegetable mould" was a nineteenth-century term for topsoil (Johnson 1999). Darwin's essays examined the relation of soils, earthworms, and artifacts. Darwin's question centered on *why* archaeologists invariably *dug* for materials that, in the case of those of Late Antiquity, such as Roman, should not be buried at all. We would call his study, today, a study of *bioturbation* or how the action of soil-dwelling organisms, such as the earthworms, creates soils. Bioturbation is not limited to worms (Johnson 1990). Larger burrowing animals such as gerbils, rodents, and insects play a large role in this phenomenon. In fluvial, lacustrine and marine environments' other burrowing organisms such as shrimp, clams, and worms play the same role. To Darwin, bioturbation worked to bury artifacts (Leigh 2001). His observations, however well worked out, were lost on antiquarians and later archaeologists mainly due to miscommunication. Geologists and soil scientists "spoke" a different language or jargon from that of the archaeologists. In today's geoarchaeology, we recognize the importance of both natural burial processes along with those of erosion. By these two processes, two archaeological surfaces are created. Following Darwin's 1859 publication of *Origin (of Species)*, Charles Lyell, one of the founders of modern geology, published *The Geological Evidences of the Antiquity of Man* (1863)—conceivably the first book on geoarchaeology.

After the great time depth of human antiquity was established in Europe after 1859, archaeologists were faced with integrating this greater temporality into the "3-Age System" of Denmark's Christian Thomsen—Stone, Bronze, and Iron. It was obvious that the Stone Age was

now vastly longer than the other two ages. John Lubbock, of Great Britain, proposed dividing the Stone Age into two, "New" and "Old," hence the term *paleo* (old) and *lithic* (stone). By extension, the "New" Stone Age was *Neolithic* or "New Stone." Lubbock and other workers used differing criteria to define the two: the Neolithic was defined in terms of industry, while the Paleolithic was based on fauna—"reindeer period," "elephant period," etc. Although a British prehistorian coined the term, the French created the chronology.

Edouard Lartet (1801–1871) developed the first useful chronology for the Paleolithic, using paleontology as a guide. He divided Quaternary (Pleistocene) into the Cave Bear Period, the Elephant Period, the Rhinoceros Period, and the Reindeer Period, from oldest to youngest. "Upper" Paleolithic cultures lived in the Reindeer Period, for example. DuPont reduced these to two—"the Mammoth, Cave Bear Period" and "the Reindeer Period."

Henri Breuil and Gabriel de Mortillet produced subsequent chronologies that quickly replace Lartet's at least in France, but even in the early twentieth century the British were using Lartet's scheme.

Lartet based his chronology on fauna ala Lubbock—not artifacts. This is a paleontological approach. Lartet's model, also, was regional in scope—not universal for all areas or regions. In this Lartet was accidentally more correct than later workers and their Paleolithic chronologies—which had differing timing of the Paleolithic phases in differing parts of the world.

Gabriel de Mortillet (1821–1898) recognized the great temporal length encompassed by the Paleolithic. He did not know exactly how much time but geology clearly inferred this. He published his ideas in 1869. His divisions of the Paleolithic were simple: Acheulean, Mousterian, Solutrean, and Magdalenian. With two additions, in his lifetime, these basic divisions are used today.

This simple system rested on some complex theoretical underpinnings. De Mortillet rejected Lartet's "faunal" ages—"Reindeer," etc. He did so for two reasons: first, paleontologists did not

agree on any single scheme for faunal successions, and, secondly, instead of using presence-absence of species, Lartet used the relative abundance of species. How to determine this? Types of fauna will vary according to the site and context. De Mortillet's solutions: Stone Tools. His divisions were materially based instead of paleontological. De Mortillet's scheme was cultural-historical in concept—culture history through typology (of stone tools). French prehistorians, like many of the nineteenth-century researchers, were trained in geology. De Mortillet simply declared it “(prehistory) to be an extension of geology” (Daniel 1967). Into the mid-twentieth century, French prehistorians continued to hue to a “paleontological” paradigm for the conceptualization of their excavations. Strata were viewed biostratigraphically but material finds—tool types (*fossile directeurs*), aka the “biota”—separated antecedent and subsequent units (Sackett 1999).

Stratigraphy was used by North American researchers in the mid-to-late nineteenth century.

Rapp and Hill (2006) give a thorough review of this in their textbook. Some of this historical context bears repeating here. In addition, like the French pioneers of Paleolithic archaeology, Americans used paleontological principles as well in their work. George Frederick Wright had advocated for an *American Paleolithic* based in part on the geological context of artifacts (Wright and Haynes 1892). The question of a geological context for this American Paleolithic at the time of Wright hinged in large part on working out the glacial sequence for North America at a level equivalent to that of Europe. The European glacial sequence owed much of its precedence to the pioneering work of Louis Agassiz in the 1840s. Along with Wright, W.H. Holmes, successor to John Wesley Powell at the United States Geological Survey (1902–1910), recognized the importance of this sequence as a reliable context for archaeological research (Holmes 1892, 1893). Key to working out the last glaciations sequence was Newton Horace Winchell, State Geologist for Minnesota, later integrating this knowledge in his book, *The Aborigines of Minnesota* (Brower et al. 1911).

An integrative framework that incorporated the geology into the overall explanatory perspective of archaeological research was necessary, and it was a product of the efforts of numerous workers across the globe in the twentieth century. Working at the Galilean cave sites of Skhul and Tabun, Dorothy Garrod, the British archaeologist, and Dorothy Bate, the British paleontologist, combined to work out the sedimentological sequences for these Paleolithic deposits. Both sites, excavated by Garrod between 1929 and 1934, revealed the richness of Middle and Upper Paleolithic archaeology in the Levant. Garrod found both Neanderthal and “Anatomically Modern Humans” (“AMH”) in the caves but not in the *same* cave. Tabun was “Neanderthal,” while more modern yet contemporary hominin occupations were identified at Skhul (McCown and Keith 1939). These researchers recognized the importance of the sedimentological context relative to the interpretation of these important sites.

The dichotomies, specialty and gender based, that existed in prewar scientific studies of Paleolithic sites are illustrated at the Mount Carmel caves. Garrod and Bate were female, albeit University trained, whereas the paleontological description of the Skhul and Tabun hominins fell to Theodore McCown and Arthur Keith, at Garrod's behest, we can be sure. These two anatomists found the nearest affinities of the Skhul hominins, who they termed the Mount Carmel people, with those found at Krapina in Croatia “...through the anatomy of the Mount Carmel people there runs a substratum of characters which link them to the Neanderthal type.” The Tabun type, plainly Neanderthaloid, may be placed at one extreme and the Skhul type at the other (McCown and Keith 1939). In these conclusions, they were proven correct. This said, the divisions between archaeology, geology, and paleontology were evident. Goldberg and Bar-Yosef (1998); Meignen et al. (2001); Vita-Finzi and Stringer (2007) represent three major modern-day geoarchaeological studies of both Tabun, Skhul, and, also, Kebara Caves.

Even in Tanzania, where Louis and Mary Leakey toiled for years before finally unearthing

the early hominins that made them, perhaps, the most recognized paleoanthropologists of the twentieth century, geology was necessary. Hans Reck worked with Leakey early on roughly and at the same time Garrod and Bate were excavating in Galilee, in the early 1930s. By being trained in both volcanology and paleontology, Reck was well suited for working out the stratigraphy of the Olduvai Gorge in two expeditions to the site in 1913 and, again, with Leakey in 1931.

While much later in terms of evolutionary time, discoveries in New Mexico, in 1927, at the Folsom site, extended America human antiquity into the Late Pleistocene. This discovery of extinct megafauna together with distinctive lanceolate tools propelled a renewed cooperation between geology and archaeology (Howard 1935). Edgar Howard integrated several lines of research—paleoenvironmental, archaeological, and geological—into an early synthesis of what became to be known as the “Paleo-Indian Period.” Better known than Howard, and Elias Sellards, who had examined the association of human remains and megafauna in Florida, was Kirk Bryan.

Bryan, according to Rapp and Hill (1998), along with Ernst Antevs, dominated the interface between geology and archaeology in the 1950s. Their work continued primarily in the American Southwest at Clovis, Chaco Canyon, and other locations such as Midland, Texas, where definitive Pleistocene-aged human remains were excavated (Wendorf et al. 1955). In the mid-twentieth century, in the United States, the use of geological methods at the Midland site by Wendorf and his co-workers, Claude Albritton, Alex Krieger, and John Miller, in the 1950s, set an important and enduring example of how geology and archaeology buttressed each other to mutual advantage (Wendorf et al. 1955).

Karl Butzer is generally recognized as one of the first, in the mid-twentieth century, to integrate geology and archeology (Butzer 1971; Hassan 1979). Gladfelter proposed a definition for geoarchaeology in 1977. He, along with Butzer together with Davidson and Shackley (1976), was the first to call the field

“geoarchaeology,” while Rapp and Rapp and Gifford (1985) helped coin the alternate term “archaeological geology.” As Hassan pointed out in his 1979 review, geoarchaeology had moved away from a set of methods in support of archaeology to one more focused on the relationships of local and regional geology to settlement locations together with the nature of site formation processes (Hassan 1977, 1978; Schiffer 1982). Butzer (1971) proposed a “contextual archaeology” of which the geological and geomorphic played no small part. He—Butzer—in 1975, wrote that the geologist should be well acquainted with the goals and aims of archaeology, while the archaeologist should be fully aware of the potential of geological investigations. Specific geoarchaeological questions should arise from a consideration of geological variables in man-earth interactive systems (Hassan 1979).

Indeed, this textbook simply reinforces similar calls by others within the geology of archaeology. These include Karl Butzer (2008), George (Rip) Rapp, Vance Haynes, Jack Donoghue, Brooks Ellwood, Reid Ferring, William Farrand, Joel Schuldenrein, and Julie Stein to name but a few of these scholars. As previously noted, above, Rapp, in his books written with John Rapp and Gifford (1985), and Christopher Hill (1999, 2006), together with works by Davidson and Shackley (1976); Gladfelter (1977); Waters (1992); Stein and Linse (1993); Stein and Farrand (2001); Bettis (1995); Pollard (1999); Goldberg and MacPhail (2006), have provided clear models for modern geoarchaeological inquiry and interpretation. Archaeological geology has become more than simply “method oriented.” While a methodology is clearly a technique-driven enterprise in the service of both archaeology and Quaternary studies, it has developed a theoretical contextualization (Goldberg and MacPhail 2006). This has been principally a recent development. In the first edition of this textbook, a draft chapter devoted to a discussion of theory in archaeological geology was deleted in the editorial process.

As a consequence of that editorial decision, the first edition of *Techniques for Archaeological*

Geology had no body of theory to discuss. While geoarchaeology has no great pantheon of past practitioners such as older disciplines like physics and chemistry (Garrison 2001), it has begun to develop a theoretical approach to its study of the intersection of earth processes and human agency. It is no great stretch for geoarchaeologists to pose questions posed as hypotheses nor to use induction as a tool to generate ideas of causation or affiliation among an observed set of variables (Buchdahl 1951). Wilson (2011) characterizes geoarchaeology as evolving into a coherent discipline no longer limited to geologists helping out archaeologists nor archaeologists simply with an interest in geology. Geoarchaeology is seen as discipline unto itself bridging its two parent disciplines of geology and archaeology (*supra*). Human life has never been distant from natural influences. Archeologists have always been skeptical of environmental determinism in explanation and would have no counsel for a geological determinism. Modern geoarchaeology tends to heed Butzer's (1982) injunction to treat neither culture nor environment as static nor separate from one another. Charting intersections of culture and nature tend to provide insight into the role of each as they influence each other in the complex coevolution of natural and anthropogenic systems in prehistory (Haynes 1995; Redman 1999; Levine 2007; Benedetti et al. 2011).

As Gladfelter, in his acceptance of the Geological Society of America's "Ripp Rapp" Archaeological Geology Award in 2001, implies, it (geoarchaeology) is an honorable enterprise (GSA Today 2002). In the past years, this observation has been made of archaeology itself (Daniel 1967). The application of perspectives and methods born in disciplines like geomorphology now are recognized as crucial to the understanding of site location, function, duration, and like questions (Jones 2007). Quoting Beach et al. (2008), "Geomorphology deals with Earth surface processes and landforms; archaeology deals with what artifacts in the landscape can tell us about the human past. Because geomorphology as a discipline was born through a mixture of physical geography and surficial geology, geomorphology can inform archaeological

studies through its focus on landscapes and formational processes over a wide range of spatial and temporal scales." Special issues of important journals such as *Geodinamica Acta* (2007), *Geomorphology* (2008), and *Catena* (2011), all devoted to geoarchaeology, emphasize its global reach (Tourloukis and Karkanas 2012) as well as the field's multidisciplinarity as a major feature and methodological strengths. Hassan in his 1979 *American Antiquity* article "Geology and the Archaeologist" may have suggested a more narrow view of the discipline than he intended. Geology as an earth science is mostly synonymous with lithology of the Earth, while geomorphology is associated with the surface of the Earth. Geology concerns itself with the Earth surface, but geomorphology is more likely found within Department of Geography. Both geography and geology are branches of earth science.

Over the latter part of the twentieth century, the incorporation of the methods of other areas of earth science—geochemistry, geochronology, and geophysics—has expanded the reach and utility of archaeological geology. As Kraft notes in a review of archaeological geology, the workers in this area are becoming more aware of the nuances of the historical and classical record (Kraft 1994). Legend, oral tradition, mythology, and the body of cultural knowledge for a prehistoric culture are being used in the search for information about ancient events—paleoenvironmental and paleogeographical (*supra*). This is the essence of a "multidiscipline" archaeological geology—the use of geological and analytical techniques in concert with archaeological expertise to gain knowledge of the past. This book echoes many of these tenets set forth by these other workers. In so doing, this work will serve to amplify that call for technical and methodological rigor in the use of earth science in the practice of archaeology as a whole.

One last note as to what archaeological geology is about, simply put geoarchaeology. In a sense, Hassan, Gladfelter, Rapp, and Gifford may have inadvertently proscribed geography and the important subfield of geomorphology by using the terminology "archaeological geology." Geoarchaeology is the more inclusive

terminology and that probably explains its more frequent usage today. This text will simply use “geoarchaeology” throughout with the understanding that the author recognizes its more common usage as well as that the discipline’s signature journal is entitled *Geoarchaeology*.

1.1 Organization of This Book

This work is comprised of 11 chapters. The contents of these chapters cover major elements within archaeological geology. One significant aspect of earth science that is omitted is that of geochronology. This was consciously done. Given the present-day literature on the use of dating techniques in archaeology, another survey of this area hardly seemed warranted. The reader is directed to the premier volume of this series by Springer-Verlag, *Age Determination of Young Rocks and Artifacts* (Wagner 1998). The focus of the book will be on a systematic approach to the archaeological site, its geomorphic/geological features, and anthropogenic materials from an earth science perspective. While geochronological techniques are central of the understanding of stratigraphic contexts of sites, their in-depth discussion will remain secondary if discussed at all. Individual chapters are discussions of those areas of earth science that bear directly on the nature of archaeological deposits and materials as interpreted from the geological perspective.

Chapter 2 will address the geomorphological and geological context of the archaeological site. Immediately obvious is the question of scale to be considered by the researcher. This devolves, in turn, on the archaeological objectives of the specific research. Regional scale mapping would be called for by a research design that seeks to determine the spatial context (location) of a cohort of sites, their cultural and temporal placement important but secondary at this stage of the inquiry. Below regional scale would be the local environment of the individual site. This is, perhaps, the most familiar type of geological mapping used in archaeology. From a geomorphological standpoint, the identification of landforms (the specific case) and landscapes

(the general case) is important (Evans 1972). From the geological standpoint, the identification of structural framework and the characterization of the area’s lithology from outcrops and exposures must be done as well. To do this, the archaeological geologist relies on traditional as well as contemporary methods.

Studies show that animals throughout the Holocene are indicators of both changing climates and cultural evolution and that coastal sites are strongly influenced by changing sea level; the history of these changes can be recreated by sediment coring studies. An understanding of site selection criteria is important for archaeological studies in of fluvial, estuarine, and coastal systems throughout the United States and the world. Earth science techniques can be deployed to quickly identify areas with a high potential as ancient habitats. Geoarchaeological evidence can be used to document neotectonism, sea-level changes, and site location.

In the area of traditional geological mapping, the researcher relies on their training in landform and soil recognition, basin hydrology, and structural geology. The basic tools are maps—geographical, geological, and hydrological—together with the compass, the inclinometer, the shovel, the rock hammer, and the hand lens. Today, there are newer tools such as satellite images, satellite location or global positioning system (GPS), laser technology as seen in the increased use of LiDAR, laser transits, and levels coupled with laptop computers and geographic information systems (GIS). The low-cost autonomous vehicle or “drone” has revolutionized the mapping of landscapes and archaeological features. Whatever the technique or tool, the aim is the same: characterize the geomorphic and geological context of the archaeological site or sites. Once this is done, the archaeologist has a better understanding of the “why” of the site’s location in a particular landscape. The past landscape or landscapes generally are masked by modern earth system processes such that the determination of the prehistoric landscape becomes an archaeological inquiry in and of itself.

Chapter 3 principal focus is the description of sediments and soils and their use in archaeological geology. The chapter, in some detail, examines ways to carry out more detailed investigation into the sedimentological context of the archaeological site and its environment beyond that of the present-day or near-surface components. The prehistoric landscape can be, and oftentimes is, more deeply found than what is capable of recovery with the shovel or even mechanical excavation. The recovery of sediment columns from hand-operated and mechanical coring devices is a favored means of geoarchaeological study and has a successful history in application. Cores produce not only sediments but macrobotanical, macrofaunal, and artifactual remains as well. Cores taken in a systematic campaign across a site, and its surrounding area, can yield significant amounts of environment, depositional history, and spatial extent. Mechanical excavation, in exposing soil and sediment profiles, are superior to coring for obtaining the “big picture” as regards the geomorphic mapping of the lateral continuity of sedimentary deposits. Both hand and mechanical methods have their place in archaeological geology. It is difficult to visualize the deployment of a large mechanical excavator or even a drill rig on a prehistoric burial mound given the rarity and uniqueness of these features. Gone are the days of total excavation of these types of structures. Careful and judicious sampling of them requires methods that give the researcher greater control (and analytical returns) over the technique to be used. Noninvasive, shallow geophysical methods, discussed in Chap. 5, are proving to be essential in the sensitive sites.

Chapter 4 deals with analytical procedures for examining sediment and soil samples acquired by excavation or coring methods. The five “p’s”—particle size, point counting, phosphorus content, pollen, and phytoliths—are discussed. Mineralogical identification of sediments will be discussed in the context of petrographic methods in Chap. 6. Many of the methods presented are hardly “cutting edge,” but they have had significant development and application across a broad range of archaeological

materials achieving reliable results. Studies of sites should include micromorphology, hearths, floors, phytoliths, and chemical analysis, especially of Al, organic C, Fe, available phosphate, and pH. Sedimentation plays a key role as a counter to erosion in site preservation and also allows dating, e.g., volcanic ash layers in Santorini and, of course, Pompeii, where recent studies have provided new insights into the timing and kind of eruptions that destroyed this city and nearby Herculaneum in AD 79. Micromorphology is a mainstream methodology for the study of deposits created or altered by human occupation; thereby, allowing for distinctions between cultural and natural transforms must be made.

In Chap. 5, shallow geophysics is discussed as a modern outgrowth of the need for techniques that can rapidly and effectively characterize near-surface geology. Overviews are cited and used to update the earlier edition (Clark 2003; Linford 2006; Gaffney 2008). This is a geophysics that is basically non-seismic in nature or one that does not use sound as the principal means to measure subsurface rock and sediment thickness. When applied to archaeological problems, this form of geophysics has been called “archaeological geophysics” or more simply “archaeogeophysics.” Weymouth (1996) has called this use of geophysics “digs without digging.” Beginning in the 1960s with the application of electrical methods such as resistivity profiling, the field has expanded with the addition of electromagnetic techniques such as conductivity meters and metal detectors, the use of magnetics in the form of magnetometers and gradiometers, and, since the late twentieth century, the increased use of ground penetrating radar (GPR). Coupled with computer software that is basically derivative from seismic-based geophysics, the expansion of geophysical prospection into archaeology has produced an extensive body of research in recent decades that is recognized within both archaeology and geology.

Chapter 6 deals with the use of petrographic methods in the analysis of rocks, minerals, sediments, and archaeological artifacts or features made up of all or some of the foregoing.

The principal discussion centers on the utility of the geological thin section and the petrographic microscope in analyses of rock and mineral items of archaeological interest. Beyond the hand lens this protocol is the geologist's most reliable and time-honored methodology. As Herz and Garrison (1998) has pointed out, it is also one of the most economical and reliable ways of determining the geological nature of artifacts. It is certainly to be considered before moving to the next level of analysis—geochemical analytical techniques. What is disquieting is how often the archaeologist does not use petrography before moving to more costly methods. In the case of ceramic studies, the use of petrography is a major and precise method of studying ceramics and their clay sources (Vaughn 1991; Velde and Druc 1998; Courty and Roux 1995; Quinn 2013).

Determining sources of raw material for lithic artifact fabrication was discussed in the context of manufacturing techniques, reasons for use of the particular raw material, source depletion, usefulness, and change of social patterns. Analysis of data obtained on physical properties such as mineralogy, petrology, and chemistry must be evaluated in the light of method of production, use of the artifact, and effects of long-term burial. Finally, interpretation of the relationship between the artifact and the ancient cultural context must also take into account the expertise of the ancient artisan.

Chapter 7 reintroduces the importance of clay minerals and cultural materials, such as ceramics, made from these unique minerals. Our discussion will center on recognition and characterization of clay minerals both as primary and secondary minerals and in particular their use by prehistoric and historic cultures. From both geological and mineralogical perspectives, clays represent a robust contemporary area of study. Much like stone, “Clay is where you find it.” We’ll examine this proposition further as well as the basic geochemistry of how clay forms as a weathering deposit (primary) of silicate minerals and secondarily as deposits of transported sediments. Consideration will be given to the wide range of ceramics from earthenwares to porcelains. A discussion

of clays and their mineralogical transformations at high temperatures provides insight into manufacturing processes. Geoarchaeological and geochemical protocols for ceramic analyses will be examined.

Chapter 8 deals with some of the more prevalent instrumental techniques that have come to be used in the study of archaeological problems. Notable among these techniques are neutron activation analysis (NAA) and mass spectroscopy of stable isotopes. Added to these are the X-ray methods of fluorescence and diffraction (XRF and XRD). The latter method has been styled as “the archaeologist’s first line of defense in mineralogical identification.” Together with the electron microprobe (EMPA), its high-energy cousins—various ion microprobe methods, inductively coupled plasma spectroscopy (ICP), and atomic absorption spectroscopy (AAS)—the archaeological chemistry of artifacts, and, increasingly, their residual contents, food, liquids, etc., are the subject of major contemporary studies across all aspects of archaeology: prehistoric and classical.

Because of the usefulness of stable isotopes in geoarchaeology, Chap. 7 will examine their worth for provenance in paleoenvironmental and paleodiet studies. Sulfur isotopes are particularly useful in the studies of handmade artifacts. The strontium isotope ratio, which depends upon sea or land source, is useful in studies of marbles, as are oxygen and carbon isotopes. Carbon, along with nitrogen, sulfur, and strontium, is also useful in determining diet and diet changes through the study of the isotope content of bone. The nitrogen content of bone can distinguish herbivore from carnivore and, along with carbon and sulfur content, is useful for determining the nature of isotope cycling on a global scale. To the question of whether trace element signatures could be helpful in determining sources of raw material used in the manufacture of artifacts worldwide, the answer was that an extensive library of samples and a wide range of archaeometric techniques would be required.

Chapter 9 recognizes the importance of the study of ores, manufacturing debris, and slags, together with research on metallic artifacts as an

increasingly important aspect of archaeological geology. The metal ages—bronze to iron—comprised two-thirds of Thomsen’s nineteenth-century classificatory system for European prehistoric cultures. The late twentieth and early twenty-first centuries have seen advances in archaeometallurgy (Roberts and Thornton, eds. 2014). An example of the intersection metallurgical techniques, used by Bantu tribesmen of Malawi, illustrates how primitive iron-making methods necessitated the extraction of iron from low-grade ore when higher-grade ore was nearby and known. Trace element variety, content, and ratios may also provide important clues to the source of raw material, but application of the data must take into account, in the case of metallic artifacts at least, the possible effects on the fingerprint patterns of any flux used in the smelting process.

Chapter 10 reprises the first edition’s review of some basic statistical methods used in archaeological geology. Updates relative to the advances in the application of multivariate methods to large data sets (Speakman et al. 2011) and the increased use of Bayesian methods will be presented.

Chapter 11 is a concluding chapter as well as a brief discussion of theory and practice in geoarchaeology. In some ways, it simply redresses the lack of such a discussion in the first edition. This textbook is not a comprehensive treatment of the field of archaeological geol-

ogy as it exists today: radiocarbon, fission track, luminescence, archaeo- and paleomagnetism, U-series, argon-argon, and aministratigraphy methods are only discussed in relation to example applications and do not occupy a chapter to themselves. Likewise, fission-track methods are especially useful in dating volcanic rocks and, potentially, pyroclastic deposits. For ages up to 350,000 years, dating by U-series isotopes has been shown to be particularly useful. Remanent magnetization and optical/thermal luminescence (OSL/TL) can both be used to date sedimentary rocks, on the bases of time of deposition for the former and time of burial and exposure to heat or sunlight. In the case of OSL, the growth of its use in geoarchaeology has been exponential.

It is a tribute to the increasing maturity of the field, as a discipline, that there is such breadth and diversity in its subject matter. What I shall attempt to in the following chapters is expose the student, and any interested colleague, to practical concerns and earth science methods that are useful in the consideration of archaeological problems. Archaeology identifies the results of this interaction between humans and nature in the material remains found in the Earth. Linking the trajectory of past human cultures to that of the earth system requires geological science. The synthesis of this interaction provides a diversity of roles for the archaeological geologist/geoarchaeologist using the techniques outlined in this textbook.

2.1 Introduction

As noted in the preceding chapter, geomorphology is a discipline more often found in the larger field of physical geography, at least in the United States and Great Britain, while sedimentology is a speciality area of geology. While some in archaeology may wonder at a partition in what is basically earth science, the location of geomorphology within geography has had some unexpected benefits, most notably the recognition and use of the burgeoning techniques of geographic information systems better known as GIS. Likewise geographers were quick to incorporate their traditional interest in remote sensing into GIS studies as well. Digitally based, these large-scale spatial analysis systems have proven to be a boon to geoarchaeological researchers. GIS frameworks, devised principally within geography, have made it possible to converge many different lines of data into synthetic map projections that can be manipulated and compared so as to yield new insights into the nature of archaeological sites and their locations. Had geomorphology been housed exclusively within geology departments, it is unlikely that GIS methodology would have entered the arsenal of archaeological geology as quickly as it has. Sedimentology and its close relationship to paleoenvironmental study, particularly in quaternary research, have continued to be a major component of archaeological geology. Likewise, the mapping the surface and subsurface

of an archaeological locale provides crucial information as to the why of a site's specific location and possible function.

2.2 Landscapes and People

In Native American mythology, the landscape is often characterized as either indifferent or even antagonistic to humanity. Descriptions of the ancient landscape by these and other cultures, Australian, for instance, ascribe it as resulting from the action of powerful forces often in zoomorphic form. Humanity inherited this landscape from more primal times (and species, "monsters," etc.), and it was only made more habitable by time and heroic figures such as the Hero Twins of Diné cosmology of the American Southwest. Today, most geologists view the Earth's surface is a transient feature changing in a kaleidoscopic fashion through eons. This was not the case for many earth scientists into the early-to-mid-twentieth century (Frankel 2012). For much of the geology's history, the Earth was a "fixed" planetary sphere whose exterior's surface was the only changing feature. This "fixist" view was eclipsed by the theory of plate tectonics by the mid-1970s (Frankel, *supra*). The interior as well as the exterior of our planet is subject to constant change.

Non-western, nativist views of the Earth often reflect this dynamic view of the Earth. Certainly

aboriginal descriptions of the early Earth incorporate change as a key process. The forces for much of this change were seen as corporeal supernatural beings or “monsters.” How else could the Earth being changed without recourse to power beyond the kin of humans? Knowledge of the land surface was critical to human survival. Prehistoric and some modern tribal peoples set great store their knowledge of their geographies. Modern cultural geographers and ethnographers have recorded this aspect of non-Western knowledge time and again.

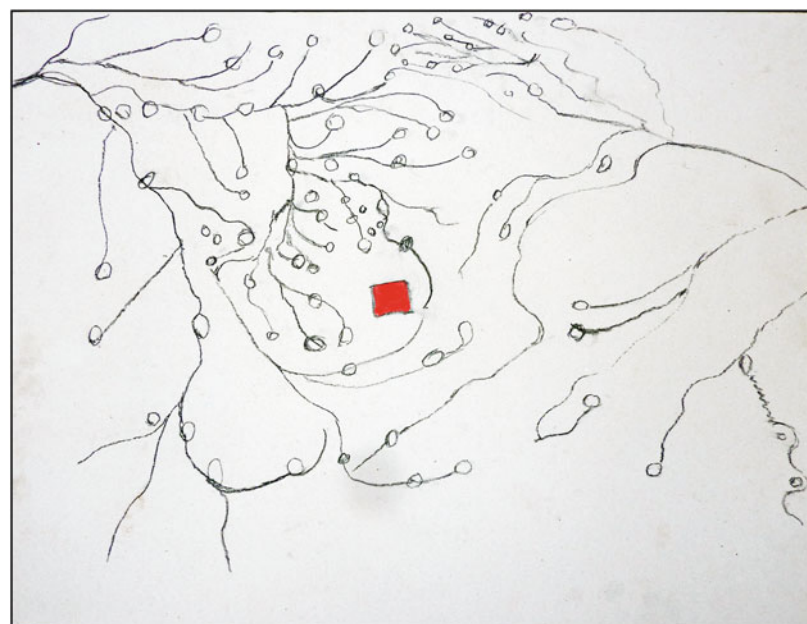
Basso (1996) in his award-winning treatment of the “place making” of the western Apache noted that “entire regions and local landscapes are where groups of men and women have invested themselves … and to which they belong.” The late Lakota scholar, Vine Deloria, Jr., observes that “most American Indian names embrace spatial constructions of history” (*supra*). Pulitzer prize-winning author, N. Scott Momaday writes: “From the time the Indian first set foot on this continent, he centered his life in the natural world.The sense of place was paramount. Only in reference to the earth can he persist in this identity (Momaday 1994:1).”

The Cherokee Indians name the double peak, in the Great Smokey Mountains of North Carolina, known to others as Chimney Tops, *Duni'skwalgun'i*. The name means “forked antler” for the great stone deer concealed there (Camuto 2004a). It is either a great stone animal or a mountain of flesh and bone. Perhaps both (*supra*). This and other ridges of the mountains are ancient storehouses and council places for animals (as well as humans) (Camuto, *supra*). The Cherokee nouns that describe these mountains are archaic and stony things. *Nugatsa'ni*, high ridge with a gradual slope, is similar in its specificity as that of the Western Apache, *Tséé Chiizh Sidilé*, “Coarse-Textured Rocks Lie Above in A Compact Cluster” (Basso 1996).

Exacting landscape descriptiveness and its relevance to non-Western cultures is further illustrated by the hand-drawn map below. Created, in less than 2 h, from memory, by a Wardaman Aboriginal Elder, it shows the locations of nearly 200 springs near his house in the Northern Territory of Australia (Fig. 2.1).

The twenty-first-century view of a malleable and changeable Earth surface echoes that of the ancient non-Western models. At geological time

Fig. 2.1 Map of nearly 200 springs around Menngen Station (in red), Northern Territory, Australia (Map drawn by Senior Elder Yidumdua Bill Harney in 2010)



scales, the surface-forming processes of erosion and deposition are secondary to the larger, dramatic forces of plate motion, tectonism, and orogeny. Such processes operate within time intervals, outside human experience, approaching that of *Wilson Cycles* wherein oceanic basins rift open and subsequently close after millions of years (Levin 1988).

The geomorphic surface is a mixture of landforms that are an expression of (1) modern geological processes and (2) geological processes that are no longer active. Landscapes reflect present and past processes of erosion and deposition. The topography of a given landscape is the result of climate-driven processes oftentimes directly coupled to tectonic activity. Rinaldo et al. (1995) presented these relationships in a mathematical model of landscape evolution which underscored the importance of tectonic uplift to the formation and persistence of geomorphic signatures. Seismicity is not a new concern in geomorphology, but its character and expression—earthquakes, faulting, and volcanism—are important to unraveling the nature and origin of various relicts and modern landforms.

In the northern hemisphere, climate-driven processes have given rise to glaciations which the geomorphologist must always be cognizant of the special character of glacial landform. The interactions of landform and environment are dramatically demonstrated in North America and Europe due in large part to their glacial past. Concomitant with Ice Ages were marine regressions, and consequent transgressions, which alter coastal and fluvial systems and play much the same role as uplift in non-glaciated regions. Coastal landforms—past and present—are the expression of glacial processes acting globally through sea-level change.

2.3 Geomorphic Concepts

Keller and Pinter (2002) review the basic principles used in the study of geomorphic landscapes. The most basic principle, in terms of modern, process-oriented geomorphology, is

that any change in a landscape implies a change in process. Other concepts include:

1. Landscape evolution can be gradual or abrupt as thresholds are exceeded.
2. The interaction of landscape changes with thresholds results from complex processes and is termed *complex response*.
3. Various tectonic fault varieties—normal, reverse, and slip-strike—are associated with characteristic landforms.

In general these geomorphic concepts apply to that part of the Earth's history called the Quaternary. The Quaternary spans, exactly, the last 2.588 million years and encompasses the largest part of hominid evolution in the later Pliocene and Pleistocene (Riccardi 2009; Gibbard and Head 2009).

One of the oldest models for landscape evolution is that of William Morris Davis who articulated the “Cycle of Erosion” (1899). In this model, brief periods of uplift are followed by much longer periods of inactivity and erosion. In Davis' view, the landscape had a “life cycle” from (1) youth through (2) maturity to (3) old age (*supra*). Young landscapes are characterized by stream incision, and deep valleys are followed, in mature landscapes, by less dramatic stream gradients and valley down-cutting. Mature landscapes have broad floodplains and meandering streams characterized by high discharge and sediment loads. In old age, the landscape has eroded to a planar or *peneplain* surface with low relief awaiting rejuvenation or the start of a new cycle. Davis put a time scale of a million years on his cycle—long but archaeologically more relevant than the longer Wilson Cycles.

In this, and, other process models, the landscape can, and will, equilibrate for thousands of years. Equilibrium is clearly a relative concept with regard to landscapes. As we will discuss in Chap. 3, paleosols typically mark these equilibrium periods of climate. Uplift can go on for millions of years however imperceptively. Likewise, subsidence and/or erosion will occur over the same time scales. In many instances, the interplay of these forces is a “zero-sum”

situation. In the contest between uplift and erosion, the latter always wins in the cycle of erosion. Small wonder that archaeology is an endeavor that deals primarily with that which is buried. Yet without uplift, the geomorphic surface of the Earth would be that of the relatively unchanging surface of Mars. In the case of Mars, landers and mapping satellites have identified what Morris would have termed “old age” with only erosion—primarily by wind—modifying a desert surface. Still, what we term “deserts” on Earth, such as Antarctica, the Atacama, or the Sahara, cannot begin to match those of Mars for stark barrenness and lack of overall change.

Some geomorphologists define a type of equilibrium termed “steady state” where the landscape exhibits a relative constancy over a period of 100–1,000 years. This conceptual view of the landscape can be called the “average” of a land surface at this particular time scale. From a process-oriented perspective, one could say the limits of equilibrium or thresholds are relatively “high” such that abrupt or dramatic landscape change is precluded at this scale.

In a tectonic sense, landscapes can be “dormant” with little actual or observable seismic activity. Generally the most active landscapes are those associated with seismically dynamic zones such as found at crustal plate boundaries. Conversely the most inactive areas, again, in the tectonic sense, are furthest from plate margins such as continental interiors. It is easy to locate tectonically active areas. They either exhibit volcanoes or earthquakes or both. Archaeological examples come easily to mind—the Apennines, Naples/Pompeii, Thera/Akrotiri, Anatolia, the Dead Sea region, the East African Rift Valley, and Pacific Rim to name the most obvious.

The “take-home message” for the archaeologist using modern process geomorphology is that the geomorphic surface on (and under) which archaeology is found is not a static surface. Even in a geological sense, the geomorphic surface changes at rates of decadal to annual scale. True, the mountain belts form at Wilsonian rates as do their valleys and adjacent basins, *but* their

surfaces are modified, daily, by gravity-driven processes—creep, erosion, etc. Because of this dynamic and changing surface, the archaeologist should never be lulled into thinking that surface is immemorial. It is not.

The landforms that we propose to study and map are the result of three factors: (1) geomorphic processes, (2) stage of evolution of landform, and (3) geological structure. To map archaeologically interesting topography, one must (a) identify the geological processes by which the landform were shaped, (b) recognize the stages of development of landform and their evolution through time, and (c) recognize the topographic expression of geological structures—dip, strike, clinal variation, etc. In geoarchaeology, the consideration of topography must include another factor—human-induced geomorphic change.

2.4 Geomorphic Setting

A brief review of geomorphic settings reminds us that there are basically only fluvial, desert/arid, coastal, glacial, volcanic, and karst/caves. Most archaeology is done in relation to fluvial landforms. Human groups have always gravitated to available water, and this is readily apparent in any study of agrarian cultures. Crops need reliable water supplies and these are most often found in drainage systems. Besides available water, there are rich, deep alluvial soils which ancient farmers were quick to identify and exploit. Geomorphic settings are the result of geomorphic processes—fluvial, aeolian, volcanic, and glacial processes—which in turn are special cases of the two primary processes: erosion and deposition. In this book, we are concerned primarily with the identification of the results of geomorphic processes than the processes themselves. The study of the latter is that of surficial process geology. In this chapter, we recapitulate the importance of these landforms to archaeology and their attributes.

2.4.1 Fluvial Landforms

Mapping fluvial systems involves both the horizontal and vertical dimensions of the riverine topography. In creating floodplains and valleys, streams alternately downcut and deposit sediments. In montane areas, alluvial fans are key features that contribute to the available sediment balance as well as the distribution of that sediment. Another key landform feature in stream valleys is terraces. It is on these topographic features that most archaeological sites are located. Determining their number and order is a primary objective in any mapping of a fluvial system. The youngest terrace (T_0) is adjacent to the floodplain, and the oldest is the highest terrace (T_n) (Fig. 2.2).

Between these terraces, the channel moves alternately eroding (cutbanks) and depositing (point bars) alluvial sediments, generally opposite to one another. Depending upon elevation and gradient (slope), which are direct expressions of uplift, stream and valley morphology vary from region to region. The hydrologic cycle (precipitation-evaporation) determines the amount of available water to the drainage system, in turn influencing the incision and growth of smaller-order streams within the drainage basin. The delta represents a major fluvial landform historically significant to human cultures throughout antiquity.

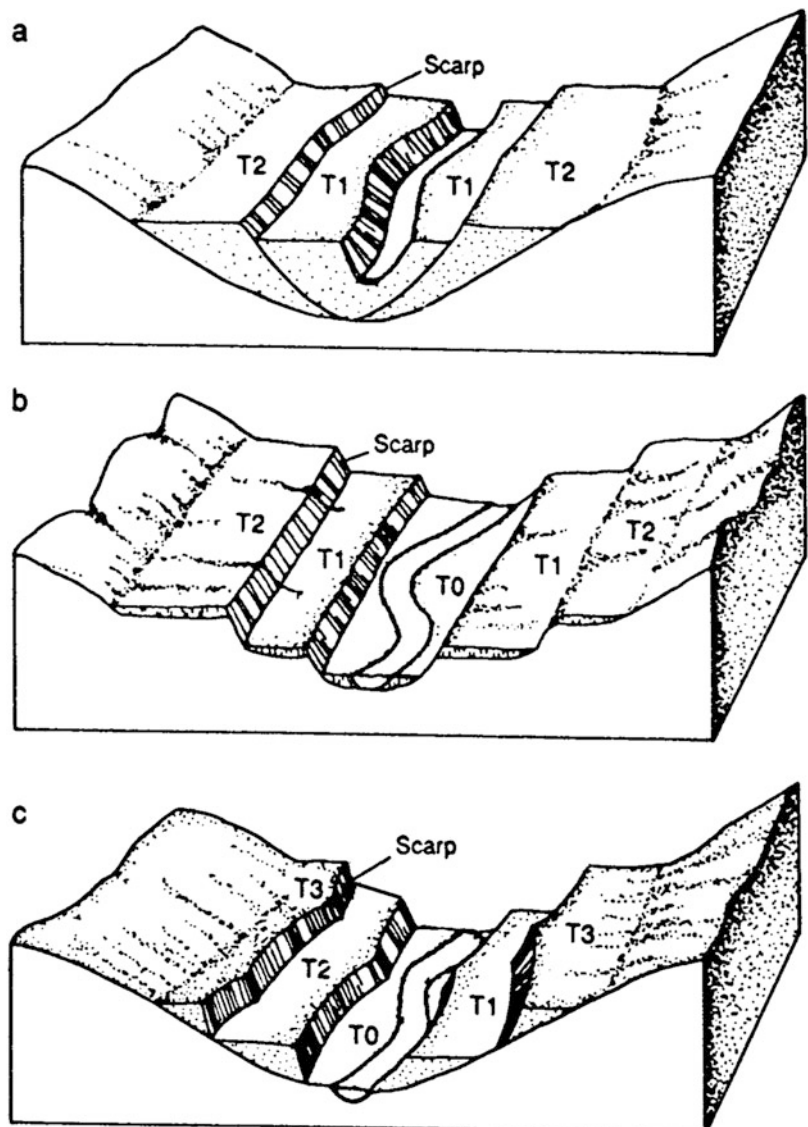
Fluvial systems, along with volcanoes and glaciers, have the role of renewing “old” landscapes and building new ones. The movement of eroded sediments is principally the role of the stream. In doing so, it transports the sediment through its valley creating terraces, levees, and floodplains and, ultimately, modeling coastal landforms—estuaries and beaches. Depending upon the factors of precipitation, vegetation cover, lithology, and gradient, the sediment load a stream carries varying with its discharge. That latter factor is dependent on climate. For geoarchaeology, the correct reading of type, texture, and distribution of fluvial sediments allows the retrodiction of past climate—the controlling factor in paleoecologies and a primary mediating element for past human cultures.

Streams incise, creating terraces and valleys, and aggrade, creating floodplains and new channel courses (Fig. 2.2). When stream base levels are lower, the stream incises even in its lower reaches. When the base level rises, due to changing climate and elevated lake/sea levels, a stream aggrades. Base level was first defined by John Wesley Powell (Leopold and Bull 1979). Powell correctly identified sea level as the ultimate arbiter—exclusive of mediating factors (geological framework, etc.)—of upstream incision. An incising stream is more of a conduit for sediment. Only when the discharge increases to flood levels does the sediment escape the channel to deposit new sediments in the floodplain. A stream carrying large volumes of sediments, such as an outwash stream, can fill its channel to the extent that an arbitrarily higher base level is established. Streams can then regularly overflow and significantly increase the volume of sediment in its valley.

In any discussion of fluvial systems, “load” and “form” are often paramount. Bed, wash, and suspended “load” characterize the finer-grained sediment entrained in a river and deposited in its floodplain. Included with discussions of load is “flow.” Flow can be described as laminar, turbulent, chaotic, etc. Flow is quantified using parameters such as Reynolds number, Froude’s number, etc. Flow and sediment load are combined in the Hjulstrom diagram (Fig. 2.3).

Recent studies (Pizzuto 2012) have shown the movement of fine sediment is less “suspended” as load than it is moved by saltation analogous to aeolian processes. Where bed and suspended load have a genetic relationship, “wash” load has none, being, rather, that portion of sediment carried entirely by stream flow with no deposition. The architecture of sediment facies within or adjacent to streams can be characterized as (1) massive, (2) cross-bedded, (3) laminar, and (4) interbedded, to name the more commonly used terms. Likewise, cross-bedded forms can be “trough-like,” “planar” within channel forms described as “m-scale,” “epsilon,” and “low-to-high angle” (Larsen and Brock 2014). This architecture is a direct reflection of stream flow and sediment depositional regimes (Tilston

Fig. 2.2 Variety of fluvial terraces, paired and unpaired, created by erosional and depositional cycles



et al. 2015). When coupled with sediment size and velocity estimates, retrodiction and modeling of systemic dynamics are possible.

Soils formed or forming on the valley floors are buried, becoming paleosols, often together with archaeological facies associated with these land surfaces (West and Dubos 2013). Streams, in incision, and meander, likewise, can exhume past land surfaces.

Weathering of the uplands, coupled with and caused in part by precipitation, is the ultimate source of the basin sediments. The sediments are

thus a direct record of their parent lithologies and, in some part, the processes active on these rocks and minerals. For instance, if we observe resistant materials, such as quartz and rutile, in large amounts in the sediments we can speculate on the nature and intensity of the weathering climate. By contrast, the finer sediments of clay and silts suggest a much different climate scenario as well as that of deposition and stream dynamics.

Human changes of landscapes can alter runoff and the sedimentological character of fluvial

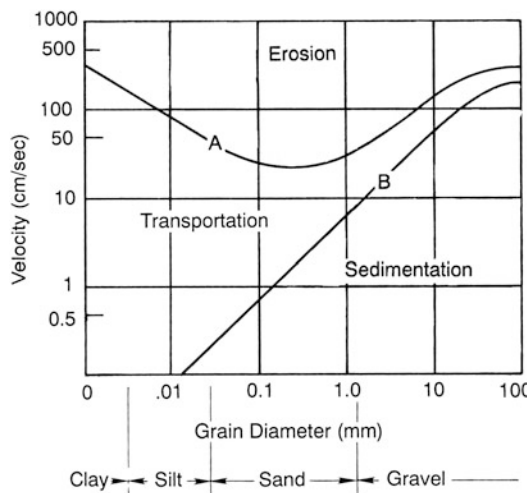


Fig. 2.3 The Hjulstrom diagram. Flow velocity is juxtaposed to sediment size to indicate “transport” (suspension) versus “sedimentation” (deposition) for various sediment grain sizes

systems. Dramatic changes in erosion, due to the clearance of forests, increase the sediment loads of streams, causing aggradation and increased recurrence of floods. Since the Neolithic, these changes have increased principally because of the introduction of plant and animal domestication. In extreme cases, the soils of the watershed are eroded to bedrock, but more often the upper soil horizons (cf. Chap. 3) are deflated, leaving the resistant soil layers such as clay-rich B horizons on which new soils and sequences can form.

Alluvial and colluvial fans—Petit-Chasseur, Sion, Switzerland—50 years ago, during the construction of a new road between Sion and Petit-Chasseur, workers discovered the remains of over a dozen Late Neolithic (ca. 2500 BC) dolmen tombs (Osterwalder and Andre 1980). Buried under deep (6 m+) alluvium, the elaborate tombs and 30 menhirs (standing stones, cf. Chap. 5, Fig. 5.7) were well-preserved along a small tributary of the Rhône (Sauter 1976; Besse 2014). During the construction, and reuse, by later peoples, of the tombs, the Late Neolithic and Early Bronze Age climate only produced nominal runoff and erosion. Sometime after 2200 BC and into the Middle Bronze Age, the

climate became much wetter. Elevated levels, in the Alpine lakes, which submerged the lake dwellings of earlier cultures, attest to this. At Petit-Chasseur, the increased precipitation, together with denudation of the surrounding slopes, led to greater erosion and runoff which, in turn, led to increased flooding by the small river. Coupled with the aggradation of the river, colluvial debris flows inundated the site as well. The archaeological site disappeared under a cone of alluvium and colluvium.

2.4.2 Coastal Landforms

The fluvial delta marks the entry of the river to the sea. The delta is the alluvial fan deposited in the sea rather than in stream valley. Coastal landforms are among the most changeable of all geomorphic settings. This is due to sea-level change wherein a rising sea level creates a submergent coast and conversely a falling sea level produces an emergent coast. In the United States, the bulk of the eastern shoreline is submergent, while that of the west is largely emergent. In the Gulf of Mexico, the shoreline of eastern Texas and that of Louisiana together with Alabama and Mississippi are submergent due to the great sediment loading of the continental shelf by the Mississippi River. Coastal down warping due to sediment loads mimics that due to little or no tectonic activity producing continental margins like the Eastern United States. Coastal landforms can challenge fluvial for the density of archaeological sites. Wherein the fluvial system provided humans with rich riparian zones, many coasts have comparably biologically active estuaries. Human cultures have taken advantage of these estuarine zones, and their settlement remains dot the shorelines of the Earth—past and present.

The most prevalent coastal landform is the beach, whether on a barrier island or simply the margin, above sea level, of a continental landmass. The beach is a transient topography changing over time with eustatic sea level and over the year according to storms and season. Ancient

beaches are of archaeological interest. Henry de Lumley, in his landmark excavation of Terra Amata, demonstrated the presence of Pleistocene hominids—*Homo erectus*—on now uplifted, exposed beaches at Nice, France (Lumley 1969). Beaches and dune systems, often found back of them, provide direct clues to sea level and climate, fauna and flora found within their sediments.

Estuaries form back of the beach and represent the juncture of the river and the ocean. They are unique landforms that are the richest, in terms of biomass, along shorelines (Odum 1995). Estuaries are transient landforms like beaches. Unlike the beach, the estuaries can penetrate inland and cover large areas of the coast. These landforms are rich in archaeological sites from the Mesolithic to the historic era. The deltas of large fluvial systems attracted early human groups to their rich alluvial deposits as well as abundant marine resources.

Geoarchaeological sediment coring of the coastal plain and estuarine deposits along the Eastern North American margin has gone on apace, in the late twentieth and, continued, into the early twenty-first century (Pavich et al. 2010). Coupled with new data from the offshore, the southeastern United States has provided a higher-resolution view of the Pleistocene and early Holocene. The penultimate glaciation (MIS 4) and interglacial (MIS 5) paleoenvironments have been characterized using pollen and macrobotanical remains from sediment cores into estuarine sediments of the Chesapeake Bay (*supra*).

As shown in the following, Chowns et al. (2008) have presented reimagined Pleistocene age paleochannels now infilled behind modern barrier islands (Fig. 2.4). Chowns and his students have posited the presence of an “inlet-dominated” coast for the Georgia Bight rather than a “tidal-dominated” coast of today. In this inlet-dominated model, coastal streams, such as the Brunswick, Ogeechee, and other coastal plain rivers, did not debouche at their modern locations but ran parallel to the coast behind barrier island systems. Figure 2.4 illustrates this scenario where the paleo-Brunswick River

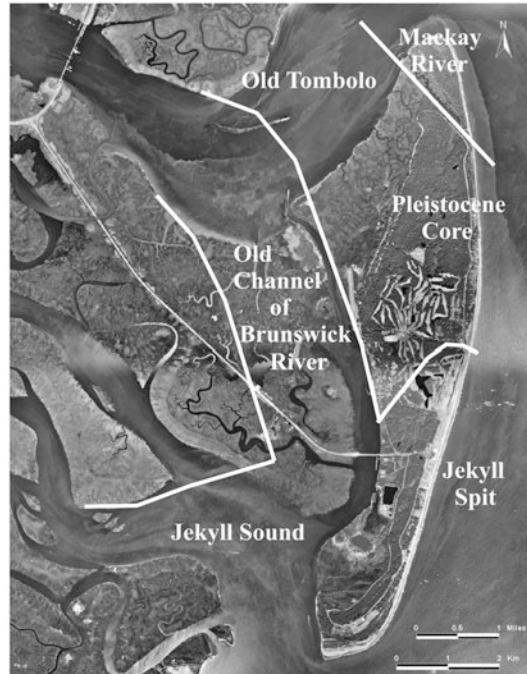


Fig. 2.4 Jekyll Island, Georgia, with overlay of a paleochannel or “Old Channel” of the Brunswick River, occupied, in part, by Jekyll Creek, today (Chowns et al. 2008, Fig. 9)

followed the thalweg of the modern Jekyll Creek, thereby emptying into the Atlantic south of a paleo-Jekyll Island (“Pleistocene core”) rather at its modern tidal delta at the north end of the modern island. Figure 2.5 shows this proposed paleochannel in its modern setting.

The Jekyll Creek area was vibracored by Chowns (*supra*), and bedforms, so described, suggested the remnant of a buried paleochannel of the Brunswick River. A later 2012 survey (Panamerican Consultants, Inc.) mapped subbottom features as stratigraphic sections of alternating beds, channel parabolic “sag” features indicating channel facies. A high backscatter sonar contact, along the channel margin, upon diver investigation, was confirmed to be a deposit made up of whole and fragments of oysters. All specimens were disarticulated, with evidence of oxidation (rust color) on many valves. The oyster shells were large, and there were equal numbers of left and right valves indicating a natural deposit of undetermined

Fig. 2.5 Present-day view of Jekyll Creek looking eastward from the “Old Channel” or “paleochannel” of the Brunswick River toward the “Pleistocene core” per Chowns et al. (2008) (cf. Fig. 2.4). Modern oyster reefs line the shoreline (Photograph by the author)



age. Based on size, alone, the oyster specimens were larger than modern populations encountered during subsequent studies (Garrison et al. 2012a).

2.4.3 Submerged Landforms

Jonathan Benjamin (2010) summarizes much of the modern archaeological emphasis on submerged coastal landforms of the continental shelf and estuaries in Europe. Specifically, focus on the inundated prehistoric terrain of the North Sea Basin which remains one of the most enigmatic archaeological landscapes in northwestern Europe. This region was submerged by the sea for 11,000 years following the last glacial maximum (LGM), and this change in sea levels resulted in the loss of an area larger than the modern United Kingdom (Coles 1998, 2000). The region therefore contains one of the most extensive and, presumably, best preserved prehistoric landscapes in Europe (Gaffney et al. 2007) and has been named “Doggerland” (Fig. 2.6; cf. Chap. 9).

This submergence of the present English Channel and North Sea was not unknown to early twentieth-century archaeologists. Writing in 1916, H.F. Osburn specifically presents strikingly accurate maps of the “English Channel

River” and its surrounding terrain (Fig. 2.6). This Quaternary Channel River had its formation on Oligocene times but occupied a repeatedly incised Pleistocene era paleo-valley (Lencolais et al. 2003) (Fig. 2.6).

Submerged landforms and oftentimes buried, prehistoric archaeological sites thereupon are difficult to discover and study. These submerged sites are extremely relevant to a fuller understanding of human colonization and expansion in Asia, Europe, Africa, and the Americas. These now drowned landforms were generally subaerial coastal plains for several millennia prior to and after the Last Glacial Maximum (LGM). Recent studies have amply demonstrated that there are recoverable cultural and subfossil faunal materials (Fig. 2.7) left behind on submerged former coastal plains worldwide (Al-Suwaidei et al. 2006; Anuskiewicz and Dunbar 1993; Dunbar et al. 1989; Erlandson et al. 1998, 2011; Faught 2004a, b; Garrison et al. 2012c; Grøn and Skaarup 2004; Grøn 2006, 2007; Kelley et al. 2013; Lavin 1988; Lübke 2002; Merwin 2010; Rick and Erlandson 2009; Rick et al. 2013).

The search for prehistoric submerged archaeological sites has gained increasing attention in both the scholarly world and in the popular imagination and is, in part, driven by modern research that has demonstrated that climate change and

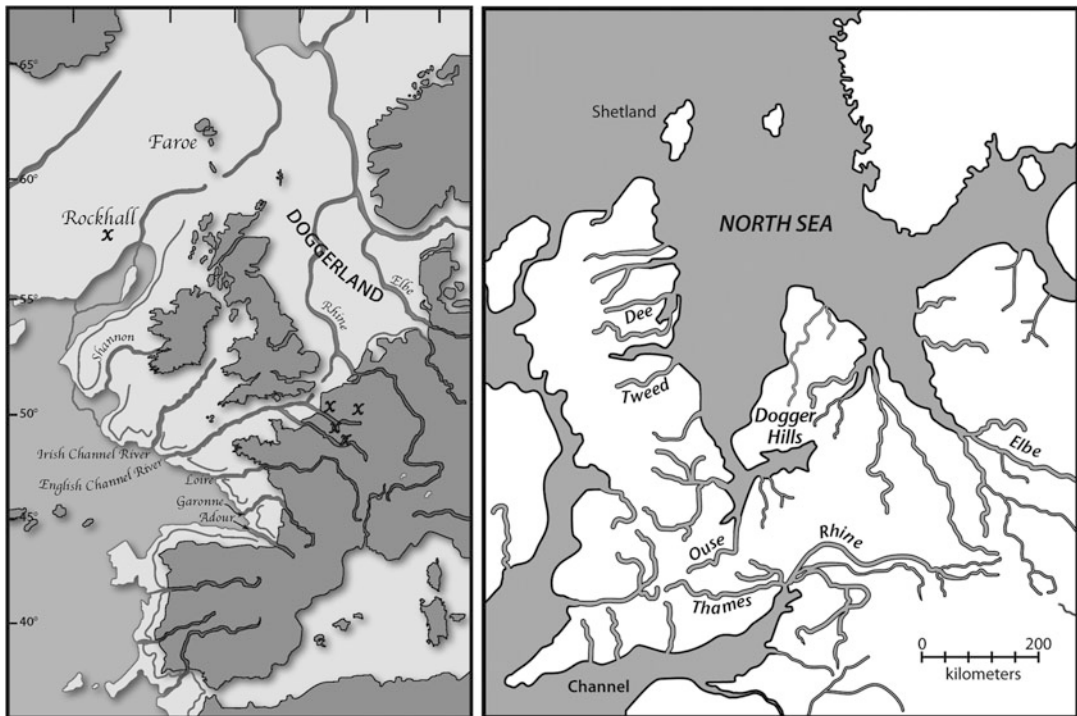


Fig. 2.6 (L) Illustration of the English Channel River (Redrawn from Osburn 1916, Fig. 26); (R) early Holocene Doggerland (Redrawn from Coles 1998)



Fig. 2.7 Lower. Maxilla of adult male mammoth dredged from the North Sea off the Netherlands (Photograph by author)

marine transgression are not gradual events to which human groups gradually adapt themselves. Instead, global research has shown that ice sheet collapse and subsequent sea-level rise often proceed in rapid pulses (Berner and Berner 2012). Likewise, the continental shelves themselves are

geologically “recent” (2012). Helland-Hansen et al. (*supra*) point out the fact: “Because we live during a glacial highstand during which previous coastal plains are now flooded, our perception is colored by the present state. For long periods of Earth history (especially greenhouse intervals), shelfal bathymetric profiles were likely *not* prominent features” (emphasis added).

Submerged, non-eroded, sites on continental shelves often have a much higher potential to preserve organic materials than similar, terrestrial sites, and one can reasonably conclude that prehistoric submerged sites have the potential to offer significant insights into human behaviors during any period of lowered sea levels and specifically badly needed insight into human behaviors during periods of rapid sea-level rise and climate change. Perhaps even more importantly, archaeological research focused on the end of the Pleistocene through the middle of the Holocene (around 20,000 BP until 5,000 BP—note that all years are given in radiocarbon years,

not calendar) can provide insights into the colonization and settlement of the prehistoric Americas. Without the inclusion of data sets gathered from submerged sites, our understanding of coastal occupations during these early periods remains incomplete, and it is impossible to understand the fuller spectrum of early human use of changing coastlines and coastal landforms (Bailey and Flemming 2008; Benjamin and Hale 2012; Faught and Donoghue 1997; Faught and Gusick 2011; Fischer 2011).

The search for prehistoric underwater archaeological sites in North America has used, primarily, a methodology that focuses on the search for terrestrial evidence of early human presence and then extrapolates that information to the near and offshore (cf. Fladmark 1979; Pearson et al. 1982; Benjamin 2010; Dixon 2013; Flatman and Evans 2014). Some of the earliest dates for human occupation of the New World come from the southeastern United States (Anderson and Gillam 2000; Faught 2008: 676, 683), while research within the last 30 years has demonstrated that coastal areas are extremely productive zones with a wide variety of food resources available year round (Reitz 1982; Rietz and Reitz 1988). Taken together, these findings strongly suggest that coastlines were probably occupied virtually as soon as human groups entered the Americas, following the so-called “coastline” hypothesis that colonizing groups from northeastern Siberia followed the now-submerged coastline during entry instead of the so-called Ice-Free Corridor between the Laurentide and Cordilleran ice sheets (Erlandson et al. 2011).

Fladmark (1979) well prior to the period of the general acceptance of a “Pre-Clovis” occupation of the Americas observed, “A wide range of data suggests that a mid-continental corridor was not an encouraging area for human occupation, if even basically inhabitable, during the climax and initial retreat of the Woodfordian ice.” In his 1970 report on the archaeology of the Queen Charlotte Islands, now Haida Gwaii, he noted that “An interesting possibility is presented by the presence of cultural remains on the islands at least 8,000 years old, and the geological

indications of ice free areas in the northeast end of, Graham Island. During, or just after a glacial maximum, decreased sea level, may have exposed the floor of Hecate Strait and opened a migration route via an exposed shelf along the eastern end of Dixon Entrance to the Alaskan Islands, and perhaps as far north as the Bering Strait region. Certainly a 250' drop in sea level would connect the Charlottes to the off-shore islands and mainland” (Fladmark 1979). Davis, in 2006, further notes that the evidence for a coastal migration route is not new, citing Fladmark as well as Gruhn (1994, 1998).

Submerged and buried prehistoric archaeological sites are, otherwise, difficult or nearly impossible to detect without the use of “heroic” or expensive and/or time-intensive marine survey methods. Typically, approaches to detection of submerged sites on the continental shelves have used geological and geoarchaeological methods. The earliest examples examined seismic data gathered for oil and gas exploration such as in the Gulf of Mexico. In Europe, seismic data of a similar origin have also been used in larger, regional scale landscape reconstructions termed “Doggerland,” now-submerged within the North Sea (Fitch et al. 2005; Gaffney et al. 2007) (Fig. 2.6).

Harris et al. (2005, 2013); Baldwin et al. (2006) have used multibeam bathymetry surveys, side-scan sonar mosaics, high-resolution subbottom profiles, and ground-truth surveys from –250 m to the modern tidewater region to characterize the well-preserved but scattered remnants of a submerged paleolandscape. By coupling the data from sediment cores (Garrison et al. 2008, 2012a, b; Chowns et al. 2008; Pavich et al. 2010; and earlier studies), with these other methods, a drowned coastal plain can be reimaged and related to Paleo-Indian cultures who exploited that landform (Russell et al. 2009) (Fig. 2.8).

Shallow features such as Pleistocene river terraces buried by Holocene estuarine sediments were examined in the Gulf of Mexico using sediment coring methods. Cores extracted at specific seismic targets were examined for geochemical

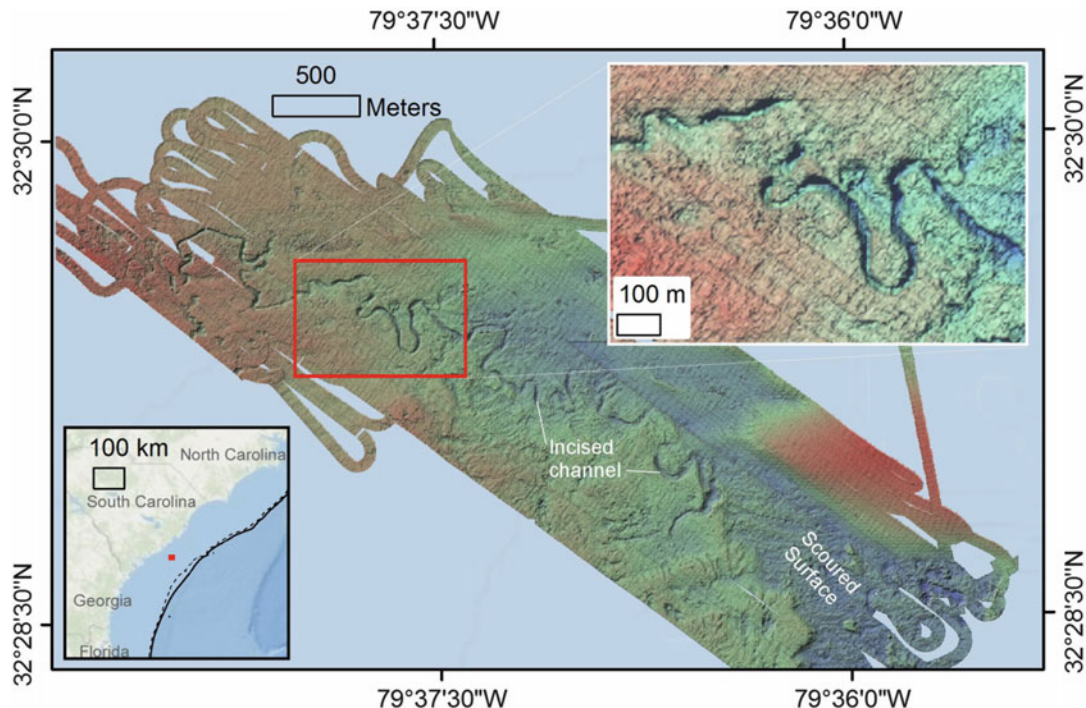


Fig. 2.8 Paleochannels of the “Transect River,” Georgia Bight, Atlantic Ocean, offshore South Carolina (see *inset, lower left*), as imaged using multibeam sonar data

(Stubbs et al. 2007; Harris et al. 2013). *Inset, upper right*, shows incision of the paleochannel into Pliocene lithology

and/or sedimentological markers for human activities such as charcoal, bone, burnt shell, and lithic debitage, and elevated Mn, Zn, and inorganic phosphate (Pearson et al. 1982, 1986, 2008, 2014; Stright 1986a, b, 1995).

In the southeastern United States, models have been predicated on sea-level position in tandem with regional geohydrology, and locations of lithic resources have been employed successfully in the Big Bend of Florida (Dunbar et al. 1989; Anuskiewicz and Dunbar 1993; Faught 2004a, b). In Europe, Benjamin (2010) proposes a generalized, stepwise methodology for underwater research known as the “Danish Model” that is extremely effective, with over an 80 % success rate in locating underwater sites in Denmark where it was developed. This methodical approach, or variants of it, has been well received due to its great adaptability to regional or local contexts and conditions (Benjamin 2010:258).

2.4.4 Mountain and Glacial Landforms

When Louis Agassiz established glacial theory for good and all with his 1840 book, *Etudes sur les Glaciers*, archaeology, as well as geology, adopted a powerful explanatory tool for landforms over much of the northern hemisphere (1940, 1967). Geomorphic evidence of former ice ages are often dramatic, notably erosional features such as sculpted mountain terrains of cirques, arêtes, horns, and hanging valleys. Depositional features, such as moraines, while less picturesque, mark the limits of advances and regressions of the ice sheets. In special cases like the Salisbury Plain, the great stones of Avebury and Stonehenge likely originated as erratics carried by the movement of the Fennoscandic ice sheet. It is their linkage to climate that makes the glaciers and landforms derived from them important to human prehistory. Like the volcano and river, the glacier has

shaped landscapes, started new soils, and, therefore, created new ecologies over 30 % of the Earth's land surface.

The development of glacial theory, in the mid-nineteenth century, paralleled that of uniformitarianism theory and that of the antiquity of the Earth. Its impact on archaeological thinking then and now cannot be underestimated. What every school child learns as the Ice Age was not patently obvious to the geologists of the past century. Prior to the development of glacial theory, glacial features-moraines, outwash deposits, kettle lakes, and erratics were simply the result of catastrophic floods aka Noachian. Lyell was more realistic about fluvial processes and suggested that icebergs during the Noachian flood dispersed rock and sediment across the Earth's surface. If this had been true, Lyell should have wondered why the bulk of these glacial landscapes only occurred in the northern hemisphere.

Alpine farmers and mountain guides knew what Lyell did not by way of daily experience. Glaciers, even in their reduced modern forms, advance and retreat, subject to climatic variation, pushing rocks, sediments, and trees before them and then leaving this as debris when they subsequently melt. Ignatz Yenetz, a Swiss Civil Engineer, listened closely to a mountain guide, Jean-Pierre Perraudin, and published, in 1821, a paper on the theory of glacial transport of exotic or erratic boulders (also called "foundlings" beyond the existing margins of Alpine glaciers (Hsú 1995)). In 1829, he went further to propose an Ice Age wherein glaciers covered nearly all of Switzerland as well as most of Europe. Most geologists doubted such a theory with the exception of Jean de Charpentier and his skeptical protégé, Louis Agassiz, Professor of Geology at the University of Neuchâtel. Because the scientific method works best when used to falsify a hypothesis or theory, Charpentier and Agassiz set out to gather data to do just that. Their work did just the opposite. In 1840, Agassiz published his seminal work on glacial theory (*supra*).

Implicit in Agassiz's newly developed theory was the variability of the Earth's climate-cold periods leading to glacial advances—warm periods leading to their retreat. The question of

what led to these cold periods or their duration was only be answered in the mid-twentieth century by the general sequence of glaciations which was established in Europe and America by the start of the twentieth century by Albrecht Penck in Germany and T.C. Chamberlin in the US Midwest (Penck and Bruckner 1909). While presented as confirmation of the uniformitarianism principle (Tarbuck and Lutgens 1984), it was perceived, at that time as anything but. Lyell's postulated uniformity of the Earth's processes from the beginning to "today" (1833, 1840) had no room for glacial theory (Hsú 1995). To make room for recent (Pleistocene) glaciations, Agassiz, with the help of Lyell's mentor, William Buckland, took Lyell to glacial moraines within two miles of his home. Glacial theory, and "Ice Ages," was accepted by the British, and Agassiz carried his message to America visiting at Harvard for some time.

Glacial theory has immediacy for archaeology that stems from its description of an Earth, in the most important period of humanity's development, the Pleistocene, so unlike that of the modern era. For the European archaeologists, no reading of fossil sites or material culture could be made without an eye toward how they fit into the ebb and flow of glaciations. For Americanists, the great continent-wide ice sheets presented a barrier to colonization of North and South America. Human settlement of the Americas, by migration from Asia, had to wait for the right convergence of natural opportunity and human necessity. This, as generally believed, came in the terminal Pleistocene sometime after 20,000 years ago.

The most dramatic archaeological discovery in the last decade of the twentieth century came at the Tyrolean glacier, on the Alpine border of Austria and Italy, with the discovery of the famed "Iceman" mummy (Spindler 1994). Found at an altitude of 3,000 m, this intact prehistoric man, and his accoutrements, reminded archaeology of the importance of glacial landforms to human society as well as their potential for study. The sacrificial mummies of the high Andes, at even higher altitudes—6,100 m—are a testament to the importance of alpine regions to ancient cultures (Carey 1999).

Mountain landscapes, while can host glaciers, can be, *and very often*, unstable landforms in and of themselves. One recent example of geoarchaeological study is a tsunami of 563 AD—Lake Geneva (SUI/FR).

In 563 AD, the mountain above the town of Tauredunum collapses in a huge “landslide”/debris flow, burying the town and “running out” across the valley of the Rhône river just above where it enters the Lake Geneva. Two contemporary accounts exist for tsunami of 563 AD:

- (a) Bishop Marius of Avenches: “This year a great mountain at Tauredunum, in the diocese of Valais, collapsed suddenly and destroyed the town and the nearby villages and at the same time, their inhabitants. The landslide also moved the length of the lake, 60 miles long and 20 miles wide, flooding both shores, and destroying very old villages along with people and animals. The lake demolished, at the same time, many churches and those that served them. Finally, the (wave?) struck the bridge at Geneva, the mills and its people entering into the town killing many inhabitants.”
- (b) Bishop Gregory of Tours: “A great event occurred at the town of Tauredunum. This town is near/above the Rhône river. After not having heard for 60 days and more, so loud the deaf could hear, the mountain, split finally, from the other nearby mountain, and crashed into the river, carrying along in the landslide the people, the churches with their valuables which were in the buildings; the two banks (of the river) were obstructed. The water rose in the rear (of the blockage), the place constricted, both shores of the valley, in whose throat the river ran. Having inundated the larger portion of the valley, it covered and destroyed that found on its banks. The waters that had accumulated suddenly dropped, drowning the people, destroying their homes and the beasts of burden perished; violently flooding all that was found on both shores of the lake unto Geneva. The mass of water spread as aforementioned and passed over the walls. The

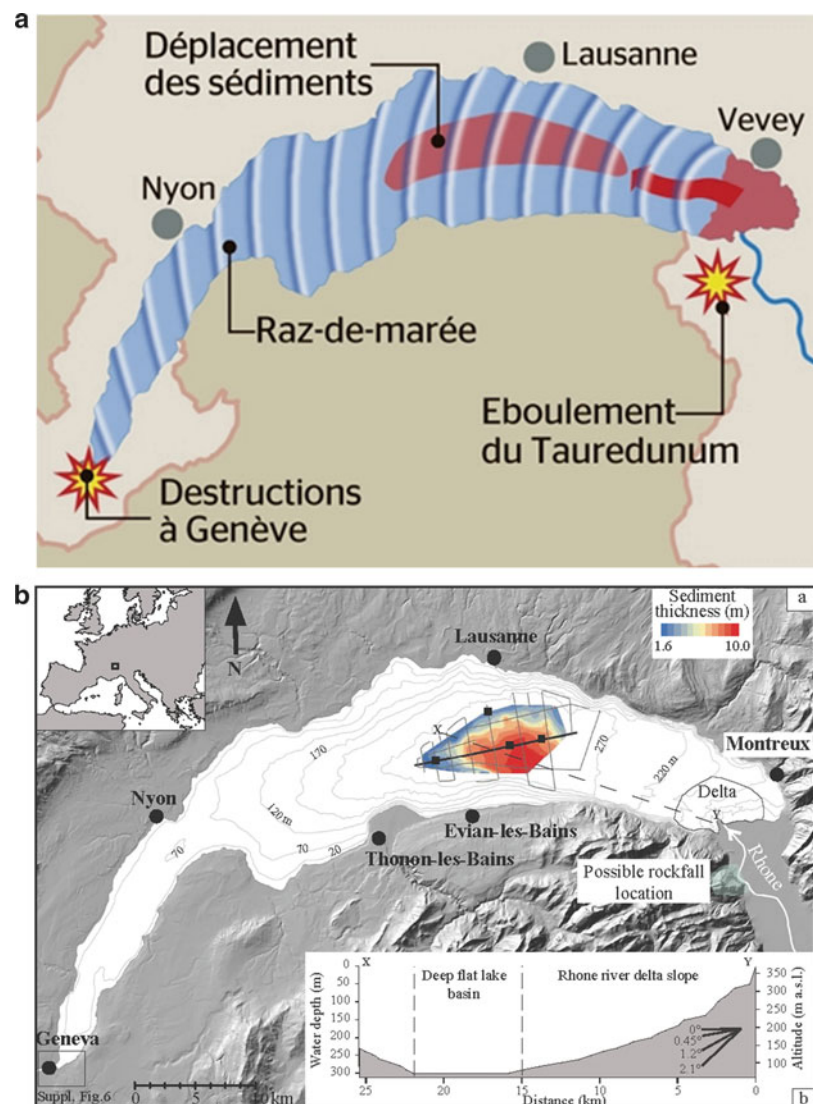
Rhône, itself, its course through the gorges being blocked, not finding any exit or course to flow, until breaking free and creating great devastation. After that, 30 monks came to the location where the town (Tauredunum) was overwhelmed and searched the earth (deposits) the mountain had brought there, finding (only) bronze and iron.”

Finding the geoarchaeological evidence for this Medieval disaster fell to Katrina Kremer, doctoral student at the University of Geneva, who first conducted a sonar/echo sounder “pinger” survey in the fall of 2010 and then took 10 m sediment cores into the lake sediments at 300 m water depths (Fig. 2.9).

Shown above, from a 2012 article (Kremer et al. 2012), in Fig. 2.9, and the cartoon, Fig. 2.9a, Kremer mapped, cored, and sampled a huge sand deposit 15 km long and 7 km wide; 250 million cubic meters of sediment, 25 m thick, was ejected into the lake, creating a giant wave or tsunami. Wood recovered in the cores, dated by radiocarbon, placed the deposit in AD 563. Kremer confirmed Gregory of Tours’ account which clearly stresses the blockage of the Rhône river and a subsequent inundation caused by the “rapid lowering” (se répandit impétuosité plus bas) of the accumulated water behind the landslide deposits, which subsequently failed. The tsunami was *not* the result of a direct debris flow *into* the lake but a later, secondary discharge of a catastrophic flood of water and sediment into the lake, creating the “bulge” of water necessary for a tsunami.

In modeling studies of the event (2012), Kremer notes: “We have not accounted for how the subaerial rockfall actually initiated failure of the delta, or the transformation of the subsequent subaqueous landslide into a mass flow, for which we have no observational data.” Further, “...it is important to recognize that our results are still strongly dependent of several key variables that are uncertain, particularly the slide volume, and the slide velocity. The slide volume used in simulations is a minimum of that actually measured and could potentially be even larger, that would generate even larger wave heights.

Fig. 2.9 (a) Shaded map showing the AD 563 turbidite deposits (“déplacement des sédiments,” in red) and the supposed propagation of the tsunami (“raz-de-marée,” blue arcs) (Source. 24 Heures, Lausanne, March 8, 2011). (b) Shaded relief map (DEM) (Swiss Federal Office of Topography) of the Lake Geneva. Water depths are indicated by bathymetric contour lines (meters). The 563 AD turbidite is color shaded (orange-blue) as to extent and sediment thickness (meters). Vessel tracks for seismic lines are indicated. Sediment core locations are indicated by black squares. The inset bathymetric profile, X-Y, shows the gradient of sediment thickness



The slide velocity could potentially be smaller than our used estimate, for example, due to interaction with the water column resulting in loss of momentum. Reducing the slide velocity from 46 to 23 km/h decreased the maximum wave height observed in Geneva from 8 to 3 m.” More recently (2014, 2015), Kremer et al. have proposed earthquake-triggered mass movements and tsunami as an alternative explanation for the observed occupation gap between 1872 and 1608 BC for Bronze Age settlements on Lake Geneva.

Less dramatic, perhaps another important aspect of glacial landscapes, has been the subject

of intense archaeological study in the twenty-first century—“ice patches”—in North America and Europe, most notably Scandinavia and the Alps (Hafner 2012; Reckin 2013).

2.4.5 Ice Patches

With the onset of twenty-first-century melting, alpine areas, once glaciated, are yielding archaeological evidence of prehistoric use (Reckin 2013). Prehistoric finds from four Swiss sites dating from the Neolithic period, the Bronze

Fig. 2.10 Schnidejoch (site circled) in the Bernese Alps of Switzerland (Fig. 2, Hafner 2012)



Age, and the Iron Age have been recovered from small ice patches (Schnidejoch, Lötschenpass, Tisenjoch, and Gemsbichl/Rieserferner). The Schnidejoch, at an altitude of 2,756 m a.s.l., is a pass in the Wildhorn region of the western Bernese Alps (Fig. 2.10). It has yielded some of the earliest evidence of Neolithic human activity at high altitude in the Alps. The abundant assemblage of finds contains a number of unique artifacts, mainly from organic materials like leather, wood, bark, and fibers. The site clearly proves access to high-mountain areas as early as the 5th millennium BC, and the chronological distribution of the finds indicates that the Schnidejoch pass was used mainly during periods when glaciers were in retreat (Hafner 2012).

In addition to the Neolithic finds, an Early Bronze Age (EBA) round-headed pin was found as well as an Iron Age coin together with significant numbers of iron nails from Roman era shoe soles.

In Scandinavia and the Yukon of North America, prehistoric and early historic finds have been found near ice patches (Reckin 2013). In Norway and the North American Arctic, animals and their hunters were actively seeking ice; ice patches with finds come in a wide variety of forms. In the Yukon (Andrews

et al. 2009), ice patch hunting focused on caribou that sought out—and still do today—these features to escape biting insects. By “yarding up” in the convenient ice patches, hunters were aware of this behavior and used it to take game. Evidence of this hunting behavior—two dart shafts are from the Northwest Territories and date from 2,310 to 2,410 cal BP and three other artifacts from the Yukon include a dart shaft (2,350–2,210 cal BP), a walking stick fragment (2,280–2,100 cal BP), and an antler point (2,755–2,727 cal BP)—have been recovered. Bow-and-arrow technology dating between approximately 800 and 150 cal BP has been found, including two complete arrows and two distal arrow shaft fragments, along with a very rare item: a partial willow bow dating to 465–317 cal BP. Researchers also found modified feathers from a large bird, presumably used as fletching, in direct association with one of the arrows. Lithic materials including a large biface and a projectile point were also located (Andrews, et al. 2012).

High mountains were often difficult landforms for humans. Quoting the Swiss writer, Charles-Ferdinand Ramuz (1983), “Les Montagnes, ils sont des milliers et vous? Vous êtes seul.” (The mountains are thousands and you? You are alone.) While Ramuz is writing

primarily about Swiss mountain peasant attitudes of the eighteenth and nineteenth centuries, he portrays the very real culturally based wariness of mountain terrains. Still, archaeologists have demonstrated early peoples armed with stone technologies and hunting skills exploited high-mountain areas even if they did so seasonally (Benedict 1985). In many areas of the world, mountains are the integral portion of the landscape. Archaeologists, working in these areas, have demonstrated that reconstruction of regional prehistory cannot be successfully achieved without consideration of the processes by which local populations adapted to mountainous ecosystems. Bender and Wright (1988) further note that an archaeological disregard of mountains probably derives from our own culturally embedded notions of mountains as inaccessible and marginal (cf. Ramuz). Archaeologists, nor geoarchaeologists for that matter, cannot *a priori* decide that mountains functioned as marginal environments in prehistory (Bender and Wright, *supra*).

Research in alpine areas have conclusively demonstrated that prehistoric hunters and gatherers seasonally scheduled occupations of mountainous areas in order to procure the wide variety of resources available there (Bender 1983; Wright et al. 1980). Local annual or even decadal scale variations in climatic conditions might curtail or prohibit occupation in any given year; the important factor is that the mountains, in general, were another stop on the round of annual movements made by Late Paleolithic and Mesolithic hunting and gathering bands. The mountains thus become intrinsic, rather than marginal, to procurement strategies. The foregoing example of prehistoric exploitation of ice patches more than illustrates this fact. The geographer Carl Sauer defined a cultural landscape which is one that has been "... fashioned from a natural landscape by a cultural group. Culture is the agent, the natural are the medium, the cultural landscape is the result" (Sauer 1925). Like other natural landscapes, mountains were the medium for cultures that utilized them.

In the Italian portion of the Southern Alps, geoarchaeological studies in Trentino region have used stratigraphic and geomorphological methods to characterize landscape evolution of the Trentino alpine region and its surroundings from the Last Glacial Maximum (LGM) to the Middle Holocene, approximately between 22,000 and 4,000 years cal BP. The oldest evidence of the late glacial human occupation along the southern margin of the Alps is recorded in the montane valleys. One of the key sites is Riparo Tagliente, in Valpantena (Verona, 250 m a.s.l.: Bisi et al. 1983; Bartolomei et al. 1985; Fontana et al. 2002; Table 2). This site was occupied from the early late glacial, with dates ranging from $13,430 \pm 180$ 14c BP (15,360–16,548 cal BP) to $12,040 \pm 170$ 14c BP (13,448–14,469 cal BP).

The site of Riparo Dalmeri (Dalmeri et al. 2005) with an earliest date of 12,900–13,303 cal BP shows clear evidence of the environmental situation during the Lateglacial Interstadial. The rock-shelter is located along a N-oriented wall at ca. 1,250 m a.s.l. Micromorphological studies have identified anthropogenic processes recorded in an Epigravettian paleosurface (EDF stratigraphic complex) that were related to the implementation of different activities: the preparation of the occupation surfaces by means of the accumulation of silty sediment that was collected from loess deposits off the site, the accumulation of fine organic waste, tool production, trampling, and the remobilization of organic debris (Angelucci and Basetti 2009).

In the Bighorn Mountains of the American west, rock-shelters, specifically, 48BH1827 (Two Moon Shelter) and 48BH1065 (BA Cave), have been the subject of geoarchaeological studies (Finley et al. 2005). Two Moon Shelter bears stratified Paleo-Indian deposits that include a Folsom projectile point fragment, a $10,060 \pm 60$ BP. radiocarbon date, and an undated Paleo-Indian component positioned stratigraphically below the Folsom occupation. BA Cave is a well-stratified and well-dated archaeological deposit, yielding cultural occupations spanning the last 4,000 years.

Geoarchaeological investigations at BA Cave describe changes in sediment depositional regimes that may reflect significant late Holocene trends in centennial-to-millennial-scale climatic changes in the Middle Rocky Mountain region (*supra*).

In Nepal, geologically grounded appraisal of the paleoenvironment and geological data of the Plio-Pleistocene and early Holocene periods allows reconstruction of the early history of man before the beginning of the historical period in the Himalayas of Nepal (Pandey 1987). In the American cordillera, yet again, workers like Cortegoso (2005), Ramiro et al. (2011); Sandweiss et al. (2009) have used geoarchaeological methods to illuminate the relationship of montane prehistoric populations to Holocene environmental change.

2.4.6 Lacustrine Landforms

This author first wrote on lacustrine or limnological processes in relation to drowned prehistoric sites in lakes in 1975. That article dealt primarily with man-made lakes or reservoirs. With the exception of the artificial dam, artificial and natural lake systems are very much alike. In the Lake Geneva example, above, and in the discussion of African lakes later in this chapter—paleo

or otherwise—lacustrine landforms are primary loci for human settlement and natural resources. François Alphonse Forel, whose father, a historian, is shown in Fig. 2.11 making what is believed to be the first archaeological dive in history, is the “father of limnology” (Edgerton 1962; Vincent and Bertola 2012).

François Alphonse Forel (Fig. 2.12) never ignored the relationship of human cultures to lacustrine systems. In his three volume treatise (1892–1904), he synthesized his physical-chemical-biotic-human-coupled approach to the study of lacustrine systems. Because of his early involvement in his father’s study of submerged prehistoric sites in Lake Geneva, F-A. Foral or “FAF” as he was known to his peers included the historical importance of a lake to people, ancient to modern (Vincent and Bertola, *supra*). Because of his lifelong interest in these ancient sites, he devoted 78 pages to them in volume III of this *Monograph on Limnology* (1892–1904). In this work, he updated the 1860 map of the prehistoric sites of Lake Geneva listing 47 sites. Most importantly, Forel was the first to propose an integrated geological and sedimentological approach to understand the location of these sites on the drowned terraces of the lake bottom (Corboud 2004:28).

Lochs are natural lacustrine systems in Scotland. There are over 30,000 lochs, large

Fig. 2.11 The first underwater archaeology dive—August 24, 1854, Lac Léman (Lake Geneva). François Marie Etienne Forel, father of a then 13-year-old François Alphonse Forel, is seated in the boat with his back turned, presumably operating the air pump for the diver (Adolphe Morot), while Frédéric Troyon holds a safety line (Water color by Adolphe von Morot)

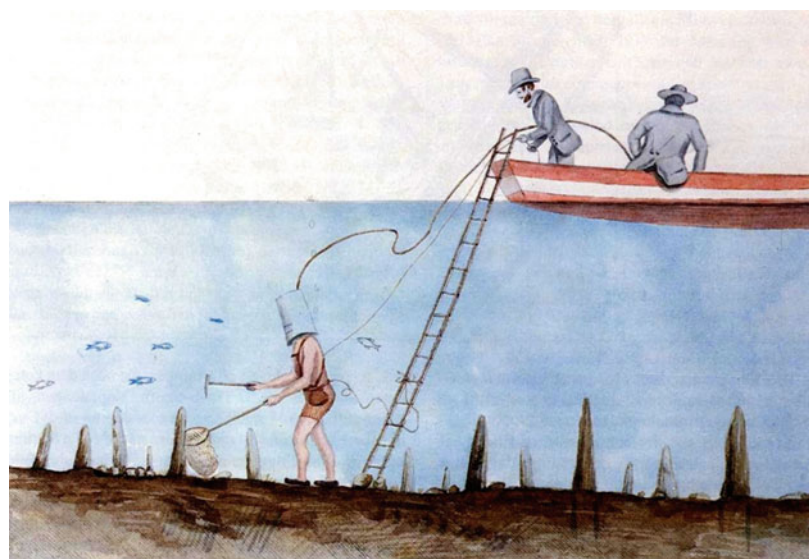


Fig. 2.12 Water color portrait of François Alphonse Forel in the room he used as his study and laboratory, at his home in Morges on the shores of Lake Geneva (Lac Léman), Switzerland (Watercolor by Ernest Bieler, no date, private collection)



and small (T. Nicholas Dixon, Personal Communication 2012). Much like the prehistoric settlements in Alpine lakes, in Scotland and Ireland, prehistoric peoples utilized the lochs for resources and settlement (Dixon 2004) from the Neolithic into the Medieval Periods. A unique aspect of this human use was the creation of pile-dwellings known as *crannogs* (Munro 1882; Morrison 1985; Fredengren 2002; Dixon 1983, 2004). Their importance of crannogs to prehistoric archaeology is uncontested, but they are understudied. One of their obvious values is the enhanced preservation of organic remains not seen on most terrestrial sites. Likewise, these lacustrine sites are underappreciated as their overall importance in prehistoric settlement systems. Unlike the shoreline villages of the Neolithic and Bronze Ages in Alpine Europe, crannogs were family-based structures built upon artificial islands of stone and clay (Dixon 2004). The very difference in the social origin of the crannog and that of larger settlements begs

for study. Certainly geoarchaeology has much to contribute to their study as well.

A recent example of geoarchaeology's contribution to prehistoric use of a lacustrine environment is the Paleolithic site of Schöningen (Thieme 1997; Stahlschmidt et al. 2015). The original excavators of this important Middle Pleistocene site proposed that hominin activity, likely that of *H. heidelbergensis*, included hunting and butchery and occurred on a dry lake shore followed by a rapid sedimentation of organic deposits that embedded and preserved the artifacts. Recent geoarchaeological analysis challenges this model. Evidence supports a different scenario where the sediments of Schöningen 13 II-4 aka "spear horizon" were deposited in a constantly submerged area of a paleolake. In one suggested depositional scenario, cultural activity occurred on a shallow frozen lake surface and during thaws and warm seasons of both remnants—butchery tools and the remains of the butchered simply fell to the

bottom—following the geological concept of dropstones, while in another the materials are relocated by geogenic processes (Stahlschmidt et al. 2015).

While Olduvai Gorge is used as an example of the geological stratigraphic section, it could as easily be an exemplar for geoarchaeological studies of lacustrine paleoenvironments of the Pleistocene. The Olduvai Basin in northern Tanzania is a Plio-Pleistocene sedimentary basin containing a succession of fluvial and lacustrine deposits that are largely derived from volcaniclastic material (Hay 1976, 1990). These well-known fossiliferous deposits contain proxy records of the evolution, behavior, and paleoecology of early hominins such as *Homo habilis* and *Zinjanthropus boisei* (Leakey 1971; Tobias 1991). Lowermost Bed II (LMBII) is \sim 1.75–1.85 myr old based on ages of the basalt “lithological floor.” The Olduvai Landscape Paleoanthropology Project (OLAPP) has sought to understand synchronic, basinwide patterns of land use by the Oldowan hominins. Paleoenvironmental reconstructions (Hay 1976, 1996; Bonnefille 1984; Cerling and Hay 1986; Sikes 1994; Hay and Kyser 2001; Deocampo and Ashley 1999; Ashley and Driese 2000; Deocampo et al. 2002) have provided a context for interpreting associated archaeological finds (Blumenschine and Masao 1991) and test aspects of recently proposed hominid land-use models (Peters and Blumenschine 1995, 1996; Blumenschine and Peters 1998). As noted in Chap. 3, Hans Reck and later Hay distinguished these beds within the Olduvai section based upon their color, sedimentological texture, and biostratigraphy.

2.4.7 Loessic and Glacial Landscapes: Midwestern United States

In the Midwestern United States are landforms that dramatically display the interplay of wind-born deposition of both sand and silt (loess). These are the sand hill regions of the state of Nebraska along with the great loess/sand prairies of Nebraska, Kansas, and the Missouri River Valley (Fig. 2.13). Most identifiable of aeolian landform are dunes—barchan, transverse,

parabolic, longitudinal, and linear. When active, these features were not likely to have been the locus of much human settlement, but after the establishment of a vegetation cover, they have occupied by both pastoralists and agriculturalists. Geoarchaeological studies of artifacts and buried surfaces in aeolian deposits can provide significant information for the archaeologist (Ivester et al. 2001; Leigh 1998).

Highway construction in Northwest Missouri exposed a stratified archaeological site that was found to contain a range of lithic materials extending into the Paleo-Indian Period (Reagan et al. 1978). The excavations carried out in the mid-1970s were characterized by the extensive use of geoarchaeological techniques to describe the deposits. The site, now destroyed, was called the Shriver site and was located in the northwestern prairie section of Missouri on a plain characterized by loess and glacial drift deposits overlying shale and limestone bedrock (Dort 1978). Its discovery and its distinctive lithic assemblage raised the possibility of it being a so-called “Pre-Clovis” site. This assignation was based on the artifactual stratification wherein a Folsom period occupation (ca. 11,000 BP) was superposed on a deeper (\sim 40 cm) assemblage of bifacial and unifacial flint artifacts containing no lanceolate projectile points (Reagan, *supra*). Because of the unusual nature of the archaeological assemblage, the excavators conducted extensive geoarchaeological studies to include geological/geochemical, soil/sediment, pollen, and geochronological procedures. The author was involved in the geochronological aspect of the study utilizing thermoluminescence (TL) to investigate flints suspected of being heat-treated (Reagan, *supra*).

From a lithostratigraphic perspective, Dort reduced the 13 units to a section of four geological units which he called: (i) Unit 1, the Bignell loess, 8,000–13,000 BP; (ii) Unit 2, Peoria Loess, 13,000–18,000 BP; (iii) other glacial and erosional materials; and (iv) Upper Pennsylvanian bedrock (Reagan, *supra*). He placed the three cultural stratigraphic units into the upper two geological units. The older of the culture stratigraphic units, “Pre-Clovis,” was located on the

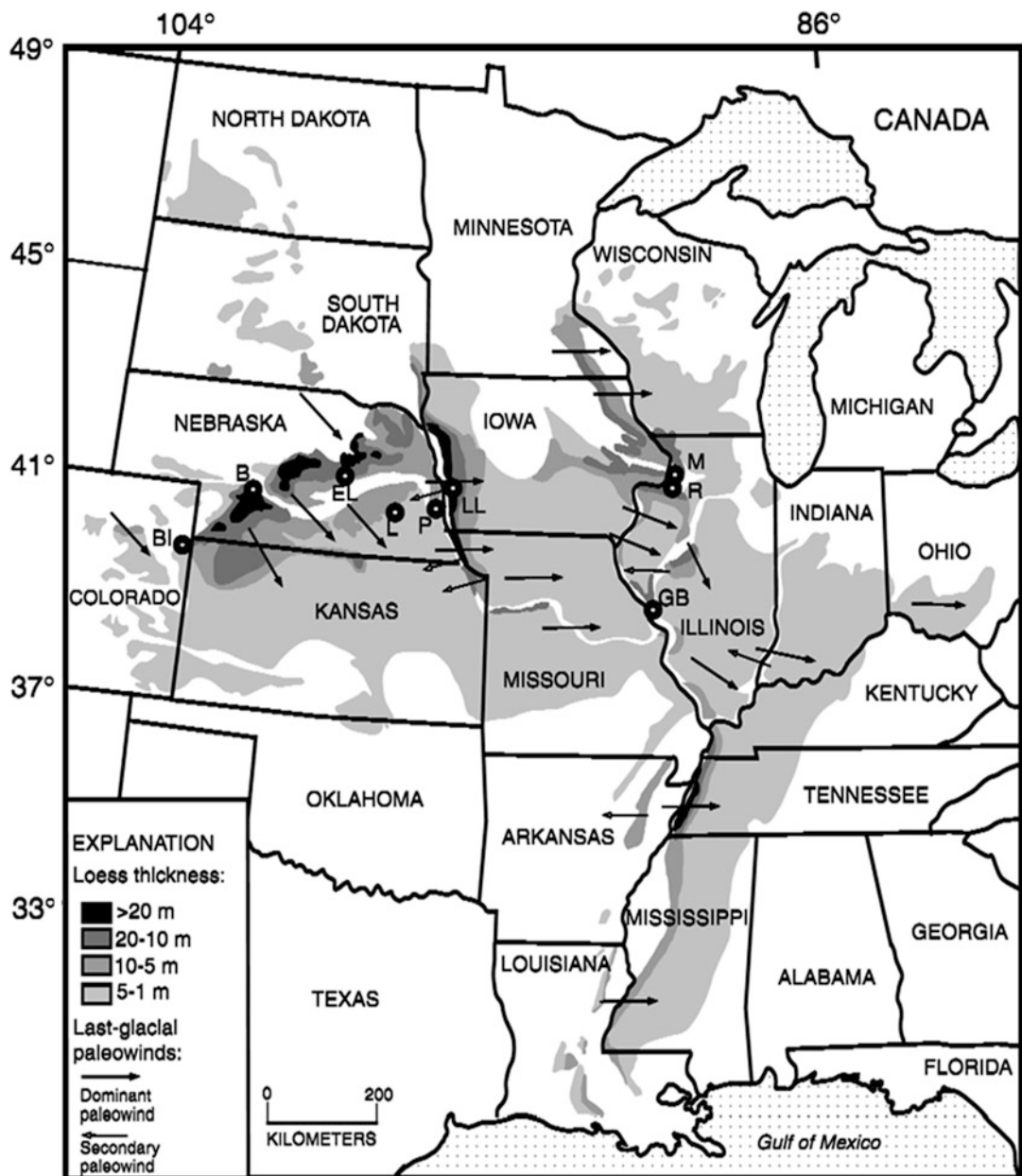


Fig. 2.13 Map by Bettis et al. (2003) showing loess distribution and thickness in the Great Plains of the United States

sub-loess (Peoria) erosional surface implying an antiquity of at least 18,000 years. Soil chemical trends, particularly the phosphorus and potassium concentrations, showed a correlative discontinuity at this stratigraphic location (65–75 cm). A similar break in the geochemical signatures was seen deeper in the section at

215 cm. Dort identified an erosional surface and probable paleosol at this location as well. No archaeological significance was attached to this lower geomorphic surface, but its paleoclimatic relevance is obvious.

The most well-described post-LGM paleosol for the Midwestern United States area is the

Fig. 2.14 The Brady paleosol (Photograph courtesy of Charles Trautmann)



so-called Brady Soil. Peoria Loess deposition in the central Great Plains appears to have occurred between approximately 20,000 and 10,500 BP (Martin 1993) (Fig. 2.14). The Brady Paleosol is identified as carbon-rich, organic layer across most of Kansas and Nebraska. Formation of the Brady soil initiated between 15,500 and 13,500 cal year BP, during a time period of much slower dust deposition ($0.1\text{--}0.2\text{ mkyr}^{-1}$), which allowed for pedogenesis and the accumulation of SOM (Marin-Spiotta et al. 2014). Increasing rates of loess deposition over time, estimated at $0.72\text{--}0.80\text{ mkyr}^{-1}$, buried the Brady soil approximately 10,500–9,000 years ago.

The work of Follmer (1982) at the central Illinois archaeological Rhoads site identified a Peoria Loess deposit on the till plain of the Illinoian (penultimate) glaciation just south of the morainic margin of the later Wisconsin glaciation. At the Rhoads site, the Peoria Loess caps sand and gravel outwash deposits termed the Henry formation, whose aggradation peak was about 17,000 BP. Follmer gives the Peoria Loess a wider time range than Dort—12,600–23,000 years—based on radiocarbon dates for its base, near St. Louis, of $23,110 \pm 280$, $23,930 \pm 280$ BP (McKay 1979). On the Peoria Loess was identified a paleudal or

buried mollisol which has the pH profile increasing with depth together with high silt (63–76 %) values typical of loesses. The observed clay ratio (0.3) in the mollisol's Ap horizon increases to a value of 1.4 in the Bt2 horizon (*supra*). Argillic horizons in mollisols have fine-to-coarse clay ratios ranging from 1.0 to 1.5 (Wascher et al. 1960). Likewise, in well-drained examples, the clay mineral alteration is minimal. Follmer noted some properties, the presence of incipient E horizon, in the mollisol that indicated the possibility of polygenesis or overprinting caused by the presence of a later forest cover (*supra*). The C horizon is the Henry Formation. Follmer does not specifically discuss the archaeological materials found at the Rhoads site, but they are later (Archaic Period) than those excavated at the Paleo-Indian Shriver site.

Balco and Rovey II (2010) have used cosmogenic isotopic dating methods and magnetostratigraphy to assess the chronology of the major Pleistocene ice advances in North America. The first two of these advances were found to correlate well with the newly proposed Pleistocene—Pliocene boundary of 2.58 Ma (~2.4 Ma) and the “mid-Pleistocene transition” at 1.3 Ma. The initial advance reached 39° N latitude or what is today the Missouri River Trench in central

Missouri (Fig. 2.6). Lithological evidence for the five advances lay in individual glacial tills. In dating the tills, the authors of this study were in fact dating underlying paleosols which had formed from the overlying tills. The oldest paleosols were named the Atlanta and Moberly Formations and were magnetically reversed, making them older than the Brunhes-Matuyama Boundary (~780 Ka). The younger tills were magnetically normal, indicating ages less than that of the Brunhes-Matuyama event. These tills were the Fulton, Columbia, and Macon Formations. All predated MIS 6 (~150 Ka). The Columbia is till dated to before this time (0.22 ± 0.16 Ma), whereas the Macon Formation was not well constrained, suggesting only that it was younger, but uncertainties in the chosen cosmogenic method ($^{26}\text{Al}/^{10}\text{Be}$) prevented reliable dating of the final till (*supra*).

2.4.8 Desert/Arid Landforms

Just as nearshore continental shelves were one coastal plain, drylands and deserts were often verdant savannahs and forests. Drylands form 35 % of the Earth's land surface (Oviatt et al. 1997). Within these drylands are true deserts (16 %). Water plays an important role in shaping dryland topography but a more significant factor is the wind. The reason the wind is important is self-evident from an inspection of the term "dry" land.

Dryland landforms created by water vary from arroyos ("wadis" in Old World parlance) to eroded mesas and buttes. Playas form in deserts where precipitation is insufficient to maintain permanent lakes. Where lakes do exist in dryland areas such as the Great Salt Lake (USA), the Dead Sea (Israel/Jordan), and Pyramid Lake (USA), snow melt and other runoff feed the basin from outside the immediate area of the lake itself. Ancient fluvial systems or paleo-drainages have been revealed in the shallow subsurface of the eastern Sahara in the driest region of southern Egypt and northern Sudan (McCauley et al. 1982). Space shuttle-based radar provided us with evidence of a long and

complex fluvial history in a now hyperarid and uninhabited region (*supra*). Well-defined networks of broad alluvial valleys, braided streams together with bedrock-controlled channels, appear in the radar images and have been confirmed on the ground by archaeologists. Along these "radar rivers" have been found evidence of some of the earliest inhabitants of northeast Africa and northwest China (Wendorf n.d.; Holcomb 1996). Allogenic streams exist in many arid lands—the Nile in Ethiopia and Egypt, the Jordan in the valley and hills of the Dead Sea, the Truckee ending in the Nevadan desert at Pyramid Lake, and the Colorado of Grand Canyon to the Gulf of California. These fluvial systems can be sensitive indicators of paleoclimate because of their aggradation and erosion due to rainfall outside the bulk of their drainages (Hassan 1988).

2.4.9 The Sahara: Geoarchaeology of Paleolakes and Paleoclimate

The Sahara is the largest of the world's hot deserts (the polar regions are deserts, too, and larger). C.B.M. McBurney, writing in 1960, stated, "The central fact of the North African environment is the Sahara (p.62)." McBurney went on to say, "...to many the name conjures up a vision of vast area covered almost entirely with rolling sand dunes and scattered here and there with oases of almost incredible fertility." It is, as he points, the largest single tract of aridity in the world spanning Africa from the Red Sea to the Atlantic. That said, natural vegetation, though rare, is not totally absent and takes the form of widely spaced clumps of desert shrub and, toward the desert's margins, clumps of bunch grass extending over perhaps 60 % of the Sahara's vast area (*supra*, 64). The southern margin is a zone of steppe and savannah some 400+ km wide grading into tropical forest. The north is steppe as well but narrower. The western half is mountainous—the Atlas Range—with coniferous scrub and forest due to higher rainfall.

In the central Sahara lie two important, in prehistory, highland areas—the Hoggar and Tibesti massifs. A third, lesser massif—the

Air—lies southeast of the Hoggar. Peaks in the Hoggar often exceed 2,500 m and two, in the Tibesti, are 3,000 and 4,000 m. These heights are equal to many well-known peaks in the Alps such as Schilthorn and Jungfrau. In prehistory, these heights are thought to have influenced climate and cultures across the heart of the Sahara (Williams 1984b). Nonetheless, vast dune fields do exist that give the Sahara its well-deserved reputation for inhospitality to all but the hardiest.

Nubian Sandstone Aquifer System underlies much of the eastern Sahara. This is the world's largest fossil water aquifer, and it spreads roughly 2,000,000 km² (772,000 sq. mi.) beneath Chad, Sudan, Egypt, and Libya to a maximum depth of 4,000 m (12,800'). The Lakes of Ounianga, 18 interconnected, freshwater, saline, and hypersaline lakes (Fig. 2.15), located more than 800 km (500 mi) from the nearest other lake, Lake Chad, are supplied from below by this aquifer. *Sahelanthropus tchadensis*, dated to over 6 m.y., was discovered in 2001 and 2002 in the Chadian desert by Michel Brunet et al. (2002) nearby. As the result of a hydrological system, all but 1 of the 11 lakes of Ounianga Serir are fresh.

The intense Saharan sun drives the evaporation at nearby Lake Yoan, lowering the water level by 6 m (19') a year. Now, and presumably

during the last 3,000 years of hyperaridity, rainfall has been measured only in millimeters a year, so the deficit must be made up by the aquifer. In the prehistoric Green Sahara era, an ancient lake, the Mega-Chad, 50 or 100 times—an order of magnitude—more extensive than the present-day Lake Yoan, may have existed. The Green Sahara, known as the African Humid Period, lasted roughly from 11,000 to 5,000 years ago. A North African savannah—now the parched Sahara—existed for elephants, giraffe, hippos, antelopes, and aurochs that once made their homes there.

In a 2008 research paper, geoarchaeologist Stefan Kröpelin challenged the hypothesis that the Sahara underwent rapid desertification in the Holocene. Advanced by P.B. deMenocal (1995, 2000), the North Africa dried from savannah to desert over the course of only a few centuries. DeMenocal et al. used the record of a marine sediment core of Late Pleistocene-Holocene terrigenous (aeolian) sediment at ODP Site 658C, off Cap Blanc, Mauritania, to document very abrupt, large-scale changes in subtropical North African climate. This terrigenous record, according to deMenocal, exhibited a well-defined period of low sediment influx between 14.8 and 5.5 cal. ka BP associated with the African Humid Period, when the Sahara was nearly completely vegetated and supported numerous

Fig. 2.15 The area of the Sahara Lakes (Adapted from: *Saudi Aramco World*, vol. 65 (3), 2014)



perennial lakes and an arid interval corresponding to the Younger Dryas Chronozone. Using new data, from Saharan lake sediments, Kröpelin asserted that it may have been a far longer, much more gradual process of desertification, one taking not centuries but millennia.

One biomineralogical piece of evidence for ancient lakes is diatomite. Diatomite is a light sediment made up of the microscopic skeletal remains of diatoms, single-celled plants that have sunk to the bottom of lakes and oceans. When the water of a lake recedes, diatomaceous earth can often be found on the walls of the sandstone escarpments that surround the Ounianga Kebir and Serir basins. Sampled, the elevation of deposits noted and carbon dated, the approximate depth and the extent of the Chadian “paleolakes” can be postulated.

In 2010, Kröpelin and Martin Melles of the Quaternary and Paleoclimatology Group at the University of Köln directed the recovery of a 16 m (52½') sediment core from Lake Yoan, in pursuit of layers from the Holocene Era. The laminated sediments have yielded a continuous, 10,940-year continental record of climate and environmental change for the south-central Sahara. Kröpelin et al. summarized, in 2008, that the Lake Yoa(n) record supports archaeological and geological data from the eastern Sahara as well as palynological data from the West African Sahel that the record of Saharan dust deposition in the tropical Atlantic Ocean is not representative for landscape history throughout dry northern Africa. The dispute based on two geoarchaeologically oriented sediment studies points out the disparity that can accrue between even the best of data sets.

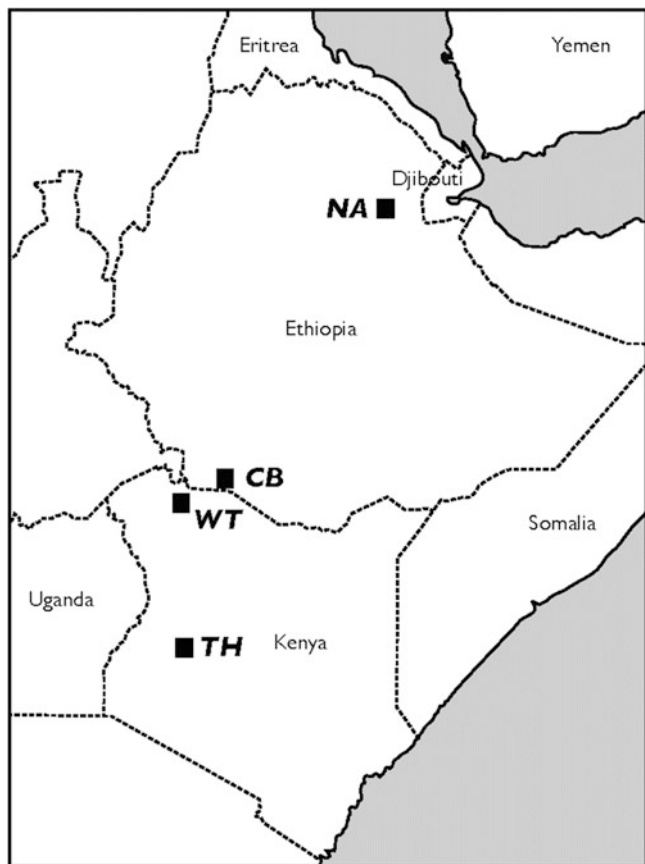
In another, recent, large-scale geoarchaeological drilling project, the Hominin Sites and Paleolakes Drilling Project (HSPDP) has begun the study of six ancient lakebeds in the African Rift (Pennisi 2013) (Fig. 2.15). In the Baringo Basin, the project has drilled to a depth of 228 m, extracting sediment cores. This study, like that of the Lakes of Ounianga research, seeks to examine the synchronicity of deep sea cores’ findings with that of the African continent.

How did climate and tectonic change interact during critical intervals of human evolution? To answer this fundamental question, recently, 2012–2013, scientific drilling teams have extracted long cores from five high-priority areas in Ethiopia (Northern Awash River and Chew Bahir areas) and Kenya (West Turkana, Tugen Hills, and Southern Kenya Rift/Lake Magadi) where highly resolved, continuous lacustrine paleoclimate records can be collected through important time intervals in the same basins that contain fossils and artifacts (Pennisi 2013) (Fig. 2.16).

The extraction of high-resolution (centennial-millennial scale) sediment cores allow acquisition of datable, geochemical, paleoecological, and sedimentological records. These proxy data from the paleolake sediments include tephra, pollen, phytoliths, macrobotanical remains, diatoms, algae, macro- and micro-invertebrate and vertebrate remains, as well as any artifacts—whole or fragmentary—fashioned by hominins.

The HSPDP seeks, much like the Sahara lakes study, to use lake sediment records, for *continental* sites, to address paleoenvironment. Where the Saharan research focuses on the Late Pleistocene-early Holocene climatic variation, the Rift’s paleolake study delves more deeply into the period of hominin evolution, the Plio-Pleistocene. With the recalibration of the base date for the Pleistocene at 2.588 m.y., more hominin genera, such as *Homo erectus/ergaster* and *habilis*, are now exclusively within this geological era. *Australopithecus* species and pre-Australo genera such as *Orrorin*, *Ardipithecus*, and *Sahelanthropus* are firmly rooted within the Pliocene and late Miocene. The Rift’s study addresses what is termed the variability selection hypothesis (Conroy and Pontzer 2012). This hypothesis attempts to widespread Plio-Pleistocene climatic and associated environmental change to important events in hominin evolution (Potts 1998). HSPDP data are hoped to be able to directly identify increased environmental variability, allowing evaluation in regard to hominin adaptations.

Fig. 2.16 The Rift
Paleolakes: *NA* Northern
Awash, *CB* Chew Bahir,
WT West Turkana, *TH*
Tugen Hills, and *LM* Lake
Magadi



2.4.10 Karst/Cave Landforms

Nowhere is the linkage of hydrology and geology so apparent than in these types of landforms and features. In some cases, the situation is one of the underground drainages carving often vast solution features rather than great fluvial valleys. Karst landforms are generally considered to originate on carbonate rocks, in most cases, limestones. This limestone can be composed of 50 % or more calcite or aragonite, both pseudomorphs of CaCO_3 . In the Ozark Mountains of the Central United States, karst forms in dolomites— CaMgCO_3 —that is more than 50 % this species, but more often limestone is the rock system (Easterbrook 1998:194). Springs are very common in these landforms. In Missouri, heartland of the Ozark Mountains, the dolomites are rich in caves and springs (Vineyard and Feder 1982). In the gold reefs of South Africa's

Witwatersrand, the massive dolomite strata contain vast quantities of water that are of concern to miners (Garrison 1999).

Precipitation is critical to the production of karst but only if the water table is high enough to facilitate the dissolution process. Therefore, development of karst is, like the fluvial landform, linked directly to climate and, importantly, the geological structure (Palmer 1991). Faults, joints, and fractures form the conduits for water and entrained chemicals, such as carbonic acid, that dissolve the limestone. Where sulfide deposits exist along fault planes, the production of sulfuric acid will accelerate the growth of karst.

The most recognized karst landform is the sinkhole or doline. These closed depressions are solution/collapse features that vary around a basic, circular or elliptical, funnel-like shape. In some of these, the local hydrology forms a

spring. For archaeology, these sources of water have concentrated both fauna and human cultures, forming deposits of both within and around the spring. Where the water has abandoned the subterranean feeder conduits of the ancient springs, caverns and caves now exist. Collapses occur over time that form *traps* for animals and humans. In Spain, collapsed limestone caves have produced some of the most spectacular evidence of early humans on the continent of Europe. The collection of sites is known as Atapuerca that lies within the northern sierra of Spain. The caves, known since 1976, have, since the beginning of serious excavations in 1990s, produced over 1,600 human bones ranging in age from greater than 780,000 to 127,000 years ago. This chronology has been derived from work in what is termed “the Gran Dolina” or Big Sinkhole (Renfrew and Bahn 1996, 2000, 2004).

The nearby site Sima de los Huesos or “Pit of Bones” has yielded the bulk of the large collection of human remains found to date and revolutionized our thinking of the colonization of Europe by early humans. Indeed, in Europe and elsewhere, some of our earliest fossil humans and their material culture has originated in caves. The first of these was Neanderthal, discovered in 1856, in its eponymous valley. A continent away, *Homo erectus* known as “Peking Man” was found in the debris of the “Cave of the Dragons”—Zhoukoutien.

In 1990 and, shortly thereafter, in 1994, two dramatic cave art discoveries were made in France. These solution features, in massive limestones, south of the Massif Central, were, respectively, Cosquer Cave and Chauvet Cave. Both contain some of the oldest Upper Paleolithic art ever discovered—29 to 35,000 years (Clottes and Courtin 1996; Clottes 2001). Both are located outside the heartland of Paleolithic cave art, the Loire River valley and northern Spain. Cosquer Cave is unique, by virtue of its discovery below the surface of the Mediterranean near Marseilles. The cave entrance was found 30 m below the sea surface by scuba divers. Its entry, by ancient artists, occurred sometime during the last glaciation (Würm/Weichsel).

Chauvet Cave, located along the Ardeche River, a tributary of the Rhône, lies on the south flank of the Massif Central and dates to the same period as Cosquer.

2.4.11 Combe Grenal

As noted in the introductory chapter, the term “Paleolithic” was a British invention, but the French applied it to their extensive variety of prehistoric sites. One such site is Combe-Grenal. The excavation and significance of Combe-Grenal is most closely associated with Francois Bordes. Francois Bordes was the leading French Paleolithic archaeologist for most of the mid-part of the twentieth century. Bordes was encouraged by Peyrony to excavate there (Dibble et al. 2009a, b). At Combe-Grenal, Bordes and his students, from 1953 to 1965, revealed a sequence of almost 13 m of rich archaeological deposits, apparently spanning the period from the final stages of the penultimate glaciation (MIS 6) through to almost the end of the Mousterian succession, from 125,000 BP to 40,000 BP (Fig. 2.17) (Bordes 1972). They excavated 64 stratigraphic levels, and using these data, Bordes refined the Middle Paleolithic stone tool typology used today by most workers in this period (Dibble et al. 2009a, b).

Bordes was trained as a geologist. As discussed in the introductory chapter, into the mid-twentieth century, French prehistorians continued to hue to a “paleontological” paradigm for conceptualizing the stratigraphy of their excavations (Fig. 2.17). Strata were viewed biostratigraphically but material finds—tool types (*fossile directeurs*)—the “biota,” separating antecedent and subsequent units (Sackett 1999). This approach to stratigraphy, Bordes discarded at Combe-Grenal. Bordes was quick to recognize the *fossile directeur* approach had two implicit assumptions: the first was the conflation of the Paleolithic record with that of a paleontological record—a one-to-one correlation between archaeological levels and “natural” stratigraphic units—and the second was the excavated material record, tool traditions,

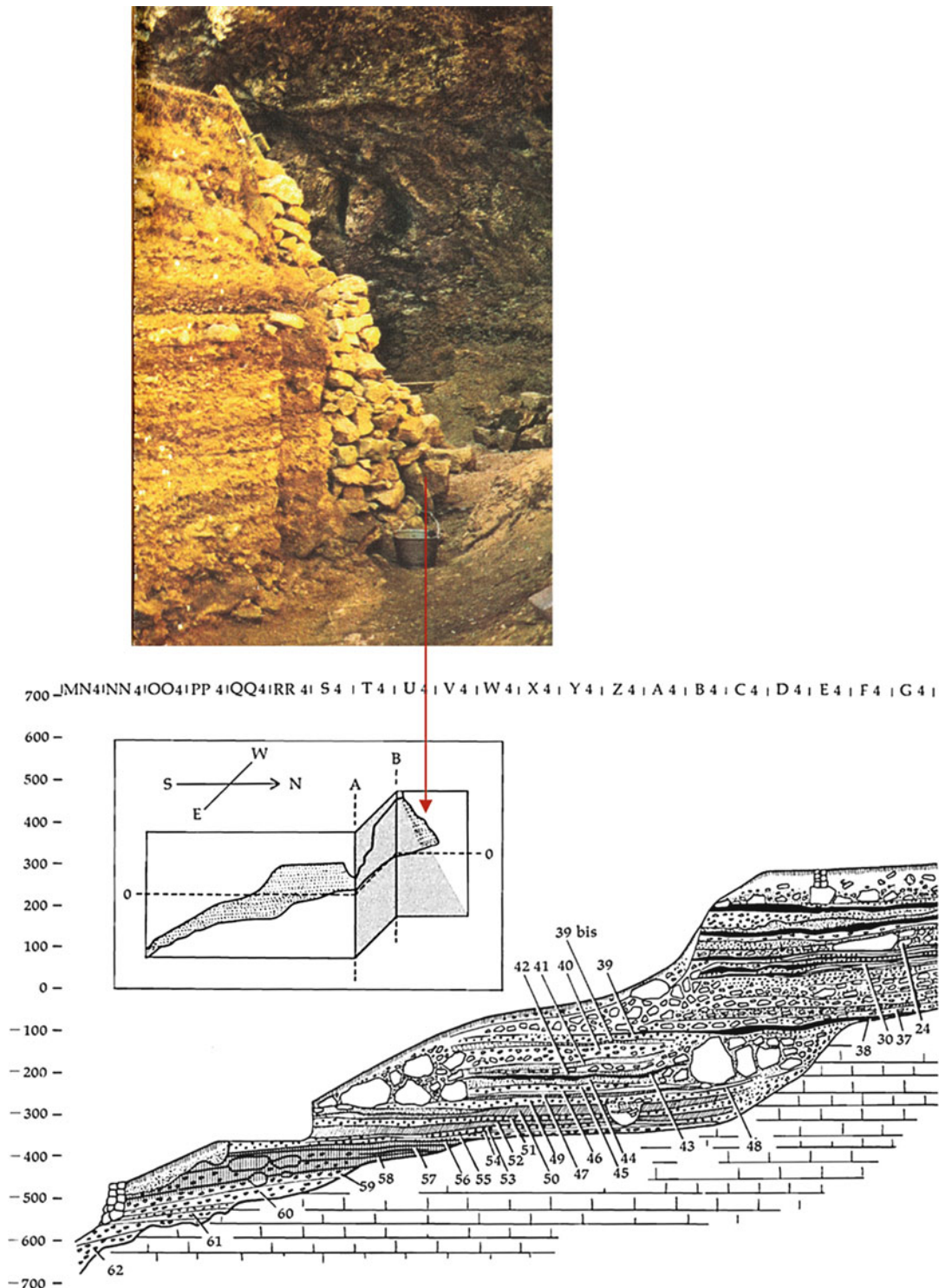


Fig. 2.17 Combe-Grenal stratigraphy—Mousterian levels 24–54 are shown in photo and inset. The rear portion of the inset fence diagram (B) is correlated with the

photograph, from Bordes (1968), above. Levels 56–64 are shown in the elevation section, below, which corresponds to the far left of the fence diagram (Bordes 1972)

features, etc., which would reflect a specific block of time in the archaeological record (Sackett, *supra*). In short, major episodes of depositional history were reflective of similar episodes of cultural history.

The Bordesian approach, as it has been termed, used well-defined artifact assemblages segregated into “occupational horizons” and the minimal sedimentological units that were discernable within these. Bordes viewed the relative frequency of tool types, ensemble, with their paleoenvironmental contexts as critical to developing a true chronostratigraphic description of a site. One glance at his stratigraphic section for Combe-Grenal will confirm this. Combining the definition of polymorphic tool assemblages with simple statistical measures, Bordes was able to wring greater complexity out of the Paleolithic record. This said, Combe-Grenal was one of Bordes’ first applications of new proveniencing methods, and it required managing these methods over a very large-scale excavation. Because of this, the Combe-Grenal collection has some serious problems, especially in terms of the stratigraphic integrity of the assemblages (Dibble et al. 2009a, b). This is troublesome because of the long sequence and also the richness of its lithic and faunal assemblages at Combe-Grenal. The site has played a central role in many of the dominant issues in French

Paleolithic research over the last half century (*supra*).

Pech de l’Azé IV is another of a complex of four Lower and Middle Paleolithic sites located in the Perigord region of southwest France. Bordes did spend extensive efforts at this site (Bordes 1972). Bordes discovered and first tested the site in the spring of 1952 (Bordes 1954) and then excavated there continuously from 1970 to 1977. It and Combe-Grenal were two of the more important examples of Bordes’ methodology—the “Bordesian approach”—and his lifelong attempt to bring order to the Middle-to-Upper Paleolithic in France. Goldberg, in 1979, and then later (Goldberg and Sherwood 2006) did groundbreaking micromorphological studies of the deposits at Pech de l’Azé IV (Fig. 2.18). At this Middle Paleolithic cave, well-rounded pebbles recovered during Bordes’ original excavations were initially thought to be hammer-stone artifact. However, they, now, appear to be fluvially transported Pleistocene endokarstic deposits that significantly predate the occupation of the cave (Goldberg and Sherwood, *supra*).

Bordes did not excavate Fontéchevade (Charente) cave, but perhaps he should have given the recent geoarchaeological reassessment of the site formation processes and taphonomic factors at play there (Dibble et al. 2006; Chase et al. 2009). The Tayacian, as an archaeological

Fig. 2.18 West profile at Pech de l’Aze’ IV. This profile typifies the deposits in this region. It consists of variously sized blocks of limestone *éboulis* fallen from the roof and walls of the cave within a sandy, iron-stained matrix. The sand is derived ultimately from breakdown of the limestone and accumulated via different sources from outside and mainly within the cave, including slope wash, creep, and solifluction (Photograph by Philippe Jugie)



Paleolithic culture, was first recognized by the French archaeologist Denis Peyrony at the site of La Micoque (Peyrony 1938), located in the Dordogne in SW France. Not long afterwards, excavations at another site 80 km to the northwest, in the Charente, yielded an even larger Tayacian (Henri-Martin 1957). It was for this reason, this latter site, Fontéchevade, ultimately, become the reference site for the Tayacian (Dibble et al. 2006).

Fontéchevade illustrates the importance of revisiting and reevaluating earlier excavations with new techniques and methodologies. Chase et al. (2009) and Dibble et al. (2006) present comprehensive reviews, based primarily on geoarchaeology, of the sedimentological context, as well as the reality of the Tayacian as a Paleolithic stone industry. When the site was originally excavated, the association of bones and stone tools in a cave was uncritically accepted as evidence of human agency in their accumulation. Re-excavation and reanalysis in the 2000s have led to the conclusions that Tayacian assemblages at Fontéchevade are primarily the result of natural formation processes. These processes probably introduced some modified artifacts into the site and clearly produced pseudo-artifacts that were originally interpreted as artifacts. It is this combination of damaged and pseudo-artifacts that became the basis for the assemblages known as Tayacian (*supra*). The authors concluded that the use of the term Tayacian should be dropped. In this regard, it could join the Osteodontokeratic “culture” (Dart 1957) as an example of an industry that simply isn’t.

Beyond Europe, most notably the above examples from southwestern France, cave sites on all continents have been extensively studied by geologists. The study of caves is, perhaps, one of the most mature aspects of modern geoarchaeology. One of the most dramatic advances in the realm of cave sediment studies involves diagenesis and mineralogical research and their implications for understanding site formation processes, human use of caves, and dating of cave sediments. Their systematic study at Kebara and Hayonim Caves during the 1990s

documented diagenetic and mineralogical processes and their ramifications for correctly interpreting anthropogenic deposits (Goldberg and Sherwood 2006).

Along the coast of South Africa are numerous Paleolithic cave sites where geoarchaeological studies have made salient contributions. Klasies River Mouth cave has produced skeletal evidence of anatomically modern humans (AMH) as early as 90,000 years BP in what is termed the Middle Stone Age (MSA) (Ambrose and Lorenz 1990). At Die Kelders Cave east of Cape Town, MSA deposits have been shown to postdate a last interglacial (OIS 5) high sea level that overlies earlier deposits (Grine et al. 1991). Farther east Blombos and Sibudu Caves have produced evidence of MSA stone and bone tools in association with early fire (Backwell et al. 2008; Henshilwood et al. 2001; Schmidt et al. 2012). The South African caves, in general, are important because of the demonstrated signatures of modern human behavior in the use of tool, ornamentation, and control of intentional fire (Klein 2000; Shimelmitz et al. 2014).

With regard to early fire and hominins, results from micromorphology and FTIR refute many of the commonly held notions regarding the intentional use of fire by humans at Zhoukoudian Cave (Goldberg et al. 2009; Goldberg and Sherwood 2006). A similar type of study was conducted at Kebara Cave, where numerous combustion features are also preserved. As at Tabun, higher concentrations of phytoliths occurred in micromorphological samples from within the cave than in those from outside. The results indicate that human transport of fuel was the major source of phytoliths into the cave (Goldberg and Sherwood, *supra*).

2.4.12 Volcanic Landforms

Not every geomorphologist considers this type of landform within the scope of basic geomorphic settings. This is somewhat surprising given the prevalence of volcanism and its impacts on humanity over time. Islands are almost always volcanic landforms. Continental terrains are

imprinted with the remains of volcanic events. The history of archaeology would have been much different if it were not for the discovery of the lost Roman cities of Pompeii and Herculaneum in the later 1700s (Corti 1951). In the modern world, we are reminded almost annually of the force of volcanoes and their disruptive impacts on nearby human groups. At the global scale, we can consider volcanism a factor in shaping climate (Bryson 1988).

Volcanic landforms range from the signature cone shape to craters, caldera, tabular mountains, basalt flows, and ash beds to exposures of intrusions of magma such as plutons, dikes, batholiths, sills, cuestas, and pinnacles. There are floodplains called llanos created by lava dams of drainages (Inbar et al. 1994). Volcanic landforms can, like the volcano itself, be categorized as active, dormant, or extinct. Iceland is both an island and an ongoing display of a variety of volcanic landform. In Western Europe, past eruptions of Iceland's volcanoes have acted as "clocks" with widespread tephra deposits blown from these sources. Geoarchaeologists can map these deposits and gain an understanding of the timing of human occupation, a location far remote from the eruption site. Deposition processes associated with volcanoes are among the most dramatic in nature. After deposition, these volcanic deposits are exposed to erosional processes common to other geomorphic settings.

The following statement from Luciana and Tiziano Mannoni (1984) provides adequate justification for archaeological geology's interest in volcanoes and tectonic processes: "The movement of the plates and continental platform within the covering crust causes volcanic eruptions and earthquakes. Crustal subduction, orogenesis, and the metamorphism associated with crystal deformation, under great pressure and temperature, at plate boundaries create earthquakes and the formation of volcanoes." All of this is subsumed under the rubric of the "Wilsonian Cycle of plate displacements" (Hsü 1995; Wilson 1966). One has to go no further than the names of Pompeii, Troy, Thera, Port Royal, Jericho, and Ceren to assign landmark

archaeological/geological significance to cataclysmic eruptions and earthquakes. Pompeii, and its neighbor Herculaneum, have the place of honor in the pantheon of archaeologically (and historically) documented catastrophes.

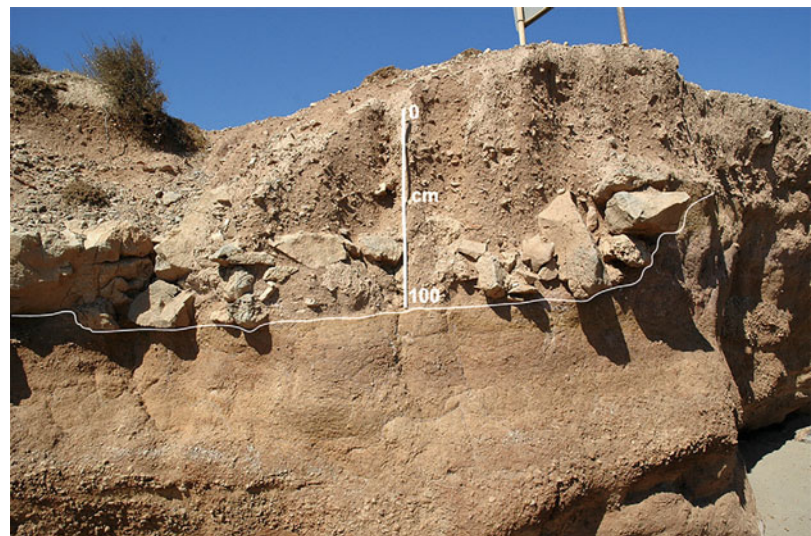
From August 24 to August 25, 79 AD, Vesuvius erupted in, what has been named for its chronicler, Pliny the Younger, a Plinian eruption. Hal Sigurdsson (1999) has published a detailed discussion of Pompeii's end. From an archaeological standpoint, Pompeii's discovery in 1748 led to at first unsystematic antiquity collecting, but by 1860, and the appointment of Giuseppe Fiorelli, well-documented excavations began and have continued to the present. Tourists, including Lyell, came to Pompeii both as antiquarians, and, in Lyell's case, as a geologist. Sigurdsson uses the Latin texts and his own analysis of the tephra deposits, in what is an archaeological study of the fatal eruptive sequence. Herculaneum was destroyed on the first of the 2-day eruption.

https://www.youtube.com/watch?v=dY_3ggKg0Bc

Thera, the volcanic island, also known as Santorini, buried the Minoan town of Akrotiri. Like Pompeii, Akrotiri was buried under several meters of volcanic ash. It was discovered in 1967. The eruption of Thera occurred along the Hellenic Island arc, a back-arc volcanic region formed in Miocene-Pliocene times (Hsü 1995). Wrapped up in the eruption of Thera, a Krakatoan-type blast has also been alternately blamed for the eclipse of Minoan civilization as well as being both the inspiration and plupical location for the Atlantis Myth.

As to the former charge, Thera has been found not guilty by both archaeology and earth science. Spyridon Marinatos, first excavator of Akrotiri, speculated on the timing of the Thera eruption being coincident with the archaeologically observed destruction of Minoan Palace culture on Crete 100 km to the south of Thera. Placing the eruption at around time of the Late Minoan 1B period (ca. 1450 BC) helped solve questions of the demise of high Minoan culture but posed other problems for later archaeologists at

Fig. 2.19 Tsunamigenic deposits for the Santorini eruption or eruptions, 17th c. BC, at East Beach cliff, Crete. The *white line* indicates the erosional contact, termed the basal unconformity, between the chaotic archaeological debris layer and the underlying geological strata. Wall remains and dislocated building stones are present as reworked material in the lower part of the archaeological layer



Akrotiri. No Late Minoan 1B ceramics have been found there, only earlier Late Minoan 1A period wares (ca. 1500 BC).

Based on this discrepancy, many archaeologists see no direct connection between the Thera eruption and Cretan problems caused by tsunamis and ash falls. The recent publication of geochemical data from the Greenland ice sheet cores (Fiedel et al. 1995) indicate a sharp increase in volcanically derived concentrations of NO_3^- and SO_4^{2-} in the atmosphere in the interval between 1646 and 1642 BC. Coupled with dendrochronological data for the same period, 1628–1626 BC, a major volcanic eruption occurred, but was it Thera? The evidence argues against a fifteenth-century BC eruption and suggests an early mid-seventeenth century BC for the Thera eruption (Bruins et al. 2008).

Recent geoarchaeological studies by Bruins et al. (2008) have produced definitive evidence for a tsunami or tsunamis associated with the Santorini eruption as shown in Fig. 2.19.

the result of fault movements, both alter landscapes—natural and cultural. Amos Nur, Stanford geophysicist, has investigated earthquakes in the Holy Land (Nur and Ron 1997). Earthquakes are the second consequence of the tectonism—volcanoes being the other. Indeed, where there is volcanism, there will be earthquakes, but the opposite is not necessarily so. In the collision of continental plates, volcanism or magmatic arcs are not present or occur only early on in the process. The collision need not be “head on,” a convergent boundary, but a “side-swipe” type of collision, called a transform fault boundary. The boundary between the Pacific and North American plates is a transform boundary as in that between the Mediterranean and Arabian Plates. Both are the seismically active zones particularly in California and the Jordan-Dead Sea Transform fault. Along the Dead Sea-Sea of Galilee axis, Nur has identified a 14 m strike-slip movement in the past 2,000 years. The observed motion of the fault accounts for only 3–4 m of this amount. Why the discrepancy? Nur suggests the occurrence of magnitude 8.0 or greater (Richter scale) event(s) in the past.

Using the literary sources, histories, and the Bible, Nur has accounts of major earthquakes in 370 AD, 31 BC, and 756 BC. Judea, half of the dual monarchy of Israel, and later the name of the

2.5 Earthquakes: Volcanic or Otherwise

While they can be a direct result of volcanism, earthquakes, whether associated with volcanic eruptions, or, as more generally the case, simply

Roman province, experienced a devastating earthquake mentioned in Josephus as the same time as the Battle of Actium (31 BC). The 370 AD quake destroyed the Roman city of Beth Shean and is mentioned by Ammianus Marcellinus (Nur and Ron, *supra*, 55). This event was recorded in Cyprus, 360 km to the southwest. Zachariah describes a major earthquake, along with the classic strike-and-dip movement, at Jerusalem in 756 BC. The strongest candidate for earthquake destruction is ancient Jericho where “the walls come tumbling down.” Jericho is no stranger to earthquakes, being struck in July 11, 1927 by a major event that destroyed major portions of Jerusalem, killing hundreds.

2.6 Mapping

Identification of particular landform is typically done by the use of (a) planimetric maps, (b) aerial or satellite imagery, and (c) ground reconnaissance. The objective is to map the principal geomorphic landform, from remotely sensed data onto maps of scales appropriate to the archaeological questions being asked. Broad geomorphic features, at local and regional scales, can be deduced from aerial/satellite images. In regions with extensive vegetative cover, conventional visible spectrum photographs are not as effective for evaluating landforms as those using infrared and microwave regions of the electromagnetic spectrum. These latter types of imaging can aid in landform classification by differing levels and types of vegetative cover, surface hydrology, and, with newer types of high-resolution imaging spectrometers, mineralogy and rock types can be examined. Ground-level studies include walkover surveys and subsurface studies using both hand and mechanical means.

From these images and ground investigations, the geomorphic map should describe (a) morphology, (b) landform, (c) drainage patterns, (d) surficial deposits, and (e) tectonic features together with geomorphic/geological processes active in the mapped area. In today's

world, this is where the value of GIS is most apparent. Once the geographic information is in digital form, GIS programs can be used to make a base geomorphic map (the *primary surface* in GIS parlance) and then as series of subsequent maps (*secondary surfaces*) showing elevation data, stream locations, soil types, landform types, and landform units such as alluvial fans, colluvial deposits, terraces, etc. By breaking up the geomorphic data into multiple displays, one can avoid the problem of complicated and difficult-to-interpret maps. In the United States and many other developed countries, it is possible to obtain geographic and geological data encoded into computer-compatible form. Again, in the United States, a primary source would be the US Geological Survey (USGS). Digital terrain maps are available from that agency, while coastal maps are available from the National Oceanic and Atmospheric Administration (NOAA). Digitized topographic maps now exist at a scale commonly used in archaeology—1:24,000—that of the 7.5 min quadrangle map. Many countries have similar maps available. The GIS base maps of Mexico, for example, are exemplary.

Much of the discussion involving geomorphic mapping is appropriate to that of geological mapping. The use of aerial and other remotely sensed data is important to the mapping of *surface* rock units. The geological map thus shows the distribution of rock units as they appear on the surface of the Earth. Like the geomorphic map, the data is overlain on existing maps at a scale chosen by the investigator. The two types of maps are similar, but the geological map uses a suite of symbols that are commonly agreed upon by geologists. Not only does the map show rock types, but it also shows elevation, strike, and dip of the geological structure. Strike or line of strike is the direction or trend of a formation relative to north or south. Dip is the angle between the horizontal and the tilt of the formation. On geological maps, these appear as t-shaped symbols (†) where long lines indicate strike and short lines indicate dip. A number can be shown by the symbol to indicate the angle of dip (e.g., 25°). As all maps *must* be oriented to the

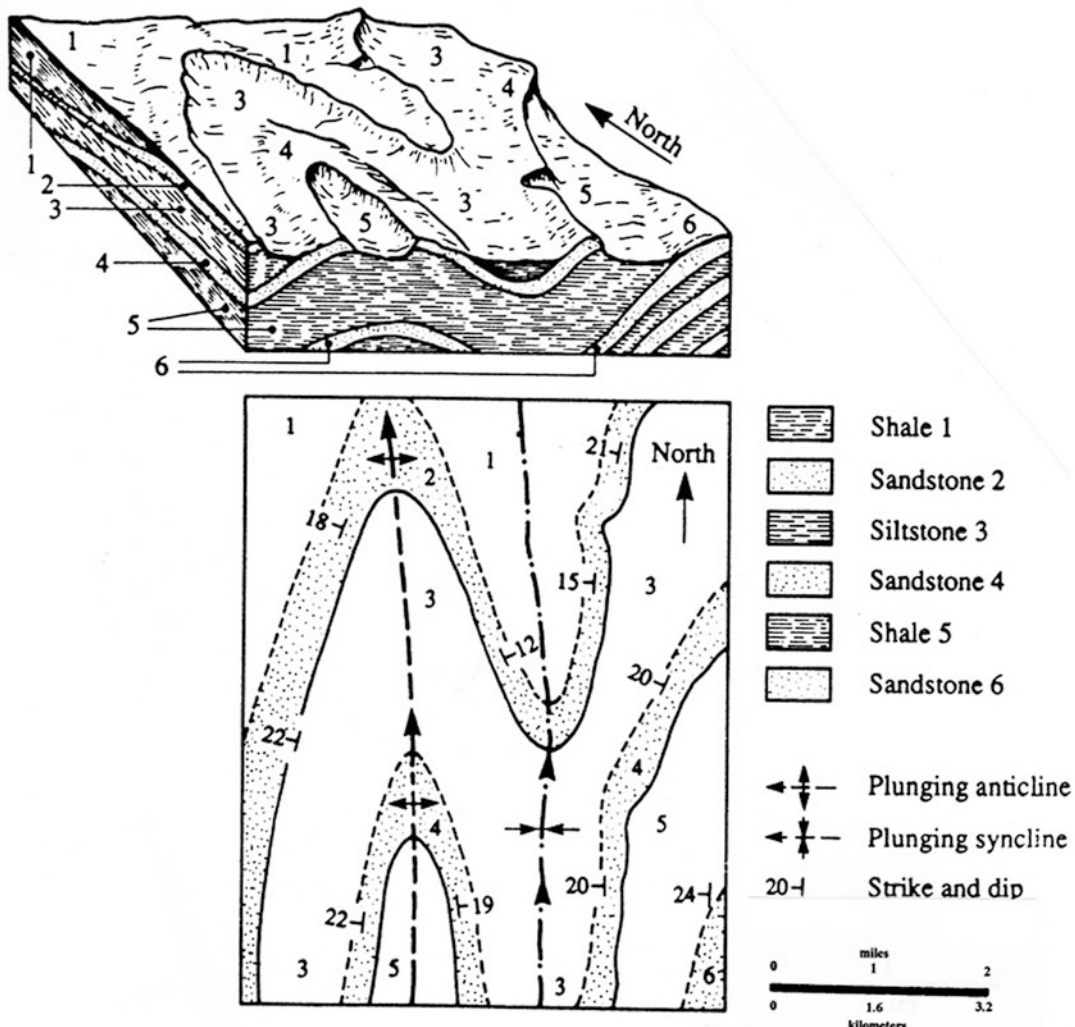


Fig. 2.20 Block diagram, with strata and folding illustrated (a) and geological map (b) further illustrating synclinal, anticlinal folding, strike-dip directions (From

Allard and Whitney, Environmental Geology Lab Manual, Wm. C. Brown, Fig. 4 (1994))

north, the angle of strike is generally deduced from the map itself.

Foliations are indicated by teethlike symbols, while multiples of this symbol indicates a reverse fault and lines with adjacent directional arrows illustrate slip-strike faults (Fig. 2.20). Chronological designations of the rock units are given by abbreviations such as "Q" for quaternary, "T" for tertiary, etc. Color-coding is often used to good effect in geological maps. Contour lines allow the inference of three-dimensional arrangements of rocks and sediments.

Topographic profiles, cross-sectional illustrations, or sections can be produced of outcrops of formations to show stratigraphy in the mapped area. These are not maps in the true sense but can be used in conjunction with the surface geological map to gain a better understanding of the rock units within the area. Structural features such as folds—synclines and anticlines, faults and unconformities—can be shown in section across the geologically mapped area. The bedding of formations—thicknesses and angularity—is also presented in this format.

The profile is indicated on the geological map as a straight line such as “AB.” On the profile, the horizontal maintains the scale of the surface map, but the vertical scale is more often than not exaggerated to several times than that of the horizontal scale. The vertical exaggeration is a ratio of the horizontal scale divided by the vertical scale such as a scale of a topographic map of 1:24,000 (2,000 ft to the inch) divided by a scale of 200 ft to the inch yielding a ratio of 2000/20 or a 10× vertical exaggeration.

Simple rules to follow involving topographic and geological maps include:

1. All points on any given contour have the same elevation.
2. Contours of different elevation *never* intersect each other.
3. Contour lines *never* split.
4. Contour line spacing—close versus wide—indicates steep versus gentle slopes; cliffs are indicated by closely spaced or seemingly coincident lines.
5. Contour lines close on themselves, either within or without the confines of a map.
6. A contour that closes on itself within a map indicates a *hill*.
7. A contour that closes on itself, with hachures, indicates a *depression*—the hachures point inward.
8. Contour lines curve up or “inward”—pointing “up” a valley. The lines cross streams at right angles.
9. Bold or darker contour lines reflect simple multiples of one another. Some maps indicate a multiple of 5, 25, etc. This is termed the *contour interval* (Fig. 2.20).
10. Anticlines have their *oldest* beds or rock units in the center.
11. Synclines have their *youngest* beds in the center.
12. Anticlines incline (“plunge”) toward the *closed end* of a geological structure.
13. Synclines incline toward the *open end* of the geological structure.
14. *Monoclinal* folds incline in only direction. Terraces act as monoclines.

Contacts of rock units with a dip greater than the stream’s slope or gradient “V” *downstream*, while those with a dip less than the gradient, “V” *upstream*.

15. Vertical beds do not “V” or migrate with erosion.
16. Contacts migrate down-dip with erosion.
17. Fault blocks erode according to their up- or downthrown aspect—upthrown eroding faster than downthrown fault blocks.
18. Contacts between horizontal rock units are parallel to the topographic contours along those contacts.
19. The top of a map is *always* north.

2.7 Map Scale

Generally, geomorphology, in the service of archaeology, is not practiced at the global scale. We are concerned, principally, with topography and its control of surface hydrology and past human ecosystems. Scale is important in the conduct of geomorphic and geological mapping. In the remote sensing of topography, from aerial- and space-based platforms, the National Aeronautics and Space Administration (NASA) has recognized three scales of interest: global scale, 1 km horizontal, 10 m vertical resolution; intermediate scale, 100 m horizontal, 1 m vertical resolution; and local scale, 10 m horizontal, 0.1 m vertical resolution. These scales apply to both visual and multispectral imaging.

Their usefulness in geomorphic mapping is fairly obvious. When mapping we refer to high resolution as small scale. In terms of map scale, this nomenclature is confusing to many. “Large-scale” maps of 1:150,000 to over 1:1,000,000 are “low resolution.” High resolution, at the local scale, is represented by ratios of 1:20,000 or smaller. Observations made at different scales are useful depending, of course, on the types of questions being asked. One must be careful, as Stein cautions (1993), in geoarchaeology, to address scale from the human perspective. This is to say that in archaeology, landscape

reconstructions must be focussed on their relevance to human cultures, their processes, and consequent stability or change over time. In this regard, geoarchaeology is differentiated from traditional geomorphology and other geosciences by its use of earth science methods to make interpretations about human groups interacting with landscape, climate, vegetation, and hydrology (*supra*). In mapping archaeology onto topography, it is done more often at local or intermediate scales.

2.8 Data Sources for Mapping

If one starts with satellite imagery such as that of Landsat—land + satellite—(hereafter “Landsat”), 3/4, then the scales of this format varied from 1:250,000 to 1:1,000,000. At the larger scale, the images are 185 km on a side with data on several spectral bands that are available upon request. The most commonly used bands for geomorphic mapping are the visible and infrared bands 4 to 7 with composites available. Band 4 is the green spectral band and is good for delineating areas of water in coastal areas; band 5 is the red band and is good for the vegetation mapping; band 6 is the

thermal infrared band which discriminates between land and water; band 7 is the near-infrared spectral band which penetrates haze, emphasizing water and boundaries in landform. Landsat 3 did not have bands 5–7. These were incorporated into Landsat 4. It did have a Multi-Spectral Scanner (MSS).

Landsat 4 was the first satellite in the Landsat program to incorporate the Thematic Mapper (TM) sensor. The Landsat 4 TM sensor is able to gather seven bands of data as opposed to the four bands of data collected from the previous Multispectral Scanner (MSS). In addition to having three more bands of data to work with, scientists are able to view the TM data at a much higher resolution than with MSS. Bands 1–5 and 7 each have a spatial resolution of 30 m, while the MSS is only offered in 79 m and 82 m resolutions. Band 6 (which is a thermal infrared band) has only a maximum spatial resolution of 120 m. The present-day Landsat 8 provides nine bands of spectral data (including panochromatic), seven of which are ETM (Enhanced Thematic Mapper) bands, with an image resolution or *pixel size* of 30 m (Fig. 2.21). The panochromatic images have 15 m pixel resolution. This is an improvement

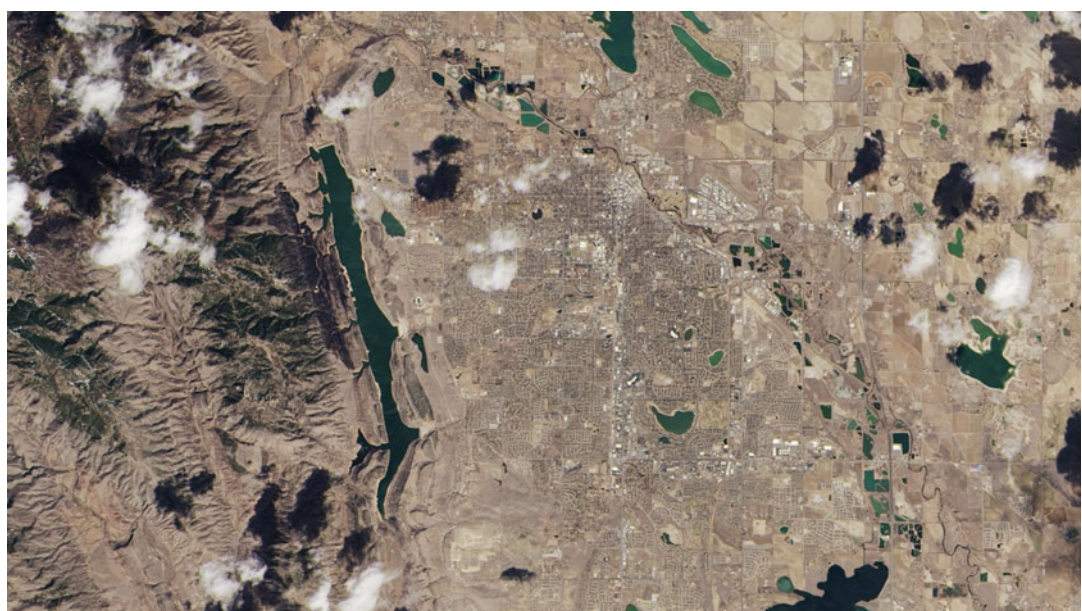


Fig. 2.21 The first Landsat 8 image. Fort Collins, Colorado (Courtesy NASA/USGS)

of original Landsat models whose resolution was 60 m. Landsat 8 has two long wavelength infrared bands (10, 11) with 100 m resolution.

Commercial satellite imaging by the IKONOS and SPOT satellite services, launched in the 1990s, regularly produces 1 m pixel visual band images. The original image cost was about \$1,000/negative, but digitization has driven those costs down significantly. This availability of high-resolution, online imagery has been a boon to archaeo-geomorphic mapping efforts.

The High Resolution Infrared Spectrometer (HRIS) on Landsat 8 has a continuous sampling range from 0.4 to 2.5 μm region with a capability of 10 nm spectral sampling intervals, thus obviating the “band” restrictions of lower spatial resolution systems such as Landsat MSS and TM as well as the French SPOT systems. The continuous spectral capability of the HRIS gives the researcher the ability to assess sediments, rock types, and minerals in exposed terrain (EOS 1987:2–3). For example, the spectral reflectance of sedimentary rocks, which constitute about 75 % of the Earth’s surface (Pettijohn 1975), varies to a degree that important facies such as calcite, which absorbs in the short wavelength infrared, can be readily identified along with limestones, shales, and sandstones. Using Landsat ETM bands 4, 5, and 7, Carr and Turner (1996) have demonstrated different spectral profiles for rock, soil, and weathered bedrock in western Montana.

Both aerial photographs and multispectral data commonly had scales of 1:80,000 down to 1:2,000. In practice, these can be co-registered with satellite data at comparable scales or simply used singularly. Aerial images are of three types—vertical, oblique, and mosaic. The most commonly used are the vertical images which when co-registered with adjacent images form the mosaic type. Both are used in geomorphic mapping depending upon the scale of interest. Oblique aerial photographs provide wide-angle, perspective view of terrain and assist in determining low-relief features in relatively flat terrain. In rough terrain, the value of oblique images is reduced. For the detection of archaeological features, the aerial image is still unsurpassed.

Again this is due to the scale of interest. Features of geomorphic interest are not necessarily those of archaeological interest, and this must be constantly kept in mind when selecting remote sensing data for mapping studies. Archaeological sites, themselves, are rarely detected from satellite images (McMorrow 1995), so *site* scale studies should rely on the advantages of aerial images of lower scale, higher resolution.

Some cautionary notes on using remote sensing imagery as a substitute for planimetric maps should be made here. When using these media either to create a geomorphic/geological map or augment a planimetric map, there are inherent problems both in spatial perspective and elevation. If an image has not been acquired at the truly vertical, then the image lacks spatial fidelity across its height and breadth. The only point on the image of spatial accuracy is directly at the *nadir* or point directly below the lens. All other areas of the image are spatially distorted with respect to their true positions. That is to say, the ground distance between geomorphic features is not in a true proportion with the photo distance between those features no matter what scale is used. Additionally, the height of features is distorted such that relief is exaggerated except in the flattest of terrains.

When photomosaics are made from a collection of vertical images, the same problems still ensue. Only the area around the nadir or principal point will have reliable spatial relationships. Those toward the edges of the images are the most distorted. This distortion can be removed by the process of *rectification* where all points on the image plane are corrected to the vertical. Vertical exaggeration is harder to remove and depends a great deal on the focal length of the lens making the image. Longer focal length lens produces less vertical exaggeration as a rule. When both image distortion—spatial and vertical—have been removed, the image is known as an *orthophotograph* or *ortho-image*. Mosaics made of these are truly picture maps and can have contour lines overprinted on them. When these mosaics are overlain on planimetric maps, the best of both worlds is achieved in the creation of the *orthophotoquad* map.

2.9 LiDAR

In the most recent past, primary data for mapping was obtained from a variety of sources such as traditional maps to satellite images. In the late twentieth and early twenty-first century, a quiet revolution has occurred involving the generation of large digital data sets using airborne and terrestrial LiDAR Systems (*Light Detection And Ranging*) for mapping. “DEMs” or digital elevation models have become the “standard” for intermediate-global scale mapping. At local scale, terrestrial LiDAR (TLS) has proven to be more and more the method of choice for archaeology.

In terms of functional use, LiDAR provides users with detailed terrain models which, after digital processing, can yield bare-earth, vegetation, features, and structures that are either natural or anthropogenic in origin. Both airborne and terrestrial laser scanners provide the LiDAR data sets. Both can be expensive but costs have fallen dramatically over the past decade with increased use of this technology. Likewise the size of the scanners has been reduced as well, making the technology more useful on a host of smaller platforms ranging from backpack to small aerial drones.

Photogrammetry is long been used in different fields, such as topographic mapping, architecture, engineering, manufacturing, quality control, police investigation, and geology, as well as by archaeologists to quickly produce plans of large or complex sites. Photogrammetric data combined with the dense range data from LiDAR scanners complement each other. Photos can clearly define the edges of buildings when the point cloud footprint cannot (Fig. 2.22). It is beneficial to incorporate the advantages of both systems and integrate them to create a useful product for geoarchaeology. Photogrammetrically derived LiDAR combines the more accurate in the x and y directions of photographs with LiDAR range data which are generally more accurate in the z direction. This range data can be supplied by LiDAR, laser scanners (using time of flight,

triangulation, or interferometry), white-light digitizers, and any other technique that scans an area and returns x, y, z coordinates for multiple discrete points (commonly called “point clouds”).

Photos can clearly define the edges of buildings and other features when the point cloud footprint cannot. A 3D visualization can be created by geo-referencing the aerial photos and LiDAR data in the same reference frame; ortho-rectifying the aerial photos, as discussed above; and then draping the ortho-images on top of the LiDAR grid. It is also possible to create digital terrain models and thus 3D visualizations using pairs (or multiples) of aerial photographs or satellite imagery, transformed through a camera model program such as 123D Catch (AUTODESK) to produce a dense array of x, y, z data which can be used to produce digital terrain model (DEM) and ortho-image products.

2.10 Structure from Motion (SfM)

Structure from Motion (SfM) has increasingly become a low-cost, easy method of accomplishing much of what, previously, had required imagery obtained from satellite and rotary/fixed-wing platforms. Using drone-mounted and handheld cameras, high-resolution images can be quickly obtained and processed using open-source or licensed software programs. The results are strikingly comparable to those from LiDAR, for instance, digital-surface, hill-shade renderings and digital elevation models (DEM). (Fig. 2.22). Figure 2.23 illustrates a simple application of SfM on an archaeological excavation. The upper image shows the various camera positions and the sequence of photographs taken to render the isometric view. The lower image is the digital-surface rendering of the same view. Compare this with the LiDAR views in Fig. 2.22. Both SfM renderings are scalable and capable of 3D rotation. Two different softwares were used in this example. The first is by AUTODESK and available at no cost. It is known as 123D Catch. The second software program used is Smart 3D offered by Acute3D.

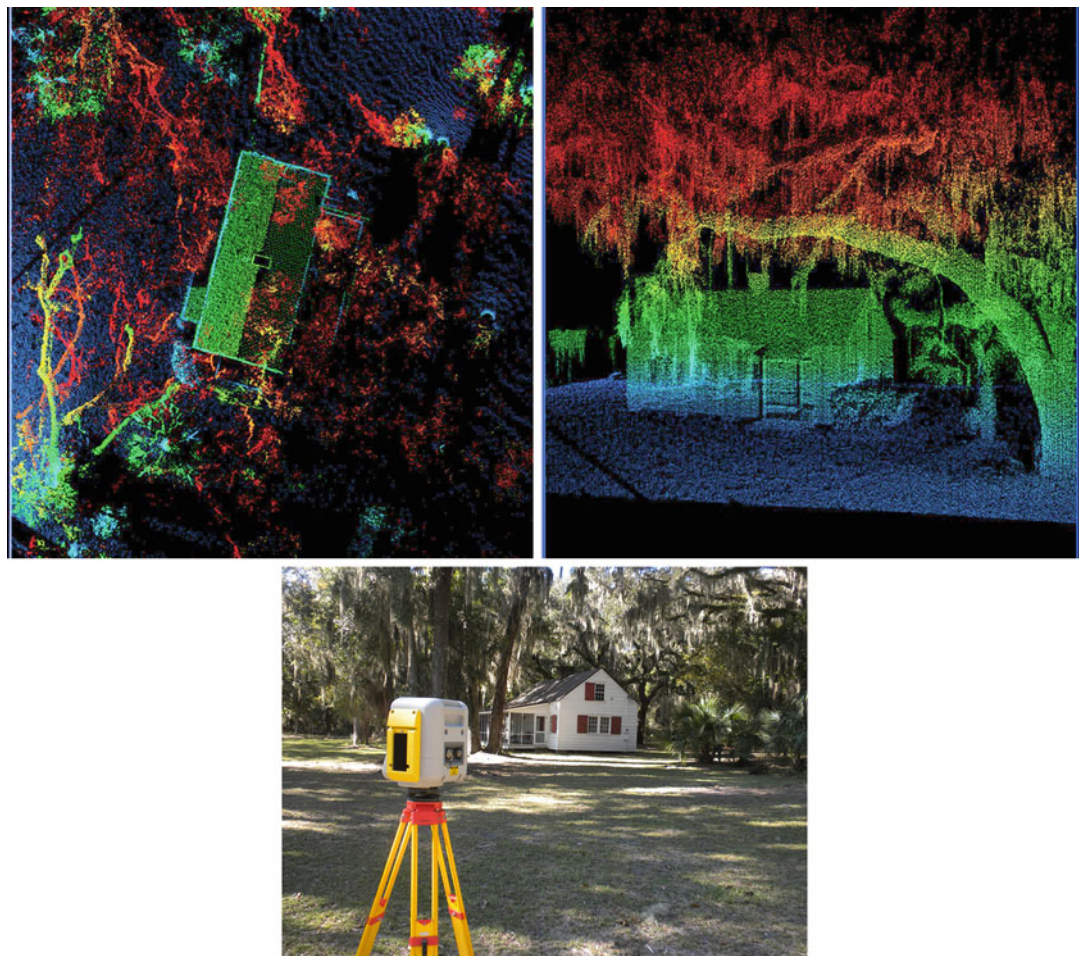


Fig. 2.22 Three views of a historic slave cabin, Wormsloe Plantation, Savannah, Georgia, USA. The upper two views illustrate LiDAR views, and the lower

view is a photograph of the cabin with the LiDAR unit shown (LiDAR and photo images courtesy Geospatial Mapping Center, the University of Georgia)

Luhmann et al. (2013) provide an overview of the diversity of close-range photogrammetry and 3D imaging available.

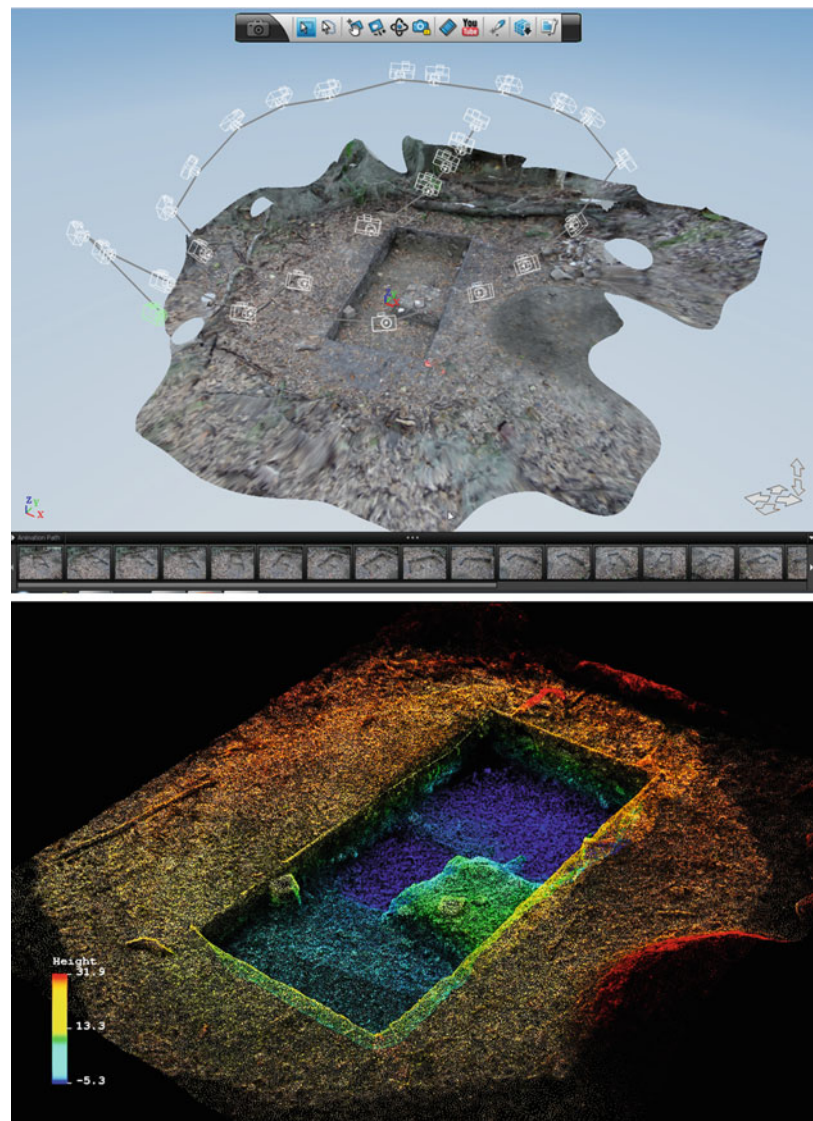
2.11 Drones

The utilization of unmanned, powered aircraft has flourished in the early twenty-first-century beginning, first, with military uses. These vehicles are either remotely piloted or autonomous (Figs. 2.23 and 2.24).

As Fernández-Hernandez et al. (2015) have pointed out, even in the early years of the twenty-first century, it was thought that laser

scanning would make photogrammetry obsolete in archaeological studies. However, digital image matching and image-based modeling, as illustrated in Figs. 2.20 and 2.21, have become alternatives to laser scanners. The use of photogrammetry in conjunction with unmanned aerial vehicles (aka “drones”) offers effective low-cost tools for the generation of 3D models and ortho-images using image-based modeling techniques without the use of laser scanners. This new flexibility and access to both open-access and proprietary software make the drone a useful tool for the imaging and modeling of complex archaeological sites. Using techniques taken for DEM methodology and presentation formats such as

Fig. 2.23 Illustrating SfM. The *upper* view of an excavation was produced using the program 123D Catch. The *lower* view is a digital-surface view of the same unit using another program, SmartD. Both views are scalable and rotatable (Images courtesy Geospatial Mapping Center, the University of Georgia)



“hillshade,” photographs taken by low-cost drones offer a rich and broader utility for the larger geoarchaeological community as a whole when compared to the LiDAR and other more costly and equipment-intensive approaches (cf. discussion on SfM).

2.12 Making the Map: ArcGIS to Google Earth

In the digital age, a geomorphic map or geological map can be produced with media most

commonly downloaded from Google Earth. Digital photographic images of the area of an archaeological site can be reconciled to planimetric maps of that same location through the use of a recent creation termed the *Geo.pdf* (Fig. 2.25). The first concerns were of *scale* and *geodetic position*. These two parameters often differ significantly, in pre-digital, “Google Earth” days such that they had to be *ratioed* where the two formats were in a realistic numerical proportion. Another concern was when the maps and the images were made, e.g., the *date* of their production. Photograph and other imagery differ



Fig. 2.24 A small, commercial drone (eBee by SenseFly) being preflight programmed for a photographic survey. The photomosaic shown on the right

is the result of this particular flight (Photographs courtesy of Chet Walker, shown programming the eBee drone)

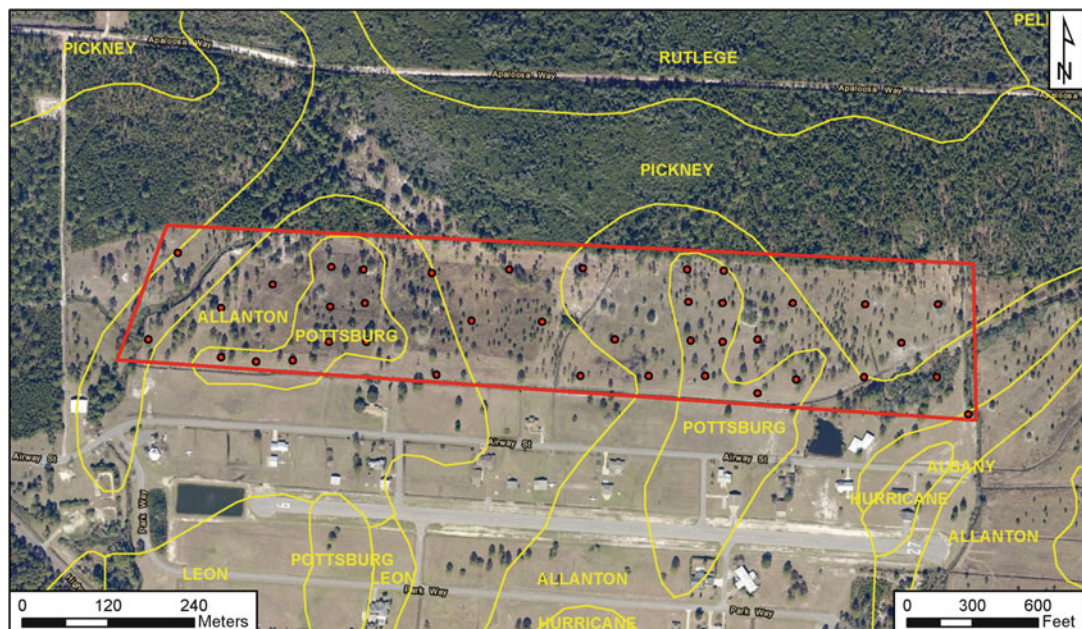


Fig. 2.25 A Geo.pdf with the capability for embedding geographic coordinate information. The red circles are location of selected test locations across the survey area (Image courtesy of ARI, Tallahassee, Florida)

significantly from maps in their dates. A map is, therefore, a synthetic creation that generalizes the temporal frame with that of the spatial or geodetic. Working with digitally based media such as the Geo.pdf (Fig. 2.25) allowed us to utilize another recently developed of the space age—Global Positioning Satellites or GPS—for location and creating reference points within the map frame (red dots in Fig. 2.25). Using

handheld receivers, one can quickly map the geomorphic and geological features.

Mobile phone applications have also been developed for as GPS, database management, and GIS use. Examples of such applications are ArcheoSurvey (<http://www.icarehb.com/index.php/field-methods-and-techniques-mz>) and Polaris Navigation GPS (<http://www.appsapk.com/polaris-navigation-gps/>).

2.13 Other Types of Maps

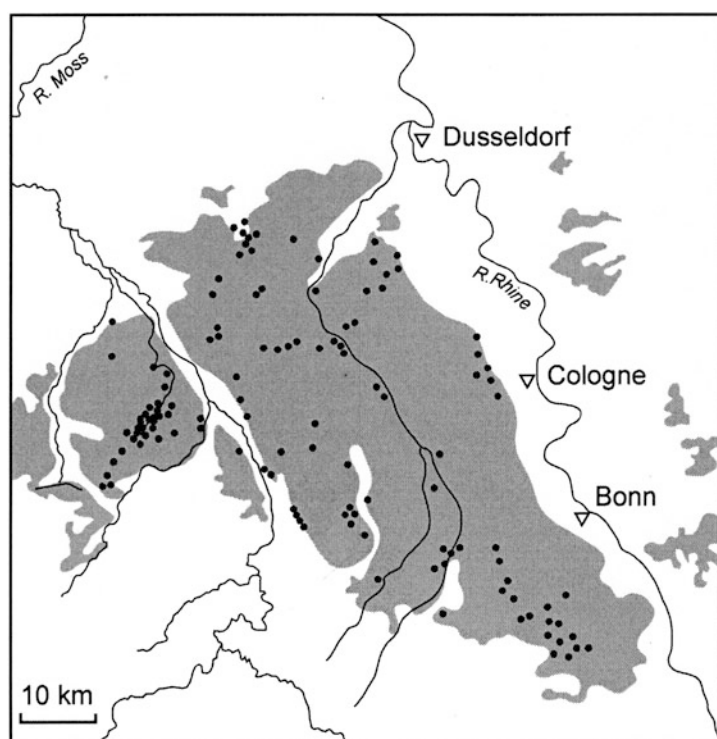
Paleogeographic—These maps are typically regional or broader in scale, showing the distribution of ancient land and sea. In Europe and North America, the most common paleogeographic maps are, perhaps, those showing the extent of the Pleistocene ice sheets relative to unglaciated terrain. Another commonly seen representation is past sea levels and coastlines in the Pleistocene. Unlike paleogeographic maps from more ancient epochs, which rely on the plotting of rock units that are time synchronous, paleogeographic maps of archaeological interest are based on more geologically recent mappable surficial features such as moraines and strandlines.

Isopach—These maps are used to illustrate the thickness of particular strata. Unlike profile illustrations, the stratigraphic unit is mapped and has contoured some selected interval. The ice sheet thicknesses illustrate a typical isopach representation. Isopach maps generally are done for buried strata and, hence, are based on core data. The use of isopach maps is infrequent in the presentation of archaeological data. As a rule,

when core data is available, a profile representation is done with the stratigraphic data overlain at specific sounding. When doing an isopach map, the upper surface is used to portray the stratigraphic unit. Isopach maps are very useful in determining the shape, direction, and depth of basin-like features and buried channels.

Lithofacies—A lithofacies is defined as that aspect or attribute of a sedimentary unit that is a direct consequence of a particular depositional environment or process. An obvious example is a fluvially deposited unit wherein the grain shape, mineralogy, surface texture, size, etc., of the sediment reflect stream transport. Another way to visualize a lithofacies map is to think of it as an isopach map without contouring. Sometimes archaeologists will use a variant of the lithofacies map in showing the association of archaeological sites with specific landforms or soils. In the latter case, Kuper et al. (1977) correlate Bandkeramik (LBK) sites with loessic soils in northwestern Germany, west of the Rhine River valley. The lithofacies map is a qualitative representation of surficial and subsurface strata known from isolated soundings (Fig. 2.26). One can assume

Fig. 2.26 Linear band ceramic (LBK) sites (black dots) plotted relative to loess soils (gray) in northwestern Germany (Adapted from Kuper et al. 1977)



the distribution of some strata will not be uniform or continuous. This is true for most intra-site mapping and limits the applicability of the technique. Where soundings are of sufficient density, the use of lithofacies maps has merit. Where a clear association of archaeological material, with a stratigraphic unit, is

demonstrated, then the lithofacies mapping of the unit, based on pedological/sedimentological features, assists in bounding the site for a specific occupational period. This method works very well in shallow (<1 m) depth sites that can be quickly sampled with hand coring equipment (see Chap. 4).

3.1 Introduction

Since the principal focus of this chapter is the description of sediments and soils and their use in archaeological geology, a programmatic approach to their study is used in modern geoarchaeology. Many of the methods, discussed in this chapter, and their use in both terrestrial and marine/lacustrine environments will be within their specific applications to paleoenvironments. For the assessment of subsurface deposits and their spatial/stratigraphic extent, these techniques provide the most reliable and efficient means of doing so. From the geomorphological perspective, any paleosol, unless found to outcrop in the vicinity of interest, is exposed and described using them. Likewise, for ground-truth purposes of geophysical data, they provide a reliable means of assessing depth of features such as subsurface contacts and anomalies. These field techniques allow the investigator to recover representative and depth-constrained sediment, soil, and rock samples for purposes of laboratory studies.

The study of sediments is the branch of geology termed sedimentology. Sediment beds accumulate on top of another, whereas soils form in place. The study of soils is the field of pedology. A “ped” is the smallest, recognizable element of soil structure. The solum is defined as the uppermost part of the Earth’s surface and is composed of the O, A, E, and B horizons (Richter and Yaalon 2012). Both sediments and soils are

important dimensions of the geological study of archaeological sites (Benedetti et al. 2011). The sediment and soil context of the archaeological site is the essential matrix for the material remains of archaeological interest. An adequate scientific description of this matrix is basic to the study of any site. Without it, artifacts and features lose much of their temporal and environmental points of reference. The pioneering Russian soil scientist, V.V. Dokuchaev, at the end of the nineteenth century, recognized that soils resulted from (a) the climate of a locality, (b) the nature of the parent material, (c) the amount and character of the vegetation, (d) the age of the landscape, and (e) the relief of that landscape (Clarke and Beckett 1971). By a close study of this context of the archaeological site, one can retrodict many of these important factors. For example, clay minerals are sensitive to most weathering environments and reflect changes in those environments—rainfall, temperature, etc.—when measured in soils. Likewise these minerals are indicative, in many cases, of the parent lithic substrate (Conklin 2013:47–48; Rye and Holland 1998). Additionally the particle size of these minerals can help the researcher to determine the past depositional environment such as that of a backwater lake (finer clays/silts) versus that of a fluvial nature (coarser silts/clays as well as sands).

Much of the modern study of sediments and soils is done in the laboratory and we shall

discuss several of these techniques in Chap. 4. Nonetheless much information can be gained in the field. The description of a sediment or soil profile is typically done in the field as many elements of the fundamental nature of those deposits would be lost even with the most careful of sampling for later laboratory description. Beyond the macromorphological information obtained from profile studies, the collection of subsamples for later study is essential. How one goes about this involves standardized and well-known tools and procedures taught at college-level courses of soil science, sedimentology, and geomorphology. Still it is important to reiterate the description of the use of these tools and techniques as this generally omitted by journal editors as too tutorial in nature.

3.2 A Brief Review of Sediments and Soils

Geologists usually define soil as a layered mixture of mineral and organic components that are physical and or compositionally different from an original, unweathered parent material (Smith and Pun 2006). To agriculturally trained soil scientists, sediments differ from soils in the capacity of the latter to support plant growth. Many definitions of these materials focus on the organic content of a soil as compared to that of a sediment. Soil ultimately originated in a rock substrate referred to as bedrock. Clastic sediment is a solid fragmental material that originates from weathering of the bedrock and is transported or deposited by air, water, or ice. The unconsolidated portion of the Earth's surface that is not soil is the regolith. The regolith is weathered rock and/or debris that overlies solid bedrock. In many places, such as the Piedmont of the Appalachian Mountains, it forms a several-meter-deep cover referred to as saprolite. Soils form over an extended period of time. Except in the most exceptional cases, soils require thousands of years to form in most regions of the world such as the formation of B_t horizons in the Appalachian Mountains of the southeastern United States in less than 4,000 years (Layzell et al. 2012).

Sediments and soils result from the chemical and mechanical weathering of rocks and their minerals. The breakdown of the lithic material and its subsequent redeposition is part of what Stein (1988) terms the "history of a sediment." A sediment's history is a function of four factors: (1) source, (2) transport, (3) depositional environment, and (4) postdepositional environment. A study of the physical and chemical properties of a sediment or soil can evaluate the nature of these factors. By using the principle of uniformitarianism (Hutton 1788)—the soil-forming processes active today are those of the past—and those of sedimentation, one can compare a sediment or soil of a known history and infer the processes responsible for the properties and characteristics of those under study. In archaeological geological studies of sediments and soils, the processes involved are generally both natural and anthropogenic (Butzer 1982). Again, by examining archaeological sediments, and comparing them to reference examples from other well-studied sites, one can infer the specific processes involved in their formation (Schiffer 1987). From the standpoint of geomorphology, there are two basic processes—erosion and deposition—which determine the location and variety of sediment and soil:

As we shall see in the following chapter, a sediment's source can be evaluated by examining its textural makeup – grain-size, grain morphology and surface features, and composition (mineralogy). These parameters give insights into the transport history of the sediment with fluvial sediments demonstrating a well-known rounding due to water transport. Aeolian sediments can be recognized by grain shape and by the grain surface "polish" or glossiness. Size gives clues to the transport mechanism – large, poorly rounded gravels are good indicators of glacial transport in terrains of the northern hemisphere. Small grained sediments are found in arid environments such as deserts and drylands as well as fan and fluvial sediments. In the Great Basin of the western United States fine-grained sediments are common in large slope-wash colluvial fans (Nelson 1992). Clays from these fans were often used by prehistoric potters (Speakman et al. 2011).

Depositional features of sediments are determined from samples either in situ or recovered en bloc. The structures, of these deposits, include

the orientation of bedding planes and laminae of various grain sizes and textures. These depositional features are observed in profiles and cores. The last phase of a sediment's history is that of postdeposition. In archaeological contexts, zonation develops either due to soil formation or cultural activities such as building, disposal of materials, and the simple act of living which produces surfaces that can be identified by their micro- and macro-characteristics (Gè et al. 1993; Courty et al. 1989; Goldberg and Berna 2010).

Soils: From the perspective of archaeology, soils and buried soils—paleosols—perhaps more so than sediments per se, provide clearly delineated markers of past landscapes and the factors responsible for their formation (Valentine and Dalrymple 1976; Mack et al. 1993; Johnson 1998). Archaeological cultures exploited soils particularly after the advent of plant and animal domestication. Beyond being the important substrate for the “agricultural revolution” (Childe 1951), soils, as *paleosols*, serve as stratigraphic horizons as well as proxies for temporal/cultural periods in the archaeological record. It is more and more common to read of a past cultural facies associated with a particular paleosol, e.g., a paleolithic cultural association with a loess- or tuff-derived soil, and the association of the Bandkeramik culture with light, well-drained alluvial soils. These early Neolithic sites are found along the Rhine and Danube drainages—specifically on gravel river terraces overlooking medium-sized drainages in areas of loessic soils (Fig. 2.25) (Howell 1987).

As Dokuchaev (1899) correctly observed, soils are the result of *in situ* formative factors. These factors have been arranged into the acronym CLORPT first introduced by Hans Jenny (1941). Jenny includes the same five state factors—(1) climate, (2) relief or topography, (3) organic(s), (4) parent rock, and (5) time as Dokuchaev—but related them into a quantitative equation: $s = f (cl, o, r, p, t, .)$. In the particular case of granite, a common soil formed under forests is the ultisol. Using the parameters of the CLORPT acronym, climatic geomorphology is an area of study that has direct relevance to archaeological inquiry. While it is important to

recognize that its influence on geomorphology is complex, the study of climate, in archaeological contexts, begins with the soil and its role as a proxy for paleoclimate.

In the absence of biologic effects, subaerial weathering would have essentially involved the reaction of rocks with the ambient atmosphere. Subaerially weathered soils sometimes dry out. As they dry, desiccation cracks may form on the top portion of the profile. If these cracks are filled by sediment and are later consolidated and compacted, they provide a clear testament to the subaerial origin of the soil.

Soils that form in place on a homogeneous substrate such as an igneous or high-grade metamorphic rock tend to exhibit unidirectional changes in texture, mineralogy, and bulk chemical composition from the unweathered parent rock to the top of the soil profile (Holland and Zbinden 1988). At their base, such soils typically grade smoothly into the parent material such as the ultisol example. The top of the mature soil generally retains few, if any, of the parent rock's textural or mineralogical features. There is usually a continuum of intermediate stages of decomposition of the original minerals and textures. As the original minerals of the igneous or metamorphic substrate break down, they are replaced by soil minerals. In a mature ultisol, kaolinite, gibbsite, and amorphous silica often dominate the mineralogy near the top of the soil. Smectite and vermiculite are common in the lower portion of the profile. Soils often develop on sedimentary rocks. Most sedimentary rocks are vertically heterogeneous. Soils that develop on flat-lying clastic sediments and other heterogeneous substrates tend not to develop textural, mineralogical, and chemical profiles that distinguish them from other clastic sediments. It is important to recognize that not all, if indeed, many, soils are the result of *in-place* weathering. Surficial processes such as colluviation, erosion, redeposition, etc. all contribute to the polygenetic origins of soils (Driese et al. 2011).

Soils are described by the use of *pedostratigraphic* nomenclature. This is in contrast to the nomenclature of lithostratigraphy which follows

the NACSM code (see below). One must consider both in many descriptions of profiles as the former “overprints” the latter in all cases. Waters (1992) discusses this in detail, noting that because a paleosol is superimposed onto a lithostratigraphic unit (alluvial deposit, dune, ash deposit, etc.), it is always younger than the unit on which it develops. Likewise, because the soil-forming processes alter original particle sizes and create new pedologic structures, the original stratigraphic features such as contacts are often obscured or otherwise made difficult to interpret (*supra*). Soil horizons have no relationship to the geological deposition in the lithostratigraphic units on which they occur. The description of soil horizons and sub-horizons will be discussed in the next paragraphs. These are typically done in the field, but sample blocks can and are described in a laboratory setting. Certainly this is true for “deep” core samples (>1+ m) obtained using devices like the Giddings-type and other mechanical coring devices (cf. Chap. 5).

Gvirtzman and Weider (2001) present an excellent discussion of a combined field and laboratory description of a 53 ka eastern Mediterranean soil-sequence stratigraphy. In a section with at least six paleosols, these researchers have used a combination of descriptive protocols, which can be used as a model for similar studies. In their study, pedostratigraphic, lithostratigraphic, and sequence-stratigraphic nomenclature are combined in full description of the soil sequence. For pedostratigraphy, the soil sequence is described from the *top down*, while the stratigraphic sequence is described from the *bottom up* (*supra*). Moreover these researchers use the terminology, and methodology, of modern sequence stratigraphy as applied to paleosol units such that the *sequence boundary* (cf. this chapter) is a surface between the top of an older buried soil or sediment and the base of a younger overlying soil or sediment.

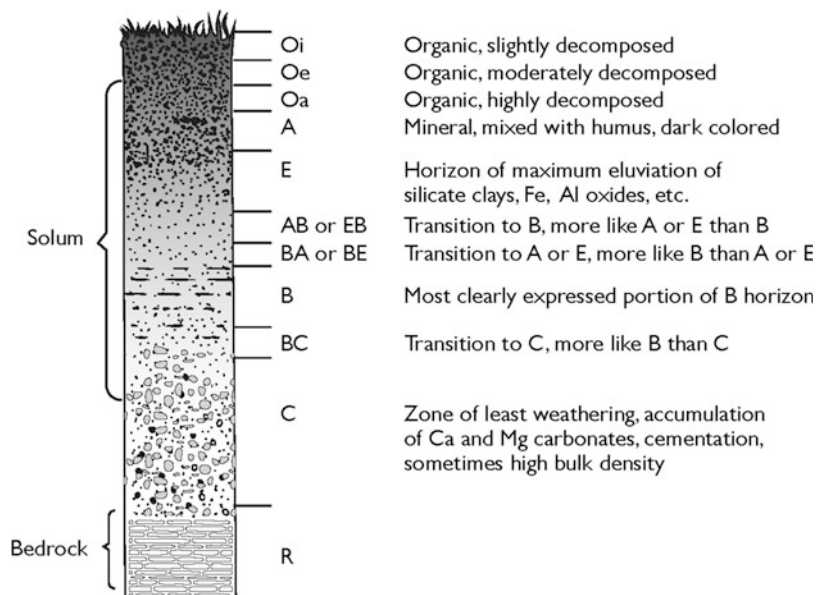
Following the standard practice in lithostratigraphic description, the paleosols were considered “lower” in stratigraphic hierarchy than “member” and were described as say a “Hamara Member” of the “Hefer Formation.” Paleosols

within the Hamara were described as “subunits,” still maintaining a valid priority in sequence terms. The subunits are separated by the use of soil-sequence boundaries as just described. This usage of sequence-stratigraphic terminology differs from its more common application to marine sequences where “sequences” are made up of *parasequences* separated by *erosional surfaces*. In the marine context, these reflect basin facies changes, whereas in a soil-sequence setting, the soils form on the “erosional” surface (s). To use sequence-stratigraphic nomenclature exclusively would require that terms like “formation” be dropped. In a lithostratigraphic context, the contacts are the boundaries or erosional surfaces. Later in this chapter, we shall discuss the role of the erosional surface for developing allostratigraphic sequences. Again, it must be plain that one must take care in the use of these nomenclature systems and be very clear in describing their use in a particular study.

Horizonation: A solum or the upper part of the soil horizons—A and B—of a buried soil, termed a *paleosol*, like a sediment, can give us information on the five factors that produced it. Paleosols are the grist of most soil studies in archaeological geology. Buried soils are characteristic of the mid-latitudes and are rare in the tropics and arctic. Russian scientists such as Dokuchaev and Sibirtsev first described soils as consisting of zones (*supra*). The American C. F. Marbut elaborated the Russian scheme giving names to differing soil types. Today we continue the use of names for specific types of soils, but the term zone, to distinguish soil profile divisions, has been replaced with soil horizon nomenclature.

The generalized soil profile (Fig. 3.1) consists of the “master” horizons: O, A, B, E, C, and R. Their formation, over millennia, occurs through the process of horizonation. O horizons are those layers above the mineral surface and consist of decomposed organic material such as leaf litter and the like. It, together with the A horizon, is also termed the “topsoil.” The A horizon is the topmost mineral horizon located just below the surface. These horizons generally have a high organic content and have lost iron,

Fig. 3.1 Soil profile with commonly found horizons



aluminum, and clays, resulting in a concentration of siliceous material. The E horizon is now generally recognized as a separate horizon although it is still common to see it considered, by some soil scientists, as a leached A or B and even a “transitional zone” between the A and B but having no specific horizon name. E horizons are those of maximum leaching or *eluviation* of soil minerals, most notably iron, alumina, and clays. The E horizon is bleached or lighter colored in appearance compared to that of adjacent horizons. The B horizon is the *illuvial* layer where the translocated mineral complexes from the A to E are concentrated. Depending upon precipitation, a B horizon will vary in the amount of redeposited minerals as well as development in profile thickness. B horizons are mistakenly referred to as the “subsoil,” by definition, making the O and A the topsoil no matter their composition and thickness. The C horizon is sometimes termed the *regolith*, but this term, as implied above, is better reserved for unconsolidated material overlying rock (Brady 1990). The C horizon may appear as rock but it has undergone pedogenic processes. Saprolytic soils are good examples of this with deeply weathered C horizons several meters thick in some regions. The R horizon is unaltered, consolidated *country*

rock or parent material. In undisturbed soils, the R horizon lies conformably with the superposed sediments and soils above it.

The relationship of artifacts to soil horizons is central to any archaeological geology of a site.

As reiterated in the upcoming discussion, there is no sufficient phenomenological relationship between artifacts, their occurrence on sites, and soils *per se*. Cremeens and Hart (1995) provide a good review of this important relationship in their consideration of chronostratigraphy and pedostratigraphy relative to the archaeological context. In that paper, the authors note the difficulty of using the North American Code of Stratigraphic Nomenclature (NACSN) pedostratigraphic term of “geosol,” which stipulates that a paleosol must be overlain by a lithostratigraphic unit—a condition rarely met by Holocene soils (*supra*, 15). Likewise, no subdivisions of a geosol are admitted which is a problem for archaeological description to say the least. Adjacent soil horizons—A, E, B, etc.—are spatially discrete but not temporally so. In this they differ, fundamentally, from the lithostratigraphic description of sediments. In even Holocene contexts, paleosols can be of three types—(1) relict or a surface, never buried paleosol; (2) exhumed or a buried paleosol now subaerially

exposed; and (3) buried or “classic” paleosol. Paleosols are recognized on the basis of their organic, textural, and stratigraphic features (Collinson 1996). Because of their antiquity, the increased exposure to diagenetic processes can make original pedogenic differences between horizons more pronounced when compared to analogous modern soils. This is observed in “red bed-type” paleosol successions such as the example given for the “Hamra” soils. The authors of that study note this in their observation that “the older hamra developed (and) enhanced the red color and increased clay content (*supra*).” In the following discussion of soil chronosequence, this “deepening” of red hues—10YR to 2.5 YR—is synchronous with increasing clay content (Layzell et al., *supra*).

In the Gvirtzman and Weiner study, the soil sequence demonstrates a common aspect of paleosols which is an overprinting of a later soil onto the preceding one. This is referred to as *polygenesis* and leads to what are termed “composite” paleosols. In particular the production of red pigments may take away from existing pedogenic features (Collinson, *supra*). When the soil sequence is not so mixed and the separation of paleosols is such that soil-forming episodes are distinct, then one must examine the nature of the geological processes that “reset” the sequence to primary stages of development. Vitousek et al. (1997), in their study of Hawaiian paleosols, suggest that glaciations and volcanic eruptions are the most likely to do this. Gvirtzman and Weiner (*supra*) observed that coastal aeolian deposition was the mechanism at their location.

In the study of the geomorphology of the Quaternary, most workers use Birkeland’s cross-disciplinary approach (Birkeland 1984). For purposes of archaeology where one may be describing a paleosol or a sediment stratum, it is important to remember that the objectives of that description may be very different, as mentioned earlier in this section, from that of a pedologic or edaphic characterization. Archaeological sediments can have lithostratigraphic differences, based on texture and composition; chronostratigraphic differences, based on temporal distinctions; allostratigraphic differences,

based on bounding discontinuities or unconformities; as well as pedostratigraphic differences, based on one or more differentiated soil horizons.

In this book, the taxonomic level of soil order is used for discussion purposes. As noted above, there is no compelling methodological reason to associate a soil with any form or period of archaeological site. Archaeological sites can and do occur on land surfaces that have the various soil orders discussed below. Still there is no particular type of cultural site that demands a particular type of soil. Prairie soils, such as mollisols, could be associated with archaeological sites of an agricultural nature, such as in the American Midwest characterized by late Quaternary lithostratigraphic units such as the Loveland, Roxana, and Peoria formations (Leigh and Knox 1994). These three younger formations date as follows: Roxana (55,000–25,000 year B.P.) and Peoria (25,000–12,000 year B.P.) loesses recognized elsewhere in the midcontinental United States.

But is it, likewise, necessary for a paleosol like the *Brady soil* (Fig. 2.12) to have formed on a widespread paleolandscape like the Peoria Loess on those same prairies? Archaeological sites ranging from the earliest periods in North America are found on both the Brady Soil and the Peoria Loess (Reagan et al. 1978). An association of a particular form of archaeological site with a soil could be called a necessary condition, in terms of logic, but hardly a *sufficient* condition. Early agriculture and early entrant hunting-foraging cultures are as easily found on ultisols (typically found in formerly forested landscapes) and on young entisols or inceptisols found on active fluvial landforms.

As such the stratigraphy of archaeological deposits can be formalized using the North American Stratigraphic Code (NACSN 1983) or, perhaps, better still by the International Stratigraphic Guide (Salvador 1994). Workers such as Stein (1993) endorse the use of cultural items such as artifacts or features to specify ethnostratigraphic differences in archaeological sediments.

Taxonomy: Soils are classified according to systematic taxonomic naming systems. The system developed in the United States is termed the

7th Approximation or Soil Taxonomy. This system was developed by soil scientists of the US Department of Agriculture and those of many other countries and was introduced in 1965, in the United States, and has been adapted, to varying degrees, by over 45 other countries. In this system, the A and B horizons become epipedons or surface horizons, and those horizons below the B are subsurface horizons. There are six categories in the classification system arranged in a descending order of scale—order, suborder, great group, subgroup, family, and series. The most inclusive category is that of order. There are only 12 soil orders but there are around 16,800 soil series recognized in the United States alone.

The soil taxonomic classification system was developed to describe and map soils found on the surface of the Earth today. As Fig. 3.2 illustrates, this is not the exclusive soil classification scheme. The American system, the FAO, and the French schemes are the most commonly used (Collinson, *supra*). The American system relies on the organic content of the near-surface layer and the chemical characteristics of the deeper horizons. The FAO scheme, somewhat simpler, recognizes basic soil types, predicated on maturity of the soil type and climate. The French system relies less on climate criteria and more on soil-forming processes.

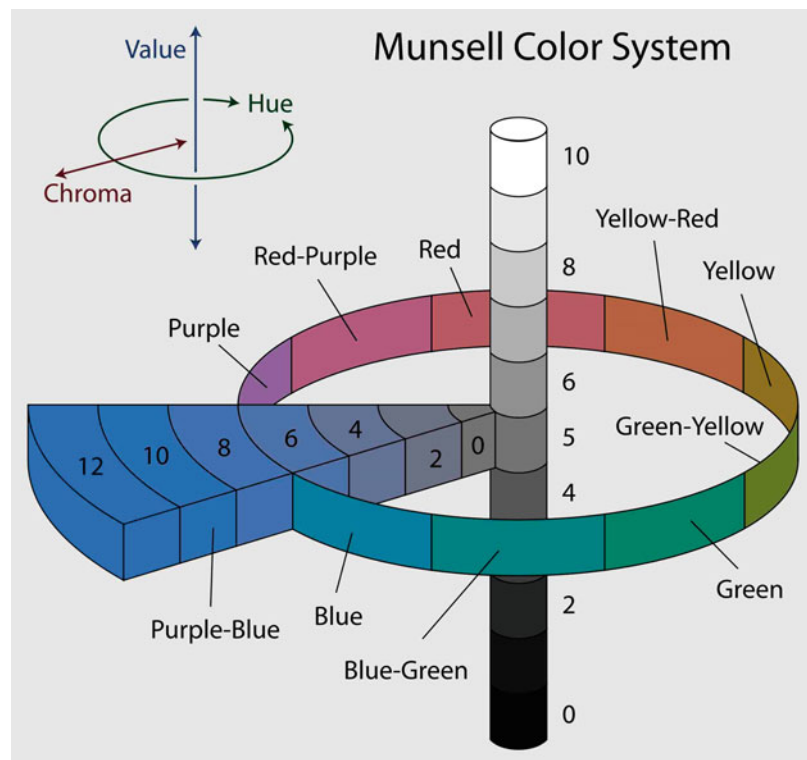
Soil taxonomic nomenclature allows a quick and thorough description of the properties of a soil. The names of the classification units are simple combinations of syllables that are derived from Latin or Greek root terms, each of which conveys some key aspect of the nature of the soil such as the Latin root *aridus* for “dry” appears in the order name Aridisol. The Latin root *mollis*, meaning “soft,” forms the order term Mollisol. The suffix *sol* is the Latin for “soil” so a mollisol is a “soft soil” and likewise an aridisol is a “dry (land) soil.” As one descends the naming system, a wet, soft soil is described by the suborder term aquoll which is the conjunction of “*aqu(a)*” and “*(m)oll*.” Note the higher taxonomic designator “*(m)oll*” appears last in the sequence. Continuing the description of the soil the level of the great group, a clay-rich, wet mollisol is a agriaquoll. If

the soil is characteristic of a subgroup, it is described a “typic,” and with the addition of textural designators “loamy,” “sandy,” etc., then a particular soil could be described as a loamy, typic agriaquoll. The final level—series—is the least informative as the series name departs from the logical taxonomic pattern using, simply, a name such as “Brookston,” “Westland,” “Fayette,” etc. to designate the soil. A buried soil or paleosol is indicated by the prefix paleo- to the great group designation such as a buried aquoll (a wet mollisol) termed a paleoudoll. In fluvial contexts, multiple paleosol sequences are very possible (see “Allostratigraphy” (Sect. 7.1)).

The 12 soil orders in the American soil taxonomic classification system are:

1. *Entisols*: soils without any distinctive layers or profile development.
2. *Inceptisols*: soils with poorly developed layers or weak B horizon, e.g., mineral translocation is not present or is poorly advanced.
3. *Mollisols*: soils with a dark A horizon or epipedon and that are base rich and have strong B horizons, typical of grasslands.
4. *Alfisols*: soils with a well-developed argillic or natric (high sodium (Na)) B horizons and are well watered forming under deciduous forests as a rule; E horizon is usually present.
5. *Ultisols*: soils with well-developed argillic B horizons, but low in base minerals (e.g., acid soils) typical of soils formed under native pine forests in humid areas such as the American South; E horizons can be present.
6. *Oxisols*: soils typical of the tropics with deep, highly weathered B horizons that are very reddish in appearance.
7. *Vertisols*: soils that are clay rich but have no B horizons and are characterized by an annual “shrink-swell” cycle producing large, deep cracks in their profiles.
8. *Aridisols*: “dry soils” characterized by ochric or pale profiles due to lack of organic matter; found in dry areas of the world.
9. *Spodosols*: soils with acidic B horizons rich in iron/aluminum oxides; A horizons are highly leached.

Fig. 3.2 The Munsell color system. Using this diagram, an example soil color such as “2.5YR5/4” can be understood as 2.5 yellow-red on the hue circle, 5 on the vertical scale for value, and 4 on the horizontal section for chroma



10. *Histosols*: soils characterized by high organic matter (>20 %) originating in bogs, marshes, and swamps; no B horizons.

11. *Andisols*: soils of volcanic origin with weakly developed or no real profile; dominated by silicate mineral—no clays—and with humic epipedon; previously included with inceptisols.

12. *Gelisols*: soils that have permafrost and many are cryoturbated (frost heaving, solifluction, etc.). These soils consist of minerals or organic soil materials or both. They commonly have layers of gelic materials and histic (high organic %) or ochric (pale) epipedons.

Acrisols: clay rich and is associated with humid, tropical climates (ultisols—all orders)

Alisols: poorly drained soils with a dense subsurface clay layer (vertisols)

Andosols: volcanic soils, containing glass and amorphous colloidal materials (andisols)

Anthrosols: formed or heavily modified by long-term human activity (various orders)

Arenosols: an entisol consisting of unconsolidated sand deposits (entisols)

Calcisols: a soil with a substantial secondary accumulation of lime (aridisols)

Cambisols: horizonation is weak; young soil (inceptisols)

Chernozems: black-colored soil containing a high percentage of humus (boreal mollisols)

Ferralsols: soils containing at all depths <10 % weatherable minerals (oxisols)

Fluvisols: a genetically young soil in alluvial deposits (entisols)

Gleysols: wetland soils (hydric soil) that develop a characteristic gleyic color (inceptisols)

The Food and Agriculture Organization (FAO) developed a “World Soil Classification System.”

In the revised FAO system, there are 28 “World Classes” formed by 106 “Soil Units” (FAO 1988).

USDA Soil Taxonomy equivalents in parentheses:

Greyzems: boreal or wetland soils (USDA equivalent—mollisols; gelic or aqualls)

Gypsisols: soils with substantial secondary accumulation of gypsum (aridisols)

Histosols: a soil consisting primarily of organic materials (histosols)

Kastanozems: rich in humus, formed from early maturing native grasslands (mollisols)

Leptosols: soil over hard rock or highly calcareous material; lithosols (no USDA equivalent)

Lixisols: soil developed under intensive tropical weathering (alfisols)

Luvisols: clay-rich soils in humid-subhumid forested areas (ultisols)

Nitisols: deep, red, well-drained soil >30 % clay content; blocky structure (alfisols/ultisols)

Phaeozems: dark soil; high base content, but without a calcareous soil horizon (mollisols)

Planosols: light-colored, coarse-textured, surface horizon; clay subsoil (alfisols/mollisols)

Plinthosols: iron-rich soils characterized by the presence of plinthite (oxisols)

Podzols: derive from either quartz-rich sands and sandstones (spodosols)

Podzoluvicols: A and E horizons leached of organic material and soluble minerals (spodosols)

Regosols: very weakly developed mineral soil in unconsolidated materials (entisols)

Solonchaks: pale or gray soils found in arid to subhumid, poorly drained areas (aridisols/mollisols)

Solonetz: soils with a so-called natic horizon, in the upper 100 cm of the profile (alfisols)

Vertisols: a soil in which there is a high content of expansive clay (see alisol)

3.3 The Soil Catena

The strict definition of a catena is a sequence of types of soil down a hill slope. These types reflect slope processes such as precipitation, evaporation, erosion, deposition, and parent material that are key variables that influence soil formation and stability. A catena can consist of simply the

same soil type such as an ultisol with only a variation in the horizonation of the down slope examples. At the top and upper slope, the horizons may be thicker in comparison with those at mid-slope where erosion has reduced the thickness. At the base of the slope the soil, there could have deep horizons similar to those of the top but, in contrast, could have a much different character due to more minerals moving down-slope. In many cases, the lower slope soil could be another type altogether such as an inceptisol or entisol. Slopes without forested cover will develop soil types consistent with edaphic conditions. A south-facing slope, well watered, could produce a parkland or upland prairie mollisol.

Bushnell (1943) links the concept of the catena to that of a catenary wherein the differences observed at points along a catenary such as a valley slope result from environmental forces at work along it. He stresses topography as a controlling variable. Parent material is another key factor.

Bushnell's catenas are made up of a series of types made up of profiles that are characterized as to number, thickness, arrangement, color, texture, structure, composition, etc.—all the categories discussed in the following section. In the ultisol example, Bushnell would call this a “simple catena” wherein the singular soil series are homologous in all features except for those due to variation in drainage. “Series” is used strictly in the taxonomic sense, wherein a specific soil is so designated.

3.4 The Soil Chronosequence

Unlike a soil catena, a soil chronosequence is “a sequence of soils developed on similar parent materials and relief under the influence of constant or ineffectively varying climate and biotic factors, whose differences can thus be ascribed to the lapse . . . of time” (Stevens and Walker 1970). If the ages of the soils of a chronosequence are known, then rates for soil formation as well as variation on soil-forming minerals and conditions can be deduced.

In a study of a southeastern US soil chronosequence of Paleudults, formed on five fluvial terraces of the Catawba River, NC, Layzell et al. (2012) estimated terrace ages based on elevation from 3 to 42 m above the modern river. The oldest terrace (Qt1) was estimated to be $1,470 \pm 180$ ka, while the youngest terrace Qt5 was dated to 4 ± 0.5 ka. In this study, soil morphological properties such as color hue, clay content, and iron mineralogy showed positive trends in concert with terrace ages.

Specifically, color hue increased from 10 YR on Qt5 to 2.5 YR on Qt1. Likewise, clay content increased, particularly in the Bt horizon from ~25 % on Qt5 to ~63 % on Qt1. West and Dubos (2013) relate this difference in hue to increasing clay and iron. Maximum clay content values reached an asymptote on terrace Qt2 (~610 ka). This compared well with Engel (1996) who measured ~53 % clay content in early Pleistocene soils (~770–970 ka).

Iron minerals converted over the chronosequence from amorphous hydroxy forms (goethite, hematite, ilmenite, etc.) to crystalline forms (oxides) (Layzell et al., *supra*). West and Dubos (2013) term the Blue Ridge and acidic upland soils as parasequic which recognizes soils with larger amounts of the iron oxides such as goethite, hematite, and gibbsite in the clay fraction. Dithionite-extractable pedogenic iron (crystalline forms) increased, progressively, in the chronosequence from 3.63 % on Qt5 to 6.37 % on Qt1, again, like clay content, reaching a maximum value on the Qt2 terrace. These minerals, together with the color and clay variables, point to a plateau in their rate of development peaking at ~128 ka. The authors of this particular chronosequence suggest that the effects of parent material and climate were overshadowed by changes in sedimentation and fluvial processes (*supra*). These changes represented a major shift in the landscape evolution for this region. An example of this shift in rates of soil formation is the rapid formation of clay-rich Bt horizons in as little as 4,000 years.

3.5 Describing Archaeological Sediments and Soils in Profile

Strata and Horizons: At a cleaned exposure or excavated profile, the first step in description is to determine the number and kind of strata or horizons present. If the deposit is not a soil, one still determines its lithostratigraphic nature. Each stratum or horizon, whichever the case, should be measured from a surface datum or downward and upward from the surface of a mineral horizon if present. These strata are sketched and characterized. If the stratum is a soil, then the presence of master soil horizons should be noted. Arabic numerals, in the master horizon designation, indicate certain key characteristics such as “O2,” an O horizon with accumulated organic materials which in the past (and in certain countries today) were indicated by lowercase letters such as “Oa.” Lowercase letters are still used today in the description of soil profiles such as the important designation for archaeological geologists—the lowercase “b” which indicates a buried soil or paleosol such as “Bb.” The accumulation of translocated clays is commonly denoted as a “Bt” horizon. A more complete listing of these designators is shown in the following table. Master horizon categories and subordinate distinctions are made depending upon the detail desired at the field site (Table 3.1).

Lithological discontinuities or contacts are indicated by Roman numerals such as a change within an A horizon from a loessic sediment to a quartzitic sand matrix which would be designated as “IA” and “IIA.” In the case of buried soils, the second or lower soil sequence is noted as follows: “A’2, B’2.”

Color: This parameter is important to be observed and recorded as systematically as possible. The method most used today is the Munsell Soil Color Chart. The color chart is a collection of color chips organized in notebook form. The color chips are arranged according to hue, value, and chroma. Hue is the principal spectral color. The pages of the color chart take their names from this attribute such as “2.5YR,” indicating

Table 3.1 Designations of master soil horizons and subordinate symbols for soils (Adapted from Olson 1981)

| Master horizons | | Subordinate symbols | |
|-----------------|---|---------------------|-------------------------|
| 01 | Organic undecomposed horizon | b | Buried horizon |
| 02 | Organic decomposed horizon | ca | Calcium in horizon |
| A1 | Organic accumulation in mineral soil horizon | cs | Gypsum in horizon |
| A2 | Leached, eluviated horizon | cn | Concretions in horizon |
| A3 | Transition to B horizon | f | Frozen horizon |
| AB | Transition to B horizon; like A in upper part | g | Gleyed horizon |
| A and B | A2 w/ less than 50 % occupied w/ spots of B | h | Humus in horizon |
| AC | Transition horizon; not dominated by A or C | ir | Iron-rich horizon |
| B and A | B w/ less than 50 % occupied w/ spots of A2 | m | Cemented horizon |
| B | B horizon w/ accumulation of clays, iron, cations | p | Plowed horizon |
| | Humus; residual concentration of clays; coatings (cutans) | sa | Salt-rich horizon |
| | Or alterations in original material forming clay and structure | si | Silica-cemented horizon |
| B1 | Transition horizon more like B than A | t | Clay-rich horizon (Bt) |
| B2 | Maximum expression of B horizon (clay rich) | x | Fragipan horizon |
| B3 | Transitional horizon to C or R | | |
| II, III, IV | Lithological discontinuities | | |
| C | Altered parent material from which A and B horizons are presumed to have formed | | |
| A'2, B'2 | Second soil sequence in bisequel soil | | |
| R | Consolidated or competent bedrock | | |

a variation from gray to black, pale red to very dusky red, reddish brown to dark reddish brown, and light red to dark red. “5YR” differs in hue from *white* to black, *pinkish* white to dark reddish brown, and reddish *yellow* to *yellowish red*. There are ten hues in the Munsell system—the two already mentioned along with 5R, 7.5R, 10Y, 7.5YR, 10YR, 2.5Y, 5Y, and gley. On each page, the color chips are arranged biaxially according to value (vertical axis) and chroma (horizontal axis). Value refers to the relative lightness (darkness) of the color, while chroma designates the relative purity of the color (red, red-orange; yellow-red, etc.) and its spectral strength increasing in numerical value with decreasing grayness. Figure 3.2 illustrates the relationships among the three variables of Munsell color. An example of a Munsell color descriptor for a sediment or soil could be “5YR2/1.” The descriptor reads: a hue of 5YR, a value of 2 and a chroma of 1. This color is black. However, a one-unit shift in the chroma to 5YR2/2 makes this color dark reddish brown.

Recording colors using the Munsell system allows for a relative standardization of the reporting of soil/sediment color but it is not an infallible tool. Too often the beginning student is not instructed properly in the use of the color chart and what the three parameters signify. Light conditions at the time of the measurement can vary significantly in the field. Measurements made in the shadows of an excavation trench will differ from those made just outside of the trench. Direct sunlight is generally avoided and many use indirect or reflected light. Colors read in the morning and evening, aside from being qualitatively darker, will tend to appear more red, e.g., 10YR is less red than 2.5 YR. Moist and dry readings are taken of the sample. The simplest procedure is to take a small sample of the material on the end of a trowel and hold it behind the appropriate page of the color chart notebook. Color matches are seldom exact and the reader must make the best judgment possible perhaps indicating the quality (poor to good) of the color match. A few archaeologists still eschew the use

of the Munsell chart, preferring to simply designate the color as “brownish red,” “light tan,” etc. While his/her system may be readily intelligible to them individually, it lacks that quality for others. While two workers may disagree on whether a horizon is 10YR8/3 or 10YR7/4, the Munsell color designation is still “very pale brown” which in another more unstandardized description could be “tan,” “light brown,” or even “buff colored”! Figure 3.2 illustrates the three components of a Munsell color designation.

Recently, Ferguson (2014) has examined the use of the Munsell color chart in archaeology. He notes that archaeologists have limited their color descriptions to those of the Munsell Soil Color Chart. While giving a fuller discussion of the variety of Munsell color charts—Plant Tissue, Bead Color, and Rock Color charts—he concluded that, given the familiarity and length of use of color names in the Soil Color Chart, it would be counterproductive to replace the system (*supra*). The point of Ferguson’s review is not to question a relatively standardized use of colors and color names in the description of archaeological materials, but rather to suggest a broader “palette” of recognized colors and color names for use in archaeology. His point is well taken as the Soil Color Chart is basically applicable to just that—soil. Not all archaeological materials—lithic, ceramic, or organic—fall comfortably within the range of soil colors. In fact, only recently have the “tropical soil colors” pages been added to the Soil Color Chart as an extra cost option—now downloadable—mainly for archaeologists since oxisols do not exist in continental North America nor Europe. In Asia, the tropics, South America, and portions of Africa, yes—but for descriptive purposes of earthenwares, in the Americas, these two pages expand the color palette as Ferguson has discussed. Those archaeologists who prefer not to use the Munsell Soil Color Chart for descriptive purposes might prefer the use of a broader color name system as seen in the other Munsell charts as well as other color naming systems such as the Inter-Society Color Council on Soil Color—National Bureau of Standards (ISCC-NBS) system which provides a full range of Munsell

names, showing values and chromas for each color name (Kelly and Judd 1976).

Texture: This parameter, also known as granulometry, along with color, is the most salient of a sediment or soil. Texture is size and proportion of the particles that make up a deposit. The four basic categories of size are gravel, sand, silt, and clay. In the United States, these size categories are divided as follows: <0.002 mm, clay; 0.002–0.05 mm, silt; 0.05–2 mm, sand; and >2.0 mm, gravel. The International Society of Soil Science scheme differs in the size range for silts and sands: 0.002–0.02 mm, silt, and 0.02–2.0 mm, sand (cf. Chap. 5). Likewise, other countries vary somewhat in their size categories so it is important to note which size classification scheme is reported (Fig. 3.1). Another size scale still in use in the United States is the *phi* scale (Φ). This classification scheme ranges from -8Φ (gravel) to $+8 \Phi$ (clay). Texture or particle size analysis is done with sieves to mechanically separate the gravel and sand grains into finer and finer divisions. Silt and clay sizes and amounts are determined by their settling rates in water.

A sandy soil consists of at least 70 % sand and 15 % or less clay. A silty soil contains at least 80 % silt and 12 % or less clay. Clay soils must contain 35 % or more clay. In the field, a rough approximation is done by “feel” or examining the texture by manipulating a sample of the material between the fingers—sands are gritty to the touch, silts are less so, and clays display a characteristic plasticity and stickiness when wet. This latter parameter is known as *consistence* and is used to describe soils (see below). Visually, sand particles are readily apparent to the eye. These are described in terms of “rounding” and “sorting” relative to grain assemblages (Fig. 3.3).

Silt, in its finer particles, and clay cannot be seen without an electron microscope.

Texture or particle size is typically represented, graphically, in ternary diagrams wherein the apices are 100 % sand-clay-silt (Fig. 3.4).

Structure: Aggregates or *peds* of soil, separated by planes of weakness, have four principal types: (1) spheroidal, (2) platelike or platy, (3) prismatic,

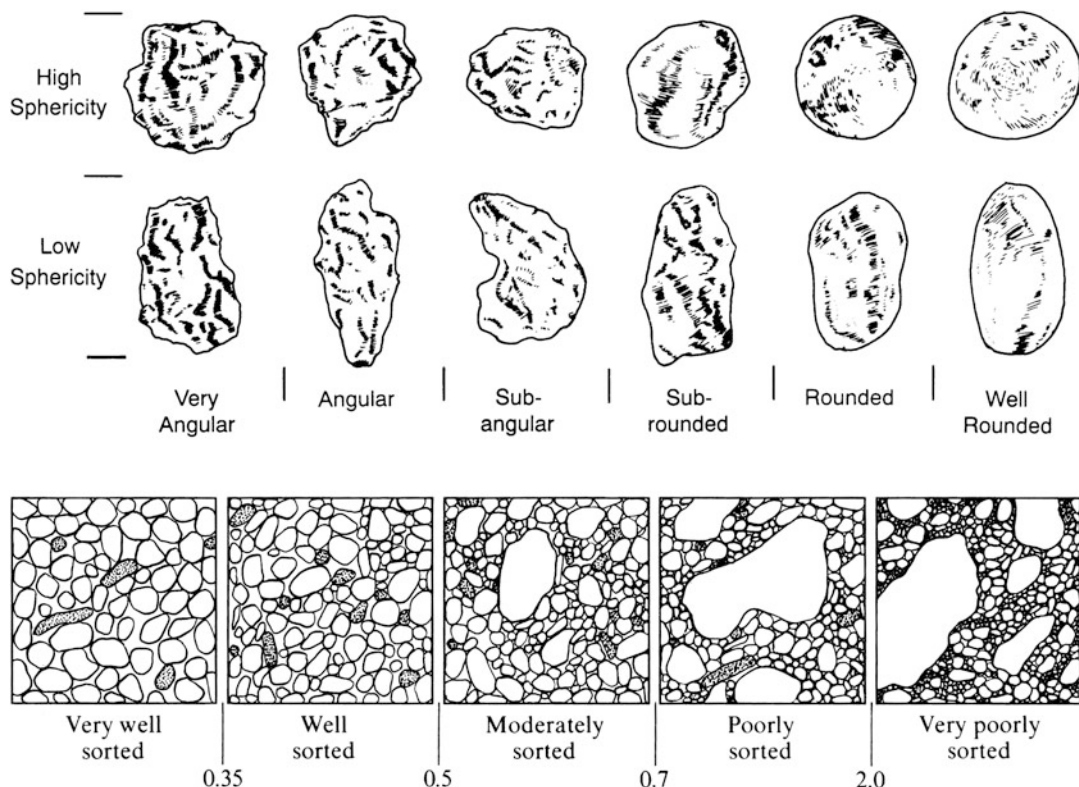


Fig. 3.3 Above, sand grains, roundness, and sphericity (Modified from Powers 1953), below, sorting of sand grains (Modified from Compton 1962, *Manual of Field Geology*)

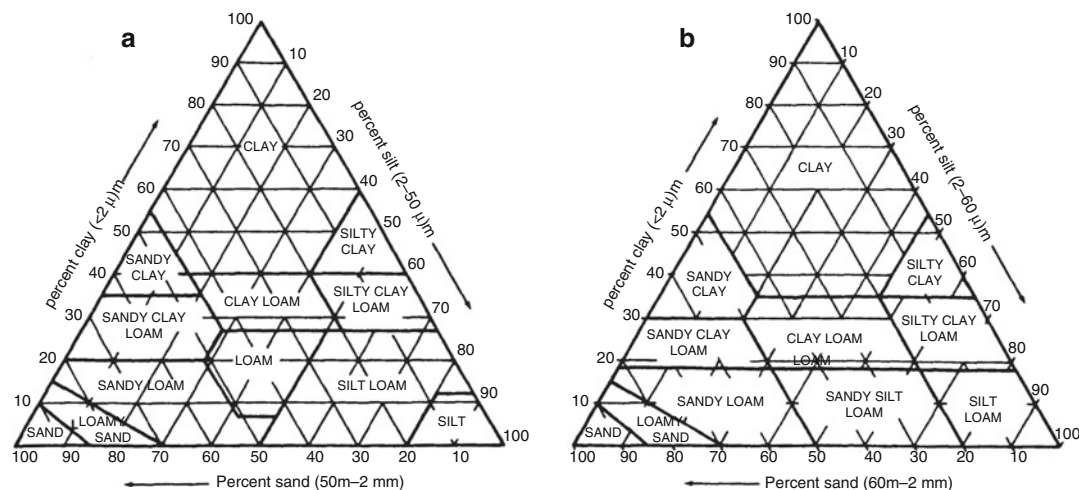


Fig. 3.4 Example ternary diagram plots for, *left*, the United States and, *right*, Great Britain and Wales

and (4) blocky. Categories 1 and 2 most often occur in A horizons, while prismatic and blocky pedes are generally found in B horizons. A key

aspect of pedes is their size. Like texture, there is a relative scale for the size of pedes in a horizon from very fine (<1 mm) to very coarse (>10 mm)

with spheroidal and platy structures. The class of spheroidal structures is subdivided into granular and crumb. Most sediment grains are not perfectly round so they will most likely fall into one or the other of the two subclasses. Blocky structures vary in size from very fine (<5 mm) to coarse (20–50 mm). Prismatic structures vary from <10 mm to 50–100 mm. As a rule, the age of the soil influences the development of structure with older soils having more well-developed or *strong* peds, and, conversely, young soils have *weak* peds.

Consistence: This property of soils is measured under three conditions—dry, moist, and wet. It describes a soil's resistance to mechanical stresses and manipulation. Most dry soils have little coherence and readily fall apart. Those that have not have been cemented by carbonates, iron/aluminum oxides, and silica minerals other than the clays. Plinthite is an example of the cementation of sediments by iron that was translocated by groundwater. Calcium carbonates and gypsum ($\text{CaSO}_4 \cdot 2\text{H}_2\text{O}$) produce cemented petrocalcic and petrogypsic horizons and are so-named in the master horizon nomenclature. This type of cementation is seen in aridisols. Generally, soil, when moist, has a coherence that varies from loose to extremely firm. Wet soil has a consistence that varies from nonsticky to very plastic as one would expect that the more plastic the material, the higher the clay content.

pH or Reactibility: Chemical solutions can provide indications of the acidity or alkalinity of a sediment or soil. Differential weathering of minerals translocates cations such as Ca^{2+} , Mg^{2+} , K^+ , H^+ , Na^+ , NH_4^+ , and Al^{3+} , creating a great variety in the geochemistry of sediments and soils. The most common chemical parameter tested for in soils is the presence of the hydrogen ion commonly expressed as pH. The acidic ($\text{pH} < 7$) or basic ($\text{pH} > 7$) character of a sediment or soil typically depends on the concentration of hydrogen (H^+) and aluminum (Al^{3+}) ions present. The exchange of cations and the relative amount of base formation is dependent on pH. In low pH (acidic) situations, cation exchange is reduced. Base-forming cations

dominate in alkaline sediments and soils. These chemical species replace the aluminum and hydrogen ions available for reactions. The chemical nature of a sediment or soil has a direct bearing on the diagenetic effects on archaeological materials such as bone, wood, or other organic artifacts. For instance, bone preservation is significantly reduced in acidic soils. Precipitation, the ultimate source of water—hence hydrogen and hydroxyl (OH^-) ions—in sediments and soils, varies and mediates their acidity. Where soil moisture is low, then one should expect a low acidity as well. Ultisols, for example, formed in semitropical and temperate regions should be and indeed are acidic in nature.

Stoniness: This category was developed by British workers. The principal parameters looked for are quantity or abundance, lithology, size, and shape. A common way of reporting stoniness is as percentage of volume. This, in itself, is somewhat misleading as most determinations of percentage are done from a profile rather than a true volume. If one extracted a volume of soil or sediment, it is easy to see that the size of the lithic materials has a significant influence on the measurement which is to say that larger stones will require larger volumes. A straightforward scale for a vertical section's percentage of rocks is slight stony (<7 %), stony (7–30 %), and very stony (>30 %) (Hodgson 1978). Again, large areas of a soil profile should be used to make this determination.

As pointed out in Chap. 1, Darwin was the first to remark on what we call bioturbation and its importance to the formation of the upper soil. If not offset by what is termed “floralturbation” (Leigh 2001; Thoms 1995), e.g., root growth, tree throws, animal burrows, and “stump burns” (the latter in forest fires), soil biota will bring fine-grained sediments to the surface. This loosening of sediments, gravity and the infiltration of water to allow larger clasts – stones/cobbles – as well as artifacts – to settle downward in the upper soil just as Darwin observed (1896). “Stone lines” form at the base of this upper biomantle (Johnson 1990).

In the Ozark Mountains of Missouri, USA, Henry R. Schoolcraft remarked in 1818 on the

general stoniness of the landscape. Schroeder (1967) describes three types of stoniness in the eastern Ozark Mountains: (1) stone-free; (2) moderately stony, and (3) extremely stony. The last category describes a soil mass and surface composed of 50–90 % rock fragments, mostly cherts, that can reach a thickness of 7–15 m (*supra*).

Organic Matter: For the soil scientist, this component defines the soil from simple sediment. In the description of master soil horizons, it is the key parameter in determining the O horizon. It is a somewhat transitory element of soils in that its residence time rarely exceeds a few hundred years unless it is depositional (anaerobic) environments that preserve it— inundated deposits such as wetlands and submarine landforms. In these environments, microbial and biochemical activity is suppressed or absent. Organic matter has a great deal to do with soil moisture. Dark, organic soils tend to indicate greater water retention, whereas soils with lesser amounts of organic matter allow water penetration to deeper depths. The amount of organic matter in soils is relatively low, being on the order of 6 % or less in topsoils and even less in the subsoil (Brady 1990). Organic matter is a rich source of ions from the breakdown of plant and animal matter into organic complexes.

Outside of the field setting, organic matter is categorized as *humus*—raw, mild, intimate, or mechanically incorporated varieties (Clarke and Beckett 1971). In the Soil Taxonomy, soils containing appreciable quantities of organic matter are described as slightly humose, humose, very humose, and organic soil (*supra*, 46). It is difficult to assess these categories in the soil horizon. To the touch, organic matter can make a soil feel like silt, but the texture is different—a silt smears evenly, while an organic soil sample will fragment or fray.

Histosols are soils rich in organic matter (>20 %). Peats, by definition, are histosols but are more closely classified by British workers into three classes—pseudo-fibrous, fibrous, and amorphous (*supra*, 72–73). Organic matter that is incorporated into the soil mass is termed *intimate* humus and can be dispersed throughout the A and B horizons, giving these a darker—brown

to black—color such as the typical mollisol. Organic horizons can be evidence of anthropic deposition of organic debris in cultural middens.

Mode: More usually used to describe the nature or distribution of minerals in a rock, it is less commonly used in describing sediments and soils. In the context of paleosols, the preservation of *primary* minerals is directly linked to time and diagenesis. When we refer to “mature” beach sands, we infer that only the most resistant minerals, e.g., quartz, have survived to make up the textural/mineralogic assemblage. The common silicate minerals ranging from quartz, through the feldspars, to olivine respond very differently to weathering with the latter species the first to disappear, while zircon, structurally similar to olivine, persists longer in the soil (Ritter et al. 1995). By and large, the heavy minerals can be used to gauge the exposure of the paleosol to normal meteoritic waters, percolating fluids such as soil acids. Certainly their presence or absence is a barometer of the “history” of that paleosol; therefore, their *mode* should be noted just as we measure the nature of the secondary minerals—clays, hydrous oxides—gibbsite, hematite, goethite, etc.

Boundaries: Transitions between strata and horizons are characterized as to their distinctness. In describing a soil, its mineralogy, texture, color, and chemistry all contribute to the determination of horizons. In archaeological settings, these attributes, plus those of cultural origin—anthropogenic—help in the delineation of stratigraphic differences. Where archaeological deposits occur as buried paleosols, one must be aware of the likelihood of overprinting by subsequent soil-forming processes. Likewise many of the changes observed in archaeological sediments may not be stratigraphic in nature. This is to say that not every *solum* in a site profile is necessarily important to its stratigraphic description. Archaeologically interesting levels, of like chronostratigraphy, may vary significantly in textural color and chemical characteristics. In general, stratigraphic differences are denoted by contacts, which in turn are most usually determined by changes in color and texture, together with inclusions—anthropogenic or otherwise.

Fig. 3.5 Bounding in a spodosol. The A horizon is bounded as “clear to abrupt”; that between the “A” and “E” is “gradual to diffuse” (Photograph by the author)



Micromorphological features such as lamellae may indicate archaeologically interesting stratigraphic relationships, and then they may not (Anderson and Schulderein 1985).

Using strictly pedostratigraphic terminology, the vertical boundaries between horizons are described as either:

- (a) Abrupt: if less than 3 cm wide
- (b) Clear: if 3–5 cm wide
- (c) Gradual: if 5–10 cm wide
- (d) Diffuse: if more than 10 cm wide

The example in Fig. 3.5 shows a spodosol with *clear* bounding between horizons.

These contacts are generally defined on the basis of lithostratigraphy where breaks in the color and textural quality of the sediments are obvious (Fig. 3.5). In geological sections, one is always cognizant of temporal gaps in a depositional sequence which are designated as conformities or unconformities. These are the boundaries between adjacent strata. Figure 3.6 illustrates pedogenic contact terminology described below. Conformities, in a geological sense, have little temporal breaks in the depositional record, whereas unconformities represent temporal hiatuses where deposition has halted and even been eroded (disconformities). Conformable contacts can be described by all of the



Fig. 3.6 Disconformable (allo)contact between the Central Builders member of the Wyoming Formation and the coarse gravel in the cutbank of Cayuta Creek in Sayre, Pennsylvania, at river km 452 (Thieme 2003)

terms listed above. Unconformities are more likely to be described as abrupt due to significant changes in the subsequent sediments. In the horizontal dimension, lateral variation in strata is described somewhat differently than in the case of their vertical relationships. These are:

1. Abrupt: the boundary between adjacent units is distinct.
2. Pinch-out: one unit thins progressively to extinction; not uncommon in archaeological deposits.
3. Interfingered: the adjacent units split into smaller divisions that interdigitate with each other.
4. Gradual: adjacent units blend into one another without abrupt lithological changes

Haplodization: In contrast to sharp or clear boundaries between the stratigraphic components of a solum, haploidization describes what some term as “regressive pedogenesis” (Johnson and Watson-Stegner 1990). The E, and sometimes upper B soil horizons, can be substantially disrupted. Some geoarchaeologists (Thoms 1995, 2007; Leigh 2001) have commented on soil haploidization as it impinges on cultural/

archaeological stratigraphy. Much of this is attributed to floral bioturbation, but this may be overstating its influence on site stratigraphy. These effects are not generally so extensive as to obliterate the archaeological stratigraphy. While Thoms and Leigh (*supra*) have studied haploidization in sandy soils, their arguments could be extended to upland ultisols where forests can produce haploidization. A common soil category in the Appalachians is the “typic hapluadult” or clay-rich, haploidized ultisol.

Goldberg (1995), following Stein, reduces the checklist for soils to the following:

1. Color (moist and dry) using the Munsell color notation
2. Lithological composition (e.g., detrital vs. chemical)
3. Geological vs. anthropogenic components
4. Texture (e.g., gravel, sand, etc.) and the morphology of the particles
5. Internal organization, such as bedding
6. Consistence (e.g., loose, riable, firm, hard)
7. Voids and porosity (types and amounts)
8. Boundaries between units (e.g., abrupt, gradual, etc.)

3.6 The Geological Stratigraphic Section

The mapping of geological sections and structures has been a traditional capstone technique taught to almost all earth science students. By understanding the horizontal and vertical relationships of geological strata across space, the extent and nature of depositional and erosional sequences are realized. The principal differences in geological and geomorphological mapping are the scale and the nature of what is being mapped. Scale is one thing while landscape and lithology are quite another. Both use the same basic protocols on different scales of lithostratigraphy. Both scales have relevance for archaeological inquiry. For instance, the location of resources such as toolstone or metal ores will generally signal the likelihood of nearby habitation and/or extraction sites. Conversely the presence of these materials in the archaeological context requires the identification of the source location. Either way the mapping of the geology of an area is required.

3.7 Nomenclature

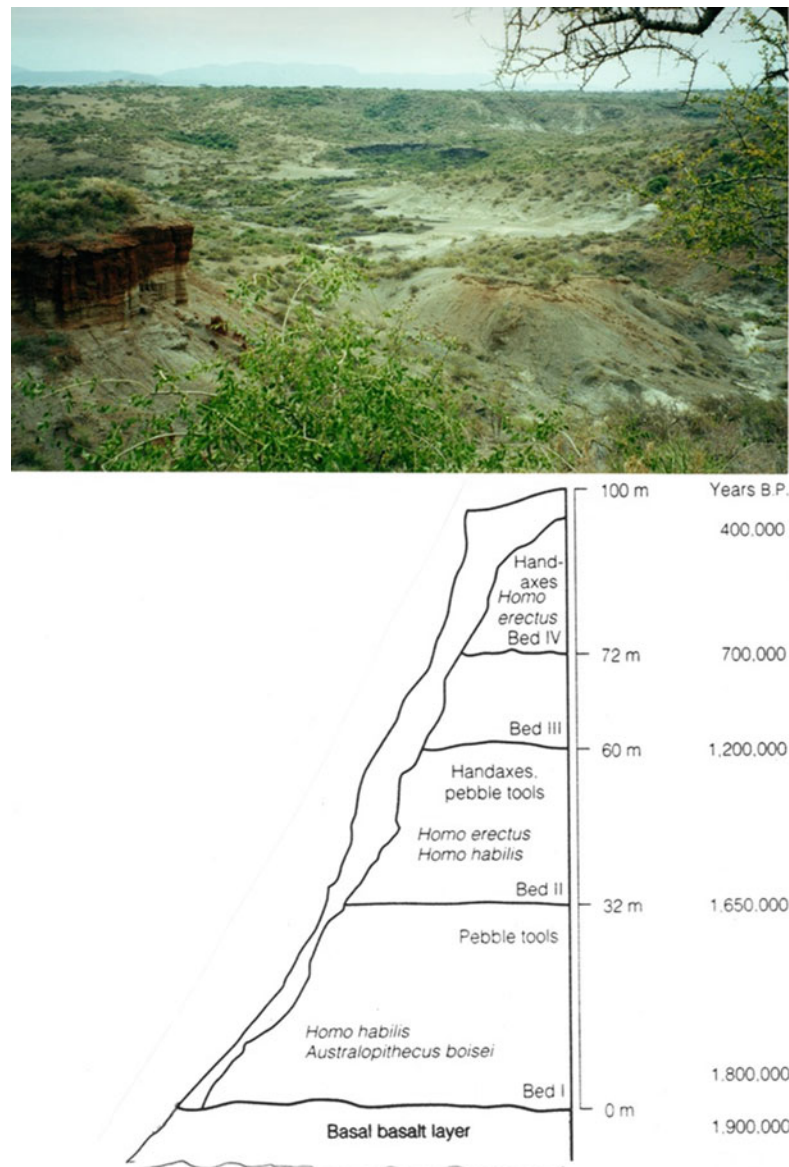
Formations make up geological sections that in turn are composed of rock *strata* or *beds* organized into *members* which, unless they are of igneous origin such as basalt or granite, were laid down according to the principle of original horizontality which presumes a depositional history of a uniform lenticular nature. Intrusive features—dikes, sills, etc.—are the result of volcanic processes which, in turn, are the result of the tectonic activity due to the restless nature of the continental plates. *Structural* features within sections such as faults, syn-and-anti-clines, folds, and the like are indicative of Earth seismicity as well. *Stratigraphic* relationships such as conformity and the lack thereof express the broad patterns of the rocks in the Earth's crust. A geologist reads the geological section as a series of pages of the Earth's history with all the twists and turns of that record imprinted therein.

For the early part of humanity's own story, the rock record was the only reliable means of assessing that antiquity with any assuredness. Following the protocols of stratigraphy, early antiquarians and later archaeologists were able to deduce precedence, succession, and simultaneity of fossils and ancient tools found within the *members* of a formation. Necessarily, the primary relation was that simply the oldest strata were at the bottom of the section—Smith's principle in its most simplistic expression of the *Law of Superposition*. As mentioned previously, Sir John Evans and Joseph Prestwich's visit to Boucher de Perthes' excavations in the Somme River terraces provided the geological framework for assigning the true antiquity to the latter's claims for the relationships between ancient fauna and tools within the gravels.

The relative age of a lithostratigraphic formation's bed or member (a bed being a sub-unit of a member) can be determined by superposition and the *Principle of Inclusions* which holds that inclusions or fragments in a rock unit are older than the surrounding unit itself. For instance, in the case of lava or tephra deposits, those inclusions, geological or cultural, are, by definition, older than the volcanic matrix. In the case of volcanic flows or ash falls, such as those of Pompeii and Ceren, cultural debris was entrained or enclosed in the deposits and provides what are termed a *terminus post quem*—that is, the deposit cannot be older than the inclusions. Before the advent of chronometric dating techniques, archaeology relied on this principle of stratigraphy without specifically stating it. In East Africa, the finds of early hominids have come from sedimentary sequences of ancient lakebeds such as Olduvai Gorge (Fig. 3.7).

Hans Reck, a member of the Geological Survey of German East Africa, and later Richard L. Hay (1976) untangled these sequences for the Leakeys—Mary and Louis—enabling the latter to more confidently assign the Pleistocene ages to finds such as *Zinjanthropus* (now classified as *Australopithecus*) and *Homo habilis* (Fagan 1994). The Olduvai sequence is a model of the use of stratigraphic principles with the

Fig. 3.7 Olduvai Gorge, Tanzania. *Upper*, the red sandstone of Bed III is clearly visible as well as the top of Bed II, lower, stratigraphy of Olduvai (Photograph courtesy of Dr. Sandra Whitney)



straightforward terminology of Bed I, Bed II, Bed III, and Bed IV.

A Bed V, relatively thin and recent, was identified at the top of the Olduvai section being what is called the *end member* as well. Reck distinguished these beds within the Olduvai section based upon their color, sedimentological texture, and *biostratigraphy*. The latter procedure relies on the identification of fossil

forms—macro and micro—to help assign a *chronostratigraphic* sequence to a section.

Lithostratigraphic units are defined by physical attributes of rocks where similarity in lithology implies a geographic, and genetic, association in the units. A lithostratigraphic correlation does not necessarily imply a temporal equivalence. At Olduvai, biozones based on fossil genera can provide a rough temporal control.

“Roug,” in a temporal sense, implies that the presence of a particular fossil type (*index fossil*) only indicates the time range of a plant or animal species—fine for geology but not very useful for archaeology. At Olduvai biostratigraphic correlation was useful because of the millions of years that the strata represented.

At Olduvai Beds I and II represent the most ancient lithified remains of sand and clay-rich lacustrine environments of a late Pliocene/early Pleistocene. Bed III represented a dramatic change in color compared to the lower two beds. It is strikingly red in color and contrasts sharply with its whiter stratigraphic neighbors. The next upper member was named Bed IV. Reck recognized the sedimentary nature of the rocks but noted the record of volcanism as well as indicated by the tuff deposits. The Rift Valley, an active seismic zone of extension where the African and Eurasian continental plates are pulling apart, has had volcanic activity throughout prehistory. The volcanic deposits provide lithological and geochemical signatures of individual eruptive events identified today through *tephrochronology*. The volcanic rocks also allow techniques such as radiogenic argon to be used to directly date them. Olduvai Gorge’s geological sequence was delineated by Reck and then confirmed by the early use of the then new potassium-argon direct dating technique. Bed I, containing both *Australthropines* and *habilines*, was found to date to 1.95 million years (Fagan, *supra*). Reck’s and Daly’s geological mapping of Olduvai demonstrated the utility of stratigraphy for elucidating the *provenance* or context of important archaeological facies.

Archaeostratigraphy, as we have seen in the section on caves, describes the sequence of the materials of antecedent or subsequent cultural deposits found in an archaeological site. This is illustrated in Paleolithic site deposits. In recent years, the interstratification of “archaeo-facies” in Paleolithic sites has led to animated discussions about their exact nature and their interpretation. An excellent example is that of Middle Paleolithic Mousterian technofacies—Quina, Denticulate, Mousterian of Acheulian Tradition (MAT), etc.

3.7.1 Allostratigraphy

Goldberg’s eighth category, boundaries between (soil) units, has taken on increased importance in mapping paleosols. Soils are soft. Typically, they are eroded prior to the deposition of younger units producing unconformities. Allostratigraphy uses unconformities in the form of soil, soils, and geomorphic surfaces to define allounits which define discrete depositional (and erosion) episodes (Morrison and Davis 1984; Morrison 1991). Alloformations are defined as “mappable stratiform bodies of sedimentary rock defined on the basis of bounding discontinuities.” This definition follows Article 58 of the Stratigraphic Code of the North American Commission on Stratigraphic Nomenclature (1983). In short an allosurface is a period of relatively stable environment where sediment deposition/soil formation occurs. Subsequent burial of that surface indicates a possible shift away from environmental and/or climatological stability. An allosequence presumes a polycyclic series of allounits in section. Allosequences can be found in almost any landform but they are most commonly found in lacustrine and alluvial landforms (Negrini 2002; Lichtenstein 2003). During periods of stream down-cutting or lower lake levels, soils can form and mature on former levees and terraces. With the return of fluvial or lacustrine sediment deposition, these surfaces and their soils can become paleosols.

3.7.1.1 Example: The Allostratigraphy of the Wyoming Branch of the Susquehanna River, Pennsylvania, USA

A recent study of ten large river basins located in the Appalachian Piedmont of the southeastern United States has quantified background erosion rates (8 m/m.y.), using Be10 dating of basin sediments (Reusser et al. 2015). Additionally that study examined the transport of eroded sediments by these rivers and found that only 6 % of the eroded sediments were transported. The non-transported sediments remain stored at the base of hillslopes and in valley bottoms

(supra). This includes the significant amount of sediments eroded after historic land and forest clearances began in the Colonial Period including, perhaps, an earlier increase due to late prehistoric maize agriculture. In the following two examples, we shall examine how geoarchaeology provides data to examine stratigraphy as well as landform history. The first example is from Pennsylvania, USA, and the second from the Piedmont of North Georgia.

The alluvial deposits of the North Branch of the Susquehanna River represent an archive of environmental change as well as a repository of artifacts and cultural features made by prehistoric people (Thieme and Schuldenrein 1998; Thieme 2006). While many local factors affected how frequently the river flooded and when it stored sediment within the valley, stratified archaeological sites exhibit remarkably consistent discontinuities that bound discrete packages seen in both culturally sterile alluvium and archaeological site profiles. These include some Paleoindian as well as Early Archaic sites (Thieme, supra).

Thieme (2003) proposed an allostratigraphic unit, the Wyoming Valley formation, for the alluvial deposits which underlie the first terrace in the North Branch of the Susquehanna River Valley (Fig. 3.6). He correlated this formation throughout the valley from Binghamton, New York, downstream to Harrisburg, Pennsylvania. The lower bounding surface is a contact with outwash or ice-contact stratified drift at the base of the alluvial terrace. Four members are distinguished within the Wyoming Valley formation on the basis of buried soils which formed on former terrace surfaces. The members were traced through 23 stratigraphic sections in the 250 km study area on the basis of field observations, thin-section photomicrographs, and laboratory analyses of grain size, soil chemistry, clay mineralogy, and magnetic susceptibility. A total of 139 radiocarbon dates constrained the age of bounding surfaces within an allostratigraphic framework.

In Fig. 3.6, two sediment (storage) units are exposed, one a member of the Wyoming Formation (Central Builders) and the other the late

Pleistocene outwash gravels. While a few hundred kilometers north of those rivers in the Piedmont study, the Susquehanna is a major Appalachian draining river, matching or exceeding the scale of the Savannah River. It intersects the more narrow northward extent of the Piedmont in Pennsylvania on its way to the Chesapeake Bay. Unlike the more southerly Savannah, the Susquehanna drained the Laurentide Ice Front.

Thieme (2003) describes an Early Archaic component archaeological site on the Central Builders member in the upper 20 cm of a buried soil (3AB horizon) with a hearth containing wood charcoal dated to $9165 +210/-205$ BP (A-10053), which calibrates to 11,070–9,699 BP at two sigma. We must not expect this date to be that of the unit itself; while the contact represents a chronological discontinuity, the gap between the outwash gravel and the Central Builders' finer-grained sediments is not well constrained. It is reasonable to assume the deposition of the finer-grained materials began in the early Holocene, sometime before the establishment of the archaeological occupation. What the Central Builders unit does provide is clear corroboration for Reusser et al. (supra) with regard to the long-term storage of eroded materials. These materials have been stable surface for the millennia needed for soils to form.

3.7.2 Sequence Stratigraphy

In modern geology, the nomenclature of stratigraphy has seen a new terminology introduced under the rubric of “sequence” stratigraphy to describe basin edge sea-level rise and fall. Here the term formation is replaced by a new term that of *sequence*. Sequence stratigraphy recognizes that sedimentary rock units, adjacent to basins, have generally resulted from sea-level change in transgression or regression. In the former, the shoreline moves landward, and in the latter, it moves seaward. A vertical representation of these processes shows different facies superposed according to the particular depositional environment. For example, a transgression

of nearshore sands (sandstones) underlies mid-shelf facies (shales) which are, in turn, overly deep sea muds (limestones) in the section. The sequence of transgression, highstand, regression, and lowstand strata, as typically seen in seismic sections, is designated as *tracts*.

A system tract is made up of *parasequences*, which, in turn, are made up of sets of facies like those just described (Reading and Levell 1996). Erosional surfaces separate parasequences. A regression or abrupt basinward shift in sedimentary facies exposes a depositional sequence to subaerial weathering and creates what traditional stratigraphic nomenclature would term an unconformity. In a sequence-stratigraphic description of a depositional system, the “formations” are replaced by “sequences” with gaps or unconformities interpreted as flooding (ravinement) intervals of a significant temporal duration.

As we have discussed in the context of the coastal landforms and prehistoric Doggerland, sea level has played a significant role in the archaeology of the Pleistocene, alternately exposing or flooding vast areas of continental margins. Worldwide or eustatic sea-level change, in the Pleistocene, has been driven by multiple periods where large volumes of the oceans have been sequestered or released during glacials, interglacials, and more transient Heinrich and Dansgaard-Oeschger (D-O) events (Bond

et al. 1999). These dramatic shifts in sea level, during regressions, opened corridors and “land bridges” between continents such as Asia and North America, the Bering Strait land bridge, and between Europe and the British Isles, Doggerland (Fig. 2.6); http://instaar.colorado.edu/QGISL/bering_land_bridge/). Both humans and other biota used these connections for colonization purposes. In the lithostratigraphy of coastal areas, we see this recorded in the sedimentary sequences for those periods.

Lericolais et al. (2003); Törnquist et al. (2003) use sequence stratigraphy to elucidate the late Pleistocene sedimentary record for the Channel River and the Rhine-Meuse delta (the Netherlands).

By subdividing the sedimentary deposits into unconformity bounded sequences, the timing of sea levels in the late Pleistocene can be examined. Lericolais (*supra*) identify a lowstand history for the Channel River at MIS stages 22, 16, 6, and 2 (LGM). Törnquist (*supra*) date the formation of the last sequence boundary using five, over 35 m in length, sediment cores, of the Rhine-Meuse delta, to shortly after 80 ka or roughly MIS 5a or a falling stage of sea level, thereafter (MIS 5/4) with subaerial erosion and sediment bypass. The subsequent lowstand for MIS 4 was either not evident in their sediment data or was not as pronounced as that of the MIS 5/4 interval.

4.1 Sampling Sediments and Soils: Monoliths to Sediment Grabs

Undisturbed Versus Disturbed Sampling—Profile Samples, Soil Monoliths, and Solid Cores: Undisturbed sampling of an archaeological sediment can be as straightforward as the description of an exposed profile in the field. It can also mean the recovery of a representative fraction of those sediments for studies to be performed in a laboratory rather than in a field setting. Disturbed samples are those taken from individual horizons or strata in which structure and morphology information is sacrificed. The sense of the term “sample” used in this discussion is not one commonly associated with statistical evaluations but simply the acquisition of a portion of the sediment or soil for analytical purposes. Sampling (statistical) procedures can, in many cases, be used to assure the representativeness of the field or laboratory fraction of the sediment or soil being examined. This issue will be addressed in the following section. In this section, we shall examine a variety of techniques commonly used to acquire data on archaeologically interesting sediments.

Profile Exposures—The simplest method of examining a profile or section is to find an outcrop or exposure. Failing this most researchers create their own by excavating one. This can be done by either hand or mechanical methods. Traditionally shallow profile exposures are dug by

hand, but in deeper sites, mechanical excavation is required. At the profile face, one can assess many of the primary parameters used in a description of a sediment or soil—color, textural changes, contacts, etc. The principal drawback in simple hand excavation is one of time. A longitudinal study of an excavation profile such as at an ongoing, relatively long-term archaeological excavation is the most appropriate way to gain an adequate field description of that profile. Such is the case in many more famous studies such as cave sites such as Abri Pataud (Farrand 1975; Stein and Farrand 1998), Combe Grenal (Bordes 1972), Tabun (Jelinek et al. 1973), and Rogers Shelter (Wood and Wood and McMillan 1975) to name but some more well-known examples.

Mechanical excavation or exposure of a soil/sediment profile is the most commonly used method in geomorphology today. The most common mechanical means is the “backhoe”—a tractor or tracked hoe-type excavator capable of digging to depths of 7 m with lengthy trench exposures. If one is interested in investigating fluvial valley, this type of excavator can expose entire terrace and flood plain systems within it. Unlike discontinuous sampling, as typical of coring studies, the continuous exposure, by use of the mechanical hoe, provides a more synthetic view of the depositional stratigraphy—in both vertical and horizontal dimensions.

Long-term studies of sediment profiles are the exception rather than the rule in today’s

archaeology. Researchers are more often than not required to get the information on an excavated exposure in a few days or less. Working under such time constraints, the field description of the exposure is important but so is the recovery of a representative sample of those sediments for more thorough study in the laboratory. Still the field exposure provides the most faithful picture of the exposure in terms of scale and setting. It is critical that the profile face be properly prepared before beginning its description. Simply excavating the profile does not provide the best view of the face. One must dress the profile face to adequately bring out the features of the deposits. The tool of choice for this task is the archaeologist's friend—the trowel. If archaeology has mastered one thing in stratigraphic studies, as first mandated by Sir Mortimer Wheeler, it is the meticulous care taken with the vertical profile. The nature of a deposit is best seen when the profile face is cleaned and made uniformly even.

After the face is adequately prepared, measurements must be taken. The establishment of a reference datum level is required. Most researchers approach this step in one or two ways—(1) establish a surface datum level or (2) establish a relative datum level on the profile face. This writer has no preference in the selection of either method. When applied with care, either technique works equally well. In this world of “automatic” laser levels, the use of a surface datum is manifold easier than in the past when workers used string levels to transits to control verticality in an excavation. Even with use of the relative datum level at some time, the stratigraphy must be reconciled to the actual topographic setting or geomorphic surface.

Using the relative datum level technique, the placement of the datum can be made at any point on the profile face as long as it—the datum line—is level. The datum line is usually a simple string level strung between two points on either end of the profile face. From this level line, the stratigraphy of the profile can be measured up and down. The result is an accurate picture of the profile to the scale that one has chosen. The surface datum level line is “zero,” and all

readings of the profile face are below this level. The result is the same—a representation of the profile face to scale. Where feasible, a photograph of the profile should be taken to assist in the interpretation of the profile after the excavation has been closed. Color photography is preferred over black and white so as to record the important parameter of soil or sediment color. Photography of a profile face is not an easy task. When they are available, a professional photographer should perform this important task. In some cases, as with an excavation trench, the focal distance to the face is such that several photographs must be taken to develop a composite image—mosaic—of the profile. Lighting is almost always difficult on a profile, and the best results are obtained in complete shade rather than in direct sunlight just as with the case of obtaining Munsell colors. Digital photography has provided significant improvement, and ease, of documenting field profiles.

Profile Samples: Soil monoliths are small vertical columnar sections of a profile. This technique was developed by Russian soil scientists in the late nineteenth century and introduced to the rest of the world at the Chicago International Exhibition in 1893 (Vanderford 1897). The monolith can function as both a permanent record of the deposit and temporary reference section from which measurements can be made. The profile can be reconstructed from a series of these smaller sections. This procedure is laborious and can be accomplished almost as well by the quicker method of coring. The advantage of the monolith is in its use in the laboratory in assessing, under more controlled conditions than those of the field, diagnostic parameters in detail and under more convenient time constraints.

To take a monolith, a container is constructed for the monolith from either metal or wood. The size of monoliths varies but commonly is about 1 m in length, 10–20 cm wide, and a few (<10 cm) cm thick. Methods vary, in detail and objectives, but the basic method is to use a wooden or metal boxlike tray that is open on one side. The monolith is excavated to the dimensions of the box and cleared on all sides

including the base of the section. Once this is accomplished, the box is placed over the monolith and pressed firmly against it to assure a firm juncture between the container and the section. Cutting the monolith away from the profile face is perhaps the most difficult task requiring patience and some skill with a sharp shovel or trowel to uniformly disengage the section. Some workers simply press a metal frame into the profile face and then excavate the monolith out along with the box. Either way collects a rather faithful representation of the profile being sampled. Of course the exact nature of the deposit will condition the ease of removing the monolith particularly in rocky sediments or archaeological deposits with many cultural inclusions. Smaller monoliths for purposes of micromorphological studies can be taken using the Kubiena frame (Kubiena 1953). These small metal boxes are, again less scrupulously but expeditiously, mimicked by the use of domestic metal food containers whose lids have been removed.

4.2 One Method for Constructing a Soil Monolith

Materials

- One metal frame: 5' × 4–6" × 1–2".
- One presentation board: made to fit sample from frame, backboard must be a 2 × 8", adding quarter round at top helps hold the sample.
- Glue for adhering sample to presentation board.
- Future Floor Wax
- Spray bottle
- Backhoe
- Three people
- Sharpshooter with flat shovel head

Method

1. Excavate a pit with a backhoe to over 5 ft deep with a clean, vertical face on one wall and room for two people to stand comfortable in front of the smoothed face.
2. Hammer the frame into the smooth face from surface to the desired depth.

3. With two people in the pit holding the frame and one at the top of the pit, the person at the top of the pit begins shoveling down parallel to and 4–5" away from the frame.
4. As the shovel removes the vertical layer of soil, the people in the pit holding the frame begin leaning the frame back as sections of the sample are added to it. (In very sandy soils during the dry season, thoroughly wet the soil overnight and remove small sections at a time into the frame.) This part may have a few failed attempts. Multiple samples can be taken from the same pit.
5. Once the entire sample is collected, carry the frame and sample outside of the pit and trim the lip down to the frame edge.
6. Add adhesive to presentation board and invert over extracted sample in frame. Very carefully press frame into presentation board and invert till sample is transferred to presentation board. Remove frame.
7. Carefully transport the sample. Clean face of sample. Dry.
8. Add full strength Future Floor Wax and thoroughly saturate soil. Apply with a spray bottle. Will dry clear.
9. Add finishing touches to presentation board.

Once the monolith, of whatever dimensions, is freed from the profile, it must be stabilized before transport. Thicker monoliths require less treatment before transport. The monoliths, particularly the larger 1 m varieties, are heavy—25 kg or more. All specimens should be carefully logged, photographed, and described before placing a coverlid over them. They can be safely transported to the laboratory where they are uncovered and more elaborate studies are begun. In some instances, the monoliths are impregnated with plastic resins for reasons ranging from the removal of thin sections to the fabrication of displays. From the standpoint of scientific studies such as textural, chemical, and age determination, it is best to leave impregnation of the monoliths to last (Fig. 4.1).

One use of impregnation of soil profiles has been used to obtain “peels” of the face of a deposit (Orliac 1975). In this method, a thin



Fig. 4.1 Cutting out a soil monolith

layer of synthetic latex is applied to the profile and allowed to harden. When dry, the latex or epoxy preserves the profile to the depth of the impregnation—a few mm to a cm or so. This image is adequate to describing color and textural differences as well as providing a facsimile of the profile that can be kept for future reference. In Switzerland, Arnold and his co-workers (1978) have used epoxy peels of entire archaeological surfaces both for study and for more elaborate particle size, chemical, or other studies such as palynological ones; the peel technique is inadequate in terms of sample size as well as adulterating the sediments of the profile.

Core Samples This type of undisturbed sediment or soil column is acquired by a variety of methods and results in specimens of varying dimensions of length and diameter. The key word in describing cores is *diameter*. The coring devices used to obtain soil and sediment samples are cylindrical as a rule. There are square coring

devices such the “box corer” used in sampling marine and lacustrine sediments. Coring devices range from gravity corers, piston corers, percussion corers, and drive corers to rotary corers. The first two types, like the box corer, are used for inundated or wetland sediments. Percussion, drive, and rotary corers are typically used for terrestrial coring although a variant of the percussion type, the vibracorer, is routinely used in wetland and inundated contexts. Vibracorers are particularly effective in penetrating unconsolidated sandy sediments. A recent, rather innovative, “coring” device is the freezing corer or “cryoprobe” which has proved effective in both inundated and terrestrial settings (Garrison 1998).

Rotary Corers These are mechanical coring devices that extract solid columns of sediment or soil that is relatively uncompacted. Unlike larger rotary drilling systems such as used in hydrocarbon or hydrological exploration, rotary corers used in archaeological geology do not usually use drilling fluids which are used to lubricate the drill bit in rock. As almost all archaeological deposits are sedimentological in nature, the rotary corer can penetrate their relative shallow depths (a few meters as a rule) without lubricants, which, in many instances, prove inconvenient for accurate chemical and textural tests. As shown in Fig. 4.2, the rotary corer is most often vehicle mounted for ease of transport to the archaeological site. The coring tool is an open cylinder a few centimeters in diameter that has a drill bit or *straight* cutting edge of hardened steel alloy. The barrel of the corer often features a screw-like exterior creating the appearance of a hollow auger that allows the central section to remain open for the acquisition of a continuous, solid sediment/soil column in all but the stoniest or wet conditions.

The advantage of the rotary corer, or for that matter any corer type, is the recovery of an *undisturbed* column of sediment or soil. The recovered monolith is reflective of the macro- and microscale stratigraphy without a great deal of compaction or mixing of sediment/soil structure and features such as lamellae. For



Fig. 4.2 Rotary corer. Shown deployed in the excavation of a Roman era cemetery in urban Tunis, Tunisia, the auger rapidly bores through the clastic sediments. Photograph by Nina Šerman

measurement of parameters such as porosity, moisture content, and consolidation of clays solid, undisturbed core samples are mandatory (Shuter and Teasdale 1989).

Percussion and Drive Corers These types of coring devices are excellent for the recovery of soft or compressible sediments (*supra*). Likewise they work well in unconsolidated sandy sediments particularly the percussion corer. The difference between the percussion and drive corers is the application of the pressure on the coring tool. The percussion corers apply intermittent impact pressure either by a hammer or by raising and dropping the entire coring tool. The drive corer applies pressure in a constant manner usually with a hydraulic booster system. The vibracorer is a percussion type of corer that

utilizes an eccentric or offset gearing system to develop a steady vibratory motion on the core barrel enabling it to “settle” into a deposit. Vibracorers can be pneumatic, hydraulic, or electric powered. Percussion corers can vary in size from a meter in length to over 10 m. Core barrel diameters can vary from a 50 to 75 mm as a rule. The most popular terrestrial drive coring device is the Giddings corer. This device applies hydraulic pressure to a core barrel of 75 mm diameter extracting solid columns of over a meter in length (Fig. 4.3).

Hand-driven percussion corers are the most popular and economical type of the coring types. These corers typically consist a solid or split-core sampler barrel, a series of solid metal extensions that terminates in a swage- or screw-type adaptor for a slide hammer. The individual hammers the core into the ground, in set increments, determined by the length of the coring tool, to the ultimate depth of interest and then extracts the solid core. A type of coring tool called a gouge auger can be used. This “auger” is a cylindrical open device for use in soft sediments. Hand-driven corers are rarely over 25 mm in diameter and obtain relatively small samples of the sediments/soils. Compared to some screw augers of 100 mm diameter, there is a clear advantage in overall sample size for the screw auger even if the sediment is a disturbed sample. Core liners of clear plastic can be used inside all types of corers from mechanical models to hand types. For maximum protection and preservation of the *in situ* context of the cored deposit, these sampling devices are recommended. This is important for the recovery of fragile macrobotanical or macrofaunal materials as well as pollen remains.

An important factor in percussion corers, most notably those that are hammer driven, is the disturbance and compaction of fine-grained sediments. This can occur in vibrating corers as well. Quantitative data is lacking on this point, but it is suspected that an increase in the driving rate, measured in blows per foot, increases the potential for disturbance and compaction in the recovered sediment column. The author has

Fig. 4.3 A Giddings hydraulic coring system. The operators are exchanging a “Kelly (extension) bar” from the adjacent rack, to increase the depth of the core. The vertical “mast” contains a hydraulic “ram” powered by a small engine (not shown) to push and pull, utilizing the lever controls (red), the core barrels used to collect sediments. The system is easily deployed using a vehicle as shown. A typical core takes less than 30 min to collect



observed this in small diameter, rigid barrel hand corers when using a 5 kg slide hammer in resistant deposits such as stiff muds or sands. If a sample requires a driving rate in excess of 25 blows per foot, then one should be on guard for sample disturbance. If the corer’s hammer is quite heavy—say, 50 kg or so—then this is particularly true with regard to compaction of the recovered core sample.

Gravity (“Drop”) and Piston Corers These corers, as previously said, are more often used to core marine and lacustrine sediments. Both types are raised and then released to rely on gravity for the force required to penetrate inundated or soft wetland sediments. In the contexts that they are deployed in, they are rarely coring into soils with the exception of soils developed on peat bog deposits such as paleohistosols. To aid in penetration of the sediments, these corers use heavy weight loads attached to the upper part of the coring barrel with as much as a ton of weight added to corers of 2–3 m in length. Needless to say, a corer of this weight is not recovered by hand.

The piston corer is a gravity corer design that uses the creation of a partial vacuum in the recovery barrel to recover wet, unconsolidated sediments. The piston corer works well in multi-bedded deposits of silts and sands. Various types are used today such as the Livingstone corer, the

Kullenberg corer, and the Ewing type. Figure 4.4 illustrates the principal components of a Ewing-type piston corer used, by the author, to recover riverine and marine sediments. A smaller, auxiliary corer, called a messenger corer, is added to a gravity corer design whose barrel assembly has incorporated a piston coupled, by a cable, to the messenger corer and the hoisting mechanism for both elements of the piston corer. As shown in the illustration, the messenger corer is cantilevered off the larger gravity-piston corer such that it will contact the sediments first, raising the cantilever arm such that a cam device, in turn, releases the cable at the point of attachment on the hoisting device along with the main corer. The heavier, main corer drops in free-fall mode, into the sediments, while simultaneously the fixed cable remains taut along with the piston. Thus, as the core barrel falls deeper into the deposits, the piston moves up the core barrel drawing sediments into the partial vacuum created by the rapid “rise” of the piston up the barrel. These corers use plastic core liners to aid in creation of the vacuum and to preserve the sample. Piston corers are sometimes prone to problems such as foreshortening or stretching of sedimentary units (Buckley et al. 1994).

Freeze Corers Hammer-driven freeze corers or “cryogenic soil probes” are a fairly recent addition to sediment sampling in archaeology

Fig. 4.4 Ewing piston corer

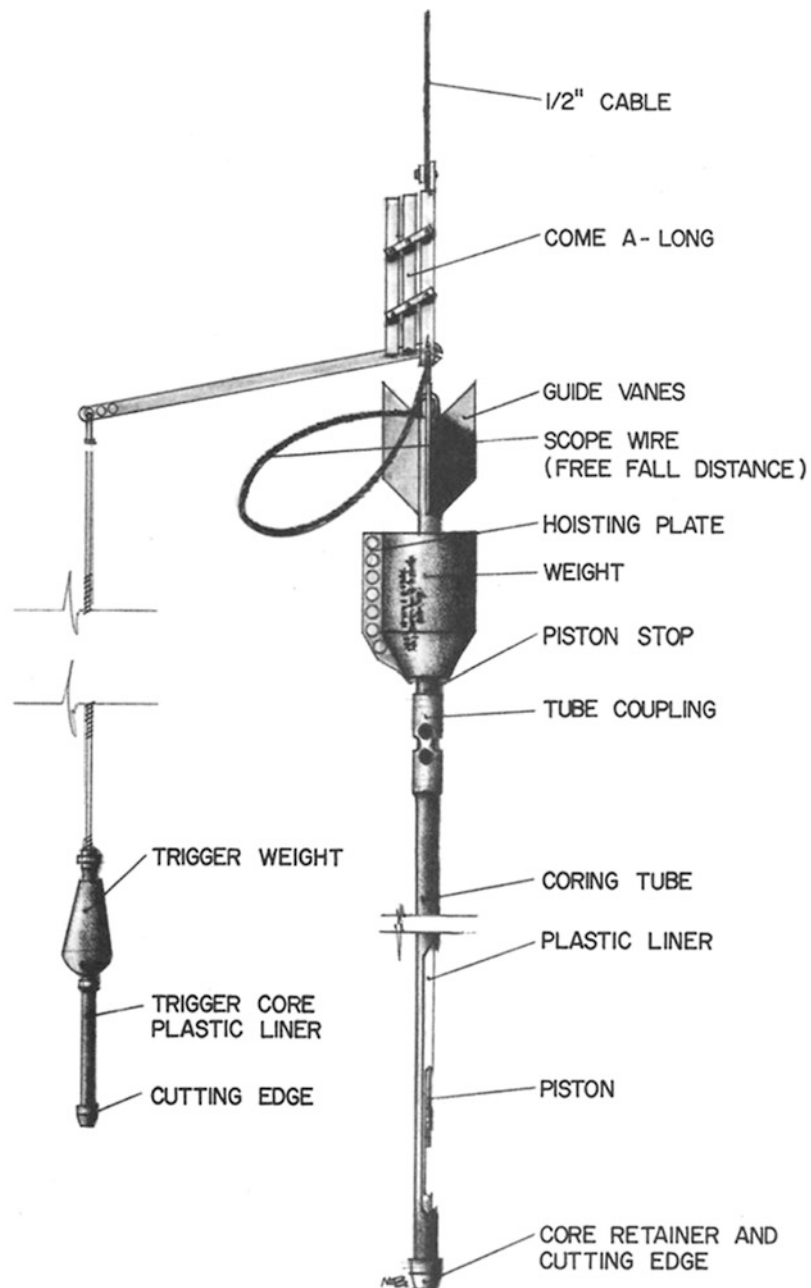


(Fig. 3.8) They have been used to sample wet sediments for biological purposes as well as those of archaeology (Greboth   et al. 1990; Lassau and Riethmann 1988; Miskimmin et al. 1996). Early in the 1990s, European and North American workers quickly moved the design of these corers forward from prototypes

to relatively standardized field models (Hochuli 1994; Garrison 1998). The principle of the freezing corer is simple—insert a closed-tip metal tube into the earth, fill it with a cryogenic fluid, such as nitrogen, and freeze the adjacent sediments to the metal tube. Extraction of the tube brings with it all the frozen sediments

adhering to the core barrel. The diameters of the freezing corer barrel have varied with development as has the freezing fluids used in these designs. The present-day archaeological designs have opted for 75 mm diameter steel barrels about the length of rotary and drive corers such as the Giddings type, e.g., 1 m or so in length. Those used in lacustrine settings are cylindrical or wedge-shaped containers of slurries of alcohol and dry ice (Lotter et al. 1997).

Figure 3.8 illustrated the design and use of a typical freezing corer. The corer is hammered into the sediments, and then a transfer hose is attached to valving on the top of the corer. Liquid nitrogen, at a temperature of -197°C , is circulated through the corer for a period of about 20 min. A mechanical extraction assembly, composed of a tripod and lifting device, are attached to the frozen core sample and it is withdrawn. The description of the recovered sample is described much the same as any sediment or soil sample—color, texture, structures, etc. Moisture content is important to the efficient use of the freezing corer, but it is surprising at the relatively small amount of moisture needed for adequate freezing in most sediments (5–10 %).

Augers and Drills Undisturbed Sampling Techniques—Rotary augers and drills have a long history in soil and sediment sampling. Recently, two noted geoarchaeologists have discussed the relative merits of small-diameter corers (25 mm) versus larger-diameter (100 mm) soil augers (Stein 1986, 1991; Schuldenrein 1991). Both types are commonly used today, and their use will continue for both practical (speed, costs) and scientific reasons. Rotary augers and drills recover disturbed samples in terms of pedologic structure and micromorphology. If the samples are in soil horizons, the stratigraphic integrity of the deposits are degraded or destroyed, but much information is retained for both field and laboratory studies. Larger sample sizes are routinely recovered using soil augers and mechanical drill systems. Mechanical drilling systems can recover sediments as effectively as comparable solid column corers.

4.3 Handling and Description of Cores: Some General Considerations

Depending on the type of core sample one has—auger, drill, etc.—some general observations should be made about the sample as quickly as possible, either in the field or immediately upon arrival at a laboratory. All samples allow the determination of the basic parameters of a sediment or soil—color, general texture, consistency, general organic content, etc. Some things must wait for more rigorous measures to be applied to the sample such as the quantitative determination of size classes, total organic matter content, macro- and microbotanical makeup, chemical attributes, magnetic properties, etc. Nonetheless, a researcher must recognize that the freshly recovered sample contains information that can be readily assessed. These data, however qualitative, in some cases, provide the investigator with firsthand information as to the general nature of the sediment or soil. Additionally, these data are not to be replicated as the simple passage of time subtly alters the core sample through changes in moisture content and chemical changes such as oxidation and the corrosion of mineralogic or organic remains. Rapid storage of the core sample, in a cold room or freezer, can do much to ameliorate or retard these changes, but even in these cases, workers typically record as much data about the sample as possible before placing the core in storage. If the core sample cannot be archived in such facilities, then it is imperative that the material be sampled and described as quickly and as fully as possible.

Rotary, Percussion/Drive, Box, and Piston Cores: These devices can extract whole core samples such that the structure of the peds and the lithostratigraphy are generally preserved. The sample can be extruded from the core barrel, a sample holder, or the subsample can be contained within a core tube liner made of a plastic material. The core sample can, in some cases, be maintained in a type of container that can be removed or detached to allow transport, storage, and examination of the sample.

Depending on the length and diameter of the core sample, analysis and storage considerations can vary. In the case of small-diameter (25 mm/1 in.), shortish (30 cm/12 in.) core samples, handling and storage protocols are not very complex. In the case of long, larger diameter, 75 mm +(3 in. +), cylindrical cores, handling, sampling, and storage become a more serious issue. With the larger core samples, it is not uncommon to section or cut the sample into shorter, more manageable lengths such as 50 or 100 cm. Again, the core may, in the case where the liner or barrel is used for handling, be sampled and then archived without too much disturbance. Cores that are not immediately placed in climate-controlled storage such as cold rooms can alter, biologically and chemically such that the peds and inclusions are adulterated in terms of shape, size, etc. Textural and color differences are typically maintained. The general nature of lithostratigraphic relationships, in the core, can still to be seen, but the absolute, metric nature of the relationships can be compromised.

Whatever the core type, the infield and laboratory description of the sediment section follows a commonsense procedure in most cases. A standardized protocol, such as the following log of the box sediment corer, shown in Fig. 4.6, is commonly used. This example is used by the Great Lakes Environmental Research Laboratory and the Great Lakes Water Institute (Edgington and Robbins 1991). The categories used in the core description can vary and be easily customized to the particular objectives of a project. The categories shown in this example were used in the description of lacustrine/marine box core samples, but they could as easily be used for sediment cores for most any application.

4.4 Standard Operating Procedure for Collection of Sediment Samples

1.0 Scope and Application

The application of this sampling procedure is for the collection of sediment cores, using a box corer, for the analysis of radionuclides to provide

estimates of the sedimentation rate and mixing depth for the GLNPO Lake Michigan Mass Balance Study.

2.0 Summary of Procedure

Before any box cores are taken, test grabs, using a ponar, will be taken to determine the suitability of the sediment for coring. If coring is possible, then the box corer will be deployed. Once the box coring is completed and box core is back onboard the ship, then four 10 cm (ID) plastic tubes will be inserted by hand into the Master box core, thereby creating four subcores (A–D). Each of the subcores will be sectioned and these subsamples stored for future analysis.

3.0 List of Equipment

| Item | Quantity |
|--|-----------|
| Modified box corer (Soutar corer) | 1 |
| Box corer extraction rigging | 1 |
| Set of critical spare parts for box corer and extraction rigging | 1 |
| Hydraulic extruding stand for 4" diameter subcores | 1 |
| Set of core sectioning gear | 1 |
| 125 ml polyethylene bottles/pre-labeled and tared | As needed |
| Ponar grab sampler | 2 |
| Winch for Ponar deployment | 1 |
| 10 cm/4" diameter subcore butyrate tubes | |
| 12 vacuum-extractor caps | 2 |
| Portable vacuum pumps with Tygon tubing | 2 |

4.0 Sampling Procedure

4.1 Test grabs, using a Ponar grab sampler, will be taken to determine the suitability of the sediment for coring. If three grabs return without a sample, then the site will be vacated. If the Ponar grabs are obtained but coring is not feasible, then surface samples from the grabs will be obtained. If coring is possible, then box coring will be undertaken as long as there appears to be a limited risk of damage to the box core.

4.2 Once the box core has been retrieved and is back on the ship's deck, then the core is examined for acceptability. This

examination is done by using the viewing window on the front side of the box core. If the core is unacceptable, then the contents of the box core will be released and the box corer redeployed.

- 4.3 Acceptable box cores are subcored by carefully inserting a 10 cm diameter butyrate tube into the core. Distortion of the sediment during the tube insertion is minimized by the application of a partial vacuum to the tube top. By continuous manual adjustment of the vacuum as the core is inserted, the interface within the tube remains in alignment with the interface of the surrounding sediment in the box core.
- 4.4 Sediments within the tube are hydraulically extruded and sectioned onboard the ship. Extrusion is done by the application of water pressure from the ship's hose line to a rubber stopper inserted into the base of the core tube. Fine control of water flow allows slow movement of the core upward into a separate short section of tube (the collar) placed in-line with the core tube top. The collar is scribed in cm intervals so as to define the amount of core section to be displaced laterally into an aluminum receiving tray.
- 4.5 Subcore taken for the analysis of radionuclides will be sectioned with plastic utensils.
- 4.6 Subcore samples are stored in conformity with EPA QA/OC requirements.
- 4.7 A backup core is taken in case of unexpected problems in analyzing the first core or if an interest in analysis of additional material develops.
- 4.8 Core lengths are expected not to exceed 50 cm in length and should more than cover the entire post-settlement history of deposition.
- 4.9 A detailed record of the sediment characteristics, as a function of depth, as well as a notation of any unusual properties (i.e., large wood chips) will be entered in the sampling log. An example of the sampling log form is shown in Fig. 4.5.

5.0 Sample Custody

After the sectioning of each core, the Co-PIs will verify that all the samples are accounted for and that they are transferred to proper storage. After sampling has been completed and the samples transported to the lab, the CO-PIs will again verify that all samples have properly transferred and stored. The location of all samples is noted in the sample log.

6.0 Sample Labeling and Logs

Prior to each sampling event, a complete set of sample bottle labels will be prepared. The number and type of these labels will depend on the length of the sediment core recovered and the estimated sedimentation rate. An example of a typical label is seen in Fig. 4.5.

Box cores are so-named because sediment samples reside in metal "boxes" (Fig. 4.6). As indicated in Sect. 4.2, the acceptable sediment core is removed from the corer, another "box" sampler is loaded, and the corer is redeployed. Also, as noted the core can then be subcored for various purposes ranging from textural analysis to age determination.

Percussion, drive, or otherwise cylindrical sediment cores, upon recovery the core will generally be "split" into equal halves using power saws. The halves were measured and described as to color and sediment texture. They were drawn on standardized recording sheets, as shown, and photographed along their entire sections. Subsampling, of the core, for textural, geophysical, chemical, and botanical analyses, is relatively straightforward.

The recovery of samples for use in age dating is relatively routine as well, but in certain cases, special handling is required. For instance, the paleomagnetic/archaeomagnetic evaluation of a core sample can only be done on intact samples. The dating is typically done *in situ* along the core using a magnetometer designed for this. Most archaeological dates are not obtained from the magnetic dating of cores unlike geological core samples where the procedure is more common. For one thing, paleomagnetism measures field reversals across a broad time range, whereas

Lake Michigan Mass Balance and EMAP Study Sediment Sampling Log

Station No:

Core No:

Date:

Time:

Latitude:

Longitude:

| Section | Description | Section | Description |
|---------|-------------|---------|-------------|
| 0 – 1 | | 29 – 30 | |
| 1 – 2 | | 31 – 32 | |
| 2 – 3 | | 32 – 33 | |
| 3 – 4 | | 33 – 34 | |
| 4 – 5 | | 34 – 35 | |
| 5 – 6 | | 35 – 36 | |
| 6 – 7 | | 36 – 37 | |
| 7 – 8 | | 37 – 38 | |
| 8 – 9 | | 38 – 39 | |
| 9 – 10 | | 39 – 40 | |
| 10 – 11 | | 40 – 41 | |
| 28 – 29 | | 59 – 60 | |

Sectioned by

Recorded by

Samples Checked by

Received & Checked by

Samples Stored at

Date

Fig. 4.5 Sediment sampling log

archaeomagnetic dating requires declination and inclination measurements which are compared to regional reference dating curves (Eighmy and Sternberg 1990). Radiocarbon dating of organic inclusions is the most typical means of age determination of cores within the practical range (~50,000 years) of the respective carbon dating techniques—beta counting or accelerator mass spectroscopy (Blackwell and Schwarz 1993).

As optically stimulated luminescence (OSL) dating of sediments has become common, the need for special handling of the particular core samples will be needed. Basically this entails the use of darkness and photographic darkroom procedures to prevent undue exposure of the core sediments, such that the remnant OSL signal is not affected (Godfrey-Smith et al. 1988). From one-half of each core sediment, samples were



Fig. 4.6 Sediment box corer

drawn at set intervals (ca. 20–30 cm). Depending on the lengths of the cores, typically 3 m, this resulted in about a dozen sediment samples of 100–300 g each. These sediment samples were placed in plastic bags, marked and catalogued as to location and time of recovery as well as depth within the individual core. The other halves of the cores were covered with mylar and aluminum wrap for their entire lengths. The sampled halves will be treated the same way as well. Both sets of cores—sampled and unsampled—were transported to laboratories for further study and subsequent storage in controlled environmental conditions and reserved for future research. Standard drill core boxes, made of heavy corrugated Kraft cardboard or corrugated plastic, are available from most geological/soil science supply houses. One box can hold up to 3 m (10 ft) of core sample.

Rotary Augers and Drills: The core samples from these devices have, by their very nature, lost pedological and lithostratigraphic information. The use of these devices is typically limited to shallow sediment/soil sampling (<2–3 m), but

as most archaeological deposits are within this range, their utility will remain high. The hand augers and drills allow very rapid sampling for small, yet representative samples. Color, textural, or even chemical analyses require only a few grams of sample in most cases, so the volume of sample needed is not that great. Again, it is the continuity and cohesiveness of the sample that is at issue, and if this not a methodological priority, then the use of the devices is feasible.

Like the more intact samples from the rotary/push/percussion corers, handling, analysis, and storage depend a lot on the sample size. Long, continuous sediment samples may be extracted using the hand drill or auger. Mechanized units certainly can do this. The length of the sample is only limited by the number of extensions that are used in the recovery of the core. Samples from the core may be placed in drill core boxes or simply placed in plastic bags. These latter items are labeled as to the location and weight of the sample as well as the other identifying information—core sample #, date, etc. One problem encountered by this author, in the use of a mechanized drill, was the difficulty in monitoring and recovering the sediment sample during the course of the coring operation. This particular unit did not have a variable speed control on the drill, so sample was simply extruded from the borehole as the drill descended. This type of drill is to be avoided if controlled sampling is a goal of the study.

Cryogenic or Freeze Cores: While relatively rarely used in coring studies today, more and more references to the use of these devices have appeared in a wide variety of literature, mostly to do with the sampling of wetland and/or inundated deposits. The freezing of soils originated in the Soviet era (Khakimov Akh 1957). The author's use of these devices has demonstrated some handling problems that are unique to them. One major difference in the core taken by a freeze corer versus that recovered by other types is temperature. Whether the coolant used is carbon dioxide (−78 °C) or colder nitrogen (−197 °C), the recovered core remains frozen to the core barrel for some time—up to over an hour in many instances. The core sample is

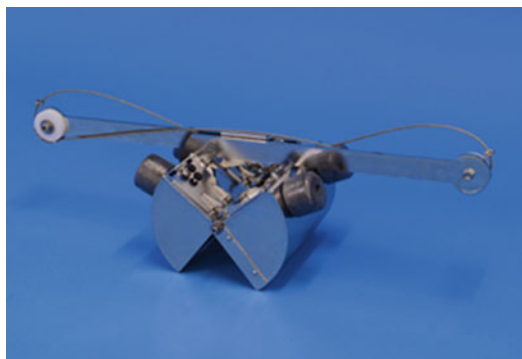


Fig. 4.7 The sediment grab sampler

rock hard until it finally melts, and even then the sample rarely loses its consistency and cohesion. This is not a bad thing. Indeed it is one of the real advantages of the freeze corer that relatively uncompressed samples can be recovered intact over considerable lengths (>1 m/core). Too many times, in inundated sediments, even with standard coring devices with sample catchers in place, some or all of the samples have been lost during recovery of the core sample. Freezing cores do not suffer from this shortcoming.

Another interesting aspect of a frozen core is the necessity, upon occasion, to literally defrost the sample. This is done using a portable propane torch. The objective is not so much as to thaw the core but to remove the frost that forms on the surface of the sample obscuring the color of the material. Once thawed, the battery of analytical techniques that can be applied to freeze core are no different from those used on other core samples. The removal of sample requires the cutting away of the core from the barrel to which it adhered. This can be easily done with a trowel where the length of the core is sectioned, to the barrel, and the sediments simply peeled back along the length. The sample can be transferred to core boxes or other sample containers.

The Grab Sampler The collection of bottom and subbottom sediment samples sediment grab sampling is a well-used technique. Grab samples are taken using easily deployed over-the-side apparatus (Figs. 4.7 and 4.8a, b). The Ponar-type grab sampler, just mentioned in the context

of box coring, is a commonly used sampler, in fluvial, lacustrine/estuarine, and marine settings, that is very versatile for all types of hard bottoms such as sand, gravel, and clay. Shown in Fig. 4.7 is the Van Veen-type self-tripping sampler with center hinged jaws and a spring loaded pin that releases when the sampler makes impact with the bottom. A simple metal pin prevents premature closing.

As long as the grab sampler is hanging freely from the hydrographic wire or line (Fig. 4.8b), the trigger mechanism will keep the jaws open. However, as soon as there is slack in the winch line, the trigger will be released. When the winch starts to raise the grab sampler, the jaws will close, thereby taking a “bite” (sample) from the bottom. Grab samples, brought aboard, are lowered into a rectangular stainless steel or wooden frame box that has a fine-to-very fine screen on the bottom (Fig. 4.9).

4.5 “1700 Sondages”: Geological Testing of the Plateau of Bevaix, Neuchâtel (Switzerland)

A geological survey using 1700 sondages (“trial excavations”) was undertaken from 1991 to 1997, along the construction right of way for the A5 autoroute, between Cortaillod and Bevaix, supplemented by a palynological study of the swamp known as the Bataillard, which has allowed the reconstruction the paleoenvironmental history of the Plateau of Bevaix, since the withdrawal of the Würmien glacier until today. This work has allowed a better understanding of the role of climate and human factors in the history of the landscape of the plateau. Figure 4.10 shows a typical set of these systematically deployed soundings across an agricultural field along the highway route.

In addition to the large number of excavated tests, the study dug 28 cross-sectional trenches to characterize the relationship of the sedimentologic and pedologic units to the underlying lithology. Across the plateau section, the paleosols

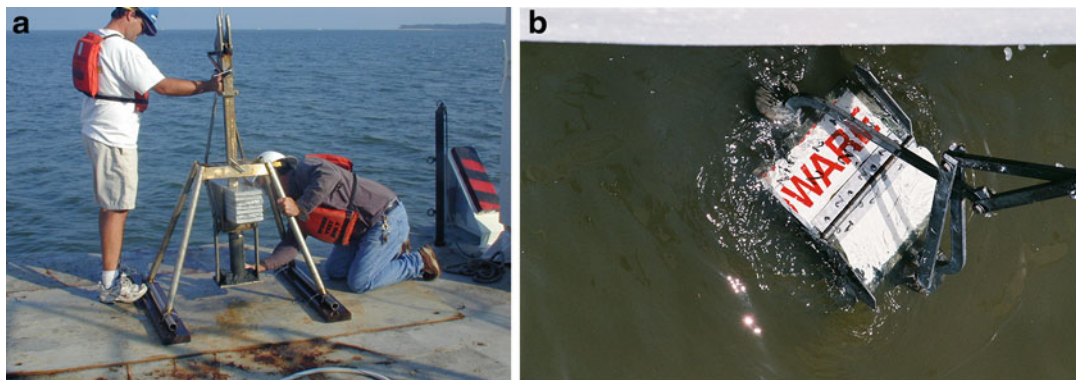


Fig. 4.8 (a) Above, shallow sediment corer; (b) right, a sediment grab deployed at Jekyll Creek, Atlantic Intracoastal Waterway (AIWW), Georgia, USA



Fig. 4.9 Sediment grab sample on a screen box

were observed to form on colluvium derived from either quaternary morainic or tertiary molasse units. The most prominent paleosol was the “Atlantic period soil” (4900/4750–3500/3300 BC) (Weber-Tièche and Sordoillet 2008). In Fig. 4.11, this paleosol is represented by complex 3. The study delineated what are termed biostatic versus rheustatic periods when the landscape was either stabilized by vegetation or destabilized by the lack of vegetation and other paleoenvironmental factors.

4.6 Analytical Procedures for Sediments and Soils

As most depositional environments, geological or archaeological, result in stratigraphic sequences or horizons such observed in the

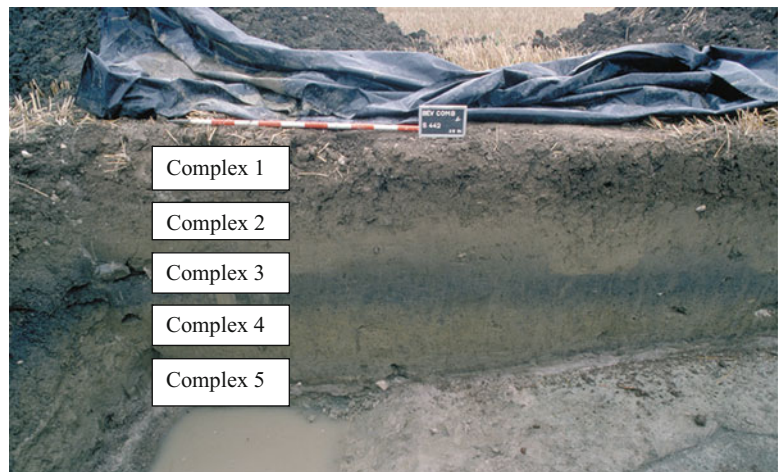
Plateau of Bevaix study and nearby Neuchâtel (Hadorn 1994). The paleoecological, sedimentological, and artifactual information must be collected level by level, evaluated quantitatively, to provide, at best, a fragmentary synthesis of a prehistoric milieu. As Gall and others have noted, the paucity of that fragmented record, plus its inherent alienness, makes understanding elusive and speculative (Gall 1983, 2012). Nonetheless, it is the record we, as archaeological scientists, must use, and the sedimentary fraction is no small part of the picture. In geology, the study of sediments is the field of sedimentology. Because of the linkage between sedimentary basins and hydrocarbons, there has been a strong focus on this aspect of earth science both in terms of theory and practice. Because of their importance in the natural rock cycle, sedimentary rocks and their genesis—mineralogy, depositional histories, and environments—have been examined to the extent that much information salient to archaeological inquiry can be deduced from the sedimentary matrix or context in the site (Soukup et al. 2008). Today, with the development of optical stimulated luminescence (OSL) technology, and cosmogenic nuclides, ^{14}C , ^{10}Be , and ^{26}Al , the “chronometric” or “numeric” dating of soils and sediments is possible (Wagner 1998).

While the possibility of directly dating an archaeological sediment facies is exciting, this only adds to the other well-established techniques used in the analysis of the sediment

Fig. 4.10 Typical sequence of sondages used to systematically characterize the landscape of the Plateau of Bevaix (Courtesy of the Archaeological Service, Canton of Neuchâtel)



Fig. 4.11 Typical stratigraphic sequence seen in the profile for a test unit. The “complexes” listed represent sediment deposits of colluvium and soils formed thereon



such as what I have called “the 5 Ps,” particle size, point counting, palynology, phytolith, and phosphate procedures. As Julie Stein, Gall, and others pointed out, the study of sediments allows us to deduce their “history” such as origin, transport, and deposition (Stein 1988). The specific study of a particle’s mineralogy (petrography of sediment particles, particle size, and point counting) is discussed in the two following chapters.

Simply studying the morphology and variety of sedimentary particles allows a rather reliable retrodiction of processes such as geological source, climate, and diagenesis. If the

sedimentary particles are found in structural materials—daub or brick—or ceramic artifacts, additional understanding of their sources, trade, or other aspects of these materials can be studied. The study of those smallest of sediments—the clays—occupies a subdiscipline of its own and has proven quite pertinent to the study of archaeological ceramics. The mean size and percentage of sediments together with the calculation of straightforward coefficients, such as (a) grain size, (b) sorting, and (c) skewness, provide significant information on transport, deposition, and diagenetic processes. For instance, the nature of cultural versus natural deposits in cave sediments

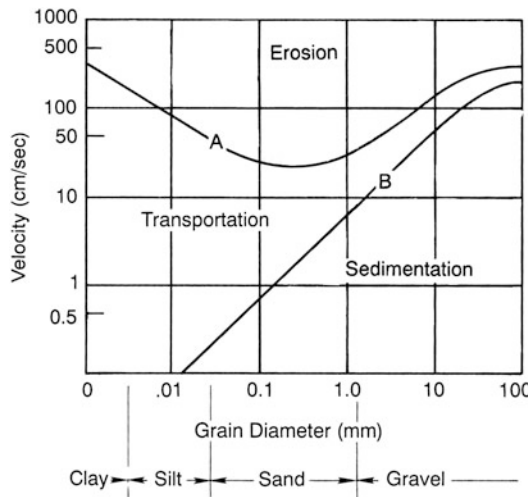


Fig. 4.12 The Hjulstrom diagram relating particle movement to size and stream velocity

can be examined by particle size, shape, and distributional (mean size, kurtosis, etc.) as well as other micromorphology procedures (Courty et al. 1989; Courty 1992; Goldberg 1995).

Bulk density and carbonate percentage are important parameters determined in the laboratory setting. The latter technique is important in the characterization of sediments and soils where the buildup of calcium carbonate is commonplace and a key parameter in soil genesis as well as sediment deposition.

In fluvial geomorphology and sedimentology, the Hjulstrom classification or diagram (Fig. 4.12) is an important nomogram to understand the relationship between particle size, suspension, and stream velocity. The size of the particle determines, in large part, whether a specific size range of bed materials will become suspended load or entrained in a current.

Table 4.1 lists specific size classes for particles: 1.0 is sand; 10 is small gravel, etc.

4.7 Particle Size Analysis

Particle size analysis (PSA) is the measurement of the size distribution of the individual particles of a sediment or soil. It involves the destruction or dispersion of sediments into their constituent

Table 4.1 The standard grain-size scale for clastic sediments

| | Name | (mm) | (μm) | φ |
|---|------------------|-------|-------------------|-----------|
| G | Boulder | 4,096 | | -12 |
| R | Cobble | 256 | | -8 |
| A | Pebble | 64 | | -6 |
| V | Granule | 4 | | -2 |
| E | Very coarse sand | 2 | | -1 |
| L | Coarse sand | 1 | | 0 |
| | Medium sand | 0.5 | 500 | 1 |
| S | Fine sand | 0.25 | 250 | 2 |
| A | Very fine sand | 0.125 | 125 | 3 |
| N | Coarse silt | 0.062 | 62 | 4 |
| D | Medium silt | 0.031 | 31 | 5 |
| | Fine silt | 0.016 | 16 | 6 |
| M | Very fine silt | 0.008 | 8 | 7 |
| U | Clay | 0.004 | 2 | 8 |
| D | | | | |

As devised by Johann A. Udden and Chester K. Wentworth (Blair and McPherson 1999), the φ scale was devised to facilitate statistical manipulation of grain-size data and is commonly used. $\varphi = -\log_2 D(\text{mm})$ where D is the grain diameter. It is a geometric scale where the succeeding size class is twice the size of the former class or size grade

particles by chemical, mechanical, or ultrasonic means and their separation into size categories or grades by sieving and sedimentation (Gee and Bauder 1986). As these particles range from rocks to clays, various methods of their classification have been developed using arbitrary size classes or limits as illustrated in Table 4.1.

After color determination, grain-size determination is the most fundamental test performed on soil/sediment samples. Three general size or textural classes are used by most investigations to show the textural divisions in a particular sample. These are plotted on ternary diagrams whose axes are 100 % clay, silt, and sand (Fig. 4.1). In the United States, the standard protocol is to use the US Department of Agriculture (USDA) classification of the texture of sediments. In Europe, and elsewhere, the particle size classes vary slightly from that of the USDA scheme. An in-depth reconciliation of the various classifications is described elsewhere (Hodgson 1978). The USDA terminology has gained wide acceptance outside the United States, but even in countries such as Belgium and the Netherlands, where the USDA

terminology is used for other soil features—horizons, contacts, mineral content, etc.—these countries have set up their own particle size classifications (*Supra*, 54). While this heterogeneity looks to be the case for the foreseeable future, the use of the ternary diagram to represent the variety of particle size classes is relatively a standard practice. Figure 5.1 shows the USDA particle size scheme (a) together with examples from (b) Belgium, (c) France, (d) Germany, (e) Switzerland, and (f) England and Wales.

Typical PSA methods require the sediment to be broken down in to its individual particles by both chemical and physical means. This two-part procedure is necessary in most sediments where clay minerals comprise a significant portion. The larger size particles (>2 mm) are sorted and sized by the use of wire-mesh screen sieves in mechanical shakers (Fig. 4.9). Of course, the sediment must be dry before either mechanical or chemical sorting is to be attempted. The ease of sorting or dispersion depends on the nature of the sediments. Because of this fact, there is no one “standard” PSA technique.

Sediments rich in organics and clays are plastic and require substantial chemical pretreatment with agents such as sodium hexameta-phosphate (HMP), hydrogen peroxide, sodium hypochlorite, sodium hypobromite, and potassium permanganate. Acid treatments are generally to be avoided because these reagents, such as HCl, can destroy the lattice of clay minerals. HMP is the most commonly used dispersant chemical and is recommended in microbotanical separations of pollen and phytoliths (Yaalon 1976; Rovner 1996a).

For small-size particle aggregates such as the clays, ultrasound is used to cause dispersion. Ultrasonic baths operate on the transmission of the high-frequency sound waves through the sediment or soil suspension. Bubbles form and burst creating a “sonic cavitation” that disperses the most highly aggregated particles without damage to the individual grains. Ultrasound can be used without chemical dispersants. Simple suspensions of distilled water are routinely used. Sediments or soils rich in calcium

(pedocals), iron oxides (pedalfers), clays, and organic matter all disperse well in ultrasound baths. Still Mikhail and Briner (1978) insist that a stepwise pretreatment of a sample with H_2O_2 , weak acid wash, and sodium hypochlorite saturation before ultrasonic treatment produces the best results.

Mechanical sieving is the first step in PSA. Screen sieve sizes have long been standardized, and the problems and limitations inherent to this method are well understood (Day 1965). Reliable sieving requires the use of mechanical shakers that are sets and forgets such that consistent results can be expected. Pansu et al. (2001) provide a comprehensive review of grinding and sieving equipment in their text on soil analysis. If one does not use ultrasonic dispersion, sedimentation techniques follow most sieving using pipette or hydrometer methods. The settling of small particle grains such as the clay minerals follows Stokes’ law in the form:

$$v = g(\rho_s - \rho_i)X^2/18\eta$$

where v (mm/s) is the settling velocity of the particle; ρ_s (kg/m^3), the particle’s density; ρ_i (kg/m^3), the liquids density; X (mm), the particle size; and η ($\text{kg}/\text{s}/\text{m}$), the viscosity of the liquid. g ($9.8 \text{ m}/\text{s}^2$) is the gravity. Stokes assumed particles to be spherical, an assumption that does not affect the results too drastically given that many particles do not meet this criterion, notably the clays. The diameter of the particle, and hence its size, is obviously more critical than sphericity. To do PSA of the sediment fraction, two methods or apparatus are generally used: (1) a pipette method and (2) a hydrometer method. Both have variants and are described in detail in most works on PSA technique. Much like one’s choice of dispersal techniques, the specific method is the one that most effectively accomplishes the goals of one’s analysis of a specific type of archaeological sediment. All are somewhat time consuming with typical times of 20 h for clay dispersal (Rockwell 2000). Examples of each sedimentation method are presented below.

4.7.1 Hydrometer Method

This technique is commonly utilized to assess the clay fraction of sediments samples. The technique allows for rapid, multiple measurements from the same solution/suspension. The standard hydrometer used in the United States is ASTM 152H model. The upper stem of the hydrometer is graduated to determine the settling depth, h , for particles of diameter, X . The settling depth (mm), h , is directly related to the graduated reading, R , (ml) on the hydrometer stem. For an ASTM 152H, the empirical calculation is

$$h = -0.164R + 16.3$$

To calculate X , the variant of Stokes' law used is

$$X = \theta t_{1/2}$$

t = temperature ($^{\circ}\text{C}$), and $\theta = 1,000$ (Bh) $^{1/2}$ where $B = 30\eta(\rho_s - \rho_i)$; the units are discussed above.

One can continue to obtain the concentration of the clay fraction in g/l from the simple calculation $C = R - R_L$ where R_L is the hydrometer reading of a blank solution. These readings are taken at the same time intervals (e.g., 1.5 h, 24 h, etc.). The term, summation percentage, P , is equal to $C/C_o \times 100$ where C_o is the oven-dry weight of the total sediment sample. For instance, the percentage of the clay fraction in the sample is given by

$$P_{\text{clay}} = m \ln(2/X_T) + P_T$$

T is the time interval and m is the slope of a summation percentage curve between two time intervals T_1 and T_2 . The hydrometer may be used to determine the sand fraction percentage which, plus the clay percentage, may be subtracted from 100 to obtain the silt percentage in the sample; % silt = 100 - (% clay + % sand).

4.7.2 The Pipette Method

The method most commonly used to determine silt and clay size fractions, in a sediment sample,

is the sedimentation pipette method as described by Day (1965) and Green (1981). The sample sediment suspension is placed in a 1 l cylinder after 10 ml of HMP has been added together with distilled water to make the 1 l volume. Using a Lowy pipette, a 10 ml sample is withdrawn from the cylinder at a depth of 200 mm at set time intervals. A typical sequence, suggested by Catt and Weir (1976), is as follows:

| |
|---|
| 57 s = 0.063 mm or 4 φ fraction |
| 3 min 48 s = 0.031 mm or 5 φ fraction |
| 15 min 12 s = 0.016 mm or 6 φ fraction |
| 1 h 48 s = 0.008 mm or 7 φ fraction |
| 4 h 3 min 12 s = 0.004 mm or 8 φ fraction |

These aliquots are drained into pre-weighed aluminum evaporating dishes. These weighing dishes are placed in an oven at 105°C to dry. The dishes are then weighed and the weight percentage per fraction calculated. The silt size fractions are determined similarly using established settling times from tables. Pearson et al. (1982), in a successful study of inundated archaeological sediments, used the following particle size analysis on an average 150 g sample, following Folk (1968), which were analyzed in a two-step procedure—coarse fraction then fine fraction:

Course Fraction (Steps 1–7)

1. Coarse fraction samples soaked in water for 24 h to disperse clays then dried (air).
2. Weigh sample.
3. Sample soaked, in water, to further disaggregate clays.
4. Sample wash through a 4 φ (0.067 mm) wet sieve screen to remove all the fine (silt and clay) fraction.
5. Sample dried and weighed.
6. Subtraction of this weight (5) from the prewash sample weight yields the fine fraction weight.
7. Depending upon the particular size classes of interest, e.g., five to eight 1 φ divisions, further separation of the coarse fraction is done by sieving.

Fine Fraction (Steps 8–11)

8. The fine fraction sample is dispersed with calgon at a concentration of 2.1 g/l.
9. The sample is placed in a 1,000 ml beaker and vigorously stirred.
10. Pipette samples, with a standard (Lowy) pipette, are drawn at various times (up to 8 h) at various withdrawal depths for a total of seven withdrawals/samples.
11. Each withdrawal is dried, weighed, and analyzed at selected size division (e.g., 4 ϕ –100 ϕ).

4.7.3 The Modified Pipette or “Fleaker” Method

A new procedure, reported by Indurante et al. (1990), has the advantage over the standard pipette method described by Day (1965) and Green (1981). The principal difference is the use of a single vessel, called a “fleaker,” to disperse and pipette the sample. The fleaker is a 300 ml vessel that is a combination of the beaker and Erlenmeyer flask forms. Aliquots are taken from the fleakers in a manner similar to that described above. These are dried and weighed to arrive at estimates of the silt and clay fractions in the following manner.

Five grams of soil is placed in the 300 ml fleakers that are tared to 0.001 g. Five ml of sodium metaphosphate solution (50 g/l) is added to the fleaker with a pipette. The mixture is then diluted to the 100 ml level, and the fleaker stoppered and put on an Eberbach shaker for 8–12 h at slow speed. After shaking, the mixture is diluted further to 250 ml, stoppered again, and vigorously shaken by hand for 1 min. The sample is then allowed to settle for a 1.5–2 min interval. A 20–25 ml aliquot is withdrawn at the 5 cm depth with the time noted. The mixture is, thus, repeatedly sampled in this manner with the respective samples being drained into weighing cups, typically of lightweight aluminum, that are tared to 0.001 g and placed in a drying oven. The

remainder of the liquid remaining in the fleaker, after the respective size samples have been withdrawn, is rinsed into a 63 μm sieve. Any sand recovered in the sieve is rinsed with deionized water and placed in a container to be dried overnight as the other samples. The containers are then weighed to 0.0001 g and the fractions compared to the particular particle size scheme used in the procedure (U.S. Department of Agriculture or GAO) (Fig. 4.1).

4.7.4 The Imhoff Cone Method

Volumetric Procedure: Fill an Imhoff cone to the 1 1 mark with a well-mixed sample.

Settle for 45 min.

Record volume of settleable solids in the cone as ml/l.

Sediments: Fill the Imhoff cone to the 1 1 mark with a well-mixed sample of 100 g.

The size fractions—sand, silt, and clay—can be estimated using the graduations on the cone.

Settle for 0.25–0.50 h, regardless of soil texture. Sofka et al. (1992) observed that even for clayey soil, settling is fairly rapid, since most of the suspension occurred as aggregates rather than individual primary particles. Furthermore, the amount of additional soil settling out of suspension from 0.5 to 1.0 h is negligible (1–2 %) and causes no serious errors if a 0.50-h settling interval is inadvertently exceeded (Carter et al. 1985, unpublished data).

Sediment remaining in suspension after 0.50 h is the nonaggregated clay fraction (Gee and Bauder 1986) (cf. Fig. 4.13). The entire contents of the Imhoff cones are then decanted, with rinsing, the volume of sediment in each sample can be measured, and each sample dried in an oven at 60 °C, weighed, ashed in a furnace at 500 °C, and weighed again to determine both ash-free dry mass and the mass of inorganic matter in each sample. The mean of replicates of both granular (sand fraction) and nongranular (silt-clay) fractions is used to calibrate the dry-weight densities of each fraction. Still, after settling, the volume of granular and nongranular sediment

Fig. 4.13 Imhoff cone and soil auger sample. Suspected B horizon shown separating in Imhoff cone



in the cone can be assessed because this interface is generally obvious, separating sand from clay-silt fraction.

In many respects, the use of the Imhoff cone mimics a settling column. Its principal advantages are its ease of use, portability, and speed. The Imhoff cone method cannot replicate the settling column nor fleaker methods for exactitude in determining particle size fractions

4.7.4.1 Statistical Parameters and PSA

Particle size analysis and all of the other four techniques, presented in this chapter, require

standard parametric statistical estimators to be applied to the data they produce. These estimators include mean, variance, and standard deviation together with parameters such as skew, sorting, etc. Some of these measures will be discussed in some depth in Chap. 8.

4.7.4.2 Point Count Analysis (PCA)

Point counting analysis is time-honored technique developed in sedimentary petrography for the determination of the proportions of various minerals in a thin section of a rock specimen (Carver 1971). The assumption is that the results

of a point count will accurately reflect the percentage of a particular component—feldspar, quartz, pyroxene, pyrite, etc., within the sample—and, to a larger degree, the percentage of that mineral (or particle size) within the source from which the sample was taken (the Delesse Relation). PCA as implied was developed by petrographers to assess the mineral content in whole rocks using what is a sampling technique. Shackley (1975) has applied point counting to archaeological sediments. In PCA studies, much discussion is given to the number of grains that should be counted. This is to be expected as PCA is a sampling, n , of a larger population, N , wherein common statistical estimators such as average, mean, standard deviation, and variance are used to characterize the relationship of the sample to the population. Chapter 8 will discuss statistical procedures commonly used in archaeological geology rather than embed that discussion in this topic. Without diverging too far from this goal, it is, perhaps, appropriate to discuss the relationship between particle size and that of the sample size to be counted, n . It is almost a mantra in statistics, that is, as one increases the sample size, n , the approximation of estimators for N , the population, is more assured by the Law of Large Numbers (cf. Chap. 8).

One cautionary side of this is that the result one obtains is uninformative as it represents estimator values that are so “average” as to be of no real value. This is to say that if one counts enough of anything—mineral grains, pottery sherds, people, etc.—the statistical estimates of those large samples will be so homogenous as to unreflective of important subpopulation differences such as the difference in igneous rock types—basalt versus rhyolite, phases of pottery, and different cultural groups. This is a conundrum present in all sampling studies—what value of n is large enough to detect important population differences yet not so large as to mask the very differences we seek to detect and reliably estimate? Another way to express this problem is to cast it in terms of randomness versus nonrandomness. Too large a sample, n , allows for the suppression of nonrandom trends or differences such that the results are reflective

of random processes at play in all populations. About PCA, much ink, and rightly so, has been spilled over the appropriate procedures to be used in arriving at reliable estimates of the constituents of rock or sediment aggregates as counted from a thin section or facsimile thereof. These discussions extend down to the grid type, size, and microscope stage to be used. The aim is the same—count enough “points” on the slide to estimate the target population correctly.

What is the sample size, n , that best estimates grains smaller than a cobble and larger than a clay? Assuming that most samples are either rock or sediment specimens with grains of sand size or less, then the grain count will fall somewhere between 100 and 1,000. Sample counts of between 200 and 400 grains are fairly standard in studies of foraminifera, pollen, and sedimentary rocks (Martin 1970; Bryant and Holloway 1983; Krumbein and Pettijohn 1938). Krumbein (1938) has graphically illustrated the estimation of probable error in varying sample sizes used in PCA (Fig. 4.3). According to that analysis, it can be seen that the probable error stabilizes between 5 % and 15 % at about 300 grains. It is easy to see why this sample count is so commonly used in pollen studies.

In microbotanical (pollen, phytoliths) and microfaunal (forams) studies, the sample is dispersed, in solution, across a counting slide which can be gridded or can be covered by a glass coverslip, appropriately divided for counting purposes. Such standardized items exist for these particular analytical procedures. In geology the most commonly point-counted sample is the rock thin section. More often today, the sediments examined by PCA are in their section mounts as well (Goldberg 1999). Still, it is not uncommon to see sediments dispersed, as evenly as possible, onto the gridded card or glass slide covered with a mounting spray cement (Gagliano et al. 1982).

Most PCA is done using stereomicroscopes of relatively low-power (7X–30X) magnification. Depending upon the specific goals of the PCA, the microscope can be either petrographic or not. If mineralogical identification is important, then a petrographic capability is required. This would

be the case in studies of archaeological stone such as marbles, granites, or other building or artifactual rock. It would be useful in the identification and characterization of temper found in earthenwares. For instance, in a thick (100 μm) thin sections, one should readily differentiate the quartz and feldspars on the basis of bright second-order interference colors under crossed polars (XPL). At standard thin section thickness, 30 μm , polarizing filters allow the full gamut of mineralogical identification (cf. Chap. 6). When examining slides for pollen and the smaller phytoliths, polarized microscopy is not required and, in most cases, would impede the PCA. This is because the transparency of the grains is important to making a reliable identification based on particle shape and texture (Rovner 1996b). A raster-type microscope stage (X-Y direction) is used to move the appropriate grid distance across the slide, counting grains at the grid intervals, until the selected grain sample count (n) is reached.

As Van der Plas and Tobi (Van der Plas and Tobi 1965) have pointed out, in their discussion of the reliability of point counting results, it is determined not only by the number of grains counted but on the distance between points as well. Their point is that there is an obvious relationship between a sample's grain size and the point distance chosen for its modal analysis. For instance, it would be patently foolish to choose a point counting distance of 0.2 mm if all or most of the grains were 2 mm in diameter. The grain/point sizes will vary, and therefore, the point counting protocol must be flexible to match analytical requirements of the specific case. Van der Plas and Tobi (1965) stress that "the point distance chosen should be larger than the largest grain fraction that is included in the analysis."

4.7.5 Organic Content Determination Methods

Other important parameters—TOC (total organic carbon) and LOI (loss on ignition) along with mineral oxides (FeO, MgO, etc.) together with water content—are provided in most analytical

packages at fee-service laboratories. Of these the organic content can be determined in most laboratories without too much difficulty. The mineral oxides are generally done with analytical methods (XRF, etc.) that may or may not be readily available in most labs. A discussion of these analytical methods is presented in Chap. 7.

Total Organic Carbon (TOC) Total organic carbon is the sum of organic carbon in the soil. While new instrumental methods have been developed in recent years, most soil testing laboratories routinely use one or the other the following: (1) wet digestion and (2) colormetric (Soil and Plant Analysis Council, Inc 2000).

The wet-oxidation digestion method uses potassium dichromate ($\text{K}_2\text{Cr}_2\text{O}_7$) with external heat (hot plate) and back titration to measure the unreacted dichromate which serves as the proxy for the carbon content. Typically 0.1–0.5 g. of soil is added to a 500 ml Erlenmeyer along with 15 ml of dichromate reagent. The mixture is then boiled for 30 min. After cooling, three drops of the indicator solution, n-phenylanthranilic acid, is added and the mixture titrated against Mohr's salt solution, ferrous ammonium sulfate, until a color change from violet to bright green is observed. The % organic matter = $\{[\text{meq K}_2\text{Cr}_2\text{O}_7 - \text{meq FeSO}_4 \times 0.3]/\text{g soil}\} \times 1.15$. Here meq. is milliequivalents.

The colormetric procedure uses the property of absorbance as discussed, in detail, below, in reference to phosphorus determination. Here, 2.0 g of soil is placed in a test tube to which 20 ml of sodium dichromate solution is added. The reaction is exothermic, and after the mixture is cooled (40 min to 1 h), it is allowed to stand for 8 h. Aliquots of the clarified solution are then transferred to the spectrometer for absorbance measurements at 645 nm wavelength (*supra*, 178). The values so obtained, when plotted in comparison to standard curves, yield the organic content.

Loss on Ignition (LOI) This method has become comparable in reporting to that done by the methods just discussed. It is equally effective for the analysis of soils containing low to very

high organic matter (OM) (*supra*). It has a sensitivity of 0.2–0.5 % organic matter. A sample of 5–10 g soil weight (W) is placed in an ashing vessel. The vessel is first placed in a drying oven at 105 °C for 4 h. Once cooled, the sample is weighed to the nearest 0.01 g and then placed in a muffle furnace at 400 °C for 4 h. The sample is removed, cooled, and weighed again. To calculate the % organic matter, one uses the formula:

$$\% \text{OM} = [(W_{105} - W_{400}) \times 100]/W_{105}$$

4.7.5.1 Bulk Density

Bulk density is the average dry weight per unit volume of soil. Depending on the nature of the sample, fine or coarse grained, the principal method is to determine the matrix bulk density by addition of paraffin and subsequent measurements. The sample is first dried and weighed then soaked in paraffin, dried, and weighed again. This determines the weight (and volume) of the paraffin. Finally, the sample is immersed in water and weighed. Bulk density, in g/cm³, is calculated thus:

$$\text{Bulk density} = (\rho_w)(WC_d)/WC_p - WC_{pw} + [(W_p)(\rho_w)/\rho_p]$$

where ρ_w is the density of water; WC_d is the dry weight in air; WC_p is the waxed weight in air; WC_{pw} is the waxed weight in water; W_p is the weight of the paraffin; and ρ_p is the density of the paraffin.

For fine-grained samples (size <<2 mm), the procedure is straightforward. With coarser, gravel-rich samples, some error can be introduced by the size of the large clasts. A sample should be broken apart to determine the amount of these clasts within a sample. As a result, the bulk density so determined is more an average value and less a specific value for an individual sample. Elevated bulk density values are typical of older soils with significant clay and carbonate volumes (*supra*).

4.7.5.2 Carbonate Content

The amount of calcium carbonate in aridisols, marine, and lacustrine sediments can be significant and must be accurately measured. Like the

straightforward manner of basic mineral determination, of the introductory geology laboratory, the use of hydrochloric acid is required. In this more rigorous determination, the HCl release of CO₂ gas is collected and measured by the use of sealed flask and graduated column apparatus called the Chittick method (Singer and Janitsky 1986). The evolved gas displaces a fluid (colored water) into the graduated column. This value is divided by the original sample weight to determine the carbonate content generally reported as percent (%) (*supra*).

4.7.5.3 Phosphorus Analysis (PA)

As Joseph Schuldenrein (1995) states “P (phosphorus) appears to be the most generic indicator of anthropogenic input...” for archaeological sediments. The importance of phosphorus analysis in archaeology was first recognized by Arrhenius (1931), but it was R. C. Eidt who established the systematic use of the phosphate method in evaluating anthropogenic sediments (Schuldenrein 1995). Eidt, his co-workers, and students established the processes, chemistry and chronology of phosphorus, as phosphate compounds, in archaeological sediments (Eidt 1973, 1977, 1985; Sjöberg 1976; Woods 1977). The assumption is that the magnitude of human impact on a landscape can be demonstrated by the total phosphorus concentration such that archaeological sites and inter-site activity areas/features can be isolated. Phosphorus occurs in sediments as either bound (non-labile) or unbound/free (labile) phosphate compounds. The labile forms correspond to Al and Fe phosphates. As we have discussed, bound or occluded forms of Al and Fe phosphates develop as inorganic compounds in soil horizons.

Inorganic compounds are (a) those containing calcium and (b) those containing iron and aluminum. The solubility of inorganic calcium compounds increases with the increased simplicity of the compound, but the simpler compounds are only available in very small quantities, and they easily revert to insoluble states. The fixation of phosphates, when the pH value is in the range of a little less than 8.0 and 8.5, is mostly in the form of calcium phosphates. In alkaline soils,

phosphates will react with the calcium ion and with calcium carbonate. The next step includes a conversion of the calcium phosphate ($\text{Ca}_3(\text{PO}_4)_2$) to insoluble compounds, such as hydroxy-, oxy-, carbonate-, and fluorapatite (insoluble apatite compounds are formed at pH levels of above 7.0) compounds, the latter being the most insoluble compound known. An excessive amount of calcium carbonate (CaCO_3) produces very insoluble compounds. At a pH level of between 6.0 and 7.0, phosphate fixation is at its minimum.

It is not within the scope of this book to fully describe the extremely complex and incompletely investigated phosphorus cycle in sediments. It is important to mention the potential sources of both anthropogenic and non-anthropogenic sources such as geology and soils. After mineral sources in sediments, and soils, the bulk of phosphorus is from organic matter such as dead plants and animals that decompose in the soil. Phosphorus is an important energy source in organisms particularly as a component of the ATP (adenosine triphosphate) molecule. As a result, all plants and animals contain significant amounts of phosphorus in their tissues which is incorporated into sediments after their deaths. In addition, humans and animals excrete large amounts of phosphorus as both feces and urine. Plant and animal decay, burials, refuse coupled with urine, and excrement increase the phosphorus content of soils above ambient levels. The accumulation of this phosphorus in anthropogenic soils, if it can be fixed into insoluble forms, can have long residence times—millennia in many cases—and provide a relatively reliable geochemical marker of archaeological interest.

4.8 Determination of Total Phosphorus by Perchloric Digestion

Information on this method is found in Eidt and Woods (1974) and Woods (1977). The methodological procedure in the chemical analysis is described through the steps noted in Fig. 4.4.

The method extracts *total phosphorus*, i.e., both organic and inorganic phosphorus compounds. The accuracy level of the method of the analysis ranges between 95 and 98 % recovery. All samples are dried overnight in an oven at a temperature of around 50 °C. Samples consisting of very fine particle sizes are ground directly after having been dried, while samples with coarser particle sizes have to be screened. The choice of sieve size was made so that the sieved sample would have the same particle size as the ground one. A half gram of each sample is put into a graduated digestion tube, to which is added 2 ml of perchloric acid (HClO_4) and nitric acid (HNO_3), respectively.

The tubes are then placed in an aluminum heating rack under a perchloric acid fume hood. The HNO_3 is boiled off at a temperature of 170 °C. After a stepwise increase to 225 °C, the remaining HClO_4 is left to boil for 1 h. The tubes are checked regularly to prevent being boiled dry. After the digestion, the volume of each tube is raised to 50 ml with distilled H_2O , stirred, and left to rest for a period of at least 12 h. A stock solution is made consisting of (a) 9.0 g ammonium molybdate ($(\text{NH}_4)_6\text{Mo}_7\text{O}_{24} \cdot 4\text{H}_2\text{O}$) and 0.2 g potassium antimony tartrate ($\text{K}(\text{SbO})\text{C}_4\text{H}_4\text{O}_6 \cdot 1/2\text{H}_2\text{O}$), which are mixed in 500 ml of H_2O and (b) 65 ml sulfuric acid (H_2SO_4) and 335 ml of H_2O . Initially mixed separately, the (a) and (b) reagents are mixed together and volume raised to 1,000 ml with H_2O .

A primary standard solution, with a concentration of 1,000 $\mu\text{g/g P}$, is made by dissolving 4.387 g potassium phosphate monobasic (KH_2PO_4) in sufficient H_2O to yield 1,000 ml. A secondary standard solution, with a concentration of 10 $\mu\text{g/g P}$, is made by adding 40 ml HClO_4 to 10 ml of the primary standard solution and dilution with H_2O to a volume of 1,000 ml. Working standard solutions ranging from 1 to 6 $\mu\text{g/g P}$ are made from the secondary standard solution. The color-developing solution, freshly made for every batch of 100 samples, consists of 2.0 g ascorbic acid mixed with 200 ml of the stock solution and raised to 1,000 ml with H_2O . Five milliliters of the color-developing solution is added to 1 ml of each of the working

standard solutions as well as to 1 ml of the samples. After 1 h, their absorbencies are read on a colorimeter at a wavelength of 740 nm. The absorbance of the standards is plotted against the known concentration.

The chemical analysis, as just described, is accurate and has good reproducibility. A linear regression of P content and absorbance gives a correlation coefficient (r) of 0.9998 (cf. Chap. 10 for a detailed discussion of linear regression). The regression line is a linear relationship between absorbance and concentration judging from the r value of 0.9998 and the straight line. Beer's law states the following: "the fraction of light absorbed is directly proportional to the concentration of the colored constituent." The phosphate determination conforms closely to Beer's law: the slope of the regression line is just below optimal linearity as is expressed by the regression equation $y = 0.0957x + 0.0028$. A direct proportionality, as stated by Beer's law, would mean $y = 0.1x$.

4.9 Absolute Phosphate Analysis Versus Qualitative Color Tests

Total phosphorus-bound fraction analysis versus those of labile or less bound phosphates has little or no comparative value. The latter phosphates can be qualitatively detected by methods similar to the familiar litmus strip test for acidic/basic solutions. In the qualitative phosphate test, one measures the intensity of color produced in a spot test on paper or in a small tube. While somewhat subjective and decidedly not quantitative, the color test has economy and ease of application in a field setting on its side. At the site of Great Zimbabwe, researches from Lund University used both quantitative, bound phosphate analysis and the field color tests with good effect (Sinclair 1991, 1996, Personal Communication; Sinclair and Pétron n.d.). The Swedish team, in extensive coring tests, extracted phosphates in column samples to measure the extent, vertical and horizontal, of the famous African Iron Age site.

Intercomparison of their data—relative color intensity and the absolute colorimetric determination—showed similar findings in the measurement of site extent (Fig. 4.14).

Like Sinclair (*supra*), Barba used the phosphate spot test. On house floors at Manzanilla (2007), Barba and Lazos (2000) detected nonrandom, linear patterns on floors in the phosphate data that suggested heavy traffic on stairs and around the altar (Barba 2007).

Cavanagh et al. (1988) utilized a "cheap, robust" colorimetric phosphate procedure developed by Craddock et al. (1985) to assess site parameters at Laconia, Greece. Craddock et al. (1985) developed the molybdenum blue method to analyze multiple samples in a relatively short time. Like the simpler, qualitative tests used at Great Zimbabwe, the procedure used at Laconia examined the total phosphorus present without the extraction of the bound (P_2O_5) "total" component as accomplished by the perchloric acid technique described. The molybdenum blue method is described as follows: (1) Beginning with excavated/cored 10 g soil/sediment samples that are (2) air-dried and screened through 1 mm metal sieves, (3) 1 g subsamples are digested in (4) 5 ml of 2 N HCl boiled for 10 min. (5) A 0.2 ml aliquot is removed and 10 ml of molybdenum blue reagent is added, and (6) the liquid is analyzed with a colorimeter standardized to zero optical density with a phosphorus-free reagent. Like the perchloric approach, a set of eight or more reference samples of known concentrations are used to produce a calibration regression line. If percent transmittance (T) is measured, this can be converted to optical density by the formula:

$$\text{Optical density} = -\log_{10}T$$

The molybdenum blue reagent is mixed from 65 ml H_2SO_4 (6N), 37.5 ml ammonium molybdate (40 g/l), 12.5 ml potassium antimonyl tartrate (2.743 g/l), and 1.32 ascorbic acid (solid) as suggested by Murphy and Riley (1962).

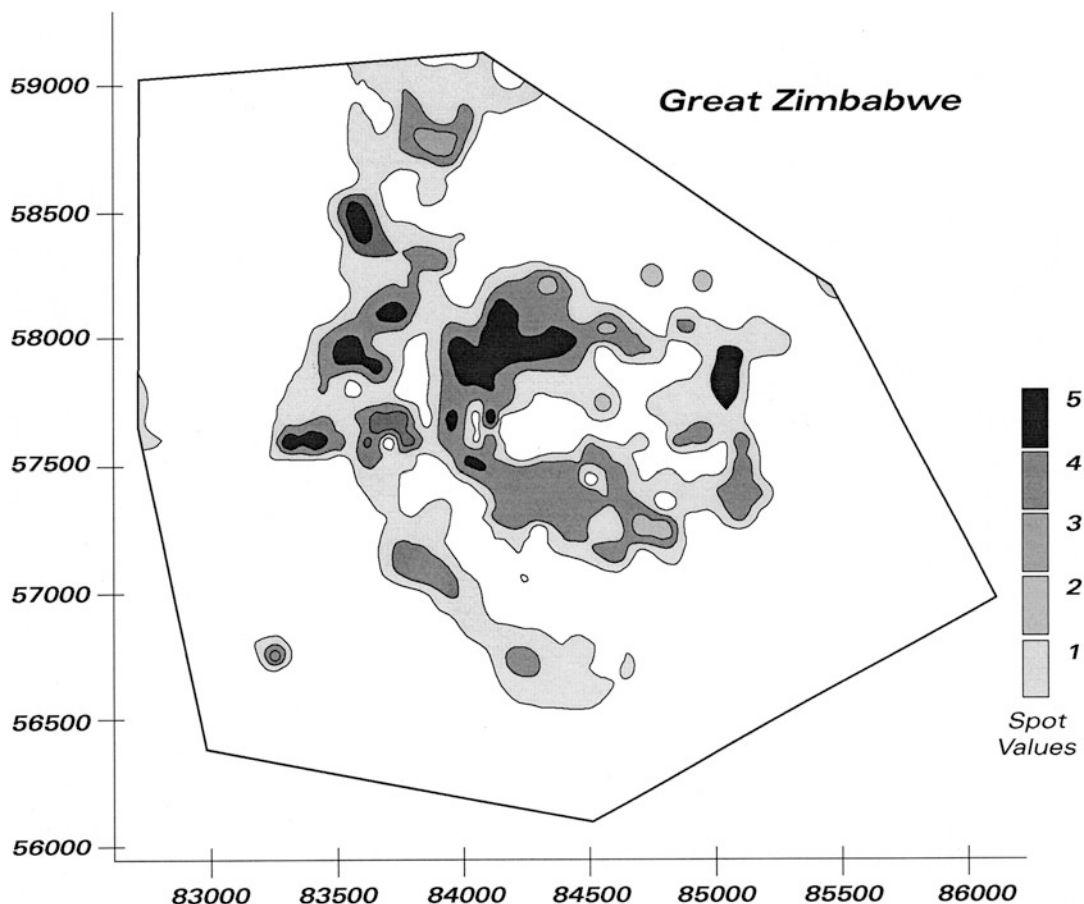


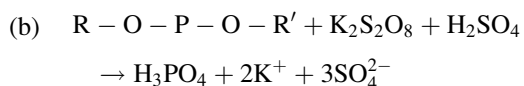
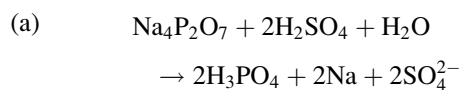
Fig. 4.14 Phosphate intensity plot for Great Zimbabwe using the colormetric method (Courtesy of Paul Sinclair)

4.10 Colorimetry and Spectrophotometry

For the geoarchaeologist, there exist relatively “quick and dirty” methods for ascertaining total phosphorus without recourse to elaborate laboratory techniques such as perchloric digestion. This latter technique is essential for a thorough, quantitative determination of the bound and “condensed” phosphate fractions. One other component of the total phosphorus is that of the labile or orthophosphate fraction. This is helpful to archaeologists as it can be readily determined in the field.

The most common procedure is acid hydrolysis of the organic and condensed inorganic forms (meta-, pyro-, and other polyphosphates) to reactive orthophosphate (Hach Water Analysis Handbook

1992). Pretreatment with an acid (sulfuric, nitric) and heat provides the conditions for hydrolysis of the inorganic fraction: (a) organic phosphates are converted to orthophosphate by heating with acid (acid oxidation) and persulfate (b).



In (b) R and R' represent various organic groups. If one determines the total phosphorus by the second method (b), it can then be followed by the reactive phosphorus test. By subtracting

that amount from the total phosphorus result, one can determine the organically bound phosphate which is a good indicator of cultural deposits of archaeological interest. The analysis of reactive phosphorus—the orthophosphate—can be done using a field spectrophotometer. Orthophosphate absorbs at the 890 nm wavelength, in the Hach field spectrophotometer, and produces reliable measurements, in mg/l of PO_4^{3-} . Using the same device, one can assess the total phosphorus (PO_4) using either the acid persulfate digestion method or the ascorbic acid method (Hach water analysis handbook, 2nd edn 1992).

Colorimetry and spectrophotometry rely on straightforward principles where the color of a molecule in solution, such as phosphorus, depends on the wavelength of light it absorbs. When a sample solution is exposed to white light, certain wavelengths are absorbed, and the remaining are transmitted to the eye or a photometer. In our discussion of the determination of total phosphorus by perchloric acid digestion, the final measurement is to test absorbance in a light cell where the absorbance and concentration of the unknown is determined from an absorbance versus concentration curve, for the element of interest, in our case, P, constructed by the use of standards. The absorbance, A , is generally defined as the $\log(P_o/P)$ where P_o = incident light intensity and P = intensity after absorption. Using Beer's law, $A = a \cdot b \cdot c$, where a = molar absorptivity (%), b = path length (μm), and c = concentration (g/ml). We hold a and b constant, and measure c concentration by the spectrometer.

structure of spatial patterns in natural and non-natural layers using microscopic techniques.

Goldberg (1995) has used resin impregnation of soil/sediment blocks as a precursor to producing thin sections of the clastic materials for use in micromorphology. Undisturbed sample soil/sediment blocks are taken from the field profile. These samples are then impregnated, in a vacuum chamber, with epoxy resin. In this matrix, after hardening, the sample can be treated like a rock sample and sawn to produce viewable thin sections of standard dimensions. This procedure is finding increasing application in the geoarchaeological studies of site deposits (Courtney, Goldberg, and Macphail 1989). At the thin section scale, undisturbed, oriented samples are examined by the microscope—petrographic or otherwise (SEM; CL) (allowing for observation of composition in mineralogical terms, texture, and fabric) the geometric relationships among constituents (*supra*).

Courtney describes soil micromorphology as the integrated use of various microscopic techniques to study the arrangement and nature of the components that comprise sediments and soils (1992).

She, particularly, discusses the micromorphologic study of sediments and soils as an essential component of environmental reconstruction. Likewise, it helps identify the various kinds of domestic and specialized activities that are involved in the formation of living floors and other anthropogenic surfaces (*supra*). Microstratigraphic changes can reflect changes in depositional processes.

Additionally, soil micromorphology has been applied to the study of stone tools (Fladmark 1982). Microdebitage is defined as all stone flaking residue less than 1 mm in maximum dimension (Susino 2010). Lithic microdebitage is produced during lithic tools and rock engraving manufacture. For tools or rocks containing quartz, small particles persist as microwaste initially on the ground surface but later as particles that are incorporated into sedimentary deposits associated with the occupation site. Experimental replication indicates that it is produced in great quantities by stone tool

4.11 Micromorphology: Describing Archaeological Sediments and Soils with the Microscope

Kubiëna (1938) first introduced the study of undisturbed soil samples using microscopic techniques. He became the founder of soil micromorphology and published in 1938 his book *Micropedology*. Soil micromorphology can be defined as follows: the *in situ* study of the

manufacture and can permeate site matrices as a permanent signature of past cultural activity.

If microwaste is distinguished from naturally occurring sediments, then microwaste and/or its surrounding sediment provides a mechanism for establishing lithic use in archaeological deposits. Identification of microwaste is undertaken by comparing the shape of microwaste particles with those from surface sediments, taking particular note of angularity and irregular shapes, and by analyzing quartz or other toolstone grain morphologies. On the basis of surface features identified on experimental microwaste, particles identified as microwaste can be separated from the sedimentary grains (Susino, *supra*). Scanning electron microscopy (SEM) and light microscopy are used to determine surface differences between pedogenic grains and anthropogenic material from archaeological deposits.

It has been noted that microwaste may lie within or close to the age boundaries of the surrounding strata/sediments but not necessarily where larger lithic material is found. Microwaste is incorporated into sediment and may not be subjected to the same degree of movement as larger lithic waste and stone tools within the deposit. Indeed, Baker (1978) noted smaller artifacts from the surface are proportionately fewer (53.3 %) compared to the proportion of smaller artifacts within a total cultural deposit (61.5 %). One possible reason for this, *per* Baker, size effect, is that smaller artifacts might tend to be trampled into the sediment or soil and larger artifacts are not resulting in an increased amount of “micro” materials in comparison to larger items—cores, grinding stones, etc.—within a deposit.

Courty (1992) describes three types of cultural deposits. The first or “primary” deposits result from utilization of an activity area (e.g., flint knapping; food preparation). Ash layers are primary cultural deposits. “Secondary” deposits are primary deposits that have suffered modifications in their original settings. Examples of secondary deposits are “dumped” ashes removed from a hearth area, shells consumed and dumped outside the eating area, etc. The “tertiary” deposit were defined by Butzer

(1982) as totally removed from their original settings and, in many cases, reused for other purposes. The most obvious example of this would be the digging of a berm or terrace where fill is “robbed” from its original deposition locale and redeposited in another.

Some skill in petrography is suggested by Courty (*supra*). This is illustrated by Angelucci’s study of knapped lithic materials in thin section (Angelucci 2010). In contrast to other types of cultural materials, microdebitage is usually not weathered to any degree. From a micromorphological standpoint, micromaterials, such as lithics, fall into the category of “coarse” components. As Angelucci points out, Courty et al. (1989) consider lithic materials as a “mineralogic” component. For instance, “Flint is easily distinguished by its petrographic properties, which include low birefringence and crytocrystallinity...and is exceedingly hard to distinguish natural from worked fragments...” (Courty et al. in Angelucci 2010). This is a bit of understatement as flints or cherts are non-birefringent to the point of optical extinction in most petrographic settings. This caveat, notwithstanding, several authors have reported identification of various lithic artifacts in thin section (Angelucci, *supra*; Bergada 1998), most notably chert or quartzite. The present author has identified toolstone microdebitage from siliceous sandstones and arenites (Garrison et al. 2012a).

Figure 4.15 illustrates the utility of micromorphological study of Neolithic settlements. Micromorphology was used extensively at the site of Arbon-Bleiche 3, a lakeshore site on the Bodensee, Switzerland (Ismail-Meyer et al. 2013).

4.12 Palynology: A Micromorphological Study of Archaeological Pollen

Jean-Claude Gall (1983, 2012), in his book *Ancient Sedimentary environments and Habitats of Living Organisms*, has recognized the kinship of archaeology and geology, in the fact that both face a “fossilized world.” If we are interested in the paleoenvironment of that world, then the only

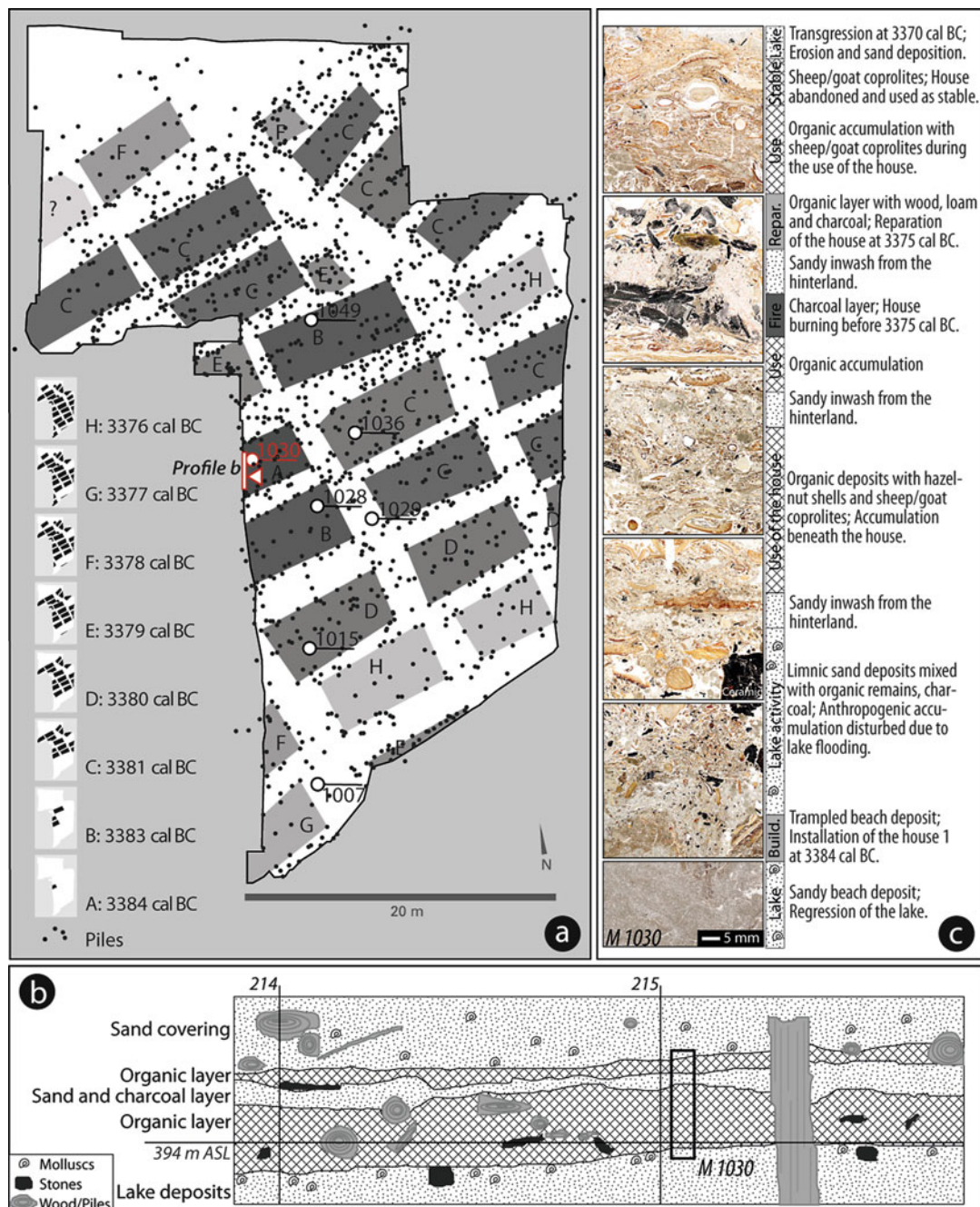


Fig. 4.15 The Neolithic site of Arbon-Bleiche 3 demonstrating the use of micromorphology: (a) site map with the ground floors of the houses and with the eight phases of the village. The pilings of the houses are marked as black dots. The position of the profile section B and the profile photograph (c) are marked with white arrows and highlighted in red. (b) The west profile through house A showing the typical sequence with two

main organic cultural layers divided by a sandy layer. (c) The Arbon-Bleiche 3 thin sections of the column M 1030 (profile B) with the micromorphologically identified phases of installation, organic accumulations beneath the house's floor and inwash of sand from the hinterland surrounding the village (Fig. 4.2 in Ismail-Meyer et al. 2013, used with permission)

recourse is “through the organisms and the sediments” (*supra*). In the case of the archaeologist, one must add cultural (artifactual) remains as well. The study of archaeological sediments and what they contain as “fossils”—organic remains such as floral and faunal materials, artifacts and non-portable cultural features, and textural and chemical indices—can provide a great deal of evidence about a paleoenvironment within which a past human population together with plant/animal communities coexisted.

Soil archives are rich. Plants and trees produce plenty of pollen, invisible to the naked eye in soil layers. Plants can be recognized by their pollen, and when well preserved per layer, a list of species can be determined (Kooistra and Kooistra 2003). Fossil pollen grains and grass spores are preserved in many soils and sediments that are not overly acidic. These elementary reproductive particles are produced in large amounts by both trees and shrubs and the grasses. Some trees, like the pines, produce millions of pollen grains annually. Other plants, by contrast, are more meager in their output such as clover (200 grains per anther). The grains themselves are larger than clay particles (10–100+ μm) and are amenable to optical microscopic study. Pollen grains are tough customers being preserved by a very resistant exine made of sporopollenin. The exine defines the basic morphology of the pollen grain and is distinctive of most higher plants. The palynologist inspects the grains for shape, size, surface texture, and apertures. As a result of over a hundred years of taxonomic studies of pollen, beginning with Lagerheim and his student, von Post (Bryant Jr 1989), in the early 1900s, we enjoy a broad and reliable repertoire of pollen identification keys (Faegri and Iverson 1975; Bryant, *supra*).

Von Post set forth five principles for pollen studies which remain valid today:

1. Many plants produce pollen or spores in great quantities, which are dispersed by wind currents.
2. Pollen and spores have very durable outer walls (exine) that can survive long periods of time.

3. The morphological features of pollen and spores remain consistent within a species; different species produce their own unique forms.
4. Each pollen- or spore-producing plant is restricted in its distribution by ecological conditions such as moisture, temperature, and soil type.
5. Most wind-blown pollen falls to the earth’s surface within a small radius, roughly 50–100 km from where it is dispersed.

As von Post observed, pollen is often produced in significant quantities that survive, in sediments, for long periods and have distinctive, often species-specific forms and is distributed over significant areas, mostly by the wind as “pollen rain.” The pollen of trees is termed arboreal or AP, that of shrubs and herbs, together with some grasses, non-arboreal (NAP). Bryant (1978) lists three factors that influence the preservation of pollen grains in sediments and soils: (1) mechanical, (2) chemical, and (3) biological. Mechanical damage occurs during dispersal and deposition generally by crushing or abrasion of the grain. Chemical corrosion of the exine is related to the pH of the depositional environment such that sediments of 6.0 or higher alkaline degrades pollen and alkaline soils that fix phosphates degrade pollen. Fungi and bacteria can breakdown the pollen. Susceptibility of pollen to corrosion results in the differential preservation of various species. Pine, although produced in large amounts, along with oak (Fig. 4.15), elm, and birch, can be over-represented in pollen spectra by a factor of 4, whereas alder and beech (Fig. 4.16) are direct reflections, percentage-wise, of their occurrence in forest (Andersen 1986).

Archaeologists, as with other scientists interested in past environments, must recognize the various factors that obscure recovered pollen percentages as representational of vegetation composition. Key factors are the biological productivity of the respective plants, dispersal modes and patterns, and grain survivability. For the purposes of archaeological geology, it is less important to this discussion to reprise the specialized discussions of varieties of pollen,

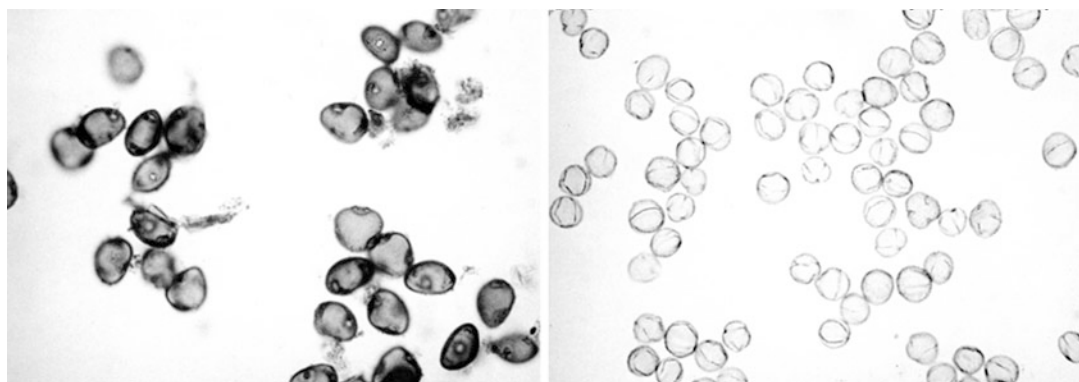


Fig. 4.16 Typical triporate pollen grains: *left*, beech; *right*, oak

their identification, and the various methodological approaches to reconciling pollen spectra to vegetational reality in the past than it is to examine methods for the recovery and extraction of pollen grains.

Pollen, itself, can and should be considered as a sediment. It is an organic component of the sedimentary matrix and *sensu stricto* a defining element of “soil.” In paleosols, pollen is preserved subject to soil geochemistry. Within the peds of a soil, the pollen grains are found with the silt-sized particles. As such, pollen grains are not recoverable with the methods typically used to separate the coarse sediment fraction. Pollen grains are separated by dispersal and digestion procedures. Unlike the techniques used in the separation and preservation of the clay, those used for pollen recovery utilize more caustic reagents such potassium hydroxide, hydrochloric acid, and the high reactive acid, hydrofluoric. Acquiring sediments for pollen extraction and analysis can be done in conjunction with the study and description of a soil/sediment profile. Similar to our example of obtaining a soil monolith, a bloc of material is removed by the use of a trowel or small shovel. Such a bloc or vertical sequence of blocks can be returned to the laboratory for subsequent, systematic removal of subsamples every few centimeters as a general rule.

Coring is a common means of retrieving continuous sediment columns. Of the various coring procedures described, the one most appropriate for the specific study depends in great part on the

sediment/soil being sampled. Cores are taken in wetlands such as bogs, sinks, and shallow lakes where sediments are conducive to pollen preservation. Short, open barrel corers can simply be pushed into soft sediments. Deep cores require mechanical or hydraulic assists. In drier sediments, the rotary, percussion, or drive corers are useful. After recovery, the sediment column is subsampled at selected intervals (ex. 10 cm).

If the sediment is in the form of a core, then some care must be taken to note not only the sampling interval but where that interval is in relation to the *top* of the core. Most investigators stress that the sample be labeled, in terms of distance (cm, mm, etc.), from the top of the core. Until just recently, the author was in complete concurrence with this procedure. Having used geological coring, as a sediment sampling method technique for some time, it now seems that using the top of core, as the point of reference, may not be as appropriate as previously thought. In situations of single cores, using the top of the core as “zero” may have merit, but in the case of multiple cores, across an uneven topography, the stratigraphic relationship between cores, in an absolute sense, may be difficult to determine without some measure of surface elevation, such that each core can be placed in correct relationship to its neighbor. One core must be a reference elevation datum and the others placed in relation to it.

Where elevation data is lacking, it is suggested that the measurement of “zero,” in

the core, may be more useful, if taken from the *bottom* or tip of the core. There is nothing arbitrary about the bottom point of a core. In sampling wetland or submerged sediments, it is not uncommon to lose portions of upper sediments due to suspension/dispersion of light fractions or simple unconsolidation of the sediment by the coring device. In these cases, one does not have a true surface measurement that is coincident with the observed top of sediment in the core sample. By measuring from the core tip, some consistency is assured. In the case of varying surface topography, this procedure “normalizes” the disparity in strata by removing the offset in altitude such that these strata will be observed at their same relative positions, in the core sample, regardless of surface elevation.

Additional caution should be taken in the removal of sediment whether from a core or profile. Scrape the sampling site’s surface removing the surface material with a spatula or trowel that is *cleaned* between samples. Take uniform samples of 0.5–1.0 cm³ (a few grams) in size. A typical extraction procedure is shown in Table 4.2. The sequence of various regents and dispersals removes the sediment matrix containing the pollen and spores. After the pollen grains and spores are extracted, stained, and mounted, a typical sample area, such as 22 × 22 mm, is called “strew” (Rich 1999).

As with point counting, the pollen grain count results in a relative sample frequency. This sample pollen frequency must be converted to absolute pollen frequencies to compensate for disparities in pollen influx at different times such as the difference between fluences of 1,000 and 100,000 cm⁻² although both represent 90 percentile samples. Davis (1969) suggested a novel method to do this by amending or “spiking” the samples with a tracer pollen type in known amounts. Using this method, the number of pollen grains of each pollen type can be ascertained relative to known ratio of the tracer species.

The spike procedure may use something like exotic pollen grains like those of *Eucalyptus*. The concentration of any pollen taxon can then be measured in ratio-proportion to this “exotic” spike by the simple relation:

Table 4.2 Sample preparation for pollen analysis

| | |
|-------|---|
| (i) | Boil sediment with 10 % NaOH or KOH to remove soluble humic acids and to break the sediment down |
| (ii) | Sieve to remove coarse debris |
| (iii) | Treat with cold 10 % HCl to remove carbonates |
| (iv) | Treat with either hot 48 % HF for a short time (up to 1 h) or cold 48 % HF for a long time (up to 24 h) to remove silicates (silt, clay, diatoms, etc.) |
| (v) | Treat with hot acetolysis mixture (9 parts acetic anhydride: 1 part concentrated H ₂ SO ₄) to hydrolyze cellulose |
| (vi) | After neutralization, stain the residue with safranin or basic fuchsin |
| (vii) | Mount the residue in a suitable medium with a refractive index (1.55 which is that of pollen grains. An excellent medium is silicone oil (R. I. = 1.4) |

Courtesy George Brook, University of Georgia Geography Department

Observed spike grains(a)

Total spike grains(b)

$$= \frac{\text{Observed grains of taxon X(c)}}{\text{Total particles of taxon X(d)}}$$

where one simply solves for (d) total particles of taxon X. Of course, using a spike of *Eucalyptus* pollen is precluded in areas where the species occurs naturally or has been introduced (e.g., southern California). Shane (1992) suggests using 7–10 × 10⁴ spike grains/ml such that by adding 0.5–1.0 ml of this spike to a 0.5 cm³ sediment, sample will yield an “ideal” 2 grains of the pollen spike to the sample (Maher 1981). In counting a spiked sample, one procedure is to use a hemocytometer, a thick, specialized slide with apertures (2) for introduction of aliquots into two, separate grids. Once the sample aliquot is placed in the hemocytometer, the grains along the parallel sides of those grid squares marked by “X” are counted and listed in pairs. A total of 30–40 grid squares are counted. The volume/square is about 0.1 mm³ so 10 squares equal 1 ml by volume. One hopes to observe at least 300 grains in a count of at least 5 squares to assure representation statistics. If the counts, done by a palynology laboratory, show a paucity of pollen grains (~300 grains/sample), they will

Table 4.3 Palynological composition of samples from Gray's Reef

| Taxon | Gray's Reef clay | Gray's Reef core 1 | Gray's Reef core 2 |
|-------------------------------------|------------------|--------------------|--------------------|
| <i>Alnus</i> | 2.3 | 1.3 | 2.1 |
| <i>Ambrosia</i> | 0.89 | 0.97 | 0.62 |
| <i>Asteroideae</i> | 1.5 | — | — |
| <i>Betula</i> | 0.59 | 0.97 | 0.98 |
| <i>Carya</i> | 3.6 | 1.9 | 1.2 |
| <i>Castanea</i> | 0.29 | 1.6 | 0.62 |
| <i>Chenopodiaceae/Amaranthaceae</i> | 15.2 | 8.1 | 5.6 |
| <i>Corylus</i> | 0.32 | 0.62 | — |
| <i>Cyperaceae</i> | 1.2 | 0.32 | — |
| <i>Fagus</i> | 0.59 | 0.32 | — |
| <i>Fraxinus</i> | 0.29 | 0.32 | 0.62 |
| <i>Gramineae</i> | 2.7 | 6.8 | 0.98 |
| <i>Iva</i> | 0.59 | 0.65 | — |
| <i>Liquidambar</i> | 1.8 | — | 0.30 |
| <i>Myrica</i> | 1.2 | 0.32 | 0.30 |
| <i>Osmunda</i> | 0.59 | 0.32 | — |
| <i>Ostrya/Carpinus</i> | — | 0.32 | — |
| <i>Picea</i> | 2.1 | — | — |
| <i>Pinus</i> | 41.7 | 56.5 | 67.2 |
| <i>Polygonum</i> | 0.59 | — | — |
| <i>Polypodium</i> | — | 0.65 | — |
| <i>Pteridium</i> | — | 0.32 | — |
| <i>Quercus</i> | 13.4 | 12.7 | 13 |
| <i>Salix</i> | 0.59 | — | 0.62 |
| <i>Sambucus</i> | — | 0.32 | — |
| <i>Sphagnum</i> | 0.29 | 0.32 | — |
| <i>Stellaria</i> | 0.29 | — | — |
| <i>Taxodium</i> | 2.1 | — | — |
| <i>Tsuga</i> | 0.59 | — | — |
| <i>Ulmus</i> | 0.59 | 0.97 | 0.62 |
| <i>Woodwardia</i> | 2.1 | 0.97 | — |
| Indeterminate | 2.1 | 2.6 | 3.7 |
| Totals | 100 | 100 | 99.4 |

Values are expressed as percent of the total identifiable pollen and spores (minimum number of 300 grains: F. J. Rich, unpublished data (in Russell et al. 2009; Table 4.4, Garrison et al. 2012a, b; Weaver 2002)

generally advise against extensive analyses (Table 4.3).

Micromorphology can identify whether pollen may occur in situ, analyze processes of redistribution, or explain why pollen are not found. Palynology can determine pollen and organic materials present in thin sections to the species level, identify the crops grown in arable fields, and explain deposition patterns. In general, micromorphology identifies abiotic conditions, palynology the biotic ones, both with such an overlap in that they can be

complementary. In an integrated approach, their application results in a more complete reconstruction of paleoenvironments and past land usage (Hadorn 1994; Kooistra and Kooistra 2003).

4.13 Phytoliths for Archaeology

Rovner (1983, 1988) describes phytoliths as botanical microfossils that can provide significant paleoenvironmental and archaeobotanical

information. Phytoliths are mineral deposits (calcium, silica) that form in and between plant cells (Mulholland and Rapp 1992). Of the two mineralogic varieties of phytoliths—calcium and silica or “opal”—the latter has formed the bulk of most modern phytolith studies. While both calcium and opal phleboliths exist as either amorphous forms or cell morphology (“cystoliths”), the opal phytoliths exist longer in sedimentary contexts. Fossil opal phytoliths have been reported in sedimentary rock millions of year old (Jones 1964). Bryant (1974) has reported both calcium and opal phytoliths in ancient coprolites, but the former are not frequent in sediments. Bukry (1979) has reported opal phytoliths preserved in deep ocean sediments.

Christian Gottfried Ehrenberg began in 1836 the systematic study of phytoliths or phytolitharia which he published in 1845, 10 years after the first published work on phytoliths by another German scientist named Struve (1835). His subsequent, extensive collection and study of phytoliths from Europe, Africa, Asia, and America led to Ehrenberg’s *Mikrogeologie* (1854). Ehrenberg’s lead inspired other German researchers to continue phytolith studies in sediments and expanded observations of phytolith sources (Grob 1896). From the beginning, the link between phytolith studies and that of paleoenvironments, a key interest of modern archaeology, was articulated by Ehrenberg and those who came after him. Increasingly more common, the phytolith studies of archaeological sediments have yet to reach the level of acceptance as palynological studies. This situation is rapidly changing, and the use of phytolith studies has proven to be of diverse benefit to both archaeology and geology (Twiss 2001).

4.14 Phytolith Identification and Morphology

Traditionally, the identification of phytoliths has been based on typologies. The most typical shapes found have been given significance for

the identification of plant taxonomy. Phytolith populations are complex and stochastic—suffering from multiplicity of shapes, subtle and not so subtle morphological variation, and duplication (redundancy) of basic forms among taxa (Rovner 1996b). In this form of systematics, differences between phytoliths are ignored in favor of their similarities. Phytoliths are grouped rather than differentiated into smaller taxonomic categories such as genus and species. Furthermore, most measurements that are taken are length and width since they are the easiest to measure manually (Rovner 1996b). Opal phytoliths are produced by angiosperms, gymnosperms, and pteridophytes (Piperno 1988). They are produced by both monocotyledons and dicotyledons. Plant families producing opal phytoliths include both Poaceae and Gramineae grasses, Cyperaceae (sedges), Ulmaceae (elm), Fabaceae or Leguminosae (beans), Cucurbitaceae (squashes), and Asteraceae or Compositae (sunflower) (Mulholland and Rapp 1992). Still phytolith production is not universal, and even when plants do so, the phytoliths are amorphous and are not distinctive.

The immense variety in shape stems both from intraplant taxonomic differences and simple cellular differences between different parts of the plant from a specific taxa. Additionally, plants produce vast amounts of these cell casts as they die and decompose in the soil. It should be noted that the two major differences exist between phytoliths and pollen besides long-term preservation: (1) phytoliths are less taxonomic specific than pollen, and (2) they are more likely to be deposited in situ rather than broadcast over large areas like many forms of pollen. When phytoliths can be reliably identified, they make up stable components of archaeological sediments (Pearsall and Trimball 1984; Pearsall 1989).

The size and shape of phytoliths vary depending on the plant in which they are deposited and the area of deposition within the plant. Monosilic acid is carried into the tissues of the

plant in groundwater and is usually deposited in stems, leaves, and inflorescences. Eventually the silica is precipitated forming opaline silica ($\text{SiO}_2 \cdot \text{nH}_2\text{O}$) in the shape of the area that contains it. These areas lie within or between cells. This forms the cystalith or morphocast of the cell. Upon decay of this plant, the phytoliths become a component of the soil which can then be studied to determine the past floral assemblages of the immediate area as Ehrenberg had foreshadowed. Guntz and Grob (1896), more than Ehrenberg, identified and taxonomically classified more phytolith varieties than their predecessor. Guntz, alone, studied 130 species of grass in attempt to link cell morphology of leaves to the area's climate in which they grew (Powers 1992).

The grass family is a monocotyledon taxon that produces an abundance of phytoliths and is also a good indicator of climatic changes. These phytoliths have been subdivided into general long and short cell categories. Distinctive grass short cells have been further subdivided into festucoid, panicoid, and chloridoid classes (Twiss et al. 1969). Festucoids include grasses that prefer cool and moist conditions and include Festuceae, Hordeae, Aeneae, and Agrostideae. Their shapes range from trapezoid, rectangular, elliptical, and acicular to crescent, crenate, and oblong. Chloridoid grasses grow under drier and warmer conditions. Their shapes are less diverse being a basic saddle shape. Chloridoid grasses occur in Chlorideae, Ergostaeae, and Sporoboleae. Panicoids include the other grass tribes of Andropogoneae, Paniceae, Maydeae, Isachneae, and Oryzeae which are located in warm, moist environments. Their short cells contain the most distinct shapes such as bilobates, cross bodies, and crenate shapes. The grass short cells and their morphology are illustrated and discussed in detail by Brown (1984). Twiss has pointed out that for grass phytolith classification, it is the costal short cells that are the most diagnostic (2001). Unfortunately, these cells comprise only a small fraction (~5 %) of the total

siliceous residue (*supra*). Most of the residue used in a phytolith sample is composed of the relatively nondiagnostic epidermal cells. Fragments of the epidermis of leaves, stems, and husks (inflorescence bracts—hair cells, papillae, etc.) offer today's worker improved chances for identification success.

In terms of agriculture, many European grasses fall into the festucoid category, while maize contains panicoid lobate shapes. Rice contains a type of phytolith known as bulliforms, while parts of other cultigens such as the rind of squash, the leaf of bean, and the sunflower as well as maize form unique shapes that were identified by Bozarth (1986, 1993). Squash, for example, forms spheroid phytoliths covered with contiguous concavities. Weed species that thrive in areas of agricultural abandonment often contain chloridoid short cells. The identification of phytoliths from these species remains important to the study of archaeology. Trees and shrubs also produce phytoliths. The shapes vary greatly and need further study to identify their taxa and origin. Grasses are largely unidentifiable below family level.

4.15 Phytolith Extraction and Counting

The technique of phytolith extraction set forth by Rovner (1996a) was used on the soil samples collected from the site. It represents a relatively simple but labor intensive and time-consuming procedure which is necessary to separate phytoliths from the other components of the soil (Table 4.4). Approximately thirty grams of soils are necessary for processing using this procedure.

Once the phytoliths have been successfully extracted, one proceeds to identify and count as many recognizable forms as possible at family or subfamily taxonomic levels. Most researchers prior to the 1990s relied on light

Table 4.4 Process of phytolith extraction

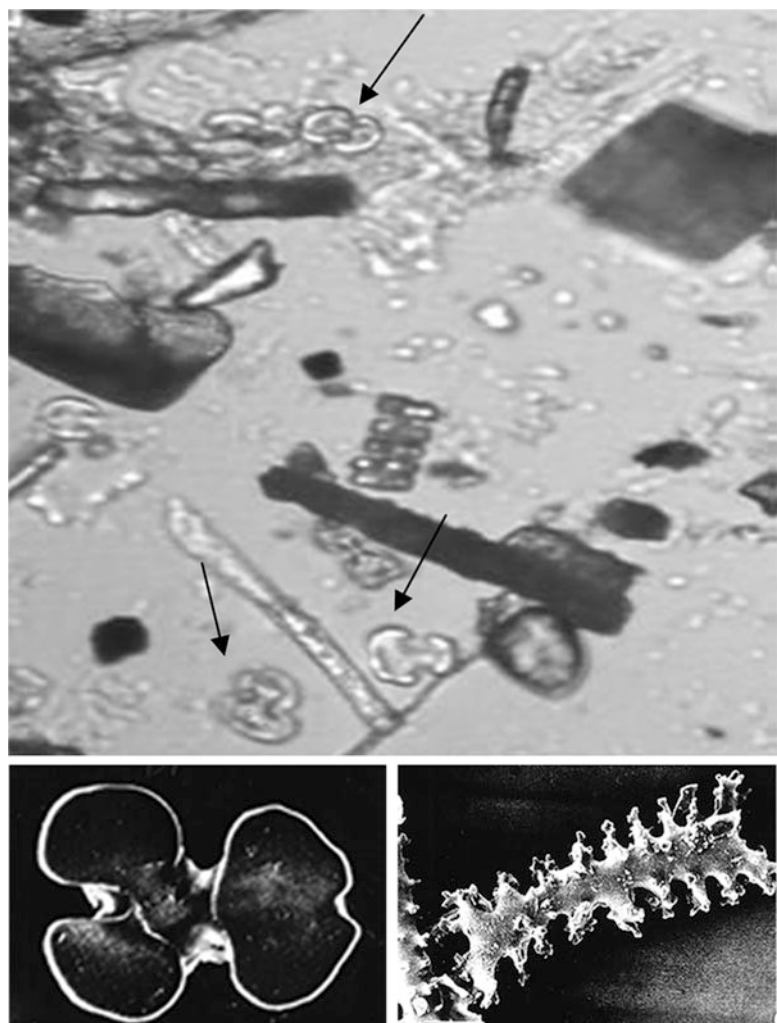
| Step | Reason |
|---|---------------------------------------|
| Distilled water | Removes organic material by flotation |
| Centrifuged | Allows phytoliths to settle to bottom |
| Decanted | Removes excess water |
| <i>Repeat 3 times</i> | |
| Bleach | Dissolves remaining organic material |
| Soaked overnight | |
| Distilled water | Rinses off bleach |
| Centrifuged | |
| Decanted | |
| <i>Repeat rinse 3 times</i> | |
| HCl | Removes CaCO_3 |
| Centrifuged | |
| Decanted | |
| Distilled water | Rinses off HCl |
| Centrifuged | |
| Decanted | |
| <i>Repeat rinse 3 times</i> | |
| Na metaphosphate | Removes clay minerals |
| Centrifuged | |
| Decanted | |
| Distilled water | Rinses off Na metaphosphate |
| Centrifuged | |
| Decanted | |
| <i>Repeat rinse 3 times</i> | |
| Dried overnight | Removes moisture |
| Placed in vials | |
| Heavy liquid (ZnBr or Na metatungstate) sp.g.2.35 | Floats off phytoliths |
| Centrifuged | |
| Decanted | |
| Distilled water | |
| Centrifuged | |
| Decanted | |
| <i>Repeat rinse 3 times</i> | |
| Placed in vials | |

After Owens (1997)

microscopy to identify and count phytoliths. The method most commonly used is the “quick scan” under magnifications of 300–500X. The slide, containing the phytoliths, is raster scanned with the observer tallies all phytoliths present as to known and unknown types. The use of scanning electron microscopy (SEM) and confocal technologies is changing phytolith analytical procedures particularly with regard to the

identification of phytolith morphology (Fig. 4.17). Both technologies are superior imaging systems compared to traditional optical microscopy. SEM is well established, and confocal laser microscopy has the like advantage of imaging the cell cast in great detail in storable digital, isometric images. The drawback to these higher-resolution imaging techniques is scale and speed.

Fig. 4.17 Various phytolith types. Arrows indicate “cross-body” chlorodoid types, whereas a festicoid type may be present, center of the photomicrograph. The photomicrograph courtesy Dr. Liovando Marciano da Costa. The two close-ups of chlorodoids and festicoid types are from Ball et al. (1996)



Because the SEM and confocal systems focus on micron-submicron scales, the investigator does not examine as many phytoliths during a scan. The identifications are more confidently made, but the overall number of individual “grains” counted is minuscule compared to the

optical procedures. Russ and Rovner (1989) have suggested the use of computer-assisted image analysis to achieve reliable, less subjective phytolith identification as well as more rapid assessment of total numbers of phytoliths per sample.

5.1 Introduction

This chapter will provide a brief but relatively comprehensive overview of geophysical techniques used in archaeology today ranging from electrical—resistivity and conductivity—to magnetic and radar methods. The methods to be discussed are the ones most commonly used in archaeological geophysics. Less frequently used methods—seismic, gravity, thermographic, induced polarization, and self-potential—to name some of the other methods used in “conventional” geophysics, will not be examined in any detail. Many of these other methods have achieved interesting results, in regard to archaeological prospection, but they remain, for a variety of reasons, of marginal interest to archaeology. As with all the geophysical methods utilized by archaeology, *none* were developed with archaeological prospection in mind. As is true with most, if not all, of the various methods used by archaeology, these methods have been borrowed and adapted to fit archaeological goals.

As Gaffney (2008) observes, the increased use of geophysical methods in archaeology is at an all time high. Linford (2006) notes that this was presaged in the 1980s. Gater and Gaffney (2003) suggested, perhaps, correctly, that the demise of the influential journal *Prospettive Archeologiche*, in that same period, contradicts Linford’s contention. The so-called golden age in development and application of geophysics to

archaeology occurred during the 1960s and 1970s (*supra*). Using the same hyperbole, perhaps, a “second golden age” is upon us.

In this survey we shall examine basic principles of the specific geophysical technique under discussion and then proceed to a brief discussion of the technique’s importance to archaeology. When illustrative, a brief example or two will be given. Mathematical formulae and equations are part and parcel of geophysics but, in this chapter, we shall only examine those most germane to the method. There are a host of works, some referenced in the following paragraph which do provide in-depth summaries of the physics and formulae involved in the use of these geophysical methods. Excellent general textbooks, on geophysics, such as those by Prem Sharma (1997), Kearey and Brooks (1991), and Burger (1992) together with field manuals (Milsom and Eriksen 2011) are readily available to those readers who seek a more in-depth understanding of the principles.

Textbooks (Scollar 1990; Clark 1990, 2003; Conyers and Goodman 1997; Gater and Gaffney 2003; Witten 2006; Aspinall et al. 2009; Conyers 2013) and major reviews (Wynn 1990; Weymouth 1996; Kvamme 2001; Aspinall et al. 2008; Linford 2006; Gaffney 2008), together with a dedicated journal—*Archaeological Prospection* (1994 to present)—are all indicators of the increased importance of geophysical techniques for archaeology. Excellent

historical background reviews appear in some of these works as well as elsewhere. Without digressing into historical perspective, it is important to remember that the use of geophysics in archaeology began in earnest after World War II, first in Europe and then elsewhere. The sequence of development proceeded from the use of soil resistivity methods by British workers (1950s) to magnetics by the Germans and Italians (1960s) and the development of ground-penetrating radar (GPR) by Americans (1980–1990s). Other geophysical techniques have found their way into archaeological use but to a lesser degree than those just mentioned. These latter methods include induced polarization (IP), conductivity (EM), magnetic susceptibility, microgravity, thermography, seismic reflection/refraction, and electrical tomographic imaging.

Beginning in the 1960s, the International Symposium on Archaeometry has prominently featured archaeological prospection in its programs. The increasing inclusion of geophysics in archaeology has seen the use of interesting terms to describe this. Wynn (1987, 1990) proposed the term “archaeogeophysics” for all ground and airborne geophysical methods applied to archaeology. In the strictest sense, most geophysical methods used today are terrestrial (“ground”) in nature although the use of airborne or space-based sensing technology (synthetic aperture radar (SAR), light distance and ranging (LiDAR)) has produced significant archaeological finds ranging from buried, “desert” rivers (Wendorf et al. 1987; Wiseman 1996) to Mayan centers hidden under tropical forests (Chase et al. 2011; Comer and Harrower 2013).

There is an additional use of geophysical methods that Wynn does not specifically include in his 1990 definition although he discusses it in his review article at some length—acoustic reflection and sonar in marine archaeology. Today, seismic/acoustic profiling coupled with magnetometers and side-scanning sonars are standard marine search procedures conducted on archaeological sites ranging from shipwrecks to drowned terrestrial landforms of archaeological interest (Pearson et al. (2008); Gaffney et al. 2007).

The suite of geophysical instrumentation developed or adapted for archaeological prospection is indeed impressive. With the concurrent usage of geophysics in mineral prospection, environmental studies, and geotechnical engineering, the development of new systems and iterations of existing ones has, indeed, been impressive. Linford (2006) and Gaffney (2008) have both noted that while the basic physical nature of geophysical methods have not changed, digitalization has revolutionized their design, application, data processing, and presentation. Along with this welcome, increased utilization of geophysics in archaeology has come to an increase in a more unwelcome aspect similar to that described for the chemical analysis of archaeomaterials (Artioli and Angelini (2011)—the proliferation of data that should never appear in scientific forums or journals.

Beyond venues like that of the International Archaeometry Symposia, papers on research and application of archaeological prospection have received more and more time at less technically focused professional meetings. Professional conferences in the earth and soil sciences, archaeology, and remote sensing commonly include papers on the theory and use of geophysical methods in archaeology. Add to this favorable trend the use of workshops on the “hands on application of these techniques” such as the US National Park Service’s annual workshop on archaeological prospection techniques entitled “Current Archaeological Prospection Advances for Non-Destructive Investigations in the 21st Century.”

Academic training in archaeological prospection has evolved as well. Important examples can be found in European (Oxford, Bournemouth, Bradford, Zürich, CNRS-France, Warsaw, Vienna, and Rome) academic settings together with the North American Universities: the UNAM (Mexico City), University of Arkansas, University of Georgia, University of Mississippi, Louisiana State University, and University of Pennsylvania. As today’s students become skilled in theory and practice, the application of geophysics in archaeology is assured.

Professionals, in the past decade, have formed a professional organization focused exclusively on the use of geophysics in archaeology.

5.2 The International Society for Archaeological Prospection (ISAP)

The inaugural meeting of the Society was held on September 13, 2003, during the fifth International Conference on Archaeological Prospection in Cracow, Poland. “The object of the Society shall be to advance the education of the public in archaeology (including the man-made landscape and the built-environment) through the promotion of high standards of research, application and communication in the field of archaeological prospection and related studies. The Society’s scope shall be international, both in activities and membership” (Armin Schmidt, Personal Communication 2015).

5.3 Electrical Methods: Resistivity

Resistivity methods have “pride of place” in archaeological geophysics by virtue of being the first geophysical method used by archaeologists (Aitken 1974). These early efforts, after World War II, consisted of much trial and error, with multiple, galvanic electrodes used as a rule. The first applications were what we will call “profiling” studies in that the electrodes—simple steel rods in most cases—are advanced over the site at a fixed interval between the probes, Wenner and Schlumberger methods (*supra*). A rough rule of thumb, still followed today, holds that the electrode separation is equivalent to the profiling depth or that a 1 m electrode separation will detect buried features at 1 m depth in the site.

Electrical resistivity or resistance survey methods measure electrical flow through soils or sediments. Most earth materials conduct currents, poorly at best, but vary nonetheless, according to mineralogic makeup and water content. Rocks are poor conductors. Some of the metallic or igneous varieties, such as the sulfide

minerals, basalt, gabbro, diorite, and magnetite, are better than the sedimentary or metamorphic rocks. Table 5.1 lists resistivity values of common sediments, rocks, and minerals. Of the sediments, clays are the best conductors, and clay-rich soils have lower resistance to electrical flow than, say, quartzitic or carbonate types. The difference in the resistance or resistivity, as it most commonly called, as measured by galvanometers or ohm/voltmeters, is used to detect and characterize buried features of an archaeological nature. The fundamental physical relation involved in resistivity is Ohm’s law.

$$R = V/I$$

In Ohm’s law, R is the resistance (measured in ohm Ω), V is the voltage (measured in volt V), and I the current (measured in ampere A). One ampere is equal to one coulomb of (electron) charge moving in 1 s through a potential of 1 V. For a current to flow, there must be a difference in the voltage potential, also termed bias. On the microscopic level, Ohm’s law can be written, in vectorial form, as

$$E = \sigma j$$

E is the electric field, σ is conductivity, and j is the current density.

Resistivity and resistance are not totally synonymous terms. Resistivity is specific resistance, expressed as ρ in the unit of ohm-meter Ωm . It is the resistance to current flow, over some distance, and is proportional to the area. In resistivity survey we measure the apparent resistivity, ρ_a , which is the “true” resistance across a nonhomogeneous media like the earth. The apparent resistivity is expressed with a geometric correction factor that is particular to a particular electrode spacing or array. The geometric factor for the Wenner array, the most commonly used array, is $2\pi a$ where a is the electrode spacing and 2π considers the half-space volume over which the current flows. With this in mind, we rewrite Ohm’s law, for the Wenner array as

$$\rho_a = 2\pi a V/I$$

A material with significant resistance to current flow is an insulator, while one that allows current

Table 5.1 Resistivity of common materials

| Material | Frequency at measurement, CPS (if not DC) | Resistivity, ohm-cm |
|-------------------------|---|---|
| Minerals | | |
| Galena | | 0.5–5.0 |
| Pyrite | | 0.1 |
| Magnetite | | 0.6–1.0 |
| Graphite | | 0.03 |
| Rock salt (impure) | | 3×10^3 – 5×10^5 |
| Serpentine | | 2×10^4 |
| Siderite | | 7×10^3 |
| Igneous rocks | | |
| Granite | | 10^8 |
| Granite | 16 | 5×10^5 |
| Diorite | | 10^6 |
| Gabbro | | 10^7 – 1.4×10^9 |
| Diabase | | 3.1×10^5 |
| Metamorphic rocks | | |
| Garnet gneiss | | 2×10^7 |
| Mica schist | 16 | 1.3×10^5 |
| Biotite gneiss | | 10^8 – 6×10^8 |
| Slate | | 6.4×10^4 – 6.5×10^6 |
| Sedimentary rocks | | |
| Chattanooga shale | 50 | 2×10^3 – 1.4×10^5 |
| Michigan shale | 60 | 2×10^5 |
| Calumet and hecla | | |
| Conglomerates | 60 | 2×10^5 – 1.3×10^6 |
| Muschelkalk sandstone | 16 | 7×10^3 |
| Ferruginous sandstone | | 7×10^5 |
| Muschelkalk limestone | 16 | 1.8×10^4 |
| Marl | | 7×10^3 |
| Glacial till | | 5×10^4 |
| Oil sand | | 4×10^2 – 2.2×10^4 |
| Rock type | | |
| Consolidated shales | | Resistivity range ($\Omega\text{-m}$) 20 – 2×10^3 |
| Argillites | | 10 – 8×10^2 |
| Conglomerates | | 2×10^3 – 10^4 |
| Sandstones | | 1 – 6.4×10^8 |
| Limestones | | 50 – 10^7 |
| Dolomite | | 3.5×10^2 – 5×10^3 |
| Unconsolidated wet clay | | 20 |
| Marls | | 3–70 |
| Clays | | 1–100 |
| Alluvium and sands | | 10–800 |
| Oil sands | | 4–800 |

flow is a conductor. Glass and silicate minerals are insulators, while the metals are conductors.

The conductance of current through soil is greatly influenced by water content. Water alone is not necessarily a conductor as distilled

water is a good insulator whereas tap water is a conductor. Why? Distilled water is free of any mineralogic salts and other ions where tap water has charge carrier ions such as sodium, chlorine, etc., that *conduct* electrical current. This property

is termed *ionic conductivity*. In sediments, the number of ionic elements is much greater than simple water. It is the water that mobilizes the ions to form the electrolytic soil/water solution. When an electrical potential is applied across a soil volume, with electrodes, the material and moisture will act first as charge carriers. After a period of time, the soil will impede the motion of ions so that they accumulate at grain boundaries wherein the ground acts like a battery. This is particularly true where direct current (DC) is applied to the electrodes. To avoid unwanted polarization effects, resistivity devices use alternating current (AC). An alternating current source, regulated by an oscillator, varies the sign of the current in +0.5 to –0.5 cycles such that the ground “battery” cannot build up charge without subsequent reversal and discharge. As a result there can be no net polarization. The early two-electrode arrays were prone to another problem known as “contact resistance” which comprises a large part of the total resistance. Workers overcame this problem by adding two additional electrodes, equally spaced apart, and the four-electrode array was born.

As stated, resistivity is the most venerable of geophysical techniques used for archaeology (Aitken, *supra*); resistivity will continue to be used into this millennium as a productive prospection method. Over a half-century of experience, in both archaeology and geology, resistivity has provided a solid conceptual as well as applied basis. To remain a productive geophysical methodology for archaeology, advances in electrode design, such as non-polarizing electrodes, together with current reversal circuitry, low power AC batteries, and low induction cables have all contributed to a more efficient modern resistivity technology. These hardware innovations have been coupled with the advances in computer design to make modern instruments more compact and flexible. Data is in digital formats making storage manipulation and modeling by geophysical software all the more routine. The most often heard problem—lack of speed in field survey—has been addressed, at least in archaeology, by the modern double-dipole array instruments and the multielectrode

array instruments. The multielectrode (25+) cable arrays used with computer-driven control units allow the rapid collection of field data in a host of array configurations—Schlumberger, Wenner, double-dipole, etc.

5.3.1 Resistivity Arrays

In archaeological prospection four-electrode arrays are most commonly used. We now review in order of popularity. The Wenner array is the “standard” against which other arrays are assessed (Milsom and Eriksen 2011).

5.3.1.1 Wenner Array

The high impedance measurement circuit used for Wenner potential electrodes (P_1, P_2) reduces contact resistance by orders of magnitude because it draws little current. It has been found that electrode size, depth, and geometry are of little importance but electrode spacing, as we have said, is more so. With the Wenner array, this relationship is fairly direct with the depth of profiling roughly equivalent to electrode spacing. Depth and spacing are generally treated as equivalent.

The diagram in Fig. 5.1 illustrates the spacing, a , is equal and set to the depth of interest for the specific traverse. To traverse a site, the array is advanced by increments equal to a with readings made. The direction of the survey will influence the appearance of most anomalies. While it is time consuming, it is sometimes useful to resurvey at right angles to the direction of the original survey. For sounding surveys the electrode spacing is expanded by increasing increments of $a = 1, 2, 4, 8, \dots, n$. It is the easiest of the four-electrode arrays to conceptualize. One simply lines up the four electrodes, at an equal interval a , drives a current, reads the resistance, and then moves the electrodes, in sequence, by predetermined interval a . This is repeated until the area of interest has been completely traversed on an X-Y grid.

All of the arrays discussed in this section can be used for archaeological profiling studies and indeed they have. The profiling method simply

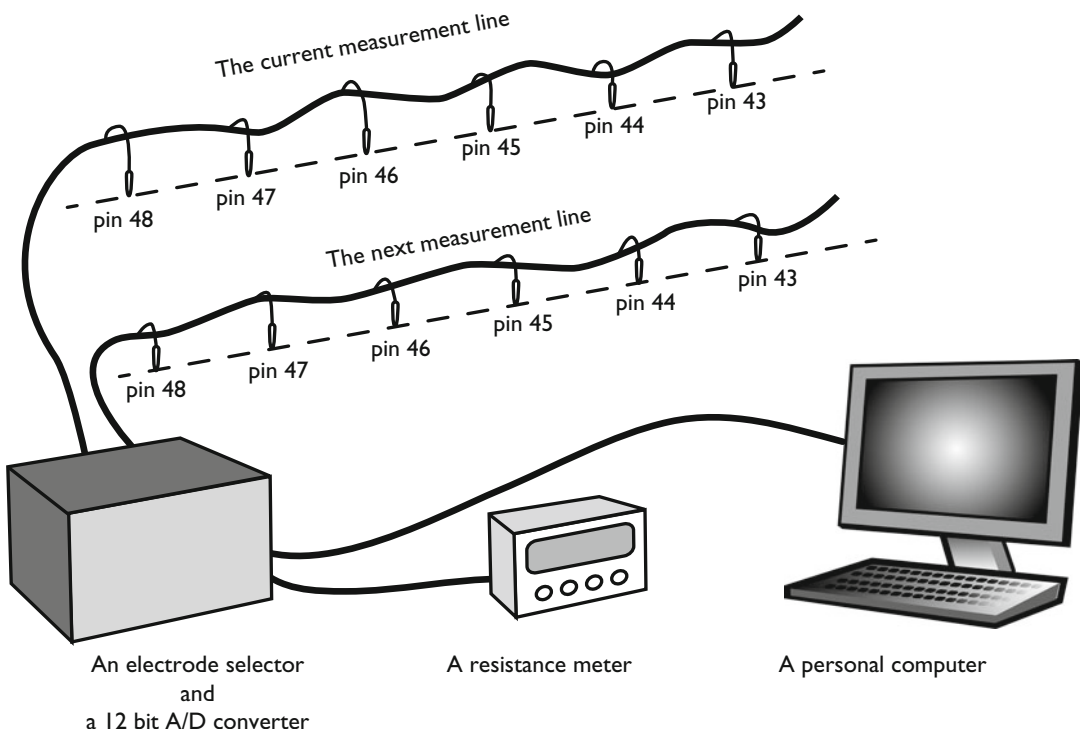


Fig. 5.1 General multielectrode resistivity system. This system can be programmed for both Wenner and Schlumberger array configurations

requires the traverse of an archaeological site using a preselected offset and sampling interval. This is termed the “constant-spread” traverse.

Resistivity Sounding This category of resistivity measurement is typically described as a sounding method (Burger 1992) but that is only if the center of the array is kept at a fixed location and the electrode spacing, a , in the Wenner method, are sequentially increased. This common variation is to simply repeat the constant-spread traverse at increased increments of (a) . Rather than construct a resistivity *pseudosection*, described in the following sections, each (a) spacing traverse’s data, for that level, can be viewed independently of preceding or subsequent traverses. This data can be modeled in an areal contour plot rather than in a depth section. Multi-level plots can be made treating each level as a “resistivity surface” (Herbich 1993). We shall provide an example of this type

of profiling in the discussion of the Schlumberger array.

5.3.1.2 Double-Dipole Array

In principle, the double-dipole array mimics induced polarization (IP) techniques in array configuration and measurement. The principal difference in the two techniques is the method of applying and measuring potentials—the double-dipole array applies a continuous potential, while IP relies on induced, remnant potentials transient in the soils. For a discussion of IP methods, see Wynn (1988). The double-dipole array has the potential electrodes separated, at some distance, from the current electrodes (C_1, C_2), while the electrode spacing, a , is the same for both sets of electrodes) involves a geometric factor that differs from Wenner and Schlumberger arrays. Here, the parameter n is the distance between the current electrodes.

$$\rho_a = \pi a n (n + 1) (n + 2) V/I$$

Williams (1984a, b, 1993, Personal Communication) touts the double-dipole array over that of the Wenner array, in archaeological prospection, primarily because of the location of the measured maximal value of apparent resistivity. With the Wenner array, the profile of a resistive feature takes on a double-peak shape and is reminiscent of the magnetic dipole shapes discussed later in this chapter with the maximal value for ρ_a , over the feature, reduced because of electrode spacing and type.

This “double-peak signature” is not seen in plots of double-dipole data as the most sensitive location for measuring apparent resistivity is measuring at (ηa). Two disadvantages of the double-dipole array are (1) overall sensitivity and (2) comparability of reading to those of other arrays. This is true for either profiles or soundings. The double-dipole array has become popular in both archaeological and mineralogical prospection using sounding data to produce 2D inversions and pseudosections (Griffiths and Barker 1994; Milsom and Eriksen 2011). Both Wenner and Schlumberger arrays produce more reliable, deep soundings.

5.3.1.3 Two-/Twin-Electrode Array

Milson and Eriksen (*supra*) characterize the modern variant of this array (double-dipole) as the one most popular in archaeological prospection today. The successful modern variant is a DC system with a fixed interelectrode distance, a , that allows the unit to be operated by a single person without cables to caddy. The use of DC, with its polarizing effect, has been ameliorated by use of a switching circuit to minimizing charging.

The twin-electrode array was especially designed for archaeological prospection (El-Gammili et al. 1999). It is basically a Wenner array divided into two parts, with a very large separation between the current and potential electrode pairs (*supra*). Aspinall and Lyman (1970) have shown that this arrangement allows for the same penetration of a Wenner array with

twice the separation between the electrodes. The thing that commends the twin-electrode array to archaeological prospection is its compact nature. The so-called mobile probes are on a fixed frame with a cable connection to the other electrode pair located at a fixed point some distance away (greater than 30 times the electrode spacing as a rule). Another benefit of the large separation in the array halves is a reduction in background resistance. Current practice in Great Britain, and elsewhere, in Europe, favors the use of the twin-electrode array. It is quick—up to 6,000 readings per day—and coverage is comparable to that of magnetometer survey, a hectare per day.

5.3.1.4 Schlumberger Array

Conceptually, the Schlumberger array is as well understood as the Wenner array and is, perhaps, more used than that array for sounding work. On the first inspection, the two arrays appear similar with the potential electrodes in the array’s center and the current electrodes on the ends. The potential electrodes are fixed in their spacing such that a minimum factor of $2.5 \times$ exists between their interelectrode distance, $2l$, compared to that of the current electrodes, L . The array can be moved as an ensemble for a profile survey or the current electrodes moved separately increasing L , by logarithmic steps, to produce sounding data. The inner electrodes are not moved until voltage levels are not measurable. The apparent resistivity for this array is calculated as follows:

$$\rho_a = \pi [(L^2 - l^2) V] / 2l$$

Williams (1982, 1998) considers a 1 m depth/electrode spacing adequate for most archaeological resistivity work. This being the case, then the use of a rigid frame resistivity meter mounting fixed-distance electrodes (a) and a data logger or portable computer is in keeping with most profiling needs of an archaeological nature. Calculation of the apparent resistivity for the two-electrode array is the same as that for the Wenner array.

5.4 Vertical Sounding Methods in Archaeology

Electrical sounding has been called “electrical drilling.” As such it can be thought of as a type of coring device to get at the depth as well as the distribution of archaeological features, i.e., pits, hearths, and remains of structures. The Schlumberger technique provides excellent profile data. It can also be used for vertical soundings, involving the expansion of the spread of current probes AB around a central point with constant position of potential probes MN, giving information on the number of horizontal resistivity interfaces at that point. The result reflects the properties of a vertical section or *pseudosection* of the subsurface, but:

- The quality of the interpretation decreases radically with depth, since the properties of larger volumes of soil are being sampled by each expanding reading.
- Each datum point will include significant contributions from volumes of soil not directly under the array—the pseudosection compresses all such effects onto a two-dimensional display of apparent resistivities onto an arbitrary vertical grid.
- The pseudosection, whether displayed as a block of numbers, a gray-scale image, or in contoured form, is not a direct representation of the subsurface and any interpretation as an image can be extremely misleading—the depth scale can be completely arbitrary. In

the past processing, filtering or smoothing of the data could not seem to overcome this fact (Szymański and Tsourlos 1993), but the use of inversion techniques have improved results significantly (Barker 1992; Sasaki 1989; Tripp et al. 1984).

Today, with double-dipole data, inversion of the pseudosection data gives a 2D tomographic image (Fig. 5.2). It is now possible to get accurate depth and location using the inversion process (Sharma 1997). By starting with an initial model—the pseudosection—which is essentially a “guess” as to what the subsurface looks like, the inversion then changes or “iterates” the model data until the model agrees with the collected data within accepted error. These are called “error-minimization” routines. It is analogous to the technology used in medical MRI and CAT scans. Barker (1992) developed an algorithm, based on the finite difference method, that inverts the pseudosection and converts the apparent resistivity measurements to “true” resistivity—an immediate gain is the adjustment of depth variation. For a detailed discussion of the inversion method, see Szymański and Tsourlos (1993) and Noel and Xu (1991) as well as Barker (1992).

Having given the reader these caveats, many current articles describe the use of electrical sounding and, in particular, suggest the use of pseudosections to aid in the interpretation of the subsurface archaeology (Dalan et al. 1992; Aspinall and Crummet 1997; Szymański and Tsourlos 1993). Griffiths and Barker (1994)

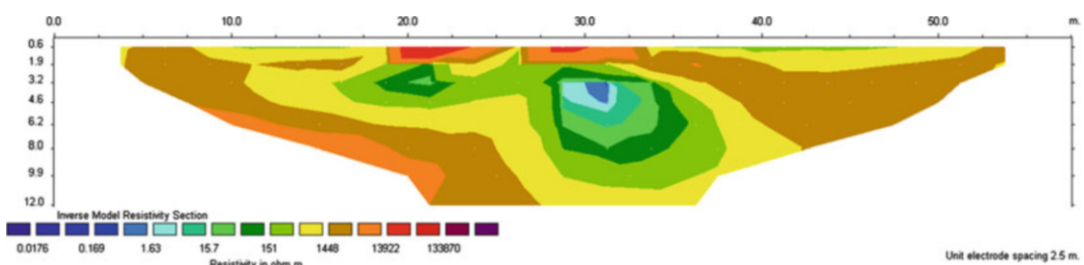


Fig. 5.2 Resistivity pseudosection of Mound A, Etowah Mounds State Park, Cartersville, Georgia, USA. This 20 m-high Mississippian period temple mound was built sometime prior to 1250 AD. It has been the subject of several geophysical studies beginning in 1993 with the author’s

initial radar studies of this and adjacent mounds B (Garrison 1998). This figure is the result of a later electrical study (Garrison et al. 2005). The near-surface features in red are well-documented “robber trenches” but the deeper anomalies, in green, are prehistoric structural features

have used a computer-controlled electrode array along a fixed-length cable such that the sequence, spacing, and array configuration are selected and manipulated by the software resident in the control unit (Fig. 5.1).

5.5 Electrical Methods: Electromagnetic/Conductivity

The reciprocal of resistivity is conductivity and is written with the Greek sigma, σ , just as in the microscopic form of Ohm's Law, so

$$\sigma = 1/\rho$$

Electromagnetic (EM) induction, avoided in resistivity measuring systems, is utilized to measure the conductance in the subsurface. Like resistivity, differences in conductivity measured in the subsurface may have as their source objects or features of archaeological interest. Induction of eddy currents is a consequence of a primary dipole field whose magnetic field lines flow through a conductor producing the weak secondary currents (electrical). Conductive minerals like clays and metallic oxides in soils enhance induction by what is termed mutual inductance (Tite and Mullins 1969; Milsom and Eriksen 2011).

A Slingram-type conductivity meter uses a source current flowing through a wire coil loop producing an alternating low-frequency magnetic field (i.e., between 200 and 20 kHz), while a second coil, at a distance L , measures two different components of the magnetic field—the inphase and quadrature components. The inphase component is a measurement of the magnetic susceptibility of the soil and that of quadrature a measurement of the soil conductivity. Inphase measurements are like those of a “metal detector,” only much more sensitive. Quadrature measurements are those of electrical properties of the soil.

The response of the conductivity meter is complex: the secondary field is not inphase with the primary field and this increases with the conductivity of the ground. The presence of this

secondary field is a direct consequence of the magnetization induced by the primary field. High-frequency waves attenuate first and quite rapidly with depth. As a consequence frequencies above 1,000 Hz are rarely used in devices for archaeological prospection. A semi-empirical formula relates soil resistivity to frequency as follows:

$$h\sqrt{f/\rho} = 10$$

h is the depth, f the frequency, and ρ the resistivity. For instance, if we solve for f with ρ equal to $10^4 \Omega\text{-m}$ and h equal to 10 m, then f should be 100 Hz.

With the continuous wave (CW), frequency domain EM devices such as the Slingram, Geonics EM 31 and EM 38, and the primary transmitter coil put out a sinusoidally varying current at a set frequency which serves as a reference for the secondary (receiver) coil whose current characteristics are compared to the primary. The amplitude and phase angle components of the current are compared, e.g., the inphase and quadrature (out-of-phase) components. These are read directly on a digital meter on the device. The principal advantage of the conductivity meter is *speed*. These units can cover a site's area as quickly as the magnetometer. Even as impressive as the new twin-electrode resistivity units are, they are no match for the ease of survey that the conductivity and magnetometer provide to archaeological prospection. It should be noted that the noncontact nature of the conductivity measurement usually results in a reduced sensitivity, ordinarily by a factor of 5, when compared to resistivity measurements, but this is usually not important in archaeological cases.

Multifrequency Devices These instruments, such as the GEM-2, made by Geophex, Ltd., and the Profiler EMP-400, manufactured by GSSI, Inc., operate over a range of frequencies. For the Profile EMP-400, it operates on three frequencies from 1,000 to 16,000 Hz. The frequency range for the GEM-2 is 300–96 kHz. They are “time domain” instruments. As we

recall the effect of frequency on the soil, generally speaking, the higher frequencies “see” all soil as conductive, and, therefore, the depth of survey is quite shallow. Circuitry and coil geometries allow the use of multiple frequencies which are particularly good at isolating shallow conductive features such as those interesting to archaeology (Figs. 5.2 and 5.4). These multifrequency devices allow for the acquisition of large, digital data sets that can be plotted and compared as to the presence of conductive features and their “depths.” True depth estimations can be problematic for EM survey results. With units like either the EM-31 or EM-38, the rough relationship between coil separation ($1.2 \times$ coil separation) and depth can be used. The EM-31 has a maximum depth of survey of about 6 m, while that of the EM-38 is only 1.5 m. This problem will crop up again in our discussion of another EM-based device: the ground-penetrating radar (GPR).

5.5.1 Application of EM Methods

EM surveys are done as traverses. Like resistivity data, the results are typically presented as (a) profiles or (b) surface plots, either plan view or isometric. The following example illustrates the use of EM deployed over the site of a historic school building.

5.6 Conductivity (EM) Survey of a Burned and Buried Cherokee Seminary Building, Tahlequah, Oklahoma, Cherokee Nation, USA

In a survey conducted over the area of a burned and buried nineteenth-century seminary building (Fig. 5.2), conductivity data was taken using the predecessor of the Profiler EMP-400, the Gem-300, a multifrequency instrument capable of up to six frequencies in a range from 330 to 20,000 Hz. Electromagnetic induction, as noted above, works by inducing and then subsequently

measuring a weak, secondary electromagnetic field/current in the ground. The ability of the subsurface materials to conduct electromagnetic energy can then be measured and used to interpret the anomalies found within the subsurface. EM surveys that can measure multiple frequencies can correlate these frequencies to different depths. Lower frequencies are able to penetrate deeper into the ground due to their long wavelengths but cannot resolve finer details. Higher frequencies may be able to resolve those finer details in the data but are unable to penetrate as deeply into the ground. By using a range of six frequencies during the Cherokee Female Seminary survey, it was possible to explore different depths from just below the ground surface down to deeper geological and embedded archaeological features.

A GSSI GEM-300 conductivity (EM) meter was used for this survey. Data were collected at stations placed every 2 ft along transects that were spaced 3 ft apart. These intervals were used because the building was constructed using feet-inch units. EM data were downloaded from the GEM-300 instrument and processed using Geosoft’s Oasis MONTAJ software. Each of the six frequencies was used to provide information about anomalies at different depths. Depths were roughly calculated using the formula for skin depth, but more accurate correlation for depth was generally found by cross-comparing EM data plots with those using GPR data (Figs. 5.3 and 5.4).

5.6.1 Magnetic Methods

The degree to which a material becomes magnetized in an applied magnetic field H is called its magnetic susceptibility. Later in this chapter, we will discuss the use of this property of rock minerals and sediments for archaeological purposes, but for the moment we will use it to examine how magnetism is used in archaeological geophysics. How a material is magnetized is termed magnetic induction. Magnetic susceptibility, χ , is defined as

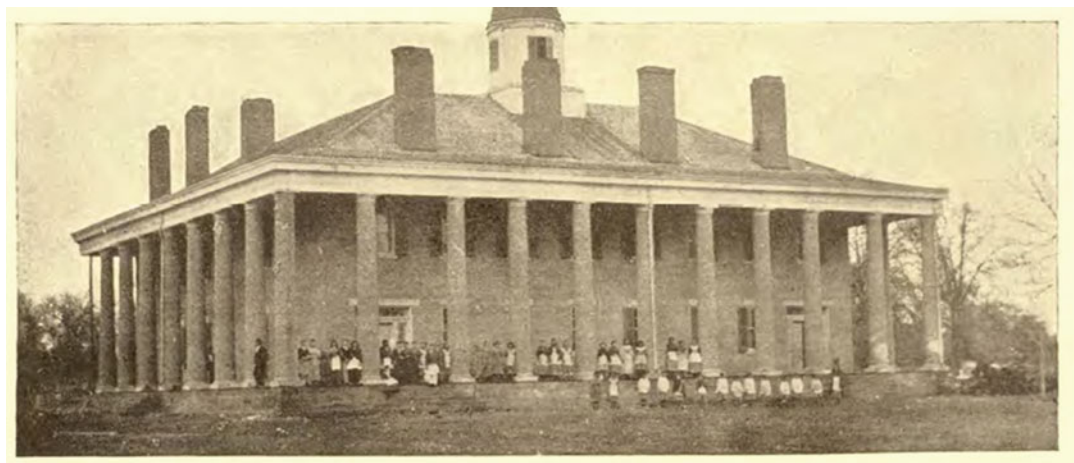


Fig. 5.3 The Cherokee female seminary, ca. 1,848. Courtesy of the Oklahoma Historical Society

$$\chi = M/H$$

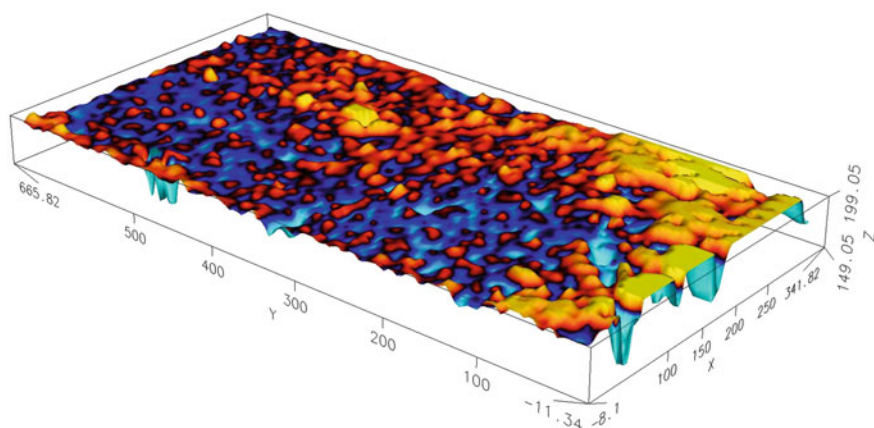
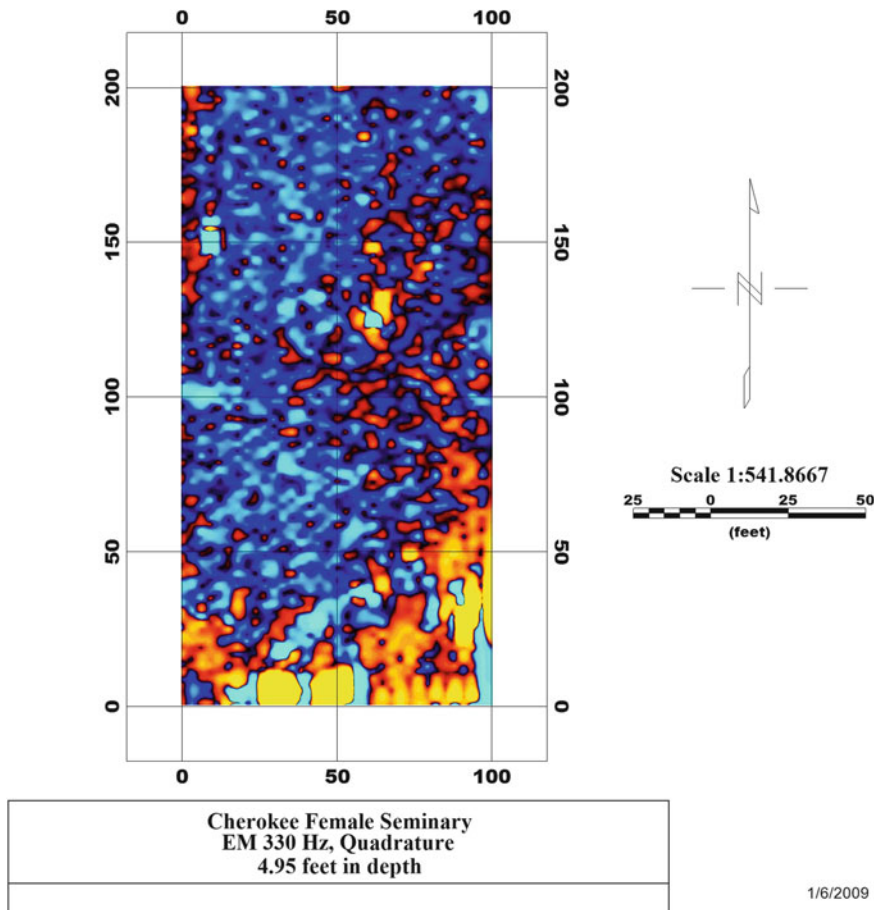
where M is the induced magnetism and H is the total magnetic intensity of the applied field.

χ is a dimensionless quantity in the cgs system and generally measured for a volume or mass. The above relation describes volume susceptibility and when divided by the material's density, χ/d , the mass susceptibility is obtained. Magnetic materials vary in susceptibility from weakly negative to strongly positive. Magnetic prospection depends on an observed contrast in the susceptibility of materials. Almost all magnetic features in archaeological sites are differentiated by the amount of the magnetic mineral magnetite, Fe_3O_4 present. Magnetism is characterized as either diamagnetic, paramagnetic, or ferri(o) magnetic. Briefly these various terms describe the magnetic response at the atomic level.

Diamagnetism arises from the distortion of an atom's electron orbits in a magnetic field. Always present, this form of magnetism is very weak (about 1 nT). When an atom has an unfilled electron shells, valence or otherwise, they will demonstrate paramagnetism individually. This latter point is important. By behaving individually, in bulk arrangements (crystals, glass, liquids), there is no net magnetic behavior or moment. Paramagnetic materials demonstrate weak magnetism in applied fields.

When a material's atoms, with unfilled outer shells, behave collectively or coupled, the

magnetism can be ferromagnetic or anti-ferrimagnetic depending on orientation of magnetic moments. Iron (Fe), cobalt (Co), nickel (Ni), their alloys, or minerals are powerfully attracted to magnetic fields ("magnetic induction"). As a result, ferromagnetic and ferrimagnetic materials are the most prevalent in producing strongly magnetic features in archaeological sites. We, therefore, characterize materials on their ability to "acquire" magnetism or their magnetic susceptibility. Typical susceptibilities are shown in Table 5.2. The reader will note that χ , in this table, is written in Gaussian or cgs units. Volume magnetic susceptibility is generally regarded as dimensionless, while the magnetic susceptibility per mass is a more useful quantity for use in magnetochemistry of archaeological materials and is given the units of reciprocal density. Rocks, artifacts such as ceramics, can acquire a permanent net magnetism termed remanent magnetism. There are various ways this can occur such as heating, chemical activity, and pressure. The remanent magnetism so acquired, by whichever physical means, is relatively permanent, over geological time, and forms the basis for paleo- and archaeomagnetic dating methods. Interaction of the induced and remanent magnetic components yield the net magnetism of a material we observe in the earth's field. To measure this net magnetism, magnetometers are utilized.



Cherokee Female Seminary
EM 330 Hz, Quadrature
4.95 feet in depth

Fig. 5.4 Three plots of geophysical data from surveys of the site of the Cherokee Female Seminary, Tahlequah, Oklahoma. The upper plots are, respectively, a plan view of quadrature phase data (330 Hz) and an isometric view of the same data. The lower

image is a GPR “time slice” of the same area showing good correlation between the two sensors. Architectural interpretation has been added to the radar plot. The area outlined in red is buried ruin of the building

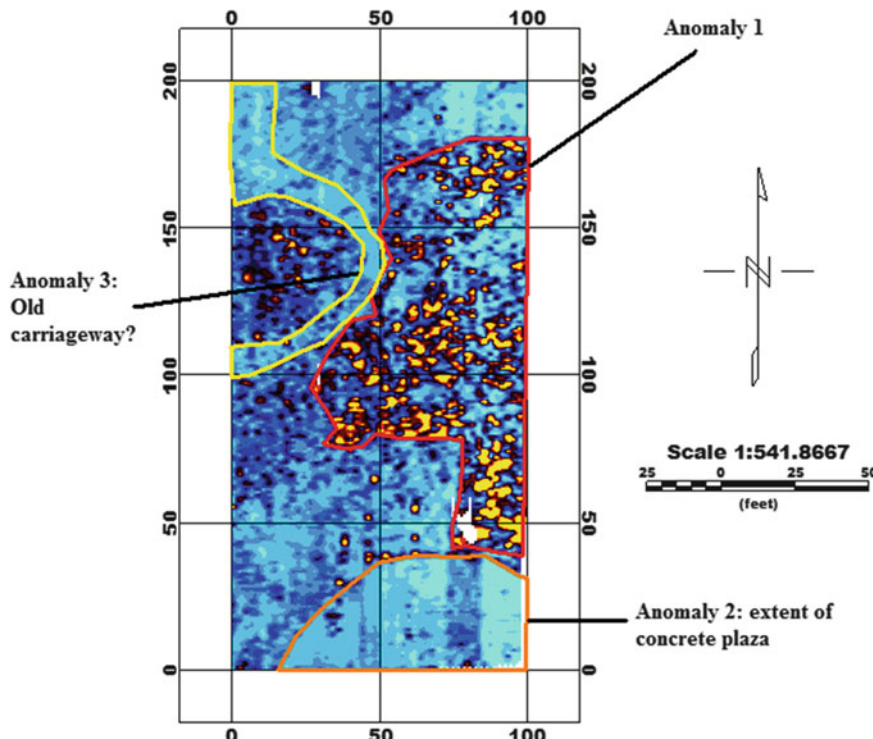


Fig. 5.4 (continued)

Iron-bearing minerals such as goethite, hematite, and magnetite (cf. Tables 5.2 and 5.3) are common in many soils that contain archaeological features. Till et al. (2015) have described soil mechanisms that increase the presence of the more magnetic of these minerals—magnetite and maghemite. Conversion, by chemical/recrystallization pathways, of less magnetic goethite and hematite forms together with either natural or anthropogenic fires to magnetite/maghemite has been documented for soils where organic matter acts as a reductant (*supra*).

5.6.2 Magnetometers

Magnetometers, unlike conductivity and resistivity devices, which actively generate electric fields are “passive” instruments. By comparison the simplest device for measuring magnetic fields is the compass. While this hardly seems to qualify this important directional tool as a prospection instrument, it was used to successfully relocate the sunken Civil War ironclad,

USS Cairo (Bearrs 1966). Geophysicists have developed several magnetometers for use in prospection. These include the fluxgate magnetometer, proton precession magnetometer, and the optically pumped magnetometer.

Magnetometers measure the sum of the induced and remanent magnetization in some absolute or relative ratio to the earth’s field depending on the instrument (LeBorgne 1960). Fluxgate models measure this along a single axis, while the other types measure the total or absolute field—the sum of all axes of the magnetic field at a location. The single axis fluxgate readings can be subtracted from the total field to obtain the remnant component that is often directly representative of archaeological features. Absolute or total field devices, proton precession or optically pumped systems, are also used to detect local magnetic materials—artifacts and architectural remains, for instance.

Fluxgate Magnetometer This magnetometer is simply a magnetic metal around which two coils, primary and secondary, are wound to form a

Table 5.2 Magnetic susceptibilities of common rocks and minerals (cgs units)

| | |
|--------------------------|-----------------------|
| Top soil | 10^{-4} |
| Clay (unfired) | 10^{-5} |
| Altered ultrabasic rocks | 10^{-4} – 10^{-2} |
| Basalt | 10^{-4} – 10^{-3} |
| Gabbro | 10^{-4} |
| Granite | 10^{-5} – 10^{-3} |
| Andesite | 10^{-4} |
| Dolerite | 10^{-2} –0.1 |
| Rhyolite | 10^{-5} – 10^{-4} |
| Shale | 10^{-5} – 10^{-4} |
| Schist and other | |
| Metamorphic rocks | 10^{-4} – 10^{-6} |
| Most sedimentary rocks | 10^{-6} – 10^{-5} |
| Limestone and chert | 10^{-6} |
| Pyrrhotite | 10^{-3} –1 |
| Magnetite | 10^{-3} –2.0 |
| Chromite | 10^{-4} –1 |
| Hematite | 10^{-6} – 10^{-5} |
| Pyrite | 10^{-4} – 10^{-3} |

Table 5.3 Magnetic properties of soil minerals

| Mineral | Formula | Magnetism |
|---------------|------------------|-------------------|
| Magnetite | Fe_3O_4 | Ferrimagnetic |
| Hematite | $\alpha-Fe_2O_3$ | Antiferromagnetic |
| Maghemite | $\gamma-Fe_2O_3$ | Ferrimagnetic |
| Goethite | $\alpha-FeOOH$ | Antiferromagnetic |
| Lepidocrocite | $\gamma-FeOOH$ | Antiferromagnetic |
| Ilmenite | $FeTiO_3$ | Antiferromagnetic |
| Pyrrhotite | Fe_7S_8 | Ferrimagnetic |
| Pyrolusite | MnO_2 | Antiferromagnetic |

transformer. In operation the introduction of AC in the primary coil produces (induces) a magnetic field in the core metal as a secondary voltage or waveform. Any external field along the axis of the core can alter the waveform proportional to the strength of the magnetic field at a sensitivity of 1 part in 50,000 nT, i.e., 1 nano-Tesla (nT). If the field vector is off the axis of the fluxgate device, then it is not as readily detected. Fluxgate devices are popular in Great Britain and the continent (Milsom and Eriksen 2011; Marshall 1999; Neubauer and Eder-Hinterleitner 1997).

A three-component fluxgate magnetometer has been described by Kamei et al. (1992). Coupling two of these devices creates a gradiometer wherein both the total and gradient fields can

be measured. The magnetometer can measure all three components of the total magnetic field's X, Y, and Z orientation. Because of the complexity of the sensor(s) output, a microprocessor is needed. In practice the x-axis is fixed to north and the Y and Z fluxgate sensors held in some fixed orientation to X. The data can be displayed as to (a) the north-south component (X) and the east-west component (Y) and the vertical component (Z).

Proton Precession Magnetometer This type of magnetometer is perhaps the most common field system used in archaeological prospection. Conceptually, it is somewhat more complex than the fluxgate design. As the name implies, the measurement of the magnetic field strength is through use of proton (the hydrogen nucleus) precession. Precession is a property of electrons and protons due to its spin (Leute 1987). An individual proton will align, as its spin generates a very weak magnetic dipolar moment, along the direction of a magnetic field such as the geomagnetic field of the earth.

Protons, such as in a fluid—water, gasoline, or alcohol—can act in a collective manner, similarly to that of ferromagnetic domains. A proton precession magnetometer has as its sensor, a container of a proton-rich fluid, encircled by wire windings that carry a current. The current, 1–1.5 A, generally, can generate a locally brief yet strong magnetic field that “polarizes” the protons. After the field is turned off, the protons precess together until their motion decays into random modes, about the field lines (of magnetic force) of the geomagnetic field. There is a known frequency for this precession about the geomagnetic field that is termed the Larmor frequency, using an average value of the earth's field of 50,000 nT; it is equal to 2,100 Hz. The protons processing in unison, at or near the Larmor frequency, induce a weak electrical current in the sensor's windings which, when amplified, converts the voltage's frequency to direct measure of the magnetic field strength to about 0.02 Hz or 0.5 nT (Leute 1987).

Optically Pumped Magnetometer In the geo-magnetic field, electronic levels will have their

orbital “degeneracy” removed such that a discrete energy, of a few electron volts, exists between the + and – energy states of an atomic electron. This effect was discovered by Pieter Zeeman in the nineteenth century and was named for him. The use of the Zeeman effect created a third type of magnetometer called the optical-pumped or absorption cell magnetometer. The electrons of a specific element such as sodium, cesium, or rubidium can move between the Zeeman levels, generally from ground (lowest) state to higher energy states by absorption of appropriately polarized light protons ($\hbar\nu$). Optical or absorption cells, filled with a vapor or sodium, for example, will experience “pumping” of ground state electrons into higher Zeeman energy states until the ground state is depleted. Absorption stops as the cell becomes opaque. Absorption is re-initiated by applying a weak high-frequency radio field to the cell, and the higher electron energy states will “depopulate” and cascade back down to the ground state. Optically pumped magnetometers have been in use almost as long as proton precession and fluxgate models. A recent use of the Zeeman effect in the proton precession design takes advantage of a resonant proton-electron coupling in an organo-electrolyte (paramagnetic) that increases the magnetometer’s sensitivity to 0.01 nT. The effect is termed the Overhauser effect and the device based on this effect is the Overhauser-Abragam magnetometer (Milsom and Eriksen 2011).

5.6.3 Gradiometers

Almost any type of magnetometer—proton, fluxgate, and optical—can be configured to function as a gradiometer. Two sensors are paired at a fixed distance apart such that a horizontal or vertical *gradient* exists between the pair. This magnetic gradient or separation is small—0.5–1.0 m—compared to most magnetic features. Gradiometers react to near-surface anomalies, with the lower sensor, if the instrument’s sensors are aligned in a vertical mode, detects the buried

feature more strongly than the upper sensor. The upper sensor can be thought to be affected more by the magnetic field of the earth rather than the feature. By subtracting the readings of the paired sensors, the gradient is obtained. In modern instruments this is done electronically and digitally displayed. To get a similar result, two magnetometers are often used with one remaining at a fixed location, the base station, and a second unit, the mobile unit, used to conduct the survey. At each location the readings, taken simultaneously, are subtracted to give what is termed the *differential* magnetic reading. This differential reading subtracts the magnetic field reading of the base station from the mobile reading. It is similar but not quite the same as the gradiometer reading.

5.6.4 Magnetic Anomaly Interpretation: Basic Principles

Magnetometers measure the field that results from the sum of the magnetic field strength induced by the earth’s field (average value = 50,000 nT) and any additional permanent magnetism or remanence. The remnant field component of the total field, at the measurement point, is often off axis to that of the earth’s field. Magnetic features are termed “anomalies” in the parlance of geophysics. Unless the anomaly has a strong remnant component, such as a hematite ore body or a buried clay hearth or kiln, most features found by archaeological prospection are the result of magnetic induction due to higher than average amounts of ferri- and ferromagnetic minerals and their increased magnetic susceptibility. Magnetic prospection relies on the contrast in terms of magnetic susceptibility among buried materials that is expressed as k and total magnetism is M . Less rigorous treatments reduce to semiempirical characterizations of the anomaly’s strength such as

$$T = k M/r^n \bullet \text{dimension/shape factor}$$

Here T is the anomaly strength, r is the distance to the anomaly from the sensor, and the

exponent, n , is the rate of decay of magnetic strength or *falloff factor* and a shape or dimension factor. M and k are as before. This expression is reduced to

$$T = M/r^n$$

Field inclination is indirectly considered by its effect on total magnetic intensity such that:

$T = 2 M/r^3$ for a dipolar anomaly along its axis; $T = M/r^3$ for a dipolar anomaly, off axis; and $T = M/r^2$ for a monopolar anomaly, any orientation. Field measurement of I is difficult and is most commonly estimated, e.g., 60° inclination at 30° N latitude. If I is known or estimated, a simple vectorial solution for the anomaly strength can be obtained.

The falloff factor is important. The field of a dipole falls off as the third power of the distance. For a monopole this is only by the square of the distance. In practical terms this implies that an anomaly's strength, measured at 81 nT, directly over the feature, will fall to 3 nT at a distance of 1 m. By way of comparison, active EM devices, such as metal detectors, have a total falloff factor of r^6 !

One, even if assuming a purely vertical or horizontal field direction, can ascertain much about the nature of an anomaly by observing the rate of falloff and the sign of the anomaly along with its strength. Anomaly shapes change with an increase/decrease in sensor height and field direction. Depth estimation is likewise important. One can use the straightforward relationship seen in the above formulae or use "rules of thumb" or nomograms. Milson estimates the accuracy of these latter methods to within 30 % (Milson and Eriksen 2014). One method is the "full-width half-max" rule (FWHM). The anomaly's maximum value for Z (field strength) is used to determine those points on the x -axis where the value falls to $Z/2$. The distance between the two points of $Z/2$ is proportional to the approximate depth of the anomaly. For a spherical dipole, the depth is $\sim x/2$ and for a monopole the depth is $\sim 1.3 x/2$. In the mid-latitudes of the Northern Hemisphere, the maximum value of an anomaly tends to occur

to the south of the actual feature at a distance equal to one-third the depth of the feature.

5.6.5 Magnetic Prospection: Practice

Many "successful" magnetic surveys have been done in archaeology without a great deal of attention paid to first principles. In those surveys the results were judged on the presence or absence together with strength of anomalies. Indeed with the first magnetometer models, this was about all one could expect before reliable digital measurement of the field strength was added. Martin Packard and Russell Varian are credited with the development of the proton precession instrument in 1954 (Weymouth 1996). By 1956 John Belshé demonstrated that a replica of an ancient kiln produced a magnetic moment. Martin Aitken and Teddy Hall, of Oxford, constructed a proton-based unit and located an actual kiln buried in a Roman site (*supra*). Linnington, at the Lerici Foundation in Rome, surveyed the Greek site of Metapontum in 1968 and began the modeling of magnetic data. By the 1960s, workers, such as Scollar, in Bonn, were doing automatic data collection and applying computers to the processing and display of that data (Scollar et al. 1986). Workers such as Aitken, Linnington, Tite, Scollar, Ralph, Beven, Weymouth, and others rapidly moved magnetic prospection, in archaeology, forward.

Understanding the susceptibility contrasts of materials greatly enhances the predictability of what one can hope to detect in differing field situations. For instance, a contrast of 10^{-2} versus one of $\Delta k = 10^{-4}$ results in strikingly different anomaly strengths, i.e., 32 vs 0.32 nT. Another factor, not mentioned in the discussion of principles, is the daily or *diurnal variation* in the earth's field. This is a real and fairly regular effect observed over the course of the day. This change is observed; field strength is a result of ionospheric currents that grow in strength over the day, with solar heating, and subside overnight. The pattern, in mid-latitude areas, follows an increase in field strength to 11 AM decrease of ten or more nanoTeslas toward dusk and then a

steady increase up to midnight. Again the increase is in the low terms of nT. Long-duration surveys must account for the diurnal variation. This is typically done by using the differential arrangement discussed previously. These changes are subtracted from the data to normalize the AM and PM components. If a gradiometer instrument is being used, then such a correction is less necessary. Another common factor that intrudes on long traverses (>100 m) is the earth's field gradient. This is a consequence of running most profiles in a N-S direction. Those readings most northward will gradually increase as a function of the normal increase in the earth's field strength as one approaches the poles. It is easily observed as slight change of profile slope and subtracted from the data.

The two principal magnetic methods, magnetometer and magnetic susceptibility, have proven successful in the search for archaeometallurgical sites and their features (Powell et al. 2002).

The former, magnetometer, "proton," "optically pumped," or "fluxgate," is considered "passive" in that the instrument produces no physical perturbation of the soil or feature and only detects the magnetization by means of sensor coils. Magnetic susceptibility systems—susceptibility meters and electrical conductivity meters—are "active" instruments in that they use an alternating current in a coil to induce or measure secondary magnetic fields in a feature (Florsch et al. 2011). As we discussed in the foregoing treatment on conductivity, induction is measured as a function of the applied frequency or frequencies. In an excellent example of one lesser used geophysical methods, Florsch et al. (2011) utilized induced polarization for the study of slag heaps.

5.6.6 Date Acquisition and Display

Magnetometer surveys, as with most of the other techniques discussed in this chapter, are done on orthogonal grids of straight headings and fixed offsets between (traverse) lines. Other than sensor height, these are the only real variables in a magnetic survey that an investigator can control.

As just discussed geomagnetic and ionospheric factors are accounted for but not chosen beforehand. Unlike other geophysical surveys, archaeological prospection involves more grid-area survey on closely spaced (0.5–2 m+) lines. The spacing of grid intervals is largely determined by the size of the feature(s) being sought and susceptibility contrasts. For small, discrete objects of low-to-moderate magnetic contrast, the grid should rarely exceed 1 m in interval/offset spacing. For larger features such as structural remains, roadways, etc., the interval can be relaxed to 5 and even 10 m spacing if the area to survey is large.

On the average, one team of two to three individuals can survey a 20×20 m area on a 1 m interval in a 6–8 h period. Speed in these surveys is determined by the cycling time of the instrument which is basically a nonfactor with any modern instrument given that the operator can occupy a point and measure, move, and repeat the sequence in a typical one-half second cycling time of a precession device. Optically pumped and fluxgate systems read continuously so one just walks, reads, etc. This aspect of magnetic survey is its great advantage. Compared even to the two-probe resistivity array, magnetic surveys in terms of time make it a tortoise-hare situation. This time the hare wins.

Other techniques comparable, in terms of speed, are some EM survey devices and, in more and more instances, GPR. Data produced by magnetic prospection is three-dimensional, that is to say, x, y, z, or "triplet form." The z value is that of the magnetic field. Because mapping software today commonly uses triplet-form data, it is an easy thing to substitute magnetic field strength for altitude producing both (a) contour and (b) isometric plots of the data.

5.6.7 Advantages and Disadvantages

Speed of survey, relative ease operation, rapid computer-based display, and manipulation of large data sets have made magnetic prospection one of the most widely used of today's geophysical techniques. The physical principles are well

understood drawing on the depth of research into magnetism at both the micro- and macrolevels. The cost of instruments has become less of a problem with the increased volume of devices available.

Of the most prominent types of magnetometers—proton precession, optically pumped vapor cells, and fluxgate devices—only the latter are relatively immune to external noise and strong local field gradients. Even these devices may have problems in some volcanic terrains. With the exception of the fluxgate systems, most magnetometers cannot be used too close to power transmission lines or large concentrations of iron and steel. A problem, but not one of the magnetometer itself, is the interference caused by modern metal commonly found on more ancient archaeological sites. In these cases the use of EM devices, in conjunction with magnetometers, has merit. Neither surface or near-surface metal debris nor strong field gradients significantly impact resistivity survey techniques.

5.7 An Abandoned Nineteenth-Century Cherokee Cemetery, Park Hill, Oklahoma, Cherokee Nation, USA

Rose Cottage (Figs. 5.5 and 5.6) was the residence of Chief John Ross, principal chief of the Cherokee Nation, 1828–1866, after the tribe's forced removal from tribal lands in Georgia, Tennessee, and North Carolina, in 1838–1839. Located somewhere near the site, the nineteenth-century home, the Rose Cottage, of Principal Chief John Ross, the “Forgotten Cemetery” grid was suspected to lie under mown, grassy pasture bordered by a low elevation on its north side by the so-called Old Road which connected the Rose Cottage with the present-day Park Hill Road. Mentioned in a 1937 Elizabeth Ross interview as “One of the oldest burying grounds in Cherokee County, now altogether obliterated, once lay near the north bank of the Park Hill branch, several hundred yards northeast of the Campbell Spring.” Relocating the Rose Cottage site as well as the nearby burial ground

was undertaken by the University of Georgia's Institute for Native American Studies (INAS), which conducted a multisensor geophysical survey of the historic Rose Cottage site and its vicinity in August 2013.

The most dramatic feature seen in the radar data is shown in Fig. 5.6. The rectangular feature that is just below the present ground surface continues to some depth, over a meter, and is clearly a “man-made” or anthropogenic feature. It is 40 m in overall length and more than 15 m in width. The north or upper portion of the feature extends beneath the elevation termed the “Old Road.” The survey grid did not extend beyond the edge of this latter topographic feature.

Within the boundaries of the large rectangular radar feature, large and sharply delineated magnetic features are clearly seen (Fig. 5.7).

5.7.1 Ground-Penetrating Radar: GPR

The publication of textbooks (Goodman and Conyers 1998; Conyers 2012) exclusively focusing on the use of fairly recently developed geophysical technique in archaeology highlights the rapid incorporation of GPR into archaeological prospection. At the end of the century, after only slightly over two decades, GPR has risen to a level of recognition among archaeologists previously reserved for magnetic or resistivity instruments. This newfound popularity of GPR in archaeology, in environmental studies, geotechnical and construction areas of engineering, as well as geology has led to new and older journals alike, devoting entire issues to the applications and methods of the technique (*Geophysics* 1986).

Principles GPR is an electromagnetic geophysical technique where a radar beam (wave) is transmitted into the subsurface and, depending on different electrical properties of materials in the subsurface, that beam can be diffracted and reflected at objects and interfaces (Leute 1987) (Fig. 5.7). The strength and the travel time, the time delay, between transmitted and returning pulses, tt , of radar reflections can be plotted by recorders and converted to depth and dimension.



Fig. 5.5 Rose Cottage, from a painting of the house done from memory. Oklahoma Historical Society

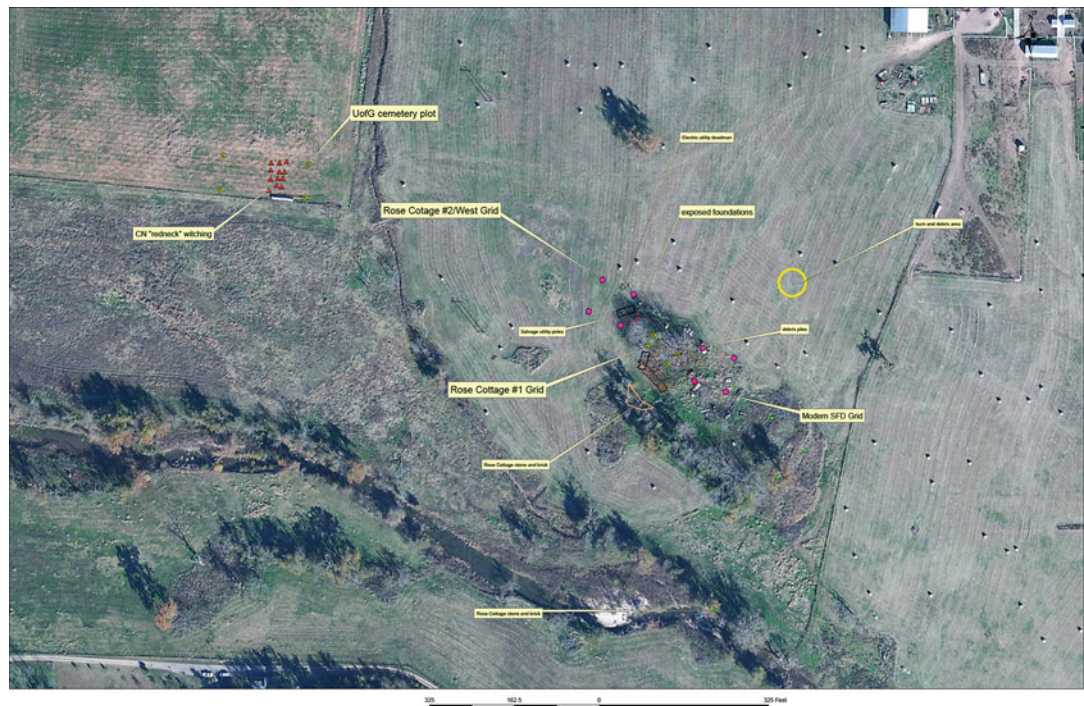


Fig. 5.6 A GeoPDF showing the location of UGA survey grids and other landmarks at the Rose Cottage site

GPR “sees” through freshwater, ice, soil, rock, brick, and paving although highly conductive materials such as seawater, clays, and metal attenuate or occlude radar propagation. The radar pulse is transmitted as a short burst of EM energy over a compact range of frequencies called a “CHIRP.” The center frequency of the antenna

plus 50 % above and below the center frequency makes up the chirp’s range. For example, a 100 MHz center frequency includes frequencies down to 50 MHz and up to 150 MHz. The general rule in estimating GPR depth of penetration is the lower the frequency, the deeper the potential survey depth. Because GPR operates at relatively

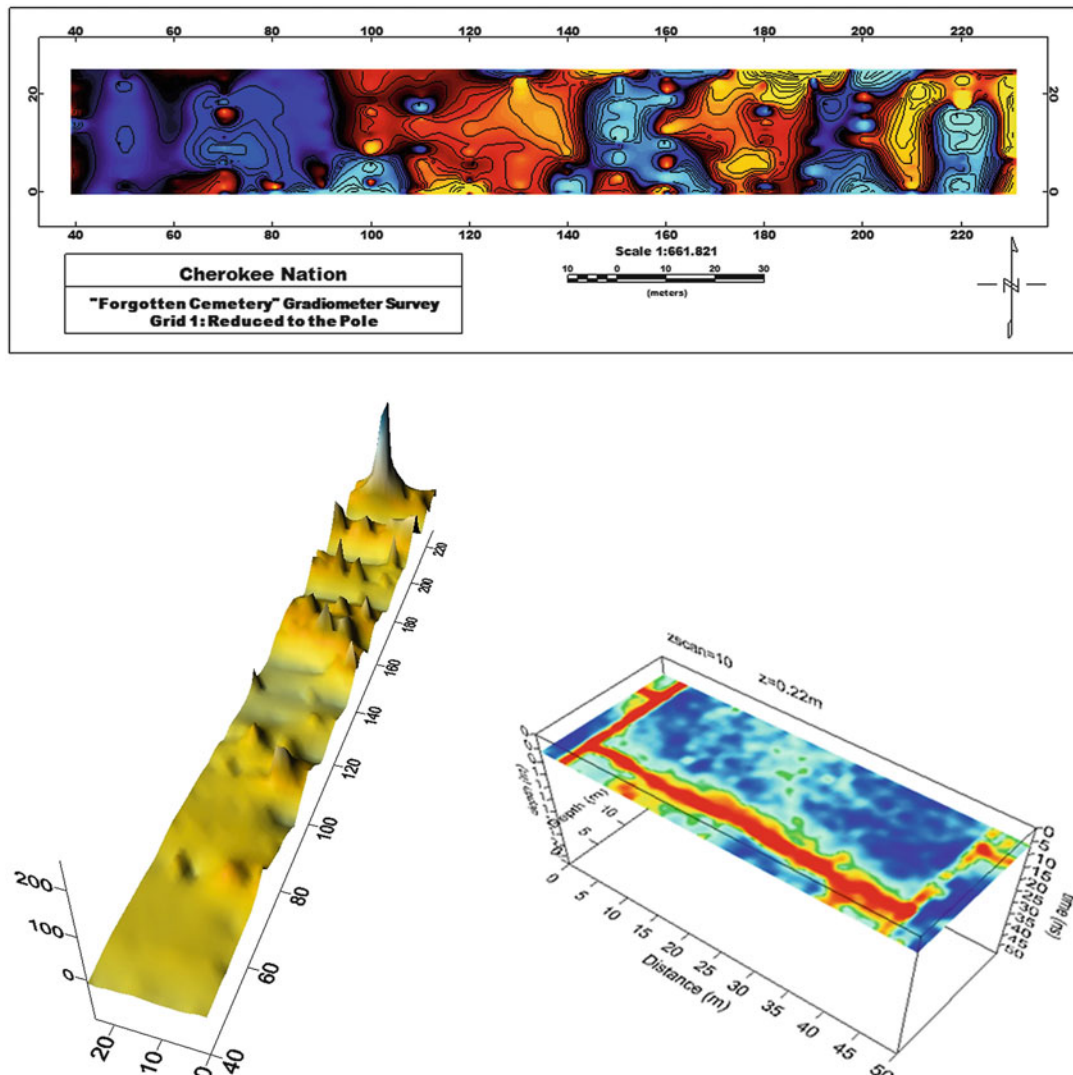


Fig. 5.7 Multisensor representations—left and above, magnetic; right, ground radar—of an abandoned Native American cemetery, Park Hill, Oklahoma, Cherokee Nation, USA. The magnetic anomalies correspond to rows of grave pits while the radargram indicates three sides of a buried stone wall. The latter

view is 1.74 m depth and clearly shows the rectangular subsurface feature interpreted as a remnant of a stone or masonry wall. The magnetic features (orange red) in the plots show linear patterns. The separation between the anomalies indicate individual graves

high frequencies 20–1500 MHz, compared to seismic frequencies where “high” is considered to be in the range of 100 Hz, penetration beyond a few tens of meters in all but the most favorable material—rock generally—is uncommon. For most antennae, used in archaeology, the depth range is 5 m or less, the working limit of 400–500 MHz models. For most archaeological

sites, this range is quite adequate as the bulk of most habitation sites seldom exceed this depth range with the exception of tells and other deeply found settlements. Even in these sites of exceptional depth, the antenna with a frequency appropriate to the survey can be found.

The resolution of a specific radar frequency is a direct function of wavelength, which, in turn, is

a function of the velocity of radar wave in a material. Velocity relies on the value of electrical permittivity or more termed, the dielectric “constant” (coefficient), ϵ . With EM techniques, it governs attenuation in both cases where induction currents extract energy from the radar pulse. The conductivity of materials generally follows an increase in the dielectric constant, but this is not so direct a relation as to have seeming contradictions where fresh- and seawater share the same value ($\epsilon = 80$) yet have extreme differences in conductivity ($\sigma = 0.5$ vs 3,000). This contradiction is better understood when the electrolytic properties—ionic vs nonionic—are considered. Permittivity is a direct reflection of the molecule’s ability to polarize. The typical values of ϵ , σ , and velocity (v) as well as attenuation factors are shown in Table 5.4.

The wavelength and velocity are given by the following:

$$\begin{aligned} v &= 1/\sqrt{\mu\epsilon} \\ \lambda &= v/f\sqrt{\epsilon} \quad \text{and} \quad v = c/\sqrt{\epsilon} \\ \lambda &= v/f \end{aligned}$$

c is the velocity of light in free space (0.30 m ns^{-1}), v is the velocity of the EM wave in the medium, f is the frequency, ϵ is the dielectric constant (permittivity), and μ is relative magnetic permeability which in most materials (except metals) is close to 1. Most calculations assume it to be unity. Velocity and wavelength change with material giving radar its ability to image the subsurface. For example, in air, a 100 MHz pulse wavelength is 3 m; in rock with a velocity reduced to 0.1 m ns^{-1} , it is only 10 cm. In wet clay this will drop to about 1–2 cm. As we have said, resolution is a function of wavelength so features, in rock, can be resolved to 10 cm but no smaller as that dimension is inside the wavelength and thus subject to refraction and blurring. In this the radar wave mimics other EM waves. Another general rule for GPR resolution is that the size of the object should be not less than one-tenth of its depth (Milsom and Eriksen 2011). As a result a 10 cm object cannot easily be detected at over 1 m unless the reflection, in terms of signal return, is exceptionally good, e.g., a good dielectric contrast and low attenuation.

Table 5.4 Typical values of radar parameters of common materials

| Material | ϵ | $\sigma (\text{mS m}^{-1})$ | $v (\text{m ns}^{-1})$ | χ |
|------------------|------------|-----------------------------|------------------------|----------|
| Air | 1 | 0 | 0.30 | 0 |
| Ice | 3–4 | 0.01 | 0.16 | 0.01 |
| Freshwater | 80 | 0.5 | 0.033 | 0.1 |
| Saltwater | 80 | 3,000 | 0.01 | 1,000 |
| Dry sand | 3–5 | 0.01 | 0.15 | 0.01 |
| Wet sand | 20–30 | 0.01–1 | 0.06 | 0.03–0.3 |
| Shales and clays | 5–20 | 1–1,000 | 0.08 | 1–100 |
| Silts | 5–30 | 1–100 | 0.07 | 1–100 |
| Limestone | 4–8 | 0.5–2.0 | 0.12 | 0.4–1 |
| Granite | 4–6 | 0.01–1 | 0.13 | 0.01–1 |
| (Dry) salt | 5–6 | 0.01–1 | 0.13 | 0.01–1 |

R , the reflection coefficient, is related to the soil permittivity, ϵ , of the upper media, ϵ_1 , and the lower media, ϵ_2 , by

$$R = [(\epsilon_1(1/2) - \epsilon_2(1/2)]/[(\epsilon_1)1/2 + (\epsilon_2)1/2]$$

This equation can be used to determine the strength of reflections at interfaces of materials of different lithology or composition.

An easy way to increase penetration and signal return is to increase power on the outgoing pulse. Increasing power (or gain) of the radar pulse can create other problems such as loss of detail in the upper areas of the trace of profile and refraction multiples from objects and secondary images such as hyperbolae and extraneous noise in the record. Many digital GPR units as well as post-processing softwares allow the operator to enhance gain losses in a GPR pulse somewhat selectively. The GPR trace is radar waveform that is perturbed as it penetrates through subsurface materials such that the returning waveform’s shape provides us information about the earth’s shallow near surface (Fig. 5.7).

A GPR profile display (Fig. 5.8) is simply a series of traces, in series, taken over a traverse of some fixed distance using a set timing interval. The height of the GPR profile is a set time interval in nanoseconds. Typically, one estimates the average velocity for the soil at the site to be surveyed and this is used to set the time “window” or interval. Dry sand’s velocity is 0.15 m ns^{-1} so a 100 ns (tt) window represents about 9.5 m depth. Before presetting an unrealistic depth for

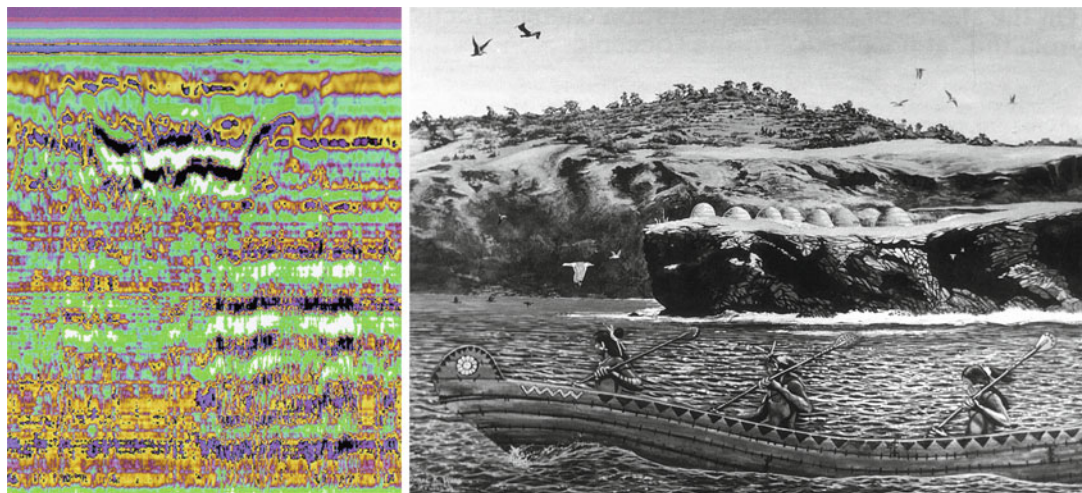


Fig. 5.8 A profile view of radar data. The image is of a Chumash pit dwelling, roughly 2 m in width, as illustrated in the artist conception adjacent. This is an idealized view

of an actual archaeological site on the island of Santa Cruz, California, USA, where the author conducted research on the late twentieth century

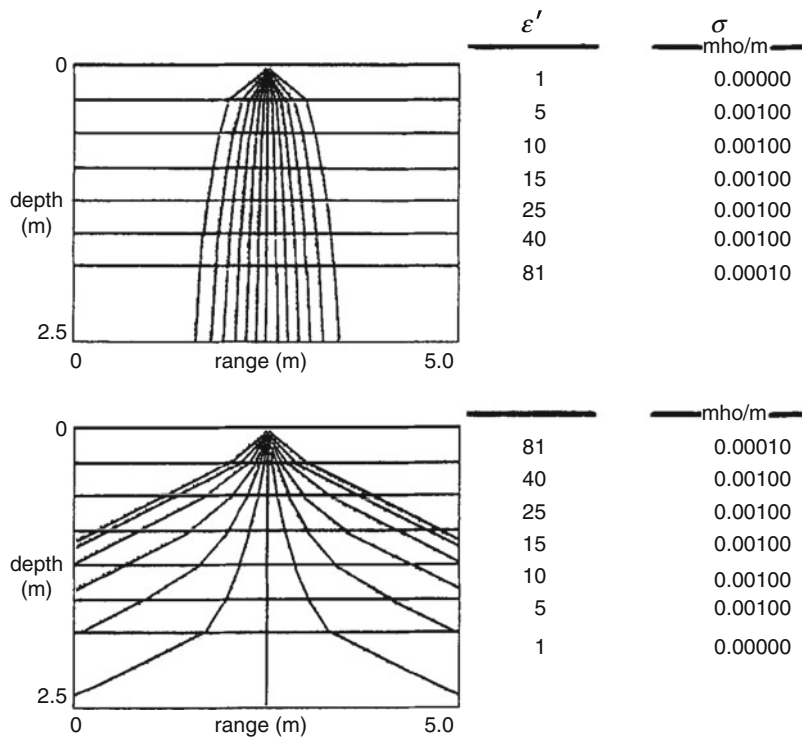


Fig. 5.9 The effects of refraction on the radar wave as the dielectric increases (upper) or decreases with depth (lower) (Adapted from Goodman 1994, Fig. 5.6)

the particular antenna type/frequency, one can estimate the realistic depth of attenuation called the skin depth by the empirical rule, $35/\sigma = \text{skin}$

depth. Here, σ is the conductivity emphasizing, again, its important role in attenuation of the GPR signal (Fig. 5.9).

5.7.2 Field Survey Methods

GPR, in seismic parlance, is a “zero or fixed offset” profiling technique, “zero” because in some antennae, using the so-called bow-tie dipole, the transmitter and receiver are in the same antenna.

Two antennae may be coupled, in bipolar or bistatic configuration, such that one is the transmitter and other the receiver yielding a small (1–2 m) fixed offset. These offsets are trivial compared to those used in seismic reflection or refraction survey where offsets can be in hundreds of meters across a geophone array. The antenna is either carried, stepped, or pulled across the ground along the preset traverse. In some cases where exceptional S/N is required, the antenna may be “stepped” along the survey line at preset intervals. This allows “stacking” of the data to be done at each station, along the traverse, thus increasing the S/N. Most field survey requires a minimum of two personnel—one the control unit operator and the other in charge of the antenna (“the mule”).

Grid size is important, particularly today, with varieties of spatial profile and three-dimensional plots available on computer programs. Unless specific parameters are maintained, the application of this data processing tools is obviated. One meter offset, for transverses, have become a default interval for most archaeological GPR surveys. Adjacent traverse lines have a good probability of crossing features at or near this size within the grid. Halving the interval doubles survey time, but almost all features at or above this size will be detected. The depth of survey is preset as we have discussed. If the site is shallow, 1–2 m, in overall thickness, then it is important to set the time window to be below this, say 2.5–3.0 m range in ns. For dry sand, this is roughly 130–200 ns, for a velocity of 0.15 ns m^{-1} . This is not an impractical setting for antennae frequencies of 100–500 MHz.

Orthogonal grid directions can be surveyed. If time permits, it should be attempted. Linear features, which the antenna may just parallel on a traverse, can be bisected by a crossing pattern survey. At the start of each traverse, no matter the

direction, a GPR must be rapidly recalibrated for comparable data across the complete grid. This is routine and requires little in the way of resetting of instrumental parameters. Generally the surface zero set and gains are all that require adjustment. Once a routine is established, and environmental conditions allow, survey progress can be steady and consistent. One GPR survey conducted in the later 1990s by a University of Georgia team covered over eight linear km of traverses in a 5-day period. This time would be significantly less today—1 day of less—using multichannel/antennae arrays.

A basic grid area is 100×100 m surveyed using a single frequency antenna on a 1 m offset interval (Fig. 5.10). A factor that has led to GPR’s rapid acceptance in archaeology is the immediate return on survey effort. GPR is a “WYSIWYG” technique—what you see is what you get. The GPR record is a digital facsimile of the subsurface immediately below the antenna along the direction of the traverse shown on-screen and most often recorded as a file. Such records are seen in Fig. 5.10. For more detailed analyses, these files are evaluated with the aforementioned post-processing routines back in the lab.

The linear feature along the left axis of both plots is interpreted as a water channel or aqueduct serving the site (Garrison et al. 2013, 2014).

5.7.3 Digital Post-Processing of GPR Data

As illustrated in Fig. 5.11, much of the enhanced interpretability of GPR records have come through the use of digital processing similar to that developed for acoustical seismic methods. Once the GPR data is logged in this format, it can be readily manipulated to remove background noise and enhance gain in weak returns by reverse time-varying gain amplification, together with the use of other filters—FIR (finite impulse response)—as well as those to compensate for spherical effects in propagation. Advanced seismic-style algorithms such as “boxcar filtering” and “Kriging” together with Fourier



Fig. 5.10 A typical survey grid and GPR units; foreground, a control unit and antenna using a survey wheel; background, another control unit mounted, along with an antenna, on a survey cart. Tapes indicate *transect lines* (Photograph by the author)

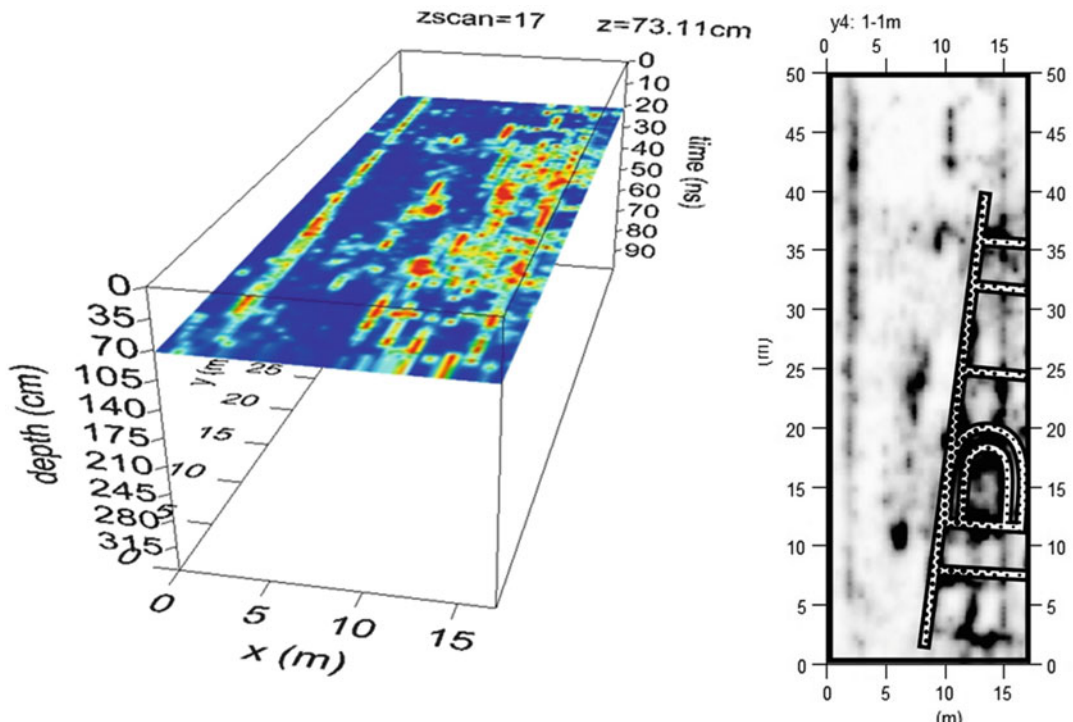


Fig. 5.11 Examples of post-processed radar data. Both represent a 2004 radar survey of a Roman villa site in western Switzerland. The plot on the left shows the burial

depth at almost a meter, while the plot on the right highlights architectural details of the villa's principal *pars urbana*

transform of frequency to time series are available which, in turn, prepares the data for deconvolution—which removes peg-leg hyperbolae and multiple reflections from the record. Migration, a common seismic technique, can be applied to profiles that are adjacent and are closely enough spaced (Meats 1996). The reader is directed to Goodman and Conyers (1997, 2013) for a good introductory review, while the advanced student is directed to their bibliography and journals such as *Geophysics*, *Applied Geophysics*, *Journal of Archaeological Science*, *Archaeometry*, *Environmental and Engineering Geophysics*, and more recently, *Archaeological Prospection*.

A useful iteration of GPR data is the so-called time slice technique (cf. Goodman and Conyers 1997, 2013). This processing method combines data from an adjacent profile at fixed intervals of time such as 30 ns, 45 ns, 60 ns, etc. Using a protocol similar in form to GIS methodology where sequential overlays or “slices” are built up gives the viewer an overhead view through the site as visualized in the GPR data (cf. Figs. 9.7 and 9.10).

5.7.4 Multiple Geophysical Techniques

Hesse (1999) has written succinctly about the combined use of multiple geophysical prospection techniques (“sensors”) for archaeology. Another excellent example is that of the geophysical study of Roman Grand, in the Lorraine region of France, presented in a theme issue of *Les Dossiers Archeologie* (1991). The point Hesse makes is that the efficacies and shortcoming of individual geophysical techniques may to a large degree offset one another in the latter case and enhance interpretability of anomalies in that of the former. Multiple sensor studies are to be attempted wherever possible. Cost and availability are prime considerations. The scale of the study is a key factor. Deploying expensive multiple sensor on relatively small sites may be a case of instrumental “overkill.” In seeming contradiction, important, very

localized archaeological features such as tombs or burials may require the use of more than one geophysical technique to adequately relocate them in many instances.

5.7.5 Underwater Geophysical Survey Techniques in Archaeology

The use of geophysical techniques in underwater archaeology began in the 1960s (Tite 1972; Aitken 1974). These rapidly moved to assemble multiple sensor arrays as these became feasible over the subsequent decades. Today, in geophysical surveys of shipwrecks and landforms, these ensembles typically include (1) a towed marine magnetometer, (2) a 100–500 MHz side-scan sonar, and (3) an acoustic “sub-bottom” profiler, more commonly of a CHIRP, swept-frequency type. In some instances, a towed pulsed EM system is used in place of or in conjunction with the magnetometer. Survey tracks are pre-plotted and tracked using high-precision line-of-sight radar transponder systems or more and more frequently with reference to GPS. Positional accuracy in dynamic survey mode regularly approach 3–5 m in accuracy. Anomalies, acoustic, magnetic, and electrical, are logged along-track to strip charts and digital files. The multiple data sets can be post-processed and reconciled just as those done terrestrially.

Two techniques that are unique to underwater survey are acoustic in nature. Deep seismic studies of the offshore for minerals have always been acoustic. Their detail, or resolution, of the seafloor and near sub-seafloor was too large scale for archaeological purposes. The late Harold Edgerton, of the Massachusetts Institute of Technology (MIT), developed a viable acoustical seismic profiler by directing a beam of a piezoelectric transducer of an appropriate frequency, 2–7 kHz, straight down to allow the beam to profile the upper sediments of sea bottom. With sound velocities in water, ca. $1,500 \text{ m s}^{-1}$, a 3.5–5 kHz transducer produces a waveform in lengths of 30–50 cm. Such wavelengths can regularly detect objects of archaeological interest much like GPR does on land.

The waves are pulsed or pinged by the transducer(s) activated by an applied voltage across condensers. Acoustical impedance differences caused by the relative compactedness or looseness of the materials appear as returning signals or reflections of differing gray scale—dark for hard and light for unconsolidated materials. The water is transparent to the sound waves so the soil/water interface is easily seen. The returning waves, although weakened, are collected by the transducer and amplified for graphical display on screen or recorder. Measuring the signal (reflector) and travel time (1 ms ~ 2.7 m at $1,500\text{ ms}^{-1}$), the depth and thickness of a sediment reflector can be measured accurately. Like GPR the waves tend to refract and reflect more than once between the sea or lake floor and the surface generating multiple reflections. These are easily detected in the acoustical record. Individual features—rocks and buried archaeological objects—appear as diffraction hyperbolae. If the object is metal, its character can be rapidly noted by use of other techniques, magnetic or EM.

Edgerton (1986) went on to quickly design the side-scan sonar after the “sub-bottom” profiler in the mid-1960s. The initial analogue models have been supplanted by digital systems, some whose design traces back to Edgerton. The side-scan sonar, by immediate reference to the output acoustical frequencies of 100–500 kHz, as are commonly used in archaeological prospection, does not attempt to penetrate the sub-seafloor. Rather, the purpose is to produce a horizontal terrain map on both sides of towed body mounting parallel transducers depressed downward at angles of 3–10°.

5.8 The Sabine River Paleovalley, Northern Gulf of Mexico, USA

In 1984, over a quarter of a century ago, Charles Pearson, Sherwood Gagliano, Richard Weinstein, and David Kelley undertook a study designed to locate submerged prehistoric archaeological deposits on the continental shelf of the Gulf of Mexico. This research was predicated on the question, raised by Melanie Stright: “Where

on the continental shelf of North America will archaeological sites dating from the Archaic Period (8,000–3,000 B.P.) occur and be preserved?” (Stright 1986a, b, 1990, 1995a, b). Her comparative analysis of published relative sea-level curves for North America indicated that Archaic Period archaeological sites may exist as deep as 22 m below present mean sea level in portions of the northern Gulf of Mexico. This early effort at submerged archaeological site discovery relied on a research strategy based on actualistic and archaeological analogues (Pearson et al. 1982) together with a series of technological approaches that have since become standard in this field of study—sub-bottom profiling, side-scan sonar, sediment coring, etc.

The study area was the now-filled and submerged stream valley of the Sabine River offshore of Louisiana and Texas (Fig. 5.12). The research involved the collection and synthesis of a large amount of high-resolution seismic data and core records in order to reconstruct the prehistoric, subaerial landscape of the region. Models of prehistoric site distributions derived from onshore analogues were extended to the offshore landscape to identify the now-submerged landforms with a high likelihood of containing preserved cultural remains. These presages, by over two decades, are the so-called Danish model popular in the literature of prehistoric underwater archaeology today (Benjamin 2010). Early Holocene climate change, reflected principally in sea-level change, was incorporated into the predictive model of site distribution and preserved landform occurrence in the offshore area of interest. More than 70 vibrocores were used to collect sediment samples from several geophysically identified high-probability landforms (Fig. 5.13). Analyses indicated the existence at least one location of cultural deposits dating to ca. 8,800 BP. Subsequent research in the region has employed a similar strategy in the search for submerged prehistoric deposits.

The Archaic Period can be called an “American Mesolithic Period” because of the extensive similarities between the cultures of both Eurasia and the Americas. Hunting-collecting economies

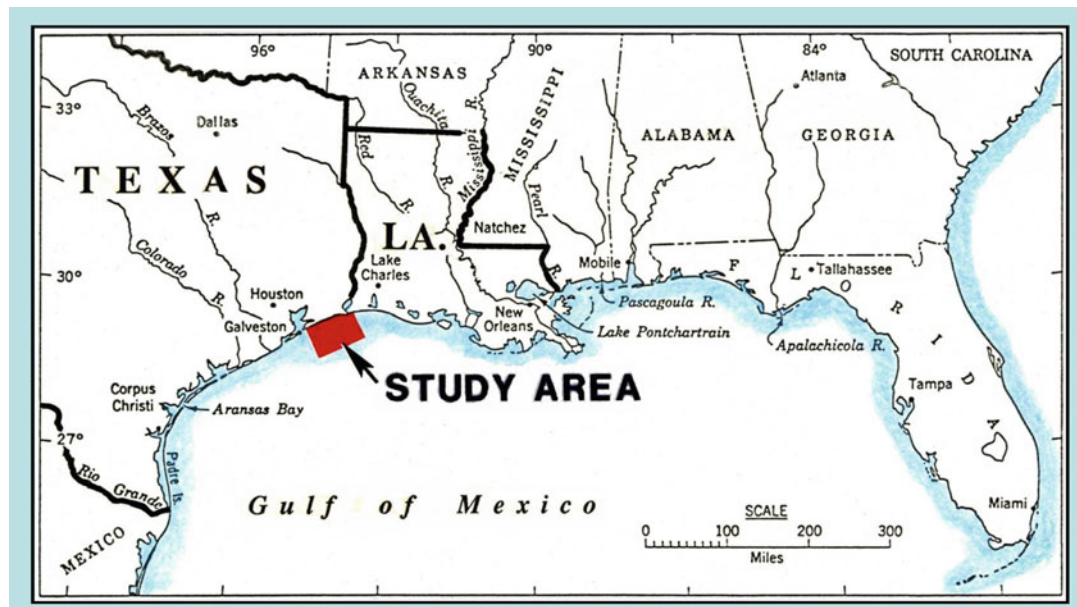


Fig. 5.12 Study area, in red, for the Sabine River paleovalley study, northern Gulf of Mexico, USA

dominate the post-Holocene. The start of the Mesolithic, in the Early Holocene, is generally regarded as synonymous with two major technological developments. The first is the development of small armaments such as the bow and arrow as opposed to spears and spear throwers of the late Paleolithic/Paleo-Indian period. Microlithic tools and the stone elements used to tip arrows appear for the first time at this period (Wickham-Jones 2005, 2010; Sassaman and Anderson 1996; Sassaman 2004; Thompson and Worth 2011). The late twentieth-century underwater study of the prehistoric northern Gulf of Mexico has much in common with the early twenty-first-century study of the prehistoric North Sea Region (Fig. 5.14).

5.9 Doggerland: Mesolithic Landscapes of the Southern North Sea

The Southern North Sea (SNS) is a marine basin that occupies a position between the European countries of Norway, Denmark, Germany, the Netherlands, Belgium, France, and the United

Kingdom and is confined in latitude between 55 and 51° north. The Southern Sector covers 6250 km² (approximately 1 %) of the total area of the North Sea (Fitch et al. 2007). To examine such a large submarine area requires large geophysical data sets. The utilization of spatially extensive oil industry data has allowed the recovery of information pertaining to the actual Mesolithic landscape of the North Sea aka “Doggerland” (Gaffney et al. 2007) (cf. Figs. 2.6 and 2.7). This information reveals the diversity of this landscape and shows that much greater consideration of submerged Mesolithic landscapes is now required of archaeologists. Indeed, Caroline Wickham-Jones (2005) recognized this situation when she suggested that “archaeologists of the Mesolithic should now investigate the potential of the undersea world.”

The North Sea Palaeolandscapes Project (NSPP) has demonstrated that recovery of archaeological landscape information through extensive 3D seismic data is both possible and desirable. The information derived provides a unique opportunity to explore human activities within a spatially extensive prehistoric landscape

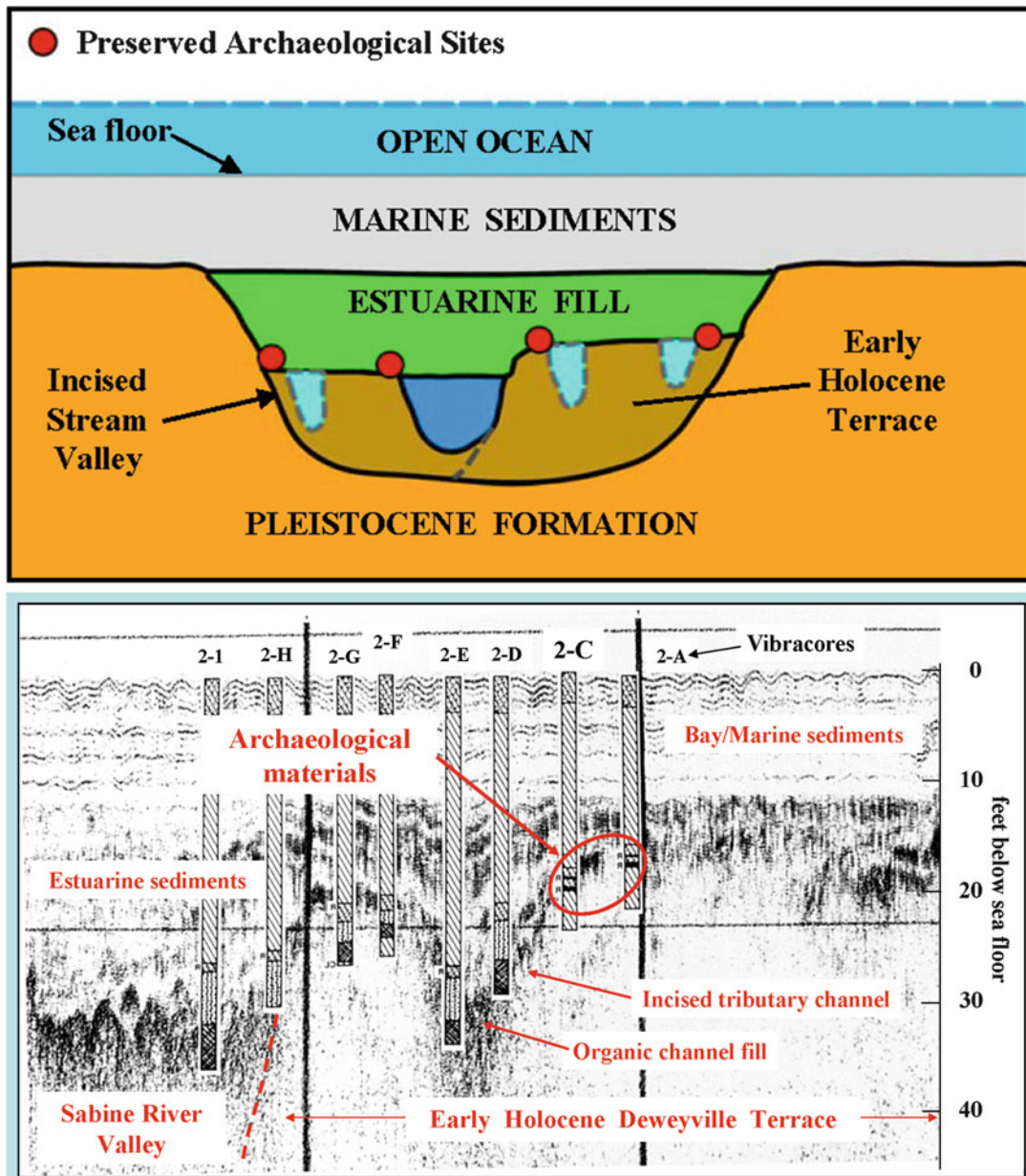


Fig. 5.13 Acoustical profile and schematic view of sonar images produced by an acoustic sub-bottom profiler of a drowned paleochannel in 15 m water depth in the Gulf of

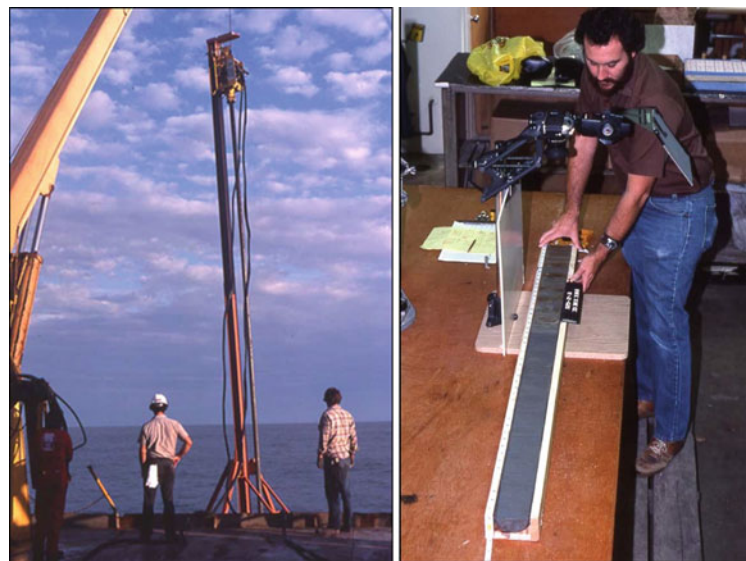
Mexico. Sediment vibracore locations (Fig. 9.14) are indicated. This ancient estuary is illustrated its drowning at transgression ca. 6000 BC (Pearson et al. 2008)

and, more fundamentally, suggests that the landscape could have contained a significant Mesolithic population. The geophysical survey data cover more than $>22,000 \text{ km}^2$ in the Southern North Sea alone (Fitch et al. *supra*), and although the potential of this data to inform submerged

archaeological prospection had been recognized (Kraft et al. 1983), this opportunity has not been realized until Gaffney et al. began their interdisciplinary study.

The Central and Southern North Sea are nowhere deeper than 60 m, and the flat-topped

Fig. 5.14 *Left*, sampling the drowned Sabine estuary shown in Fig. 9.13 with a vibracore; *right*, analyzing the sediments in a vibracore taken from the estuary (Pearson et al. 2008)



Dogger Bank rises to within 15 m of the surface, providing a total relief of 45 m over a distance of about 500 km east to west. The objective of the NSPP was to analyze the upper part of the seismic profile and to extract from that record the sedimentary facies (“seismic facies”) and topographic changes which indicate past landscape surfaces during the Mesolithic period from 10,000 to 5000 BP. Geographic information systems (GIS) were used to extract time slices

from massive blocks of raw data. Subsequent 2D and 3D views illustrate river channels, estuaries, beaches, marshes, lagoons, and braided/overlapping drainage patterns much like the earlier Sabine River paleovalley study. The success of the project depended upon access to massive computing power available to the project team through the Hewlett-Packard Visual and Spatial Technology Centre at Birmingham University (Gaffney et al. 2007).

6.1 Introduction

In the first edition of this textbook, it was asserted that the most common artifactual material of prehistory is lithological—rocks and/or minerals. This is still the case. Stone is, and was, the most durable of all materials available to early humans and, in most environmental settings, the most readily available. Its durability made it desirable for a multitude of tasks as well as helping insure its survival in archaeological sites. For the archaeologist, the survival of ancient human stone tools and artifacts has been both a blessing and a source of unintentional biases in terms of the reconstruction of past cultural behavior. Even with the earliest of human culture surely, there were other implements other than those of stone, but by their durability, the latter have survived, while other materials have long ago perished from the archaeological record.

The model in Fig. 6.1 is wearing only five items—6, 7, 8, and 9—that can be classified as stone per se. Item 9 might be hedging the definition of stone, a bit, but fossilization is basically lithification; thereby it is fair to classify this item as “stone.” More specifically, in this chapter, the use of stone for adornment or decorative purposes will be classified as “art stone.” Two other categories will be used—toolstone and dimension stone. The former will encompass those types of stone used in functional categories related to tasks. A toolstone can be used for stone

axes or as a grinding stone for a Roman hand mill. Dimension stones are used in construction of structures—buildings, dams, canals, roads, etc. Art stone will, of course, include portraiture, statuary, and monuments such as tombs, stelae, etc. Because of stone’s durability and availability, it has fulfilled all three of these roles admirably over eons of human existence.

For much of human prehistory, beginning in the Pliocene, “tools” were fashioned of durable stone; archaeology has been forced to focus on the nature of these tools and the stone—toolstone—from which they were made. In 1894, W.H. Holmes outlined the steps for the analysis of stone tools:

The first necessary step is their identification as implements as distinguished from allied forms, natural and artificial, that have no claims to be called such. The second step is a consideration of their natural history, which embodies two distinct lines of development, one of the individual from its inception in the raw material, through a series of steps of technical progress, to the finished result; the other the species or group from a primal culture germ through countless generations of implements; with these goes the evolution of form and function. The third step consists in regarding implements as historic records, first, with reference to questions of time; second with regard to questions of culture, and third, to the history of peoples. (Holmes 1894: 121)

In terms of the first step, the stone tool industry from the lowest levels (Bed I) of Olduvai



Fig. 6.1 Ancient and historic jewelry (Source: *National Geographic Magazine*). 1 Pendant of perforated shell ca.1000 BC; Syria. 2 Seal, shell, 7000–4000 BC; Syria. 3 Tubular bead, bone, 3000 BC; Syria. 4 Eye pendant, glass, 2000 BC; Egypt. 5 Pendant, glass, at least exterior; 600 BC; Punic-Phoenician? 6 Object made of carnelian,

600 AD; Central Asia. 7 “Bat wing” object—“parietal”? Jasper; Mesoamerica. 8 Bead, *lapis lazuli*, 1000 AD; West Asia. 9 Object fashioned from fossilized shell, 1000 AD; West Asia. 10 Incised disk, shell, 1900 AD; Mauritania. 11 Kiffa bead, powdered glass, 1930 AD; Mauritania. 12 Glass art depicting Marilyn Monroe, 2004; USA

Gorge was among the first implements definitively identified as made by hominins (Conroy and Pontzer 2012: 329–330). These tool forms have been found elsewhere, in earlier deposits but their forms are in all cases, manufactured. Pertinent, in particular to this chapter, is the “natural history” that includes consideration of the geological formation of rock types and their sources, e.g., the stone itself. Finally, how these implements function as historic records will be touched upon in the context of our modern analyses of them. One such example are the bluestones of Stonehenge.

6.2 Major Rock Types and Archaeology

The three rock types, sedimentary, igneous, and metamorphic, appear throughout prehistory as the materials for simple domestic tools to major masonry construction. In this section, most important archaeological rocks and minerals will be discussed with some illustrative examples from archaeology as well as a listing of their key petrographic properties that can be used in their identification using optical and instrumental methods.

This discussion begins with sedimentary rocks (Blatt 1982; Flygel 1982; Garrels and Mackensie 1971; Pettijohn et al. 1973; Rapp 2002) (Fig. 6.2).

As illustrated in Fig. 6.3, the rock cycle represents the continuum of lithogenesis wherein the formation of one type of stone may entail the destruction or alteration of another type such as the magma melt of accretionary sediment wedges in subduction and a subsequent re-extrusion as igneous rock types. Lithified shells—micro and macro—form the carbonate structure of limestones and other biogenic rocks which, in turn, undergo metamorphic alteration into that ubiquitous art stone, marble. Shales become slates; sandstones alter to quartzites.

6.3 Sedimentary Rocks

We begin with sedimentary rocks. Sedimentary rocks are formed by the consolidation of sediments. In the rubric of geology, they are termed the “soft rocks” although the hardness of some bioclastic limestones, as we shall see later in this chapter, is formidable enough to be used as grinding stone. Of the many sedimentary classification systems or schemes, most can be

Fig. 6.2 Dimension stone. Middle Jurassic sandstones. Dun Beag Broch, west coast of the Isle of Skye, Scotland. Historic Scotland

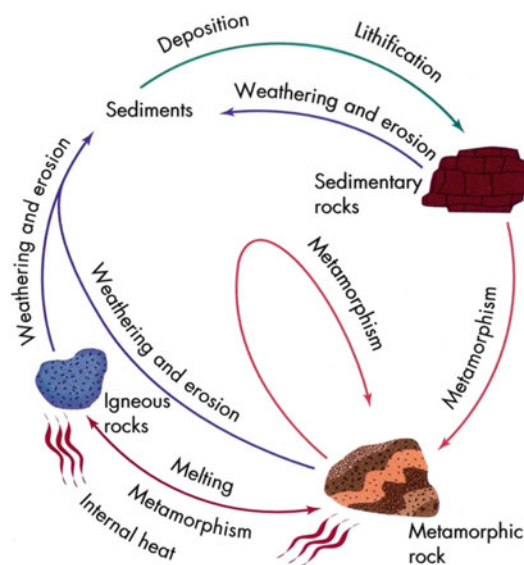


Fig. 6.3 The rock cycle

reduced to three groups of rocks, principally clastic, biogenic, and chemical (Andrews et al. 1997a, b), which in turn can be termed clastic, carbonate, and evaporites. Another way of viewing these rocks is simply *textural*. Clastic texture refers to the mineral fragments and rock debris which comprise the material. Non-clastic texture is that produced by the chemical or biogenic processes which form the rock. Within the non-clastic forms are the textures—crystalline,

skeletal, and oolitic. This discussion will follow the former classification terminology of clastic, chemical, and biogenic (Table 6.1).

Earth scientists understand that organic remains are most prone to diagenesis—the process of the chemical recrystallization or replacement in a substance, buried in the Earth, when given enough time, will change almost any natural material, even stone. Diagenesis might be confused with weathering which is the physical and chemical disintegration of rock and Earth materials upon exposure to atmospheric agents. In the case of most rocks and minerals, the time needed for diagenetic change to occur is much longer than that which alters organic materials such as the bone and botanicals. There are instances, numerous in some geological epochs, where even these latter materials become mineralized during diagenesis and are no different from stone. Happily, for paleontologists, most past life forms are fossilized and preserved for study. For archaeology, subfossil and fossil bone could become toolstone, art, and dimension stone (Figs. 6.1 and 6.2).

Clastic Rocks Fragments of rocks are called *clasts*. Clasts are the product of the weathering, physical or chemical, of rocks. Clastic rocks are classified on the basis of grain size, ranging from gravel-sized fractions in conglomerates

Table 6.1 Classification of sedimentary rocks

| Texture | Composition | Rock name |
|--|--|--------------------------|
| A. Clastic rocks | | |
| Coarse grained (over 2 mm) | Rounded fragments of any rock type—quartz, quartzite, chert dominant | Conglomerate |
| | Angular fragments of any rock type—quartz, quartzite, chert dominant | Breccia |
| Medium grained (1/16–2 mm) | Quartz with minor accessory minerals | Quartz sandstone |
| | Quartz with at least 25 % feldspar | Arkose |
| | Quartz, rock fragments, and considerable clay | Graywacke |
| Fine grained (1/256–1/16 mm) | Quartz and clay minerals | Siltstone |
| Very fine grained (less than 1/256 mm) | Quartz and clay minerals | Shale |
| B. Chemical and biogenic (some of them are not chemical but biological) | | |
| Medium to coarse grained | Calcite (CaCO_3) | Crystalline limestone |
| Microcrystalline, conchoidal fracture | | Micrite |
| Aggregates of oolites | | Oolitic limestone |
| Fossils and fossil fragments loosely cemented | | Coquina |
| Abundant fossils in calcareous matrix | | Fossiliferous limestones |
| Shells of microscopic organisms, clay soft | | Chalk |
| Banded calcite | | Travertine |
| Textures are similar to those in limestone | Dolomite $\text{CaMg}(\text{CO}_3)_2$ | Dolomite dolostone |
| Cryptocrystalline, dense | Chalcedony (SiO_2) | Chert, etc. |
| Fine to coarse crystalline | Gypsum ($\text{CaSO}_4 \cdot 2\text{H}_2\text{O}$) | Gypsum |
| Fine to coarse crystalline | Halite (NaCl) | Rock salt |

and breccias through sandstones, siltstones, and fine-grained shales. The grain-size scale for clastic rocks is exactly that for sediments (Table 6.1).

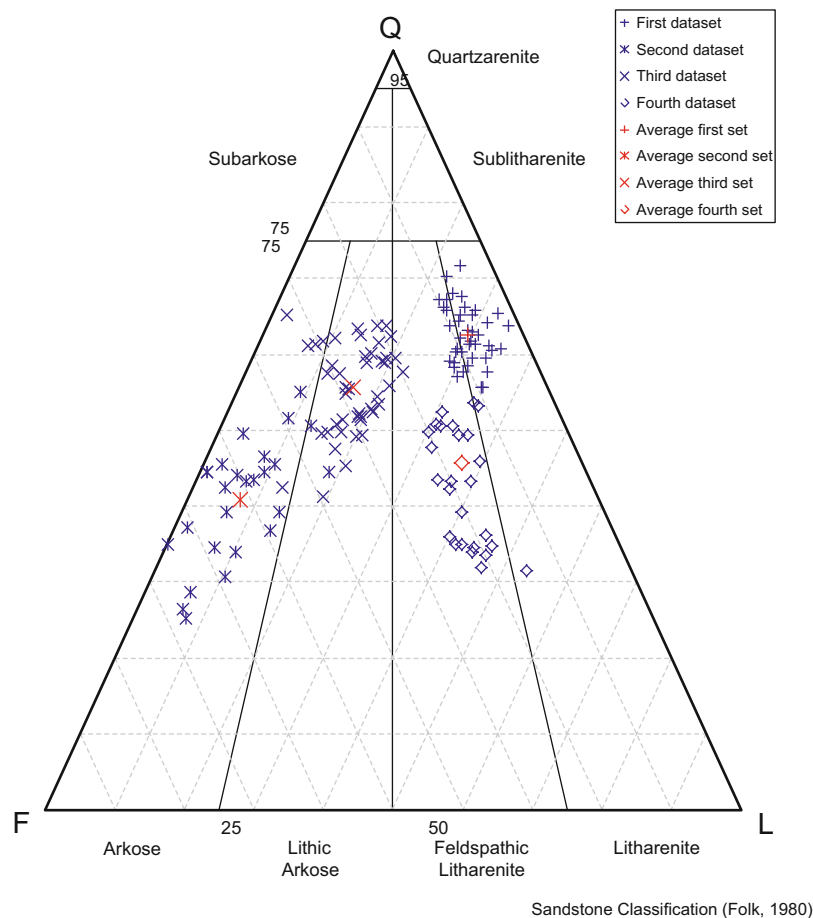
Sandstones Of the clastic rocks, the sandstones are familiar archaeologically as building stone. They are the easiest to recognize as they are cemented sand grains as their name so aptly implies. One scarcely needs more than a hand lens to initially determine this class of rocks. Within the class of sandstones are (a) the arenitic or “quartz sandstones,” composed mostly of quartz; (b) arkose, made up of feldspars rather than quartz; and (c) graywackes which contain 15 % finer-grained materials—clays and silts.

6.3.1 Arenite or Arenitic Sandstone

General properties: While the name “arenite” is a bit dated, simply implying a quartz-rich sandstone, it still commonly appears in texts. Similar terms, not used in this chapter, are “rudite” or a conglomerate or gravel-rich stone and “lutite,” a clay-rich stone (claystone). Of the general class of “sandstones,” quartz arenites are greater than 95 % quartz. The grain matrix is well cemented. Orthoquartzite is an arenite cemented with quartz. Other arenites may be cemented with calcitic, dolomitic, clayey, or ferruginous material. Figure 6.4 illustrates a ternary diagram using Folk’s classification for sandstones. As a rule, these hard,

Fig. 6.4 Ternary diagram using Folk's sandstone classification (1948, 1980) (Reproduced from Zahid and Barbeau (2011)).

Arenitic, arkosic, and lithic categories are subdivided according to the percentage of each within the diagram. Subcategories, such as lithic arkose and feldspathic litharenite, are illustrated following a 75–50–25 % breakdown



tough rocks are less well suited as archaeological toolstone and are better used as dimension stone. Figure 6.5 illustrates sandstone used for megalithic monuments.

In thin section, the quartz grains of an arenite are closely bound and relief is contingent on orientation (Fig. 6.6). In plane-polarized light (PPL), single crystals are rarely euhedral. In cross-polarized light (XPL), quartz grains exhibit classic undulatory extinction. Interference colors are low order but bright.

6.3.2 Arkose or Arkosic Sandstone

General properties: Arkoses are defined by the abundant presence of feldspar (>25 %). The feldspar may be either plagioclase or orthoclase. Arkoses are considered to be more reflective of

source environments than depositional processes (Williams et al. 1955). In thin section, feldspars appear brown in PPL, colorless, otherwise (e.g., not pleochroic). In XPL the twinning of the feldspars can be observed (Fig. 6.6). The “Carlsbad twin” is common in alkali feldspars but is seen in plagioclase as well. Fine parallel twinning (“albite”) is seen in the anorthites and microcline varieties. Relief is low or negative in both alkali and sodium/calcium feldspars (oligoclase, anorthite).

6.3.2.1 Silcrete

As chemical sedimentary rocks, silcretes are akin to calcretes and ferricretes (the former being cemented by calcite and latter by crystallized iron oxides). In South Africa where this rock type is common, it forms an indurated duricrust of silica-cemented sands and gravels—a



Fig. 6.5 Sandstone Pictish standing stone. Perthshire, Scotland. So-called Class 1 Stone by virtue of only “pagan” Pictish symbols used in its decoration (Photograph by author)

resistant capstone. It is prevalent in Australia as well. Silcrete is found in Europe, notably England and France but less so in the Americas. Arakawa and Miskell-Gerhardt (2009) have, however, identified silica indurated sandstones in the Four Corners region of the American Southwest. This silcrete-like stone has been incorrectly labeled as “quartzite” by many archaeologists (*supra*). These authors have identified a silica indurated shale facies in the same region. Both rock types were commonly used for toolstone by prehistoric groups. Both rocks are lower Cretaceous in age.

In thin section, silcretes are dominated by quartz clasts (Schmidt et al. 2012). These undergo extinction in XPL. The microquartz cement, at least in South African samples, is relatively variable, ranging from fine to coarse grained (*supra*). As a toolstone, silcrete usage extends well into the upper Pleistocene in both South Africa and Australia. By the Middle Stone

Age (MSA), 40–90 ka, in the Cape area, heat treatment of this rock has been documented (Schmidt et al. 2012; Brown et al. 2009).

6.3.3 Graywackes or Clay-Rich Sandstone (“Lutitic”)

General properties: These are sandstones with greater than 15 %—silts and clays—as a matrix. Like the arenites, the graywackes vary, in name, according to the dominant grain types—quartzitic, feldspathic, and lithic. These sandstones are generally darker in color and poorly sorted. The argillitic grains in the matrix are not visible to either the eye or under the optical microscope due to their small size ($\sim 2 \mu$).

A typical graywacke, under PPL, shows an opaque fine-grained matrix with larger quartz, feldspar, accessory mineral grains, and rock fragments. As with other sandstones, the optical properties of quartz and feldspars in PPL show coloration and shape according to their specific mineralogy. The XPL views show extinction and twinning are apparent in quartz and feldspars. Rock fragments and clays will show coloration, in PPL, such as brown-colored iron oxides in the cement, pale green chlorite and black in XPL, and brownish-green of glauconite. In XPL, amphibole will show an orange interference color. Lath-like mica, particularly, muscovite, will show the birefringence colors of blue-red and orange, much like the expanding clays (illite, chlorite, etc., cf. Chap. 7) (Fig. 6.7).

6.3.3.1 Siltstone, Mudstone, Claystone, and Shale

These clastic sedimentary rocks are composed of silicate minerals, mainly quartz and clays less than 5 μ in diameter. Interestingly, they are the most abundant of all sedimentary rocks but, compared to the harder sandstones and limestones, have less archaeological importance than that of a geological nature with the exception of shale. Siltstones occur in basin-edge successions between sands and muds (Emery and Myers 2009). These rocks also occur in foreland basins as erosional depositional sediments.

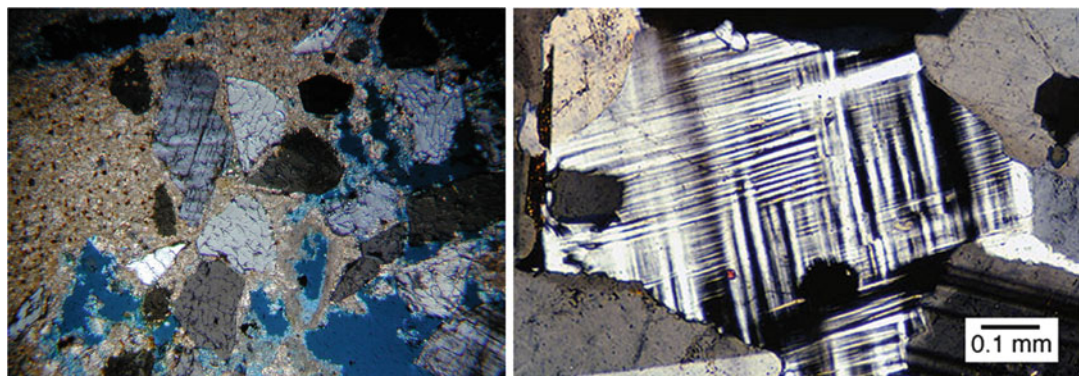


Fig. 6.6 Two thin-section views of arenitic sandstones. *Left*, XPL showing undulatory extinction of the quartz grains (black grains). Crystals of sparite cement are clearly seen along the edges of holes (blue voids) in the

thin section. The quartz grains show shattering due to sawing. *Right*, XPL image showing “twinning” of feldspar grains (*Left* image by author, *right* image courtesy of the University of North Carolina-Chapel Hill)



Fig. 6.7 Neolithic Period stelae carved from sandstone, from the megalithic site of Petit-Chasseur, Sion, Valais, Switzerland (Musée d'histoire du Valais, Sion, photograph by R. Hofer)

Figure 6.8 shows a stone of the latter type—a “green molasse” siltstone from the Jura Mountains.

In grainstones and mudstones, the former variety is composed of calcite grains cemented by spar. Mudstone is pretty much as the name implies—consisting mostly of small silt-sized grains. The sediment is not overly compacted and the grain structure or shapes, in grainstones, are oolitic to peloidal. Bioclasts can occur as well. Mudstone, also known as claystone, is most commonly named shale. Shales, because

of their habit of fracture along bedding planes, had been used from tabular artifacts to roofing material in the past. For structural purposes, even shale is too fragile for building proper.

Because of the small grain sizes common in these rocks, petrographic microscope techniques can do little than to observe small-scale sedimentary structure and describe larger-grained siliciclastic inclusions. PPL and XPL properties such as birefringence will show the presence of clay minerals and micas, such as chlorite and muscovite. In XPL, rotation of the thin section

Fig. 6.8 Rear, a siltstone, green “molasse” dimension stone; foreground, a “grès coquille” or bioclastic limestone (Photograph by the author)



will often demonstrate extinction. Also in PPL and XPL, the differing optical properties of adjacent laminae will appear as lighter and darker bands. The authigenic crystals of calcite, dolomite, siderite, etc. will appear highly birefringent as a rule (Fig. 6.8).

6.3.3.2 Breccias and Conglomerates

If one considers grain size as a continuum, clasts offer clues to the source of the sedimentary rocks—shales form from micron-sized minerals and sandstones from millimeter-sized minerals, while breccias and conglomerates are composed of the largest clasts. Morphologically, the breccias and conglomerates are differentiated on the basis of surface roundedness—the latter are more rounded than the more angular breccias. The lack of angularity in conglomerates is considered to be the result of fluvial action. Both terms for these rock types denote their structure and not their composition. As one would expect, their mineralogical makeup can be, and is, quite varied, ranging from carbonate to volcanic in composition.

The identification of the breccias and conglomerates rarely requires more than a hand lens due to the size of the fragments ranging up to pebbles. The identification of the binding matrix

of the specific rock type does require a hand lens and, in many cases, recourse to microscopes. This is due to the different depositional environments in which the rocks originate. If the rock was deposited in a marine or lacustrine setting, then the matrix can be calcareous and clay rich together with significant amounts of sand. If the rock is more the result of fluvial action, the matrix will reflect this with interstitial silts and clays bound by carbonate cements. Their matrices can vary from limonitic, calcareous, and siliceous to lithified clay-rich cements. Breccias and conglomerates are important rocks, from an archaeological standpoint, with their use in both artifacts (toolstone) and buildings (dimension stone) (Lucas and Harris 1962; Mannoni and Mannoni 1984; 159; Winkler 1994; Mazeran 1995).

6.3.3.3 Carbonates: Limestones and Dolomites

Of the carbonate or calcareous sedimentary rock, limestones are the most common. This is because their origins are most frequently in marine basins. In the ocean, the shells or skeletons of small animals rain down constantly, forming thick layers of carbonate “*Globigerina*” ooze (Thomson 1877). These muds lithify into the

skeletal limestones. As a rule the limestones, skeletal and otherwise, are authigenic in nature that is to say they have formed *in place*, at that place of deposition. The lime carbonates or limestones are made up, chiefly, of calcite (CaCO_3), dolomite ($\text{Ca}(\text{Mg})\text{CO}_3$), and ankerite $\text{Ca}(\text{Mg},\text{Fe},\text{Mn})\text{CO}_3$.

Rocks that are primarily calcite are termed limestone. Those with dolomite are dolostone or simply dolomite; and mixtures can be dolomitic limestone. Some limestones have a large proportion of the calcium carbonate *pseudomorph*, aragonite. In most limestones, particularly those exposed to meteoric water, the aragonite exsolves and recrystallizes to calcite. Such limestones are “old” limestones or compact limestones. Returning to the allogenetic forms of limestones, these clastic rocks consist of calcite of either terrigenous, organic, or oolitic origin (Williams et al. 1955). Most are of marine origin. The fragments are cemented by additional carbonate that precipitates into the pore space between the calcite grains. If the number of silicate grains increases, the rock is a calcareous sandstone rather than a calcareous limestone or calcarenite. Some limestones are made up of small (<2 mm) roundish grains that appear to be organic forms or tiny geoids. These rather unusual grains are ooids that are composed of carbonate formed around a detrital silica nucleus. If these forms are larger than 2 mm, they are called pisoids or oncoids. Bioclastic limestones are made of cemented shell and skeletal fragments. These clasts can consist of molluscs, brachiopods, corals, forams to algae, and worms. Peloidal limestones resemble ooids but the grains lack nuclei and are completely micrite.

Micrite or microcrystalline calcite has a diameter of $5\text{ }\mu\text{m}$ or less (Adams et al. 1997). Sparites are calcite grains over $5\text{ }\mu\text{m}$ in size (Fig. 6.6). The presence of these forms of calcite in limestone gives them their respective names—micritic or sparry limestones. Micritization is the process that clastic limestones, particularly bioclastic varieties, lose their original texture and form fine-grained forms. Micrite is a major cement in limestones along with carbonate mud sediments. Loss of grain texture or clastic inclusions, in

limestones, can result from processes like micritization but also can result from pressure that compacts the pore space between grains.

By simply calling the most abundant carbonate rocks either limestones or dolomites belies their petrographic complexity with diverse textures from clastic to organic accretion. Optically, it is difficult to differentiate the two, and the dye Alizarin Red S is used to do so much the same way sodium cobaltinitrite is used to distinguish the feldspars. Etching limestones with weak (10 % by volume) HCl or 2N formic acid is another technique. Calcite is more soluble than the rhombohedral dolomite which stands out in relief on either hand sections or uncovered thin sections. After extensive etching, only the non-carbonate minerals remain such as chert, clay, feldspar, and quartz.

Limestone, as a rule, does not make good toolstone, but as dimension or art stone, these rocks found great utility in antiquity. The most spectacular use of limestone as dimension stone is the pyramids. In the Americas, notably Central America and southern North America, limestone was commonly used for building purposes. The Maya use of limestone rivaled that of ancient Egypt.

Abundant as karst, the Yucatan, and areas southward, Mayan cities and infrastructure—temples, causeways, cisterns, etc.—were built using limestone. As stelae, limestone recorded the accomplishments of Mayan rulers from Copan to Tikal.

Roman stone portraiture used limestone when and where marble was not available either physically or economically. Roman—both western and Byzantine—mosaicists preferred limestone for tesserae.

It was cheap, available, and found in a variety of colors from gray/green to yellow. If the limestone colors were not acceptable, there was always paint as the Romans used on reproductions of Greek originals (Abbe 2011). Even when not used as a colorant on portraiture, monuments such as Trajan’s Column has clear evidence of the extensive use of paint and gilding. In historic America, limestone quarries in the Missouri portion of the Ozark Mountains

produced dimension stone as well as polished limestone (“white marble”) (Rovey et al. 2010).

6.3.3.4 Organic or Bioclastic Limestone

Components of these rocks are diverse calcareous organic materials characterized by (a) overall particle size and shape and (b) internal wall structure of the organism. This latter quality is one aspect where the use of XPL has a significant role in thin sections—level studies of these limestones (Adams et al. 1984). The age of limestones can be relative to the percentage of aragonite if it was there at the formation of the stone. Over time, it will revert to granular calcite. In oysters and corals, both calcite and aragonite appear. The structural shape or form will remain after dissolution or recrystallization of the aragonite unlike those forms which only secrete pure calcium carbonate whose shells or skeletons are lost.

The identification of a pseudomorph of calcite is beyond the hand lens and the microscope unless it is an electron-based unit. Even then it is perhaps best to leave the identification to techniques such as X-ray diffraction or WDS analysis on an electron microprobe. Fine sediments or micrite cement can fill in the voids or molds of lost organisms leaving casts. Identification of the organisms and the overall porosity of cement is typically done in thin section. Most examinations are done in PPL on stained specimens. As mentioned, XPL observation has advantages in examining organic structures. If the bioclasts are intermixed with sediments, the crossed polars can differentiate these mineral grains. Bioclastic limestones are used for dimension stone (Fig. 6.7).

6.4 A Roman Quern Production and Smithy Works

The main phase of the site of the Roman site of Châbles (Canton of Fribourg, Switzerland) dates to the turn of the first and second centuries AD and comprises a quern quarry, a road, a smithy, and a house (Anderson et al. 1999, Anderson 2003). The quarry was exploited for small,

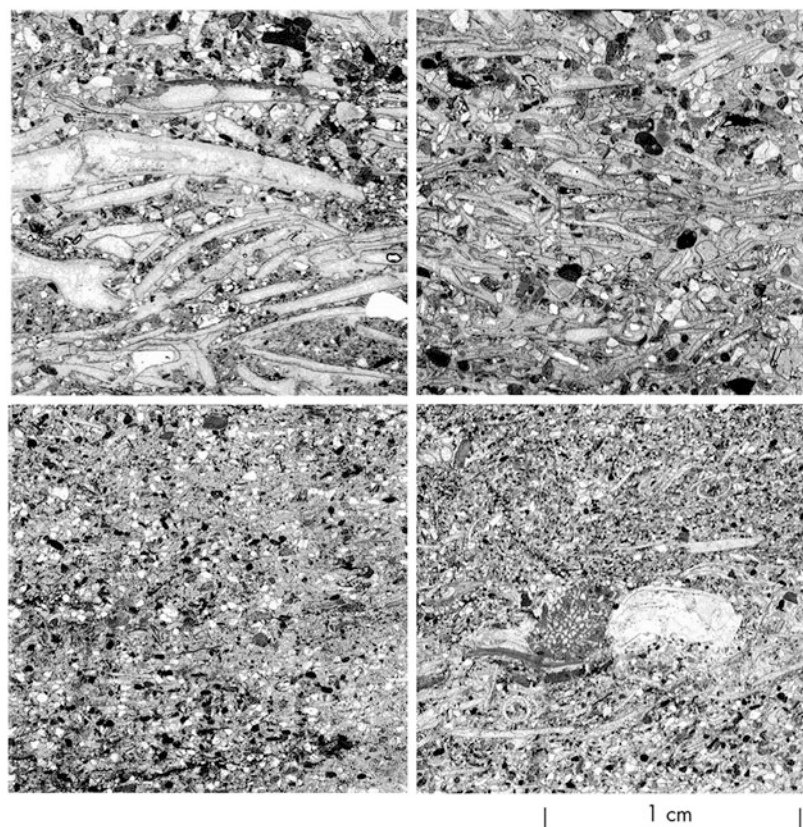
hand-operated mills known as rotary querns. The tool marks visible on the quarry faces and on a series of aborted quern extractions recovered both in the quarry backfill and along the surface of the road allow reconstruction of the operational sequence of quern production. This small quarry is beside a road 6 m wide and excavated over a length of about 300 m. This road was a major thoroughfare linking the Roman cities of Yverdon with Avenches and served to export the querns. The smithy, installed on the other side of the road, a stone’s throw from the quarry, included about 750 kg of smithy slag and about 3,000 metal objects. A wooden construction is interpreted as both the house and workshop of the blacksmith. It is obvious that the smithy repaired and maintained the tools of the quern maker. There is also evidence that the smithy served more than the quarry and made other tools for a local clientele. Finally a small wooden house, built with posts, was set along a space between the road and the quarry. It is possible that it served to lodge the quern maker.

Because of the rock’s hardness and durability, it was an excellent stone for crushing grain to flour. During excavations along an autoroute in western Switzerland, a millstone quarry, forge, and outbuildings adjacent to a Roman road were uncovered (Anderson 2003). Petrologically this particular stone is marine in origin with an extremely high density of lenticular shell and quartz cemented in a micrite matrix (*supra*) (Fig. 6.9). Besides millstone, the rock was, and still is, used for walls, curbing, steps, borders of windows, etc. In antiquity it served as the base for columns and protective caps or coping on Roman tower tombs at the *Chaplix* cemetery, *Aventicum*.

6.4.1 Clastic or Calcarene Limestones

Made up of calcite fragments, these rocks are cemented by micrite or sparite. Sorting of the composite grains is just as with sandstones. The particles of calcarenites are either organic fragments, ooliths, or carbonate rock fragments. Here the grains are predominantly carbonate

Fig. 6.9 Thin-section views of Grès coquille bioclastic limestone, western Switzerland. The high density and lamination of shell and quartz are clearly visible (Image courtesy of the Archaeological Service, Canton of Fribourg, Switzerland)



rather than silica. Nearshore beach deposits and dunes materials form into calcarenites. These deposits are rapidly cemented into rock by additional carbonate chemically precipitated in the pore spaces. Cementation can be rapid forming what is termed “beach rock.” In areas of multiple transgressive-regressive cycles, micritization and dolomitization can both cement these carbonate rocks in submarine and subaerial conditions. Hand lens examination of calcarenite samples can lead to misidentification as bioclastic sandstones. In some instances, the difference is truly one of degree so the difficulty is real (Fig. 6.10).

Grain size and texture are the first parameters easily distinguished in PPL. Porosity varies widely from tightly welded to poorly sorted varieties. In XPL, where the calcarenite grains are tightly packed and cement over growth has occurred, both the over growth and clasts will appear dark due to a uniform extinction color for grains and

cement. Micritic cement can appear greenish-brown, in PPL, while sparite is colorless. If dolomitization has affected the rock, then rhombs of this mineral can be seen in PPL or XPL. Recall that our previous discussion on the distinctive optical properties of the carbonates—high birefringence, sharp relief, and birefringence—can be used to characterize the limestones.

6.4.2 Aphanitic Limestones

General properties: Fine grained, by definition, the grains are difficult if not impossible to see with the unaided eye or even a hand lens. Color is generally white-gray although the presence of iron or organic carbon can create pink, red, and gray-black varieties. Fracture is chert-like, that is, almost conchoidal due to the very fine grain of the stone. Fossils are not uncommon in these rocks. Karstic terranes are often aphanitic

Fig. 6.10 The Roman millstone quarry at Châbles-les-Saux, Switzerland (Photograph courtesy of Dr. Timothy A. Anderson (shown in lower left))



limestones. Most limestones do not make good stone tools due to their inherent low hardness. Exceptions, such as the Roman mill stones, do occur in the archaeological record.

Fine grained and dark in PPL and the increased argillaceous content will enhance the XPL image's optical properties. Where clays are concentrated in laminae, the thin section reflects this texture as well. Intercalated calcite veinlets will give the section a weblike appearance.

6.4.3 Dolomite and Dolomitic Limestones

$\text{Ca}(\text{Mg})\text{CO}_3$ is a major component of limestone although of a secondary origin, replacing preexisting carbonate minerals (Adams et al. 1984) unless the euhedral, rhomboidal, and dolomite can be seen microscopically (Fig. 6.11), it can only be distinguished by staining, after etching, of the thin sections with Alizarin Red. The presence of dolomite in a limestone does not make it a dolomite. If the percentage is less than 10 %, it is limestone; if the percentage is less than 50 %, the rock is dolomitic limestone; and only when 50 % or more dolomite is present is the rock strictly

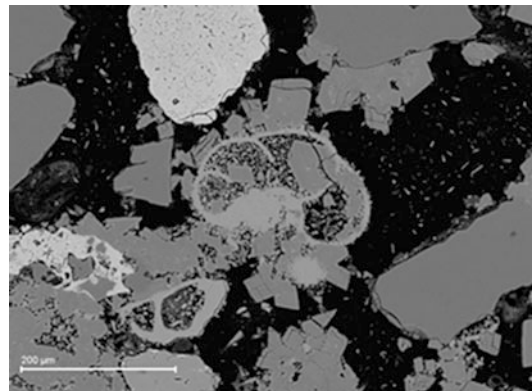


Fig. 6.11 Backscatter electron (BEI) image showing dolomite rhombs in thin section. A large rotaliid foraminifera (center) is surrounded by dolomite rhombs; large apatite grain appears in the upper, center portion of the image (SEM image by author)

termed a dolomite. Dolomitization is the replacement process that limestones undergo. As dolomitization is not observed in today's oceans, by the logical extension of the uniformitarianism principle, it is hard to visualize it as a primary process in earlier times. Whether a direct chemical precipitate or diagenetic replacement mineral, dolomites and dolomitic limestones are more resistant and harder than calcitic carbonates. For these properties, these rocks

have been regularly used in building throughout antiquity.

Dolomite, as a mineral, is a major component of many limestones (Adams et al. 1997). The macroscopic appearance of dolomitic limestone is generally fine grained although not as fine as the aphanitic forms nor as coarse as some of calcarenites. In some thin sections, the dolomite preserves the original texture or structure of the calcite protolith. Two key properties distinguish dolomite from calcite—the first is the distinctive rhombohedral shape of the single dolomite crystal and the second is its non-uptake of Alizarin Red stain. The euhedral rhombs of dolomite scattered through a limestone's calcitic matrix are singularly recognizable (Fig. 6.11). Calcite, by comparison, is generally anhedral. In closely spaced dolomitic-calcitic matrices, the dolomite rhombs become subhedral or even anhedral, making the necessity of staining obvious. Where dolomite has replaced calcite, the grain shape is calcitic.

6.4.4 Cherts, Gypsum, and Ironstones

These rock types, taken ensemble, make up only a small fraction of the sedimentary rocks, but, from an archaeological point of view, some—notably chert and gypsum—have an importance beyond that of sheer geological abundance. Others like ironstones have had economic importance in the industrial past. Because of its use as tools since great antiquity, we shall begin our review of these rocks with chert. Chert is a hard stone, very durable yet workable in the hands of artisan.

Chert/Flint Perhaps the most pervasive of all archaeological lithic materials, these are rocks composed of silica rather than carbonate (Leudtke 1992). They form within aqueous environments and are found within limestones or interbedded with them in section. It can occur as either primary or secondary—the first by precipitation and the second by the process of replacement of a limestone matrix. The silica can occur in three forms—amorphous, such as opal; cryptocrystalline; and microcrystalline. All these

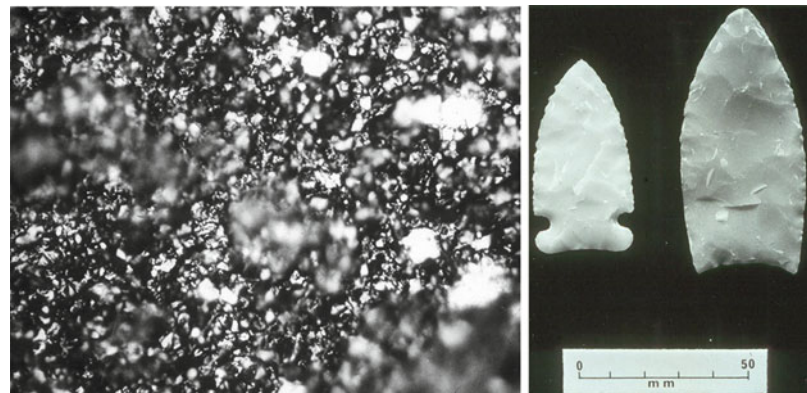
forms are found in the chert varieties. The most common of these varieties are flint, jasper, and novaculite. In cherts composed in large amounts of fibrous chalcedony, these are called by that name. Cherts are generally some admixture of all or some of these forms. “Flint,” in most English-speaking contexts, is the other common name for chert. In a strict sense, it refers to gray-to-black cherts composed mostly of chalcedony and/or cryptocrystalline quartz (Williams et al. 1955). It occurs in both nodular and bedded forms. One of the most famous archaeological localities for flint is that of Grimes Graves, Norfolk, England, site of extensive mining activities in the Neolithic Period.

Much like dolomite, chert, although silica, is thought to be a metasome as well being less a precipitate than a diagenetic production deposited in shallow seas. The nature of cherts takes three forms or “habits”—chalcedony, opaline, and crystalline. Most cherts are either crystalline or chalcedony as opal is less stable over time. Opaline chert is found, but it is more likely to find a chert with amorphous opal in a matrix of quartz—fibrous (chalcedony) or crystalline (chert/flint). Cherts may have abundant impurities such as clay minerals, feldspars, dolomite, and, in the case of the radiolarites, abundant microfossils. Conchoidal fracture is diagnostic of almost all chert. This property plus its durability and sharp edges made this rock a favorite with almost all prehistoric cultures.

As a silicate rock, the crypto- to microcrystals of quartz will demonstrate the optical properties of that mineral (cf. section on sandstone). Staining with Alizarin Red identifies any calcite in the chert. Quartz replaces calcite (metasomatic) in limestones, and in thin section, this will be observed as anhedral grains exhibiting the extinction and birefringence of quartz. Because the cherts are aggregates, the extinction pattern is “patchy.”

Novaculite is a material used in hone or whetstones and is gray-to-white chert that is crypto- to microcrystalline whose texture is almost granular to the touch. The true grain texture can only be observed by a petrographic microscope (Fig. 6.12). Novaculite has been

Fig. 6.12 Novaculite. *Left*, in thin section; *right*, projectile points (Flenniken and Garrison 1975; Used with permission of Maney Publishing)



studied as a subject of the thermal pretreatment of cherts to improve their working qualities for the production of flaked stone tools (Flenniken and Garrison 1975).

Jasper is a brown-to-red chert often difficult to differentiate from chalcedony (Fig. 6.1). The reddish color originates from ferric oxides in the material. Chalcedony, as seen in X-ray studies, is microfibrous as a rule but contains amorphous silica as well. This gives this chert a glossy, slick feel to the touch and, in some varieties, an almost gemstone quality. Chalcedony is an opaline chert and as a result is very hard. Opal is not stable and will recrystallize over time; thus, some cherts which may have been opaline have reformed into chalcedony and crystalline forms. Carnelian, a reddish-orange variety of chalcedony (Fig. 6.1), was used as jewelry in the fifteenth to thirteenth century Bronze Age Canaanite sites such as Hazor, in modern-day Israel.

Radiolarites are cherts with large proportions of the skeletal remains of radiolarians, diatoms, and sponge spicules in the stone matrix of quartz and opal. These are very hard rocks and used in prehistory to make durable tools. Jurassic radiolarites are found in California's prehistoric cultural middens.

Rock Gypsum After carbonates, the hydrous sulfate mineral, $\text{CaSO}_4\text{H}_2\text{O}$, precipitates in the evaporation of marine basins. The production of gypsum or its chemical replacement anhydrite is temperature dependent. Above 42 °C, gypsum will precipitate; below this temperature,

anhydrite-anhydrous CaSO_4 forms. At or near the Earth's surface, and exposure to meteoritic waters, gypsum replaces anhydrite.

Classified here under the sedimentary rocks, these forms are more correctly minerals. While less durable as a dimension stone in antiquity (ex. Knossos), alabaster has been mined and used for veneer slabs as well as for sculpture. Rock gypsum is a massive, coarse-grained, gray-to-white rock composed almost exclusively of aggregates of gypsum. Where iron oxides are incorporated into the matrix, it is colored with various shades of orange to red.

Gypsum, in thin section, is readily distinguished from anhydrite. Gypsum exhibits low birefringence and negative relief compared to higher birefringence and lighter relief of anhydrite. The interference color of gypsum is green, while that of anhydrite has bright interference colors.

Ironstone Deposited in marine contexts, this carbonate rock is more than 15 % iron. The iron can be in the form of siderite (FeCO_3) and chamosite). The latter can oxidize to the iron oxide limonite. Limonite can appear in oolitic form. Hematite, Fe_2O_3 , is more stable in terrigenous ironstones than either siderite or chamosite. Ironstone can be bioclastic and some are banded with chert layers (Adams et al. 1997).

Travertine Deposited in caves, this carbonate is also known variously as "flowstone" or "dripstone." It is distinguished by its lamellar or

banded nature which reflects its origin in the waters percolating into solution features such as caves. Archaeologically it can occur as a finish stone because of its beauty, but more recently it has become the object of paleoenvironmental studies wherein the bands of the rock are equated to the “growth rings” of trees. It has been demonstrated that *speleothems*—stalactites and stalagmites—can be dated using techniques such as U-Th, ESR, and radiocarbon. Coupled with examination of stable isotopic ratios in the growth bands, it is possible to retrodict past climatic conditions (Hendy 1971; Shopov et al. 1994; Brook et al. 1996). In the situation of cave sites, the presence of flowstone coating prehistoric artifacts, skeletal remains, or art can reassure researchers of their veracity and relative antiquity. Examples of this are found at Petralona Cave (Greece) and Cosquer and Chauvet Caves in France. At Petralona Cave, a skull of an archaic *Homo sapiens* was encrusted with travertine which attested to its age geologically and geochronologically (Schwartz et al. 1980; de Boris and Melentis 1991). At Cosquer and Chauvet, particularly at the former locations, the spectacular ancient cave art has calcite encrustations over some paintings and engravings (Clottes and Courtin 1996; Clottes 2001).

6.5 Igneous Rocks

Igneous rocks are formed by the solidification of molten magma or rock that has been melted in the upper mantle. This rock has been incorporated into the mantle from various sources, but in general they are the stuff of crustal rock which has been subducted at plate margins after crustal plate collisions. As such, the rock to be melted can be sedimentary, metamorphic, or igneous in nature. The type of rock melted determines the nature of the chemical components of the magma. Igneous rocks are mainly composed of the eight rock-forming minerals—quartz, plagioclase feldspar, K-spar or orthoclase, muscovite mica, biotite mica, amphibole, pyroxene, and olivine.

The most common classification of igneous rocks is that of the International Union of Geological Sciences (IUGS) Subcommission on the Systematics of Igneous Rocks (Streckeisen 1979). Beyond, and before, the IUGS classification scheme, several others used in the study of igneous rocks have produced hundreds of names. The names used in this text will be those of the IUGS system. The IUGS classification of plutonic or intrusive igneous rocks is less debated than that for volcanic or extrusive igneous rocks due to the fine-grained character of these rocks. The color index—light to dark—is commonly used along with mineralogy and texture in describing igneous rock. In our discussion of igneous rocks, we emphasize their modal mineralogic classification rather than their chemistry.

The texture of igneous rocks ranges from coarse to fine grained or pegmatitic/phaneritic to porphyritic/aphanitic (Andrews et al. 1997a, b). Texture refers to the size and shape of individual mineral grains. Phaneritic texture is visible to the unaided eye, while aphanitic texture is not. The texture of an igneous rock is an indication of the cooling rate of the parent magma. Large-grained or very coarse (pegmatitic) igneous textures are found in the plutonic rocks, while finer-grained textures are found in volcanic rock. Obsidian is the finest “grained” of all igneous rocks being in actuality a volcanic glass. In the field, an archaeological geologist can usually only evaluate color and texture if the grains are phaneritic and estimate the mineralogy of an igneous rock sample. The latter property, in its most generalized form, grades igneous rock mineralogy from felsic (feldspar-silica rich) to mafic (ferromagnesian rich) (Table 5.2).

Igneous rocks are found in almost all areas and are either intrusive, plutonic forms or the more localized, extrusive volcanic varieties. In the former, we see more metamorphic rocks associated with the intrusive geology. Sedimentary facies can blanket more ancient igneous structures, or the igneous rocks can force their way up through layers of older rock. Either process results in the presence of igneous rock that was recognized in antiquity for its durability and utility, hence its presence in archaeological

deposits. In the case of obsidian, this volcanic glass became one of the earliest economic rocks.

At Franchthi Cave, Greece, on the Argolid coast, obsidian is present in low percentages (~5 %) in Mesolithic levels increasingly through the Neolithic to 95 % of the lithic archaeological assemblage (Cherry 1988). This obsidian has unique provenance. It was quarried on the island of Melos 150 km distant meaning that sea-going watercraft, in the Aegean, has great antiquity. At the Anatolian site of Catal Hüyük, which flourished between 7500 and 6500 BC, obsidian was a prominent trade mineral being mined in the volcanic flows of the Konya region (Cunliffe 1988). The quantitative characterization relies on many of the optical techniques already described in this chapter. To the archaeological geologist examining igneous rocks, the questions are mainly of archaeological provenance—economic, cultural, cosmological, etc.—rather than geological provenance, e.g., magmatic type, temperature, etc. The composition of the rock will assist the researcher in determining the cultural history of the material.

To do this, the investigator must determine the mode (mineralogic content), texture, and color. The latter parameter, formalized originally by Johanssen (1938), into the color index, is based on the percentages of light and dark minerals present. When and where possible, the characterization should proceed to optical studies and, where necessary, instrumental examination. Many of the following descriptions are based on the excellent *Atlas of Igneous Rocks and Their Textures* (Mackensie et al. 1982). Where terminology differs from that of American

petrological usage, this book will attempt to use the terms more familiar to the American student, recognizing the equal status of the more international terminology.

6.5.1 Granite

General properties: Granites are intrusive, phaneritic rocks with a low or leucocratic color index consisting of mainly quartz, feldspars, and micas. Of the feldspars, potassium feldspar is the most prevalent form. The granites are therefore classified as *felsic*. This ferromagnesian rock is typically made up of suites of minerals such as biotite (mica), hornblende (amphibole), and augite (pyroxene). Granite has been a principal building stone through antiquity. The Egyptians used Aswan granites in the Giza pyramids for lining material of passages, for chambers, and for doorframes (Lucas and Harris 1962). In contrast to the Egyptians, granite was little used by the Classical Greeks (Higgins and Higgins 1996). Where granite makes up the cores of Greek islands, weathering of this rock results in fertile soils (Melas 1985).

Quartz appears featureless in PPL as a general rule. The feldspars will vary in the property of twinning ranging from microcline's cross-hatched variety to simple twin patterns in potassium feldspar. Plagioclase shows albite twinning. Accessory minerals such as the micas are recognized by their interference colors in XPL and their pleochroism in PPL (Table 6.2).

Table 6.2 Common igneous rocks

| SiO ₂ , Na ₂ O, K ₂ O; felsic minerals → CaO, MgO, FeO; mafic minerals | | | | |
|---|-------------------|--------------|--------|-------------------------|
| Chemical type | Acid | Intermediate | Basic | Ultrabasic |
| <i>Texture</i> | <i>Rock names</i> | | | |
| Fine grained, | Rhyolite | Andesite | Basalt | |
| Extrusive | Obsidian | Dacite | | |
| Volcanic lavas | Pitchstone | | | |
| Medium to | | | | |
| Coarse grained | Granite | Diorite | Gabbro | Peridotite ^a |
| Plutonic | Granodiorite | | | Pyroxenite ^a |

^aMetamorphosed equivalents are soapstone and serpentine

6.5.2 Diorite

Sometimes termed the “black granite,” diorites are medium-to-coarse-grained igneous rocks. It has less than 5 % silica by definition and is mineralogically 50 % ferromagnesian. Granodiorite, by contrast, has more than 10 % silica as feldspar (orthoclase), along with amphibole and pyroxene. Many of these intermediate color index rocks are melanocratic or dark colored, hence their common name. The mafic crystals of pyroxene and hornblende along with biotite are mainly responsible for the coloration. Quartz and potassium feldspar, if present, occur in trace amounts. Diorite was used in sculpture by the Egyptians in the Neolithic into Pharaonic times (Lucas and Harris 1962). The cosmetic palettes, so popular with ancient Egyptians, were made from diorite as were mace or axe heads, bowls, and vases (*supra*). Caton-Thompson and Gardner (1934) reported diorite artifacts from the Fayum Neolithic sites as well. In Egypt, there occurs a dioritic-gneiss often called diorite by early authors.

Plagioclase crystals are lath-like in thin section. Twinning is common with the single Carlsbad Twin to multiples of the Albite variety. Potassium feldspar will be interstitial to the plagioclase. Interspersed through the thin section will be the brown and green crystals of the ferromagnesian minerals—hornblende (amphibole) and biotite.

6.5.3 Andesite

General properties: Andesite is considered to be the extrusive equivalent of diorite (Andrews et al. 1997a, b). Most andesites are porphyritic. Colors range from gray to dark gray. The rock contains ferromagnesian minerals—pyroxene, amphibole, and biotite—with feldspar phenocrysts. Fine-grained nature andesite was used for hand axes in East Africa. This “andesite” is only so based on its chemistry—it is not

representative of most andesites formed in volcanic arc areas.

The PPL and XPL views of andesite clearly demonstrate the microcrystalline ground mass of plagioclase. The ferromagnesian crystals together with larger phenocrysts “float” in the andesine.

6.5.4 Basalt

Basalt is the most common extrusive igneous rock. Basalts form at the mid-ocean ridges, rifts, and hot spots. Basalts are all the ocean’s floors. Basalt is the most abundant fine-grained igneous rock.

One form of basalt is “pillow lava” commonly seen in ophiolites (Fig. 6.13). Basalt has a long history of human use from grinding stones and hammers to construction stone and sculpture. In the last category, the great carved heads of the Olmec culture were made from basalt (Winkler 1994). Basalt was quarried in the Old Kingdom of Egypt in the Fayum, west of modern-day Cairo (Lucas and Harris 1962). Because this rock does not demonstrate conchoidal fracture, some archaeologists have difficulty in recognizing intentional fabrication of the stone as tools.

Commonly, basalts are composed of plagioclase and ferromagnesian minerals—magnetite, olivines, pyroxenes, etc. However, the relative abundance of these minerals is quite variable. Poldervaart and Hess (1951) stated the following: “In most basalts of oceanic islands and in many other alkalic basalts, orthopyroxene or pigeonite is generally absent. Olivine appears as early phenocrysts and continues to crystallize for a considerable interval.” The glass in basalts will appear as a dark groundmass—genuinely so in XPL—and form the backdrop for the plagioclase laths and ferromagnesian crystals. The optical properties of the plagioclase have been detailed earlier in this section. By far the most colorful mineral in a basalt thin section will be the highly birefringent olivine with blues, pinks, and reds prevalent.

Fig. 6.13 Pillow lava basalts in road cut, Curaçao, the Netherlands Antilles. Clipboard for scale (Photograph by author)



6.5.5 Rhyolite and Obsidian

General properties: An extrusive porphyritic volcanic rock but unlike basalt, it is felsic in nature. Some geologists carry the definition into the category of felsic volcanic glasses making obsidian a variety of “rhyolitic” rocks. Taking this approach, the rhyolites can range from totally crystalline to totally glassy hyaline. Quartz and feldspar phenocrysts are common in fine-grained rhyolites and obsidians (Mackenzie et al. 1982). In antiquity, in igneous terranes, early humans used rhyolitic rock for tools such as hand axes and crude flake implements. Obsidian, which does fracture conchoidally, was a favorite material of early lithic technologists as discussed earlier. This volcanic rock has, by far, the sharpest edge of any cutting medium and was also recognized for its beauty. Melrose green rhyolite, from southeast New England, was used for Middle Archaic to Late Woodland Period artifacts and has been described by Hermes et al. (2001). This pale green rock was confused by several archaeological workers before being characterized, mineralogically, using optical and geochemical methods (*supra*).

Coincident with expanded archaeological investigations at the site of Stonehenge,

geologists renewed a long-running attempt to provenance the famous bluestone rhyolite building stones. Recent geological research by Rob Ixer (University College London) and Richard Bevins (National Museum of Wales) suggests that many of the bluestones came from the north side of the Preseli Hills (Ixer and Bevins 2010). At Craig Rhos-y-felin in the Brynberian valley, a tributary of the Nevern, the quarry for one of the rhyolite monoliths whose debitage has been found at Stonehenge (Fig. 6.14). The rhyolites are fine grained in character and lack any obvious distinctiveness, in hand specimen or thin section (Fig. 5.14). This makes determining their provenance difficult. Zircon mineral chemistry argues persuasively that rhyolitic rocks cropping out in the Pont Saeson area of north Pembrokeshire, located on low ground to the north of Mynydd Preseli, are the source of the informally termed “rhyolite with fabric” which occurs as field debris at Stonehenge. This represents the first authoritative provenance of any of the rhyolitic component of the Stonehenge bluestone assemblage.

Because of their felsic nature, thin sections of these rocks can be pretty colorless in thin section. Indeed, the only birefringent crystals will be those of an accessory or accidental origin. The

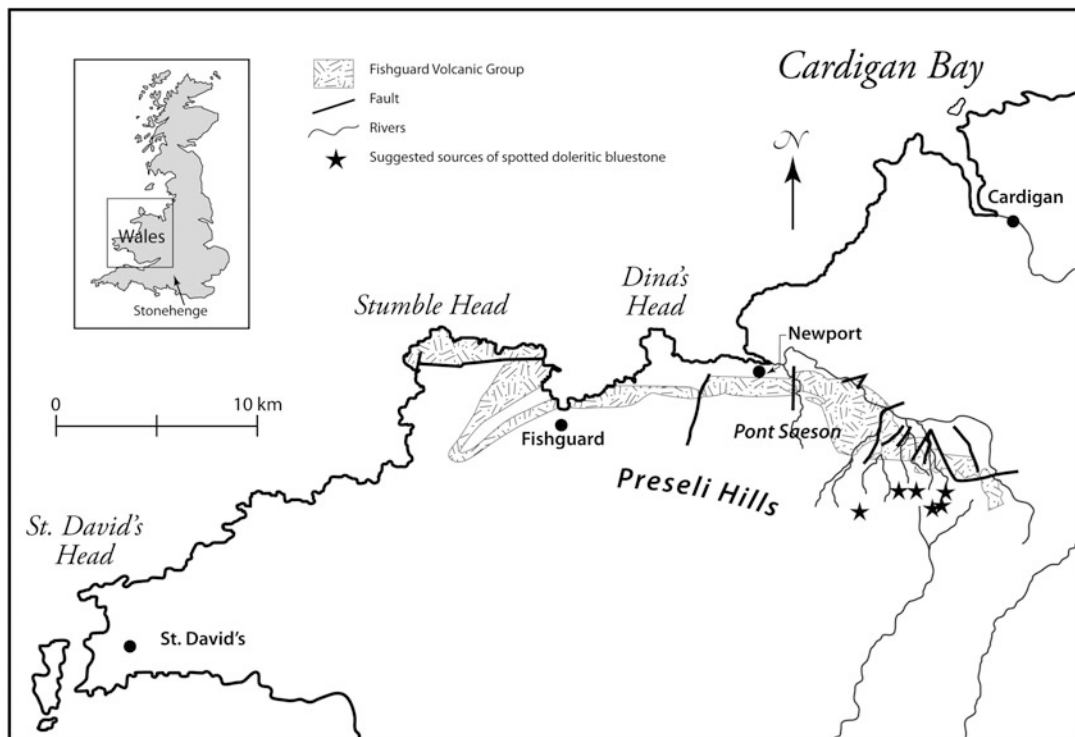


Fig. 6.14 Bluestone rhyolite quarries, Fishguard Volcanic Group at Pont Saeson, North Pembrokeshire (Map modified from Fig. 1, Bevins et al. 2011)

microcrystalline to glassy ground mass will be brown to gray in PPL and quite dark in XPL. The phenocrysts of potassium feldspar will show little twinning, while those of plagioclase will demonstrate abundant twins. The quartz phenocrysts will be of a higher relief than the groundmass but appear clear to colorless in PPL and gray in XPL with some extinction (Fig. 6.15).

6.5.6 Gabbro/Diabase

General properties: An intrusive, mafic igneous rock seen in the dikes of ophiolites. A fine-grained gabbro often found in ophiolites dikes and sills is given the name “diabase” by European workers. In the section, the gabbroic layers lie between upper pillow lava basalts and the lower mantle rock. Varieties range from olivine-rich gabbros to plagioclase-rich varieties. Gabbro contains no quartz, by definition. These rocks are coarse grained (phaneritic) and are generally dark. The gabbros were used in

antiquity only rarely for building stone because of the friable nature of the rock matrix. It was not uncommon to see this material used in smaller artifacts such as polished implements and items such as cups, bowls, plates, and ceremonial items such as mace heads. Egyptian culture of prehistory used both diorite and gabbro in all these categories (Caton-Thompson and Gardner 1934).

In the olivine gabbros, augite and plagioclase enclose equant and round olivines (Mackensie et al. 1982). Plagioclase generally occurs in laths, particularly in intergranular forms although the laths are not aligned or oriented as in trachytic gabbros where this is seen. The optical properties of the dominant plagioclase, augite, and olivine are colorful under XPL. Diabases in thin section vary from olivine to pyroxene-rich plates and laths of these minerals as well as ilmenite and magnetite. Calcite is often seen with its bright colors in XPL. Diabases show wide textural variation, even in thin sections, and some are notably porphyritic (Williams et al. 1955).

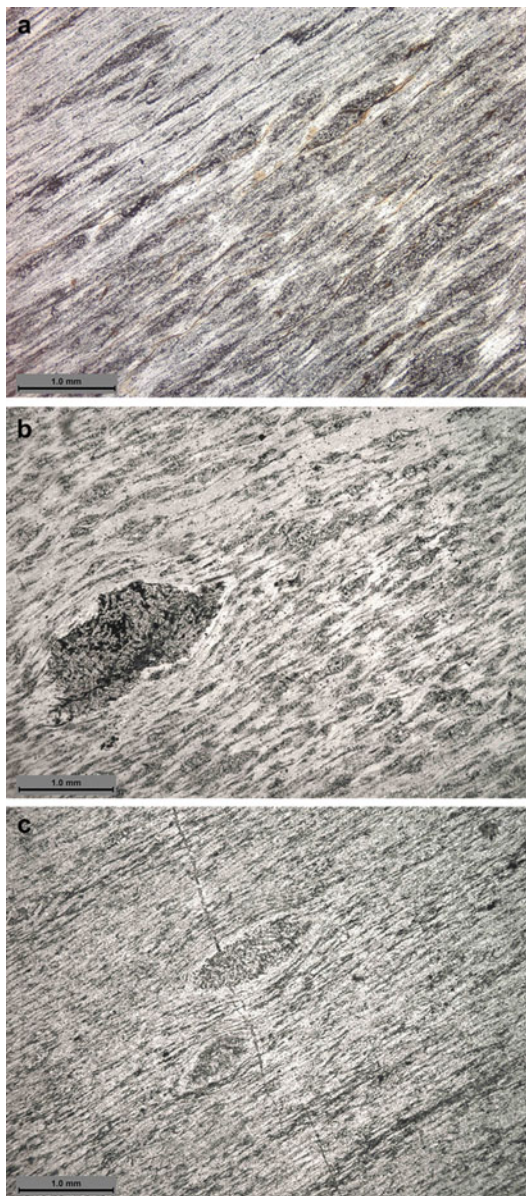


Fig. 6.15 (a) Thin-section views of strongly foliated rhyolite with small, dark (1 mm) lenses elongated in the plane of foliation. Sample 142/1947.22 from Wilsford, described originally by Stone (1948) and subsequently by Ixer and Bevins (2010) (Courtesy of Professor Michael Parker Pearson). (b) Photomicrograph of strongly foliated rhyolite with small, dark (2 mm) lenses elongated in the plane of foliation. Sample SH08/265 from the 2008 Stonehenge excavations (Courtesy of Professors Tim Darvill and Geoffrey Wainright). (c) Photomicrograph of strongly foliated rhyolite with small, dark (0.5–1.5 mm) lenses elongated in the plane of foliation. Sample PS8 from the Fishguard Volcanic Group at Pont Saeson, North Pembrokeshire (cf. Fig. 6.14) (Photomicrographs per Richard E. Bevins; the National Museum of Wales and Wiltshire Studies)

6.5.7 Tuff

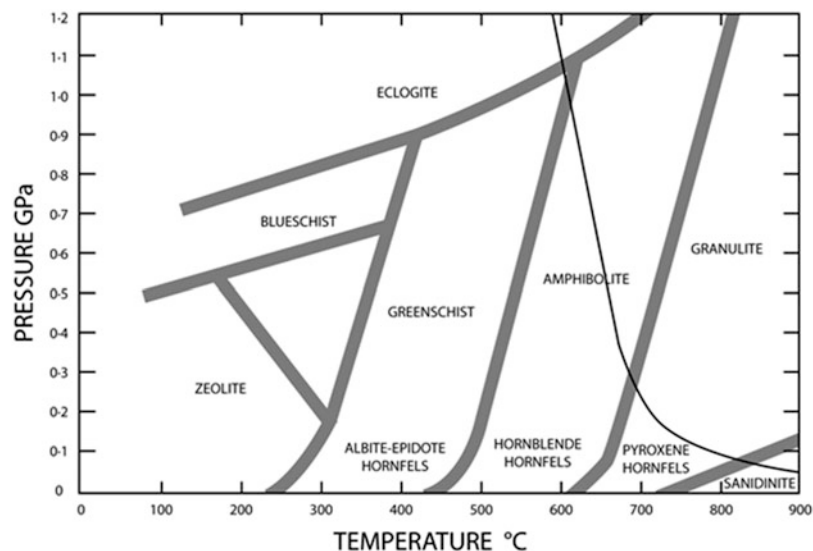
Tuff is an extrusive felsic-to-intermediate pyroclastic igneous rock composed of volcanic ash and a variety of mineral grains and rock fragments. Its color ranges from dull earth tones of light brown-pink to grays. Crystals and inclusions of sedimentary rock, lava fragments, and other pyroclasts are common within tuffs. Tuffs do appear in use for construction in antiquity but rarely. In ground or polished stone vessels, the use of tuff does appear in early dynastic Egypt. A very small fraction (4 %) of stone vessels found in The Old Kingdom (First Dynasty) tomb of Hamaka, at Saqqara, were of “ash” or tuff (Emery 1996).

At low power magnification, the heterogenous texture of this rock is quite apparent. Ash will appear as dark inclusions, while the glass inclusion will be colorless and opaque or translucent in PPL. Welded tuffs will have a glassy ground mass, with lamination apparent. The quartz and feldspar crystals will be elongated or flattened with little crystal shape evident except in the unwelded tuffs.

6.6 Metamorphic Rocks

Metamorphic rocks represent rock that “changed form”—recrystallized due to changes in temperature and/or pressure. These changes typically take place along plate junctions and intrusive/extrusive igneous boundaries. The most restricted form of metamorphism is that of contact metamorphism directly adjacent to intrusive igneous bodies where heat and hydrothermal fluids can cause new crystallization (neomorphism) and precipitation or replacement (metasomatism) of minerals. Most metamorphic rocks result from regional metamorphism which occurs over large areas associated with mountain building. Within mountain belts are slates formed from shales, quartzites from sandstones, gneisses from sediments and granites, serpentine and steatite from olivine-pyroxene-talc-rich rocks, marbles from limestones, and greenstone from basalt and andesite. The time

Fig. 6.16 Metamorphic facies by pressure and temperature. “Low” temperature or “blueschist” facies are typified by steatite (talc); marbles are more “greenschist” facies



scales are long in most instances ranging from thousands to millions of years.

Metamorphic rocks are described by texture and mineralogy. These rocks can have igneous, sedimentary, or metamorphic origins and as such retain much of the character of the original lithology while being the changed species that they are. Some of the most archaeologically important metamorphic rocks are marble, quartzite, and soapstone. Upon finding such rocks away from an orogenic zone, such as on a coastal plain with nothing but sedimentary facies for hundreds of kilometers, an archaeologist must seek cultural (trade, exchange, curation) reasons for their presence in these sites. Metamorphic rocks are classified according to their mineralogy, texture, facies, or grade. In terms of their mineralogy, V. M. Goldschmidt, in 1912, correctly observed that most metamorphic rocks contain only a few—four to five—major minerals (Philpotts 1989). The mineral assemblage, in a metamorphic rock, helps the petrologist to interpret its thermodynamic history. This is less important to the archaeological geologist, but the relationship between metamorphic grade—low, intermediate, and high—and texture is good to know. Grade refers to temperature and pressure, with a high-grade metamorphic rock more recrystallized than a

low-grade metamorphic rock. Texture refers to a metamorphic rock’s fabric orientation and direction or the lack of it, e.g., foliated versus non-foliated. The bulk of metamorphic rocks demonstrate some form of foliated texture (Fig. 6.16).

6.6.1 Metamorphic Rocks: Foliated

Slate: a very planar, parallel foliation.

Phyllite: Foliation of fine-grained sheetlike minerals such as muscovite and biotite. Phyllites are known for a glossy luster called “phyllitic sheen.”

Schist: Fine-to-coarse-grained platy minerals are aligned in parallel to subparallel fabric which is obvious to the eye. Like phyllite, such a rock is said to have “schistosity.” Schists fracture along the foliations. The variety of minerals in schists is diverse, e.g., chlorite, tourmaline, muscovite, biotite, garnet, hornblende, staurolite, kyanite, and sillimanite.

Gneiss: Gneisses have alternating layers of different minerals such as quartz and biotite. In Europe, gneiss refers to coarse-grained, mica-poor rocks irrespective of fabric (Yardley et al. 1990).

6.6.2 Metamorphic Rocks: Non-foliated

Hornfels: The minerals in hornfels are micro-crystalline giving the rock the property of conchoidal fracture like chert and obsidian.

Granulite: This is an even-grained garnet or pyroxene-rich rock lacking the micas or amphiboles. Its essential components are orthoclase feldspar, plagioclase, and quartz. This texture is observed in marble, quartzite, greenstone, serpentine/serpentinite, and skarn. It is plane foliated that can be laminated parallel to the foliation. This characteristic leads to slablike breakage and usage in construction in antiquity.

Amphibolite: This rock is medium to coarse grained. The rock is mainly hornblende and plagioclase. The parallel alignment of the hornblende crystals gives the rock its character but seldom produces a foliation.

6.6.3 Metamorphic Rocks of Archaeological Interest

6.6.3.1 Quartzite

General properties: This metamorphic rock generally originates as a quartz-rich sandstone facies such as an arkose or arenite. It is a product of regional metamorphism. As a rule it is a white rock weathering or stained to colors, such as cream or orange, in iron-rich sediments. Quartzite can appear gray when minerals such as biotite or magnetite are present with the quartz grains. Quartzite is very hard and durable but difficult to work. As an archaeological material, quartzite appears as a variety of implements such as spear points, knives, perforators, or almost any stone tool form. Because of its texture and coloration, the whiter varieties were fashioned into adornment such as beads, pendants, and the like. In some of the earlier literature, on the use of quartzite in antiquity, such as Egypt, the rock was described as “hard sandstone” (Lucas and Harris 1962). This “quartzite,” if indeed it is of

metamorphic origin, was used in making sarcophagi and statuary.

Under the microscope, quartzite is a fabric of interlocking quartz of varying grain size. Smaller grains are seen in quartzites that have undergone more intense deformation (Philpotts 1989). The grains of quartz will show the optical properties of this mineral—low relief, little or no birefringence, colorless, and some undulatory extinction in more isotropic grains. Unlike a traditional sandstone, a quartzite can show a lamellar or parallel fabric to the grains.

6.6.3.2 Marble

Marble is one of, if not, the most archaeologically important of the metamorphic rocks. Fine-grained varieties have been used for sculpture since antiquity in both the Old and New Worlds. In the classical period of Greco-Roman tradition, marble became a preferred building stone and continues to enjoy a wide usage today as both an interior and exterior stone. In the Aegean, marble appears as a quarried stone and sculpture media in the Cycladic islands third millennium BCE (Cherry 1988). Cemeteries of islands such as Melos, Naxos, Paros, and Andros have produced thousands of marble figurines and vessels. In the case of Melos, the marble must come from adjacent islands as it has none of its own Melos as we have seen was an early (Neolithic) source for obsidian.

In Egypt, marble was used in the Neolithic for bowls and vases (Mannoni and Mannoni 1984). By the Old Kingdom, at least at Saqqara, site of the first pyramid—the so-called Step Pyramid—a royal tomb was constructed of calcareous marble in the twenty-eighth century BC. In Archaic Period Greece (ca. seventh century BC), the use of marble for statuary increases with its use in life-sized, and greater than life-sized, representations of young men (*kouros/kurai*) and young women (*kore/korai*) (Fig. 6.17). Antecedent to classical statuary, these *kurai* were almost always portrayed nude or nearly so, while the *kore* was elaborately swathed in gowns called *peplos*. Diadems were commonly seen on the heads of *kore*. The *kouros* and *kore* were not the initial artstone products of Greece.

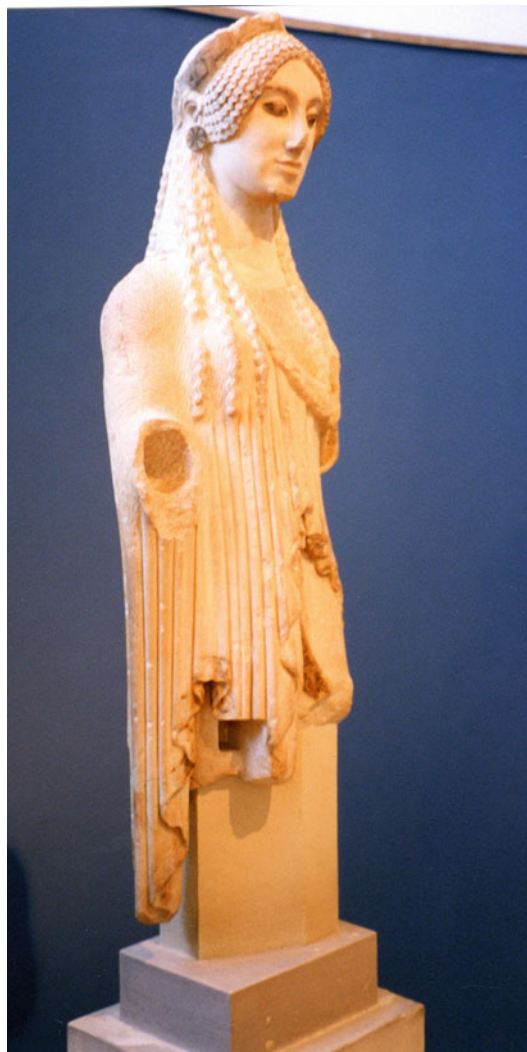


Fig. 6.17 The “almond-eyed korai” at the Acropolis Museum, Athens (Photograph by the author)

This honor falls to the Cycladic island figurines first seen in the Early Bronze Age (3700–2700 BC). Contemporaneous with the marble statues were marble bowls and marble-tempered ceramics (Rapp 2002).

Into the Classical and through the Hellenistic Periods of Greece, the demand for marble for both building and sculpture opens quarries across the Mediterranean adding to those of Egypt and Greece, with sites in Anatolia, Sicily, and Italy, most notably Carrara. In Chap. 8, a detailed



Fig. 6.18 Livia. Marble portrait (Courtesy the Estate of Dr. Norman Herz)

isotopic study of a Classical Period Aphrodite, whose origin was likely Carrara, is presented.

Marble is a granular rock, composed principally of calcite and is derived from limestones. This, of course, oversimplifies the diversity encountered in marble texture and coloration which, in the latter, ranges from the whites of Greece’s Pentelic facies to the gray marbles of Vermont (USA) and pinks to reds of Georgia and Alabama, USA, and Carrara, Italy. Richly colored banded or “streaked” varieties are found in Italy and elsewhere and doubly metamorphosed brecciated varieties (Carrara). The color and textual variety of those marbles is, of course, the result of their precursor minerals and their metamorphism. The marbles of peninsular Italy (Fig. 6.18) are generally formed at depth by regional metamorphic processes, while those of the Aegean islands can be the result of contact metamorphism.

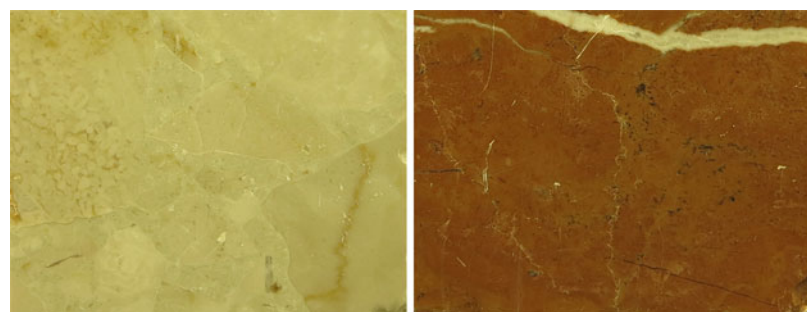
The white marbles, like Pentelic, are almost 100 % calcite while impure quartz, carbon, clay, and iron give color to others—quartz, clay, and iron produce yellow or pink color; carbon and other organics produce gray-to-black marbles; and greenish clay-rich marls, micaceous minerals, and serpentines produce gray-to-green colors. Marble colored by its component minerals is termed idiochromatic and those by inclusion pigments in cements between grains or in veins and intertices are called allochromatic.

6.6.3.3 “Marbles” or When Is a Marble Not a Marble?

“The stone found in the Brescia quarries (Italy) is a sedimentary limestone. It is called a marble because it is a hard limestone” (Giuliano Ghirardi quoted in *Stone World*, 2011). The particular “marble” referred to by this geologist is the Botticino Agglomerate (Fig. 6.19). Another famous “marble” is Rojo Alicante marble (Fig. 6.19) that is petrographically a biomicritic limestone (López-Buendía et al. 2010). “Carthage marble” was quarried in the southwestern portion of Missouri (USA) from before the 1860s and used extensively for paving and dimension stone (Rovey et al. in Hannibal and Evans 2010). It, too, is really a hard limestone classified as a “marble” stone.

Four varieties of breccias and conglomerates have been identified and characterized relative to use in Gallo-Roman architecture in southeastern France (Mazeran 1995). Within this suite of materials was a range typical of the variety rightly imputed to “marbles.” The “breccia” of Vimines, used in Roman decorative plaques and columns, has a carbonate cement of a micritic/microsparite nature. The “Bordeaux Conglomerate,” classified as a “pudding stone,” is held together by a molassic-glaconitic-cement of strictly marine origin. It is termed “breccia frutticulosa” by Italian archaeologists. In PPL, the grains of the cement show a characteristic green of glauconite and, in XPL, weak birefringence. The cement was rich in calcite that is given to bright, high-order colors. Oxidation of ovoid glauconite grains will produce brown margins because of their ferrous iron content.

Fig. 6.19 *Left*, Botticino Agglomerate limestone (Italy); *right*, Rojo Alicante limestone (Spain)



Tectonic breccia, such as that of Trets-Pourcieux (France), is a truly a metamorphosed rock. The metamorphism of this calcarenite shows features such as stylolitic (“tooth edged”) hematite crystals and mylonization (Mazeran 1995). The breccias of the French Maritime Alps are not metamorphic and are calcareous and dolomitic avalanche breccias. The matrix is a calcareous-argillaceous cement rich in hematite. The metamorphosed Italian breccias (“Dorata,” “Giallo Broccatello,” “Rossa”) have been studied petrographically with their provenance near Sienna (Bruno and Lazzarini 1995). The Breccia Rossa Appenninica, in thin section, shows its marine origin with abundant pelagic bivalves, radiolarites, and brachiopods embedded in a dark-brown micritic cement, hence its name. Breccia Dorata, a favorite for Roman monuments, has clasts of microcrystalline calcite, with quartz cemented with calcite. The cement varies from golden-yellow to pink.

Figure 6.20 is an excellent example of limestone playing the sculptural role of marble in antiquity. The sculpture, from relief of a tower tomb, found at the Germania Superior city of *Aventicum* (modern-day Avenches, Switzerland), as reconstructed, is typical of marine-themed funerary sculpture. The particular subject in this work is Triton abducting a sea nymph or Nereide. Discovered in 1989, during a salvage archaeological project, the sculpture illustrates the artistic usage of high-quality local limestone for large-scale mortuary architecture (Castella 1998).

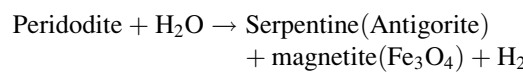


Fig. 6.20 Limestone used for sculptural relief of a Roman tower tomb, *Aventicum, Germania Superior* (modern-day Switzerland). The subject is that of Greek mythology,

Triton abducting a sea nymph or Nereide. Roman Museum of Avenches (Photograph by the author)

6.6.3.4 Serpentinite and Steatite

Serpentinite is a low-grade metamorphic rock originating from recrystallization of mafic minerals such as olivine and pyroxene (Williams et al. 1955).



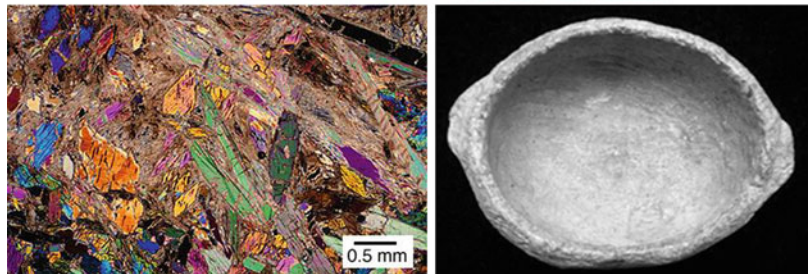
Olivine, in hydrothermal fluids, reacts to form serpentine at low temperatures, in the near surface (Yardley 1989). Some European texts (Monttana et al. 1977) as well as most early archaeological workers have had difficulty differentiating serpentine, the ultramafic mineral, from the metamorphic rock, serpentinite. Indeed, the terms serpentine and serpentinite appear interchangeably for the description of the metamorphic rock. Brecciated rock such as the ophiocarbonates of Northern Greece (Thessaly) produced from peridotites, mistaken or miss-named as “marbles,” gives interesting textural and color patterns (Mannoni and Mannoni

1984). These rocks are serpentines with veins of carbonates.

Steatite or soapstone is a general term used to describe metamorphic rocks that are composed primarily of talc, hydrous magnesium silicate, but which may contain varying quantities of other minerals, carbonate, amphibole, magnetite, and chlorite. Steatite deposits form as a result of regional or contact metamorphism due to the metasomatic alteration of an original parent body. These parent bodies are normally ultrabasics, such as serpentinites, peridotites, dunites, and pyroxenites, or in some rarer cases, the original deposit may be a carbonate sedimentary rock. In any provenancing study, it is important to recognize the nature and extent of utilization of the artifacts derived from the raw material of interest (Bray 1994).

Steatite, in the United States and Canada, is a talc or “olivine-talc-carbonate rock,” such as actinolite, low in serpentinite and the accessory talc which grades into high talc (~10 %) ultramafic metamorphic rock. Steatite is also known

Fig. 6.21 Soapstone Ridge, Georgia, USA. *Upper*, bowl “blank” in situ; *left*, thin section showing high birefringence of talc; *right*, bowl



as “soapstone” in the New World. It is also called “potstone” in the Old. The latter term reflects its use in Stone Age cultures as a vessel material. In eastern prehistoric North America, soapstone/steatite vessels appear from the Late Archaic Period to the Early Woodland Period cultures (1800 BC–AD) of the Appalachian Mountains (Fig. 6.21) (Wells et al. 2015). In the prehistoric sites of the Chumash and Gabrielino cultures of California, soapstone was used in vessel manufacture. The famous pipestone steatite quarries of eastern South Dakota were used by American Indians to fashion elegant “pipestone” pipes for tobacco. In many steatites, chlorite appears as an important accessory mineral. The color of serpentinite and steatite generally runs from dark green to lighter gray-green varieties due, in the latter case, to talc and chlorite.

The serpentine crystals of serpentinite and steatite are generally replacement of preexisting olivines and pyroxenes and the fabric may reflect this in PPL. The texture is lamellar in most cases with crystals of pyrite, magnetite, and regrown olivine sometimes present. Some serpentinites

are completely recrystallized with no trace of relic grains. These are quickly differentiated from the dark serpentine, in XPL, due to their relief, birefringence colors, and other optical properties (Fig. 6.19). The talc, in steatite, will be especially birefringent showing bright yellow and other colors reminiscent of muscovite.

6.6.4 “Greenstone”

“Greenstone” is defined as any altered basic igneous rock which is green in color due to the presence of chlorite, actinolite, or epidote (Parker 1994); this rock is metamorphic and, as a category, is used by archaeologists to describe stone artifacts such as axes. The coloration and texture give the material its name rather than a strict reading of its mineralogical makeup. Actinolite schists have both the desired color—green to almost black—and the hardness that a tool or implement must have. The rock polishes into what is termed “ground stone.” It is its hardness and toughness which make this material so

attractive to human groups and dominate the way it is worked. While it takes a moderately good edge, it withstands shock well and so can be used for artifacts which might shatter during use. In the late Neolithic Europe, Switzerland, and neighboring lands—Austria, France, etc.—both solid and shaft-hole axes are quite common (Desor 1873; Petrequin et al. 2005).

These axes are made from a variety of “green-stone” or “*roche verte*” (Ramseyer 1992; Petrequin et al. 2005). The shaft-hole axes are also known as “battle axes” or “hammer axes” (Briard 1979; Champion et al. 1984). Also termed “jadeite,” which produces some confusion as jadeite, *per se*, it is mineralogically a pyroxene. What we can say is the axes are uniformly made of a green “rock”—light to dark—that takes a good polish. Swiss geologists identify polished stone materials ranging from serpentine and quartzite to diorite (Winiger 1981). Seen in western Switzerland and elsewhere in the Alps is a suite of metamorphosed oceanic/pelagic sediments within which occur the serpentized peridotites (Hsu 1994). During subsequent glaciations of the Pleistocene, the ophiolitic rocks were deposited along the morainic margins of the Rhône Glacier and readily available for the Neolithic artisans.

Elsewhere, ophiolites occur along other subduction zones such as that of the Aegean basin. An example is the use of metamorphic rock, in particular jade, in which, as we have seen, either jadeite or nephrite, is the dominant mineral (Higgins and Higgins 1996). On the Cycladic island of Syros, serpentinite and jadeite rocks occur in quantity and were used for axe manufacture. “Greenstone” (nephrite and bowenite) was a major resource for the human occupants of New Zealand prior to contact with Europeans. The sources for this material are found in a number of locations within the South Island.

Given the disparity in the identification of archaeological “greenstone,” it is likely that the choice of specific material was simply made to fit local lithic resources and we, as archaeological geologists, apply our specificity to the individual case. As such the general and optical properties of the rock will follow that of the specific mineralogy involved. For instance, the “*roche verte*” of

western Switzerland’s perforated “battle axes” is clearly metamorphic, and in most cases, the material is either a schist—specifically a schist rich in actinolite, chlorite, and/or epidote—or a serpentinite. The texture of the former is rough or raw rock is schistose where, in the finished artifact, the polished stone is dominated by the color of the actinolite and limonite grains. In thin section the amphibole actinolite appears green, while the quartz and feldspar are granoblastic with attendant optical properties of these minerals. Actinolite grains will show a pronounced pleochroism. In XPL, the epidote will show bright birefringence colors. As we have previously said, serpentinite—a greenish facies rock as well—is fine grained with low birefringence. In PPL jadeite crystals demonstrate a high relief and they typically appear as platy and interlocked. Under XPL, the jadeite grains show a low birefringence.

6.6.4.1 Slate

A common regional metamorphic rock of pelitic or pelitic-arenaceous origin, slate’s most recognized precursor, is shale. It is fine grained and demonstrates a planar fabric that gives rise to the definition of slaty foliation. The slates are uniformly gray to black, and the principal components of the fine-grained ground mass are chlorite, muscovite, quartz, and hematite (Yardley 1989). Other minerals are andalusite and cordierite which can form elongated crystals (porphyroblasts) as do tourmaline, rutile, and pyrites (Williams et al. 1955). Graphite represents the lowest grade of metamorphism. This rock is found throughout antiquity with its usage as palettes in Egypt, for flooring and roofing, and in its most ancient archaeological appearance as a slate “tablet” for Paleolithic etchings of mammoths and figures at Gönnersdorf (Bosinski 1992).

In thin section, the fine-grained layering of the parent facies is often preserved in the ground-mass. XPL illuminates the micaceous minerals present with high birefringent colors. Porphyroblasts will demonstrate the appropriate optical properties for the specific mineral: in reflected light pyrites appear yellowish-white in

PPL; rutile with red-brown pleochroic colors in XPL; and chlorite with high relief, more brightly colored in PPL but less so in XPL.

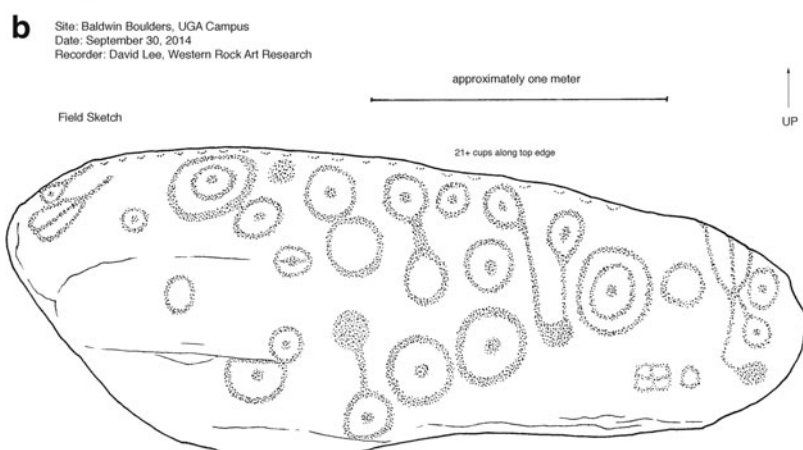
6.6.4.2 Gneisses and Schists

The varieties of these rocks are extensive usually related to their mineralogy. Grain size is medium to coarse in both types with augen gneisses having a porphyroblastic texture. Most gneisses appear lineated or banded with alternating quartz/feldspar and amphibole/biotite. Schists are foliated. Figure 6.22 shows a petroglyphic granitic gneiss boulder found in Forsyth County,

Georgia, roughly 3×1 m in size. It is covered with, on its upper portions, concentric circle motif petroglyphs of unknown age. It was first described by C.C. Jones in 1873 in his *Antiquities of the Southern Indians* (Smith 1964). It has been suggested that the stone originally stood upright in the manner of a *menhir* with the “upper” end (left in the picture) being an effigy. Schists are diverse reflecting their parent and metamorphic mineralogy.

Commonly found schists include quartz-biotite schist, hornblende schist, muscovite schist, chlorite schist, and talc schist. Most schists form from shales and the classic

Fig. 6.22 Petroglyphic boulder. Granitic gneiss



metamorphic sequence for this process is (chlorite) slate, schist, biotite-garnet schist; staurolite kyanite schist; and sillimanite schist. Previously illustrated in Fig. 2.3, the dolmen tombs of Petit-Chasseur used extensive amounts of gneiss and schist for their construction of 13 megalithic tombs of which the more imposing had stelae erected around 3000 BC by Neolithic communities living just to the east of the modern city of Sion. After functioning for more than a millennium, the cemetery was abandoned around 1600 BC, disappearing from human memory until its rediscovery by archaeologists in 1961. A stela made from schist is shown in Fig. 6.23.

The *grade of metamorphism*—low to high—is indicated by the mineral assemblage with the micas at the low end and sillimanite at the high end. As we shall see in the last section of this chapter, the firing of clays, in ceramic manufacture, closely follow the metamorphic mineralogy of shale with the low–high-grade minerals—mostly Al_2SiO_5 polymorphs—forming as the firing temperature is increased from earthenwares to porcelains.

Gneisses contain layers of quartz and feldspar along with other minerals. In thin section, the low relief and birefringence of the quartz and feldspar contrast with the darker minerals. The mineral assemblages of schist are related to the grade of metamorphism. Where the schist has formed from sandstone, the rock will have extensive quartz and feldspar in layers much like the more common micaceous varieties. Because of the deformation of these minerals, the grains will be elongated and, in the case of the feldspars, lath-like. The PPL and XPL properties will be consistent with those we have listed previously. As the metamorphic grade increases, the XPL of their thin sections produces a riot of highly birefringent colors starting with the micas continuing through the higher temperature minerals of the sillimanite group—staurolite, andalusite, kyanite, and sillimanite. Most of these minerals have a relatively high relief and a few have distinctive colors. Staurolite is pleochroic yellow–pale brown. Sillimanite and kyanite have moderate birefringence and are fibrous to prismatic with clear-cut extinction.

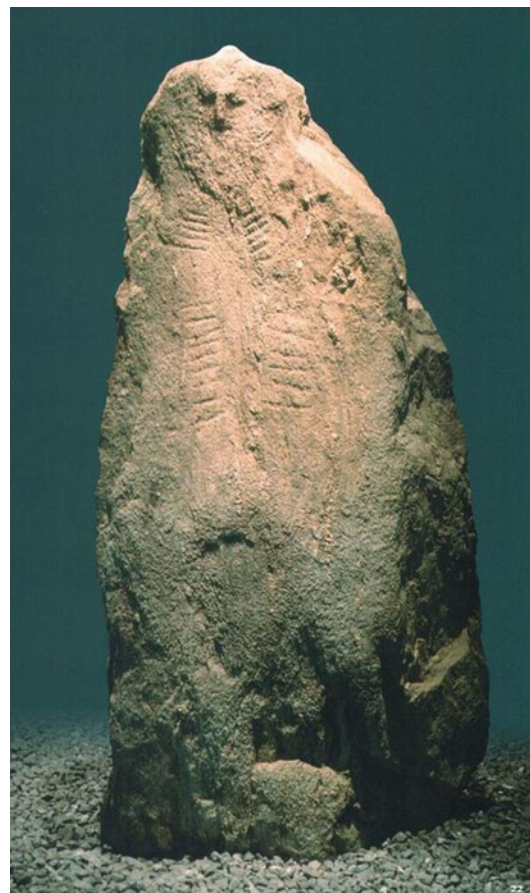


Fig. 6.23 Menhir carved from schist discovered in the Canton of Neuchâtel, in 1997, during excavations along the then proposed autoroute A5, in the vicinity of the village of Bevaix. The stone is clearly carved as *stelae* and is dated to the Neolithic Period, ca. 5000 BP. The height is 3.2 m and the weight is 2,800 kg. On exhibit, Laténium Museum, Neuchâtel, Switzerland (Photograph by the author)

6.7 Techniques: Optical and Otherwise

As rocks are collections of minerals, so their identification is the principal goal of petrography. The most straightforward means is as just mentioned—a 10 \times hand magnifier. Again, the key to one's choice of identification method is specificity. If one's goal is a simple determination of the class of rock being examined, it is reasonably sure that a distinction between sedimentary, igneous, and metamorphic rock types

can be accomplished with a good hand magnifier. If one wishes to ascertain a specific type of sedimentary rock—clastic, carbonate, or evaporate—then this too is possible for the trained eye. Beyond this level of classification becomes increasingly more difficult. The next level in petrographic identification requires the optical microscopes. This can be done with a low-power binocular microscope using reflected light or a more powerful, high (optical)-resolution petrographic microscope used to study thin sections of rocks and minerals. Beyond the optical methods are X-ray, electron, particle beam, and magnetic instrumental techniques, of which X-ray methods are the most common (Chap. 8). In this chapter are presented both hand-specimen and thin-section examples of rocks and minerals important in archaeology.

6.7.1 Hand-Specimen Macroscopic Analysis of Rocks and Minerals

Color This is one of the most obvious physical properties of lithic materials. It can be diagnostic but as a rule it is not the major identifying characteristic as it is in the studies of soils and sediments. The reason for this is relatively simple. There are 12 soil orders while there are over 2,000 minerals. Add to this fact that many archaeological rocks and minerals vary in their color (*allochromatic*), even within a specific type. Quartz has “smoky,” “rose,” and “amethyst” color varieties even though they are all quartz. The same thing is observed in flint or chert which has a host of varieties in different colors (cf. section later in this chapter). Some minerals, such as the metallic ones, tend to have reasonably characteristic shades of one basic color (*idiochromatic*) such as copper ores: blue (azurite) and chrysocolla (blue to green)—and the very commonly occurring malachite is green. Chalcopyrite, a common copper ore in antiquity, is yellow. Native varieties are generally more predictable—sulfur is yellow, copper is reddish brown, slate and graphite are gray to black, etc. The best one can say of the property of

color is that it should be used in concert with other criteria to assure confidence in identification.

Streak Streak is the color of powdered minerals. This property is a more reliable indicator of color than that of the visual color of the hand specimen. One can either rub the mineral sample on a porcelain tile or powder the sample to obtain the streak. Hematite streaks red; galena, silver-gray; hornblende, green; talc, white; azurite, blue; and magnetite, black.

Luster This is the property that describes how the mineral absorbs, reflects, or refracts light. Broad categories of luster are “metallic” and “nonmetallic.” Pyrite and galena have metallic luster. Quartz has a “glassy” luster as does olivine; soapstone (steatite) has a “greasy” or “resinous” luster as do many flints.

Cleavage and Fracture The crystalline structure of the particular minerals is observable in their geometric shapes showing clear membership in one of the six crystal systems: cubic (pyrite), monoclinic (gypsum), triclinic (plagioclase feldspar), orthorhombic (sulfur), tetragonal (chalcopyrite), and hexagonal (apatite). A *euhedral* shape is one where the mineral grain has distinguishable crystal faces on all sides such as calcite. Some mineral grains have only a few crystal faces and are *subhedral*, while grains with no crystal faces showing in a rock are *anhedral*. Most minerals are subhedral as a rule. Minerals break or cleave along planes that reflect the crystal system. In general, minerals with low crystal symmetry (triclinic) exhibit distinctive cleavage such as the feldspars. Other minerals with high symmetry are less likely to exhibit distinctive cleavage. Fracture in rocks must be distinguished from that seen in minerals. Likewise fracture is not cleavage. Cleavage planes are bonding surfaces of the crystal. Fracture can occur along cleavage planes but it does not have to. Fracture surfaces can be nonplanar, nonparallel because a rock is a collection of minerals reflecting this heterogeneity in its overall response to breakage. A good example is the important archaeological

material—flint—which does not exhibit cleavage but rather fractures in a distinctive, conchoidal manner. Obsidian, a volcanic rock, does not have a crystalline structure and, hence, no cleavage property. Obsidian does fracture conchoidally. The other common fracture forms are irregular and fibrous. An archaeological material that fractures irregularly is basalt as does most quartzite although the latter can exhibit conchoidal fracture.

Hardness Hardness is a reliable property of minerals that have not been weathered or otherwise altered. Ten minerals have been arranged in a scale known as the Mohs hardness scale. The following list gives the range of hardness relative to some common minerals:

- 10: diamond—the hardest material; can't be scratched
- 9: corundum—can be scratched with diamond
- 8: topaz—can be scratched with emerald
- 7: quartz (also flint, olivine, garnet)—can be scratched with steel
- 6: feldspar and opal—can be scratched with quartz
- 5: apatite (also hornblende)—can be scratched with ordinary knife
- 4: fluorite (also dolomite, many copper ores)—can be scratched with glass
- 3: calcite (also mica, halite)—can be scratched with common wire nail or a penny
- 2: gypsum—can be scratched with the fingernail
- 1: talc—can be crushed between the fingers

Twinning This property is observed in a host of minerals in several colloquially named forms such as the “fairy cross,” seen in staurolite, and the “fishtail” observed in some gypsum and the “dovetail” in calcite. Other commonly used names for twinned minerals are “albite twins,” “penetration twins,” “iron cross,” “spinel twins,” and “star twins.” This short list does not exhaust the varieties of twins that are seen across a large number of common minerals such as calcite, feldspar, galena, gypsum, pyrite, quartz, rutile, spinel, sphene/titanite, stibnite, and wurtzite. Of

the silicate minerals, all of the feldspar groups—albite to sanidine—form twins. Calcite is distinguished, by twinning, from its close mineralogic cousin, dolomite.

Twinning is observed at the hand specimen level and seen under the petrographic microscope where it is used, in the latter case, to identify minerals in thin sections. Twins result from errors in crystal growth. These errors result in characteristic twin forms and follow what are called “twin laws”—the Spinel law, the Albite law, the Carlsbad law, etc. Orthoclase twins according to the Carlsbad law. Microcline—a potassium feldspar with some sodium—is recognizable for its characteristic “crosshatch” or plaid-like twinning which follows the Albite law.

6.7.2 Optical Properties of Minerals

Minerals, optically, come in two forms—isotropic and anisotropic. The isotropic minerals have the same optical properties in all directions within the crystal structure (recall that one of the definitions of a mineral is it must have crystalline structure—obsidian does not, so it is simply a “rock”). Anisotropic minerals vary in their optical properties—ray paths and angles (Perkins 2011). All minerals belong to six crystal systems with isotropic minerals comprising one system and the other five anisotropic.

Light microscopy and quantitative mineralogy have been the cornerstones of any study in rocks and mineral in geoarchaeology. Yual Goren (2014) points out that several aspects of geoarchaeology require the optical microscope as their primary tool. The instrument of preference is usually the polarizing—or petrographic—microscope. The most common usages are, respectively, petrography and micromorphology. While borrowed from earth sciences, these two areas have developed a slightly different meaning within the archaeological context. While optical microscopes are also used in numerous other science-based fields of archaeology—such as metallography, archaeobotany, palynology, etc.—their use for micromorphology and

petrography for archaeological purposes has increased over the last few decades.

Petrographic thin sections are just that—paper thin (30 μm) slices of a rock sample that are mounted and polished on glass slides. These slides are then examined using the petrographic microscope invented in 1828 by William Nichol (Ford 1918). The use of thin sections was pioneered by Henry Clifton Sorby in his examination of Jurassic limestones from Yorkshire, England, in 1851 (Adams et al. 1997).

The petrographic microscope is distinguished from other types of optical microscopes by its reliance on polarized light. Polarized light is light that vibrates in one specific plane. Historically, petrographic microscopes use a Nicol prism (so-called for William Nicol) made of calcite to produce light that vibrates in only one plane (plane-polarized light or PPL). Modern petrographic microscopes use an organic film as a filter to produce PPL.

PPL is produced by one polarizing filter located below the sample stage. A second, moveable, polarizing filter, with vibration direction set perpendicular to the lower polarizing filter, is located above the sample stage. The light ray emerging from the lower filter vibrates perpendicular to the upper filter's vibration direction. With both filters in the light path, we observe the property of extinction. This arrangement is termed crossed polars or XPL where the lower filter is the polarizer and the upper filter is the analyzer. When a thin section of a mineral or a rock with a variety of minerals is placed between the two crossed polars, one can observe various intensities and colors because the light is passing through anisotropic material, such as a carbonate, that bends the PPL such that not all the light is extinguished by the upper polar. The resultant light is called birefringence.

Birefringence is a diagnostic property of anisotropic minerals—it is not seen in isotropic fluorite, garnet, and spinel or amorphous (glass, man-made, or volcanic) minerals—those materials in which the light ray travels unaffected through the material. It is observed in XPL. Polarized light, upon entering a crystal, will split (refract) into two components traveling at

differing velocities. Upon recombination, the two light paths interfere and create interference colors. As seen in Fig. 5.16, talc is highly birefringent. The index of refraction and birefringence are consistent optical properties of minerals used by petrographers. The law of refraction, called Snell's law (see Chap. 7, XRD) after its discoverer, in 1621, Willebrord Snellius, proposed the following familiar form:

$$\sin i / \sin r = n$$

where i is the angle of incidence for the light beam and r the angle of refraction as the light beam exits the material and n the index of refraction or geometric ratio of i and r . Values of n fall between 1.4 and 2.0 for most minerals. Typical values are apatite, 1.624–1.667; calcite, 1.486–1.740; fluorite, 1.434; gypsum, 1.519–1.531; olivine, 1.63–1.88; quartz, 1.544–1.553; and zircon, 1.923–2.015. A few transparent minerals like diamond (2.418) and rutile (2.605–2.901) exceed the typical range for the index of refraction.

The difference in the highest and lowest indices of refraction in a mineral results in its birefringence. In petrography, it is termed weak, moderate, strong, very strong, and extreme. Using PPL, alone, it is generally possible for an experienced observer, to estimate the refractive index and make distinctions between different birefringent minerals.

Another important aspect of a mineral's color is pleochroism. This optical property is observed in a few common anisotropic crystalline minerals, biotite and hornblende being examples. Isotropic minerals do not exhibit pleochroism. When the petrographic microscope's stage is rotated in PPL, anisotropic minerals will demonstrate this property by changing colors. Biotite mica, a common pleochroic mineral, is easily identified by this property coupled with its high birefringence. Pleochroism is easily observed at the hand specimen level in transparent varieties of cordierite and spodumene.

The final optical property, on grain mounts, sometimes mentioned in the identification of minerals, that is only observed in thin sections is relief. Relief, like the properties of

birefringence and dispersion, is directly related to the refractive index. Relief is basically a subjective and relative characteristic of a mineral (MacKenzie and Adams 1994). Here the difference is not between the path difference and wavelength of the light in the mineral but the difference between the mineral, on the thin section, and its mounting medium—epoxy, Canadian balsam, etc. Most mounting media have a well-known refractive index of 1.537 (1.54) such that minerals with a higher refractive index than 1.54 will demonstrate what is termed “positive” or moderate to high relief where the mineral appears as bolder than media in PPL. Low or negative relief would be where the mineral appears less distinct than the mounting media. The refractive index is very useful in determining the identity of a mineral, particularly those isotropic varieties like fluorite. A general rule among petrographers is that felsic minerals—quartz and feldspar—typically show low relief and are almost colorless. By comparison, ferromagnesian (mafic) minerals exhibit high relief and color, e.g., olivine.

6.7.3 Quantifying Minerals in Thin Sections

Rocks and minerals, where pertinent their general—hand specimen or grain mount—and thin-section properties, express definite optical properties, like that of the macroscopic indices.

One of the earliest and most common optical techniques of the so-called areal method for quantifying volume percentages of minerals was that of Delesse in 1847 (Holmes 1930; Jones 1977). Delesse studied polished blocks, traced the outline of minerals onto paper, then transferred the pattern to tinfoil, and cut around the boundaries. The tinfoil pieces were sorted into mineralogical classes and weighed to yield relative percentages. The volume percentage of a mineral was determined by comparing the weight of each cut pattern representing a mineral species (WA) to the total weight of cut pieces (WT).

$$\text{Percentage mineral} = (\text{WA}/\text{WT}) \times 100 [1]$$

This and other methods equated measured weights or areas to volume equivalents. To measure the volume of clay skins, Buol and Hole (1961) projected the microscope image onto a ground glass, traced the image on translucent paper, and then cut and weighed each piece. They measured clay skin volume as a function of horizonation and genesis of translocated clay. Johanssen (1938) and Fry (1933) used a camera lucida attached to a microscope to project the image. The periphery of each mineral was traced with a planimeter to yield relative proportions. Despite the awkwardness of area measurements, recent developments in computer image analysis utilize this principle.

The Linear Method – In 1898, Rosiwal developed a much simpler method of measuring the volume percentage of minerals (Holmes 1930). This technique measures lengths of line segments rather than areas and samples a portion of the mineral area rather than the whole area, as in the Delesse Method. It measures the frequency with which a mineral is encountered during the transect. The proportion of the length of the line crossing a mineral species (LA) is compared to the total length of the traverse (4). The percentage of a mineral in the specimen is given by

$$\text{Percentage mineral} = (\text{LA}/4) \times 100 [2]$$

The theoretical basis and statistical accuracy for this method are discussed by Lincoln and Rietz (1913).

Reflected Light Microscopy Many minerals, particularly the metallic ones, do not transmit light no matter how thinly they are ground. To examine such opaque minerals, in polished section, plane-polarized light is reflected off the upper, polished surface. Many research-grade petrographic microscopes are equipped with both transmitted and reflected optics. One can differentiate isotropic and anisotropic minerals under reflected light. Most isotropic minerals will remain an unchanging dark color as the microscope’s stage is rotated. Anisotropic

minerals, while never going completely to extinction, will lighten and darken four times as the stage is rotated through 360°.

The author has used reflected light microscopy extensively in the study of archaeomaterials—lithics, ceramics, metals, and slags, along with fossiliferous materials as well. A transmitted light microscope will typically be of little use to anyone wanting to examine the structure of metallic samples or the surface of ceramics. Most research microscopes can be fitted with both transmitted and reflected systems. In a reflected system, light must be directed onto the surface and eventually returned to the microscope objective by either specular or diffused reflection. Light reflected from the surface of the specimen re-enters the objective and passes into the binocular head where it is directed either to the eyepieces or to a port for photomicrography.

One of the most powerful techniques for introducing contrast into reflected light microscopy is differential interference phase contrast optics. These special optics allow the visualization of minute elevation differences on surfaces. To produce interference, a birefringent prism (also known as a Wollaston or Nomarski prism, depending upon design) is introduced into the light path just above the objective, and a polarizer is installed in the vertical illuminator (similar to polarized light). The prism splits the polarized light into two orthogonal polarized beams on their way to the specimen. These

perpendicular light beams reflect off the specimen to create a lateral wave shift/displacement in regions where surface relief exists. If the surface is completely flat, nothing is observed. However, if there is, for example, a small difference between the two wave fronts, one of the beams must travel a path that is longer and is assigned this path difference. Upon recombination, an “interference (phase) contrast” is observed, giving, in many instances, a “three-dimensional effect” to the surface. It has to be kept in mind that this is an optical effect and the relief does not necessarily resemble the actual condition of a surface. Petrographic usage of reflected light microscopy rarely requires the resolution that Nomarski optics provide, but it is there if needed.

Lithic and ceramic studies routinely use reflected light microscopy as well as transmitted microscopy. The latter cannot examine unprepared surfaces of an artifact or item directly as can reflected microscopes. So-called stereomicroscopes are most commonly used in petrographic studies. These microscopes do not have the magnification capabilities of the petrographic microscope, but, in most cases, this magnification is not needed for evaluation of surfaces on tools or fabric or temper in pottery. Pioneering studies by Semenov (1964), Tringham et al. (1974), and Odell (1975, 2001) in microscopic use were relied exclusively on reflected light microscopy.

7.1 Introduction

The study of ceramics and the clays used to produce ancient earthenwares fill detailed and discursive publications in archaeology. Geoarchaeology chiefly concerns itself with those aspects of ceramics and clays wherein it can make the most pertinent contributions in geology, petrology, and mineralogy, to name the most obvious areas. As an aluminosilicate mineral, clay is practically ubiquitous. As a marine sediment, it floors the deepest portions of the world's oceans (Thomsen 1877). Because of its geological commonplace, clay is the potter's equivalent of ore for the metallurgist.

There is no one explanation for the first transformation of clay to ceramic. Suffice to say, the association of fire and clay, in some happenstance setting—a hearth fragment, the accidentally fired clay figurine, etc.—inspired early humans to systemize the manufactured fired clay objects and, ultimately, pottery (Vandiver et al. 1989). Pottery's antiquity has doubled in the past decade with discoveries in China pushing back pottery's invention to the late Pleistocene ~18–17,000 calendar years before the present (BP) first, at Yuchanyan Cave (Hunan, China) (Boaretto et al. 2009) then over 20,000 years ago with discovery of a pottery at Xianrendong Cave with round bottoms and stripe-marked designs, tempered with coarse quartzite grains (Keally et al. 2004; Wu et al. 2012). These findings, in

contrast to earlier archaeological theories linking pottery to plant and animal domestication or “the Neolithic Revolution” (Childe 1948), indicate that pottery was a hunter-gatherer innovation that first emerged in East Asia between 20,000 and 12,000 years before the present, toward the end of the Late Pleistocene epoch (Craig et al. 2013).

Pottery represents a fundamental shift in human dietary history, conclusively demonstrating that hunter-gatherers, not early farmers, in East Asia used pottery for some 10,000 years before they became sedentary and began cultivating plants. The age for pottery production at Xianrendong of ~20,000 years ago coincides with the Last Glacial Maximum, MIS 2, when there was a decrease in the productivity of regional food resources. Used for cooking, pottery allowed the preparation of energy-rich starch foods and meat. Scorch and soot marks on shard exterior surfaces indicate that Xianrendong pottery was used in cooking, but complete physiochemical studies have not been reported yet. However, lipid residues on 15,000–11,800 BP pots (the Incipient Jōmon period) are unequivocally derived from processing and cooking freshwater and marine organisms (Brown 2000; Evershed 2008; Craig et al. 2013).

Rice, writing in 1999, states “that objects of unfired and low-fired clay were created as part of early “prestige technologies” of material

representations beginning in the Upper Paleolithic and are part of an early “software horizon.” Clay began to be more widely manipulated by non-sedentary, complex hunter-gatherers in the very Late Pleistocene and early Holocene in areas of resource abundance, especially in tropical/subtropical coastal/riverine zones...” The reliance on archaeological discovery of ancient pottery, its age determination, and chemical analysis seems to leave little room for geoarchaeology if it were not for the familiar names associated with these discoveries such as Bar-Josef and Goldberg (Xiaohong, et al. 2012). In the geoarchaeological analyses at Yuchanyan and Xianrendong, mineralogical and micromorphological analyses of the sediments both indicate that ash calcite was a major component of almost all samples, implying that they were produced mainly during periods of human occupations. Another unusual anthropogenic activity is indicated by the clay-rich sediment formed into lenticular bands that must have been brought into the cave by humans and functioned as prepared surfaces (*supra*). Understanding the geologic—sedimentologic and mineralogical—context is crucial for a comprehensive understanding of clays and pottery.

7.2 Clays

Clays as noted are geologically ubiquitous minerals. This one fact may be, in large part, a major factor in the almost universal and independent occurrence of pottery in the world. In a geologic sense, all clays are “secondary” minerals. They are formed by the breakdown of other minerals, such as feldspars or the diagenetic solution of carbonate rocks such as limestones containing clayey impurities, which, being insoluble, are deposited as clay. Clays are formed by the disintegration and solution of shale as well. In this sense, clays are all secondary, but their deposits are termed “primary” (authigenic) or “secondary” (allogenic). Thus, “clay” is a term applied to a variety of earth materials of different origins and composition. The actual definition depends on the field of

interest so that most archaeologists and potters have a different idea of what constitutes clay than do geologists, pedologists, or agronomists. To the potter, clay is any earthy aggregate that (a) when pulverized and mixed with water exhibits plasticity, (b) becomes rigid on drying, and (c) develops hardness and strength when heated to a sufficiently high temperature.

For the geologist, clay is a fine-grained weathering product of silicate minerals. The structural breakdown of minerals to form clay is caused by natural geochemical reactions induced by atmospheric and meteorological agents including water, vapor, and gasses rich in oxygen, carbon dioxide (CO_2), and sulfur oxide forms (SO_x), as well as by various biological agents, such as lichens and anaerobic bacteria. Depending on the parent rock composition, the end result of weathering can be a variable mixture of clay, quartz, hydrous ferric and aluminum oxides, resistant detrital minerals, and micaceous material such as vermiculite. Texturally, clay is characterized by extremely fine particle size, below 2 μm in diameter, and with highly variable chemical and physical properties.

As noted, clays can form either in place as “primary” or residual weathering products generally overlying their source rocks, or as “secondary,” sedimentary clays that formed elsewhere and were transported by water from their source, or as clay-size particles formed from sediments, transported and refined by water, and redeposited as sediment. In the state of Georgia, one of the world’s principal kaolin resources, the kaolin deposits of Cretaceous age are primary and higher grade; the tertiary deposits are secondary with more impurities. The secondary kaolin formed by weathering of crystalline rocks on an upland surface then was transported away from their source; refined to finer-grain sizes and picked-up impurities, especially organic matter; and redeposited where they are found today. Other clays such as montmorillonite and bentonite are also found as primary or secondary deposits. Since secondary clays are carried by water, they tend to pick up many impurities which affect the manner in which the clay may be fashioned, tempered, and fired.

Because of abrasion and alteration during transport, the particle sizes tend to be finer than in primary clays. Their fine-grain size and decayed organic matter tend to make them generally more plastic than primary clays.

Clay has the general formula of an “alumina–silicate–hydroxyl” mineral. Clays are fine particulates that are $>2\text{ }\mu\text{m}$ (microns ($1\text{ }\mu\text{m} = 1/1,000\text{th mm}$) or less of triclinic crystals (ex. kaolin). Clays are sheetlike structures. Clay minerals are characterized by substitutional cations such as Si^{4+} , Al^{3+} , Fe^{3+} , Mg^{2+} , K^+ , and Na^+ .

Cations are common in the interlayers and not in the silica-alumina structural units. The “2:1; 2:1:2 clay minerals” are more cationic than the 1:1 clay minerals, e.g., kaolin. Kaolinites have few if any cations in the interlayer. Structurally, Fe^{3+} , Al^{3+} cannot form tetrahedra, while Mg^{2+} can form octohedra along with Fe, Al. Illites have one-sixth of Si^{4+} replaced with Al^{3+} with a charge deficiency of +1 usually balanced by potassium K^+ . Montmorillonites have many cations in the interlayer, whereas Na^+ , Ca^{2+} are common in smectites.

Rocks with high glass weather more rapidly than those with lower glass (e.g., tuffs). Fine-grained rocks weather more slowly than coarse-grained rocks. Biotite-bearing rocks (granites) weather more rapidly than those without (basalt). Sedimentary rocks weather according to grain size and to some degree, clay content. Fine-grained sedimentary rocks weather more slowly as a rule. Cements in sedimentary rocks impact weathering—silica cements are typically stronger than carbonate (micrite/sparite) cements.

A “rock stability scale” is as follows: quartzite, chert–granite, basalt–sandstone/siltstone—dolomite/limestone (bioclastic, silica-cemented “limestone” is an exception). Climate/weathering of the same lithology can produce differing clays (Table 7.1; Fig. 7.1).

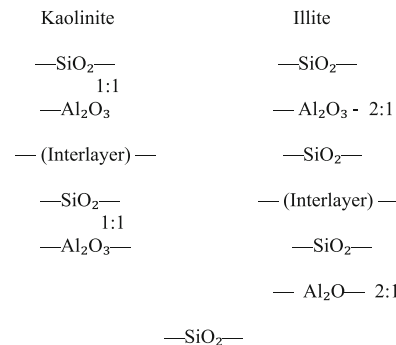
Clay “sheets” are composed of silica sheets—silica units are tetrahedral (four-sided—shown below).

Alumina sheets—alumina units are octahedral (eight sided).

Table 7.1 Climate and weathering of silicate precursor minerals

| Climate | Mineral | Clay(s) |
|----------------|---------------------|---------------------|
| Arid | Biotite | Smectite |
| | Plagioclase | Kaolinite |
| Temperate | Biotite | Vermiculite |
| | Plagioclase | Smectite, kaolinite |
| Tropical | Biotite | Kaolinite |
| | K-spar | |
| | Plagioclase | |
| Humid tropical | Biotite | Kaolinite |
| | K-spar, plagioclase | Kaolinite, gibbsite |

The structure of kaolinites is 1:1; the structure of illites and smectites is 2:1.

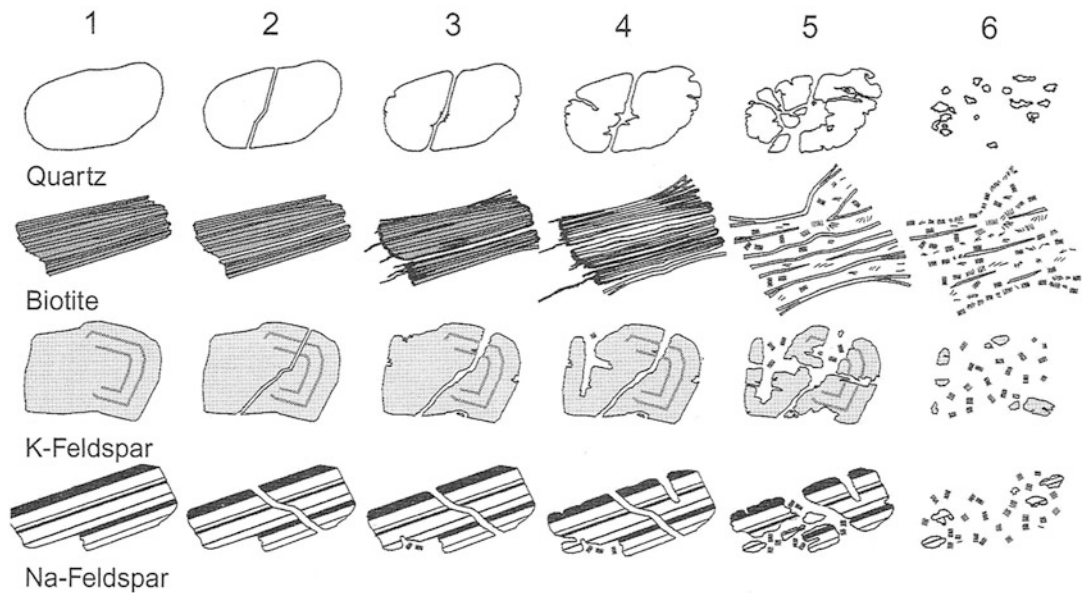


The interlayer, in illites, is filled with cations and, therefore, makes illites more rigid than montmorillonites. Kaolinites are the most rigid of all clays. The property of rigidity is related to plasticity, an aspect very important to the potter.

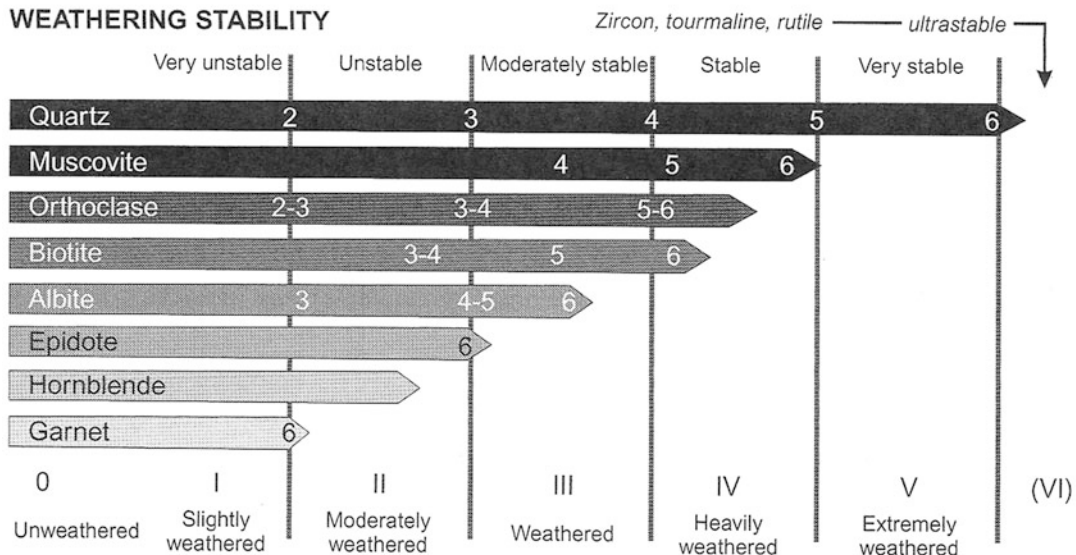
7.2.1 Clays in Paleosols

While the foregoing suggests that most primary clays originate from silicate rocks, a large number of clay-rich or “terra rossa” soils do not. In many instances, clay-rich soil such as ultisols (USDA) forms on carbonate bedrock (Driese et al. 2011). Terra rossa soils across the globe are characterized by red and yellow colors on the Munsell scale (cf. Chap. 3). Likewise, they have clay-rich B horizons (*supra*). On paleosurfaces

WEATHERING STAGES



WEATHERING STABILITY

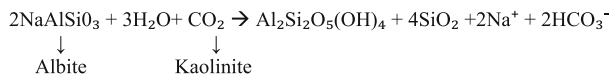


DEGREE OF WEATHERING

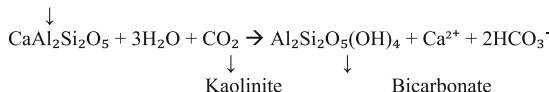
Fig. 7.1 Weathering of silicate minerals (After Horgen 2000). Granites gneisses of the Appalachians produce kaolinite with gabbros yielding smectite and olivine-rich rocks yielding montmorillonite via the mechanisms illustrated below

Hydrolysis:

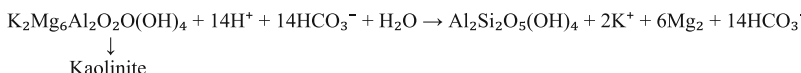
Carbonic Acid +Plagioclase [anorthite (Ca), albite (Na)] → Kaolinite



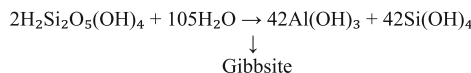
or Anorthite



or Biotite



- Kaolinite can be altered to Gibbsite by weak acids.



- Plagioclase can alter straight to Gibbsite

where clay-rich horizons indicate a paleosol or Paleudult, for example, that may have formed from limestone or dolomite bedrock and are indicative of a temperate to tropical paleoclimate. Additionally, these ultisols tend to indicate geologically old land surfaces but the kandic (argillic) B horizons can form in as little as 4,000 years due to the high rate of clay formation and illuviation (Layzell et al. 2012).

In mixed (ionic) charge sediments, constant-charge clay minerals (aluminosilicates with a permanent structural charge) interact with oxide minerals of Fe and Al, which are negatively and positively charged, respectively, at the normal pH of groundwater. Iron oxides or oxyhydroxides are known to form close associations with clay minerals, forming discontinuous layers or small aggregates on the negatively charged surfaces of clays (Bertsch and Seaman 1999; Bunn 2002; Hong and Xiao-Nian 1992; Seaman et al. 1997). Some studies have suggested that the “binding agents” providing physical stability in soils are mainly poorly crystalline or amorphous phases of Fe, Si, or Al (Arias et al. 1995; Swartz et al. 1997) and that crystalline phases are more likely to form discrete aggregates.

Studies of Southeastern United States Paleudults in the eastern Tennessee Valley-and-Ridge Physiographic Province suggest rather complex origins for these ancient soils (Driese et al. *supra*) where the bedrock is undisputedly a carbonate lithology. The clay mineralogic analyses support the formation of pedogenic kaolinite, halloysite, and hydroxyl-interlayer minerals along with illites (see above) derived exclusively from the carbonate bedrock. With these ancient soils, a hypothesis of the so-called top-down pedogenesis due to *in situ* weathering was rejected for a more polygenetic origin that involved alluviation and colluviation as contributing influxes of detrital minerals such as quartz and, of course, feldspars.

7.2.2 Clay Deposits

Most clay deposits are found with an admixture of silt, sand, and other impurities including organic material, micas, and iron hydroxides. The impurities may constitute over 50 %, so such deposits must be refined before they can be used for pottery making. The differentiation among clay, silt, and sand is by particle size, but

unfortunately, there is no agreement on where the size boundaries should be drawn. In most widely accepted granulometry scales used by agronomists, engineers, and geologists, clay is smaller than either 0.002 or 0.004 (Wentworth Scale) mm in diameter (2–4 μm), silt up to 0.05 mm, sand 0.05–2 mm, and gravel is greater than 2 mm. The name assigned to mixtures of the first three depends on the relative amount of each component present. Soil scientists call clay any mixture with more than about 40 % clay, and mixtures with much silt and sand are called loam. Potters don't classify clays on mineralogical basis. Rather the terminology one sees used among ceramicists is:

China clay: hydrated kaolin

Pipe clay: kaolin with large % SiO_2

Potter's clay: smectites, illites, bentonite, e.g., montmorillonites—not kaolin group

Brick clay: clay with sand and Fe in large %

Fire clay: clay with no lime, iron, or alkaline earths; very refractory, resists fusion

Ball clays: white or gray with large alumina—silicate %; e.g., kaolinite principal clay mineral (35 lb. "balls," British term)

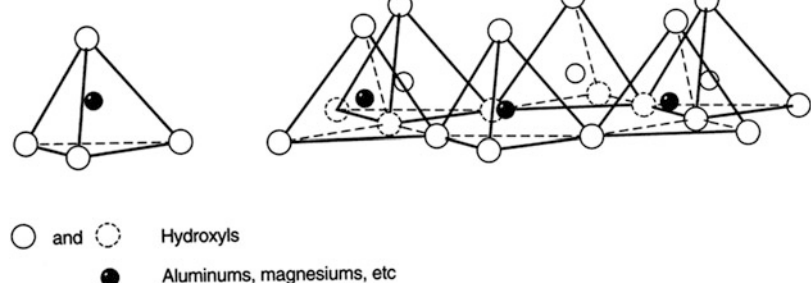
Virtually any clay can be used for making pottery, depending upon the skill of the potter. The main clay mineral groups include (1) kaolinite, which has a relatively fixed structure, (2) a group of expandable clays called smectites, whose most common member is montmorillonite, and (3) the illite group with a structure similar to smectite but is not expandable. The sum of a layer plus an interlayer is a structure unit in

clay. The structural properties of these groups govern many technological choices by potters.

1. As indicated above, the structural unit for kaolinite is a 1:1 layer, consisting of one tetrahedral sheet with one octahedral sheet (Fig. 7.2). The space between two successive 1:1 layers represents an interlayer which will be devoid of any chemical elements if the layers are electrostatically neutral, i.e., with no excess valences. Since this is true in most kaolins, the interlayers remain relatively free of cations or water. The simple rigid structure of kaolin does not allow for much substitution by exotic elements (alkali elements lower melting temperature). In addition, it has the highest Al:Si ratio of the clay minerals (higher Al means higher melting temperature) and is least able to absorb water (lowest plasticity). The use of pure kaolin clays in ceramics is thus restricted to the most advanced ceramic technologies.

2. The smectite structure unit is a 2:1 layer in which two tetrahedral sheets sandwich an octahedral sheet. The position of the two tetrahedral sheets is inverted so that all apical oxygens point to the octahedral sheet where they are shared by both sheets. Most 2:1 clay minerals have an excess layer negative charge produced by unbalanced ionic substitutions, such as Mg^{2+} for Al^{3+} or OH for O . This is neutralized in the interlayer by various cations, mainly Na and Mg, hydrated cations, hydroxyl groups, and water. Abundant substitution for Al and the presence of interlayer cations makes smectites less refractory than other clays. They are also expandable because

Fig. 7.2 The silica and alumina tetrahedral/octahedral units



their charge deficiency is in the interior alumina layer. At lower firing temperatures than other clays, about 600 °C major dehydroxylation occurs which causes irreversible structural changes. Smectites also have higher shrinkage in drying and firing than other clays.

3. The illite group of clays have structures similar to micas as well as to smectites. In the illites, about one-sixth of the Si^{4+} is replaced by Al^{3+} leading to a charge deficiency that is balanced chiefly by K^+ but also by $\text{Ca}^{2+}/\text{Mg}^{2+}$ and H^+ . The charge deficiency in the illites is primarily in the outer silica layers and therefore closer to the surface than in the smectites. The excess negative charges on the illite interlayers are satisfied by cations which accounts for a more rigid structure. Because of their fine particle size and low shrinkage which helps produce a natural luster through minimal mechanical treatment, illite clays are desirable as pottery slips.
4. Other less important clay minerals are vermiculite and the chlorite group. Vermiculite, so-named because it looks like small worms (Latin: *vermiculus*) when heated, is related to the smectites. Vermiculites also have an expanding lattice but not as great as in the smectites. The chlorite group are light green, mixed layer minerals common in low-grade metamorphic rocks and sediments. They can form in a variety of ways: as alteration of ferromagnesian silicate minerals or authigenically in sediments. They are commonly mixed in with other clay minerals and are thus hard to identify. Thus, the two-layered kaolinite and the three-layered smectite clays, including montmorillonite, are expandable, but the three-layered illites are not.

The exact chemical compositions of most clay deposits are quite variable, especially between beds; their physical properties vary as well, creating serious problems for the potter. Substitutions of water and different cations in clay structures, as well as indeterminate mixtures

of different clay and detrital minerals can make drying and firing behavior hard to predict. This explains why the choice of clay and the preparation recipe can be the most conservative aspects of ceramic production by traditional potters.

Because chemical compositions of clays vary widely in both elements present, especially trace elements at the ppm level, and water content, a structural determination by XRD analysis is more important than a chemical analysis to identify individual clay minerals. This is especially important for characterization of provenance and technological studies.

7.3 Ceramics and "Ceramics"

In the field of archaeological ceramics, there is extensive variety in the nature of the specific wares or types of pottery manufactured at any one time in any one place throughout antiquity. To the earth scientist, not versed in the complexity of archaeological ceramics, or the variety of way archaeologists look at ceramics, confusion is not a surprising first reaction. In large part, archaeologists tend to rely more on stylistic/morphological variation in ceramic wares than on petrographic parameters. A key concept for archaeological studies, not just for ceramics, although the concept was first used in ceramic analysis is that of "type." A type is a category of archaeological artifacts defined by a consistent clustering of attributes such that an item, such as a pottery vessel can be considered a member of a class/category (Clarke 1968; Thomas 1998a, b). Variation or consistency in types is used to evaluate the geographical extent and chronological persistence of a particular type, which in turn, is often used as a proxy for cultural variability or persistence. The type-variety of ceramic typology uses the type concept for vessels and groups successively finer categories into "varieties" based on some combination of variables, such as paste, decorative treatment, and surface finish. The most common form of type is that of the "descriptive type." It inheres no chronological nor functional dimension although from the

adoption of ceramic typology, these categories have been so used. For instance, if a type persists over a relatively long period of time the term “ceramic tradition” is often applied (Willey and Phillips 1958). Likewise the term “ceramic horizon” is used to describe the “rapid” appearance of a type, in a short time span, across a relatively large area or region (*supra*). This system of classification is more commonly found in the study of prehistoric earthenwares, whereas the term “ware” is more commonly used in discussions of historic ceramics (Majewski and O’Brien 1987).

Rarely does the field archaeologist look much beyond the form/shape, color, or decoration of a ceramic artifact except, perhaps, to remark on the type of temper used (in earthenwares, mostly). No archaeologist, working in Neolithic-Post-Neolithic or equivalent periods (Woodland; Pre-Classic, etc.), can ignore the ceramic artifact as (a) most of these archaeological cultures made and used pottery and (b) by definition, the “Neolithic” is often characterized by the presence of pottery. As we noted in the introduction of this chapter, early pottery appears in the Mesolithic Period in Asia, specifically in the early Jōmon Period of Japan, ca 10,500 BC (Ikawa-Smith 1976; Rice 1999). The recent discoveries in Jiangxi Province, China, Xianrendong Cave, have pushed back its invention into the late Paleolithic ca. 20,000 years ago (Wu et al. 2012). It was independently invented and used in all parts of the world with the exceptions of Australia, the far north of North America, and Eurasia. It is as ubiquitous an artifact in late Holocene archaeological cultures as those made of lithic materials.

The ubiquity of pottery as an artifact can be as much difficulty as it is an advantage for archaeology. The sheer amount of pottery, mostly recovered as shards, must be seen to be believed. Pottery is recovered in metric ton amounts on many prehistoric sites. The author participated on two excavations, one a Late Bronze Age village site in western Switzerland and another, much smaller fourteenth- to fifteenth-century habitation site in coastal Georgia, where, in the first case, over 20 tons of pottery was recovered

and, at the second, over 20,000 shards were found (O’Keene 2004; Keene and Garrison 2013). No archaeologist, nor geoarchaeologist, examines this amount of pottery as a rule with rare exceptions. Bishop (1994) reports on a massive neutron activation analysis (NAA) study done on over 12,000 Mayan pottery samples. More and more pottery analysis projects are to be mounted on a similar scale.

At the Dove Creek site (Colorado), for example, an Ancestral Puebloan/Anasazi Period site (ca. AD 900–1,050), Till (2006) in the wake of a topographic and geophysical mapping study, evaluated 8,976 shards. Till points out the use of 4 “working types”—categories used for analysis but not formally recognized as “types” per se—out of a suite of 31 types. Ancestral Pueblo farmers settled the central Mesa Verde Region of southwestern Colorado in the seventh century AD, the Basketmaker III Period (Diederichs et al. 2013). The Basketmaker III Period (AD 600–750) was part of an important cultural shift in the history of the American Southwest, when a new technological package—including “the maize suite”—enables direct precipitation or “dry” farming, due in part to the recognition of the deeper soils’ potential (Fadem et al. 2014). These innovations—including pottery—enabled the rapid expansion of Puebloan populations, thereby representing a material culture (“ceramic”) horizon in the archaeological record (Lipe 2015; Diederichs, *supra*). This change is an American version of the “Neolithic Revolution” (Lubbock 1865; Childe 1948), which emphasized the introduction and use of pottery.

The ceramic “sample,” nonetheless, in many archaeological instances can, therefore, be a reality that challenges analyses. Another aspect, beyond sheer numbers, is the salient difference, often overlooked, that exists between pottery and other artifactual remains such as lithics. That difference lies in the phenomenological nature of pottery itself. Ceramic assemblages, unlike lithic materials, are pieces of the “whole cloth” or the vessel of which they were a part. Lithic residue often represents all or portions of the *chaine d’opératoire* as originally defined by the French Paleolithic archaeologist, Leroi-Gourhan

(1993). This is to say a reduction flake is just that while the biface from which it was removed is the finished artifact temporally and spatially separate from that fragment of its manufacture. The shard is basically a smaller "vessel" in and of itself. It is not a fragment of a manufacturing process. It can yield information of that process but it is the product. This phenomenological reality gives greater credence to descriptive analysis of these singular fragments of the whole. They are, in a real sense, the "whole." This gives the shard an analytical standing that belies its humble nature. A ceramic analysis of a single shard can be much like a mineralogical study of fragment of a stone outcrop or facies in that the same relationships here, for instance, use of the Delasse Method of calculating volume percentages of minerals in a specimen (cf. Chap. 5). What is generally technologically true for the shard is true for the pot as a whole.

Archaeological analytical protocols for prehistoric ceramics have led to many important key insights. One of the first and most famous uses of a systematic examination of ceramic types was that of Sir Flinders Petrie (1904) in his use and expansion of ceramic seriation/typological sequence analysis for chronological purposes. For our purposes, the Earth science study of ceramics, specifically petrography and geochemical, provides additional ways, in the rubric of epistemology, giving independent evidence, for suppositions and hypotheses about the manufacture, technological evolution, and use of ceramics in the past (Hayden 1995, 1998; Tite 1999; Vandiver 2001).

7.3.1 Ceramic Properties of Clay

In the making of ceramics, it is crucial that the potter know how the clay body will behave during the different stages of fabrication: aging the clay, forming the matrix, finishing the ceramic, drying, and finally firing. The properties that determine the usefulness and problems for each clay raw material are (1) plasticity in forming, (2) shrinkage by drying, (3) thermal during

firing, and (4) other esthetic properties, including color, etc.

7.3.1.1 Plasticity

The addition of water to raw clay will produce a plastic mixture which can readily be shaped without rupture. Clay exhibits plastic properties for primary reasons: the clay particles themselves are platelike, a reflection of their crystalline structure; the small size of particles, clay sized, is below 0.002 mm in diameter; and the presence of water, called "water of formation" between the clay particles. Water acts as a lubricant and allows the clay particles to slide across each other rather than rupture when a shear force is applied.

The development of plasticity in clay is critical to the manufacture of a ceramic, and depending on the composition of the clay, plasticity will develop over a narrow range of water content. Dry clay is nonplastic, and as water is added, the clay will become plastic, and finally, with too much water, it will become too fluid to retain its shape when formed (Table 7.2). Kaolinite has a non-expanding two-layer structure and forms relatively large particles, 0.3–2 μm in diameter; smectites have an expandable three-layer structure with a finer-grain size. Thus, kaolinite has much lower plasticity and undergoes much less shrinkage than does smectite upon drying. If a potter has access to clays which are highly plastic, this property can be modified by the addition of nonplastic materials (soil, less plastic clay, crushed rock or pottery, or organic material) as temper.

Of the many factors that control the plasticity of clays, the most important is the shape and size of the clay particles themselves. Clay is very fine grained and crystallographically platelike with a thickness to diameter ratio of about 1:12. When

Table 7.2 Consistency water %

| | |
|---------------|-------|
| Dry | 5–18 |
| Stiff | 10–20 |
| Stiff-plastic | 12–25 |
| Plastic | 15–30 |
| Oversoft | 15–35 |
| Liquid | 20–50 |

water is added to clay, it acts as a lubricant, surrounding the clay platelets and allowing them to glide over each other. Surface tension forces acting on the water and the clay bind them weakly together and allow a molded object to retain its shape. When excess water is added, more than the minimum needed to maintain surface tension, the water and the mass will start to flow.

Other important factors which affect plasticity are the nature of adsorbed ions and clay particle size. Large monovalent ions, including Na^+ , K^+ , and ammonia, NH_3 , diminish plasticity; smaller di- and trivalent ions including Mg^{2+} , Fe^{2+} and Fe^{3+} , and Ca^{2+} enhance plasticity. The large monovalent ions, too large to fit into the clay lattice, tend to disrupt the nonliquid water structure promoting disorder. The smaller, more highly charged ions easily fit into the space available in the lattice and thus do not exercise any disordering effect.

7.3.1.2 Shrinkage

After the ceramic has been formed, the wet clay must be dried. Water will be lost in two phases. During the first phase, the water of formation will evaporate freely and the ceramic will contract. As the water is removed from around the clay particles, the particles will draw closer together until they eventually touch each other and start to adhere. The ceramic will contract no farther at this stage. The next water loss takes place more slowly, and it will come from the pore spaces between the clay particles.

Internal stresses are set up in the ceramic if it loses water too fast at this first stage.

The rate of evaporation is critical to prevent the clay from cracking or breaking up. Again, different clays vary greatly in their drying shrinkage, that is, the reduction in size upon evaporation of water. Clays also vary in their dry strength, that is, the resistance to breaking when a force is applied after the water of formation has been removed (Table 7.2). This property is important to potters who scrape and smooth vessel walls at this stage, perhaps prior to applying a slip.

Paste and Temper A ceramic vessel or object—figurine, statue, bead, etc.—is composed of clay and its impurities, generally accidental or accessory minerals and, in the case of low-fired earthenwares, some form of tempering agent which is often mineralogical in nature. There are a few commonly used terms to denote paste and temper—matrix, fabric, body—are frequently encountered. Stoltman (1991) considers paste to be “The aggregate of natural materials, ie, clays and larger mineral inclusions, to which temper is later added....”. Kamilli and Steinberg’s definition was paste “consists of a coarse mineral fraction, a fine-grained matrix, and perhaps some plant material” (Kamilli and Sternberg 1985). Body, as defined by Stoltman (*supra*), is the “bulk composition of a ceramic vessel including clays, larger natural mineral inclusion in the silt, sand and gravel size ranges, and temper (emphasis added).” Body is equivalent to the term fabric (Shepard 1936, 1954). It is temper that differentiates body/fabric from paste. Temper, by extension, is that which is not naturally occurring within the paste of a ceramic—e.g., it has been added by the potter.

Temper varies widely, in early ceramics, imaging from organic materials such as plant material, bone, and shell; mineral temper such as rock of many varieties; sand or volcanic ash or tephra; to grog or ceramic fragments reused to temper subsequent vessels. Because temper, other than that of organic origin, is similar to naturally occurring minerals and rock, some authors simply use size as a discriminating factor (Lombard 1987; Ferring and Perttula 1987). The identification of temper, because of its similarity to the materials of the paste, is oftentimes difficult (Stoltman 1991), but the petrographer must make the attempt wherever possible. Where the distinction is straightforward, the temper becomes a useful tool in distinguishing ceramic types. Even in cases, such as were there the coarser added material may be differentiated from a fine-grained matrix by textural analyses.

Potters use temper to help the clay dry and fire uniformly:

- Grog temper (basically ground up pottery)
- Shell (after it has been fired)
- Sand/stone—like marble
- Tuff
- Organic (Spanish moss, grasses, other fibrous plants)

Studies of temper and actualistic studies have yielded significant insights into the function of this amendment to clays in terms of “performance characteristics” which the ability of the vessels to retain their contents and to survive impact without cracking; heating effectiveness and the ability to survive rapid changes in temperature without cracking, in the case of cooking vessels; and cooling effectiveness, in the case of water storage vessels (Tite 1999; Schiffer 1988, 1990; Skibo et al. 1989; Skibo and Schiffer 1995; Kilikoglou et al. 1995, 1998.) One area, other than temper per se, was the importance of surface finish in preventing water loss. Resin, as we shall see with a Navaho example, applied to the surface, notably the interior, minimizes water loss (Schiffer 1990). Interestingly, simply finger-smoothing of the interior surface accomplishes the same effect (*supra*). But it is the role of temper, type density, and size that most determines the strength and “toughness” of the vessel (Tite 1999).

Ceramic “toughness” is difficult to define. Resistance to fracture is primarily the best definition.

Repeated exposure to heat and subsequent cool downs test the ability of a pottery vessel to resist fracturing. Prolonged exposure to cooking fires increased with the specific foods such as the example of beans in the Basketmaker III Period. Kilikoglou et al. (1995, 1998) showed ceramic toughness increased within an increasing number of quartz inclusions as well as an increase in their particle size. Feathers (1989) and West (1992) further showed that the type and morphology of the temper is particularly relevant. Platy or fibrous temper, such as mica or shell, greatly increases toughness when compared to angular temper such as limestone, marble, quartz, or grog (*supra*).

This morphological difference results in both resistance to crack propagation and thermal shock fracture.

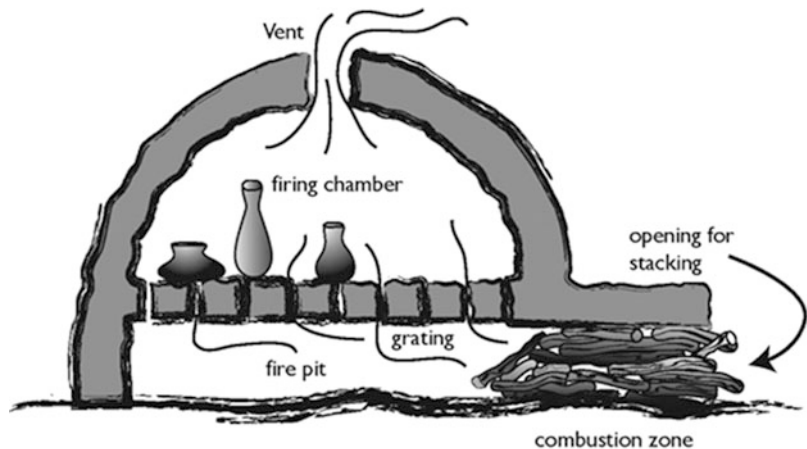
Temper morphology and size were illustrated by (1984) Moundville (Alabama) prehistoric ceramics of the Mississippian Period (ca. AD 1,000–1,500). Temper gradually changed from coarse quartz then to fine quartz, grog, and finally coarse shell. Shell-temper became one principal characteristic of evolved Mississippian ceramics. Steponaitis showed that the shell resisted thermal expansion better than other tempers and required lower firing temperatures (~700 °C.) or the shell would decompose to lime. Additionally, rehydration of the decomposed shell would cause failure in the vessels as well (*supra*).

7.3.1.3 Firing and Thermal Properties

Before firing any ceramic, the first stage—drying—is considered “air drying” and is generally carried out <150 °C. During drying, the mechanically admixed water, which is present as films surrounding clay particles, is lost. The clay mixture shrinks and loses its plasticity. As the clay particles come closer together, they may come into contact with each other. Stresses set up at this stage may later lead to structural damage to the body. During this period of drying, the body will undergo its maximum shrinkage and exhibit its maximum water loss.

Water first evaporates from the surface of the body. Then by capillary action, water rises from the interior to the surface and in turn evaporates. To ease the process of evaporation, nonplastic fillers, called temper, earlier added to the clay paste, help provide pathways for water to escape. Other materials or characteristics may be present or added to help bind the clay together and strengthen it during drying and shrinkage. This includes fine rather than coarse particle size clay, the presence of Na⁺, and added organic materials such as flour or gums of various trees. All these will help bind the clay particles together and help prevent uneven drying which may cause cracking or warping.

Much early pottery was fired in open fires, but with the passage of time, more and more firing has been in periodic kilns. The process of firing takes place in distinct phases: setting up the kiln, firing the air-dried clay bodies, cooling down the kiln, and finally, withdrawing the pottery. The

Fig. 7.3 Closed kiln

design of such kilns varies widely through time and place. Most are so-called “open-flame” kilns where the heat is used directly. The fire box is in the fire pit directly below the ware and surrounded by flames (Fig. 7.3). The combustion gases generated in the fire box move directly upward into the firing chamber by convection.

Temperature control, both in absolute degrees Celsius and in the uniformity of heating throughout the firing chamber of open flame kilns, is very poor. The temperature throughout the kiln will vary widely, with both vertical and horizontal gradients. Vertical gradients are controlled by the distance to the bottom of the kiln where it is the hottest and horizontal gradients develop by the flow of combustion gasses toward the vent. Some areas within the kiln will have a reducing atmosphere, especially nearer the bottom where highly reducing combustion gasses enter the firing chamber, and other areas nearer the vent will be oxidizing, where a strong draft exists, oxygen is readily available, and the combustion gasses themselves have become oxidized, e.g., CO_2 has become CO_2 —indeed, temperature gradients exist within single vessels, varying according to size and wall thickness.

Time of firing and peak temperature are two principal factors, beyond temper, in determining the strength of pottery vessels. Pit kiln firings were shown by Shepard (1956), and kiln firings have been demonstrated to produce very

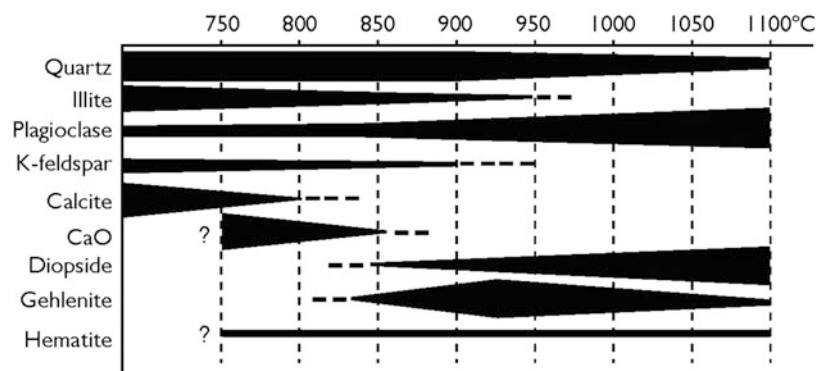
different results in the production of earthenwares (Gosselain 1992; Kingery and Vandiver 1988). In pit kilns, maximum temperatures ($\sim 600\text{--}800\text{ }^{\circ}\text{C}$) are reached within 20–30 min. Because of the rapid heating rate, coarse pottery fared better.

Thin-walled fine ware survived equally as well because of its ability to allow steam to escape the vessel (Tite 1999). Closed kilns greatly enhanced the control and quality of earthenwares (*supra*).

Firing the clay body to the hardness of a ceramic body is the next critical stage in manufacture. The ceramic then acquires its hardness, toughness, and durability. Original mineral and clay structures are transformed, and chemical compositions change as the body loses its basically sedimentary condition becomes its metamorphic equivalent. The principal changes that take place are by (a) oxidation or reduction, (b) loss of volatiles and dehydration, principally loss of hydroxyl ion (OH) from the clay structures, and (c) creation of higher temperature phases and finally, at very high temperatures of firing, vitrification.

As we will detail in the following section, clay minerals undergo important structural and chemical changes, due primarily to dehydroxylation, when they are fired at temperatures over $600\text{ }^{\circ}\text{C}$, and particularly at higher temperatures of $\sim 1,200\text{ }^{\circ}\text{C}$. These changes are important to

Fig. 7.4 Phase changes in pottery



convert the clay into a useful ceramic. High temperatures dislodge ions from original positions held in the clay structure into more favorable sites, thus converting the clay into chemically stable and structurally stronger material. Chemical changes that take place during firing of clay are shown in Fig. 7.4. The exact changes that take place for each stage of firing depend on many variables, including those that are material dependent:

1. The chemical, mineralogical, and structural composition of the clay and the nature of included materials.
2. The wall width of the ceramic body.
3. The nonplastic temper added by the potter. At 450–500 °C, water that is chemically combined in the clay structure is lost. The clay crystalline structure itself will break down above 800 °C and be largely converted to new mineral phases. Above 1,800 °C, the ceramic body will fuse, a temperature far above the possibilities of any ancient technologies and those that are dependent on firing conditions.
4. The rate of firing, allowing gases including those formed by the breakdown of organic material and carbonates to escape. Too fast a rate will trap gases and result in higher porosity.
5. The duration of firing. The longer high temperatures are held, the more complete will be mineral reactions forming glass and high temperature mineral phases, such as spinels and mullite which lead to a stronger ceramic body

6. The atmosphere in the kiln, whether reducing or oxidizing. Color is strongly dependent on this: ferrous iron can cause a green color, ferric, and unoxidized organic material black.

Tite et al. (1982) in a study of Greek Red and Black Figure pottery demonstrated the use of the three-stage oxidizing-reducing-oxidizing firing cycle to produce the reduced iron-oxide pigment

Studies of firing temperatures have proven to be capable of ascertaining both the ranges of temperatures and firing times (Tite and Maniatis 1975; Tite 1995; Wagner et al. 1986; 1998; Kingery and Friermanm 1974; Kingery 1992a, b).

7.3.1.4 Oxidation and Reduction

If materials such as dung, straw, etc. are utilized in the making of the ceramic body, then, when heated to 200–500 °C in an oxidizing atmosphere, such organics will oxidize and be given off as CO₂, leaving vacant spaces and a porous body. If, on the other hand, the ceramic body was heated under reducing conditions, in those parts of the kiln where oxygen was not available, then the organic material is only charred and a residue of elemental carbon is left. Under these conditions, a gray-black ware will result. Commonly, firing is timed to allow oxidation to go to completion so that no organic matter is trapped in the fired clay before the stages of dehydration of clay and the formation of new mineral phases and glass begin. However, much archaeological pottery with a gray core shows that oxidation does not always go to completion.

As the temperature is raised, and a good draft is obtained in the kiln, the clays themselves will start to oxidize. Clear colors such as red, buff, or yellow suggest an oxidizing atmosphere at firing temperatures of about 700–900 °C. If the draft is cut off preventing outside oxygen from entering, the entire kiln will be filled with reducing gases. The most important oxidation-reduction reaction affecting color is the change from red ferric oxide and hematite Fe_2O_3 to black ferrous oxide FeO and magnetite Fe_3O_4 .

7.3.1.5 Loss of Volatiles and Dehydration

When temperatures of firing reach about 200–300 °C, all mechanically bound or pore water still present after ambient drying is vaporized and driven off. As the kiln temperature rises, hydroxyl ions that are chemically bound within the clay lattice start to be lost. The rate of loss depends on the clay species with halloysite and kaolinite abruptly losing most hydroxyls about 4,000 °C (Fig. 7.4). Other clays, such as smectites, start to lose interlayer water (held between the silicate sheets) at lower temperatures. They then continue to lose water but at a slower rate than kaolinite.

In addition to water, as the temperature rises to over 200 °C, any carbon or organic matter in the clay will start to oxidize and escape as CO or CO_2 . The rate and completeness of oxidation depends on the rate of temperature rise, the length of time the maximum temperature is held, the wall width of the pot, the clay composition, and the nature of the paste. On average, organic carbon is not completely eliminated until temperatures of about 500 °C are reached.

7.3.1.6 High-Temperature Phases and Vitrification

Dehydroxylation or the loss of OH⁻ from the clay molecules causes major structural and chemical changes. Heating kaolinite above about 500 °C results in a disordered crystalline form which is still reversible by rehydration back to its ordered kaolinite structure. At 900 °C and higher temperatures, all water is lost and the crystal lattice is completely destroyed. If high firing

temperatures are maintained for a long enough period, high-temperature aluminum silicates will start to form. Depending on the (1) length of time held, (2) the temperatures attained, as well as (3) other minerals present, such as micas, that may react with the clays, a variety of higher-temperature mineral phases may crystallize. These include, from lower to higher temperature, feldspars, spinels, and above about 1,050 °C mullite ($3\text{Al}_2\text{O}_3 \cdot 2\text{SiO}_2$). Mullite is a synthetic aluminosilicate used in the manufacture of high-temperature and high-shock ceramics, such as automobile spark plugs. Identification of such high-temperature minerals can be important clues to a vessel's firing history.

Starting about 600 °C, vitrification or "sintering" starts in the more fusible impurities. Feldspars, among the most common impurities, and commonly added to the clay paste as a flux by modern potters, will melt: pure Na-feldspars at 1,118 °C and pure K-feldspars at 1,100 °C; solid solution mixtures will melt at lower temperatures. Many potters, both ancient and modern, recognized a variety of other materials that can act as fluxes, including illitic clay, iron oxides, etc. When enough vitrification has taken place to give a moderate degree of hardness, the clay is considered baked.

Full firing, or the burning stage for most clay bodies, begins at about 850 °C. Two baked vessels struck together will emit a dull sound, whereas when fully burned, that is for some mixtures fired as low as 850 °C, for most about 1,000 °C, the vessels will emit a ring. To summarize, the following are the expected changes in the clay paste during firing:

150–200 °C: All mechanically combined adsorbed water is lost from the clay. Much interlayer water will also be lost from smectites.

200–400 °C: Organic matter begins to oxidize and migrate to the surface, blackening the clay body before finally being driven off as CO_2 .

450–550 °C: Chemically bound water is lost from clay lattice, dehydroxylation. The loss

takes place abruptly in kaolin in the structural transformation to metakaolin with minor shrinkage and a great increase in porosity. In illite and smectite, the loss is more gradual. At 470 °C, a red glow can be seen in the dark; at 550 °C, all organic matter is oxidized.

550–750 °C: Quartz inverts at 573 °C from the alpha, low-temperature form, to beta, the high-temperature form, accompanied by a volume expansion of 2 %. Beginning at 600 °C, micas lose structural hydroxyls from their lattice.

750–850 °C: Most organic water has been successfully burned out of the clay. Kaolin and smectite begin to lose their characteristic crystalline structure.

850–950 °C: By 870 °C, CaCO_3 decomposes to CaO and loses CO_2 gas. Beta quartz inverts to a higher-temperature form, tridymite, but the reaction is very sluggish and will only take place if the firing temperature is held for a relatively long period of time.

950–1,100 °C: The structure of most kaolin and smectite is irreversibly lost, but some illite may persist. With the breakdown in clays, high-temperature alteration and reaction products can form, accompanied by pronounced shrinkage.

Above 1,000 °C: Wollastonite (CaSiO_3), calcium ferrisilicates, and, in a reducing atmosphere, hedenbergite ($\text{CaFeSi}_2\text{O}_6$) with reduced Fe^{2+} iron are typical reaction products. Other high-temperature phases expected to form are spinel (MgAl_2O_4) and mullite ($3\text{Al}_2\text{O}_3\cdot2\text{SiO}_2$).

>1,100 °C: Feldspars melt dissolving silica and initiating a glassy phase of the ceramic. Porosity diminishes rapidly.

production of earthenwares by indigenous artisans. Some authors suggest that primary evidence for pottery manufacture is rare (Sullivan 1988). In defense of Sullivan, most modern indigenous pottery is *not* made for the same set of cultural uses as in the premodern era. Much of the modern ceramic output of the American Southwest is for consumption as art rather than as utilitarian or ceremonial use. The reader should not view this statement as in any way critical of the modern indigenous potter. Rather, the appeal to collectors and museums of modern production has allowed traditional designs to survive into the modern era. Likewise, there are continued cultural uses for modern-day vessels beyond their sale outside the native culture.

Indeed, the genesis of this study of Navaho ceramics with a similar pronouncement by a tribal official in Arizona on the Tohono O’Dodom reservation (Robert S. Hill, Personal Communication 2011). The official, when queried about local potters, opined that “no one made pottery anymore.” Such was not the case, happily. A brief drive around a neighborhood produced the names and vessels of more than one local potter. Unfortunately, the Tohono O’Dodom artisans were less able to share cultural knowledge than those of the Navaho; hence, this section’s subject is of the latter’s ceramics and not the former.

Pottery has “meaning” in Native American cultures. It is more than just utilitarian in nature. Pottery contains a large amount of cultural information as noted not only by Longacre and Kramer (*supra*). This section is entitled “ethnotechnological study” rather than “ethnoarchaeological” to stress the technological aspects of Navaho pottery manufacture over the specific cultural context within which it resides. The study did ascertain that, for the Navaho, pottery connotes:

- Symbols of nationality/identity.
- Spirituality/belief systems.
- Natural world in motifs of animals, nature.
- Vessel forms indicate use as well as aesthetic.

Among the Navajo (Diné), the Changing Woman story is not told until after the first

7.3.2 Ceramic Ethnotechnological Study: Making Navaho/Diné Pottery

Kramer (1985) and Longacre (1991) have described the importance of ethnography as an important method in understanding the

Fig. 7.5 Forming the “wet” pot. Note appliquéd



frost. Changing Woman is the first woman in the Navajo belief and mother to the Hero Twins, Monster Slayer and Child-Born-of-Water, who rid the world of monsters so humans could inhabit the earth. Navajo and native potters, in general, do not refer to the vessel clay as “paste”—but rather it is the “clay body.” Paste is an archaeological term.

Manure is used for fuel particularly in the American Southwest, whereas wood was used in the Southeast. There are more sheep and cows on the Navajo Reservation than useable trees.

In the present study, dung was the preferred fuel source (Fig. 7.3). All the Navaho potters observed in the 2011–2012 study dug their own clay. The location is closely held but shared among fellow potters in many cases. Navaho is a huge place, being nearly as large as the whole of New England. Clay sources abound. One potter specifically sought out “brown clays” to help ensure a firing to a high-red color. This particular potter applied an iron-bearing slip to the drying vessels and burnished them.

Temper was usually crushed pottery or grog, ground up, and worked into the clay. Sand was used as well. Some potters, working in more traditional forms, shaped the vessel, first with a corncob then burnished using a smooth stone during the drying process (Hill 2012). As noted above, slips can be used besides appliquéd and piñon pitch applied after firing. In comparison, Santa Clara pueblo potters use a 1:3 ratio of tuff temper to clay for their ceramics.

Several techniques can be used to form pots. Three of the most used by the Navaho are:

1. Anvil—paddle
2. Draped clay—on/in basket
3. Pinch—coil

In the 2011 study, the pinch-coil method was primarily used although the anvil technique was demonstrated. The potter kneads the clay to remove air, pinching the clay – “pull-and-in”– to shape the coils. Navajo potters start with the small “pinch pot.” Coils are laid, sequentially, on top of the pinch pot base (Fig. 7.5). “Bé-ho” or *biyo*—an appliquéd of beaded clay can be used on the rims. These help with handling of a hot pot. The appliquéd is never closed—it can overlap but is never closed. This allows spirits to enter and leave the vessel. This spiritual aspect extends to pottery manufacture. The Navajo only make pottery for use in eating. Therefore, they do not make ceramic dolls. The mud dolls are unfired. Small pots are manufactured as containers for the sands (and clays) used in Navajo sand painting ceremonies.

When firing their pots, Navajo potters particularly appreciate the “fire clouds” that manure fires create (Fig. 7.6). These fire clouds add interest to the pot’s surface. Piñon pine tar is used to “glaze” pot exteriors. It is applied to hot pots allowing a sheen to form on the pot’s surface (Fig. 7.7). Santa Clara potters use the so-called saggar firing instead of pit kilns (Fig. 7.3). They can fire pots in trash cans—aka a “saggar.”

Fig. 7.6 Modern Navaho pottery (Photograph by Robert Hill)

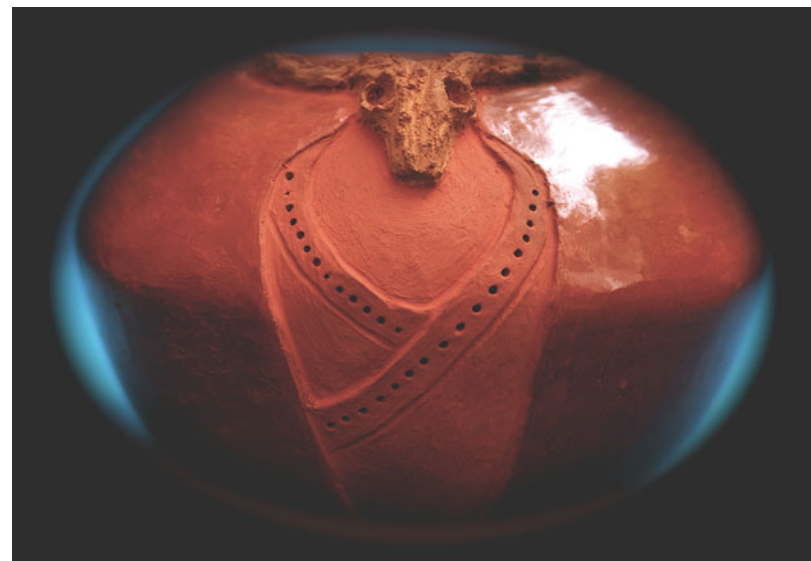


Fig. 7.7 Two thin sections of late prehistoric earthenwares, Georgia, USA. In the *left*, firing differences—black indicating reducing conditions and red-brown, oxidizing. Such differences are not unusual for pit kiln-fired wares. The thin section on the *right*

illustrates more uniform firing conditions as well as a more uniform grain-temper sizes. The temper in both is primarily quartz-dominated medium sand. Both photomicrographs were in PPL (Courtesy of Mark Williams)

7.3.3 Geoarchaeological Study of Ceramics

Pottery then is the general term used here for artifacts made entirely or largely of clay and hardened by heat. Today, a distinction is sometimes made between pottery, applied to lower-quality ceramic wares, and higher-grade porcelain. No such distinction will be made here so the term pottery alone will be used. Raw material that goes into the making of a pot includes primarily the clay body, but also varying amounts of "temper," added to make the material more manageable and to help preserve the worked shape of the pot during firing. Of primary interest in ceramic studies are:

- (a) The nature and the source of the raw materials (clays, temper), the "slip" (applied surface pigment) and a reconstruction of the working methods of ancient potters
- (b) The physical properties of the raw materials, from their preparation as a clay body, drying and firing, and through their transformations during manufacture into a final ceramic product
- (c) The nature of the chemical and mineral reactions that take place during firing as a clue to the technology available to the potter
- (d) The uses, provenance, and trade of the wares produced

Neff (1993) defines “compositional” analyses as the characterization of the ceramic fabric, either by chemical or mineralogical analysis. Indeed, trace element studies are foremost among the methods to study earthenwares (Vandiver 2001). Compositional approaches typically seek to recognize cultural transmission by use of material characterization to differentiate local from nonlocal ceramics by their clays or tempering agents. Efforts to recognize local versus nonlocal wares derives much of their impetus from exchange studies, wherein the assumption is made that local pottery is likely to pertain to a single (local) tradition within which pottery-making information was perpetuated over some period of time. Chemical data (e.g., Foust et al. 1989; Olin and Blackman 1989) or petrographic data (Stoltman 1989, 1991, 2001) seek to refine these local or nonlocal ceramic typologies (Neff, *supra*). Not all archaeologists agree with a strictly compositional approach. Sullivan (1984:77) questions the value of technological attributes (including mineralogy) in southwestern ceramic taxonomy, arguing that decorative attributes provide a superior foundation for ceramic taxonomy because they may be shared across local technological bases, thus facilitating description and comparison of assemblages.

Much of the information needed to answer compositional questions is, as Neff (*supra*) suggests, available through the use of standard geochemical and petrographic analysis of ceramic artifacts. Insight into the working methods of ancient potters also has been obtained through ethnographic studies of cultures where, either because of isolation or conservative traditions or both, ancient methods have been

preserved. Pottery is classified as a “ware” largely on the basis of its firing characteristics and surface treatment/decoration (Table 7.3). A distinction is made between vitrified ceramics, i.e., high enough firing temperatures to fuse the clay into a glassy matrix versus lower-temperature unvitrified, porous material. The former include stoneware and porcelain; the latter terracotta and earthenware.

The earliest fired pottery worldwide are terracottas. They are fired at relatively low temperatures, usually below 900 °C. Terracotta vessels, sculptures, and tiles are generally not glazed, although they may be surface treated by roughening, to absorb heat and prevent slipping when wet, or covered with a slip. The slip is a suspension of fine-grained clay and water that may be added to enhance the beauty of the pot by coloring and smoothing, as well as to reduce porosity and retard leaking.

Earthenware bodies are also porous and unvitrified but are fired at higher temperature than terra-cottas, up to about 1,100–1,200 °C. Because of the higher temperatures of firing, material at the surface might fuse and form a natural glaze or they may also be unglazed. When fired at lower temperature, they grade into terra-cotta. The clays used in the manufacture of earthenware are generally coarse and plastic when wet and many are red firing. Earthenwares include a wide variety of products, ranging from “coarse” such as bricks and tiles to “fine” wall tiles and majolica, tin enameled and made from a good-quality white-burning clay.

Stonewares are fired at temperatures that are sufficiently high enough, 1,200–1,350 °C, to achieve partial fusion or vitrification of the clay

Table 7.3 Characteristics of ceramic bodies

| | Porosity | Firing temp | Applications/notes |
|-------------|------------|----------------|---|
| Terracotta | High:~30 % | <1,000 °C | Roof tiles, bricks unglazed, most prehistoric coarse |
| Earthenware | 0–25 % | 900–1,200 °C | Coarse: tiles, bricks glazed or fine: wall and floor tile, unglazed majolica, unvitrified |
| Stoneware | 0.5–2.0 % | 1,200–1,350 °C | Roof tiles, tableware, glazed or artware unglazed, vitrified |
| Chinaware | <1 % | 1,100–1,200 °C | Tableware, white, vitrified |
| Porcelain | <1 % | 1,300–1,400 °C | Fine tableware, hard body, artware, fine, “rings” when tapped |

From Rice (1987)

body. The body itself is medium to coarse grained, opaque, and commonly light brown or gray. Modern stoneware is usually made of sedimentary clays that are transported rather than residual deposits, such as ball clays which are highly plastic and low in iron. Archaeological stonewares may or may not be glazed.

Porcelains were first produced in China during the time of the T'ang dynasty in the ninth to tenth century AD. They are fired at 1,280–1,400 °C or even higher, required to vitrify the highly refractory white clay, kaolin, used in their manufacture. The clay is relatively pure and mixed with quartz and alkali feldspars which act as a flux, allowing lower firing temperatures than needed to vitrify pure kaolin. At 1,150 °C, K-feldspar (microcline and orthoclase) melt, and at 1,118 °C, Na-rich plagioclase (albite) melts, giving the porcelain a translucency, hardness, and ring when tapped. Porcelains today are made up of about half kaolin plus roughly equal amounts of feldspar and quartz.

A major Chinese production center, 600 years ago, and today is Jingdezhen. AD 907–960, the “5 Dynasties Period.” Other major periods are as follows: Shufu (12th c.), Qingbai/Yingqing (12th–13th c.), “Blue and White” (post-14th c.), Ming Period (1368–1644), and “Monochromes” (post-18th c.). Today, Jingdezhen, produces 300 million pieces of porcelain a year.

Vogt, in 1900, established the chemical and mineralogical nature of Chinese porcelain. He determined the major minerals present were kaolinite; potash mica; soda feldspar, albite; and quartz (SiO_2).

The kilns at Jingdezhen became the main production center for large-scale porcelain exports to Europe starting with the reign of the Wanli Emperor (1572–1620).

Kaolin and pottery stone—*pu-tan*—were mixed in about equal proportions (d'Entrecolles 1743) identified this as “Best Quality or equal parts *petuntse* and kaolin” (Pollard and Wood 1986). Kaolin produced wares of great strength when added to the paste; it also enhanced the whiteness of the body—a trait that became a

much sought after property, especially when form blue-and-white wares grew in popularity. Pottery stone could be fired at a lower temperature (1,250 °C) than paste mixed with kaolin, which required 1,350 °C.

In Ming porcelains, cobalt was used for underglaze blue decoration. Prior to this, the cobalt had been brilliant in color, but with a tendency to bleed in firing; by adding manganese, the blue color was duller, but the line crisper. Xuande porcelain was the finest of all Ming output. During a significant portion of the Ming Dynastic period, exports of Chinese porcelains were banned. This allowed Vietnamese porcelains and stonewares to become widely traded. Evidence of this period of a Vietnamese ceramic florescence comes from both early kiln sites excavated in the 1990s as well as South China Sea shipwrecks of both Chinese and Vietnamese origins: Chu lâu-My Xa kiln site and in the Cù Lao Chàm (Hôi An) cargo (~250,000 ceramic vessels). The latter shipwreck was excavated by a team led by Oxford University's Mensun Bound, in cooperation with the Vietnamese government. Elements of the Hôi An cargo were sold at auction (Pope 2014).

The importance of Vietnamese ceramics produced during the fifteenth century has been established beyond any doubt. At this time, the ban on Chinese ceramic exportation by the Ming dynasty offered an open market to Vietnamese products: blue-and-white porcelains, celadons (jade-like monochrome) and *tam thai* (three colors, to be compared with the Chinese *sam cai* equivalent) overglazed wares. The Vietnamese learned ceramic skills while under Chinese domination up to the 11th c. AD and continued their indigenous development thereafter. They were experts in both porcelains and elegant stonewares. The latter fall under the heading of celadons or jade-like, colored stonewares (Colomban et al. 2004). Likewise, the Vietnamese used color to great advantage in their designs.

The constituent elements as well as the structural phases of the blue-and-white and *tam thai* glazes of the fifteenth-century Vietnamese

ceramics have been determined by a combination of XRF, EDS, and nondestructive Raman spectroscopy. The transparent glaze is an aluminosilicate glass, with CaO as the chief fluxing agent. The firing temperature for this base glaze was as high as the sintering temperature of the body, that is, more than 1,200 °C. The jade-like color of the celadon glazes was achieved by iron doping in the glazes, while the black colors or metallic-black dendrites were obtained by the dispersion of FeO and/or Fe₃O₄ under the transparent glaze (in a very strong reducing atmosphere). The blue decoration under the transparent glaze was achieved using Co-containing manganese ore. In some cases, the addition of iron made a dark greenish-blue color.

Cyfflé's Terre de Lorraine manufacture in Lunéville (1766–1780) produced some of the first European porcelains (Maggetti 2011). The diversity of Cyfflé's production is now better recognized. His trial-and-error experiments made use of a remarkably wide range of paste mixtures, with porcelain bodies in the French (soft-paste) and the German (hard-paste) tradition (*supra*).

An example of soft-paste (artificial) porcelain body (10 % water adsorption), contained quartz, calcic plagioclase (An 88–95) in a glassy matrix. Electron-backscattered diffraction analysis (EBDS) revealed a coronitic reaction rim visible around the quartz. The K-rich and Na-poor frit is a mixture of potassium nitrate, alum, calcined gypsum, sand, and moderate amounts of salt and soda. The water adsorption values indicated a somewhat underfired condition. In other samples, Maggetti (*supra*) found evidence of the high-temperature silicate mullite typical of hard-paste porcelains.

In another study employing a comparative approach to technological characteristics, Vandiver (1988) reconstructed and compared the forming and firing practices of Neolithic potters in northwestern Iran and northern China. She argues that the complex technological differences between pottery from Hajji Firuz, northwestern Iran, and Yangshao pottery from

northern China result from the divergent evolution in distinct ceramic environments. Chaff temper and sequential slab construction in northwestern Iran were adaptations to highly plastic montmorillonite clays, while coiling and tamping with paddle and anvil were adaptations to the gritty loess-derived illitic clays of northern China. In addition, the northern Chinese clays were more forgiving over a wide range of firing temperatures, permitting higher firing temperatures in China. Coincidentally, the uniform refractory properties of loess soils of northern China favored high-temperature firing in subterranean kilns, whereas Near Eastern potters developed aboveground kilns, the temperatures of which could usually be maintained below the level at which montmorillonitic kiln walls would fail.

7.4 Provenance

Determining the provenance of clay used in the manufacture of a pot is an important problem that is traditionally attacked by geochemical techniques. Many studies have used trace element analysis to compare the possible sources to a fired ceramic. However, conclusions of such studies must be carefully interpreted since ceramic pastes will not always be similar mineralogically or chemically to their sources, except in the cases of unrefined clay, typical of very ancient potters and very low-temperature firing. Most ceramic clay has been refined and mixed resulting in a great variation in particle size distribution and mineralogical variations. Blackman (1992) found that levigation of the raw clay resulted in major changes in mineralogy and chemistry if silt and finer sizes were removed. If only sand size particles were removed, the changes were not as serious except for trace elements that were concentrated in the accessory minerals.

A study by Kilikoglou et al. (1988) found that most trace elements showed great variations in comparing the raw to the fired clay. Whether the

elements increased or decreased upon firing and purification depended on many variables including their:

1. Physical nature—whether they were held in fine- or coarse-grained material, organic matter, in the clay, or in detrital minerals
2. Chemistry—whether they were present as oxides, hydroxyls, carbonates, and on their position in the clay lattice, i.e., interlayer, adsorbed on the surface, or within a sheet
3. Physical properties—most important, the temperature at which they volatilize

The conclusion of their study was that under no circumstances can the chemistry of raw clay be compared to that of a finished pot. To demonstrate the provenance of the clay in the pot, the steps taken by the potter in making the pot must be followed: the clay must be purified and fired under analogous conditions. The analytical methods then used to compare the synthetic pot to the original should be sensitive to elements present in trace amounts and include optical emission spectroscopy, neutron activation, X-ray fluorescence, SEM, or the electron microprobe. Then, so that meaningful statistical analysis can be carried out, (1) the number of elements determined should be as large as possible, and (3) a large number of samples should be analyzed.

7.5 Methods

Geochemical and petrographic analyses are widely used to characterize archaeological ceramics (Tite 1999; Vandiver 2001). As noted above, bulk trace element analyses with either NAA or ICP-MS methods are foremost among studies of trade and provenance and determining manufacturing/geologic sources. After trace element analysis follows petrographic analysis, bulk chemical analysis, and microstructural studies (Vandiver, *supra*). Important problems of sourcing raw materials and characterizing

manufacturing technology can be resolved by using the complementary techniques of petrographic and geochemical analysis to determine mineral and chemical compositions.

The hand lens, binocular microscope, optical (polarizing) microscope, scanning electron microscope (SEM) equipped with analytical capabilities (EDS), X-ray diffraction (XRD), and electron microprobe (EMPA-WDS/SXES) are the most important of these tools. The initial study of a potsherd should begin with a hand lens, followed by thin sections and a petrographic microscope. These studies are done at low magnification, that is, <200 times magnification. Textures, including pore spaces, and mineral inclusions or phases can be identified. At this point, unknown fine-grained minerals and phase reactions at mineral boundaries can be labelled for detailed study by EMPA or SEM. A preliminary grouping of the potsherd samples can be made, and, in conjunction with the archaeologist, decisions made on what other types of analysis, and perhaps field sampling, are needed to obtain further information.

7.6 Optical Petrography

A pottery sherd may be regarded as a metamorphosed sedimentary rock and clearly amendable to petrographic analysis. Quinn (2013), Stoltman (1989, 1991) and others (Kamilli and Sternberg 1985; Kamilli and Lamberg-Karlovsky 1979; Rice 1987; Whitbread 1989; Williams 1983; Williams et al. 1955), in recent years, have reiterated the importance of petrography to the study of archaeological ceramics championed, earlier, by Shepard (1936, 1942, 1954, 1966) as well as by Matson (1960, 1966) and Peacock (1981, 1970). A relatively steady volume of studies, of both Old and New World focus, have continued utilizing tried-and-true geological protocols such as point counting (Chayes 1954, 1956; Galehouse 1971) and optical/instrumental petrographic procedures

(Freestone and Middleton 1987; Garret 1986; Lombard 1987; Maggetti 1982; Vaughn 1990, 1991).

There are many good arguments for beginning a pottery study with petrographic analysis. Not only is this the cheapest kind of analysis, but information can be obtained that cannot be satisfactorily obtained by any other method. In petrographic and textural studies of ceramics, four major elements can be readily evaluated:

1. Minerals—major and accessory minerals can be examined by both petrography and particle size studies.
2. Clay minerals—well-fired pottery does not contain true clay minerals since they have reacted and transformed to other minerals.
3. Non-mineral inclusions—both petrography and textural analyses are productive methods.

The use of particle (grain) size analysis, combined with the low-power study of grain morphology, has much to offer the ceramic petrographer.

Because clay mineral identification is not typically done with the petrographic microscope, we will hold our discussion until the following chapter where more appropriate instrumental techniques are examined. It is important to note that response of clay minerals and inclusions to firing temperature produces progradational mineralization, as in metamorphism, as well as melting and recrystallization of the clays and accessories (Herz and Garrison 1998). A common reaction seen in highly fired wares is the formation of mullite ($3\text{Al}_2\text{O}_3\cdot2\text{SiO}_3$) its antecedent minerals such as kyanite and sillimanite (cf. preceding section). Other minerals such as hedenbergite and fayalite (pyroxene and iron-rich olivine, respectively) form as well, given the appropriate clay matrix. All of these crystal minerals are readily identified by their optical properties—kyanite, in particular, with its rich blue birefringence as well as the bright greens of the pyroxene.

In certain ceramics such as faience and porcelains, the effects of firing are defining elements in the identification of these varieties.

From the perspective of optical petrography, the procedure is that for the study of archaeological rocks and minerals:

1. Prepare a thin section. Two examples are shown in Fig. 7.7.
2. Stain, etch, or otherwise pretreat the thin section.
3. Examine the thin section under the low-power PPL/XPL microscope, determining minerals/phases by optical properties and the proportion of each observed.
4. Quantitatively evaluate the thin section using standard point-counting procedures.
5. Examine the thin section under high-power PPL/XPL for relief, color/birefringence, etc.

An integrated petrographic and chemical approach (NAA) to ceramics of all varieties as commonplace has been employed in the provenance studies of amphoras, Egyptian and Canaanite jars, as well as Minoan ceramics (Day et al. 2011; Hancock et al. 1986; Hancock and Betancourt 1987); American Southwest prehistoric ceramics (Carr 1984, 1990); joining a host of studies enumerated in monographs and books (e.g., Bronitsky 1989; Kingery 1984, 1990, 1993; Nelson 1984; Plog 1980; Rice 1987, 1996a, b, 1999, 2001; Sassaman 1993; Sinopoli 1991; Skibo and Feinman 1999; Glasscock et al. 2007a, b)—all studies of ceramic technology.

Josephs (2005) makes good case for a standardization of terminology in the use of micromorphological analysis of thin sections. Thin sections of ceramics have much in common with those of sediment and soil. Whereas protocols for the micromorphology description of soils and sediments are well established (Goldberg 1995; Courty et al. 1990; Kooistra and Kooistra 2003), the same cannot be said for micromorphological studies of ceramics (*supra*; Courty and Roux 1995).

In ceramic studies of archaeological interest, rocks and minerals continue to play an often decisive role in questions regarding ceramic technology, provenance, trade, and linkages to belief systems; gender relations and power; as well as art and aesthetics in the past cultures. In

the next chapter, we shall examine instrumental procedures in greater depth, while we close this chapter with a continuation of our discussion of radiographic and chemical methods.

7.7 X-Ray Radiography

Hidden features that can be detected radiographically include coils, slabs, their size, morphology, methods of joining; the material type, approximate mineralogy, size, density, and orientation of aplastic inclusions or voids; fracture systems; paste texture; and hidden vessel parts. Under certain conditions, these features can be used to sort shards by their vessels of origin, to identify the primary and secondary methods of vessel manufacture (Carr 1990). As Carr notes (*supra*), X-radiography had been used occasionally by archaeologists to study ceramics since at least the 1930s. Titterington (1935), Digby (1948), and Shepard (1956) defined a limited set of tasks to which radiography is applicable. They focused largely on documenting vessel manufacturing techniques. Radiographs can be used to reveal the primary and/or secondary formation procedures by which a vessel was constructed: pinching, slab building, drawing, coiling, throwing (wheel), and molding/anvil, for example. This application was first suggested by Shepard (1956) and then systematically investigated by Rye (1977).

Radiographs of a vessel can allow one to determine the volumetric density, size distribution, shape, material type, and general mineralogy of temper inclusions. The material type or general mineralogy of temper inclusions can be inferred from their relative grey levels on a radiograph supplemented with size and shape information. This temper mineralogy is usually further deduced using other X-ray analytical methods such as XRF and SEM-EDS or WDS.

Braun (1983) and Carr (1990), for example, have shown that temper volumetric density of a vessel can also be estimated more accurately by radiography. Temper particles can have a clustered rather than a random distribution within the paste of a vessel as a result of poor kneading or pounding. Temper density can vary from coil to

slab to slab, or pulled/pinched section to section. In coarse-tempered coiled vessels, clustering can also result from the rolling out of their coils. Coarse particles are driven to the centers of coils (Carr, *supra*). Braun (1982) is more cautionary stating that tempering inclusions of crushed sherds or simply crushed fired clay, for example, may be no more or less radiographically dense than the surrounding matrix. Radiographic experimental trial was unable to detect crushed shard tempering in Woodland Period pottery from the south-central Illinois. Nonetheless, where tempering raw materials do not impose limitations, the use of radiographic methods for analyzing temper appears both feasible and, for several large areas of research, highly desirable (Braun, *supra*).

Computed tomography (CT) and computed radiography (CR)—digital X-ray methods—have rapidly joined the earlier conventional X-ray methods of years past (Kim and Liaw 1998; Casali 2006). In a study of Late Bronze Age cremation urns, Harvig et al. (2011) used both CT and CR. CT scanners are common in today's hospitals and are equipped with various computer programs allowing rapid image building and three-dimensional visualization, but the software has been developed for medical purposes. Harvig et al. (2011) utilized a program package (MIMICS®, from Materialise®, Belgium (<http://www.materialise.be>) developed at the Laboratory of Biological Anthropology in Copenhagen. After importing the CT scanner data file, the single-slice images were accessible and the program allowed immediate multiplanar reformatting and editing of single-image elements.

7.8 Chemical Analysis

After petrographic and optical examination, chemical analysis is generally carried out.

Much chemical information could have been obtained using X-ray diffraction (XRD), the analytical scanning electron microscope (SEM-EDS), and the electron microprobe (EMPA), and, in many cases, could be enough

to answer all important questions of provenance or technology of firing or both. If more detailed information is needed, especially quantitative chemical analysis of major and trace elements of the paste, temper, slip, and detrital minerals for provenance determination, or for technology of firing, then a method of analysis can be decided upon. Many methods of chemical analysis are available, and some, such as neutron activation analysis (NAA), are very expensive and may not produce the needed results. This is a critical step in a ceramic study; before one kind of analysis is decided upon, the following should be considered:

1. Some methods can only analyze material within a few mm of the surface, such as SEM and electron microprobe, but give exceptional small-scale detail on chemistry and phase changes.
2. Each method involves a varying degree of destructive or nondestructive sample preparation.
3. If samples are to be compared against an existing database, it is preferable to use a like type of data - XRF, NAA, ICP - for the comparative database. The same elements measured by NAA and XRF, for example, will show completely different abundances.
4. Chemical analysis by itself generally does not resolve what parameter is responsible for which element. This is best done by other methods where optical control is maintained, such as SEM and the electron microprobe. However, NAA has been used for a relatively long period, and NAA data bases have been established for ceramic provenance studies. ICPS (inductively coupled plasma emission spectroscopy) is a relatively new technique used in archaeology with many advantages over other analytical systems. Suites of major elements as well as trace elements are routinely determined with a high degree of precision and at relatively inexpensive cost.

Numerous example studies abound where examination of thin sections has proven to be a successful method for discovering provenance

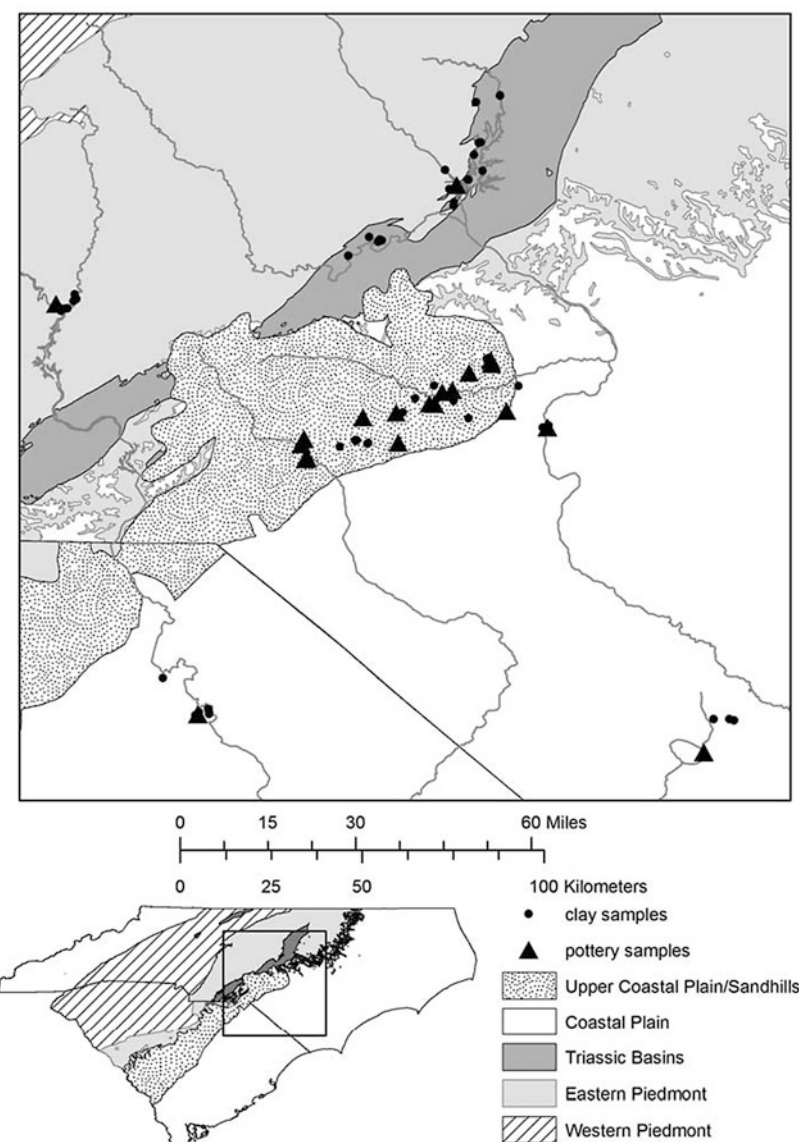
groupings of archaeological ceramics. Non-clay inclusions in pottery paste can be identified with petrographically distinctive geologic sources. When this is not the case, geochemical analysis such as NAA can be employed to search for more subtle, chemical evidence of such groupings. Where the objective is to discern local or subregional patterns of pottery manufacture and exchange, this has proven to be informative (Stewart et al. 1990; Speakman et al. 2011a, b).

7.8.1 An Example of Chemical Analysis Using X-Ray Diffraction (XRD)

This instrumental analysis foreshadows a broader discussion of the use of these techniques across geoarchaeology. While Tite (1999) is on record that because of the breakdown of clay minerals during firing, infrared spectroscopy nor X-ray diffraction are useful methods to determine the original clay minerals, McReynolds et al. (2008) have used X-ray diffraction analysis to examine local clays from the Piedmont and Coastal Plain regions of North Carolina in a study exploring residential mobility and resource use (Fig. 7.8). Variability in mineral assemblages, across 42 clay samples, were examined in the context of region (Piedmont/Sandhills) in order to identify potential sources for the prehistoric pottery found in the Sandhills region (Fig. 7.9). While clay, as a pottery resource is relatively common across the Carolina landscape, compositional analyses of prehistoric ceramics indicated that a relatively fewer number of specific were utilized. Availability was not necessarily a criterion for selectability.

As will be noted in the following chapter on instrumental techniques, XRD is uniquely capable of detecting structural differences among clay minerals of unfired samples. As we have seen in the foregoing discussion of effects of firing temperatures—decomposition of existing minerals and the formation of new phases—unfired clays preserve the most mineralogical information. XRD retrieves this information in the form of diffractograms produced by

Fig. 7.8 Sandhills regions, North Carolina. Clay sample locations are marked (Fig. 7.3, p. 34, Herbert and McReynolds 2008)



monochromatic X-rays bombarding a crystalline mineral such as clay. The reference variable is that of the so-called d-spacing or the interatomic layers or crystallographic planes of the mineral (cf. Chap. 8). Specific d-spacings identify specific minerals when compared to reference materials (Stanjek and Häusler 2004).

The Sandhills clay study examined ten clay-like minerals grouped within three primary groups based on general d-spacing intervals—7,

10, and 14 Å. Within the 7 Å group were the kaolins; the 10 Å group, the illite/micas; and in the 14 Å group, the hydroxyl-interlayered vermiculites/chlorites/smectites. Of these groups, the 14 Å group clay minerals dominated in the Sandhills samples with several being enriched in the 7 Å kaolin group minerals. The Coastal Plain clays, by comparison, were rich in the 14 Å group minerals and poor in the 10 Å illite/mica minerals (Fig. 7.10).

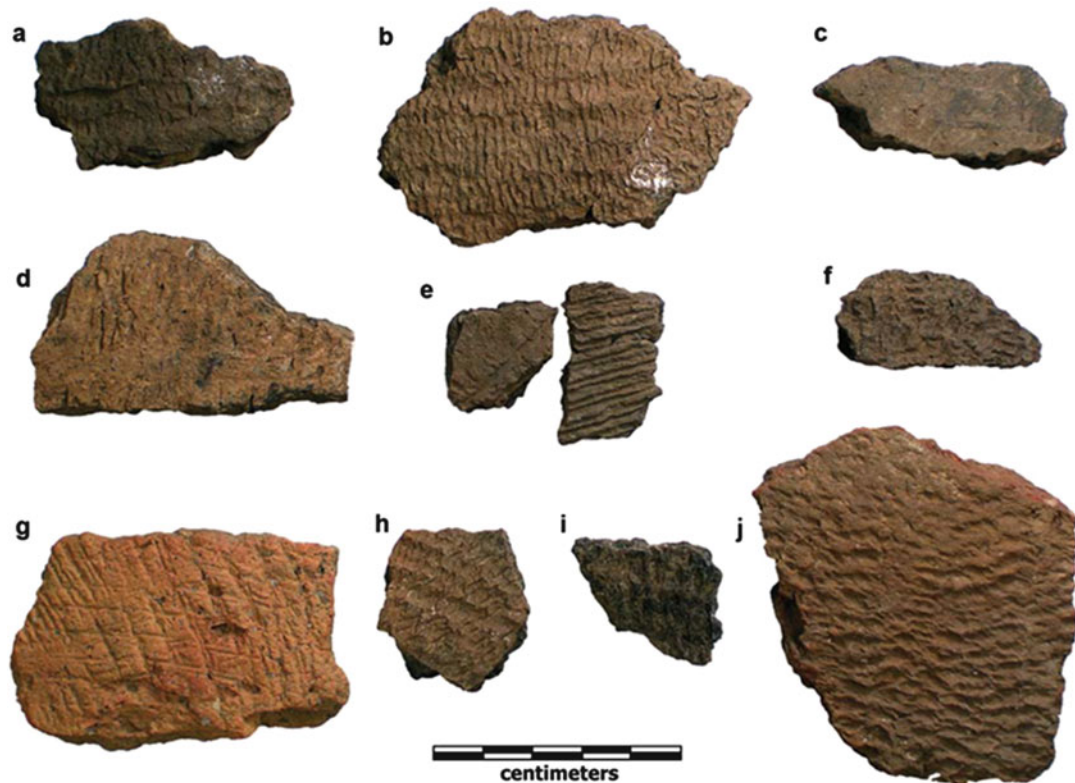


Fig. 7.9 Various pottery shards from the Sandhills regions. Pottery samples from the Kolb site (38 Da75): (a) JMH051, Yadkin Fabric Impressed; (b) JMH052, Yadkin/Hanover Fabric Impressed; (c) JMH053, Yadkin/Hanover Cord Marked; (d) JMH054, New River Cord Marked; (e) JMH055, Yadkin Cord Marked; (f)

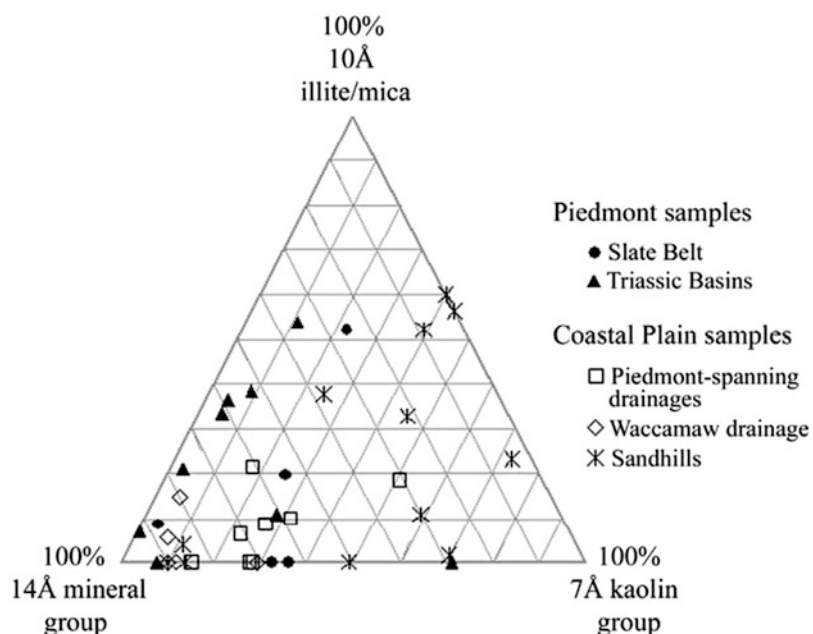
JMH056, New River Fabric Impressed (flex warp); (g) JMH057, New River Cord Marked; (h) JMH058, Cape Fear Fabric Impressed; (i) JMH059, Cape Fear Fabric Impressed; (j) JMH060, Hanover I Fabric Impressed (Fig. 7.8, p. 28, Herbert and McReynolds 2008)

Plagioclase feldspar is generally considered to be the “parent” mineral for most Piedmont clays (McReynolds et al.), whereas the Coastal Plain clays are potassium feldspars (K-feldspar) derived primarily from the Cretaceous-aged Cape Fear Formation (Sohl and Owens 1991). When included in the potting clay, the feldspars, most notably the K-feldspars, gave greater overall strength and durability to the pottery produced from them. Likewise, it was observed the smectitic (14 Å) clays were generally more plastic than the kaolin-rich Coastal Plain (7 Å) clays. The XRD study of the suite of 42 clay samples was able to clearly differentiate the mineralogy of the source clays. This information, in turn, at least in the case of the feldspar minerals, can aid archaeologists in assessing the production and movement of pottery within the Sandhills regions.

7.8.2 Diagenetic Changes

During burial elements of the pot will be subject to both infiltration of new material and dissolution of some original constituents by solutions passing through and organisms present in the environment of burial. Unfortunately, in many cases, the nature of diagenetic changes is destroyed by archaeological treatment. On most digs, pottery is cleaned with relatively strong acids which dissolve much of the products of diagenesis, including the carbonates and zeolites. Since both gypsum and calcite will be leached by this treatment, important information will be lost. Gypsum is a product of cementation during burial; the form of the calcite, either powdery or crystalline, will reveal whether or not temperatures of lime formation were reached

Fig. 7.10 Ternary plots of Sandhills' clay groups (Fig. 7.2, p. 117, Herbert and McReynolds 2008)



and if soil processes caused the formation of secondary calcite.

Diagenetic changes during burial are an especially serious problem for low-temperature ceramics, that is, those fired about 500–700 °C. Such pottery is generally very porous allowing easy access for outside solutions. Dissolution and neocrystallization will take place: deposition in pore spaces, replacement of primary minerals by secondary carbonates, hydrates, oxides, hydrosilicates (zeolites), and sulfates (gypsum). The initial porosity is due to the manufacturing and firing processes, the chemistry and mineralogy of the starting material, and the loss of other substances.

7.8.3 Analysis of Residues

Analysis of organic materials has been carried out to determine reactions that may have taken place between the food or perfume and the pot in which it had been stored or cooked. This type of analysis is generally carried out by FTIR (Fourier Transform Infrared) Spectroscopy or by similar specialized means—chromatography—that can identify organic molecules. A leading proponent

of this type of study is Richard Evershed (Heron and Evershed 1993). An interesting application of residue analysis involved the dating of prehistoric steatite vessels from the Piedmont region of the southern Appalachians wherein charred residues adhering to the interior surface have been used to determine the age of the vessel (Truncer 2004).

Chemical analysis of food residues is associated with Late Pleistocene pottery, focusing on one of the best-studied prehistoric ceramic sequences in the world, the Japanese Jōmon (Craig et al. 2013). The results of residue analyses demonstrate that lipids can be recovered reliably from charred surface deposits adhering to pottery dating from about 15,000 to 11,800 cal bp (the Incipient Jōmon period), the oldest pottery so far investigated, and, that in most cases, these organic compounds are unequivocally derived from processing freshwater and marine organisms.

The most useful surviving organic compounds are lipids, which are the constituents of fats, oils, waxes, and resins (Heron and Evershed 1993; Tite 1999). Because of hydrophobic properties, lipids survive on pottery. The lipids are extracted in a solvent, and the individual lipids are separated out, using gas chromatography. The

mass associated with each lipid can then be determined by mass spectrometry. Identification of the lipids is based on a combination of the retention time in gas chromatography and their mass spectra. Alternatively, the pattern of lipids separated out from the archaeological pottery vessel by gas chromatography can be compared with the patterns obtained from modern examples of the different animal and plant species which the vessel could have contained (REF).

Fatty acids can provide a broad classification into animal fats, dairy products, vegetable oils, or fish oils, but it is not normally possible to identify the actual animal species from the fatty acids alone. However, on the basis of the stable carbon isotopic composition of the fatty acids extracted from pottery, it has been possible to distinguish between fats from ruminant (i.e., ovine and bovine) and nonruminant (i.e., porcine) animals (Evershed et al. 1997).

As mentioned earlier in this chapter, Diederichs et al. (2013) and Lipe (2015) assert the Basketmaker III Period was part of an important cultural shift in the history of the American Southwest, when a new technological package—including cooking with pottery—enabled the rapid expansion of Puebloan populations and represents a material culture horizon in the archaeological record. The addition of beans to the dietary repertoire of this farming society

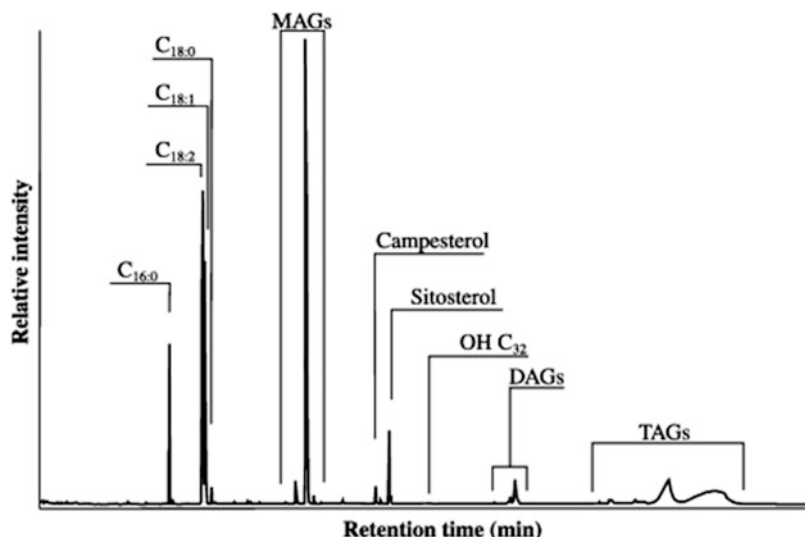
provided a vegetable protein which compensated a lack of essential proteins in a predominately (75 %) maize-only diet (Lipe, *supra*).

Beans require(d) longer cooking times than does maize. Basketmaker III groups adopted ceramic wares as a result. To chemically distinguish food like beans, one can use sterols present to distinguish animal products (cholesterol) from vegetable products (campesterol or sitosterol) (Evershed et al., *supra*). This example of the need for the adoption of pottery by a culture may be a further corroboration of Brown's (1989) contention that the adoption of pottery as a container was "a response to conditions in which the rising demand for watertight, fire-resistant containers is coupled with constraints in meeting this demand." Thus, pottery was adopted when existing other forms of containers failed to meet the increasing demand brought about by new types of food processing particularly that of beans rather than corn/maize.

In Fig. 7.11, Reber and Evershed (2004) illustrate the chromatographic spectrum of lipid residue of maize from Mississippian ceramics. Much like the example of maize and beans in the Colorado Basketmaker III discoveries, maize, beans, and squash were the requisite staples of the Mississippian cultural florescence in the central Mississippi Valley and across the late prehistoric American Southeast.

Fig. 7.11 The total ion chromatogram (TIC) of maize lipids. This shows primarily the plant and/or fish fatty acid ratio (more unsaturated C18:1 than saturated C16:0), plant biomarkers (sitosterol), and acylglycerols.

Triacylglycerols are referred to as TAGs, diacylglycerols as DAGs, and monoacylglycerols as MAGs (Reproduced from Reber and Evershed 2004, Fig. 7.1)



Reber and Evershed (supra) term this food residue approach as “biomarker analysis.” It is the second approach used to identify the original contents of vessels through absorbed organic residue analysis. Biomarkers are unique to a single source or group of foods. Lipid biomarkers survive well and are more easily analyzed than other

classes of compound. Cholesterol is a lipid biomarker for meat (Heron and Evershed 1993), sitosterol and other plant sterols are lipid biomarkers for plants (Heron 1989; Evershed et al. 1992; Evershed 1990). The presence of a lipid biomarker allows a more specific identification of the foods once cooked in a sherd.

8.1 Introduction

A simple search of either modern scholarly or popular scientific literature confirms the relevance of chemical analyses to archaeology. Chemical analyses are not only used to determine the chemical makeup of an artifact but also to reveal clues to age, diet, and health when applied to both organic and inorganic materials. Chemistry is equally important in the preservation and restoration of archaeological materials. The first use of chemistry in the study of artifacts can be traced to German chemist Martin Heinrich Klaproth's 1796 studies of Greek and Roman coins, other metal artifacts, and some Roman glass in which he pioneered the use of gravimetric analysis (Goffer 2006). Gravimetric analysis is the determination of an element through the measurement of the weight of the insoluble product of a reaction with that element. Since Klaproth's first foray, there have been numerous examples of the application of analytical chemistry to archaeological materials of all sorts by historical figures in both chemistry and physics—Sir Humphrey Davy, Jon Davy (Sir Humphrey's brother), Jöns Jakob Berzelius, Jon Voelker, Michael Faraday, Marcelin Berthelot, and Friedrich August von Kekulè (various in Meschel 1980; Goffer *supra*; and Pollard and Heron 1996).

According to Robinson (1995), one important function of analytical chemistry is to provide data to other scientists. When applied to

materials of art and archaeology, the methods must oftentimes be nondestructive or, at the very least, destructive of only a small portion of the material under examination. To Sir Humphrey Davy's chagrin, his 1818 attempt to unroll Pompeian papyrus scrolls met with less than success when all of the eleven scrolls were effectively destroyed before any decipherment could be done (Herz and Garrison 1998). In contrast, analytical chemistry's exposure of science's most famous fraud—Piltdown—using the quantitative determination of the elements fluorine, nitrogen, and uranium in the “fossil” hominid remains and their comparison to both modern and prehistoric bones, in the mid-twentieth century, was the watershed event that brought analytical chemistry into the forefront of subsequent scientific studies of archaeological materials.

The chemical examination of the physical properties of artifacts and other materials of archaeological interest generally requires instrumental assistance. In the last chapter, that instrument was the petrographic microscope, which, as we have seen, is a very useful tool in the service of archaeological geology. A mineral's optical properties are attributes which aid us in identification and, by extension, the characterization of the archaeological item. With this characterization, we can, as archaeologists, hope to use this mineralogical information to pose pertinent inquiries as Freestone and Middleton (1987) have aptly suggested in the following:

1. The characterization of the material from which an object was made
2. The reconstruction of the technology involved in its manufacture
3. The inference of the place of manufacture or source of raw materials
4. The changes that have occurred in the object during burial or storage

The reader can certainly suggest other important questions, but these are surely common to most inquiries. Nikischer (1999) has reminded us that contrary to popular belief, there aren't any foolproof *single* (author's emphasis) technological innovations that can produce an accurate identification *every* time for *every* mineral (or material for that matter). Frequently, two or more confirming techniques are needed. "This sentiment is echoed by more than one compendium on techniques used in the chemical/mineralogical analysis of archaeological materials (Artioli and Angelini 2011; Ciliberto and Spoto 2000; Garrison 2001; Glasscock et al. 2007b; Henderson 2000; Tite 1999; Vandiver 2001).

In the application of analytical techniques to archaeological materials, one can seek data at (1) the molecular level and (2) the elemental/isotopic level in archaeological geology. In archaeological geology where this would be illustrated by either examining a lithic (marble) sample as to its mineralogical (molecular) form, such as calcite (CaCO_3), or assessing the metallurgy of an early Bronze Age axe wherein the presence or absence of the alloying metallic *element* tin (Sn) is critical to its classification, both typologically and chronologically. Likewise, a second important distinction can be made in the analysis of materials—that of (a) qualitative or (b) quantitative. The former simply answers the question, posed in our axe example, "what kind?" A quantitative study asks a second level of question—"how much?" Returning to the axe, if all we want to know is whether the artifact is a copper axe or a later bronze type, then a qualitative study is appropriate to the question. But, if we desire to classify the axe, assuming our

analysis determines it is bronze, as to its appropriate typology, then we must do a quantitative assessment.

Tite (1999) observes that in the early days of provenance studies, using chemical analysis, the principal techniques were quite different from those in use today. For instance, optical emission spectroscopy (OES) was superseded first by atomic absorption analysis (AAS) then by inductively coupled plasma mass spectroscopy (ICP MS). AAS, itself, has continued to be used in many labs but the rise of ICP MS, particularly; laser ablation (LA) ICP MS has impacted its usage as well. Neutron activation (INAA), ICP MS, and X-ray fluorescence (XRF) along with newer techniques, such as proton-induced X-ray emission (PIXE), have found the widest applications (*supra*).

8.2 Analytical Techniques and Their Pluses (and Minuses) for Archaeology

Techniques commonly encountered in the study of archaeological materials include:

1. X-ray diffraction spectroscopy (XRD)
2. X-ray fluorescence (XRF) spectroscopy
3. Electron microprobe/analytical scanning electron microscopy (EMPA/SEM)
4. Atomic absorption spectroscopy (AAS)
5. Inductively coupled plasma emission spectroscopy/mass spectroscopy (ICP-ES/MS)
6. Mass spectroscopy (MS)
7. Neutron activation analysis (NAA/INAA)
8. Infrared and Raman spectroscopy (IR/FTIR/ Raman)

European laboratories commonly use emission spectroscopy, atomic absorption spectroscopy, X-ray fluorescence and diffraction spectroscopy, and neutron activation (Collon and Wiescher 2012). Additionally, ion probes (PIXE; SHRIMP) and types of mass spectroscopy are commonly found. North and, to a somewhat lesser degree, South American laboratories

mimic that of the Old World in the diversity of analytical methods regularly used on archaeological materials as do Asian labs, particularly in Japan and China. The European Union (EU) Geochemical Facility at Bristol University (UK) has a comprehensive suite of modern analytical instruments that are available to member European Union states together with 15 non-EU members in eastern Europe and the Near East. The instrumentation includes electron microprobe (EMPA), ICP-MS, laser ablation (LA) - ICP-MS, XRF, ICP-AES, XRD, Mössbauer spectroscopy, Raman spectroscopy, Fourier transform infrared spectroscopy (FTIR), nuclear magnetic imaging (NMR), and SEM (with analytical EDS). Surface analysis can be done using Auger electron, secondary ion mass, and X-ray photoelectron spectrometers.

From the perspectives of (1) molecular versus elemental and (2) qualitative versus quantitative, each technique has strengths and weaknesses. The X-ray techniques of XRD and XRF are good examples of this, XRD being a powerful instrumental technique in the qualitative and quantitative determination of the molecular nature of a material. XRF, by contrast, is a routine method for the qualitative study of elements with atomic numbers higher than $Z = 10$, including both metals and nonmetals. Additionally, it is a very sensitive and reliable method for the quantitative study of elements of high atomic weights.

The electron microprobe/scanning electron microscopic instruments (EMPA/SEM), like that of XRF, have the capabilities of performing both molecular and elemental analyses as well those that are qualitative and/or quantitative. In terms of surface analysis, the SEM techniques are highly sensitive to the number of atoms detected but not their respective percentages (Robinson 1995). Also, electron spectroscopy is used only in a semiquantitative way. Newer electron systems such as "analytical SEM" models have built-in X-ray energy dispersive spectrometer (EDS) capabilities that allow them to perform qualitative analyses.

AAS or atomic absorption spectroscopy is not used in qualitative analyses except in single element studies. It is, perhaps, the most accurate and

sensitive method for the quantitative study of metals with detection limits down to 10^{-12} g. It is not generally used in the detection of nonmetals. Newer AAS instruments have had to expand as to rapid multielement, solid sample analyses because of the introduction of ICP or inductively coupled plasma spectroscopy.

In its original form or in newer hybrid configurations with mass spectrometers and lasers, ICP has rapidly challenged AAS with regard to the analyzable range of elements as well as to quantitative sensitivity. Unlike AAS, ICP is restricted to the elemental analysis of materials. By itself, ICP is good for the analysis, like AAS, for metals. Coupled with mass spectroscopy, ICP is routinely used for analyses of both metals and nonmetals. It has a wide, linear sensitivity range from parts per billion (ppb) to percent levels.

Mass spectroscopy is used in both qualitative and quantitative studies of molecular, elemental/ionic, and isotopic forms up to very high atomic mass. At the quantitative level, the mass spectrometer is a commonly used tool for the determination of liquid and gas samples and, when combined with lasers, solid samples as well.

(Instrumental) Neutron activation analysis (INAA/NAA) requires either nuclear reactors or accelerators. The former are common in most developed countries, but the reactors must be lower power, research types rather than the more frequently found power generation reactors. NAA is an extremely sensitive analytical method that can reach the part per billion range (ppb = ng/g), in many materials, with ease. It is used for both qualitative and quantitative elemental analyses.

Infrared spectroscopy has been a staple chemical technique for the qualitative and quantitative study of organic compounds. It was the first technique that the author first became acquainted with in its use on the adsorption of contaminants on surfaces. The literature is vast on this particular technique but its use in archaeological analyses has not been as extensive as many of the other techniques we will survey. Newer variations on IR spectrometers such as the Fourier transform (FTIR) designs hold

significant promise for the study of archaeological materials such as clays and particularly in field settings.

Raman spectroscopy is, as promoted by Killick (2014), a powerful and swift alternative to powder XRD (Smith and Clark 2004). It is nondestructive, except for some compounds like some silver minerals that are degraded by exposure to laser beams. It can be used on polished blocks and thin sections of metallic ores as well as unprepared specimens. Raman and infrared spectroscopies measure the same phenomenon, which is the momentary absorption and loss of vibrational energy by molecular bonds.

Both Raman and infrared peaks correspond to molecular bonds rather than crystal plane d-spacings as in XRD and work well in identifying cryptocrystalline minerals. With regard to Killick's observation concerning the speed of analysis using Raman spectroscopy, it can take 1–2 h to obtain a publication-quality spectrum using powder XRD, whereas a spectrum of comparable quality can be obtained by Raman spectroscopy in as little as 5 min or a spectrum sufficient for chemical identification in as little as 30 s making it, like SEM-EDS, an excellent technique for use in the rapid screening of samples.

In addition to these methods, we shall briefly examine other analytical procedures, such as those listed for the EU facility, whose usage has produced insights into archaeological questions. Electron spin resonance (ESR), cathodoluminescence (CL), and magnetic susceptibility will be mentioned relative to specific archaeological findings such as provenance studies of marble, cave sediment, and climate. A major consideration in discussing this particular suite of instrumental techniques is their common usage in the analysis of materials of archaeological interest. All have long track records in both their theoretical underpinnings and their practical usage. For the archaeological researcher, other considerations enter into the selection of the instrumental technique or techniques for his/her particular needs. Key among these practical considerations are:

1. Nondestructiveness of the technique
2. Accuracy and reliability of the results
3. Availability of the technique
4. Cost

The first consideration—nondestructiveness, by the technique, of the archaeological sample of interest—is not a trivial one. Because of the rarity and uniqueness of many archaeological objects, any damage to them, beyond that of a natural, diagenetic origin while unexcavated, is generally to be avoided. Archaeologists and museum curators are loath to expose unique collections to scientific analyses that pose the threat of damage or destruction to the artifacts. As an archaeologist, the author has had to deal with just this problem when presented with the choice between preservation of an excavated item and the determination of a much-needed absolute date. In this specific case, the decision to sacrifice the archaeological sample—a prehistoric corn cob, rare in the context in which it was found—proved too compelling when its preservation was weighed against the need for a reliable age determination of an incidence of prehistoric farming in the southeastern United States. This is not usually the case in other situations. Preservation of the analyzed archaeological material is considered paramount.

The accuracy and reliability of the analytical results are key considerations in the choice of an instrumental technique. All the techniques we shall discuss have varying levels for the detection of elemental or mineralogical parameters. Some can regularly achieve accurate determination of trace levels ($\leq 1 \mu\text{g}$) of interest. Others can only achieve accurate results at the percentage level of analysis. It is perhaps important to digress here and eliminate any confusion about what is meant by “accuracy” and, its oft-confused adjunct, “precision.” Accuracy refers to the *correct* measure of a particular physical property such as temperature, mass, age, etc. The precision of that measurement refers to its replication with reliability and, most importantly, repeatability. If the true mass of an artifact is 30 g, then a measurement of 20 g is obviously in error.

Should an instrumental technique repeatedly measure the instrumental mass as 20 g to three or four place precision, it is still an inaccurate measurement; however, it is a “precise” inaccurate measurement.

The mineralogists Artioli and Angelini (2011) caution that present-day trends in archaeometry, in the service of cultural heritage, are in danger of a proliferation of “approximate” protocols and nonstandard instrumentation that can rapidly produce data that are simply wrong and misleading. Other workers have raised similar warnings (Shackley 2011b; Speakman et al. 2011a, b; Speakman and Hunt 2014). The potential to mass produce data that should never enter the scientific literature is very real.

Reproducibility and reliability are, therefore, measurement-bound in that one seeks to achieve accurate evaluations with instrumental methods. The eight listed techniques have established reliability to differing measurement levels. Of them, neutron activation analysis (NAA), a gamma-ray spectroscopic technique, can lay claim to the crown of the most accuracy and precision at trace element levels of over 70 elements. ICP, inductively coupled plasma spectroscopy, is rapidly approaching NAA’s analytical standard and will likely supplant the older technique by virtue of greater availability and cost per analysis.

The last two parameters—availability and cost—are, likewise, important to the choice of analytical technique. Again, in comparing NAA and ICP, they are nearly comparable in terms of measurement accuracy, precision, and repeatability. The availability of NAA is constrained, in part, by that of nuclear research reactors, but more readily available (and less politically controversial) particle accelerators can provide adequate neutron fluxes for most archaeological studies. Nonetheless, both these types of NAA facilities are capital intensive and limited by real concerns about radioactive wastes produced by their use. As ICP and other high-precision techniques produce little contaminates, like radionuclides, and have the advantage of lower cost and size, they will likely supplant NAA as a principal analytical technique of choice in the future.

8.3 X-ray Diffraction (XRD)

Spectroscopy is the determination of the physical properties of a material—rock, mineral, biologic, solid, liquid, or gas phase—by the absorption and/or emission of energy. The spectra of absorption and emission can be characteristic of a material thus allowing its identification and measurement. The following sections discuss the properties and characteristics of individual instrumental techniques beginning with the X-ray spectroscopic techniques of XRD and XRF.

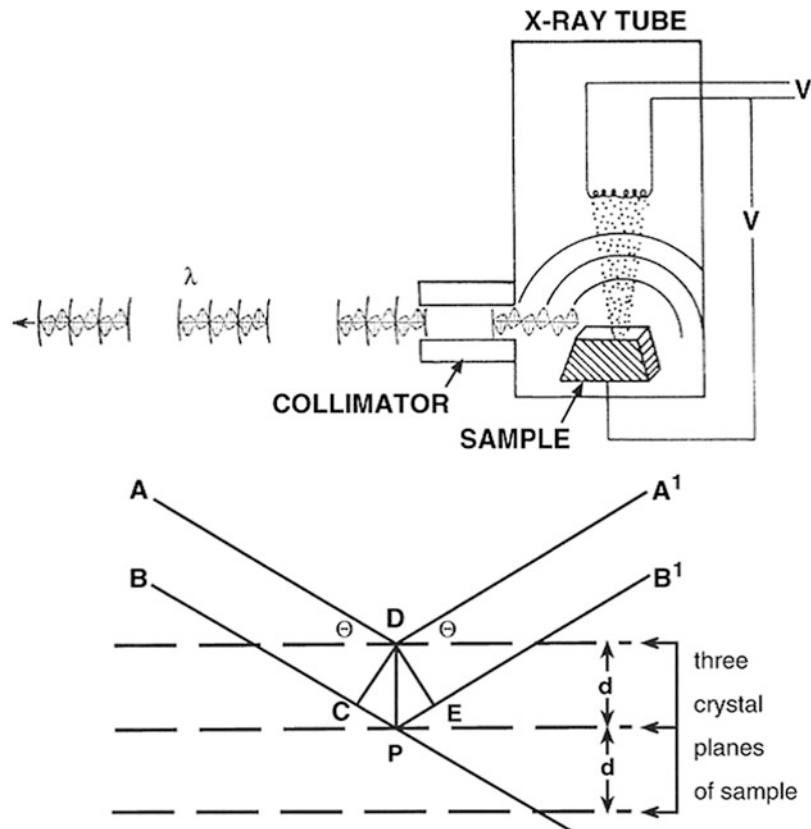
A colleague has called XRD the “first line of defense for archaeological (analytical) analyses” (Paul Schroeder, 1996, personal communication). XRD is a technique that yields a mineralogical identification rather than an elemental characterization. XRD is a monoenergetic spectroscopic technique based on Bragg’s Law:

$$n \lambda = 2 d \sin \varphi$$

where (n) is the order of wavelengths, (λ) the wavelength, (d) the interatomic spacing in a crystal, and (φ) the diffraction angle of X-ray leaving the mineral’s lattice (Robinson 1995). This is shown in Fig. 8.1. For XRD to work, the archaeological material *must* be crystalline. With the exception of glassy materials like obsidian, most minerals are crystalline.

In XRD analyses, monoenergetic collimated X-rays are allowed to fall on specimens, and a proportion will be diffracted at angles (φ) depending on the crystal structure of the specimen (Fig. 8.1). An essential feature for diffraction is that the distance between the scattering points is the same magnitude of the wavelength of the incident radiation. XRD works only on crystalline materials, as we have said, as there is no refraction in a glass because there is only random intercrystalline structure. The orderly arrangement of atoms in crystalline minerals is seen in the repeating structure of the *unit cell*. Every mineral has a unit cell dimension that is specific to it. In practice, the XRD device scans a sample, generally a powder, with a fixed X-ray wavelength of 1.54059 Å, the K_n X-ray (L-shell

Fig. 8.1 Schematic of X-ray diffraction. The diffractometer measures the “d-spacing” between the crystal planes following Bragg’s Law, $n \lambda = 2 d \sin \varphi$, where n is the integer representing the peak of interest, d is the lattice spacing of the specific crystallized mineral or element, λ is the wavelength of the incident light, and φ is the angle between the scattered X-ray and the incident radiation, and l is the wavelength of the incident light



to K-shell) for copper. By comparison, the unit cell spacing for silica is 1.6 Å.

XRD has a long and successful record in mineralogical identification, most notably the clays and phyllosilicate minerals—smectite (montmorillonite), illite, halloysite, vermiculite, chlorite, and serpentine. Because of the importance of ceramics in archaeology, the utility of a spectroscopic technique which identifies and quantifies respective clay varieties should be readily apparent. In XRD, the angle, φ , of the diffracted X-ray radiation is different for the different crystals due to the various interatomic distances. The detector is swept through 2φ to get our measurement of φ which can yield very good resolution ($\mu\text{g/g}$ -range). XRD is commonly used to study fine-grained/cryptocrystalline minerals too small to be examined optically.

For metallurgical studies, XRD has the capacity to evaluate the state of an object’s anneal. In well-annealed metals, there is clear crystal order

yielding sharp diffraction lines. If the object has been hammered, drilled, or otherwise worked as is typical of early metallurgy, then this will contribute to the blurring of the diffraction spectrum due to the effects on crystal order. Additionally, corrosion can be examined in the artifact. Recently, XRD, coupled with XRF-EDS, was used to analyze pigments from Trajan’s Column (Del Monte et al. 1998). In that study, the researchers isolated hematite and *minium* (HgS) or cinnabar that had been applied over an underlayer of plaster indicating the ancients’ use of color for this monument. Pretola (2001) has demonstrated XRD’s potential for determining varieties of cherts and their possible source locations. In this study, XRD’s ability to differentiate variations in the mineralogy of silicates, in particular “moganite,” a quartz polymorph much like those of calcium carbonate, e.g., calcite and aragonite (moganite is not currently approved as a formal mineral name (*supra*)).

Since this quartz variety cannot be easily discerned optically, XRD is the instrumental method of choice in its study.

An interesting aspect of this quartz form is its diagenetic alteration to quartz over time ($>10^6$ a) implying that cherts older than 100 Ma will have little or no amount of the polymorph (Heaney 1995). This *metastability* of a mineral is similar to that of anhydrite/gypsum and calcite/aragonite (cf. Chap. 5). Jercher et al. (1998) have used “Rietveld” XRD analysis for the study of Australian aboriginal ochres. The Rietveld method is powerful method of fitting observed spectra to structural models of specific mineral phases (Rietveld 1969). XRD, although a powerful technique, cannot differentiate certain minerals from others such as gold and silver.

Additionally, the presence of certain elements and their oxides, such as those of iron, can cause nondirectional scattering and increase background interference or scattering. Alumina and opaline silica can cause these effects as well. Any significant increase in background scattering decreases the sensitivity of the technique for other minerals.

Particle size is critical as well. Particles greater than 10 mm in diameter create a reduction in diffraction intensity as do smaller particles (0.02 mm). Heterogeneous samples must be treated carefully because of these size effects. Some workers use internal standards to offset nonrandom scattering, self-absorption, and other problems. One can then examine diffraction-to-intensity ratios for the sample and the standard to obtain mineral composition by weight (Whittig and Allardice 1986). The archaeological geologist must be aware of these effects and the realities of XRD analysis when deciding to proceed with this line of instrumental inquiry.

Preparation procedures of samples for XRD analyses are determined by the nature of the material to be studied. In archaeology, the material will generally be either a ceramic or a lithic material such as flint or marble. If the material is a sediment or soil, preparation will be much the same as a ceramic particularly if the pottery is earthenware. Finer-grained wares, including

porcelain, will be less sensitive to particle size considerations. Separation of textual classes from ceramics will produce relatively distinct fractions of the paste or body and, again, in the case of coarser earthenware, the temper. Specific techniques for particle size determination were discussed in Chap. 3. The reason samples are separated as textural sizes is that almost all XRD study samples are mounted as either a (a) random powder or (b) oriented aggregate. The powder mount, favored by most labs, enables one to obtain as many possible diffraction spacings in the minerals present. Relative diffraction intensities from a random powder mount are more nearly proportional to the actual amount of crystals present than those obtained in an oriented aggregate.

8.4 X-ray Fluorescence (XRF)

In X-ray fluorescence (XRF) spectroscopy, the specimen is bombarded by X-rays from a conventional X-ray tube and, in turn, emits a secondary (fluorescent) spectrum of X-rays whose wavelengths are *characteristic* of the elements present in the specimen. It is important to enlarge on the distinction between the wavelength dispersive spectroscopy (WDS) and energy dispersive spectroscopy (EDS). WDS is the older variety of XRF wherein the secondary X-ray's, produced by the X-ray rather than by electrons (primary excitation), *characteristic wavelength* is measured. Wavelength dispersive spectrometers are better suited to accurate quantitative analyses. By the use of a diffracting analyzer crystal in an accurate circular geometry (Roland's circle), coupled with exit slits (on the crystal), only X-rays of a specific wavelength are counted on a proportional counter. The three analyzing crystals commonly used are TAP, PET, and LIF.

Using Bragg's law, the crystals diffract X-rays within the energy range of 0.5–14 keV (Takahashi et al. 2014).

EDS is the measurement of the secondary X-ray's energy that is characteristic of a given element by use of a scintillation detector, either

composed of silicon/lithium (Si/Li) or germanium/lithium (Ge-Li). These crystals will fluoresce when struck by secondary X-rays generating a signal which is amplified and sent to a multichannel analyzer. In general, EDS has a 0.5 % detection limit making it a fast but qualitative technique for elements with Z greater than 5. This detector system experiences a lot of “dead time” and does not work well for the heavy elements because their X-rays typically have high energies which allow them to pass through the detector. EDS is a good method for the rapid, qualitative characterization of a sample to determine the variety of elements present. The SEM (scanning electron microscope) is optimized to use the EDS spectrum for image formation.

XRF can perform in both modes, and it has been in WDS that most studies prior to the 1990s have been made (Jones 1991). Due to advances in both detector crystals and analytical software, energy dispersive spectroscopy (EDS) has seen a significant increase in its usage because it is (a) faster than WDS, (b) has detection limits of 0.1 % by weight, and (c) resolves more elements with fewer peak overlaps than WDS (Nikischer 1999).

WDS has better detection limits, approaching the parts per million (ppm = $\mu\text{g/g}$) range, but significant time, compared to EDS, is required (*supra*; Potts et al. 1985. In many modern XRF instrumentals, both capabilities are available. Much as an EDS system, XRF can be applied to both powderlike and solid samples. In qualitative EDS studies, very little sample preparation is required such as those used in the aforementioned study of Trajan’s Column (Del Monte, *supra*). Rock can be placed in the XRF sample holder, up to reasonable sizes; soils and sediments can be simply poured into Teflon cups and placed in the spectrometer; and ground ceramic material can be spread on Mylar tape and scanned by the XRF. Some commercial laboratories grind and press the powder into disks similar to XRD studies. Others will fuse the sample into a glass, with a borate flux, that forms a disk at 950 °C (Jones 1991).

The detection of several elements (over a dozen) is readily done by XRF. These include

Mn, Fe, Ni, Cu, Zn, As, Br, Rb, Sr, Zr, and Pb. Sodium and magnesium are not easily done, and elements below $Z = 20$ are somewhat more difficult than those just noted. XRF is extremely useful for the analysis of both metal and nonmetals with $Z > 12$ and has the distinct advantage over both emission spectroscopy and AAS because neither method can directly determine nonmetals.

Scott (2001) has demonstrated the use of XRF in scanning both ceramics and paintings at the Getty Museum. This scanning X-ray microfluorescence system was used on an Attic lekythos (vase) and a seventeenth-century Dutch painting measuring five elements on the former and seven elements on the latter. In particular, this system can examine lead white and vermilion along with the high Z elements. In the instances where SEM-EDS has problems with peak overlap such as with Ca K_{α} (4.04 KeV) and Sb L_{β} (4.38 KeV), the XRF can rapidly measure the calcium, a common mineral pigment of “bone black” (*supra*). For rapid assessment of painted surfaces, XRF, UV, and IR together with XRD form an excellent instrumental ensemble. Guineau and coworkers have examined black pigments in paints from prehistoric cave paintings at Pech Merle (France) (2001). XRD analysis of the paint pigments indicated that the prehistoric artist(s) used the manganese minerals hollandite ($\text{BaMn}_8\text{O}_{16}$) and romanechite ($\text{BaMn}_9\text{O}_{16}(\text{OH})_4$) mixed with common black.

More recently, an Orpheus Relief copy made from an Athenian marble was examined by Abbe (2013) using an ARTAX micro-X-ray fluorescence spectrometer (abbreviated micro-XRF) which was recently used to examine painted and unpainted areas on the Orpheus Relief (Fig. 8.2). The ARTAX is a semiportable open-beam XRF machine used for nondestructive elemental analysis of surfaces. The instrument has a built-in camera that allows the analyst to view and capture an image of the area that is being analyzed. By understanding what elements are present in a given area, it is possible to identify some types of paints that would have used to decorate the relief. For example, modern white house paints typically contain large amounts of the elements titanium and/or zinc

Fig. 8.2 Micro-X-ray fluorescence spectrometer examining painted and unpainted areas on the Orpheus Relief (Photograph by Jeff Speakman)



to produce the white color. Black paints can be made from minerals containing iron, manganese, or chromium, from carbon-based materials (“lamp black”), or even from charred bone (“bone black”). Finally, red and orange paints can contain iron-oxide pigments, lead oxides, cadmium, or even the mineral cinnabar (mercury and sulfur)—just to name a few examples.

The results of an XRF analysis comprise what we refer to as a spectrum—the graphical representation of the elements present in the analyzed area: (1) the analysis of an unpainted area on the Orpheus indicating the stone is calcitic marble; (2) a modern paint was dripped onto the sculpture probably when an exhibit gallery wall was being repainted sometime during the twentieth century (the high titanium); and (3) an iron red paint was used to decorate the Orpheus after it was carved.

8.5 Is pXRF a Revolution or Just the Latest Development in XRF?

While portable or pXRF (Fig. 8.3) has both become very popular as well as highly criticized, this is to be expected in a discipline that borrows much, if not all, of its analytical technology (Liritzis and Zacharias 2011; Shackley 2011a, b). What seems to be most problematic is that

these portable instruments were originally designed for mining and industrial applications seeking only qualitative results. Most of these instruments, unlike lab/desktop EDXRF, did not allow the user to generate their own calibrations; indeed, most relied solely on routines that are often standardless and could not be modified beyond factory settings. The criticisms have had their effect, and many of the manufacturers are now generating software that allows the user to employ linear calibrations by ratioing peaks/counts to the Compton scatter and thus eliminate the problem of differing sample sizes for lab EDXRF instruments.

Given these important shifts in the ability of pXRF, it will be possible to take a sensitive instrument to the field or museum settings and nondestructively analyze at least volcanic rocks with a similar instrumental precision and accuracy of lab XRF instruments. Most of the pXRF systems now available do not acquire the range of elements that laboratory systems do (i.e., Na through U), but the mid-Z (i.e., $Z = 19-41$) sensitivity seems to be very good. There may come a time in the near future when portable systems will acquire the typical sodium through uranium elements that laboratory instruments can today, but it is not here yet. Nonetheless, pXRF is likely the future of XRF in archaeology (Williams-Thorpe et al. 1999).



Fig. 8.3 Typical handheld pXRF instrument. Bruker Tracer pXRF model

Speakman and Hunt (2014) have recently determined that although modern pXRF spectrometers have lower detection limits and better resolution than those of decades past, portable instruments remain subject to the same limitations as benchtop ED-XRF instruments, particularly with respect to sample preparation, instrument calibration, and ability to accurately quantify low-Z elements (cf. foregoing discussion of WDS). Modern pXRF instruments have become little more than point-and-shoot devices requiring little-to-no specialized knowledge. The desire to use these instruments as inexpensive shortcuts to quantitative bulk chemical analysis of archaeological materials, such as ceramics and sediments, is understandable and has resulted in numerous studies that would not have been possible otherwise.

Nonetheless, Speakman and Hunt (*supra*) conclude that under the right conditions, such as a matrix-matched calibration, He flow and prepared samples pXRF can perform similar, if not identical, to benchtop ED-XRF spectrometers for certain elements. However, a pXRF spectrometer cannot accurately quantify Na, P, V, Cr, Co, Ni, and the L lines of Ba in an archaeological ceramic or sediment matrix at the concentrations in which they are typically present. As a result of these limitations, compositional analysis of archaeological ceramics and sediments by pXRF cannot and should not be considered a substitute for fully quantitative analysis by WD-XRF, NAA, and/or ICP-MS (*supra*).

8.6 Electron Microprobe Analysis and Proton-Induced X-ray Emission (EMPA and PIXE; SEM)

The combination of thin-section petrography with instrumentally based chemical analysis has proven to be one of the most useful associations, for archaeology, in recent years (Freestone and Middleton 1987). Thin-section petrography of archaeological materials can provide significant insights. The use of electron microprobe, proton-induced excitation emission spectroscopy, and the analytical (SEM) scanning electron microscope can enhance and extend the information obtained by optical petrography.

One of the reasons that studies of metals, both modern and ancient, progressed more rapidly in the twentieth century than studies of ceramics (and the development of new ceramic materials) is simply because clay particles are so much smaller than the grain size in most metals processed by traditional means that probes of much finer magnification are required to see the submicron and micron particle sizes (Tite 1999). In 1992, Kingery (49), in a study of the history of sintering, alluded to the fact, as did Smith (50), that material interactions can be viewed at interfaces with a variety of high magnification probes such as EMPA, SEM, etc.

All the systems—EMPA and SEM—are “scanning” systems which imply the particle beam, electrons in EMPA and SEM; (protons (hydrogen ions) in PIXE), can be focused and rastered (X-Y) across the surface of an example. This use of the electron/proton as the exciting particle is the difference between these instruments and the X-ray systems. Additionally, the interaction of the incident beam, while physically similar to XRF, has the advantage of deeper, and more energetic, penetration of the subsurface of the material under investigation. The energy and mass difference between XRF’s photons, SEM/EMPA electrons, and PIXE’s protons means that EMPA/SEM can only excite the near-surface atomic layers due to the dispersive nature of the incident beam, XRF significantly

deeper (>5 μm) by virtue of its high-energy, collimated X-ray beam and PIXE the deepest (>15 μm) of all. Research at the Ruhr-Universität, on Roman coins, using both XRF-WDS and EMPA-EDS, illustrates this. The surface analysis of these coins typically found a penetration depth of 3 μm using the latter technique, while a penetration of 30 μm was achieved using XRF-WDS (Klockenkämper et al. 1999).

Analysis by electron microprobe (EMPA) and by proton-induced X-ray emission (PIXE) has become widely used in elemental analysis of both geological and archaeological materials (Reed 1996; Henderson 2000). In electron microprobe analysis (EMPA), electrons from a filament are accelerated to about a 30 keV and directed at a specimen and focused to a spot 0.001 mm in diameter. When the beam strikes, the specimen X-rays are produced that are characteristic of the elements present in the specimen. These X-rays are analyzed by a spectrometer as in the XRF technique. In PIXE analysis, the electron is replaced with a proton as the incident particle. The technique is based on the excitation of the surface atomic electron shells by the particle beam.

In theory, both EMPA and PIXE are nondestructive techniques, but this is only relative to the sample size. To acquire the specimen or sample may not be nondestructive. EMPA and PIXE samples are small less than a few millimeters as a rule so as to be able to fit in the sample chambers of the analytical devices. EMPA sample chambers, and early PIXE models, are kept under a vacuum so the particles are not scattered or absorbed by air particles in their paths. As result, small samples are taken from the larger object resulting in some damage to the object or artifact. Newer PIXE designs allow the particle beam to be operated in air allowing for analyses to be performed without recourse to destruction of the subject object.

An advantage of either technique is their capability of analyzing small areas in great detail and precision. Both EMPA and PIXE can achieve lower levels of elemental detection than XRF—typically ppm levels for the former and % levels for the latter—thus achieving good

accuracy in the quantitative results. Using the EMPA, researchers have the advantage of (1) quick, quantitative elemental determinations, (2) the use of the dispersive nature of X-rays for a semiquantitative characterization of large suites of elements, and (3) the production of secondary, back-scattered electron (BSE/BEI) images of the sample surface. The back-scattered (secondary) electrons (BSEs) are the result of elastic scattering of the primary electrons in the EMPA. BSEs pass through the atomic electron cloud and change direction without appreciable energy loss. They may travel into the sample or escape from the surface in fluxes that are proportional to the atomic number (Z) of the material.

The higher the atomic number, the smaller the mean free path between scattering events and the higher the probability for scattering (Rigler and Longo 1994). As a result, lower Z elements in a material allow primary electrons to penetrate deeply and reduce the number of BSE. Conversely, higher Z elements retard the beam's electrons and emit larger numbers of BSE. This difference in BSE emission as a function of atomic number can, and is used to, map the distribution of different elements across the surface. Images (BEI) produced by BSE have excellent resolution and provided the SEM/EMPA observer with surface compositional detail by rastering, in an X-Y pattern, the beam over the sample.

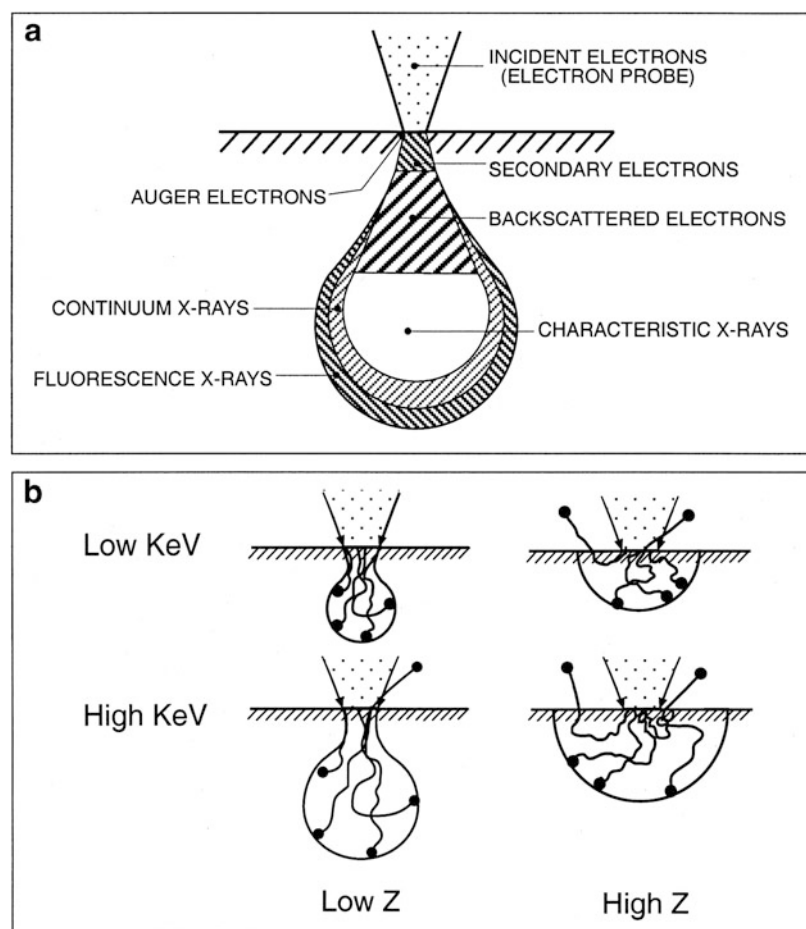
The analytical SEM combines the superior imaging capability of electron microscopy with semiquantitative chemical analysis using EDS. In ceramics and sediments/soils, the SEM can examine the microstructure of these material-grain morphology, crystal size and shape, etc. Coupled with this imaging capability, the analytical SEM's EDS can move, seamlessly, to a semiquantitative analysis of crystalline and glassy forms as minerals and slags (Freestone and Middleton 1987). Studies of Bronze Age coinage corrosion products, by SEM-EDS, have elucidated mechanisms for the formation of two differing patinations (Robbiola and Fiaud 1992). The principal differences, in the analytical SEM and the EMPA, are in accelerating current voltage, higher in the EMPA, and the beam diameter, a larger diameter in the EMPA.

The source of electrons used by the SEM or EMPA is heated filament just as with the XRD and XRF devices. These electrons are not allowed to strike a metal plate to produce X-rays but are accelerated by an electron gun much like a television set and, in the case of SEM, are rastered, by the gun, across the sample. The system is under vacuum. For imaging purposes, the backscattered electron (BSE) spectrum is used (Fig. 8.4). The relationship between penetration depth, energy, and the sample's atomic number (Z) is important. The higher the atomic number, the smaller the mean free path between electron scattering events (e.g., 528 Å for Al versus 50 Å for Sn at an accelerating voltage of 30 keV) and the higher the probability for scattering. Normal voltages for EMPs are 10–15 keV, so this example is quite

high by comparison. New SEM models can have voltage ranges of 40–200 keV. As we have noted earlier, the difference between the SEM and the EMPA is that the former is optimized to use the EDS spectrum for good images while the EMPA is optimized to provide analytical results—e.g., an EMPA beam is focused at 0.1–0.5 μm while the SEM focuses at 10–1000 nm!

Polished thin sections, such as used in optical petrography (cf. Chap. 6), are generally used with the EMPA, thereby achieving greater precision and accuracy—true quantitative analysis. A SEM optimized for obtaining images, even with the EDS detector present and without the use of polished thin sections, produces significant surface spectral interference reducing the accuracy and precision of the data.

Fig. 8.4 Electron and X-ray emission for EMPA showing the relationship between penetration depth, energy, and the sample's atomic number (Z)



Holton (2012) evaluated the efficacy of SEM-EDS and EMPA asking the question if the former was a substitute of EMPA. His conclusion, much like a similar comparison, later in the chapter, between other “competing” analytical methods—ICP MS and NAA, pXRF versus XRD, etc. is as follows.

In Holton’s evaluation, EMPA, in a nutshell, is superior for the reliable quantification of minor and major trace elements, particularly when the sample is basically of unknown composition (*supra*). Where trace element amounts are less than 0.1 %, EMPA must be used rather than EDS.

The comparison is really that of WDS versus EDS.

PIXE instruments use in comparison to photons (XRF) or electrons (EMPA, SEM) the rather more massive proton (2000× the electron mass). Accelerating these particles to high voltages allow greater subsurface penetration with very high analytical resolution (ppb range). All these techniques use the characteristic X-rays for these analytical procedures. PIXE proton beams, like electrons and X-rays, upon collisions with the inner atomic electrons, cause the emission of electromagnetic radiation, mostly X-rays (Collon and Wiescher 2012). Besides the X-rays, a major component of the energy emitted, by a sample, as a result of primary beam interaction with the material, are secondary electrons. The depth of penetration (up to 50 μm) of the proton, into the typical archaeological material, is comparable with EMPA/EDS instruments (Henderson 2000). The most significant difference between EMPA and PIXE is the reduced X-ray background in PIXE. The higher velocity of the protons entering the materials produces less scattering of the incident beam, thereby producing an X-ray background up to ten times less than EMPA, allowing for the detection of low-level amounts of certain elements (*supra*).

Use of PIXE microprobe is illustrated in a study of pre-Columbian metallurgy by Palmer et al. (1998) wherein quantitative analyses of minor ($>100 \mu\text{g/g}$ or 0.01 %) and trace ($<100 \mu\text{g/g}$) elements were done on copper bells or “crotals.” Combined with analytical SEM results from the same artifacts, the study

found six compositional types within the 24 bells inferring several prehistoric workshops of a trade-linked Hohokam-Anasazi period in the Southwestern United States. In addition to the southwestern metal, black-and-white ceramics have been examined for mineral or organic pigments used in the paint to determine provenance (Collon and Wiescher 2012). PIXE instruments are operated across Europe (Paris, Florence and Seville) and at US locations like the University of Notre Dame’s Snite Museum of Art (*supra*).

Electron Microprobe Analysis—Some Examples (EMPA): The EMPA works by focusing an electron beam at the sample. Before the electron beam reaches the sample, it moves through a voltage potential. The voltage potential of the machine used was 15 keV. When the electron beam reaches the sample, electrons are knocked out of the outer energy levels of the atoms in the sample. When the electrons are knocked out, an X-ray is emitted. Each element has a characteristic X-ray that is emitted, and these characteristic X-rays are used to identify the elements present in the sample.

For the analysis of data, wavelength dispersive spectroscopy (WDS) was used to analyze the two samples. WDS operates with a small fraction of the X-rays that escape from the sample. A WDS is tuned to one wavelength and remains stationary and counts the number of X-rays of that wavelength that pass it, through the particular analyzer crystal (TAP, PET, LIF) during the experimental time. A typical analysis uses four specific wavelengths which can be sampled at once. The one disadvantage of the WDS method is that in order for data to be obtained, there must have some preconceived idea which elements are present in the sample. The wavelengths of the expected elements then must be entered into the machine before the analysis is done. An analysis can be run, but only the preset wavelengths, within the energy range of the analyzer crystal, can be detected. This means that the sample may contain a large amount of a particular element, but if the machine is not set to detect that wavelength, it will not show up in the data. For this reason, it is

typical that energy-dispersive spectroscopy (EDS) is run before WDS because it provides a record of most of the elements present in the sample.

The data given by WDS is quantitative, in that it gives the relative amounts of each element (or oxide) detected. These relative amounts can be standardized to 100 so that the relative amounts of each can be compared. The WDS can also provide a backscatter image of the surface of the sample. The backscatter image uses the electrons that are deflected off of the sample in order to make an image. The denser portions of the sample would deflect more electrons and therefore appear darker on the backscatter image.

Recently, Takahashi et al. (2014) have described a soft X-ray emission WDS spectrometer (WD-SXES). It is particularly good for the detection and analysis of low-energy X-rays. The spectrometer is a straightforward add-on to any EMPA system. This analyzer was first developed by Terauchi et al. (2001). One potential application is the analysis of light elements such as lithium, carbon, fluorine, silicon, as well as aluminum that can be done using the K-shell X-ray lines.

L-shell X-ray lines from important elements such as Ti, Cr, Mn, V, and Fe are realizable. This addition to EMPA-WDs systems can be useful in studying archaeometals (Chap. 9).

8.7 Examples of Chemical Analysis of Nineteenth Century Transfer Printed Whitewares Using EMPA

Douglas (2000) examined the glaze and pigment mineralogy of a suite of transfer printed British whitewares. The largest number of pottery samples (18) was provided by the Spode Museum Trust. In addition, Douglas analyzed seven pottery samples excavated in the Savannah, Georgia (USA), vicinity. All the samples were nineteenth-century materials ranging from 1815—modern for the Spode samples (see below discussion of eighteenth-century Spode

porcelains). The Georgia samples were typical of mid-to-late-nineteenth-century designs.

Analysis of the glaze and pigments was done using a JEOL 8600 Superprobe (EMPA). Examples of the results for two pottery shards (Fig. 8.5) are shown in Tables 8.1a and 8.1b. These two shards were from the Georgia collection. They are undistinguished, but typical examples of these decorated whitewares. Douglas demonstrates the ease with the EMPA can examine both glaze and pigment minerals as well as acquire quantitative data using both the EDS and WDS modes typical of EMPA instruments. In the blue-printed shard, cobalt was the pigmenting agent of choice, whereas copper was used to produce the green coloration of the second shard.

In the study of nineteenth-century Spodeware, Douglas was able to detect a change in Spode glaze recipes coincident with a change in ownership of the pottery in 1833. The primary mineralogic change was in the lead percentage used in the glaze. After 1833, the lead content in the glaze was found to be a third less than pre-1833 amounts (*supra*) (see Chap. 10 for a discussion of the statistical methods utilized). As a tool for determining the general chronologic placement of a Spodeware shard, unmarked as many archaeological samples are, a simple EMPA chemical analysis of the glaze would place the find in the early or later nineteenth century. In Chap. 10, Douglas's use of discriminant function analysis will complete this discussion of the use of EMPA for characterizing historic Spodewares.

In reading Tables 8.1a and 8.1b, it must be noted that the microprobes like other probe techniques are “micro” in nature. This is to say that the area being analyzed is small—microscopic—micron sized in terms of the area actually analyzed by the beam, electron, X-ray, etc. Glasscock et al. (2007) even characterize laser ablation, inductively coupled plasma mass spectroscopy (LA-ICP-MS) as “microprobe” in nature.

In “Response to the Market: Dating English Underglaze Transfer Printed Wares,” Patricia Samford (1997) discusses the thematic motif trends in the designs for these nineteenth-century

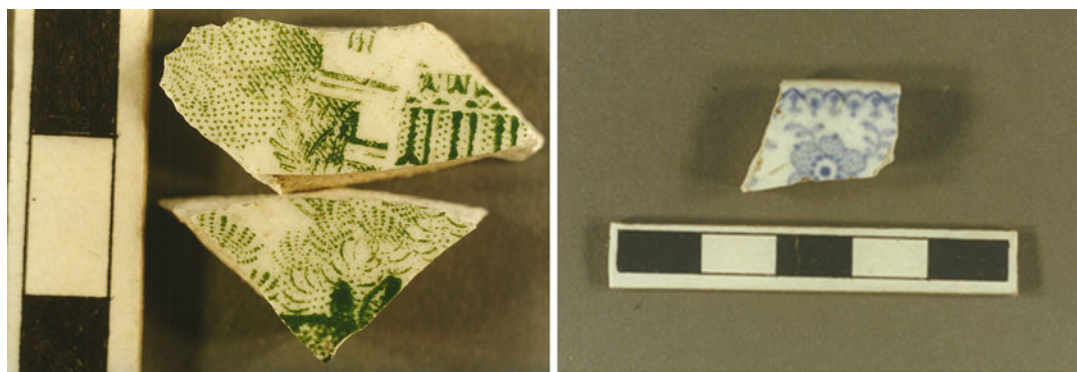


Fig. 8.5 *Left*, green transfer printed whiteware shards; *right*, flow-blue transfer printed whiteware shard (scale bars = 1 cm)

Table 8.1a Green sherd, WDS data

| Oxide | Green 1 wt.% | Trans. 2 wt.% | Trans. 3 wt.% | Trans. 4 wt.% | White 5 wt.% |
|--------------------------------|--------------|---------------|---------------|---------------|--------------|
| SiO ₂ | 39.27 | 55.25 | 51.35 | 45.86 | 39.12 |
| Al ₂ O ₃ | 3.99 | 5.02 | 4.94 | 4.19 | 5 |
| TiO ₂ | 0.03 | 0.09 | 0.13 | 0.1 | 0.16 |
| FeO | 0.42 | 0.42 | 0.54 | 0.39 | 0.34 |
| MgO | 0.11 | 0.11 | 0.18 | 0.1 | 0.05 |
| MnO | 0.01 | 0.08 | 0.05 | 0 | 0.12 |
| CaO | 0.7 | 0.95 | 0.88 | 0.83 | 0.75 |
| Na ₂ O | 0.41 | 0.21 | 0.31 | 0.23 | 0.42 |
| K ₂ O | 1.18 | 1.42 | 1.49 | 1.3 | 1.41 |
| CoO | 0 | 0 | 0.01 | 0.11 | 0 |
| CuO | 3.05 | 2.15 | 2.4 | 2.49 | 0.46 |
| PbO | 52.69 | 40.67 | 44.31 | 50.31 | 52.55 |
| Total | 101.85 | 106.36 | 106.58 | 105.89 | 100.39 |

Table 8.1b Blue sherd, WDS data

| Oxide | 1 wt.% | 2 wt.% | 3 wt.% | 4 wt.% |
|--------------------------------|--------|--------|--------|--------|
| SiO ₂ | 48.28 | 44.23 | 48.36 | 44.29 |
| Al ₂ O ₃ | 7.08 | 6.78 | 7.24 | 6.28 |
| TiO ₂ | — | — | — | — |
| FeO | 0.34 | 0.37 | 0.27 | 0.32 |
| MgO | 0.10 | 0.07 | 0.11 | 0.05 |
| MnO | — | — | — | — |
| CaO | 3.38 | 3.23 | 3.29 | 2.82 |
| Na ₂ O | 0.94 | 0.71 | 1.09 | 1.09 |
| K ₂ O | 1.48 | 1.33 | 1.50 | 1.22 |
| CoO | — | — | 0.46 | 3.16 |
| CuO | — | — | 0.08 | 1 |
| PbO | 40.25 | 42.32 | 40.63 | 41.73 |
| Total | 101.9 | 99.26 | 103.2 | 101.1 |

earthenware. She notes that, as is readily seen, upon inspection, most of these wares used underglaze designs in blue (cf. Fig. 8.5). As technology improved and glazes became clearer, other colors such as green (Fig. 8.5), brown, purple, pink, red, lavender, and black appeared (*supra*; Majewski and O'Brien 1987). The metallic oxides of cobalt, copper, manganese, and mixtures typically produced many of these colors.

Students of historic earthenware such as Samford can utilize the extensive scholarship on these wares to ascertain a general chronology for motifs and colors. For instance, blue, as stated, was the earliest and continual popular dye color throughout, but other colors were introduced and achieved varying degrees of popularity. Brown was used prior to 1829 but was more common in the 1830s (*supra*). Red was the most difficult color to produce and perhaps many of the pinks and lavenders were, in essence, “failed” reds. By 1848, most of the colors such as red, brown, yellow, as well as brown and green were better handled and even used in combination (Majewski and O'Brien, *supra*). One of the more interesting color varieties was developed by Staffordshire potters, and this was “flow blue.” The blue shard in Fig. 8.5 is an example of this color. It is a softer effect created by the use of the volatilization of ammonium chloride or lime during glaze firing. This style appeared in the 1830s (*supra*).

Other research has examined, instrumentally, glazes in historic eighteenth century soft-paste

porcelains (Owen and Hansen 1996). These researchers examined British soft-paste porcelains. These wares fall into three categories based on end-member composition—"frit" porcelains (cf. Chap. 7; Magetti, *supra*), phosphatic porcelains using bone ash recipes, and magnesium porcelains using talc in the recipe (Owen and Hansen, *supra*). Spode (see above) successfully used bone ash, kaolinite, and "China stone" (cf. *puten*, Chap. 7), and this recipe became the successful "bone china." In their study, like Douglas, Owen and Hansen used the electron microprobe.

8.8 Atomic Absorption, Inductively Coupled Plasma/Atomic Emission Spectroscopy (AAS, ICP/AES)

Atomic emission spectrometry (AES) relies on the property of the spectral emission of photons specific to an element at a rate and proportion to the amount of that element and the temperatures of the flame of a burner/furnace similar to that of our AAS example (Fig. 8.6). In AES types of analysis, the intensity of the selected wavelength is compared to that of some standard. As anyone who has done the simple flame emission test for sodium knows, the color (yellow) of the flame is directly a result of the wavelength of photons emitted by the stimulated sodium atoms. Flame temperature is central to this stimulated emission. In most AES systems, the physics requires increased (flame) energy as the wavelength (of the element) decreases. Shorter wavelengths always correlate with higher energy—X-rays are

longer in wavelength than gamma rays, for example.

Atomic spectroscopy is the most widely used technique for the determination of elements in most materials especially the metallic elements. The most common techniques include (1) flame atomic absorption, using the hollow cathode lamp (HCl), (2) graphite furnace AAS, and (3) inductively coupled plasma/atomic emission spectroscopy. Coupled with mass spectrometry, ICP has become one the most versatile of the modern atomic spectroscopic techniques becoming both the atomizing and ionizing device in these hybrid systems.

The HCl or flame AAS has been the standard unit of small labs. It is, as we have said, an efficient and robust instrument for the quantitative study of a single element at a time to relatively acceptable levels for most metallic elements of interest ($\sim \mu\text{g/g}$). A drawback of the flame method is difficulty in determining refractory elements like boron, tungsten, zirconium, or tantalum because the flame is not hot enough. The graphite furnace method typically has two orders of magnitude advantage in detection limits but suffers the same problem with refractory elements as with the flame method.

AAS has a long record in archaeological studies far too numerous to recount here, but by way of illustration, a recent study of protohistoric/historic Wichita ceramics, in eastern Oklahoma, demonstrates the utility of AAS. Singleton et al. (1994) examined eight elements in the 62 sherd samples from a large American Indian site to examine the heterogeneity in the clays and the linkage of this variation (or lack of same) to manufacture/trade practices among the members

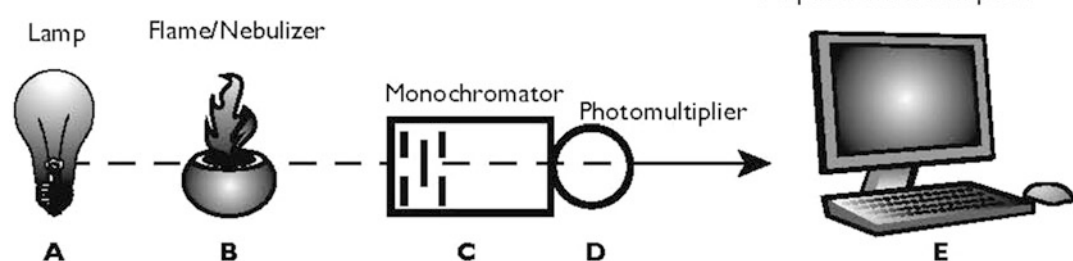


Fig. 8.6 Schematic of atomic absorption spectrometer

of this regional tribal group. The use of AAS was made on an economic, as well as a methodological, basis—to wit, less expensive, than say, NAA, and certainly more accessible in terms of the ubiquity of AAS instruments in most college chemistry units. True to its long record of success in archaeological chemistry, this use of AAS, in concert with modern multivariate statistical analysis, discriminated three different locations of manufacture that could reasonably be correlated with cultural behavior of the groups responsible for the ceramic assemblages.

To achieve the temperatures necessary for viewing elements with analytical wavelengths below 250 nm spectrometers is beyond the capacity of chemical flames such as those of air/nitrous oxide and acetylene (Ure 1991). To achieve these temperatures, radiofrequency plasma sources have been developed where the plasma flame is produced (induced) by a high-energy radio source, e.g., “inductively coupled plasma” or ICP. With flame temperatures of 4000–10,000 K, emission spectra of elements lying below 200 nm are achieved.

LeBlanc (2001) reviews current solid-sample methods approved by the US Environmental Protection Agency (EPA) that involve acid digestion-extraction for 30 analytes from solid-phase samples. He discusses five so-called “dilute-and-shoot” methods of sample preparation for AA or ES analytical systems. These are:

1. Soxhlet extraction (EPA 3540C): Used for over 100 years, this technique uses a porous cellulose thimble with the solvent, below its boiling point, to digest the sample over a 16–24 h period at four to six cycles per hour.
2. Automated Soxhlet extraction (EPA 3541): This procedure has a higher cycle time—every 2 h, yielding more samples for analysis.
3. Pressurized fluid extraction (EPA 3545): Sample cell is loaded with solvent and constant heat and pressure applied. The cell is flushed with clean solvent and then purged with nitrogen gas yielding the extract/analyte. This method has the advantage of producing samples at a rate of every 10–20 min.
4. Microwave extraction (EPA 3546): The sample is sealed in the extraction vessel with the solvent above its boiling point. It compares in speed to EPA 3545 and has a performance comparable to the Soxhlet method.
5. Ultrasonic extraction (EPA 3550C): The solvent and sample are exposed to ultrasound for 2–3 min and centrifuged. It does not compare well with the Soxhlet method in terms of analyte extraction. Extraction of analytes from paleosol samples is not very thorough.

The vaporized/atomized sample is injected, with a carrier gas, such as argon, and the particle atom experiences ionization as well as excitation. Excited atoms emit photons proportional to the atom’s electronic structure and the energy it experiences. Because of the high temperature in the central plasma flame, high ionic-excitation emission occurs. As noted in Chap. 8, Rychner and Kläntschi (1995) have used ICP-AES to good purpose in a comprehensive study of bronzes from the Middle and Late Bronze Ages. In 941 spectrometric analyses, the researchers, using 11 metallic elements, were able to address questions of copper technology, typology, and provenance for these Swiss finds. Linderholm and Lundberg (1994) utilized ICP-AES in their attempt to characterize archaeological soils using 12 elements. ICP is a much faster technique than AAS, being capable of multielement analyses, whereas AAS is not. To achieve multielement analytical speed while gaining the detection sensitivity of graphite furnace AAS, ICP was combined with the mass spectrometer. Before discussing the ICP-MS and its variations, we are best served by first discussing mass spectroscopy.

8.9 Mass Spectroscopy

Positive ions in an electrical discharge are repelled from the anode toward the cathode as noted by the discoverer of “positive rays,” Sir J.J. Thomson in 1913. Francis W. Aston, in 1919, invented the principle of the modern mass

spectrograph where positively charged particles (ions) are placed in a varying electrical potential and thus accelerated through the magnetic field (H). The ions curve according to their respective masses according to the relation:

$$R = mv/eH$$

where R is the radius of the curvature, m is the mass of the ion, e the charge, and v is velocity. In gas source instruments, the ions strike targets called Faraday cups, and their incidence and mass are measured and displayed. Today, software allows a rapid display of the masses and their amounts such as the important isotopes of carbon— ^{12}C , ^{13}C , and ^{14}C . Isotopes are nuclides with differing atomic masses of the same element such as the carbon isotopes just mentioned. They differ in the number of neutrons present in the nucleus while the proton or atomic number, Z , remains the same.

Mass spectroscopy is an analytical technique that provides both qualitative and quantitative data on the elemental and molecular forms of inorganic and organic materials. If the material can be readily vaporized then mass spectroscopy can directly detect molecular weights from single digit values to those of six figures typical of the complex organic varieties. As a quantitative tool, it can evaluate concentrations at the ppm level. The real value of the mass spectrometer is its ability to resolve particles of differing masses, a property termed resolution.

The early mass spectrometers and, indeed, most analytical types are based on the separation of mass by magnetic fields. The modern Nier type of mass spectrometer, developed by Alfred Nier in 1938, consists of three parts—a source of a positively charged ionic beam, a magnetic analyzer, and an ion collector. By varying the magnetic field or the accelerating voltage, one can generate a mass spectrum consisting of a series of peaks and valleys where the respective peaks represent an isotope whose abundance is proportional to the peak height (and area). A common variant of this design is the 60° magnetic sector mass spectrometer used in stable isotopic studies of elements such as hydrogen, carbon, oxygen,

nitrogen, and sulfur. For heavier masses, the double-focusing thermal ionization mass spectrometer (TIMS) is used. These instruments are also termed “gas-source” (carbon/oxygen isotopes) and “solid-source” (strontium) mass spectrometers.

Two non-magnet instrument designs commonly found in today’s labs are (1) the quadrupole mass spectrometer and (2) the time-of-flight mass spectrometer. The quadrupole MS uses four electrodes or poles, hence the name, to produce an oscillating magnetic field wherein the ion, if the mass and the oscillatory frequency are compatible, will pass through to the detector without any deviation. The quadrupole mass spectrometers are smaller than the larger magnetic sector designs and generally cheaper. They do have the resolution of the conventional designs but not the accuracy or precision. The time-of-flight designs (TOF-MS) likewise do not use large magnets to separate the charged ionic particles. The time-of-flight MS separates the ions by differences in their velocities after they leave the acceleration chamber. This type of mass spectrometer is a configuration more and more used in geochemical analyses—the SIMS or secondary ion mass spectrometer. This instrument uses the velocity of the secondary ions, ejected from the surface of a sample, which is indicative of their respective masses, in determining their arrival times at the detector. TOF-SIMS has large mass detection range. Patel et al. (1998) have used TOF-SIMS in the surface analysis of archaeological obsidian to determine its utility in determining weathering profiles as a substitutive for light microscopic measurement used in hydration dating. Perhaps, most importantly, the SIMS-MS and TOF-MS units, in concert with high-resolution TIMS and SHRIMP (Super High Resolution Ion Microprobe), can rapidly assess the isotopic lead ratios and amounts of uranium and thorium—a “revolution” (Stos Gale 1995) in uranium series disequilibrium dating. Unfortunately, SHRIMP instruments remain somewhat limited in their distribution and it is sometimes difficult to access these facilities as a consequence (Fig. 8.7).

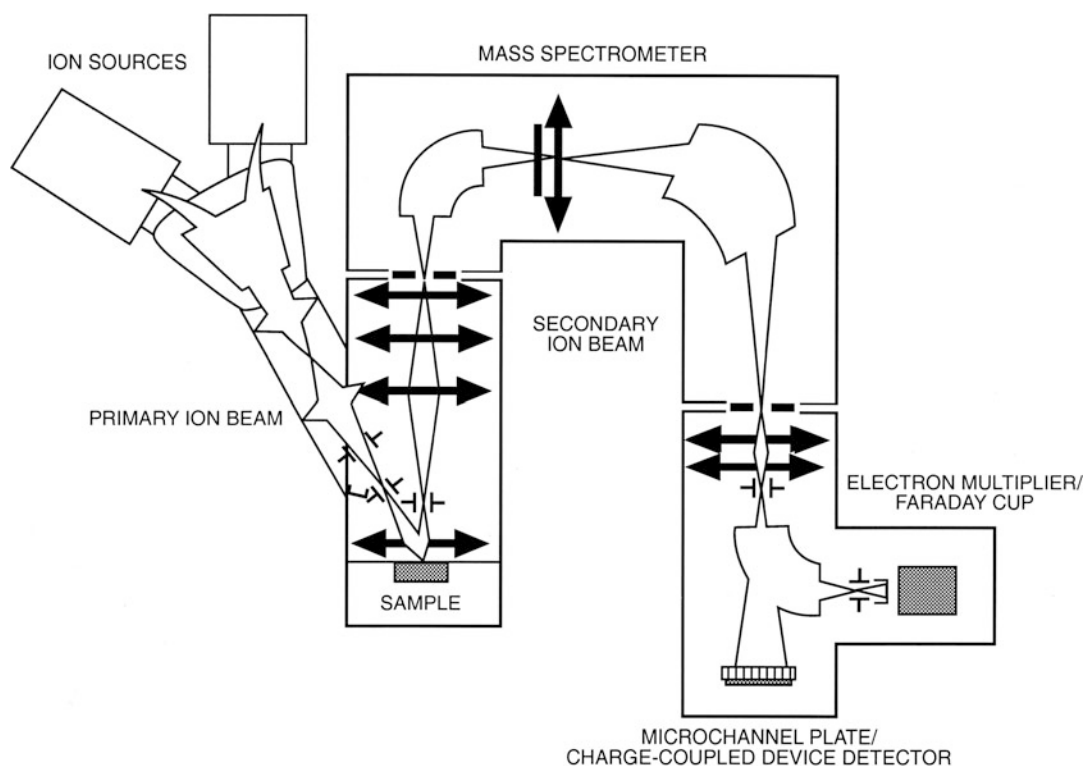


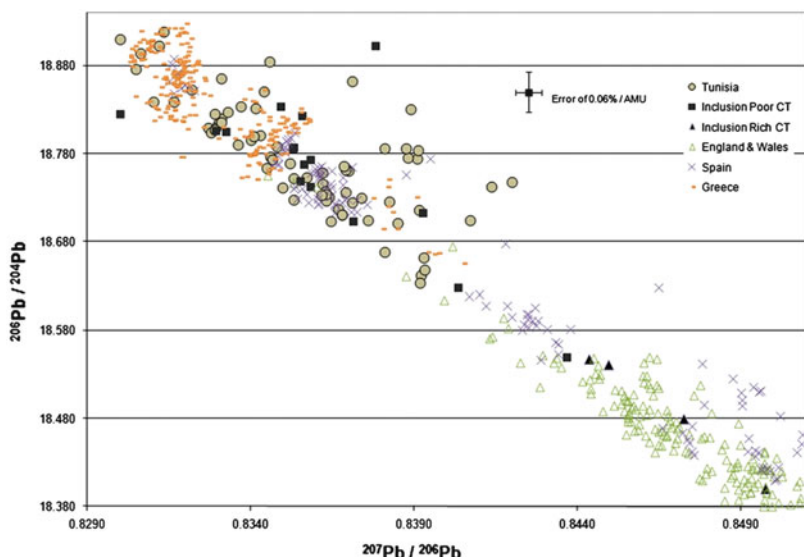
Fig. 8.7 Schematic for a modern thermal ionization mass spectrometer (TIMS)

Thermal ion mass spectroscopy or TIMS remains a standard method for the analysis of heavy isotopes such as rubidium (Rb), strontium (Sr), and lead (Pb). Skaggs (2007) and Skaggs et al. (2012) examined Roman lead curse using thermal ionization mass spectrometry (TIMS) analysis of lead isotopes and EMPA X-ray mapping for arsenic, antimony, copper, and silver. A total of 96 Roman lead curse tablets from Carthage, Tunisia, were screened with EMPA and 20 selected for TIMS to determine the ore sources of the lead used to manufacture the tablets. EMPA narrowed the sample of curse tablets to those most likely produced from Tunisian ores. Comparing the lead isotope ratios of 12 of the 16 tablets most likely to be made of Tunisian lead to samples of Tunisian ores suggests that the Romans were mining lead in Africa Proconsularis and were not relying solely on imports (Fig. 8.8).

A new analytical instrument design pairs the Nier-type MS with gas chromatography (GC) (Robinson 1995). Chromatography analysis,

while not treated in depth here, is a proven and powerful analytical technique for organic macromolecules of archaeological provenance such as residues on prehistoric vessels and even those purported to be the blood residues of butchered animals on ancient tools (Malaniney et al. 1999; Charters et al. 1993; Loy and Hardy 1992). The GC-MS Nier-type systems have the advantage, in resolution, over quadrupole designs and, when coupled with a pyrolysis furnace for sample combustion, permit the rapid analysis study of samples that can be readily done at well below microgram levels. The GC has been coupled to the Fourier transform infrared spectrometer (FTIR) as well. This device provides a rapid approach to characterizing complex mixtures. An interesting avenue of study in regard to the GC-MS systems is the splitting out of carbon and other light stable isotopes for later analysis in AMS systems. The realization of the last method has been difficult given the need for microgram quantities in AMS machines and the much smaller samples typically produced in GC studies.

Fig. 8.8 Lead isotope ratios of lead curse tablets and those of potential ore sources in Greece, England, Spain, Tunisia, and Wales (figure 5, Skaggs et al. 2012, p. 980)



Isotopic analysis of the lighter elements—hydrogen, carbon, oxygen, and nitrogen—in both rock and organic samples is done using a gas source, magnetic sector mass spectrometer. Because elemental and isotopic differences exist in food chains of both marine and terrestrial organisms, the isotopic analysis of inorganic and organic constituents of bone can provide a record of long-term dietary intake. The isotopes of choice in these types of archeological studies are carbon and nitrogen. The carbon isotopes of ^{12}C and ^{13}C allow us to evaluate the metabolic paths of the two photosynthetic classes of plants—C3 and C4. The C3 plants include all the trees, shrubs, and grasses from temperate and forested environments, while C4 plants are grasses from the subtropics and include maize. Important C3 grasses are the wheats and other cereal grains domesticated in antiquity. C3 plants tend to have more reduced (or negative) carbon isotopic values compared to those of the C4 plants, e.g., -26.5 ‰ versus -12.5 ‰ (Van der Merwe 1992). Although significantly fractionated in an organism, these isotopic ratios track in relatively predictable proportions such that an animal or human consuming these plant types will exhibit values that have direct dietary implications.

Workers like Van der Merwe, Price (1989), Sealy and Van der Merwe (1985), and others

have demonstrated the mass spectroscopic analysis of carbon, nitrogen, and strontium isotopic ratios that can differentiate the types of foodstuffs being consumed by ancient populations—both terrestrial and marine resources. Beyond paleodiet, studies of paleoclimate have benefited from the evaluation of oxygen isotopes in marine foraminifera which act as proxies for sea surface temperature (SST)—the heavier ^{18}O is enriched in colder climates (SST $<20\text{ }^{\circ}\text{C}$)—by the preferential evaporation of the lighter ^{16}O isotope. Herz (1987) had basically reinvented the field of marble provenance by using carbon and oxygen isotopic ratios in the study of marbles. A student of Herz's has continued these isotopic studies in a comprehensive study of the Pentelic quarries of Athens (Pike 2000).

8.10 Aphrodite? An Example of Isotopic Analysis Using Mass Spectroscopy

The National Gallery of Art (NGA) possesses an Aphrodite whose pedigree is, as is true of most of her sister replicas, shady (Fig. 8.9). According to Allison Luchs, Associate Curator of Sculpture, when first acquired, the Museum was told that

the earliest known owner of the torso acquired it as a Greek work. If true, then this Aphrodite should be Hellenistic in age and was exhibited as such for many years. However, the curators were doubtful about such an assignment. While very similar to examples in the Metropolitan Museum of Art in New York and in the Uffizi stylistically, a slightly narrower waist and fuller breasts implied a post-Greek age. Small holes in one arm suggested a pointing technique was used in the sculpture's manufacture, which if true makes the statue no earlier than 1790. As a result of these concerns, the official attribution of the work was changed over the years, from Greek to "possibly" Hellenistic or Roman.

The NGA Aphrodite was a perfect candidate for isotopic analysis. If its marble turned out to be Greek, then it could very well be Hellenistic. However, if the marble came from an Italian Carrara quarry, then it could not be Greek but had to be post-first century BC of any age up to today. Stable isotopic analysis showed a good match with Carrara, possibly from the Miseglia marble quarries, and similar to that found in Italian Renaissance and later works. While this information rules out a Hellenistic origin, it makes a Roman or later provenance almost certain. Since most Aphrodites in other museums are generally considered to be Hellenistic based on documents of acquisition or stylistic grounds, they were considered to be excellent candidates for isotopic testing.

Isotopic analysis provides three tests for falsification of classical marble. The standard procedure to follow for testing is as follows:

First, determine the quarry source of the marble by any standard geochemical method including isotopic signatures. Then compare its claimed archaeological date to the known time of operation of the quarry (Herz 1987). Thus, a third C. BC Hellenistic head cannot be made of Roman Carrara marble which was only quarried during and after the first C. BC. Second, for repaired marbles or a pastiche, the principal pieces including the head should be from the same quarry source, preferably the same block of marble (Wenner and van der



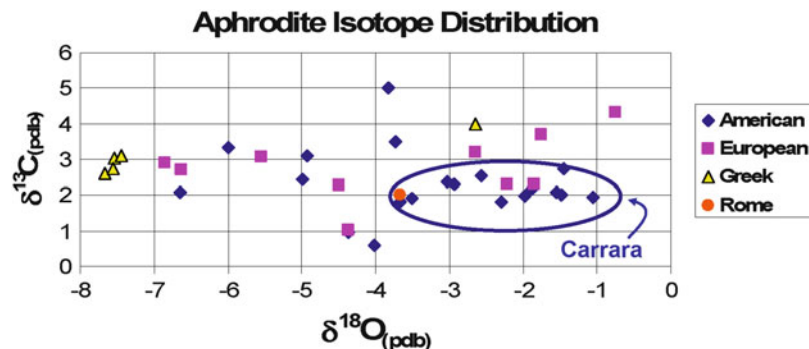
Fig. 8.9 National Gallery of Art, Aphrodite

Merwe 1987). The isotopic variation within a marble block of several cubic centimeters is small, under a few tenths per mil which allows correlations of broken fragments.

Third, compare the isotopic signatures of the weathered marble surface to those of the fresh interior (Margolis 1989). Although classical marble statuary has been copied, and much has been copied many times, a natural weathering patina cannot be falsified.

Mediterranean white marble varies isotopically from -1‰ to $+6\text{‰}$ for $\delta^{13}\text{C}$ pb and

Fig. 8.10 Distribution of isotopes for various Aphrodites relative to known isotopic fields for ancient Mediterranean marble quarries (Herz and Pike 2005)



from -11‰ to $+1\text{‰}$ for $\delta^{18}\text{O}$. Meteoric water around the latitude of the Cyclades is $\delta^{18}\text{O} \sim -32.4$ and ocean water is $\delta^{18}\text{O} \sim -29.47\text{ ppb}$ (Faure 1986). These strongly negative values indicate that any process of weathering in the region should lead to lower $\delta^{18}\text{O}$ in the patina of naturally weathered statuary but no great change in $\delta^{13}\text{C}$ unless there is also a change in the mineralogy of the patina compared to the fresh marble interior.

The National Gallery of Art's Aphrodite had been labeled Hellenistic, as are most of the Aphrodites scattered in museums worldwide. After testing revealed it was made of Carrara marble (Fig. 8.10), its official attribution was changed from Greek to "possibly" Hellenistic or Roman.

8.11 Inductively Coupled Plasma: Mass Spectroscopy (ICP-MS; LA-ICP-MS)

The "marriage" of the ICP to the mass spectrometer has produced one of the most versatile analytical instruments for use on archaeological problems (Speakman and Neff 2005). By combining the ICP's high ionic efficiency, almost 100 % for most elements of the periodic table, and low incidence of doubly charged ions (a problem with other conventional MS), with quadrupole and magnetic sector mass spectrometers, the mass spectra are relatively simple and elements and their isotopic ratios can be straightforwardly determined. For example, a 20 ms scan covers

the entire mass range of the periodic table with a sensitivity (0.1–0.2 ng/g) comparable to AAS. The mass spectrometer becomes the detector for the ICP (Fig. 8.11). The greatest advantage of the ICP-MS is that it can be used to analyze *both* metals and nonmetals. Kennett et al. (2001) have termed the increasing use of the ICP-MS as a "revolution in archaeological provenance studies."

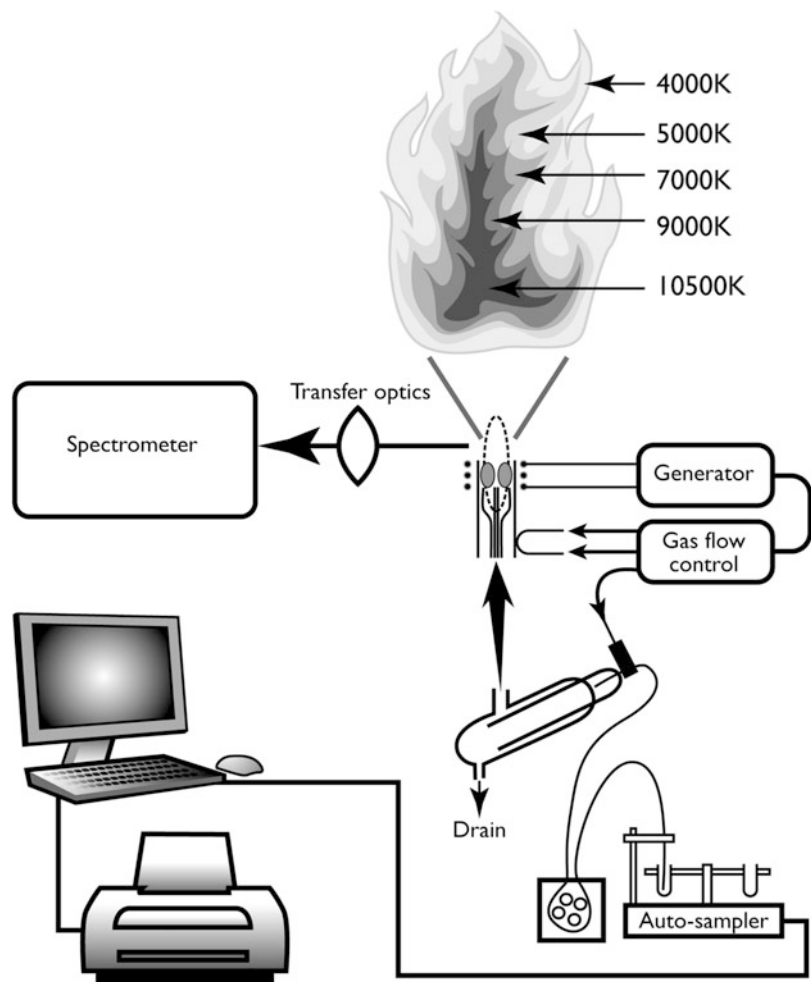
A recent variation of the ICP-MS is the Laser Ablation ICP-MS or LA-ICP-MS (analytical terminology is almost as replete with acronyms as that for computers!). The laser ablation ICP-MS was first developed in 1985 with several custom-built units operating in 1991. By using a laser such as the Nd-YAG type, small ($\sim 50\text{ }\mu\text{m}$) ablation pits can be drilled into sample surfaces with the vaporized ions entrained in an argon gas flow and thence to the quadrupole or magnet-type MS. The ICP-MS can rapidly assess 70 about elements at the ppb level (Kennett et al., *supra*).

The key to the ICP instrument, as we have seen, is the RF inductively coupled flame which will ignite nebulized liquid sample, mixed with argon gas, that has been injected into it (Fig. 8.12). The torch burns at $8000\text{ }^{\circ}\text{C}$ and ionizes the sample into a plasma. The ionized gas is injected into the mass spectrometer. In the quadrupole instruments, rapid alteration of the voltage across the pole rods allows the transmission of elements of differing mass/charge ratios. In the magnetic sector instruments, the plasma ions enter a curved flight tube where they are separated by their mass/charge ratios. The ion beam can be tightly focused in these instruments allowing discrimination of masses

as close as 0.0001 atomic mass units (amu) (*supra*). Laser ablation ICP-MS has been used in the characterization of Egyptian basalt quarries by Greenough et al. (1999) together with the elemental analysis of clays of Egyptian ceramics (Mallory-Greenough et al. 1998a, b) as well as other materials (Gratuze et al. 1993). An attractive feature of the laser ablation instruments is their relative nondestructive nature, providing one can get the sample beneath the laser. In most cases, this is possible. Compared to the nebulized or otherwise digested samples, the artifact remains relatively undamaged (typical damage pits, etched by the laser, are only tens of microns in diameter (Jarvis et al. 1992)).

Glasscock et al. (2007) raise the question of LA-ICP-MS being the answer to *in situ* bulk analysis of ceramics and their answer is “no.” They correctly point out that laser ablation is basically a microprobe analytical procedure. Because of the heterogeneity of pastes (and clays, in general), sampling becomes a real issue when attempting to characterize a ceramic vessel (*supra*). LA-ICP-MS does show real promise in the analysis of pigments and glazes. Additionally, it has yet to be demonstrated that LA-ICP-MS data has long-term replicability to generate large compositional data sets together with the issue of interlaboratory comparability of such data sets. LA-ICP-MS does not have the long-term track record (over three decades) for

Fig. 8.11 Schematic of an inductively coupled plasma (ICP) spectrometer



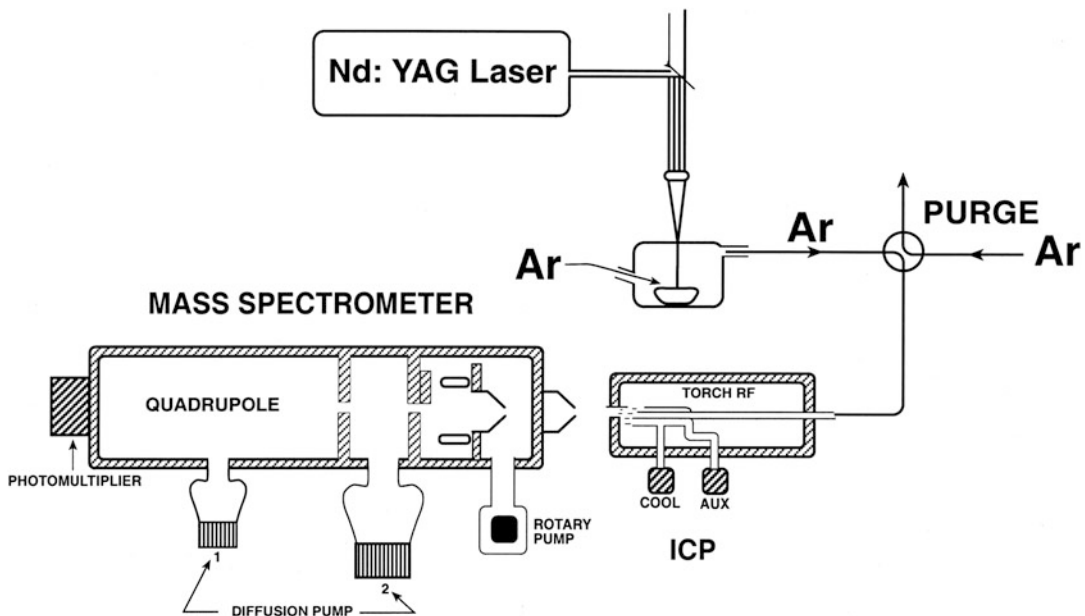


Fig. 8.12 Schematic of a laser ablation inductively coupled mass spectrometer (LA-ICP-MS) system

a technique like NAA in this regard. Glasscock et al. (*supra*) conclude that while the proliferation of ICP-MS, in general, has resulted in many excellent compositional studies (Speakman and Neff 2005), NAA remains the best analytical method of choice.

8.12 Neutron Activation Analysis (NAA/INAA)

Neutron activation can be used to determine either the absolute or the relative quantities of specific isotopes present in a sample. In practice, it is a simple matter to calculate the weight of the element being determined in the sample from the relationship:

$$\begin{aligned} \text{Weight of element in sample } \mu\text{g/g} \\ = \text{ weight of element in standard } \times C_r/C_s \end{aligned}$$

where C_r is the observed counting rate of the sample, and C_s that of the standard, measured under comparable conditions.

Nuclear reactions caused by neutrons are of interest in archaeological geology and geochemistry because such reactions are used for

analytical purposes to measure the concentrations of trace elements in both archaeological and geological materials. Neutrons produced by fission of ^{235}U atoms are emitted with high velocities and are called “fast” neutrons. For a controlled reaction, the fast neutrons must be slowed down because the fission reaction requires other than “fast” neutrons. Slowing down neutrons requires a “moderator” such as water or graphite with which the fast neutrons can collide without being absorbed. Ordinary water typically serves this purpose in the so-called swimming pool reactors.

Slow neutrons are readily absorbed by the nuclei of most of the stable isotopes of the elements. The neutron number of the product nucleus is increased by 1 compared with the target nucleus, but Z remains unchanged, so the product is an isotope of the same element as the target. The product nucleus is left in an excited state and de-excites by emission of gamma rays. The absorption of a slow neutron by the nucleus of an atom can be represented by the following equation:

$$X_Z^A(n, \gamma) Y_Z^{A+1}, \text{ for example, } ^{35}\text{Cl}(n, \gamma)^{36}\text{Cl}$$

The products of (n,γ) reactions may be either stable or unstable. Unstable nuclides produced by neutron irradiation are radioactive and the product nuclides decay with characteristic half-lives. As a result of slow-neutron irradiation, a sample composed of the stable atoms of a variety of elements produces several radioactive isotopes of these “activated” elements. This induced activity of a radioactive isotope of an element in the irradiated sample depends on many factors, including the concentration of that element in the sample. This is the basis for using neutron activation as an analytical tool.

In routine laboratory practice, neutron activation involves (1) the irradiation of some sample with neutrons to produce radioactive isotopes; (2) the measuring of the radioactive emissions from the irradiated sample; and (3) the identification, through the energy, type, and half-life of the emissions, of the radioactive isotopes produced. Irradiation of a sample with neutrons is carried out with one of three types of neutron sources—reactors, accelerators, and radioactive sources. Neutrons produced in nuclear reactors represent the strongest source of neutrons in the sense of producing the most induced radioactivity in the sample. In this case, the sample is directly inserted within the reactor. In the other two types of neutron sources, very often, the radioactivity induced, within a sample, may be too weak to measure when produced by neutron bombardment in ways other than nuclear reactors. The least desirable technique for neutron irradiation is through the use of radioactive sources. Radioactive sources such as Californium do emit neutrons, but others produce alpha particles that are absorbed by materials wrapped around the source to produce neutrons.

The stronger the neutron source, therefore, the more isotopes will reach a detectable level of radioactivity. The measuring of radioactive emissions from the irradiated sources almost always involves the detection of the gamma radiation from the sources. There are two reasons why gamma rays are used. Firstly, of all the radioactive emissions, gamma rays are the least influenced by the structure of a material. A sizable fraction of the gamma rays, which escape

the radioactive material, usually do so with their energy unchanged. Secondly, since gamma rays are emitted in monoenergetic groups, gamma energies can be used to determine the isotope which has emitted them. The half-life of the nuclide, which emitted the gamma rays, serves as an additional check on the radioactive isotope created by neutron bombardment. The gamma rays are detected and displayed using devices called gamma-ray spectrometers, which exhibit the energies of the detected gamma rays as a series of peaks. The spectrum is calibrated by use of an energy-versus-intensity plot made with reference to gamma rays of known energy. These spectra have a tendency to have relatively sharp peaks, which correspond to gamma ray absorption in the detector through the photoelectric effect. These sharp peaks are usually superimposed on and/or interspersed with relatively broad peaks, which result from scattering of gamma rays through the Compton Effect. Few, if any, investigators use the Compton peaks for interpretive work. Most work is done with the relatively sharp photoelectric peaks, which will be spread along the energy spectrum. The height of the photoelectric peak, if it is not superposed on the broad elevated background energy caused by Compton scattering, is directly proportional to the intensity of the radioactivity of the isotope that produces the peak. The photopeak plot can still be used in quantitative analysis but is less sensitive because of the presence of background.

Generally, more than one gamma-ray energy spectrum is taken at successive periods of time, which are on the order of the half-life of the radioactive isotopes expected. In successive spectra, some series of peaks diminish in height faster than others and in a manner predictable from the half-life of the isotope producing the particular gamma rays. Good examples of this are the isotopes of metallic elements typical of ancient coinage such as silver (Ag) and copper (Cu). Typical isotopes of copper are ^{64}Cu and ^{66}Cu , and those of silver are ^{108}Ag and $^{110\text{m}}\text{Ag}$. For example, silver-108 has a half-life of 2.4 min while silver-110m's is 253 days. Their respective gamma ray energies are 636 KeV (^{108}Ag) and

412 KeV (^{110m}Ag). NAA, like ICP, requires very little of the artifact, mg-level amounts as a rule, to do the analysis. In this regard, NAA can be considered “nondestructive.”

8.12.1 Provenance Determination

Provenance studies involve characterizing and locating the natural sources of the raw materials used to make artifacts of clay, stone, and metals and thus establish the pattern of trade and exchange (Tite 1992). For ceramics, the use of neutron activation analysis began early on with pioneering work done by Edward Sayre and, later, with his colleague Garmon Harbottle, at Brookhaven National Laboratory, in the United States (Sayre and Dodson 1957; Harbottle 1976). For most elements, the ratios of stable isotope abundances are invariant. The relative abundances of elements found in a particular sample are a function of where the sample is found. This makes the identification of prehistoric ceramics and trade goods, such as flint and obsidian, by element composition possible (Bishop 1992; Glasscock 1992; Hoard et al. 1992; Glasscock et al. 1994, 1996; Ambroz et al. 2001, Descantes et al. 2001). Tykot (1996) asserts that NAA, together with XRF, and increasingly ICP have proven the most successful in determining sources of obsidian.

Ceramic sourcing involves the definition of compositionally homogenous samples of unknown origin (Arnold et al. 1999). The pottery of a particular group of people can be traced through the location of the source of clay used for the pottery and determination of the trace elements in that clay. This is at the heart of what is called “the provenance postulate” which assumes groups of homogenous pottery samples, of unknown origin, represent geographically restricted sources (*supra*). However, inclusion of temper in the clay before firing might vary the trace elements characteristic of the clay deposit itself. Even when inclusion of temper creates a problem in variation of trace elements of the clay deposits, the temper might itself be characteristic (cf. Greenough, *supra*). The

elemental composition of the temper, if sufficiently specific to a particular group, might then serve as a marker of that group regardless of where the clay was obtained.

The digestion and removal of tempering materials, such as shell, can be done using relatively weak acids without altering the bulk composition of the ceramic clay. If this is done, the neutron activation of the clay can address the question of the clay source without the interference of extraneous, non-source minerals introduced by the temper. Whatever the specific sample preparation, the application of NAA in ceramic studies has been legend and immensely productive for archaeology. In a recent study of Mayan ceramics, the authors conclude that “Clearly, NAA ‘works’ in differentiating production communities that use discrete source areas” (Arnold et al. 1999). In numerous other preceding studies, the same can generally be said of the success of NAA as a technique for the study of archaeological provenance.

8.13 An Example of Neutron Activation Analysis: Coinage and a Celtic Mint: The Titelberg, Luxembourg

The Titelberg is a massive flat-topped mountain of Jurassic limestones and clays, which stands 100 m above the Chiers River’s course in southwestern Luxembourg. Atop this mountain, a tall rampart, up to 9 m high at present, typical of *oppida*, enclosed a 50 ha settlement, most famous for its Augustan and Imperial Gallo-Roman remains including extensive metallurgical evidence of foundries for the production of coinage—a mint. The Titelberg is commonly regarded as being the main *oppidum*, or fortified town, of the Treveri.

Since coins normally attributed to the Treveri are found in the pre-mint-foundry levels, at the site, obviously these are not the oldest of the Treveran mints. The mints themselves provide affirmation that Allen’s and Nash’s contention that the bulk of bronze Celtic coinage came

after the Roman Conquest applies to this part of Gaul (Allen in Nash (ed.) 1980).

Ceramic coin molds have long been known as a common find in Iron Age *oppida*, but rarely has the structure in which coinage manufacture took place been identified. One of the few such finds is a middle La Tene village cellar in northern Champagne at Celles-les-Conde (Aisne), France, and may have been the workshop of counterfeiters rather than an official mint. Thus, the virtually unique identification of a structure as a Celtic mint north of the Alps gains added significance from the fact that a number of mint foundries from different times have been uncovered, here, making it possible to follow the onset and development of coinage at the Titelberg. Among the coins recovered are a silver “seated person” coin, a Republican Roman coin of 155–133 BC, and a coin showing a person with dressed hair, in the bottommost layer of the house cellar.

The lowest-lying Gallic coin is the type depicting confronted wild boars.

The Dalles House saw the greatest production of coin flans, to judge from the fact that 16 % of the 1179 coin molds recovered were found in this level. An iron nozzle of a bellows was still in place at the bronze-smelting pit (Fig. 8.13). The Dalles (House) Floor dates to the Early Augustan Period of 30 BC–1 AD by both dendrochronology and by artifact typology (Rowlett et al. 1982). The Dalles Floor of the mint foundry measures somewhat wider than the Foundation House, and one of its fireplaces lay farther to the north (Fig. 8.13). Another fireplace was in the middle of the rather narrow early cellar at the south end of the building. Both fireplaces had clay linings as did an outside fireplace built up of dry stone walling, found much collapsed, which apparently served as a baking oven at the end of the SE corner of the cellar. In any case, this exterior fireplace was virtually devoid of the numerous fragments of slag and metal droplets and coin molds so common in these buildings and most frequent in the Dalles Floor mint.

The author analyzed several coins and coin mold fragments (Fig. 8.14) from the Dalles

Floor using neutron activation analysis (NAA) (Garrison et al. 1977) (Table 8.2).

The focus of this study was to assess the efficacy of NAA as a means of detecting and characterizing metals used in the minting process. The mold fragments were the primary items analyzed because of their sheer number in relation to the much fewer coins or coin blanks recovered at the site. Less than a dozen coins were included in the analysis.

The assay of the coins and molds using NAA demonstrated the method’s efficacy in detection of metal type using the isotopes of silver, gold, copper, zinc, and tin (Table 8.4). The challenge was greater in the case of the molds because of the lack of any obvious macroscopic evidence for metal. The ten coins were examined, parsed as six and possibly a seventh being copper based with three being silver based. The rubbings of 14 mold fragments were divided into one set of six samples taken within the “holes” and a set of eight samples from the “sides.” Of those six rubbings taken within the holes, only two samples produced evidence of metal—15.0; 22.2 $\mu\text{g/g}$ of Ag. No samples from within the holes produced evidence for copper. The samples from the mold sides were basically negative with only one sample producing evidence for metal—Cu—in the amount of 10.7 $\mu\text{g/g}$.

Six scrapings taken from within (4) and without (2) the holes produced consistent evidence for metal coinage. Oddly, only noble metals were detected with absolutely no evidence for copper.

In the four scrapings from within holes, the Au/Ag ratios and total amounts were largely consistent with amounts expected for Augustin Period coinage. The highest amounts measured, in Au/Ag ratio amounts, were 172:84.5 and 349:252. The ratios for the other two hole scrapings were 13:6.5 and 18:19.5. The two samples of scrapings from the sides of molds produced ratios of only 3.7:5.8 and 3.9:6.2. While scrapings and rubbings produced evidence for the presence of metal, scrapings were, by far, the more effective means of adequately determining metal type and amount, yet, even there, the results are not entirely definitive. A more

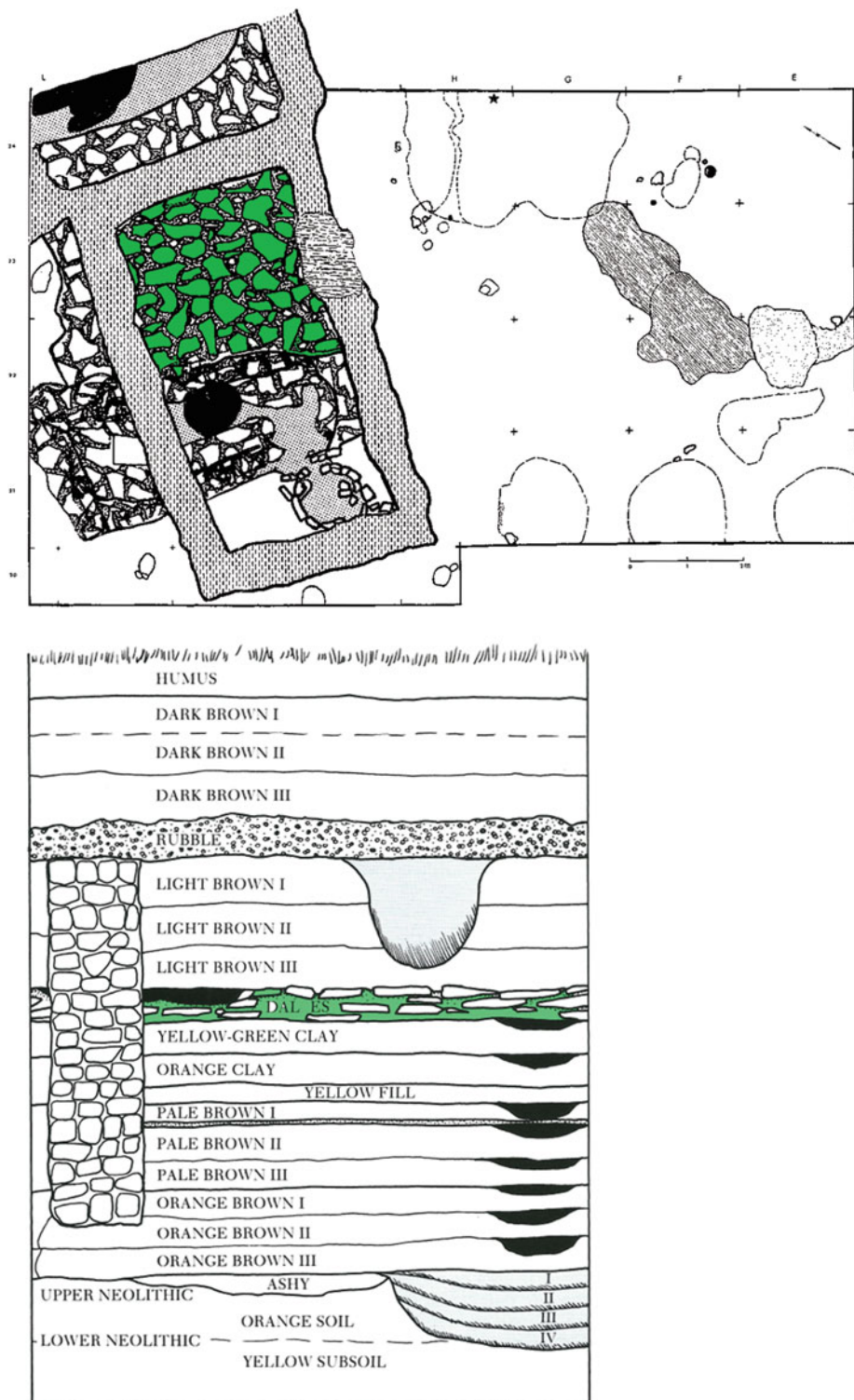


Fig. 8.13 *Upper*, plan of Dalles Floor (green); *lower*, Dalles Floor (green) in stratigraphic section

Fig. 8.14 Coin mold fragments and coin flans from the Dalles Floor, Titelberg

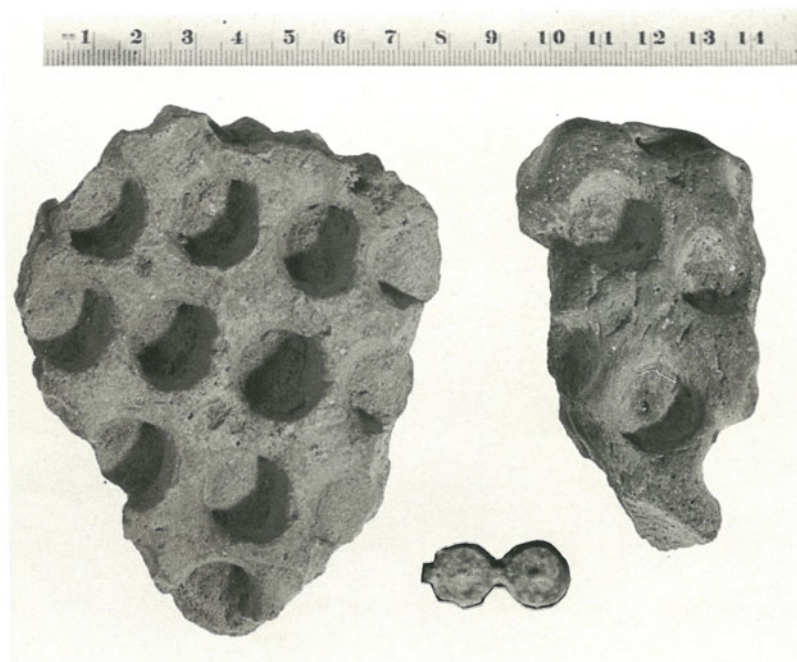


Table 8.2 Isotopes utilized in NAA analysis of coins and molds from the Titelberg

| Element | Isotope half-life ($t^{1/2}$) | Energy of gamma-ray (keV) |
|--------------------|---------------------------------|---------------------------|
| Silver (AG) | 253 days | 412 |
| ^{110}Ag | | |
| Silver | 2.4 m | 636 |
| ^{108}Ag | | |
| Gold (Au) | 2.7 days | 412 |
| ^{198}Au | | |
| Copper (Cu) | 5.1 m | 1039 |
| ^{66}Cu | | |
| Zinc (Zn) | 13.7 h | 439 |
| ^{69m}Zn | | |
| Zinc | 243 days | 1115 |
| ^{65}Zn | | |
| Tin (Sn) | 9.5 m | 325 |
| ^{125m}Sn | | |
| Tin | 245 days | 55 |
| ^{119m}Sn | | |

comprehensive study using many more of the over 1100 mold fragments would surely produce a more complete picture of both adequacy of this procedure for assessing Gallo-Roman minting technology.

Molds from strata Light Brown I and II are both dated to the Augustin Period. The relatively high Au/Ag ratios are consistent with Roman coinage of this period. These results were not consistent with a later study of mold fragments from the sites of Villeneuve-St. Germain and Mont Beuvray (Bibracte) (Chevallier et al. 1993) where X-ray fluorescence was used to basically do a qualitative “presence-absence” of coinage metals. The detection limits of that instrumentation resulted in largely negative results demonstrating the need for the use of more quantitative procedures such as NAA or ICP.

8.14 Electron Spin Resonance (ESR)

Stern and Gerlach, in a landmark experiment, demonstrated that the electron has the property of spin. As such, it has a component known as the spin angular momentum. The spinning electron behaves like a small bar magnet or magnetic dipole in that it has a magnetic moment defined as:

$$W = - : \cdot H$$

Here μ is the magnetic permittivity (also referred to as permeability) and H the external magnetic field strength. If an orbital shell is unfilled, it will have unpaired electrons in any subshell for which $L \neq 0$. A free atom or ion will have no orbital magnetic moment if it has no resultant spin ($S = 0$).

If a sample of free electrons is placed in a magnet and illuminated with microwave photons such that $h\nu$ or $\Delta E = g\beta H$, we have a resonance absorption of energy from the microwave beam as electrons are excited from E_- to E_+ . H is the external field strength as before; β is the Bohr magneton, and Landé g spectroscopic splitting factor or “ g -value” representing the frequency of the rotation of the electron (Ikeya 1985).

Transitions between these Zeeman levels involve a change in the orientation of the electrons’ magnetic moment. In most evaluations, the g -factor contains all the microscopic information that can be obtained from an analysis of the experimental data. Departures from the “free spin” value of g , 2.0023, tell us the species and atomic (crystalline or otherwise) environments within which the unpaired electrons found. Based on this straightforward information, we can rapidly identify elements, of archaeological significance, such as Mn in marbles (Fig. 8.15).

Two other features of an ESR spectrum can also give detailed information on the electron wave function and its environment:

1. *Fine structure*: If the total spin of the system involves several interacting electrons, we may

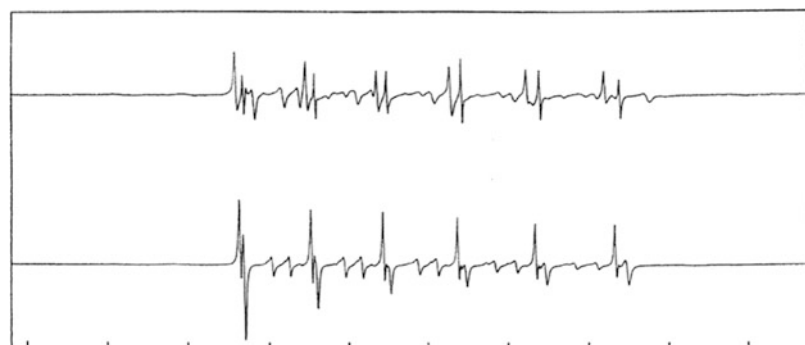
have $*S_z \geq * > H/2$ (but always integral or half integral). Then the interaction with microscopic electric fields can split some energy levels even in the absence of a magnetic field. These electric field splittings can also be measured by ESR and serve, for example, to define the local symmetry.

2. *Hyperfine structure*: If a nucleus with a magnetic moment is in the vicinity of an unpaired electron, the effective magnetic field acting on the electron is the sum of nuclear and applied fields $H = H_0 + H_{\text{nucleus}}$. The quantity H_{nucleus} depends on the possible quantized orientations of the nucleus, S , that each ESR line splits into several components. This can be a valuable diagnostic tool (e.g., in studies of ancient marbles), where the hyperfine spectrum is a direct “fingerprint” of this element thus aiding in differentiating marble facies.

ESR works only on paramagnetic materials—those with unpaired electrons. As we shall see in the following section on magnetic susceptibility, most solids have their electrons in closed (paired) shells and are dia- or non-magnetic as a result. Because paramagnetism is in complete alignment with the magnetic field, the net magnetic moment is significant in most cases.

To induce paramagnetic behavior in a material, it is placed in an ESR spectrometer which is an apparatus with an electromagnet with a sample holder between the poles at the end of a brass microwave (radiation) wave guide. The sample is placed between the magnet’s poles and microwave radiation, at a constant frequency, ca. 9.3 GHz, and a spectrum is “swept” between

Fig. 8.15 ESR spectra of marble showing typical hyperfine splitting of manganese (Mn)



the levels of magnetic field strength, say 100 Hz. Recalling the basic equation for ESR spectroscopy, the sample will absorb the microwave radiation (resonance) at some value of the g-factor.

To date, in archaeology, ESR has been increasingly used, in the last two decades, for dating purposes (Wagner 1998), whereas in mainstream chemical analysis, it has been used for studies of the properties of numerous compounds and materials. In some recent cases, ESR has been used to evaluate heat treatment of flints (Dunnell et al. 1994) and to provenance marbles (Baietto et al. 1999).

8.15 Magnetic Susceptibility

The impression of a magnetic field on a material will induce a magnetic response. The nature of that response is a direct result of the electronic structure of the material's constituent atoms. We have seen that the source of a paramagnetic response, ESR, is the unpaired orbital electrons in the valence (outer) shell of the atom. Diamagnetic magnetism results from the precession or distortion of electronic orbitals in a magnetic field. *All* materials are diamagnetic (Verhoogen 1969). Certain crystalline materials have an overlaps of the electronic orbitals of their constituent atoms. This “coupling” of the orbital magnetic moments results in coupling in either parallel or antiparallel directions producing a strong spontaneous ferromagnetic response such as magnetite. The antiparallel response is found in an antiferromagnetic material. Strong magnetism is observed in ferrimagnetic materials. The response is qualitatively similar to ferromagnetics. The difference between the two is that the magnetic ions in the ferrimagnetic material align more readily in an antiparallel direction. The ferrimagnet's crystalline structure is more complex than the ferromagnet with sublattices that create the parallel or antiparallel magnetic response. The overall response, in an applied magnetic field, is either ferri- or antiferromagnetic depending upon the material. Spinel and garnet are two ferrimagnetic minerals.

To measure magnetic susceptibility, we place the material in the magnetic device—a balance, bridge, or meter. The susceptibility measurement is obtained by measuring the net magnetic moment, I , per unit volume or mass in the applied magnetic field, H . The equation to do this is as follows:

$$I = \kappa H$$

where κ is the susceptibility. For paramagnetic materials, κ is positive. For diamagnetic materials, it is negative; for ferro- and ferrimagnets, it will be strongly one or the other. The magnetic susceptibility measure is dimensionless which means it has no units, it is simply a number. Except in devices like the Guoy magnetic balance, the paramagnetic response will be ferro- or ferrimagnetic, in either modes $-/+$.

The induced magnetism of common ferro- or ferrimagnetic materials is shown in Tables 8.1a and 8.1b. As a general rule, rocks, particularly igneous ones, are more magnetic than sediments or soils. Rocks can range as high as $10^{-1}/\text{g}$ to 1, while sediments are more commonly in the range of 10^{-5} to $10^{-6}/\text{g}$ (cf. Table 9.3).

Magnetic susceptibility measurement devices are the simplest of all magnetic instrumentation. The measurement of magnetic susceptibility, for the study of chemical species in solution, has a long history. The body of magnetic theory that supports these inquiries is some of the better understood principles in recent science. Only recently have earth scientists—geophysicists mostly—and some archaeological geologists have taken an interest in the use of susceptibility as an analytical tool. In the latter case, it is because the magnetic susceptibilities of soils reflect their parentage (Sharma 1997). Soils derived from igneous and metamorphic rocks, notably those of more mafic character, have greater amounts of magnetite and, therefore, appreciable magnetic susceptibilities. Soils of a highly organic nature, as can be found in archaeological settings, can have elevated amounts of maghemite, as can be seen, which is significantly stronger than hematite. Because of the

production of both maghemite and the increase in remnant magnetization due to fire such as hearths and conflagrations (Le Borgne 1960; Mullins 1974), the anthrosol has magnetic variations just beginning to be appreciated in archaeological geology (Marmet et al. 1999).

Tite and Linington (1975) suggested that magnetic susceptibility of anthropogenic sediments and soils could be viewed as a proxy for past climates. Magnetic susceptibility is viewed as a result of paleoclimatic controls such that when pedogenesis is high, as during interglacials, so is magnetic susceptibility (Kukla et al. 1988; Ellwood et al. 1994, 1995). Magnetic susceptibility of Swedish soil catenas has shown a close association of susceptibility with particle size—alluvium showing low values and coarser grained sands and gravels showing higher values (Linderholm 2007). Studies of deep sea sediments have shown a close correlation of magnetic susceptibility to mineralization and grain size as well (Maslin 2000; Kennett and Baldauf et al. 1994; Bond et al. 1993; Seidov and Maslin 1999).

8.16 Cathodoluminescence Microscopy (CL)

Cathodoluminescence (CL) is the emission of photons in the visible range of the electromagnetic spectrum after excitation by high-energy electrons in an electron microscope. CL occurs when a valence electron is excited to the conduction band in a solid and another conduction band electron “falls” into the valence level vacancy with an emission of visible light photo at varying frequencies (Heard 1996; Barbin et al. 1992; Ramseyer et al. 1989). It is an effect coincident with several other forms of stimulated emission such as primary and secondary X-ray emission and secondary and backscattered electrons. The energy difference between the conduction and valence levels, only a few eV, determines the wavelength of the luminescence.

The CL emission spectrum typically lies within the 200–900 nm range.

Beginning in 1965, CL became of interest to geologists. The hot-cathode CL microscope consists of a hot tungsten cathode under a vacuum, the accelerating voltage ranges between 2.5 and 50 KeV, and current densities are between 5 and 10 nA/mm². A monochromator with a spectral range of 350–850 nm is fitted between the cathode and viewing optics. CL microscopy is practiced in two differing procedures: hot-cathode CL and low-temperature CL. To date, the hot-cathode method has been most used in archaeological geology.

In archaeological geologic studies, CL has made its biggest impact in the provenance studies of white marbles. CL studies have divided white marbles into three major families based on luminescent color. Calcitic white marbles have a dominant orange or blue luminescence, while dolomitic marbles show a red luminescence. By combining CL with grain size, texture, and, most important, stable isotope analysis, finer distinctions can be obtained between marbles (Barbin et al. 1991, 1992). The excited mineral, calcite, dolomite, etc., produces different colors of luminescence that originate from various impurities in the crystal lattice. The lattice defect in carbonates, most used for CL, is that of Mn²⁺, zircons with Dysprosium (Dy³⁺) and Europium (Eu²⁺); apatites with Mn²⁺, Dy³⁺, and Samarium (Sm³⁺); and Fluorite Eu²⁺ and Eu³⁺ centers.

The orange luminescence family contains most of the calcitic marbles from quarries such as Mount Pentelikon and Thasos in Greece; Naxos, Paros, and Pteleos in the Cyclades; Carrara and Lasa in Italy; and Dokimeion in Turkey. Blue luminescing marbles are less easy to characterize because the cause of the CL coloration is not established. The blue emission is observed in marbles with manganese present in the calcite at levels below 5 µg/g. Red luminescing marbles are exclusively dolomitic (greater than 50 % dolomite). Representative marbles include those from Carrara, Italy; Marmara, Turkey; and Paros and Naxos, in the Cyclades (see following Table 8.3).

CL can be used to characterize surface texture and composition of minerals in geologic and ceramic materials. Traditional

Table 8.3 CL and other characteristics of selected white marbles

| Locality | Texture | Grain size (min.–max.) | Mineralogy | Cathodoluminescence | | |
|-----------------|-------------------------------------|---------------------------|------------|------------------------|---------------------|-------------|
| | | | | Color | Intensity | Int. distr. |
| Thassos-Aliki | Homeoblastic | 1.4–5.0 | Calcite | Orange | Medium-strong | Homogenous |
| Thassos-Vathy | Slightly cataclastic | 0.4–1.8 | Dolomite | Red | Medium-strong | Homogenous |
| Paros-Stephani | Homeoblastic-weakly porphyroblastic | 0.3–1.5 | Calcite | Dark blue to blue-pink | Faint | Homogenous |
| Paros-Chorodaki | Slightly porphyroblastic | 0.5–3.7 | Calcite | Reddish-brown | Faint-medium | Homogenous |
| Pentelikon | Slightly porphyroblastic | 0.3–1.0 | Calcite | Orange | Faint-strong | Patchy |
| Usak-Kavacik | Highly porphyroblastic | 0.4–2.0 | Calcite | Orange-brown | Faint-strong yellow | Zoned |
| Carrara | Homeoblastic | 0.06–1.3 | Calcite | Orange | Medium-strong | Homogenous |
| Afyon | Porphyroblastic | 0.5–1.4 | Calcite | Orange to blue | Very weak | Patchy |
| Marmara | Porphyroblastic | 0.2–3.6 | Calcite | Blue | Very weak | Homogenous |
| Naxos-Flerio | Porphyroblastic | 0.7–7.5 | Calcite | Orange | Medium | Homogenous |

Adapted from Barbin et al. (1991)

optical microscopes can be fitted with CL stages such that low-voltage electrons are produced which can produce CL in materials under examination. While useful, it is best to use the broader range and higher accelerating voltages produced by SEMs for high-resolution and precise CL measurements. These devices can readily measure both color and intensity rapidly and quantitatively.

Research (Heard 1996; Yacobi 1994) suggests that the combination of CL and other forms of spectroscopy (BSE, EDS, etc.) can provide important information on the composition and uniformity of ceramic materials such as clays, cements, and silicate glasses that readily luminesce. For instance, the temperature of heating or firing can be examined by the presence or absence of CL related to monoclinic phases of oxides such as CaO. Heating to a degree that eliminates the monoclinic phase removes all CL. Additionally, quartz grains, seen in BSE images, of relatively uniform density, have intensities related to grain growth and boundary behavior. Such behavior should be related to phase changes in quartz found in ceramics as either temper or as amendments to the mineral suite used in the particular ceramic such as porcelains.

Picouet et al. (1999) have used CL in the study of quartz, feldspar, and calcite grains in pottery as potential tool for provenance studies—the separation of late Neolithic-early Bronze Age pottery, from archaeological sites in western Switzerland and eastern France. Akridge and Benoit (2001) have examined the CL in chert artifacts from the Ozark Mountains of the central United States. These cherts showed predominately orange CL with an occasional blue CL observed. As chert is principally considered a microquartzite (Gerrard 1991), the CL properties are those of quartz. In a study of geological quartz, Walderhaug and Rykke (2000) suggest that the crystallographic orientation of the quartz grains may have a significant effect on observed CL.

8.17 Infrared and Raman Spectroscopy

Single atoms do not emit or absorb infrared radiation (Goffer 1980, 2007). Molecules absorb infrared frequency radiation in the 2.5–16 μm wavelength range. As a consequence, nearly all molecular compounds show some degree of absorption in the IR part of the electromagnetic

spectrum. It is best used as a qualitative rather than a quantitative technique.

As such, it is the most widely used spectroscopic method for analysis of organic compounds and mixtures. Double-beam IR, NIR (near-infrared), and FTIR (Fourier transform IR) have come to dominate this area of spectroscopy, and as a result of the new chemometric computing methods used with these instruments, the quantitative capabilities have increased dramatically. Field-hardened FTIR units have been deployed at Kebara Cave in Israel (Weiner et al. 1993).

The use of FTIR at the Kebara site illustrates the potential of the use of IR spectroscopy in archaeology. The researchers were able to detect the presence/absence of calcium hydroxyapatite or dahlite—in cave sediments. FTIR was thus able to map the concentrations of bone and to discriminate these areas from those of bone dissolution, due to diagenesis and areas of partial bone preservation (*supra*). As mentioned above, in the section on mass spectrometry, FTIR has been coupled to gas chromatography with potentially interesting results for archaeology.

Shoval and Beck (2005) point to minerals formed during firing such as sanidine, mullite and other the temperature minerals—(cf. Chap. 6) as “fingerprints” in IR spectra for production methods of ceramics. Using FTIR, these authors identified Si-O/Al-O deformation consistent with firing temperatures between 800 and 900° C in Mesoamerican ceramics. Additionally, IR spectra can identify rock and mineralogic inclusions in heterogeneous ceramic samples. Ostrooumov (2009) has created a spectra database of more than 250 different mineral and stone materials for use in geoarchaeological studies using IR methods.

Emerson et al. (2013) and Wisseman et al. (2012) have utilized near-infrared spectroscopy (NIS) to examine various “pipestone” quarries that were sources of stone during the Hopewell Period (100 BC to AD 300) principally in the midwestern United States. These studies build on earlier XRD studies conducted by Gunderson (1987). NIS, as a quantitative instrumental technique for chemical/mineralogic

analysis, compares well with XRD. Wisseman et al. (2012) report results accurate to $\pm 1\text{--}2\%$ at the 95 % confidence level for oxides in the pipestone such as hematite, for example. They cite these results as more accurate than XRD using good standards (*supra*). Since many of the pipestone sources, but not all, “catlinite,” for instance, were flint claystones, the instrumental comparison is probably valid as both techniques give robust spectra for clay minerals. Both NIS and XRD provide high precision within the same sample (cf. Chap. 10 for a discussion of accuracy and precision).

Raman spectroscopy has developed into a much-used instrumental technique for archaeological science and cultural heritage studies (Smith and Clark 2004; Dubessy et al. 2012). As noted, it uses the Raman Effect wherein a laser beam (532 nm (green), 488 nm (blue), 785 nm (IR)) produces nonresonant excitation. There is an energy shift (ΔE) between the incident and scattered photons which can be used to characterize molecules. Recognizing this effect won Raman the Nobel Prize in 1930. Typical outputs of a Raman instrument are, of course, characteristic spectral peaks which can indicate chemical bonds in materials. Metals, unfortunately, do not produce Raman spectra due to their high-order crystalline nature. Peak width is a measure of crystallinity, whereas peak intensity indicates orientation and thickness of a crystal.

For example, however, magmatic materials do lend themselves to Raman analysis. In polished thin sections, carbonates, apatite, are easily seen as well as silica, plagioclase, and epidote. Combined with SEM-EDS as on some instruments (Wall et al. (2014), phase mapping and chemical analysis can be done effectively and quickly.

The major limitations of Raman spectroscopy for mineral, notably metals, identification, as pointed out by Killick (*supra*) are:

1. As noted above, some crystals with face-centered cubic (fcc) crystal structure are not Raman active (i.e., do not produce Raman peaks). These include metallic Al, Ni, Cu, Rh, Pd, Ag, Ir, Pt, Au, and Pb and the mineral galena (PbS).

2. Fluorescence can sometimes overwhelm the Raman peaks. For this reason, most Raman systems are equipped with at least two lasers of different wavelengths (typically 514/532 and 782 nm). The longer wavelengths are less susceptible to fluorescence but produce smaller peaks.
3. Raman spectra vary with the orientation of the lattice in the crystal under investigation and with ionic substitutions. It is essential to bear this in mind when attempting to match unknown and reference spectra.

With the exception of metals, Raman microscopy may be the best single technique for identifying and studying inorganic solids, especially when they are heterogeneous mixtures on a micrometer scale (Gendron et al. 2002). Raman spectroscopy is a fingerprinting technique whereby materials are identified by comparing their characteristic vibrational spectra with those in a database (Smith and Clark, *supra*). A particularly useful database of reference spectra is the RRUF website (<http://rruff.info/>). This site provides free downloadable XRD, infrared and Raman spectra, as well as chemical compositions (by EMPA) for multiple reference specimens of more than a thousand minerals.

Raman spectroscopy has proven useful in pigment studies of Greek ceramics (Pérez and Esteve-Tébar Perez 2004). As previously noted, Tite 1999 and Magetti et al. 1981 have pointed to reducing kiln atmospheres as an important condition for the formation of black surfaces in Classical Period earthenwares. Raman spectra of pigments indicate a strong correlation between color and iron oxides, e.g., red and hematite and black and magnetite (Pérez and Esteve-Tébar, *supra*). As Tite has previously suggested, a sequential kiln firing, where oxidizing and reducing atmospheres are used, produced the requisite colors—red/oxidizing and black/reducing. White pigments were identified by Raman analysis as alumina (α - Al_2O_3), likely the result of thermal decomposition of Greek bauxite below 1100 °C (*supra*).

8.18 Instrumental Geochemical Techniques and Their Availability to Archaeology

Modern instrumental geochemical analyses are available on a fee basis throughout the world. In most research universities, many, if not most, of the methods discussed in this chapter can be found. The important thing for the archaeological investigator to determine is which technique is best able to assist in evaluating the specific research question. Shackley (1998), by way of illustration, has discussed just this question with reference to archaeological obsidians. In the late 1960s and early 1970s, XRF and NAA were increasingly used to deal with issues of obsidian exchange and interaction. By the 1980s, this interest had blossomed with archaeologists, in every part of the world, where obsidian was used, engaged in geochemical studies of this material. The range of instrumentation has expanded as well to include ICP, PIXE, together with the newer models of SEM. Shackley's comparison of the three top techniques in obsidian analyses illustrates points the archaeologist need to consider in choosing an analytical technique.

NAA endured into the late twentieth century as the geochemical method perhaps best known to archaeologists. Part of this was due to the almost missionary zeal of some archeometrists in proselytizing their archaeological fellows for its use in provenance and characterization studies from ceramics to obsidians. NAA does, as Shackley and others (Glasscock 1991; Neff and Glasscock 1995; Glasscock et al. 2007) point out, have two primary shortcomings—it is a destructive technique and it cannot analyze samples for barium (Ba) and strontium (Sr). While NAA labs pride themselves in the small portions (~ mg) that is ordinarily used in their analyses, the point is that the artifact, if indeed, it is such, must be broken however small the damage. Additionally, the material can be radioactive, depending on the mineralogical nature of the sample, for years. Finally, realistic or not, the general public has developed a general fear of radioactivity.

Archaeologists, while more scientifically versed than most, can and do share these concerns. For museum specimens and artifacts that are subject to repatriation (see the discussion in the last section of this chapter), NAA is not the method of choice.

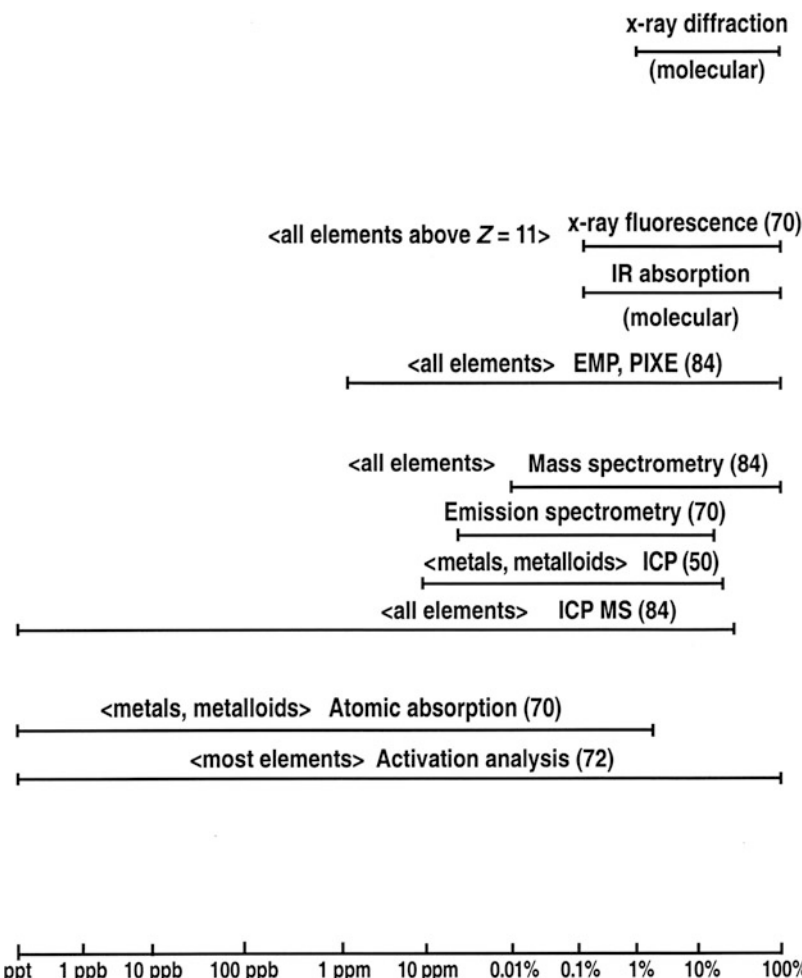
XRF and NAA are remarkably comparable in their results for obsidians particularly in the mid-Z and part of the high-Z region for more than 17 elements analyzed in common. This comparability of analytical results now extends to ICP-MS and PIXE as well. What this means to the archaeologist is that any laboratory employing XRF-EDS, XRF-WDS, NAA, PIXE, or ICP-MS will provide valid and comparable results. To a great degree, Shackley's conclusions concerning the applicability of analytical techniques to obsidian studies can be extended to the great majority of archaeological materials—either inorganic or organic in nature.

When the researcher is not comfortable in their own knowledge, consultation with either specialists or commercial laboratories can help. This is not to say competency in assessing the relative merits of instrumental geochemical techniques will not increase. Today it is common for the field archaeologist to select, collect, and submit radiocarbon samples without consultation unless it is to decide whether to choose the conventional, beta-counting radiocarbon technique, or the atom-counting AMS method.

It is also not uncommon for more and more archaeologists to subscribe to or be familiar with international specialty journals on archaeometry and archaeological science such as *Archaeometry*; *Revue d'archéologie* and the *Journal of Archaeological Science*. Add to this trend the gratifying addition of more technically oriented articles in more traditional archaeological journals such as *Antiquity*, *Journal of Field Archaeology*, and *American Antiquity*. Articles on the geochemical analysis of English ceramics have recently expanded the format of the journal *Historical Archaeology*. All of this reportage of instrumental geochemical analysis in publications commonly read by the archaeological community increases both knowledge and awareness of their usage on commonly held research questions.

Archaeological science has presented a veritable cafeteria spread of both geochronological techniques—radiocarbon, uranium series, electron spin resonance (ESR), optical-and-thermoluminescence (OSL, TL)—and geochemical methods. As archaeological geologists, it is appropriate to increase the application of both these dating and analytical tools in archaeology. In a personal survey of brochures and catalogues from commercial analytical laboratories preparatory to this book, I noted offerings of routine assays of 66–70 elements by ICP-MS and 29 elements by NAA. In the XRF of common metallic oxides, 11 were routinely analyzed by the WDS method. As we have seen in the discussion of obsidian, the University of California's Hearst Museum routinely analyzes 17 elements. Table 8.4 summarizes the analytical methods and their detection limits. The latter analytical parameters occur in relatively higher concentrations ($\mu\text{g/g}$ to %), while trace elements and rare earth elements (REE) are more often found $\mu\text{g/g}$ to ng/g concentrations. In the decision on which geochemical protocol to use, the X-ray and electron probe techniques provide relatively inexpensive and quick analyses of the higher concentration elemental parameters.

For parameters that occur in lower frequency and concentration, the ICP and particle-based methods (NAA, PIXE) provide equal analytical access for archaeological inquiry. Almost any archaeological material is analyzable ceramic, lithic, faunal, botanical, sediment, and soil. If the technique requires digestion of the sample and is, thus, destructive, the compensation is that relatively small amounts are needed (mg-g levels). In one study of archaeological sediments where we recovered in only a few gram amounts, it was gratifying to find that only milligram amounts were needed to assess elemental and minerals present. At the end of the study involving textural, geochemical, and modest geochronological analyses, we were left with some remainder of all our samples. Given the analytical power and precision of conventional instrumental geochemical techniques, there are few items of archaeological interest that cannot be examined with little or no sacrifice of that material. Where even the destruction of any

Table 8.4 Instrumental techniques and their detection limits

part of an artifact is unthinkable, the nondestructive whole sample methods—XRF, NAA, EMPA/SEM, and LA-ICP-MS—are available.

Having reported so glowingly to the reader, it is instructive to recall my own frustration with the loss of a singular piece of early horticulture in the United States—a small, carbonized corncob—in a desire to obtain chronological information with the AMS radiocarbon technique. One of the major “selling” points of AMS is the proportionally small sample needed to calculate an artifact/item’s age. While it is true that μ g samples can be used, most dating laboratories will insist on the sacrifice/digestion of as much of the sample as possible. Theory and practice are often at odds in

the specific analytical case such as that of the small corncob. In that case, the results were (1) a reliable age determination of direct evidence for early corn horticulture in the American Southeast and (2) the loss of a singular, exhibitable example of that early plant domestication.

8.19 A Closing Quote or Quotes

Stos-Gale (1995) in her review of isotope archaeology quotes Gunter Faure’s introduction to his 1977 book on isotope geology, and it seems as appropriate in this context as hers: “The time has come to introduce this subject into the curriculum

in order to prepare geologists in all branches of our science to use this source of information. Although the measurements on which isotope geology is based will probably continue to be made by a small but expanding number of experts, the interpretation of the data should be shared with geologists who are familiar with the complexity of the geological problems.” Stos-Gale suggests perhaps the time has come to substitute the word “archaeology” for that of “geology.”

Where Stos-Gale specifically speaks of isotopic studies, David Killick, writing in 2015, observes, more broadly, “The practice of archaeology has been utterly transformed over the past 15 years by an infusion of (or greatly improved) scientific methods.” To complete Killick’s statement, I would simply add “archaeological science.” Scientific, instrumental techniques, as described herein, have, indeed, been transformative in the practice of modern archaeology.

9.1 Overview

This chapter may seem somewhat unusual to those readers more accustomed to other discussions of archaeometallurgy. Typical of those researches, one often finds the focus on the metal artifact foremost with ancillary areas such as manufacturing, utilization, and provenance archaeological/geochemical examined at various levels of detail. These emphases are important and well placed particularly from the standpoint of the materials science, but it is the aim of this chapter to characterize archaeological metals, minerals, and ores from a geological perspective. By this, we mean to discuss the geology of ancient metallurgy without any special emphasis on the end product, e.g., the metal artifact.

Indeed, even the emphases or at least the breadth of archaeometallurgy is shifting from a detailed description of the form and fashion of metal item to a wider discussion of the role of metals in human social groups. By expanding its methodological frame of reference, archaeometallurgy has widened its scope to the consideration of metals and humankind. Indeed, that relationship is a continuing dynamic in the modern world system that metallurgy helped create (Glumac 1991; Ehrenreich 1991; Roberts and Thornton 2014). In this chapter, we will, briefly, (1) review copper/bronze and iron metallurgy in antiquity, (2) review metallic mineral and ore

genesis in light of contemporary geoscience, and (3) discuss ways archaeological geology can contribute to the study of ancient metallurgy.

9.2 Early Metallurgy: Copper

The development of metallurgy was first assumed to be the province of the cultures of Mesopotamia. The development of metallurgy comes in the Neolithic Period and appears in Europe (Spain, Balkans) and the Near East (Anatolia) as well as in Southeast Asia. While contemporaneous with ceramic manufacture as a technology in some areas, such as Anatolia and China, the early metallurgy may have actually preceded or was roughly contemporaneous with the production of pottery (Herz and Garrison 1998). In the New World, early metallurgy's evidence of a "forged, native metal" metallurgy has been found (Lechtman 2014) in the Andes by the late-third millennium but after ceramics were in evidence by the fourth millennium BC in South America and by the third millennium in the North. In the north of the Americas, metal usage never moved beyond cold-hammered native metals until the Euro-Colonial Period.

Recent studies have revealed two related facets of early metallurgy—(1) it was obviously originated in different places in the Old World as well as the New World, albeit the dates for early Pre-Columbian metallurgy, in the Andes, are

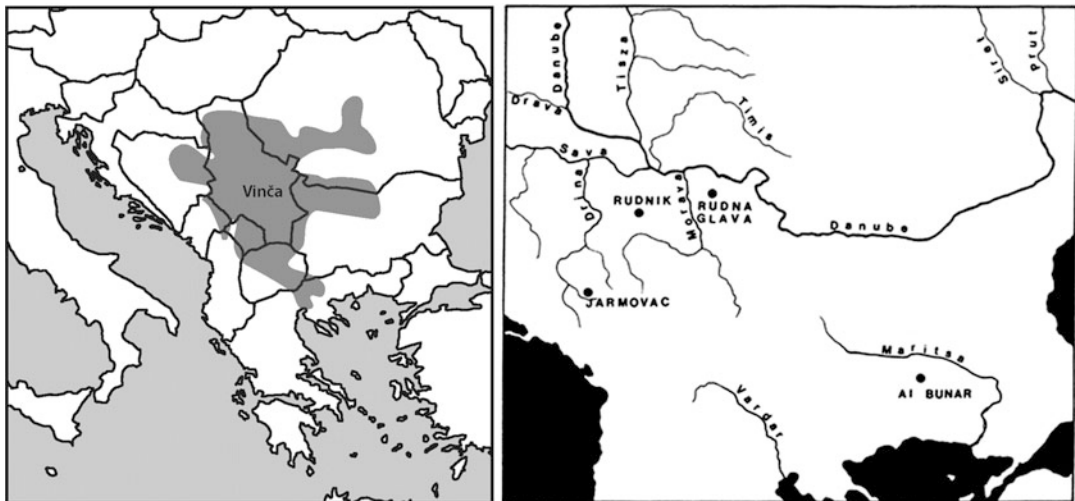


Fig. 9.1 Central Vinča culture area (*left*); detail showing early Balkan mines (*right*)

roughly contemporaneous with those of Early Bronze Age (EBA) (second millennium BC) of central Europe, whereas its appearance in western Mesoamerica is contemporaneous with the much later dates for that of the African Iron Age, ca. 7th c. AD (Hosler 2014; Childs 1991), and (2) the higher cultures of antiquity (Sumer, Egypt) did not invent metal working. Increasing evidence, in Europe, points to metal-using sites as early as 4500 BC along the Danube at sites such as Vucedol (Durman 1988, 2004, 2007). Close by, in the Balkans, the Vinča culture (5200–4600 BC) is found, archaeologically, in western Bulgaria, Romania, Serbia, eastern Bosnia, and Macedonia/Thessaly. Major Vinča sites include Gornja Tuzla, Pločnik, Rudna Glava, Selevac, Tărtăria Turdaş Vinča-Belo Brdo, and the type site, Vršac. Three major phases have been described for the Vinča culture—early, Vinča troodos; middle, Gradna; and late, Vinča.

The Vinča site of Pločnik has produced the earliest example of copper tools in the world. However, the people of the Vinča network practiced only an early and limited form of metallurgy (Radivojevic 2012). In 2010, the site of Belovode, Serbia, has produced definitive evidence of copper smelting at 5000 BC becoming the earliest evidence of smelting/melting

technology in Europe or SW Asia (Radivojevic, *supra*). Copper ores were mined on a large scale at sites like Rudna Glava, but only a fraction were smelted and cast into metal artifacts. Likewise, ores from Rudna Glava, surprisingly, do not appear to have been used in the earliest Balkan metallurgy (*supra*; Pernicka et al. 1993).

The 7000-year-old metal-smelting remains from the ancient settlement of Belovode suggest, strongly, that copper smelting may have been invented in separate parts of Asia and Europe at that time rather than spreading from a single source. Other important early metal sites occur at Los Millares (Spain), northern Italy, Ireland (Mount Gabriel), and Anatolia (Halicar and Çatal Hüyük). The Vinča culture mining site Rudna Glava (Bulgaria) was active around 5000–3000 BC. The Vinča culture also utilized copper ore deposits in Transylvania, Bosnia, Serbia, and Macedonia, as well as those at Rudna Glava (Fig. 9.1). There, archaeologist Boreslav Jovanovic (1988) found vertical mine shafts up to 30–40 m deep. The miners obviously followed the ore seams using simple deer antler picks and fire/water mining methods.

Early copper technology and hence metallurgy were developed by various technical specialists in these early Balkan and Southwest

Asian cultures. The task was not easy as copper had a high melting point—1080 °C. Experiments to try and reproduce pure copper metal, using ores and materials available to early metallurgists, have met with mixed results (Killick 2014). Perhaps, the use of compounds or alloys—copper- antimony, copper-arsenic, or copper-tin—creating a eutectic (lowered melting point) was accidentally discovered early by these specialists. Without present-day archaeological evidence, this is purely conjecture.

Killick (2014) and Notis (2014) both give excellent reviews of the geochemical and thermodynamic barriers that early metallurgists had to surmount. These chemical and physical constraints determined, in large part, which ores and subsequent metals were possible given the primitive technology of the Neolithic.

9.3 Metallurgy: Copper to Bronze

Durman (1988, 1997) distinguishes three major steps (and several intermediate stages) in the development of copper metallurgy. These are cold hammering, the “lost wax” or “cire perdue” casting technique, and the metallurgy of arsenic bronze. In light of more recent discoveries, this scenario is overly simplistic. In the following chronologue, a progression that will be discussed, further, is shown.

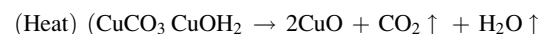
Early Metallurgy: A Chronologue

- I. Native metal as stones/nuggets
- II. Native metal stage (cold hammering cutting, of copper, gold, silver, meteoric iron)
- III. Ore stage (from ore to metal). Smelting of ores, then, alloys invented with composition of the primary factor. (Copper combined with arsenic (in ores), with tin as additive producing bronze; antimony and zinc for brasses; gold and silver naturally or as alloy to form electrum in coinage)
- IV. Iron stage (processing as primary factor—cast iron; wrought iron; steel)

The production of copper by the ancients required a pyrotechnology that could smelt the copper-bearing ores such as malachite CuCO_3 , Cu(OH)_2 , chalcocite Cu_2S , and chalcopyrite CuFeS_2 .

Notably, first the oxide then sulfide ores together with other ores such as the *fahlerz* or “gray ores” and arsenates were important sources for smelting purposes. It is the oxide and sulfide ores (cf. Tables 9.2a, 9.2b and 9.1) that were demonstrably used first by ancient metallurgists. However, the presumed sequence of use—oxides then sulfides and arsenates as well as *fahlerz*—has been called into question by recent research on early smelting sites. Bougarit (2007) has examined slags from 20 early sites, and his results indicate a contemporaneous exploitation of oxide and sulfide ores at least five of these. The following reactions have been suggested for early, simple hearth/crucible smelting:

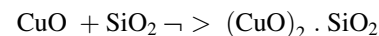
The two reactions in the copper smelting of oxide ores are



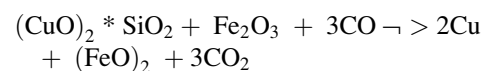
and then CuO is reduced by carbon monoxide,



Silicate impurities in the ore react with the CuO to form the slag



Iron oxides, intentionally or accidentally, in co-smelting with the copper ores, increased the copper yield thusly:



Heat is not enough to extract the metal from the ore—metal minerals plus *gangue*—the host or country rock. As we see in the above reactions, carbon monoxide, from charcoal, was necessary to reduce the metal. The presence of iron oxides, which often occurred naturally, increased the copper yield (van der Merwe and Avery 1982).

The carbonate ores presented less of a problem to the smelters and were processed in the simple bowl-shaped hearths or small, open

Table 9.1 Major mineral processes and deposits by origin (Carr and Herz 1989)

| Genesis | Process | Representative deposits |
|---------------------------------|---|--|
| <i>1. Igneous processes</i> | | |
| Intrusive rocks | Cooling from magma | Construction materials |
| Magmatic processes | Crystallization or concentration by differentiation of mafic magma at great depth | Diamonds, nickel, platinum group, chromite, titanium iron |
| Hydrothermal | Form from felsic, water-rich near surface magma | Copper, lead complexes and sulfides, tin, pegmatites feldspar, beryl |
| Hydrothermal alteration | End stage of magmatic activity, water-rich solutions | Clays, porphyry copper, sulfides |
| Replacement and vein deposits | Final stage, fills fractures, and replaces original minerals | Lead and zinc sulfides, silver lead, gold, tin |
| Porphyry deposits | Disseminations into country rock and borders of intrusive | Copper, tin, molybdenum |
| Extrusive rocks | Low temperature in volcanic rocks | Silver, gold, sulfur |
| Exhalative | Submarine volcanogenic, “black smokers” | Iron-copper-zinc sulfides |
| <i>2. Sedimentary processes</i> | | |
| Solution transport | Precipitates by changing Eh-pH | Iron ore, limestone, copper, manganese, phosphorus |
| Bacteriogenic | Anaerobic sulfur-fixing bacteria organic reduction | Sulfur, gypsum, uranium, iron, manganese, sulfides |
| Evaporation | Evaporation of seawater in enclosed basins, lagoons, etc. | Gypsum, salt |
| Clastic | Weathering and transport of heavy residual minerals | Placer deposits, gold, gems, cassiterite |
| Residual | Weathering in place, residual “lag” minerals | Clay, iron |
| <i>3. Metamorphic processes</i> | | |
| Contact metamorphism | Around or near igneous intrusions | Graphite, Al silicates, tin, gold-silver, lead |
| Regional metamorphism | Widespread, associated with orogenesis | Slate, marble, serpentine, asbestos, graphite, talc, emery, garnet |

crucibles to form small “puddles” of 98–99 % pure metal. In low-grade ores (less than 2 % copper), such as those from porphyry, the copper must be concentrated by smelting procedures. In the Anatolian region, experimentation may have been as early as the eighth millennium BC. Sites such as Çayönü and Çatal Hüyük in Anatolia are where native copper implements date to the seventh century BC at the former (Braidwood et al. 1981) and beads of copper and lead were found in Levels VII (ca. 6200–6500 ± 100 BC) and VIII (ca. 6250 BC) (Mellaart 1966).

By the early sixth millennium, smelting, as we have seen, was used to produce copper tools in the Balkans, and shortly thereafter, assuredly, in Anatolia, such as knives, sickles, and woodworking adzes. Copper metal in pure form is quite malleable and has decidedly less tensile strength

(<3000 kg cm²) than stone or the latter alloy of copper—bronze. This tensile strength was enhanced by hammer working of the tool after casting.

To produce metal from the sulfide ores, early smiths may have resorted to “roasting” also known as “dead-roasting” the sulfide ores to oxidize them of “impurities” such as arsenic (As) and antimony (Sb). Cu₂S remains as a calcine. If the gangue, generally siliceous rock, such as a chalcopyrite (Fig. 9.2), is part of the smelt, then it will naturally “flux” the melt. “Matte smelting,” was a technique within the capabilities of early metallurgists, and along with “co-smelting” was described by Agricola (Hoover 1912; Dibner 1958). Matte smelting of sulfide ores involved the production of a “matte” by open hearth or crucible smelting. This matte is

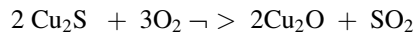


Fig. 9.2 Chalcopyrite ore with a replica of Neolithic copper axe shown (Photograph by the author)

then roasted to remove sulfur as a gas, instead of a slag as with dead roasting, leaving the copper and iron as oxides. When this residue is smelted, a flux such as quartz—as a sand—was added, thereby producing a fayalitic slag which could be “poled” or skimmed off leaving the copper.

Besides roasting and matte smelting, workers like Lechtman and Klein (1999) and Rostoker et al. (1989) have suggested the use of “co-smelting” oxide ores with sulfide ores to produce copper.

As a process, co-smelting proceeds as follows:



then



In the first step, chalcocite yields cuprite, and in the second, these are reduced to copper metal.

Epstein (1993) identified a type of slag which has been termed “slag sand.” It was produced by successful efforts, by the ancient smiths, to remove gangue materials by the simple crushing of mattes and then re-smelting the metal thus separated. As a process, it seems more feasible for use in early metallurgy than slag-producing processes such as co-smelting or matte smelting. In the case of co-smelting, access to both oxide and sulfide ores is presumed, and that may not have been the case except in rare instances, prehistorically.

As smelting techniques were extended in intensity and efficiency, the demand for ore increased. It was probably due to the inadvertent experimentation with various ores that led to the discovery of bronze in either one or two forms—arsenical or tin bronze. Arsenical copper ore such as enargite, Cu_3AsS_4 , can produce a natural bronze alloy, but it would have been difficult using the open hearth/crucible methods of early metallurgy. The arsenic (and antimony as well) would have been driven off, thereby reducing the remaining amounts to 2 % or less. If the arsenic content (up to 10 %) could be maintained through the smelt, a natural alloy would have resulted. Budd et al. (1993) and Pigott (1999) discuss the direct smelting of arsenate ore to obtain arsenical copper.

Arsenic improves the tensile strength properties of the alloy to roughly double that of the unworked pure metal. It is possible to form tin bronze from stannite, Cu_2FeSn_4 , by direct smelting (Wertime 1978). As either an accidental alloy or by 3000 BC an intentional metal process, bronze was the predominant metal until the development of iron as a useful metal by 1000 BC. The transition from arsenical copper to tin bronze is suggested by the host of artifacts showing percentages of copper of more than 5 % tin from Europe and the Near East for the periods ca. 2700–2200 BC and 2200–1800 BC.

Major tin sources include Cornwall (Britain), Spain, Turkey (Anatolian plateau), SW Asia, and South America. Sources for Egyptian tin have been identified in the Sudan during the reign of Pepi II (twenty-second century BC). Outside Europe and the Near East, major Bronze Age cultures are known for Thailand (Bai Chang) and Northern China (Hunan—the Shang Dynasty ca. 1400 BC) which have access to tin deposits.

The central Danubian area site of Vucedol (Fig. 9.3) excavated by Aleksandar Durman has produced extensive use of sulfide and fahlerz ores to produce bronze in the Early Bronze Age (EBA) (Durman 1988, 1997; 2004). Two metallurgical culture periods have been identified at Vucedol—first, the Baden Culture with a northern Balkan extent dating to 3500–3000 BC followed by the more widespread Vucedol



Fig. 9.3 Early metal site of Vucedol, located overlooking the Danube River, in eastern Croatia (Photograph by author)

culture (3000–2400 BC). In Fig. 9.3, the Baden Culture level is easily seen by virtue of the large trash/storage pits across the site. The succeeding Vucedol levels are indicated by Durman on the profile shown in Fig. 9.3.

The Baden Culture exemplifies the early smelting of sulfide and fahlerz ores. The latter, characterized by tennatites and tetrahydrites, contained significant quantities of arsenic and antimony. As noted, the more technologically simple, open smelting process, allowed both elements to evaporate at 600 °C but as assayed in two Baden daggers at 1.5 and 5.5 % arsenic contents which were retained and adequate to increase their hardness (Durman 2004). These ores were extracted nearby in the Vrbas Valley of modern-day Bosnia (*supra*). In the succeeding Vucedol culture, metallurgists cast large numbers of implements, as indicated by hoards of up to 50 artifacts, made from both arsenical bronze and copper metals (Durman, *supra*).

In the late Vucedol period, and into the later Vinkovci-Somogyvar Culture, the switch is made from sulfur fahlerz ores to chalcopyrite ores (Durman 1997). The resultant copper was soft and required alloying. Without natural mineralogic alloys like arsenic or antimony, this copper required addition of cassiterite. Like Peru, this tin was available both in *in situ* deposits and placers in streams. In western Serbia and Bosnia, the mountains of Cer and Bukulja



Fig. 9.4 Experimental archaeology. Melting bronze ingots for casting in the stone mold shown in the foreground (Courtesy Latenium, Hauterive, Switzerland)

contained tin deposits. Pernicka et al. (1997) caution against the use of tin in southeastern Europe before the third millennium BC.

Southward of the Balkans, by roughly 500 km, in northern Greece, the site of Sitagroi, excavated by Colin Renfrew et al. (2003), has produced evidence of extensive copper-based metallurgy but no direct evidence of smelting—melting, yes, but smelting, no (Muhly 2006).

Sitagroi was originally thought to be an early tin alloying site (Muhly 1985), but this opinion is now in question (Muhly 2006). It is moot to note, here, the strict injunction from Muhly (1985), “Most important of all is the absolute geological principle that without granite there is no possibility of tin (cassiterite) ever having been present....” No granite, no tin (Fig. 9.4).

Copper metallurgy of the Balkans and the eastern Aegean saw a dominance of arsenical copper in the period 4000–2000 BC (Muhly 2006). Durman (1997) echoes this conclusion in his assessment of Balkan copper metallurgy. Arsenical copper artifacts of the Early Cycladic Period, from Kythnos, have shown arsenic in amounts averaging 3.2 % (Sherratt 2000). More important, for the confirmation of a smelting arsenical copper metallurgy, is the discovery of both arsenic in slags and copper mines on the island (Hedges et al. 1990) (Fig. 9.5).

On Thassos, researchers have confirmed a sequence of metallurgy from hammered silver/gold through smelted copper and iron (Nerantzis and Papadopolous 2013). The site of Limenaria



Fig. 9.5 Experimental archaeology. Cast duplicate of a bronze spear (Courtesy Latenium, Hauterive, Switzerland)

on southwestern Thassos has, in its Late Neolithic levels, produced a clay crucible together with copper slag. Litharge fragments indicate a silver-lead metallurgy using argentiferous lead ores similar to those of Laurion. Excavations on the bay of Aghios Ioannis produced significant hearths and ovens dated to 3700–3025 BC or the Final Neolithic/Early Bronze Age transition period (*supra*). Copper artifacts in the form of pins and pendants were recovered. In 2009–2010 during rescue excavations of the Aghios Antonios site, clay mold and tuyere fragments from an Early Bronze Age context were recovered along with slag and crucible fragments (Papadopolous 2008). Copper artifacts were rare at the site by contrast. Compositional analysis using pXRF showed the slag commonly had copper and arsenic suggesting either smelting of sulfide ores or some form of alloying. SEM-EDS analyses of the slags indicated the presence of malachite and weathering products. Matte fragments suggested, again, smelting and secondary treatment of indigenous (to the island) polymetallic or sulfide ores (Papadopolous 2008; Lespez and Papadopolous 2008).

Extensive smelting of Alpine fahlerz ores occurred in the Late Bronze Age (LBA) across Switzerland (Rychner and Kläntschi 1995). In the Bronze Age phases of the Hallstatt (Ha) Culture Period, notably, HaA2, ca. 1100 BC, the dominant As/Ni, low Sb, and Ag metal type is derived from these ores. In his analysis of nearly 1000 bronzes ($n = 941$), Rychner, in collaboration with Niklaus Kläntschi, observed these ores used throughout the succeeding phases

of HaB1 and HaB2, up to 900 BC and the beginning of the Hallstatt Iron Age at ca. 850 BC.

Fahlerz ores, because of their extensive presence in the central Andes, came into wide use in the Middle Horizon (AD 600–1000) metallurgy of that area's Wari and Sicán Cultures up and into the succeeding Inca Period or Late Horizon (Shimada 2000; Lechtman 2014). Tennantite ($\text{Cu}_{12}\text{As}_4\text{S}_{13}$) and tetrahedrite ($\text{Cu}_{12}\text{Sb}_4\text{S}_{13}$), along with enargite, weathered from these hypogene deposits, as we have seen, will produce "natural" bronze alloy without the addition of tin. Unlike the low percentages of arsenic in the European examples, Shimada and Merkel (1991) reported smelted averaging 6 % arsenic. Clearly, the Andean metallurgists had mastered the processes to retain the arsenic in their metal.

The only secure evidence for extractive metallurgy in lower Egypt comes from a little after 3000 BC. At Wadi Dara, in the eastern desert between the Nile and the Red Sea, three-sided boxes of stone slabs were lined with clay to make copper-smelting furnaces about 30 cm in internal diameter (Killick 2009). These furnaces were apparently not hot enough to drain the iron-rich slags that they produced, so the slags were crushed to liberate the copper prills (*supra*; Craddock 2001).

In the South Central Andes, the use of tin, via cassiterite ores, came into use, along with arsenical bronze in the Wari, Tiwanaku, and Aguada Cultures. The core areas of the latter two cultures range south of Lake Titicaca on the border of Bolivia and Peru, while that of the Wari Culture extended almost to the northern end of this large Andean lake. The Tiwanaku and Aguada culture areas encompassed much of the Altiplano as well. All three cultures used arsenical bronze, but the Tiwanaku in its late phases (AD 600–900) used tin bronze almost exclusively, while the Aguada Culture, centered in northwest Argentina, emphasized and excelled at the production of tin bronze (Lechtman 2014). This is particularly interesting as it is not obvious that cassiterite, which is a heavy dark brown or black mineral, contains a metal. Still, there is no good reason why alluvial cassiterite should have been ignored (Killick 2009). Gonzalez (2004) stresses the two preeminent aspects of Aguada metallurgy—tin

bronze alloy and casting by use of the lost wax process (*cire perdue*).

In Grecian antiquity, bronze was utilized in building as fasteners and even for truss in the Pantheon. Beyond these uses, the metal was used primarily in weaponry and tool manufacture. Bronze was important from the physical metallurgical standpoint in that the armor of ancient Greeks probably conferred military advantage in Battle of Marathon. Persian arrows failed to penetrate Greek armor largely because the “dents” caused by the arrows were not fractures or penetrations that could cause serious wounds or death. This was in part due to the energy of the arrow itself which was reduced by the use of sinew or tendon bowstrings, which, upon flexure, had a lower Young’s Modulus and therefore less stiff. The toll at Marathon was over 6000 Persians lost compared to 192 Greeks. Archery and Young’s Modulus were factors 1700 years later at Crecy, France, in 1346, where English bows, strung with stiffer flax, would impart kinetic energy to the arrows more efficiently allowing iron-tipped English arrows to penetrate French armor. The French iron armor, unlike the Greek bronze, fractured and the arrows penetrated to kill thousands of French cavalry and infantry. Blyth examined this technological effectiveness of Greek armor against arrows in the Persian War (490–479 BC) (Blyth 1977).

9.4 Iron Metallurgy

The first smelting of iron may have taken place as early as 5000 BC in Mesopotamia (Craddock 1980). Throughout the Bronze Age, iron was produced sporadically. Iron droplets, a by-product of copper smelting, formed lumps in and on top of the slag produced by smelting.

To reduce iron in large amounts required a CO/CO₂ ratio of 3:1, whereas only 1:5000 CO/CO₂ was required for the reduction of CuO. Typically, such a ratio was not technologically possible in antiquity. Forging these lumps of early iron was difficult as the iron contained copper and sulfur. By 1200 BC, the smiths had begun to roast Fe₃O₄ in smelting furnaces. In this process, at 1200 °C, the iron did not melt as did

copper, but only became a pasty mass of iron and impurities. The production of iron in antiquity was not a melting operation; it was a reducing operation. Too much heat, such as the 1540 °C necessary to liquefy iron, would in ancient furnaces only serve to reoxidize the iron, thereby producing no metal. The object is to reduce Fe₃O₄ to metallic FeO.

Today, this is accomplished with blast furnaces, but in the early days, the smiths roasted the iron ore in a forge called a “pit forge” or later a “bloomery forge” (Fig. 9.6). To achieve the required temperature, some form of device was needed to create a draft. The first smiths utilized blow pipes illustrated here. The result of this crude smelting was a pasty mass of iron, slag, and charcoal called a “bloom.” With further heating and hammering at 1250 °C, the bloom could be consolidated into a wrought iron implement. When hammered, the fluid slag and oxides were squirted out and the iron particles welded together. This slag “gangue” was termed fayalite.

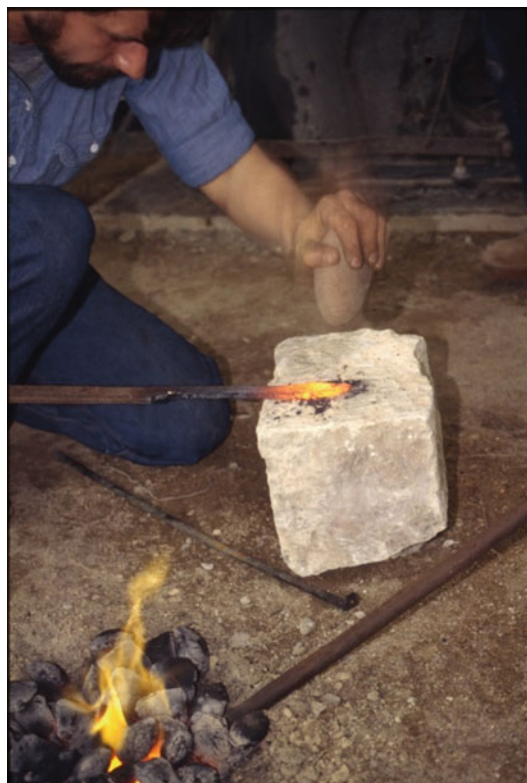
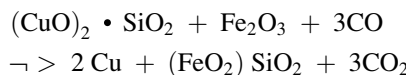


Fig. 9.6 Experimental iron metallurgy. A pit forge, stone hammer, and anvil (Photograph by author)

Seventy percent of iron comes in Fe_2O_3 , the hematite form; Fe_3O_4 magnetite is a major ore; and siderite, FeCO_3 , or carbonate ore. Iron oxides, such as hematite, increase Cu yields.



Magnetite can be “calcined” to Fe_2O_3 (Fe_3O_4). Siderite, after being calcined, yields FeO :



By further reduction, at melting, the metallic iron remains.

However, unlike copper reduction, the endothermic requirement for actual reduction to iron metal was beyond the technological capabilities of early metallurgists. Fifteen hundred degrees Celsius was out of reach to early metallurgists except in China and Southwest Asia/India. The “west” or Europe was constrained to a bloomery technology which only partially melted the iron leaving silica impurities in “bloom” ingot that had to be further refined and hammered by the smiths.

Bloomery iron was a poor substitute for a well-made bronze—with a tensile strength of about 40,000 psi compared to the strength of pure copper at 2250 kg cm². Hammering brings the strength of iron to almost 7000 kg cm². A bronze with 11 % tin has a tensile strength after casting of 4500 kg cm² and a strength after cold working of 8500 kg cm². Further, bronze could be melted and cast at temperatures reached by early furnaces. Iron could be cast only after adding as much as 4 % carbon to the bloom which in turn caused the cast metal to be extremely brittle. Bronze corroded little, iron rusted properly easily.

By 2500 BC, an iron industry existed in central India and by 1500 BC sites have large heaps of cinders and slag. Hittites developed iron for weaponry by 1400 BC as well (Soucková-Sigelová 2001; Killick 2014) which also attested by Egyptian accounts of the in 1274 BC. Cast iron metallurgy was developed in the Far East as well as Southwest Asia. By 500 BC, China was

producing “cast” iron. In China, the bloom was left in the furnace until it melted. Since the melting point of steel falls with increasing carbon content, if it absorbs over 2 % C, it will then melt at 1150 °C, forming a liquid called “cast iron” (Williams 2009). Such high carbon content iron is brittle and impractical for weapon and tool manufacture as it can be “cast” but not forged.

Why did iron, then, replace bronze? One theory suggests that iron properly carburized (the addition of carbon) produces an alloy with desirable cutting and durability properties. This alloy is steel. A carbon content of 0.2–0.3 % gives steeled iron a strength equal to that of unworked bronze; raised to 1.2 %, the steeled iron has a tensile strength of 140,000 psi. If the blacksmith then cold hammers the steeled iron, a tensile strength of up to 245,000 psi can be obtained—more than double that of cold-worked bronze!

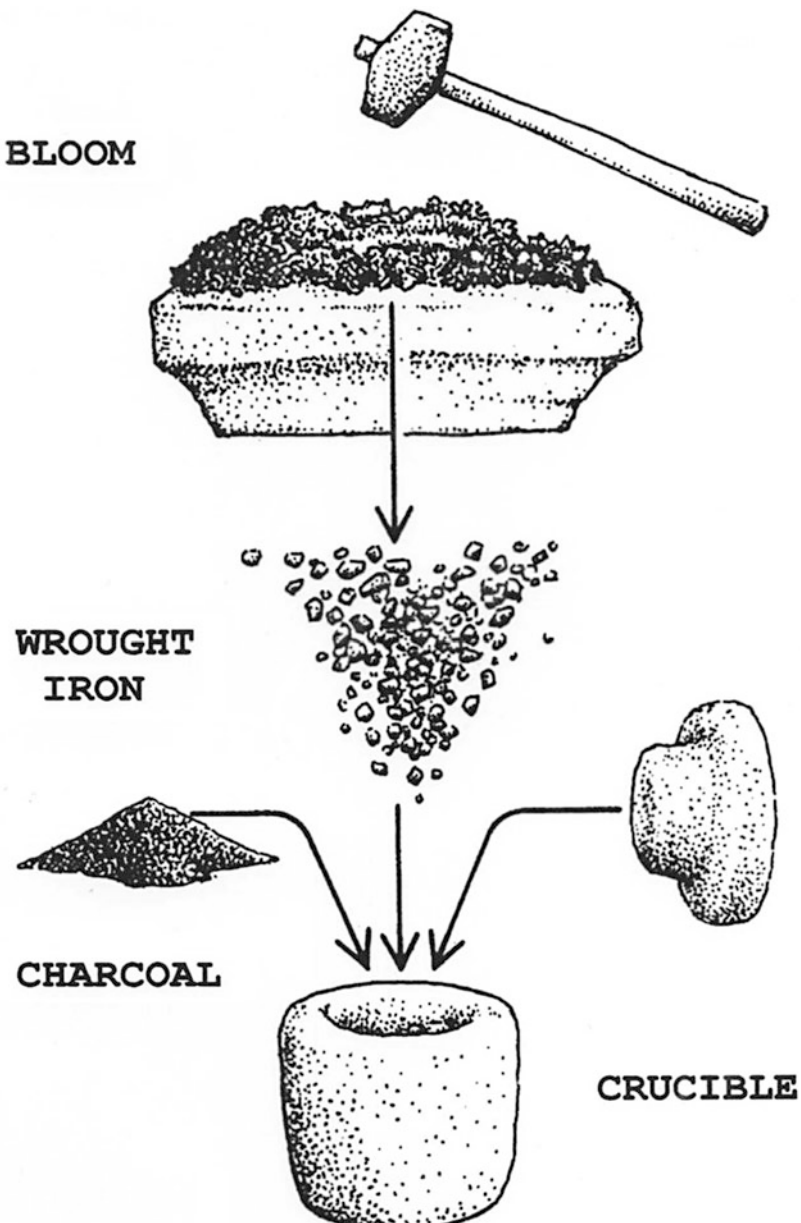
In the bloomery furnace, the fuel and ore charge pass down the stack where at 800 °C CO reduces the FeO to FeO flakes. With rising temperature (~1200 °C), the metal agglomerates and forms wustite (FeO ; iron II) subsequently forming a wustite-fayalite slag. This allows the iron-silica particles to pass the high temperature, oxidizing zone above the tuyeres, unscathed (with high-grade ores, SiO_2 must be added to form the slag). Below the tuyeres, the furnace atmosphere is reducing again. Slag flows to the bottom of the furnace, being tapped off, where possible, with the bloom forming a layer above the bowl (van der Merwe and Avery 1987). The bloom is ready for the forge where it can be steeled by the introduction of carbon. The carbon was picked up by the iron from the white hot charcoal at 1200 °C.

Before the introduction of blast furnace, the forced-draft bloomery furnace was the pinnacle of early iron-smelting technology. Recently, archaeology has produced a heretofore unknown furnace type—a wind-driven technology that took advantage of monsoon winds of the Indian Ocean. Found on the island of Sri Lanka by Gill Juleff, this unique furnace design was found at 77 sites on west, windward-facing ridges. The front wall of the furnace faced the wind rising

to the ridge crest with the multiple tuyeres introducing a strong draft to the ore charge. The genius of this furnace design uses the larger fraction of the airflow passing over the front wall to create a pressure gradient between the tuyeres and the top of the wall thus enhancing the flow through the bloom¹⁴. Juleff reports temperatures of 1500 °C concentrated inside the front wall yielding up to 17 kg of bloom and high-carbon iron metal per charge.

This latter product may be a predecessor to the famed but, as Bronson (1986) notes, “romanticized and (over) hyped” wootz steels of Medieval times. The appearance of this technology in the first millennium AD adds to the preeminence of the Indian subcontinent (including Sri Lanka) in the evolution of iron metallurgy (Forbes 1964; Bronson 1986). The diffusion of carbon into the iron, within a sealed crucible (Fig. 9.7), is temperature dependent—after 9 h

Fig. 9.7 A hypothesized crucible steel—“wootz”—process



at 1150 °C, the concentration of carbon is 2 % at 1.5 mm. In modern metallurgical terms, the carburized iron has a microstructure known as austenite. As the temperature falls to 727 °C, the austenite breaks down into ferrite, pure iron, and iron carbide or cementite. The reaction is called the Eutectoid Reaction. The new microstructure is called pearlite with alternating layers of ferrite and cementite. If the iron contains 0.8 % carbon, the entire (100 %) microstructure will be pearlite.

Developed in was a very slow-cooled ingot which preserved large crystals of cementite within the steel, which could then after etching generate a characteristic pattern (“watered silk”) on the surface of the blade. This was to be called wootz or “Damascus steel” reflecting the “damask” pattern rather than the place name (Bronson 1986; Williams 2009).

The ancient smiths developed a method to harden steamed iron even further. This method was quenching or rapid cooling in air or water. Rapid cooling from the austenite phase prevents the formation of ferrite and cementite and produces the iron microstructure called martensite which is hard but brittle. A third technique for manipulating the end result of forging steamed iron was tempering. When the ancient smiths realized that quenching made hard but brittle steel, they learned the process of tempering where the steel was heated to the temperature of transformation, 723 °C. The iron carbide (in the cementite) precipitates and coalesces, thereby increasing ductility of the metal by creating a finer grained pearlite on the cutting edges of tools and weapons.

Forging iron was and remains an art. Smiths were the first technological “nerds,” e.g., they controlled understanding of an important technological process. This was a knowledge bound up in secrecy. Forging iron created desired iron form—soft, malleable, hard, etc. Forge work basically involves:

1. “Heats”
2. “Quenches”
3. “Tempering”

In the quenching process, the blacksmith observes the “run” of color in the cooling:

Quenching by “Run of Color”: An Example

230 °C—straw color
250 °C—yellow color (knives)
260 °C—brown color (chisels)
270 °C—purple color (tools, etc.)
290 °C—blue color (springs)
320 °C—blue/black (saw blades)

Carbon % and Iron Mineral Phases

If 0.9 %—pearlite
>0.9 %—cementite and pearlite
<0.9 %—ferrite + cementite
If 0.8 %—all pearlite

Celtic tribes of Transalpine Europe became master iron smiths producing tons of iron in the form of mails, spikes, weapons, chariot tires, and other implements. Far to the east, in north China, the Shang culture (1850–1100 BC) was smelting bronze on a par with Anatolia, and by the sixth century BC, the Chou Dynasty was casting iron.

9.5 A Metallurgy for the Common Man: African Iron

Iron metallurgy in Africa—smelting and mining—has enjoyed a well-deserved scrutiny in recent years (van der Merwe and Avery 1987; Killick 1991, 2014; Childs 1991; Perret and Serneels 2006). The origins and timing of the first metallurgy of the so-called Great Lakes area of Africa are still unclear (Killick 2009). The origin of iron smelting in sub-Saharan Africa has been the subject of intense controversy over the last 60 years. Its appearance is generally thought to be between 800 and 400 cal BC, but exactly where and exactly how is, as stated, still unclear although (*supra*). In southern Africa, iron and unalloyed copper were the only two metals used before c. 1100 cal AD (Killick 2009).

Sub-Saharan iron metallurgy represents a contrast in the evolution of the acquisition and use of

Fig. 9.8 The Ncherenje mine on the Malawian Nyika Plateau (Photograph by David Wenner)



metals. Here, the copper-bronze metallurgy common elsewhere—Northern Africa, Asia, Europe, and the New World—was not dominant in central and southern Africa where bloomery iron rose to prominence. This iron metallurgy, like its copper counterpart, was small scale and is characterized by a simple, relatively uniform technology 100. While conducted by iron smiths at small furnaces, the demand for iron in Southern Africa after 1000 AD can be described as universal. The beginning of the second millennium AD saw the growth of towns with widespread trade in metals. Major sites such as Great Zimbabwe and Botswana show significant change in the elements of fabrication technology, diversification in the metals mined to include tin and gold, and the trade of cast ingots of copper and tin, particularly at Zimbabwe.

An example of a study of this African metal tradition is illustrative of the role geology has in the archaeology of metallurgy. This study was carried out by David Wenner and Nicholas Van der Merwe on iron mining and smelting in Northern Malawi. Their research was carried out at two contrasting, well-preserved Iron Age mines on the Nyika Plateau of Malawi. The first mine, Ncherenje, had around 1600 m^3 of ore mined over a linear distance of 3 km from shallow pits, large excavations, and a number of

underground shafts and tunnels (Fig. 9.8). The second mine, Mbiri, is a single excavation where only about 15.5 m^3 of magnetite-rich gneiss was taken. It is the difference in the ore quality between the two mines that Wenner and Van der Merwe's study centered on determining why the largest quantity was mined at the site of poorest ore—Ncherenje.

The Ncherenje ore was truly low grade, ranging from only 6.6 to 21.3 wt.% Fe_2O_3 . The Mbiri ore averaged 58 % magnetite (Fe_2O_3). Why would the metallurgists focus on the extraction and use of such poor ore? Wenner and van der Merwe determined the answer lay in the indigenous smelting technology available. The geological settings of the mines are described in detail. Nchenenje and Mbiri both lie within a heterogeneous association of Precambrian Age igneous and metamorphic rock, termed the Malawi Basement Complex. Much of the bedrock is covered by an extensive regolith that varies, below the soil, from 1 to 8 m in thickness. Ncherenje contains three basic rock types—gneiss, cataclastite, and granite. The Early Iron Age miners obtained their ores from the soft, highly weathered material in their varied workings abandoning these as they encountered unweathered rock. Four weathering types defined at Ncherenje. Analyses of these types indicated

that the illite replaced feldspar in the quartz feldspathic zones with kaolinite and fine-grained iron oxides forming from the mafic phases. It is in the highly weathered type 4 rock that the iron oxides (and clay) are most abundant (5–20 %).

The Mbiri mine occurs within a single homogenous rock unit mapped as cordierite gneiss although most of the mining activity took place in the regolithic portion. Magnetite veinlets (1–2 m wide) occur within this partially weathered bedrock. Table 9.2a lists the sample descriptions for the Mbiri mine. To corroborate their initial suspicions as to the variety in grade of the two mines, ores Wenner and van der

Table 9.2a Whole-rock chemical analyses of samples from the Mbiri mine

| | 14 | 14 V | 15 |
|--------------------------------|--------|-------|-------|
| SiO ₂ | 15.66 | 11.37 | 40.70 |
| TiO ₂ | 4.94 | 5.07 | 5.07 |
| Al ₂ O ₃ | 13.07 | 10.77 | 14.92 |
| FezO ₃ | 58.71 | 64.82 | 47.48 |
| MnO | 0.28 | 0.85 | 0.26 |
| MgO | 0.40 | 0.38 | 0.42 |
| CaO | 0.00 | 0.00 | 0.01 |
| Na ₂ O | 0.16 | 0.18 | <0.1 |
| K ₂ O | 2.97 | 2.62 | 2.68 |
| P ₂ O ₅ | 0.14 | 0.20 | 0.13 |
| H ₂ O- | 0.56 | 0.50 | 0.57 |
| LOI | 3.52 | 2.66 | 4.97 |
| Total | 100.41 | 99.42 | 99.59 |

LOI loss on ignition

Merwe carried out XRF studies reproduced in Tables 9.2a and 9.2b. The difference in the iron content is obvious.

Surely the ancient smiths had a practical understanding of ore quality. This was apparent after further study of the slags produced by the respective ores in earlier ethnographic studies (Schmidt 1978, 1981; Killick 1991; Childs 1991). The modern smiths of Malawi, using a two-step natural-draft and forced-draft smelting procedure maximized the iron-poor Ncherenje ore's potential in one critical aspect of iron manufacture—production of slag (SiO₂). While rich in iron, the Mbiri magnetite could not produce fayalitic slag (Fe₂SiO₄) due to a lack of silica. Additionally, the low-temperature (1200 °C) natural draft furnaces could not melt the high-grade Mbiri ore. To circumvent this conundrum, the ancient smiths chose the “best” ore for their metallurgy. That ore was the silica-rich, iron-poor Ncherenje stock. The slag and free iron produced in the first smelt was followed by a second re-smelting of the fayalite in the smaller forced-draft furnace. The product was a bloom sufficient to produce the utensils and tools required by the consumers—farmers and herders of Ancient Africa. So common yet so abundant an ore was largely the reason iron metallurgy spread throughout Africa and elsewhere (Fig. 9.9).

In modern-day Tanzania and Malawi, van der Merwe and Avery (1987) and Killick (1991)

Table 9.2b Whole-rock chemical analyses of samples from the Ncherenje mine

| Sample number | 1 | 2 | 4 | 8 | 9 | 10 | 11 | 12 | 13 |
|--------------------------------|-------|-------|--------|-------|-------|-------|--------|-------|-------|
| SiO ₂ | 56.95 | 37.37 | 41.07 | 35.73 | 51.47 | 52.46 | 68.06 | 48.25 | 40.94 |
| TiO ₂ | 1.38 | 1.16 | 2.21 | 2.29 | 1.45 | 1.38 | 0.66 | 0.22 | 1.10 |
| Al ₂ O ₃ | 19.73 | 31.5 | 30.33 | 27.37 | 22.21 | 20.41 | 15.27 | 4.05 | 28.26 |
| Fe ₂ O ₃ | 11.57 | 15.22 | 12.91 | 21.30 | 11.72 | 14.11 | 6.55 | 35.38 | 12.87 |
| MnO | 0.00 | 0.08 | 0.08 | 0.18 | 0.32 | 0.12 | 0.08 | 2.41 | 0.12 |
| MgO | 0.56 | 0.56 | 0.22 | 0.26 | 0.88 | 0.96 | 1.18 | 0.48 | 3.04 |
| CaO | 0.02 | 0.00 | 0.00 | 0.00 | 0.02 | 0.02 | 0.00 | 0.00 | 0.00 |
| Na ₂ O | 0.12 | 0.92 | 0.00 | 0.00 | 0.34 | 0.42 | 0.26 | 0.08 | 1.10 |
| K ₂ O | 3.30 | 5.96 | 0.18 | 0.10 | 4.96 | 3.06 | 1.76 | 0.76 | 7.00 |
| P ₂ O ₅ | 0.10 | 0.38 | 0.06 | 0.3 | 0.30 | 0.64 | 0.24 | 0.60 | 0.10 |
| H ₂ O- | 0.34 | 0.06 | 0.50 | 0.14 | 0.58 | 0.24 | 1.78 | 0.08 | 0.18 |
| LOI | 5.84 | 6.38 | 12.12 | 11.57 | 5.79 | 6.25 | 5.74 | 5.99 | 5.24 |
| Total | 99.93 | 99.51 | 100.06 | 99.66 | 99.58 | 99.75 | 100.30 | 99.64 | 99.93 |

LOI loss on ignition

Fig. 9.9 One of the deep pits used to extract ore from the Mbiri iron mines, northern Malawi (Wenner and van der Merwe 1987) (Photograph by David Wenner)



describe the production of high-carbon, “stealed” blooms. In Tanzania, the iron process is called Buhaya technology (van der Merwe and Avery, *supra*). The process used in Malawi has no particular name. In the former, long tuyeres (60 cm) extend into the shaft furnace and a bellows provided forced air to the interior. The air is drawn back and forth by the bellows allowing heated air to reenter allowing high temperatures of upward to 1800 °C. In this hot, reducing environment, the wustite-fayalite slag passed to a bed of wet grass on the furnace bottom. The slag is reduced, growing an iron-rich bloom on the furnace floor.

The Malawi smiths use draft furnaces, one tall (>2 m) and the other type only 1.4 or so meters in height. Traditional Phoka smelters, of northern Malawi, use a two stage smelting process. Their drafts typically do not produce high furnace temperatures (*supra*). The first stage of the Phoka smelting procedure involves a natural draft furnace operating at or below 1200 °C which processes the low-grade Ncherenje ore into slag and some free iron metal (Fig. 9.10). The slag is then re-smelted in a smaller forced-draft furnace at 1400 °C (Fig. 9.10). The iron is produced from the fayalite. The low-grade iron, lateritic, as described in the foregoing on open

mines, produces 20–30 kg blooms after 5 days (Killick 1991).

9.6 Metallic Minerals and Ore Genesis

Carr and Herz (1989) summarize, in Tables 9.2a and 9.2b, the origins for most metallic minerals. Bateman, in his earlier synthesis (1950), makes clear the diversity of geologic sources for metallic minerals and their ores. As Rono (1984) points out, the recognition that metallic mineral deposits are concentrated by hydrothermal processes at seafloor spreading centers together with ore-forming processes such as massive sulfides in volcanogenic rocks on land, was a major consequence of the plate tectonic revolution (Frankel 2012). Whereas the genetic role of tectonogenesis was geology’s signal contribution to twentieth-century science, the association of igneous activity with metallic mineral deposits had a long history beginning with the nineteenth-century French geologists Elie Beaumont and Gabriel Auguste Daubrée and the German Theodor Scheerer.

Hydrothermal activity first associated with volcanogenesis then oceanic spreading centers



Fig. 9.10 Malawian iron manufacturing, 1982, Chulu, Malawi; *above, left*, furnaces prior to firing; *above, in operation*; *above, right*, micrograph (1000 \times) showing iron (bright spheres) in bloom matrix; *right*, bloom

showing large (macroscopic) iron inclusions produced by the smaller, forced-draft furnace (Photographs by Nicholas van der Merve)

is, today, considered the *prima facie* reason for ore-forming processes (Keith et al. 2014).

Metals such as copper (Cu), molybdenum (Mo), gold (Au), tin (Sn), and tungsten (W) in porphyry and related epithermal mineral deposits are derived predominantly from the associated magmas, via magmatic-hydrothermal fluids exsolved upon emplacement into the mid- to upper crust (Richards 2011). The bulk of the metal flux into the porphyry environment may be carried by moderately saline supercritical

fluids or vapors, with a volumetrically lesser amount by saline liquid condensates. However, these vapors rapidly become dilute at lower temperatures and pressures, such that they lose their capacity to transport metals as chloride complexes. They do retain significant concentrations of sulfur species, and given propitious geochemical conditions such as pressure, temperature, and oxygen fugacity of mineral solutions— fO_2 —a primary control over magma sulfide which, in turn, accounts for differing

amounts of copper, gold, and siderophile elements in sulfide ore mineralizations (Keith et al. 2014; Jugo 2009).

Operative to hydrothermal settings is Nernst's law—the intermixing of two solutions containing salts of varying solubility which result in the precipitation of one salt at the expense of the other by the decrease of the one salt's solubility in the presence of another salt with the same ion.

Ex : $\text{Fe CO}_3 - \text{Zn CO}_3 - \text{CaCO}_3$ or Siderite
— Smithsonite — Calcite.

Likewise, ores may replace other minerals in host rock by *metasomatism*. It is associated with metamorphism. The hydrothermal fluid solutions—either diffusional or infiltrational—act as a solvent thereby replacing one mineral with another without melting, a mass transfer process.

The underlying concept of metasomatism is the acid-basic interaction of hydrothermal fluids and their general evolution as they cool through time from an early alkaline to an acidic stage. This process is termed *epigenetic* through *paragenesis*. Minerals so produced are called *metasomes*.

Skarns (Goldschmidt 1912) are typical of metasomes and can form flat bodies along the metamorphic contacts as veins, pipes, etc. crossing the carbonate and/or the silicate rocks.

Metasomes form at the contact between a silicate rock (or magmatic melt) and a carbonate rock. These rocks consist mainly of Ca-Mg-Fe-Mn silicates. In the so-called magnesium-rich skarns, the creation of new, metasomatic facies depends on P-T conditions and chemical activity that are typified by phlogopite-diopside, phlogopite-forsterite, magnetite-forsterite, diopside-monticellite, and monticellite-brucite as examples of replacement “pairs.”

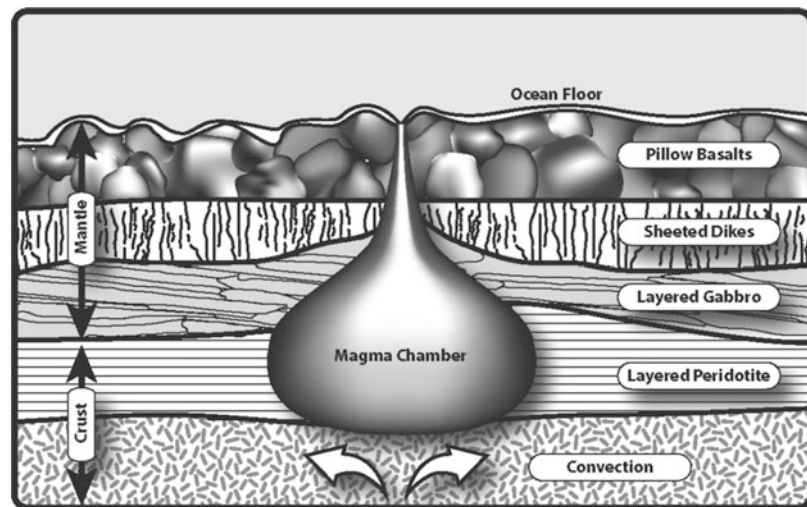
In the tectonic setting, of a subduction zone, most base and precious metals would be expected to have at least moderate solubilities in the hot, relatively oxidized, saline aqueous fluids exsolved from the downgoing slab. Pb, As, and Sb are strongly mobilized by such fluids. Lead, which is significantly enriched in the continental crust (and crustally derived sediments) relative to the mantle, is the only metal for which a clear sedimentary source can be inferred in some island arc magmas.

Porphyry Cu-(Au) deposits are found in association with mantle derived arc magmas worldwide, regardless of crustal type (oceanic or continental) or thickness (Kesler 1973). Tin and especially tungsten commonly accompany molybdenum into porphyry deposits as trace metals and by-products, but they also form a class of porphyries on their own, associated with S-type granites in continental orogens (Hart et al. 2005). The Hercynian tin granites of Europe and the Bolivian and SE Asian tin belts are examples of such deposits, with mineralization occurring in skarns and greisens around the granite intrusions (Meinert et al. 2005).

Ore minerals are typically classified as either hypogene or supergene, which indicates the direction of the fluids involved in their creation—*hypo*, from “below” or ascending, and *super(ra)*, from “above” or descending. This mineralization is also characterized as “primary” and “secondary.” Bateman (1950) correctly notes confusion arose from the use of “secondary” so *supergene* has subsequently been used as the better term. The Troodos massive sulfide complex, on Cyprus, provides an excellent example of ore formation via these two mechanisms. Hutchinson (1965) identified deposits with a sulfide content of 40–99 % with those with the highest copper and zinc content having the highest sulfide content. The ore bodies were composed primarily of pyrites with chalcopyrite, the most prevalent, and marcasite, a minor component. Pyrrhotite is absent in Cyprus ores. Sphalerite is found. These were hypogene deposits but the Troodos ore bodies have been exposed to extensive surface weathering thereby permitting supergene formation of secondary copper sulfides to include chalcocite, bornite, and covellite along with secondary sulfates. Gold and silver are present at Troodos but in only minor amounts. Killick (2014) notes that supergene enrichment results from the oxidation of pyrite yielding sulfuric acid and ferrous sulfate. The former leaches copper from the oxidized hypogene deposits precipitating the copper as chalcocite at the top of the hypogene zone.

An ophiolite is a section of the Earth's oceanic crust and the underlying upper mantle that has

Fig. 9.11 Characteristics of an ophiolite complex: axial magma chamber; pillow lava basalts; sheeted basaltic dikes; layered gabbro; dunite/peridotite



been uplifted or emplaced to be exposed within continental crustal rocks. *Ophio* is Greek for “snake”; *lite* means “stone” from the Greek *lithos*. The term ophiolite was originally used by Alexandre Brongniart (1813) for an assemblage of green rocks (serpentine, diabase) in the Alps. Steinmann (1927) later modified its use to include serpentine, pillow lava, and chert (aka “Steinmann’s trinity”), again based on their occurrences in the Alps.

With the recognition that ophiolite sequences being formed at oceanic spreading centers, in the late 1950s to early 1960s, these assemblages provided structural analogs for oceanic crust and seafloor spreading. It is widely accepted that ophiolites represent oceanic crust that had been emplaced on land. Ophiolites have played a central role in modern plate tectonic theory by virtue of their creation at intraoceanic subduction zones followed by collision of the subduction zone with a continental margin. The sheeted dike complex within the Troodos ophiolite, on Cyprus, was recognized by Gass (1968), Hutchinson (1965), and others as having formed by the intrusion of magma, since no older wall rocks are preserved within the complex. The Eastern Mediterranean region is characterized by one of the largest concentrations of ophiolites anywhere in the world, thereby providing much of the porphyry ores exploited in antiquity.

As shown in Fig. 9.11, an ophiolite complex consists of a stratigraphic sequence trending upward from the ultramafic mantle through gabbro thence sheeted dikes and pillow basalts all beneath a sedimentary cover. In sequence, 1.5 km of basalt overlies roughly 1.5 km of diabase dikes which, in turn, overlie 4 to 5 km of gabbro. The gabbro overlies the mantle rock (dunite/peridotite) at its base (Carlson and Miller 2005). At Troodos, Hutchinson (1965) identified the bulk of the ore bodies in the upper and lower pillow lavas.

As mentioned, current thinking has ophiolites being primarily the result of volcanic activity at an intraoceanic subduction zone, and this followed by collision of the subduction zone with a continental margin. Ophiolites that were emplaced associated with active margin settings range from large accreted thrust sheets to small slices within accretionary prisms and back-arc basins (Robertson 2006).

Whichever their origin, the Troodos pyrite deposits are some of the best described and oldest mined deposits in the world. In the central Mediterranean, it has long been known that some of the richest copper deposits in Europe are located in the eastern Alps including the Trentino-Alto Adige/Südtirol region in Italy (Preuschen 1973) (Fig. 9.12). The Alpine deposits encompass copper and iron-copper sulfides, fahlores (polymetallic sulfides), and occasionally galena (Oxburgh

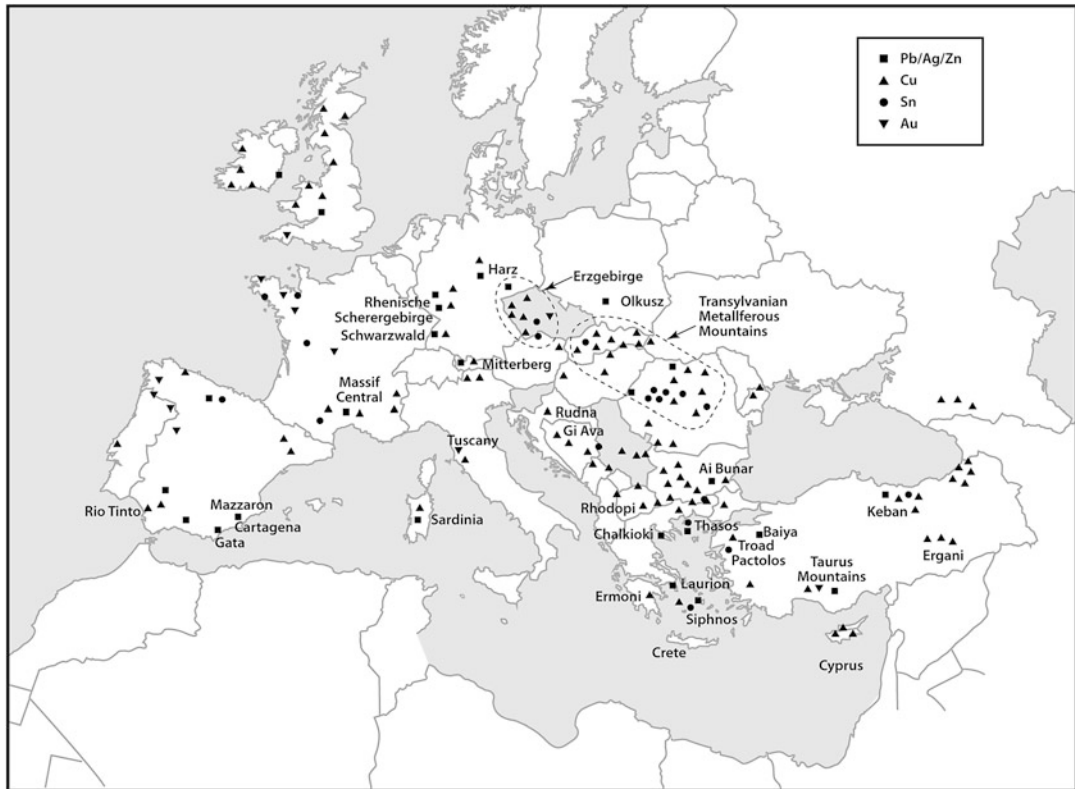


Fig. 9.12 European metal deposits with central European mines highlighted

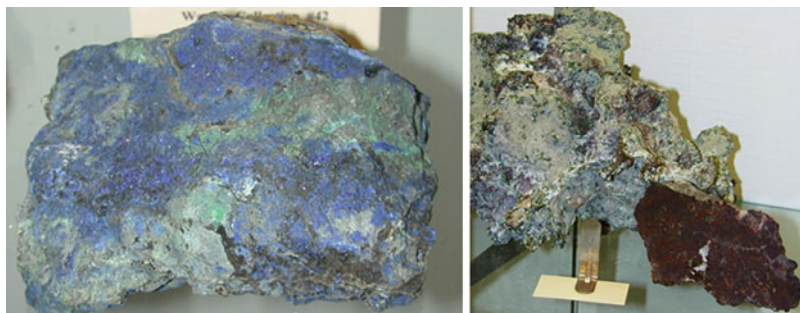


Fig. 9.13 Copper ore, azurite (left); native copper (right)

1968; Zuffardi 1977; Lutz and Pernicka 2013). Fahlores are important European and Andean ores. Most famous of the central Mediterranean ore deposits are those of Laurion (Fig. 9.13).

Figure 9.14 illustrates the geologic situation at Laurion. It is basically an alternation of schist and calcite layers with the argentiferous lead ores

deposited mainly where impervious schists overlie the more porous limestones/marbles. Mined levels are conventionally referred to as the first (1) (uppermost) and third (3) (lowest) contacts. The illustration (Fig. 9.14) shows how the ancient miner might follow the contact level. Also shown are rows of ancient galleries at Thorikos itself,

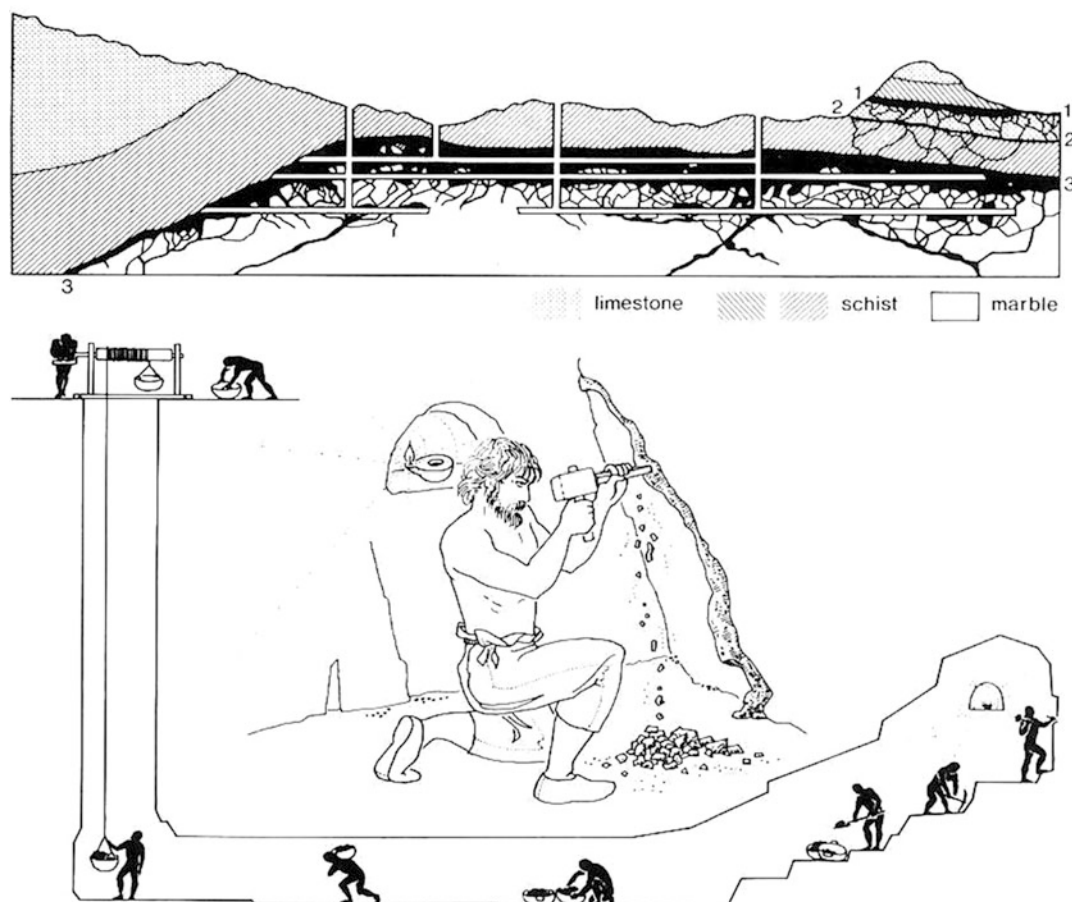


Fig. 9.14 Schematic of Laurion's geology of alternating schist and limestone with metal bearing contacts (1–3) between them. The ore contacts, 1 and 3, the richest. Argentite: “silver ore” is associated with the lead ore,

cerussite (PbCO_3). The principal silver ore mineral is silver chloride, cerargyrite (AgCl), and silver sulfide (Ag_2S). The latter is mixed with galena, PbS

more or less horizontally driven into the lower slopes of the Velatouri hill (Jones 1982).

Meixnar and Paar (1982) identify three groups of minerals at Laurion—primary mineralization (hypogene), oxidation minerals (supergene), and secondary minerals (supergene). The oxidation zone minerals—cerusites (carbonates), arsenates, chlorides, and sulfides—made Laurion the source of Athenian wealth in the Periclean Age (Garrison 1999) (Tables 9.1 and 9.3).

Hypogene subsumes hydrothermal ore formation. Supergene implies oxidation/hydration to secondary deposits. Hematite is listed as “sedimentary,” for instance, because of its extensive presence as a precipitate in banded iron formations (cf. Table 9.1).

9.7 Model Studies for the Analysis of Metal in Archaeological Geology

9.7.1 Slag: “The Archaeometallurgist’s Friend”

The careful study of slag can:

- Provide proof of metallurgy on an archaeological site
- Demonstrate the type of metallurgy present at a site, e.g., “common” copper, bronze, iron, etc., “noble”—gold, silver; coin manufacture (cf. Titelberg metallurgy below)

Table 9.3 Principal metallic ores

| Group and name | Formula | Geologic origin(s) ^a |
|--------------------------------|---|---------------------------------|
| <i>Sulfides</i> | | |
| Galena | PbS | Hypogene |
| Sphalerite | ZnS | Hypogene/sedimentary |
| Covellite | CuS | Supergene |
| Chalcocite | Cu ₂ S | Supergene/sedimentary |
| Argentite/acanthite | Ag ₂ S | Supergene |
| Stibnite | Sb ₂ S ₃ | Hypogene |
| Pyrite | FeS ₂ | Hypogene |
| Chalcopyrite | CuFeS ₂ | Hypogene |
| Bornite | Cu ₅ FeS ₄ | Hypogene |
| Stannite | Cu ₂ FeSnS ₄ | Hypogene |
| Arsenopyrite | FeAsS | Hypogene |
| <i>Oxides</i> | | |
| Cuprite | Cu ₂ O | Supergene |
| Magnetite | Fe ₃ O ₄ | Hypogene |
| Hematite | Fe ₂ O ₃ | Hypogene/sedimentary |
| Limonite | Fe ₂ O ₃ ·3H ₂ O | Supergene |
| Goethite | FeO(OH) | Supergene |
| Cassiterite | SnO ₂ | Hypogene |
| Ilmenite | FeTiO ₃ | Supergene |
| <i>Carbonates</i> | | |
| Malachite | CuCO ₃ ^a Cu(OH) ₂ | Supergene |
| Azurite | 2CuCO ₃ ^a Cu(OH) ₂ | Supergene |
| Siderite | FeCO ₃ | Hypogene/sedimentary |
| Smithsonite | ZnCO ₃ | Supergene |
| Cerussite | PbCO ₃ | Supergene |
| <i>Chlorides and silicates</i> | | |
| Cerargyrite | AgCl | Supergene |
| Atacamite | CuCl ₂ ^a 3Cu(OH) ₂ | Supergene |
| Chrysocolla | CuSiO ₃ ^a 2H ₂ O | Supergene |
| Hemimorphite | 2ZnSiO ₃ ^a H ₂ O | Supergene |
| <i>Arsenates</i> | | |
| Enargite | Cu ₃ AsS ₄ | Hypogene |
| Olivenite | Cu ₂ (AsO ₄)(OH) | Supergene |
| Domeykite | Cu ₃ As | Hypogene |
| Tennantite | Cu ₁₂ As ₄ S ₁₃ | Hypogene |
| Tetrahydrite | Cu ₁₂ Sb ₄ S ₁₃ | Hypogene |

^aNo distinction is made between a massive sulfide or porphyry hypogene deposits

- Illustrate technology and general chronological period for the site, e.g., if % high, metal ~ “early” or % low, metal ~ “late,” well-developed metallurgy
- % of SiO_2 fluxed ~ high temperature processes, “later” metallurgy
- Point to oxidation products that were present

Henderson (2000) notes that the earliest firm evidence for a smelting technology comes from the Feinan area (Jordan). Hauptman (1989), Rothenberg and Merkel (1995), Kafafi (2014), and Levy et al. (2014) emphasize the importance of the Feinan to early metallurgy. A full-fledged smelting technology converted gangue to liquid (slag), which was tapped or poled off (cf. earlier discussion re: matte smelting, etc.). Rothenberg and Merkel (*supra*) report the presence of bowl-shaped hearths for Chalcolithic copper production at Timna.

Henderson reiterates the point that the archaeological evidence for smelting has always been “thin on the ground.” If the archaeologist is fortunate to recover the actual metal, then impurities may provide clues as to smelting. Fayalitic residues point directly to high temperature

smelting by virtue of iron minerals being able to combine with silica. At Feinan sites like Timna (Fig. 9.15), copper has been found below the slag.

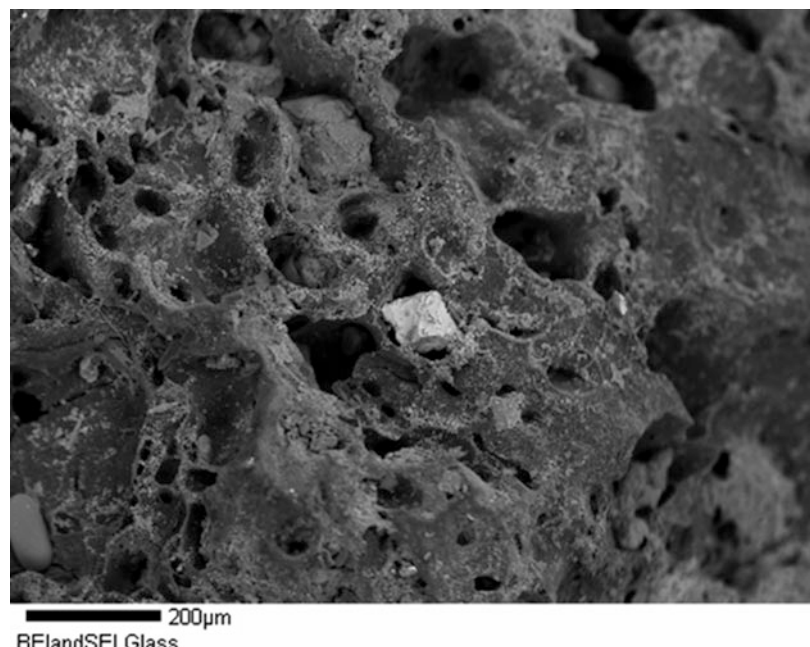
Whereas evidence for early copper smelting may be “thin on the ground” by the Iron Age, notably Iron Age IIB–IIC (ca. 900–500 BC) smelting sites at Feinan and Khirbet en-Nahas show massive evidence ($>100,000$ tons of slag!) (Rothenberg and Merkel 1995; Hauptmann et al. 1985; Hauptman z1989; Levy et al. 2014).

In iron slags, the following minerals can be seen microscopically (after Williams 2009):

Ferrite crystals are pure iron, Fe, and appear as irregular white areas. Only the grain boundaries are actually visible. Vickers hardness is 80–120 HV. Pure iron does not harden on quenching.

Pearlite is a mixture of iron and iron carbide containing up to 0.8 % C. It has a gray, lamellar appearance. It forms when steels are cooled in air after forging. Vickers hardness can be up to 250–300 HV. Most steels (hypoeutectoid, below 0.8 % C) are mixtures of ferrite and pearlite.

Fig. 9.15 Back-scattered electron image of iron slag



Martensite forms in quenched steels. It appears like laths, with some triangular symmetry. Vickers hardness, depending upon C%, varies from 200 to 800 HV.

Bainite also may appear in quenched steels. It appears as a feathery or needlelike material. Vickers hardness is 200–400 HV.

Cementite, iron carbide, Fe_3C , may be found as part of pearlite, or as separate areas in a network, or even appearing like needles, in hypereutectoid (above 0.8 % C) steels and also in cast irons (over 2 % C). The Vickers hardness of cast iron can be 400 HV, although pure cementite is much harder. Cast iron does not harden on quenching. In annealed cast irons, the cementite may break down into iron and carbon (graphite).

9.7.2 Example

9.7.2.1 The Gallo-Roman Forge at Chbles les Saux: Scories and Slags

In a comprehensive excavation report of a Gallo-Roman millstone quarry and associated smithy-forgo, the analytical extensive study of iron slags was detailed (Anderson 2003).

Located during archaeological studies prior to highway construction in Canton Fribourg, western Switzerland, a limestone quarry used for the extraction of millstones had, in close association, a smithy-forgo for maintenance of quarry tools. The site was occupied from the second half of the first century to the third century AD. The coauthor of the study, Vincent Serneels, carried out the metallurgical study of the smithy.

While the forge site produced a significant range of manufacturing debris, no evidence was recovered to indicate it ever functioned as a bloomery (*supra*). The principal artifact categories included tools or tool fragments, amorphous iron debris, cuttings, hammer scales, and scories containing slag. Slag dominated in terms of amount present. It was found in an area interpreted as a dump or rubbish heap along with two adjacent pits. The scories were very heterogeneous in form, material, and color such as

partially fused sandy clay; some had large grains of quartz and feldspar and varied from black, brown, yellow brown to gray, or whitish in color. Fayalite, along with wustite, iron oxide, was present mineralogically.

The slag varied macroscopically in texture and/or color from sandy-clay slag, gray dense slag, to iron oxidized slag. Figure 9.15, a back-scattered electron image, shows a typical slag texture. Also found were slag droplets, nodules, and hearth bottom slags.

The plano-convex hearth bottom slag was the most common form. Again, Serneels interpreted it as representative of a smithy and not a smelting operation. Estimates of the quantity of iron worked, at the site, were 5000 kg over a period of 10–20 years.

9.8 Artifacts: “When Fortune Smiles”

9.8.1 Example

9.8.1.1 Ulfberht Swords

About 100 Viking-era swords bearing the maker’s inscription, +VLFBEHR+T (for *Ulfberht*), have been found scattered around northern Europe. There is a general agreement in archaeology that the genuine Ulfberht blades were made in Christian environments familiar with the use of the Latin alphabet. This excludes the heartland, Viking, Baltic area, which was not Christianized until Ulfberht swords were no longer produced (eleventh century and later). Christianized Europe and the Middle East were prime suspect areas for the production of these weapons.

The normal procedure in metallographic investigations of edged weapons and tools is to analyze the full or, alternatively, the half section of a blade (Astrup and Martens 2011). For swords, this includes both the edges and the central part of the blade and discerns differences in materials between these parts and how they were welded together.

Standard metallographic techniques that compare samples with published atlases of alloy

microstructures were unable to determine the carbon contents of Viking-age swords. An analysis of supposed Ulfberht swords in the Wallace Collection, London, by the United Kingdom's National Physical Laboratory (NPL) used scanning electron microscopy (SEM) to determine the carbon contents of the steel samples provided. NPL analyzed very small specimens (1 mm in diameter) from Viking-age swords obtained from various museums in Norway and Finland.

NPL results showed that the swords were made of imperfectly melted steel—consisting of a mixture of iron and carbonaceous materials heated together to give high-carbon steel (~1.4 % C). The NPL results match descriptions of ancient sword making in Herat (in modern Afghanistan) described by ninth century Arab philosopher and writer Al-Kindi (Bronson 1986). Al-Kindi specifically mentions Herat as well as "Serendib" (modern-day Sri Lanka) as wootz steel centers (Bronson 1986). Crucible processes were in use outside of the subcontinent in Iran and Syria as early as the twelfth century AD and perhaps earlier (Bronson 1986).

Asian steel was, thus, made by the crucible process known as the "wootz process," which involved heating pieces of bloomery iron for hours to days, in sealed crucibles, with a carbon-containing material—charcoal or leaves—until enough carbon had been absorbed to form steel

(*supra*). WDX microanalysis of another wootz-type Medieval period sword using a CamScan MX2600 gave a carbon content from point analyses which varied from 0.59 to 2.33 %. An average of 15 points gave 1.4 % C, which is in accordance with a wootz-type steel (Williams 2009).

The carbon so absorbed into the iron produced a "wootz" steel which is characterized by its hardness. Such stealed iron could be brittle as well (Bronson 1986) but, in general, the Ulfberht-type swords with either all-steel blades, or blades with large and hard steel edges, achieved superior strength and hardness (Hošek et al. 2012).

The recent analytical results at NPL and Cambridge suggest that Vikings had brought crucible steel back to Scandinavia and integrated ancient Arab steelmaking methods with their own sword smithing. It would confirm, by extension, the existence of an important trade route from the Middle East to the Baltic area—down the Volga and across the Caspian Sea to Iran—that was in use until at least the eleventh century. On the Iranian Plateau, as we have seen, crucibles were used, as opposed to furnaces, in copper production until 3000–2500 BC (Frame 2009). While this does not imply a direct technological link in the use of crucibles for a much later wootz steel production of the Middle Ages, it serves to remind us that crucible use had a long history in SW Asia and India.

10.1 Introduction

Waltham (1994) considers statistics the most intensively used branch of mathematics in the earth sciences. His textbook, along with that of Robert Drennan, *Statistics for Archaeologists* (1996), is an excellent introduction to statistics appropriate for archaeological geology. Following Waltham, the definition of a statistic is simply an estimate of a parameter—mass, velocity, dimension, etc.—based upon a sample from a population. Unless that population is composed of a relatively small number of items or objects, then it is almost certain that estimates must be made of the populations using independently drawn samples. As archaeology is largely a study of population of “things,” reliable estimates of these collections are best made using statistical techniques. These techniques include parametric measures of central tendency and dispersion such as the mean, the standard deviation, and the variance.

Samples are observations of larger populations. For geological samples, they are the actual rocks and measurements. Taken on specific variables—the parameters such that a set number of observations on these variables make up a sample set. Dispersion is quantified and compared by statistical tests such as simple regression analysis on two variable or bivariate data. Additionally, a central question for archaeological questions of interest is that of “how big”

a sample set is needed to adequately test a difference in sample set means.

In earlier chapters, we have already alluded to statistical issues in our discussion of scale and sample size, particle size analysis, sample size, and regression or line of best fit. These are very common issues in both archaeology and geology. The justification of including an introductory chapter on statistics stems from the real need to evaluate one’s data for insights that are not that readily apparent. It is a necessary part of any rigorous science. The popularity of statistics in archaeological geology can be appreciated by a simple survey of any major journal wherein these techniques commonly appear. For example, in just one recent issue of the *Journal of Archaeological Science*, 8 of the 12 articles used statistical techniques of one form or another to present their data. While less common in journals of archaeology per se, even there one observes the increasingly frequent use of statistics. A 1999 issue of *American Antiquity*, alone, produced an impressive range of statistical methods, ranging from regression analyses, Bayesian estimations, and diversity measures to spatial and multivariate analyses in *all* five of the major research reports of that issue. Neither of these examples is unusual.

The focus of this chapter will be to list, and briefly describe, commonly used concepts and techniques in *data analysis*. It is beyond the scope of this book to attempt anything more

than this. As well as basic concepts, we shall look at ways used in the examination of large data sets that involve more than two variables—the so-called multivariate analytical methods. A few, brief examples, from archaeology and modern DNA studies of early hominids, will be used to illustrate the techniques or topics under discussion. The reader should take away in this chapter a sense that statistics offer ways to solve problems that may not be done otherwise.

10.2 Descriptive Statistics

Descriptive statistics consists of the methods for organizing, and summarizing information in a clear and organized way. In contrast, inferential statistics consists of the methods used in drawing conclusions based on information obtained from a sample of a population (Weiss and Hassett 1993). Inferential statistics is, sometimes, today, referred to as “frequentist statistics”—using measures such as sample size and so-called p-values (Flam 2014). Modern statistics is principally that of inferential statistics. We begin our discussion with descriptive statistical measures.

Scales: One area that will not be examined in any depth is that of nonparametric statistics or the techniques used in the evaluation of issues using ordinal or nominal scaled data. One important technique is that of *chi-square* (χ^2) and that will be discussed in some detail. Additionally, many data sets have non-normal distributions. These either have to be transformed to normal form or dealt with using nonparametric tests such as chi-square. With these caveats stated, we shall, nonetheless begin the discussion with these and other types of scales.

Scale types include (1) nominal, (2) ordinal, (3) interval, and (4) ratio. The types of scales differ on how the observations that make up a sample relate to one another. The simplest relationship between observations is that of the nominal scale. The nominal scale accounts only for identity such as “type A,” “type B,” etc. That is to say, it is “categorical,” non-ranked data. An example would be rock or pottery types. Within “type A,” there may be ten observations; “type

B” may have five observations. Presence-absence data are nominal scaled.

For ordinal scales, ranking is implicit although the ranks may not be of equal magnitude such as the Moh’s hardness scale (cf. Chap. 6). Observations within ordinal classes have an order. Grade categories are ordinally scaled, e.g., A, B, C, D, and F imply rank within the grade categories of an A → F order. Ranking is relative just as is magnitude.

Most observations, in what is termed parametric statistics, are interval scaled. Interval scale data improves on ordinal data as this scale has a continuum of integers divided as equal whole or decimal numbers. Size is scaled along interval scales as is temperature and dates. Interval data is arithmetic such as $2 + 2 = 4$; $2 - 1 = 1$.

Ratio scale data are typified by geometric or progression relationships. For instance, $2 \cdot 2 = 4$; $8 \div 2 = 4$ is ratio scale data. The distinction to be noted is that when one converts between interval scales addition and multiplication is necessary. When one converts between ratio scales (e.g., length in centimeters to inches), only multiplication is necessary, hence the term ratio. The ratio scale has an absolute difference in observations, and it has a natural, non-arbitrary zero point. Measurements of mass, length, time, velocity, etc. are scaled on a ratio basis.

10.2.1 Variables

Mention should be made of the important distinction between the characteristics of the observations we collect as data. Characteristics of the members of a population vary and are termed *variables*. The two kinds of variables are either (1) continuous or (2) discrete. An analogy from human genetics illustrates this difference—the gene(s) for human skin color are basically continuous—the wide range in human skin coloration from white through brown to black, while the gene for human eye color, and that for blood groups, is relatively discrete, e.g., blue, brown, or gray/green; A, B, AB, and O.

The continuous variable may assume any value within a set range such as fractional

numbers such as 30.5, 63.4, 73.5, or 75.1. By comparison, the discrete variables would take on only whole number values such as 30 coins, 25 rocks, etc. One normally does not refer to fractional values of coins such as 30.5 “dimes,” but it is perfectly appropriate to describe height as 30.5 cm or mass as 125.25 g. For populations, the values of variables are parameters; for samples, they are statistics. Measurements on variables are observations or data. Sets of data drawn from a population of variables are samples—the business of statistical inquiry.

10.2.2 Frequency Distributions, the Normal Distribution, and Dispersion

Table 10.1 lists the relation between types of scales and their various statistical measures of central tendency.

In this table, we observe that mode and median are calculated for nominal and ordinal data, respectively, but one may use them for interval and ratio scales as well. In many cases, they are appropriate measures of central tendency. Under the tests of significance, chi-square examines the dependence between characteristics or “types” in a population. How well they might be associated is contained in the value of the chi-square statistic—if the calculated chi-square value exceeds the tabulated value, at the predetermined level of significance, then the parameters are dependent or associated. Likewise, the interval and ratio scales examine central tendency—dispersions—and association is examined by correlation coefficients and comparisons between sample means are made

using the *t*- and *f*-tests. These will be discussed further in the following sections.

Even in this world of spreadsheet software and the graphical presentation of data, the need for an extended description of frequency plots exists. The frequency plot-bar graph, pie chart, etc. shows, in graphical form, how often a particular variable is observed. The variables are discrete in nature. A hidden danger with the ease with which software makes the production of these presentations is that of appropriateness. Frequency data should be displayed with bar charts, but *X-Y* data should be shown using *X-Y* plots. Data visualization is the first step in data analysis; therefore, care should be exercised when applying software to data. This injunction extends from statistical packages included in spreadsheet programs to the more sophisticated forms like SPSS.

A plot of a set of continuous variables will produce a similar looking graph, but since the data is continuous, intervals must be chosen within the continuum. An example is that of a frequency spectrum such as encountered in a conductivity meter’s data set. The frequency spectrum can be displayed continuously from, say, 300 to 19,000 Hz. Values within this range can be measured and displayed as continuous data. In actuality, most conductivity data is displayed within set frequency intervals such that only values at specific frequency settings are plotted such as 300, 3500, 8250, 19,000 Hz, etc. Counts or values of either discrete or continuous data produce histograms.

10.2.3 The Normal Distribution

A histogram or the frequency observations of variables is often confused for the probability

Table 10.1 Scales and statistical measures

| Scale type significance | Measures of central tendency | Measures of dispersion | Measures of tests of association |
|-------------------------|------------------------------|--------------------------------|--|
| Nominal | Mode | | Chi-square |
| Ordinal correlation | Median | Percentiles | Rank |
| Interval | Mean | Average and standard deviation | Correlation ratio; <i>t</i> -test <i>f</i> -test |
| Ratio | Geometric mean | | |

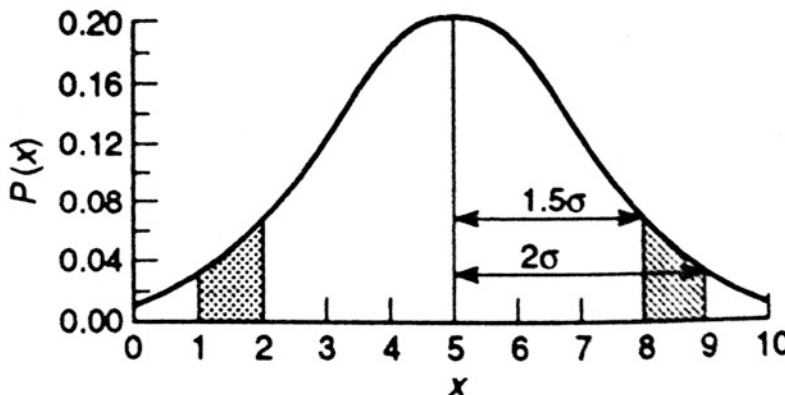


Fig. 10.1 The normal distribution. (a) The area under the curve is, by definition, 1; (b) the measure of central tendency is the mean, which is, again, by definition, zero; (c) the curve is perfectly symmetrical about the mean; (d) the standard deviation, along with mean, completely defines the normal curve; (e) the mean, mode, and the

median *all* have the *same* value. The probability $p(x)$ of occurrence of any observed values from 1 to 2 and 8 to 9 (a two-tailed σ is shown in shaded areas). The range of values in this example is 0–10 with the mean (x) = 5.2; 1.5σ indicates the standard deviations from the mean (Adapted from Waltham 1994, fig. 7.7, p. 119)

distribution. The latter are histograms of the probability of a variable and not its observed frequency. One of the most common probability distributions is the normal distribution. The normal distribution can represent either discrete or continuous variables. The great German mathematician, Carl Friedrich Gauss, in the context of determining the frequency of observable stars in a quadrant of the night sky, developed the basis for the normal or “Gaussian” probability distribution. The importance of the normal distribution lies in its central role in statistics. Because it introduces probability, it lies within the province of inferential statistics. A major assumption of normal distribution is that it characterizes the frequency of occurrence of most continuously distributed populations such as Gauss’ stars. The normal distribution is graphically familiar as the normal or bell-shaped curve (Fig. 10.1). Key mathematical properties of the normal curve are:

The normal distribution is a statistical construct which may or may not apply to any given data set. There are other types of probability distributions of discrete variables that are important to statistics such as the binomial distribution, the Poisson distribution, and the negative binomial distribution. The most important of these is the binomial distribution. It is the most widely

used discrete probability distribution. By its name, it implies that it is used in the study of two variables. It is like the normal distribution, and the other types have an area of 1. However, a mean of zero is singular to the normal distribution alone. Other distributions where the mean, mode, and median are not the same and display *skew*. This parameter is commonly calculated in sediment textural analyses typical of those outlined in Chaps. 4 and 5. The skewness of the grain size or other particulate distribution, e.g., phytoliths, can be instructive. Another way of thinking of skew is in terms of the symmetry of a distribution. The normal distribution is symmetrical with no skew. Other distributions—Poisson, Gumbel, Pearson Type III, etc.—can, and typically will, display, nonsymmetrical curves. In fact, the Poisson is recognized by its sharp skew to the left axis and hence tells one that the sample population can be described thus.

It is the normal distribution that is most commonly assumed to underlie most phenomena. This is formalized in the Central Limit Theorem. The Central Limit Theorem states that the means of samples from a population have a normal distribution provided the sample size, n , is large enough. Notice that the Central Limit Theorem does not require the sampled population to be normally distributed. This is important,

conceptually, as it allows inferential statistical tests, such as the *t*-test, discussed below, to be used on non-normal data.

10.2.4 Central Tendency

In Table 10.1 are listed the measures of central tendency appropriate for variously scaled data. The normal distribution's most common measure of central tendency is the mean. It is used to measure data on interval or ratio scales. Here, the mean may not be such a good choice particularly if the distribution is asymmetrical. In this case, perhaps, the mode—that data value which occurs most frequently—is a more representative measure. The measure of central tendency for ordinal data is the median. In the normal distribution, whose mean is zero, the median is likewise (see above) (Hampton 1994). Unlike the mean, the median is some value that has an equal number of items above and below its value. This is to say that data value is exactly in the middle of an ordered list such as with the case of the following seven values—2 2 2 3 4 4 5. In this sequence, “3” is the median value. For nominal scales, the measure of central tendency is the mode or the most frequently occurring item in the data set. In a set of ten flint artifacts, eight basalt artifacts, and five quartzite artifacts, the mode is “flint artifacts.”

There is no simple rule for choosing one of the three—mode, median, or mean—to measure central tendency. For instance, if the data is bi- or trimodal, then using either the median or mean seems to be poor choices, whereas the mode is more representative of central tendency in these cases.

Another example could be that of cathodoluminescence observed in a suite of marbles such as what we have seen in Chap. 7, Table 7.3. We see that the researchers have reported the “mode” for the CL color for the marbles, e.g., Thassos-Vathy, a dolomitic marble, is “red”; Carrara marble is “orange”; etc. Had the researchers quantified the CL in interval terms, then we might use either the median or mean to describe the “intensity” of the “red” or “orange.” Be this

as it may, it is the arithmetic mean that one encounters most often in parametric statistics and this is what we shall discuss now.

10.2.5 Arithmetic Mean and Its Standard Deviation

The mean of the overall population is symbolized by μ , whereas the sample mean is denoted as \bar{x} . It is calculated as follows:

$$\bar{x} = \Sigma x/n$$

or the sum (Σ) of the x observations of a variable divided by n observations. The standard deviation, σ , is the mean squared difference between an observation and the mean. The calculation of the standard deviation requires that one must first determine the total variation or variance (s^2) within the sample. The population variance, σ^2 , is often illustrated in textbooks but rarely used. To calculate s^2 , the sum of squares (ss) is first calculated. The formula is

$$ss = \Sigma(x - \bar{x})^2$$

Here, the mean is subtracted from each value of the data set. These differences are then squared and summed. The parameter obtained is divided by, n , the number of observations.

$$\sigma^2 = ss/n$$

This is the population variance which can rarely be determined so one uses $n - 1$ in the denominator to determine s^2 or simply: $s^2 = ss/n - 1$. The standard deviation is simply the square root of the variance.

In the normal distribution, the standard deviation is mathematically the point of maximum inflection tangent to that normal curve. Under the normal curve, one standard deviation represents 34.13 % of the total area under the curve. This is for one “tail” or side of the curve, so for the total curve, one standard deviation represents 68.26 % (Fig. 10.1). Typically, the reporting of a radiocarbon date is at one standard deviation from the mean age.

10.3 Inference: Hypothesis Testing, Types of Error, and Sample Size

10.3.1 Hypotheses and Testing

In the Scientific Method, the approach to evaluation of phenomena is through the use of hypothesis testing. Statistics—those which we term *inferential*—aid in the evaluation of hypotheses. A hypothesis is simply a statement that something is true. As such, this statement can be tested. The *null hypothesis* is that which is actually tested. An example of this method can be illustrated by use of the CL of marbles. We can assert “All Carrara marbles show orange CL.” To test this “null hypothesis,” we then examine a sample population of Carrara marbles. If one sample is found not to be orange, then the null hypothesis is found to be false. A key aspect of scientific methodology is that a hypothesis must be falsifiable. If the null hypothesis is incorrect—not necessarily “untrue”—then maybe an “alternative” hypothesis is better such as the statement “*MOST* Carrara marbles show orange CL.” Another way of looking at this is to say that “there is a high probability that a sample of Carrara marble will show orange CL” and that this *mode* will be observed in almost all cases. This second hypothesis is *confirmed*.

10.3.2 Probability

Probability is conceptually central to inferential statistics but not so for descriptive statistics. Probability is the relative frequency with which an event occurs. It is also possible to discuss distributions and many of their descriptive parameters without recourse to a discussion of probability as well.

Classical probability for independent events with equal outcomes: This rule states that for independent events that are equally probable, where an event does not in any way determine the occurrence of another event, such as height and eye color, then by knowing the total number

of possible outcomes, we can calculate the probability for a particular outcome or event. If f is the observed outcomes or events and N is the total number of possible outcomes or events, then the probability $P(E)$ is

$$P(E) = f/N$$

The classic example for this is toss of the coin with the “head or tail” outcomes so that $P(E)$ is

$$1/2 \text{ or } 0.5.$$

One notes that since the two possible outcomes, head or tail, cannot happen at the same time, they are termed mutually exclusive. Independent and mutually exclusive outcomes are sometimes confused. They are not the same.

Another illustration of rule 1 would be the presence of seven basalt stone tools in a sample assemblage of 40 tools where $P(E)$ for this occurrence is 7/40 or 0.175.

By use of a rule termed complementation, the probability of a non-basalt tool ($P(\text{not } E)$) is simply

$$P(\text{not } E) = 1 - P(E) \text{ or } 1 - 0.175 = 0.825$$

These rules are central in the calculation of expected probabilities used to determine the chi-square statistic as we shall see.

Other fundamental laws of probability are:

- A probability of zero means the event cannot happen.
- A probability of one means the event must happen.
- All probabilities must be between one and zero.
- The sum of the probabilities of all simple events must equal one.

Probability distributions are models of a specific kind of random process. Key to any discussion of probability is the assumption of randomness or that the occurrence of a thing or event is unpredictable. Returning to the coin toss, we know the outcomes must be head or tail, but we cannot predict which outcome will occur on any particular toss. Probability estimates

quantify uncertainty. By rule (c) above, the uncertainty lies between 1 and 0 with an increased certainty (or concomitant reduction of our uncertainty) if the value lies closer to one than zero.

10.3.3 Types of Error

In statistical inference, a decision to reject the null hypothesis when it is really true is called a Type I error. Likewise, the acceptance of the null hypothesis when it is false is called Type II error. The probability of making a Type I error defines the *significance level* or α . The probability of making a Type II error is denoted as β . To illustrate this, we can suppose that the rejection region for a hypothesis is at the two standard deviation level or has a probability of 0.9544. If our estimate—mean—falls within the rejection region and it is really a member of that population, then we have a Type I error. Cannon (2001:186) illustrates this with regard to zooarchaeological assemblages. In his example, if one concludes there is a trend in relative abundance (of species) in sample assemblages when in fact there is not, then this is Type I error.

10.3.4 Confidence Interval and the Z-Score

To use statistics in the tests of hypotheses, we can examine a set of sample values and determine their mean and compare that to an expected value or a hypothesized value. Generally, we have an idea of the “population” mean so we can assess our samples against this parameter. Additionally, the use of mean implies a range of values for the population. Anything outside this range, typically expressed in terms of the standard deviation, is considered in rejection region of the population. We name the range of values in our population as the *confidence interval*.

The confidence interval, or CI, can be observed or calculated as we shall see in our discussion of the Student’s *t*-distribution below. The CI is simply an interval of numbers about a

mean, and a *confidence estimate* is a measure of how sure or confident we are that an observed value will lie within that interval.

One way of expressing the distance of an observational measurement, x , away from the mean is the Z-statistic or Z-score. The Z-score is calculated as follows:

$$Z = (x - \mu) / \sigma$$

For example, a $\mu = 728$ mm and $\sigma = 73$ observation, $x = 801$, we define—as a new statistic—the standard error of the mean, given by

$$\sigma_{\bar{x}} = \sigma / \sqrt{N}$$

$z = 1$ means the value of x is exactly 1 standard error from the mean and will occur, in the one-tailed case, 34 % of the time. Here again, it is best to use the parameter, s_0 , for the sample distribution’s standard error rather than that of the population, or instead of N , we choose $n - 1$ for the denominator and derive the square root. The standard error of the mean observed from the samples was drawn from the sample population. To calculate the Z-score, one *must* use sigma (σ) or the population parameter.

For our example:

$$Z = (801 - 728) / 73 = 73 / 73 \\ \text{or } z = 1$$

One can use the Z-score to determine the probability of finding a specific value in a normally distributed population. One must use a table of Z-scores to convert to curve area. For $Z = 1$, this is self-evident, but for fractional values, a table of Z-scores is necessary. I have introduced this technique for inference more to illustrate the concept of standard error than to imply it is commonly used. Because the sigma is so rarely known, the Z-score is of limited value. Statisticians such as W.S. Gossett, in 1908, developed the Student’s *t*-distribution and the *t*-test, which are more commonly used than Z. The *t*-distribution has a similarity to the normal curve and as sample sizes become large enough closely approximates it.

The *t*-score, determined by the *t*-test, differs from the Z-score in that the standard deviation of the population must be estimated. This is not

surprising as most population parameters are not well known at first if ever. The confidence interval, CI, used in the *t*-distribution is calculated as follows:

$$C.I. = \bar{x} + (t_{0.05, n-1})(s_{\bar{x}})$$

We can intuitively estimate the age range of an archaeological site based on ceramics or we can estimate the range in the size of ceramic vessels of a particular phase or period. From that intuition, we can then estimate the standard deviation to a first approximation. After more rigorous study of a large suite of samples that estimate can be refined such that the population's variability is more correctly known₁.

In calculating the *t*-score, the value is very much dependent on sample size because the standard error is that of the sample, *s*, where *n* is now *n* – 1. The calculation is similar to that of the *Z*-score. The direct calculation of *t* is as follows:

$$t = (\bar{x} - \mu) / s_{\bar{x}}$$

This score can be compared to tabular values of *t* to examine whether a mean lies within a specific confidence interval. For example, if a *t*-score of 2.3 is calculated, it exceeds the tabulated *t*-score of 1.984 so this mean is unlikely to be within the sample population's range or exceeds the significance level for the test.

Another measure of variation one can use, as it is expressed as a readily identifiable percent value, is the coefficient of variation (CV). It is calculated using the standard deviation and the mean:

$$CV = 100s/\bar{x}$$

Notice that this parameter is unadjusted for the sample size.

10.3.5 Sample Size

More often, the question facing a researcher is how large a number of observations is sufficient to draw a valid statistical conclusion as to a population's underlying characteristics. How

many coins must we examine with microprobe or PIXE analysis before we can make valid inferences as to their composition as a group? How different this can be since by inspection of formulae like that for the standard error of the mean has *n* clearly defined, e.g., $S_{\bar{x}} = \sigma / \sqrt{n}$. If we know the standard error and the standard deviation, then *n* is immediate. Generally, we do not know the parameters for a population we wish to study.

An important element in the discussion of how large a sample, *n*, is necessary for valid estimates of population mean follows from considerations of the probability of that sample estimate being reliable for the population. A basic definition of the probability of a mean is:

$$P_r = \lim_{N \rightarrow \infty} \frac{1}{N} \sum_{j=1}^N \delta(\bar{x}_j - \mu)$$

As the limit approaches some *N*, the value of *P_r* will be equal to 1 (Johnson and Leone 1964). It follows from this that as *n* increases, so will the probability that the sample mean will approximate that of the population. This is the Law of Large Numbers. Another important factor in choosing sample size is the homogeneity or heterogeneity of the population. Homogeneous populations require smaller samples and heterogeneous ones require larger samples. What is the difference between two means? If the difference is large, then the estimate is "crude" and requires fewer observations. If the difference is a fine one, then *n* will increase accordingly. There is some help in the concept of detectable difference as one does not need to know σ precisely, only the ratio between the difference, *S*, and σ (Sokal and Rohlf 1981).

For purposes of discussion, let us examine an example using *Homo erectus* skulls.

10.3.6 Example 1: Cranial Capacity in *H. Erectus*

- Given the following cranial capacity parameters: $\bar{x} = 935$ cc; $\sigma = 132$ cc for

Homo erectus samples, how large a sample would be required to be 90 % confident that they would average greater than 920 cm³ in cranial capacity?

In this problem, we set the level of probability, e.g., how probable is our estimate. This done, the sample size determines precision and not population size (Kish 1965). This is echoed by Lazerwitz (1968) in the statement that population size has nothing to do with the size of the probability sample from that population. Certainly, as Lazerwitz points out, the relative homogeneity of the population will influence the sample size.

The Central Limit Theorem (see Thomas 1976) states that if “random samples are repeatedly drawn from a population with a finite mean μ and variance σ^2 , the sampling distribution of the standardized sample means will be normally distributed with $\mu_0 = \mu$ and the variances $\sigma^2 = \sigma^2/n$. The approximation becomes more accurate as n becomes larger.

Key to all this discussion of sample size is that for valid implementation of any of these formulae, one must draw the sample in a manner such that the assumptions of statistical theory are applicable (Cowgill 1964). This necessitates that the samples be drawn in a randomized manner.

With these assumptions and the new parameter σ_0 , we can now calculate the sample size by suitable manipulation of the following two formulas:

$$Z = 0 - \mu/\sigma_0 \quad (10.1)$$

and

$$\sigma_0 = \sigma^2 // n \quad (10.2)$$

From the above problem, we substitute the following values into (10.1); 935 cm³ = μ , 920 = 0, and $\sigma = 132$ cm³. Solving for σ_0 ,

$$\sigma_0 = \frac{920 - 935}{1.29}$$

where $z = 1.29$ and is determined by our level of confidence, 0.10. Hence, $\sigma_0 = 11.627$ and by formula (10.2), after rearrangement,

$$\text{or } n = (132/11.627)^2 \\ n = 129 \text{ skulls}$$

Having reached this value for n , it is equally valid to ask if sample size of 129 *H. erectus* skulls is really realistic given the rarity of fossil remains of this hominid. It probably isn’t.

This determination of sample size assumes σ is known. If σ is not known, then a preliminary sample is necessary to estimate this parameter. Past surveys can aid in this problem. Kish (1965) has suggested that if σ is not known, we can guess CV, the coefficient of variation, where $CV = \sigma/0$. CV is far less variable than hence with an estimate of CV and 0 we can “guess-timate” σ .

Another, more common method is suggested by Thomas (1976) where

$$\mu = np$$

where n = no. of trials and p = the probability of occurrence and, from the rule of complementation, $q = 1 - p$, implying that

$$\sigma = /npq$$

This approach assumes that some notion of probabilities for events is known.

Lazerwitz (1968), when p and q are not known, utilizes the fact that the numerator in the formula for the variance of a sample proportion reaches its maximum value when the proportion is 0.5. Utilizing this value, a conservative estimate for sample size by the following formula:

$$n = \frac{(2)^2 pq}{(2SE(p))^2} \\ \text{where } SE(p) = /pq/n.$$

The general formula is:

$$n = 1/k^2$$

where k is the desired interval about 0.5 at the 95 % confidence level (cf. Chebyshev's rule).¹

10.3.7 Scale and Size: Adequacy of the Sample in Geomorphology and Pedology

Sample size is also relative to the nature of the deposits being examined. One must always be cognizant that the volume of sediment recovered in the average diameter corer or auger barrel is inconsequential compared to the overall volume of most deposits being studied. Understanding this simple fact places a premium on the logical extension of a description of a small sample to the larger whole of the sediment or soil volume. A common sense approach is to obtain the largest sample possible relative to the research question being asked.

If the question is one of a correspondence of a sediment or soil type with your description, then a statistical approach to establishing commonality or difference is appropriate. It is a question of the adequacy of a sample for determining paleoenvironmental data from soil/sediment structure, geochemical properties, and pollen and other micro-botanical or micro-faunal inclusions such as phytoliths or foraminifera. Understanding the relationship of soil or sediment properties with respect to sample size is

essential to the design of effective sampling strategies. In a paper by Starr et al. (1995), the effect of sample size on common soil properties—bulk density, moisture content, pH, NO₃, and P—was measured across five different corer diameters (17–54 mm) and a 20 × 30 cm monolith. The findings indicated that smaller diameter samples gave sample means, greater skewness, and higher variances than the larger block sample (Starr et al. 1995). Replicates, or several repeated samples, using the smaller corers could compensate for the variation in the data. This is simply increasing the sample size. With an eye to the debate between Stein and Schuldenrein concerning corers versus augers, at least with hand-driven types, the larger diameter augers (100 mm) are less likely to be prone to statistical variability.

Still the problem of arguing from the sample level to that of the population, as a whole, remains both a question of sample size and *representativeness*. The latter property relates directly to the location of the sampling. This is less a size problem than it is a spatial one. In statistical sampling theory, the issue of randomness of the samples is a key one. Many samples are taken on grids set across vertical profiles or across horizontal plots using a systematic approach—that is, every point on the grid is sampled. This is much the same as point counting procedures of grains of sediments or soils. It is practical but non-probabilistic in nature. The author has used both simple random and stratified random sampling where sampling locations are assigned by use of randomization such as using a random number generator (calculator) or a table of random numbers. This has been done in samples from soil horizons as well as across archaeological site grids. The effect of random sampling is to improve the representativeness of the sample and to reduce the overall sample size. Without delving into statistical models at this point, it is suffice to say that one must be aware of *what* one is sampling.

Measuring correspondence between sample populations is generally done by bivariate comparisons of soil or sediment properties. With multiple samples or replicates, then one

¹ Chebyshev's Rule for Samples and Populations

The Russian mathematician P.L. Chebyshev formalized the rule that holds for any data set. The first property of this rule states that 75 % of all observations will lie within two standard deviations of the mean; the second property states that ~90 % will lie within three standard deviations on both sides of the mean (Weiss and Hassett 1991:98). Recalling our discussion of the Z-score, its meaning now should be more apparent. Chebyshev's rule gives us the means to constrain the variability inherent in our samples.

For example, property three of this rule states that for any number, k , greater than 1, observations in a data set, at least $1 - 1/k^2$ of the observations, must lie within k standard deviations of the mean.

may resort to multivariate methods which will allow the evaluation of likeness or difference in the sample populations. In the rubric of statistics, one measures the parameters versus the specific cases, or vice versa. Those samples with similar variability, which meet statistical tests of similarity such as chi-square, Kolmogorov-Smirnov, Mann-Whitney U, Student's *t*-tests, etc., can be reasonably assumed to represent the same or similar populations (Hawkes 1995). Underlying these tests is the assumption that most parent and sample populations are *normally* distributed, that the average or mean of the population of sand grains—grain size—lies near the center of the size distribution, and that all other sizes lie to either side of the mean creating the familiar bell-shaped curve or frequency distribution. If all is well, and your distribution is normal, then sampling measures will work. If not...

10.4 Data Analysis

10.4.1 Example 2: Single Variable Data-Phosphorus in Soils

In this example, observations are made on the presence of P_2O_5 in the sediment samples. From Chap. 7 we have seen that the analysis of labile or bound phosphorus is an important chemical indicator of archaeological sites. In nine samples (n), we observe a range of phosphorus from 192 to 228 $\mu\text{g/g}$. The calculated mean is 218 $\mu\text{g/g}$ P_2O_5 in the sediments. The variance, s^2 , is 124.36 and the standard deviation, s , equals 11.1 $\mu\text{g/g}$. The standard error of the mean, s_0 , is 3.7 $\mu\text{g/g}$.

What is the variability? If we use the coefficient of variation, it is

$$CV = (11.1)(100)/218 \text{ or } 5\%$$

a somewhat “large” variation. Using the *t*-score, we can establish a confidence interval such that 95 % of the time our sample mean will lie within it. From $t = 0 - \mu/s_x$, at 8° of freedom (9–1), $t_{0.05} = 2.306$, and $s_x = 3.7 \mu\text{g/g}$. So our 95 % C.I. = $218 \pm (2.306)(3.7)$ which means that the $0 = 218$ will be found within the interval of 209.51 – $226.51 \mu\text{g/g}$. Any phosphorus value outside this range is outside the sample population

and its (assumed) normally distributed variation. The value of 228 $\mu\text{g/g}$, in our data, is outside this population.

10.4.2 Data Analysis of More than One Variable

The eminent statistician, John Tukey, enjoins us to plot the data...“there is no excuse for failing to plot and look” (1977). This should be the first step in data analysis. In plotting single variable data, we look for the central tendency in the distribution of the occurrences of that variable in populations. Our measures of dispersion and tests for fit or membership, within a sampled population, validate (or invalidate) the behavior of that variable. For instance, if the amount of bound phosphorus is increasing in an archaeological site, then we can speculate on the intensity of the occupation at that location. If we take our inquiry a step further, we may wish to examine the variation in phosphorus amount relative to a second variable such as either time or space. Pollen studies of sediments of archaeological interest reveal variations in individual plant species, arboreal or non-arboreal. These variations in particular plant species are typically plotted in so-called pollen diagrams. In these familiar bivariate plots, the pollen amounts for a species are compared to their distribution across time. If we assign the variable name, y , to the pollen amount of a given plant species, then, in mathematical parlance, it can be viewed as functionally related to a second variable, x , which in the example here is time. Written as a function of time (x), pollen intensity is:

$$y = f(x)$$

10.4.3 Covariation-Correlation, Causality or “Not”

The basic question for most studies of relationships in two or more variables is: “Does x cause variation in y ?” If not, there is no functional relationship between x and y . Even if there is covariation in two variables, there may not be a

causal relationship. Correlation does not imply causality. In the study of causality, we try to discover for the underlying conditions that exist between x and y such that (1) y may never occur without x , a logically *necessary* condition, or (2) x is always followed by y of which it is “a” cause, but necessarily the only cause. This second situation is termed a logically *sufficient* condition. It is possible to establish correlation with statistics but not causality.

In statistics as in other experimentally based inquiry, experimental design provides greater certainty and, certainly, increased efficiency in testing relationships in x and y . Good experimental design attempts to formulate exploratory studies that will hopefully isolate variables who do exist in some causal relationship and then design tests that accurately portray the frequency of occurrence that supposed relationship.

Implicit in the determination of the frequency of the concomitant occurrence of x and y is an increased reliability in the suspected causation. Another aspect of good experimental design is the accuracy of measurements of x and y . Repeatable replicates (precision) of accurate measures of x and y increase the reliability of observed correlations and reduce or minimize bias in an experiment. Bias is related to error, systematic or otherwise, and is generally related to measurement in statistical tests (Kempthorne and Allamaras 1986). One can express bias as the residual errors in a data set as that of the root-mean-square (RMS) error of an estimate (mean, average).

10.4.4 Least-Squares Analysis and Linear Regression

The simplest relationship between more than one variable is bivariate— x and y . The simplest relationship between x and y is linear such that

$$y = a + bx$$

e.g., the slope-intercept equation for a line. The general linear model for n the regression of one

variable Y on another variable x , which exist in direct variation, is:

$$y = \beta x$$

where β is the population parameter for slope and whose range is $-1 \leq \beta \leq 1$. In a perfect correlation between x and y , $y = x$ and $\beta = \pm 1$. The perfect negative correlation is the case of minus (-1) . If there is no correlation, $y \neq x$ and $\beta = 0$.

In common practice, the correlation coefficient is written as r and is equal to $r = b_{y,x} \cdot s_y / s_x$.

Here, b is the slope of the regression of x and y , and this is multiplied by the ratio of the standard deviations of x and y .

Graphically, we can examine correlation in the regression of a least-squares plot (Fig. 10.2): (a) one is a case (least-squares fit without Snaketown) of a relatively strong correlation in x and y and (b) a case (least-squares fit with Snaketown) of a strong but somewhat reduced correlation. The least-squares method is so named for the procedure’s criterion on making the sum of squares for deviations (Δy), from the regression line, as small as possible (Pentia 1998: Personal Communication). Another way of stating this is that the mean square (Δy)² difference between the data and the straight (regression) line should be a minimum. A brief explanation of this is as follows: The equation $y = a + bx$, based on two values of x and y , clearly defines a line, but when we introduce a new, second, value for x , simply called, x_1 , the solution is not y but y_1 which is now equal to $a + bx_1$ and differs from the line $y = a + bx$ by Δy . The process for fitting a line to a series of x_n, y_n pairs is called linear regression. From this procedure, we can evaluate the correlation coefficient, r .

Two ways of calculating r involve (a) calculation of b , the slope $(y_2 - y_1)/(x_2 - x_1)$ or (b) a direct method of using x and y . The first, (a), is:

$$b = \left[\sum (x - 0)(y - \bar{y}) \right] / \sum (x - 0)^2$$

and

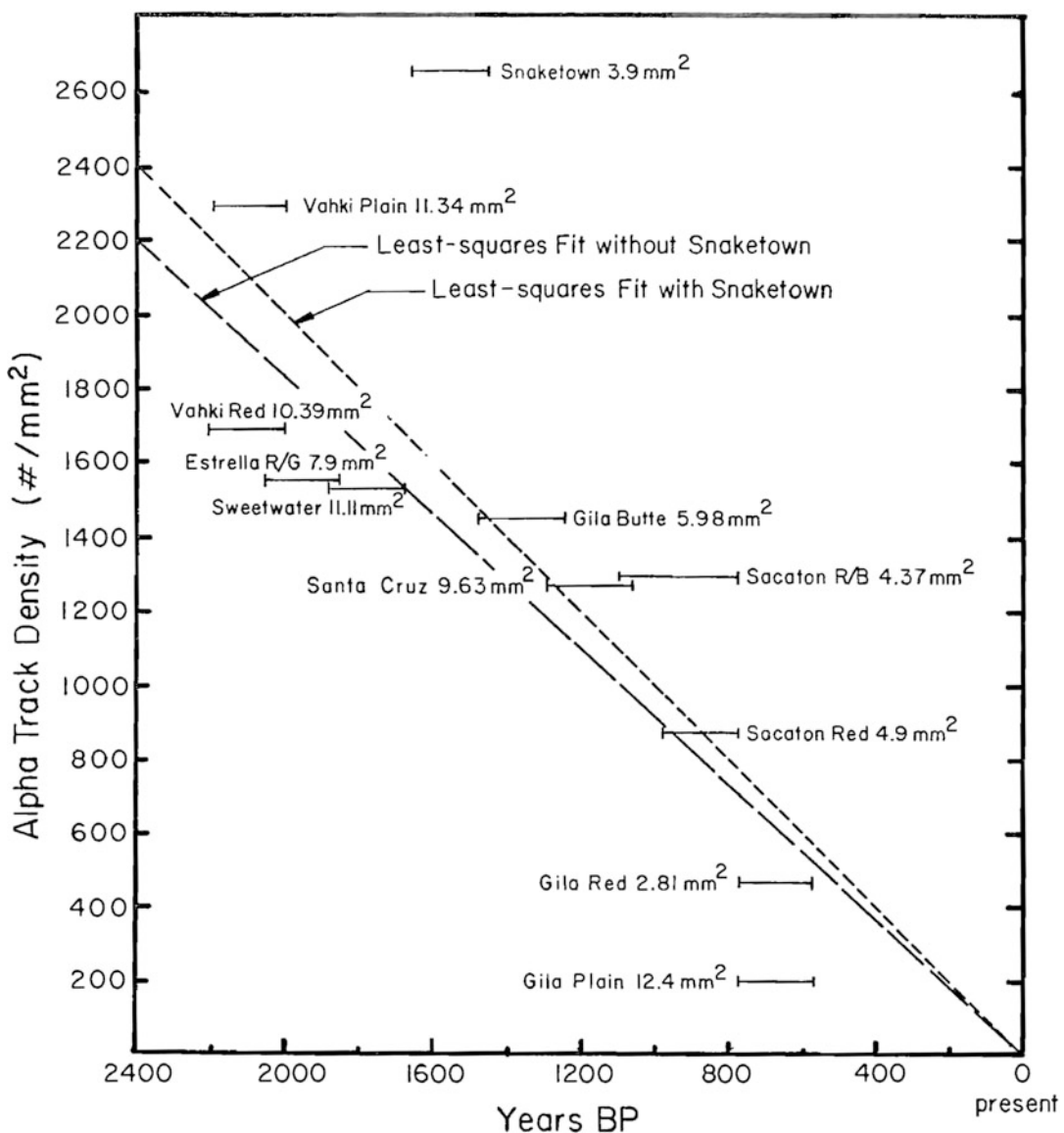


Fig. 10.2 Linear regression. Two correlations between the observed alpha-recoil track (ART) density in mica inclusions used as a tempering agent for prehistoric Hohokam pottery (“Sacaton Red,” “Vahki Plain,” etc.) versus

age in years before the present (BP). The line width for each pottery type track density value is the standard deviation (Garrison 1973; Garrison et al. 1978)

$$r = b \cdot s_0 / s_1 \{$$

where s_0 and s_1 are standard errors of the means for x and y . The second, (b), is more direct:

$$r = \sum xy / \sum x^2 y^2$$

Most regression lines do not cross the y -axis at zero so the y -intercept value has implications for assessing a data set. For instance, if the y -intercept, for a set of alpha track density versus time, is found to be greater than time (t) = 0 (y -axis) and is rather, for purposes of demonstration, equal to 1550 years, then the regression line is not appropriate for samples less than this age.

The correlation coefficient, r^2 , is a ratio of the variance—that of the original variance in Y to that the sum of squares of residuals or deviations, Δy , from the regression line of best fit (Fig. 10.2). Values of r^2 could be 1 or zero with the values somewhere in between. A high correlation coefficient means a good fit of the regression line to the observed data.

For example:

$r^2 = 0.78$, a high, positive correlation in x and y ;
or $r^2 = 0.25$, a weak correlation

The case, least-squares fit without Snaketown, has an r^2 of 0.8, while the other case,

least-squares fit with Snaketown, has an r^2 that is slightly less, indicating that the correlation between the two variables, alpha track density and age, is strongly positive (Fig. 10.2).

Hawkes (1995) lists the following descriptions for the correlation coefficient.

| | |
|-------------------|---------------------------------------|
| $r = 0$ | no linear relationship |
| $-0.5 < r < 0.5$ | weak negative linear relationship |
| $0 < r < 0.5$ | weak positive linear relationship |
| $-0.8 < r < -0.5$ | moderate negative linear relationship |
| $0.5 < r < 0.8$ | moderate positive linear relationship |
| $-1.0 < r < -0.8$ | strong negative linear relationship |
| $0.8 < r < 1.0$ | strong positive linear relationship |
| $r = 1$ | exact positive linear relationship |
| $r = -1$ | exact negative linear relationship |

10.4.5 Example 3: Alloys in Iron Age Metallurgy

An example least-squares analysis of data from a rather straightforward PIXE study of the compositional makeup for a suite of Iron Age (800–58 BC) metal artifacts to ascertain their nature as to either: (a) copper, (b) bronze, or (c) brass. The difference being based on the occurrence of tin (Sn) is less than trace amounts in bronze; the occurrence of zinc (Zn) is similar compositional amounts (~10 %) in brass, while only copper (Cu) predominates at levels of 97–100 % in “pure” copper artifacts. In the data from Table 10.2, one observes little variation in Zn, which is consistently at trace levels, while the variation in Sn is such as to suspect a separation in

these artifacts into bronze and copper artifact classes. Simple regression analyses for bivariate pairs of x , (in all three cases the value of Cu) and y , (alternately Sn then Zn). The correlation coefficients for each paired regression were:

1. Cu vs. “high” Sn (greater than 5.19 %) artifacts, $r = 0.97$, $r^2 = 0.94$
2. Cu vs. “low” Sn (less than 5.19 %) artifacts, $r = 0.53$, $r^2 = 0.28$
3. Cu vs. Zn ($n = 21$) artifacts, $r = 0.68$ $r^2 = 0.46$

Only in case (1), Cu (x) vs. “high” Sn amounts (y) is the correlation significant ($r^2 = 0.94$).

To determine the significance of the r value, in this case 0.97, a t -test should be done on either the slope parameter, β , or on the r value itself. Either is easily done. For β , or b , the test is

$$t = b - 0/s_\beta$$

For a t -test of r , we use the following formula: We compute the standard error, $s_{y,x}$, by

$$s_{y,x} = \sqrt{1 - r^2}/n - 2$$

where n is simply the number of x - y comparisons. The t -test becomes

$$t = (r - 0)/\sqrt{1 - r^2}/n - 2$$

Note its similarity to the test using the slope parameter, β .

In regression studies, there are two variations, termed Model I and Model II or Bartlett’s method. They differ in how the variable x is handled. In Model I regression, x is fixed and set as such in the experiment; in Model II both x and y are random. Model I regression studies are common in psychological, educational, and agricultural testing. In most instances, and in particular when dealing with archaeological and geological phenomena, Model II regression is done. Thomas (1976) states that “ r ” is meaningless in Model I regression. The correlation analysis assumes a bivariate normal distribution which is not the case when x is nonrandom and fixed. This is to say the statistics of r and r^2 are

Table 10.2 Compositional data (in %) for Iron Age artifact

| Artifact | | Sn | Pb | As | Sb | Ag | Ni | Bi | Co | Zn | Fe | Cu |
|----------|-----|-------|-------|-------|-------|-------|-------|-------|-------|-------|-------|-------|
| 170 | 2P | 9.87 | 0.041 | 0.085 | 0.052 | 0.012 | 0.069 | 0.001 | 0.035 | 0.022 | 0.064 | 89.7 |
| 171 | 3P | 6.13 | 0.017 | 0.165 | 0.060 | 0. | 0.187 | 0. | 0.027 | 0.014 | 0.027 | 93.4 |
| 172 | 3N3 | 5.23 | 0.198 | 0.182 | 0.105 | 0.019 | 0.56 | 0.002 | 0.033 | 0.015 | 0.094 | 93.6 |
| 173 | 6N2 | 9.69 | 0.044 | 0.34 | 0.62 | 0.020 | 0.25 | 0. | 0.014 | 0.008 | 0.007 | 89.0 |
| 174 | 5N1 | 9.00 | 0.27 | 0.108 | 0.193 | 0.094 | 0.137 | 0.011 | 0.024 | 0.018 | 0.030 | 90.1 |
| 175 | 1P | 9.42 | 0.61 | 0.093 | 0.092 | 0.133 | 0.065 | 0.021 | 0.026 | 0.056 | 0.23 | 89.3 |
| 176 | 1P | 0.135 | 9.19 | 0.032 | 0.018 | 0.140 | 0.004 | 0.033 | 0.007 | 0.55 | 0.77 | 89.1 |
| 177 | 5P | 0.017 | 0.50 | 0.020 | 0.085 | 0.061 | 0.034 | 0.011 | 0.061 | 0.24 | 1.89 | 97.1 |
| 178 | 2P | 0.121 | 0.47 | 0.32 | 0.007 | 0.075 | 0.071 | 0.031 | 0.060 | 0.64 | 1.02 | 97.2 |
| 179 | 1P | 0.81 | 0.046 | 0.072 | 0.005 | 0.119 | 0.002 | 0.017 | 0.021 | 0.021 | 1.60 | 97.3 |
| 180 | 1P | 9.69 | 0.49 | 0.090 | 0.074 | 0.099 | 0.041 | 0.021 | 0.034 | 0.060 | 0.60 | 88.8 |
| 181 | 3N2 | 10.70 | 0.30 | 0.139 | 0.075 | 0.085 | 0.26 | 0.019 | 0.025 | 0.030 | 0.43 | 87.9 |
| 182 | 6P | 0.050 | 0.41 | 0.030 | 0.077 | 0.056 | 0.030 | 0.012 | 0.053 | 0.174 | 0.90 | 98.2 |
| 183 | 3P | 0.110 | 0.061 | 0.017 | 0.006 | 0.074 | 0.035 | 0.001 | 0.034 | 0.134 | 2.02 | 97.5 |
| 184 | 4P | 0.016 | 0.57 | 0.018 | 0.020 | 0.097 | 0.042 | 0.021 | 0.042 | 0.24 | 1.35 | 97.6 |
| 185 | 2P | 0.095 | 1.16 | 0.030 | 0.018 | 0.079 | 0.024 | 0.003 | 0.025 | 0.34 | 0.193 | 97.3 |
| 186 | 2P | 0.083 | 0.047 | 0.054 | 0.007 | 0.044 | 0.020 | 0.003 | 0.069 | 0.029 | 0.98 | 98.7 |
| 187 | 3P | 0. | 0.009 | 0.003 | 0.001 | 0. | 0.008 | 0.006 | 0.001 | 0.003 | 0.018 | 100.0 |
| 188 | 6N2 | 5.19 | 1.38 | 0.23 | 0.48 | 0.157 | 0.23 | 0.013 | 0.034 | 0.008 | 0.016 | 92.3 |
| 189 | 6P | 11.21 | 0.41 | 0.083 | 0.119 | 0.086 | 0.075 | 0.016 | 0.021 | 0.019 | 0.031 | 87.9 |
| 190 | 6P | 7.70 | 0.099 | 0.048 | 0.081 | 0.065 | 0.045 | 0. | 0. | 0.010 | 0.101 | 91.9 |

grounded on very different assumptions depending upon whether the data are collected using Model I or Model II (*supra*). Many researchers today prefer to use what is termed Major Axis Regression Analysis rather than Least-Squares Regression (Model I) recognizing that both x and y vary at random (Steve Holland, 2002, Personal Communication).

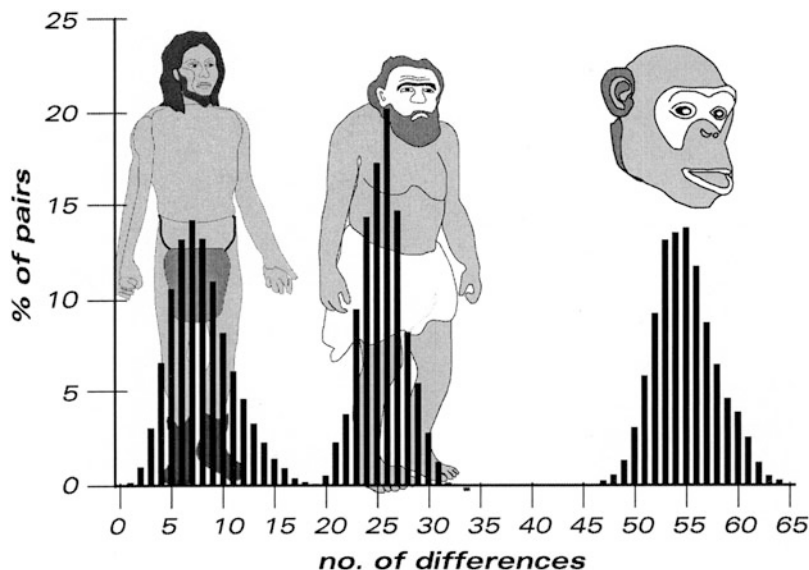
10.4.6 “SHE” Measures of Variability of Assemblages

Variation in the size and the composition of artifact assemblages makes them scale dependent. Likewise, the scale and variability are the result of the “type” of processes that created an assemblage at a particular site or sites (Shott 2010). The parameters of diversity (S), heterogeneity (H), and evenness (E)—“SHE”—can allow the archaeologist to gain entry into the articulation of past activities/processes with that of their

surrounding environment and, in the best of cases, support inferences about those activities. Assemblages have intrinsic properties that can be defined and measured. These include size, composition, and spatial distribution.

Size is simply the number of objects in an assemblage; composition is the count of proportion of types of objects in an assemblage. These parameters lend themselves to quantification and numerical analysis. Assemblages are objects or materials and thereby subject to inquiries based on materialist methodology. This methodology uses “derived measures” much like ecology—ratios, indexes, and diversity/heterogeneity measures (“SHE” measures) (Shott 2010). These derived measures can be used to analyze site assemblages. The size of assemblages, their richness, diversity, and evenness can be assessed based on count data across well-recognized typological classes to be acquired during this study. The composition of assemblages is known to change with occupation span and size.

Fig. 10.3 Pair-wise comparison of mtDNA sequences of observed differences in human-Neanderthal sequences and human-chimpanzee sequences



10.4.7 Paired Comparisons or Paired Difference Experiments

One can view paired difference comparisons as “before-and-after” types of tests. For instance, one can, say, map the positions and/or the amounts of elements in artifacts for comparison before-and-after something has been done to the material such as the weathering of a surface.

One can use a reference material for comparison as well. What the paired comparison test seeks to discover is the presence of any difference in the two samples and to quantify that difference (Hawkes 1995). One could use the sequence of two tree-ring samples for comparison. Certainly, a comparison that yields no difference in two ring sequences implies a similar age for both. This is what is done in dendrochronology to achieve a “match” between two sample sequences. The dendrochronologist, in this case, desires to find no difference in the match between the unknown and the master reference tree-ring sequence. In paired comparisons of sequenced data, one can be looking for similarity or difference. An excellent example of both the type of data and the utility of the test can be found in recent studies of Neanderthal mtDNA sequences.

Recently (1997), the fossil remains of the original 1856 Neanderthal find were assayed using modern DNA analysis (Krings et al. 1997). A sample of the right humerus from the ancient hominid was used to obtain a 360 base pair (bp) sequence of mitochondrial DNA (mtDNA). This sequence was then compared to modern human reference standard as well as 994 contemporary human mitochondrial lineages (478 Africans, 494 Asians, 167 American Indians, and 20 Australian/Oceanian individuals) together with 16 nonhuman, chimpanzee, lineages for a total of 2051 human and 59 common chimpanzee sequences. This study was done to address questions of the phylogenetic relationship of Neanderthals to modern human populations as well the great apes. The null hypothesis would be something of the nature of no difference in the 360 bp Neanderthal mtDNA sequence and modern humans. A second null hypothesis might be no difference between Neanderthals and the great apes based on the DNA comparison.

In a pair-wise comparison of the respective mtDNA sequences, some interesting results were obtained. As illustrated in Fig. 10.3, the observed differences in human-Neanderthal sequences averaged 25.6 ± 2.2 differences, between

human-human sequences an average of 8.0 ± 3.0 differences, and between human-chimpanzee an average of 55 ± 3.0 differences. Using a calculated rate for mutations to arise in the sequences, a common ancestor for humanity (including Neanderthal) existed up to a divergence at 4–5 Ma ago and a divergence in the human and Neanderthal lines around 550–690 ka ago. The researchers concluded, on the basis of this pair-wise comparison, that the mitochondrial DNA sequence for Neanderthal lies outside modern human variation. What the researchers do not report is a test of significance for their paired comparison results. This can be done using the *t*-test. For paired comparisons, the *t*-statistic is found as follows:

$$t = \bar{D}_D - \mu_D / S_D / \sqrt{n_D}$$

Here we examine the sample differences, \bar{D}_D , using the standard deviation of the differences, S_D , where n should be apparent; the population mean, μ_D , is presumed to be zero.

An important footnote to this earlier DNA study is that of the larger sequencing of the Neanderthal genome completed in 2010 (Green et al. 2010) which shows that Neanderthals shared more genetic variants with present-day humans in Eurasia than with present-day humans in sub-Saharan Africa, suggesting that gene flow from Neanderthals into the ancestors of non-Africans occurred before the divergence of Eurasian groups from one another. Modern Eurasians can have between a 1 and 4 % genetic contribution from Neanderthal (*supra*).

the calculations where, in sets of data of n greater than 3 variables, the use of matrix algebra was required. In the last decades of the twentieth century, the use of vector-based multivariate analytic techniques has increased in almost all sciences. The most frequently encountered multivariate technique(s) are found under the general heading of factor analysis.

Factor analysis methods—principal components, Kaiser image, Harris image, and iterated principal axis, to name but some of the more common—are described and discussed in detail elsewhere (Gorsuch 1984; Mulaik 1972; Davis 1986). In factor analyses, linear algebra is used to manipulate variables in a data set to examine possible relationships and associations among them. Each variable is treated as a vector within n -dimensional space where n is equal to the number of variables, e.g., 12 variables, 12 vectors. The data set of a matrix of n variables measured against n number of samples (cases).

Two patterns of relationships can be examined using factor analysis- *R* and *Q*-modes. The former, *R*-mode, factor analysis attempts to isolate relationships among the variables in the data set, whereas *Q*-mode factor analysis attempts to examine relationships among the various samples or cases. On most archaeological or geological studies, *Q*-mode is the factoring technique most used. The end result of either approach is a series of “factors” or members that determine the commonality estimates among the variables. The key characteristic of a factor analysis is that, if done correctly, it will reduce the number of “variables” needed to describe the data. The new “variables” are called factors and are linear combinations of the original variables. Generally, in factor analyses, the rule of thumb is that the maximum number of factors is no more than one-half the number of variables being analyzed. In practice, the number of factors are well below half and number about four to six in even the largest data sets. The objective is to account for as much of the variance as possible in the original data set. Factor analysis algorithms operate on matrix data that is sets of linear operations of either the raw data (variables). The basic linear equation is:

10.5 Exploration: Multivariate Approaches to Large Data Sets

10.5.1 Exploring Correlation Among n Greater than 2 Variables: Some Multivariate Statistical Techniques

Multivariate or multidimensional data, before the advent of digital computing, was difficult to analyze statistically due to the laborious nature of

$$S_n = f_1 c_1 + f_2 c_2 \dots f_n c_n + R$$

S_n is the bulk amount of the variables, 1 to n , in a sample; f is the fraction of the factors, 1 to n , in the sample; C is the amounts of the variable in the factors; and R is the residual terms for error. For eight variables, there will be eight linear equations. The mathematical strategy involved is the determination of a best estimate for values of factors extracted by minimizing the values for the residual errors in R . The method most often used to do this is the now familiar method of least squares.

A principal assumption for justifying the use of least squares is that the data are normally distributed. The least-squares approach minimizes the sum of squares of the residuals, R . A cutoff value for the final number of factors can be done in several ways. The most commonly seen are to choose the number of factors that account for at least 95 % of the total variance. It is common for the first factor to account for nearly 50 % or more of the variance, with the other factors accounting for less and less. A rule of thumb is that as the amount of variance accounted for by a factor decreases, the variance of its components increases. In the principal components method of factor extraction (PCA), eigenvalues (and eigenvectors) are used as the second way of factor selection. An eigenvalue can be viewed as a characteristic root of the matrix. Because of the n -number of equations, there are n -eigenvalues, but not all are important in accounting for the total variance of the data set.

In general, the number of significant factors extracted by a factor analysis is equal to the number of eigenvalues determined: One rule of thumb in the use of eigenvalues is that the variance accounted for must be at least 75 %. Another selection criterion for factors is the eigenvalue be greater than or equal to 1. The maximum or largest eigenvalue is equal to the variance of Y . Therefore, for a matrix of r (non-zero) eigenvalues, there are exactly r principal components.

10.5.2 Discriminant Function Analysis (DA) and Principal Components Analysis (PCA)

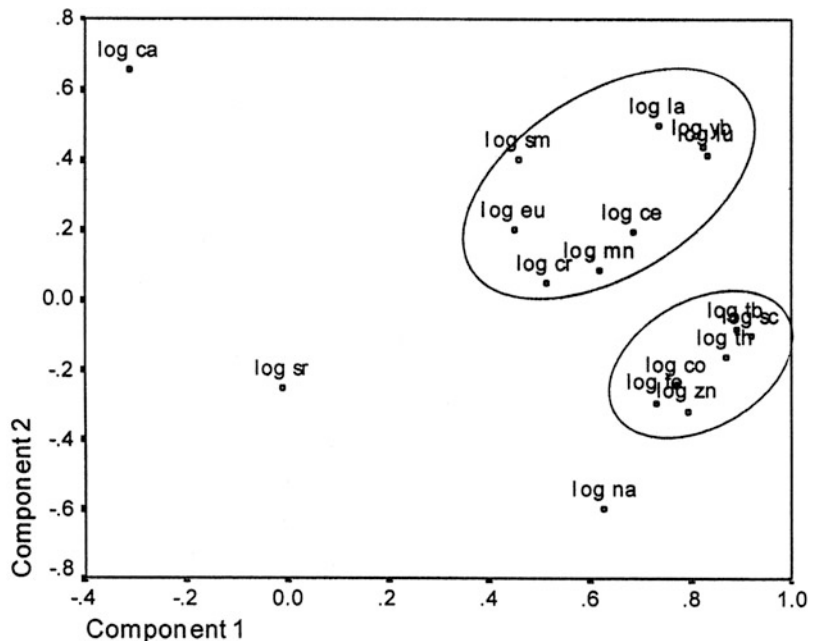
Discriminant (function) analysis (DA) presumes that a set of variables, such as elemental data, can distinguish (*discriminate*) between groups, for example, pottery clay sources, that contain these elements. DA improves the distinction between sources by statistically removing variables (elements in this case) that have any or no discrimination value (Klecka 1975). Discriminant analysis works best between a priori defined groups.

In discriminant function analysis, the “distance”—near or far between two groups (minerals, artifacts, etc.) in a statistical sense—is compared by use of what is termed *pair-wise generalized squared distance function*, D^2 . The main idea behind discriminant function analysis is to define a function, Y , which will discriminate between groups of p variables. For the best discrimination, the respective group means, of say, two groups, Y_1 and Y_2 , should be widely separated.

An analytical software program (SPSS) calculates the coefficient vector and the distance function then projects the groups onto a *linear discriminant function*, Z , defined by variables within the groups (e.g., SiO_2 , Pb , Mg , etc.). Using the value $D^2(E)$, which some readers will recognize as the Mahalanobis distance, a *posterior probability*, P_r , for a sample (E) belonging to different groups. In general, membership of a sample, E , in a group is indicated by a high P_r , say, 0.8–1.0. A low P_r , e.g., less than 0.5 or so, indicates nonmembership in a group.

In principal component analysis, or PCA, the factors extracted from a correlation matrix are presented as axes. The first principal component or axis accounts for the maximum possible variance and the second the maximum remaining variance, and so one can use this axis extraction for two-axis plots wherein the number of samples are displayed as a scatter plot. Clusters can be seen in many of these plots that infer

Fig. 10.4 Bivariate plot of elements within Pentelic marble. Two ellipses denote specific marble groups based on discriminating elements (Courtesy Scott Pike)



relationships between the samples based on the derived and measured distance from centroids of the clustered samples. Figure 10.4 illustrates the use of PCA to isolate elemental groupings in marbles from Mount Pentelikon, Greece. Pike (n.d.) has evaluated the use of NAA data of Pentelic marbles in an exploratory study of discriminating prehistoric quarries. We see a typical bivariate plot or “biplot” of the first two principal components illustrating correlation of elements in the marbles. Closely spaced elements indicate strong correlations.

An important question raised by Baxter and Jackson (2001) concerns variable selection in artifact compositional studies. These authors point out that compositional studies such as those just described proceed from a first principle used in biological numerical taxonomy—“the greater the content of information in the taxa of a classification and the more characters on which it is based, the better the classification will be” (Sneath and Sokal 1973). Because instrumental methods, such as NAA and the ICP variants (cf. Chap. 7), routinely determine 30–40 elements per sample, it would appear that they meet the foregoing injunction. Harbottle (1976) affirmed this approach in his influential paper. Baxter and

Jackson take issue with this approach suggesting, instead, that “less is more” with regard to the number of analytical variables used in certain analyses (Baxter and Jackson, *supra*). Their point, in the context of multielement-multivariate analyses, is that too often the choice of many variables may obscure the perception of actual patterns (*supra*; Fowlkes et al. 1988; Kzanowski 1988). Kzanowski illustrates this by pointing out that sample size may militate against the use of too many variables, particularly where, in cluster or factor extraction, the number of cases, used in the analysis, must exceed the number of variables used. Instances where this injunction has been ignored extend back to the early days of the use of multivariate statistics in archaeology, in general, and in archaeometry, in particular. Certainly, in these cases, some form of variable reduction seems mandated along with the use of PCA.

A good example of not only variable reduction but variable selection is that of Speakman et al. (2011a, b). In this study, Speakman and his coresearchers compare the discriminatory capability of pXRF and INAA for prehistoric Mimbres pottery. PCA of compositional data from both instrumental procedures were

performed. For elements analyzed in common (Al, K, Ca, Ti, Mn, Rb, Sr, Th), the variance-covariance structure illustrated in biplots showed more-or-less similar group structure. However, PCA results using five elements measured by INAA (Cr, Cs, Eu, Ta, Th) showed excellent discrimination between eight compositional groups.

Discriminant function analysis must provide a group assignment for each individual/item and that the analysis is designed to maximize differences between the groups. This results in an overall tendency to correctly assign individuals/items at a higher rate than that expected by chance alone, even if the data set itself is comprised of predictor variables that in fact bear no real relationship to the groups one is trying to discriminate. A result like this can be mistakenly interpreted as representing the successful attribution of individuals/items to their groups on the basis of meaningful functions, when the correct assignments are merely the result of an inherent property of the analysis (Korarovic et al. 2011). In archaeology, observations used to build discriminant functions must be independent if at all possible (*supra*). Likewise, proper sampling is important. This speaks to the need for large enough/adequate sample sizes and a sampling strategy that accurately encompasses the breadth of variation within each group.

The use of the discriminant function, as well as principal components analysis, has a long

history in attempts to classify archaeological materials (Sieveking et al. 1972; Ward 1974; Picon et al. 1975; de Bruin et al. 1976; Leach and Manley 1982; Craddock et al. 1983; Rapp et al. 1984; Vitali and Franklin 1986). The discriminant function, in particular, mathematically generalizes the characteristics of a group of objects and can be used to evaluate the probability of membership of any object of a group (Vitali and Franklin 1986). The underlying assumption in these types of provenance analyses is that the elemental composition of pottery is characteristic of its clay and thus of a particular site or place of manufacture.

Douglas (2000) has extended this type of analysis to historic English ceramics in a study of pigmenting elements used in the dyes used for the printed designs found on nineteenth century pottery. This study concentrated on 16 samples of Spode pottery manufactured at Stokes-on-Kent, England. A JEOL 8600 Superprobe (EMP) was used in all the instrumental analysis of the underglaze dyes (Fig. 10.5). Table 10.3 lists Douglas' use of the discriminant function on these 12 ceramic samples based on SiO₂ and PbO content.

The analysis clearly shows two distinct groups of "Age 0" and "Age 1" which stand for Spode pottery manufactured before 1834 (Age 0) and after 1834 (Age 1). A Spode pottery sample, of unknown chronological provenance, can be examined instrumentally and classified with some confidence (Fig. 10.6).

Fig. 10.5 *Left:* Spode blue printed design.
Right: back-scattered electron (BSE) image of dye, with brighter areas those of high cobalt content

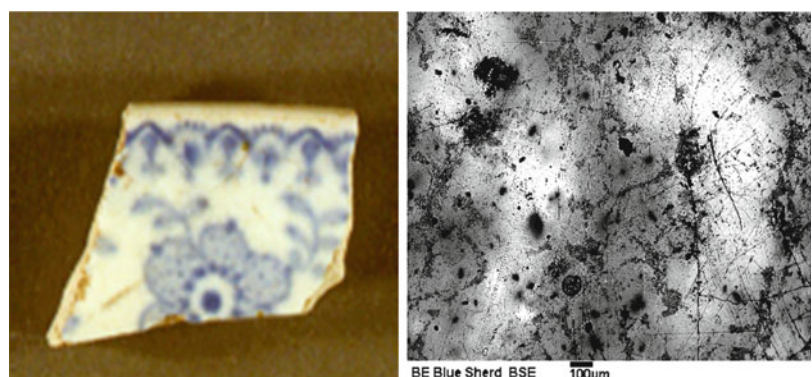


Table 10.3 Spode pottery statistical analysis (Douglas 2000)

Resubstitution results using linear discriminant function

| Obs | From AGE | Classified into AGE | Posterior probability of membership | |
|-------|----------|---------------------|-------------------------------------|--------|
| | | | AGE 0 | AGE1 |
| BS-1 | 1 | 0 | 0.78 | 0.22 |
| BS-2 | 1 | 1 | 0.0354 | 0.9646 |
| BS-3 | 1 | 1 | 0.1627 | 0.8373 |
| BS-4 | 1 | 1 | 0.0073 | 0.9927 |
| BS-5 | 1 | 1 | 0.0003 | 0.9997 |
| BS-6 | 1 | 1 | 0.0034 | 0.9966 |
| BS-7 | 1 | 1 | 0.0018 | 0.9982 |
| BS-8 | 1 | 1 | 0.0002 | 0.9998 |
| BS-10 | 1 | 1 | 0.0041 | 0.9959 |
| BS-11 | 0 | 0 | 0.7305 | 0.2695 |
| BS-13 | 0 | 0 | 0.9185 | 0.0815 |
| BS-14 | 0 | 0 | 0.9784 | 0.0216 |
| BS-15 | 0 | 0 | 0.9849 | 0.0151 |
| BS-16 | 0 | 0 | 0.9998 | 0.0002 |
| BS-17 | 0 | 0 | 0.9998 | 0.0002 |
| BS-18 | 0 | 0 | 0.9996 | 0.0004 |

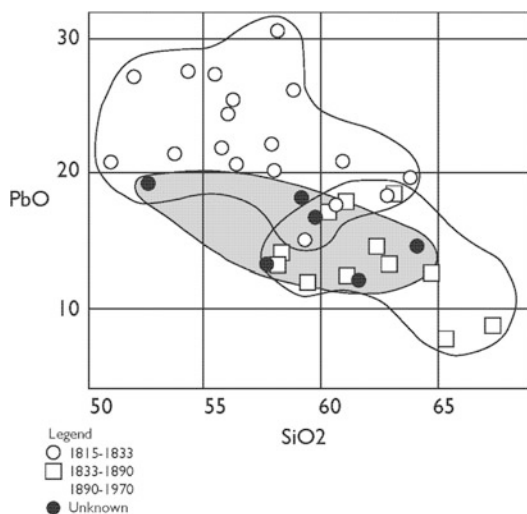


Fig. 10.6 Binary diagram of PbO and SiO₂ data for all Spode samples. Clusters of “open” samples manufactured before and after 1833, correlating with a change in ownership at the Spode factory (cf. Table 10.3); the “unknown” (closed) samples are highlighted in gray and occur in their respective manufacturing group

10.5.3 Cluster Analysis

A variant of multivariate analysis is termed average-link cluster analysis, and it seeks to measure association in the samples, but unlike

principal components analysis, it provides little information about the variables themselves. Cluster analysis starts with determining similarity (distance) coefficients computed between pairs of samples rather than variables. Papageorgiou et al. (2001) point out a “problem” with methods of cluster analysis in that there are so many of them. Cluster analysis is the most widely used multivariate technique in archaeology (*supra*). Again, as pointed out earlier in this chapter, the output of instrumental analyses of artifactual and geoarchaeological materials produces extensive bodies of measurement data across many variables. Since most of these studies are exploratory in nature, a family of statistical methods such as those of cluster analysis will continue to enjoy popularity.

A common form of representing the output for cluster analysis is the dendrogram. The dendrogram presents the samples ranked in association with those most similar. If the distance or similarity coefficients are printed for each set, then those values most different (e.g., 1.15 and 0.092) mark boundaries between clusters. An interesting use of cluster analysis, on data from instrumental analysis—XRF and PIXE—was done by Kuhn and Sempowski (2001). In this study of artifactual material from early members of the Iroquois

League, ca, 1590, the Mohawk and Seneca tribes were examined as proxy data for increasingly strong political ties—a league between these widely separated Great Lakes cultures. A cluster analysis of elemental means (13 elements) was done for each archaeological case (site) to identify natural groupings in the data and to indicate whether the site samples clustered into Seneca-Mohawk groups. Kuhn and Sempowski's results support a coalescence of the powerful League at the end of the sixteenth century or the early seventeenth century. Kuhn and Sempowski utilized principal components and discriminant function analysis as well.

In all cases of factor analysis, it is often difficult to determine precisely what the new grouping of variables or cases means. In the analysis of ancient coins, the separation of key elements—noble versus base metals—can enable the investigator to assign, with some confidence, identities to the factors separated on the basis of these metallic elements. In ceramics, the compositional variability of differing wares can often be used to isolate distinctness or similarity. This is particularly useful when one routinely can obtain reliable estimates for 30 or more elements using ICP or NAA making factor analysis methods essential for discriminating association among the key combinations of variables represented by the factors. Singleton et al. (1994), in their study of prehistoric pottery clays with AAS (cf. - Chap. 7), have utilized both cluster analysis and DA. Their results, first using DA to discriminate key chemical elements, led the researchers to refine their analysis to four elements that defined the spatial variability of the pottery.

10.5.4 Chi-Square: “Nonparametric” Calculation of Association

Not all data require comparison using the normal distribution and its associated parameters—mean, standard deviation, etc. Rather than using “parameters,” we can choose to use the observed proportions in our sample to measure association by means of the chi-square statistic. The chi-square statistic and the chi-square distribution allow us to use the observations within the

predetermined categories—vessel types, axe varieties, weapons, sites, etc.—to make tests of association, independence, and significance. The chi-square statistic basically measures departures for the average (Drennan 1996).

Categories are often called nominal data. They allow us to simply enumerate observations within them—87 hand axes, 13 Solutrean points, 23 burins, 47 dolmens, etc. If the categories are arranged in some rank order, then we are dealing with the next scale of data—*rank*. Categories contrast to *measurements* made on interval or ratio scales. These measurements are quantified and used in the parametric tests we have discussed earlier. In the use of the chi-square, we assume no order or rank and we simply examine the proportion of the observations within categories such as those of types. Types cannot be ranked, whereas categories of size can. Still we count the representative shards of types we recover and arrive at their numerical proportions. These values can then be used in the calculation of the chi-square statistic.

The chi-square statistic is calculated as follows:

$$\chi^2 = \sum (O_i - E_i)^2 / E_i$$

where O_i is the observed number in any category and E_i is the expected number in any category.

The number of items in category is counted and then compared to those of another category by use χ^2 . This value is then compared to some chi-square distribution (Fig. 10.7). By way of example, the simplest chi-square comparison is that of the 2×2 chi-square table.

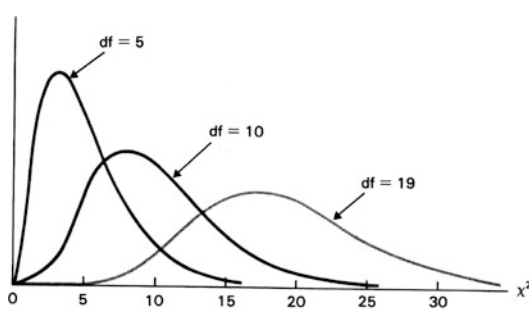


Fig. 10.7 Three chi-square distribution curves. Note the higher degrees of freedom (df = 19) approximate the normal distribution

Table 10.4 Contingency table for winged versus socketed axes

| | Winged axes | Socketed axes | Total |
|---------|-------------|---------------|-------|
| Level A | 20 | 30 | 50 |
| Level B | 20 | 10 | 30 |
| Total | 40 | 40 | 80 |

In the table are listed the number of observations of, say, the occurrence of Bronze Age metal axe types—winged and socketed—in two levels of a site. We ask the question whether there is a measurable difference in the occurrence of the axe types found in these two excavation levels. The table is constructed thus (Table 10.4):

The observed values are apparent. To arrive at the expected values, E_i , for winged axes in level A, required by the chi-square formula, 1 multiplies the row total, 50, by the column total, for winged axes, 40 and divides this value by the grand total 80. Each “cell” of this table is calculated in a similar manner. These individual cell values are then summed as follows:

$$\begin{aligned}\chi^2 &= (20 - 25)^2/25 + (30 - 25)^2/25 \\ &\quad + (20 - 15)^2/15 + (10 - 15)^2/15 \\ \chi^2 &= 1 + 1 + 1.66 + 1.66 \\ \chi^2 &= 5.33\end{aligned}$$

Comparing this value to tabulated chi-square values gives a measure of the similarity or difference in these categories from level A to level B. The number of degrees of freedom for a table is the product of one less the number of columns and one less the number of columns. Since the number of rows and columns are equal to two, the calculation is $1 \times 1 = 1 \text{ df}$.

At one degree of freedom, $\chi^2 = 5.33$ and 5.33 lies between the tabulated values of 3.841 and 5.412. These values represent significance at the 0.05 level (3.841) and the 0.02 level (5.412). Our measured value is closer to that of the 0.02 level so the similarity is significant at a very high level of confidence. In this result, it is highly plausible that the materials are contemporaneous and differ from the other level. Like our multivariate examples, the statistical analysis has

provided some quantitative measure of group (level, type, age, etc.) membership and difference.

Similar to the normal distribution, the area under the chi-square curve is equal to 1. In Fig. 10.7, one quickly observes that these curves are skewed to the left for smaller degrees of freedom. It is also apparent that as the number of degrees of freedom increases, the chi-square distribution approaches the shape of the normal distribution. Chi-square is used on large and small samples. In small samples, only a very strong difference/similarity is significant as in our example. In larger samples, weak or small differences are magnified. Recall our recent discussion of variable selection here as well. In terms of significance, the larger the sample size, exaggeration of small differences, within categories, is a possibility. As in all cases of the use of parametric and nonparametric statistical measures, one must always consider sample size.

To end this chapter, and overall, this discussion of techniques for archaeological geology, let me paraphrase Simon A. Levin, in his MacArthur Award Lecture of 1989 (Levin 1992), wherein he notes that “the simple statistical (or analytical) description of patterns is a starting point; but correlations are *no* substitute for (a) mechanistic understanding.” Statistics, and the other techniques, discussed in the preceding chapters, allow us to describe phenomena and patterning in archaeologically interesting phenomena across a wide range of scales. It is, however, for the archaeological geologist to use these techniques to infer conclusions of archaeological consequence.

10.5.5 The Next “New” Thing?: Bayesian Analysis and Archaeological Age Determination

Thomas Bayes, an eighteenth-century English Presbyterian minister, versed in mathematics, attempted to calculate the probability of God’s existence (Flam 2014). With his attempt, the

English cleric unknowingly founded a “school” of modern statistics termed “Bayesian” in his honor. We do not know if Reverend Bayes succeeded in his quest but the basis of his method—the use of *prior* knowledge to improve probabilistic calculations, using “Bayes’ theorem” (Bayes 1763), has become the “next new thing” in modern statistics.

In general, Bayesian models include three fundamental types of probabilities: *prior*, *likelihood*, and *posterior*. *Prior* information refers to estimates that are made about an event before any data are collected or observations are made. In archaeological analysis, prior information may include an age estimate for the beginning of a depositional event, such as the initial construction of a stone structure based on associations with a historically known event. Prior information also can include the relative order of stratigraphic units *in situ*. *Likelihood* refers to the probability density functions introduced by the data measurements themselves. In the case of ^{14}C dating, likelihood information derives from the absolute dates as measured through a ^{14}C probability function (Williams 2012). *Prior* and *likelihood* probabilities are formally integrated into a statistical model using Bayes’ theorem. The resulting information is referred to as the *posterior* probability (Buck and Millard 2004).

Referring back the earlier discussion of basic probability, we can briefly illustrate Bayes’ use of prior knowledge in shaping the probability of an event or occurrence.

The product rule for the probability that X is true as well as Y is true is stated as:

$$\begin{aligned} \text{Probability } (X, Y) &= \text{probability } (X|Y) \\ &\quad \times \text{probability } (Y) \end{aligned}$$

The transpose of this—the probability (X, Y) —is likewise true. Dividing through the transpose by the probability (Y) yields Bayes’ theorem:

$$\begin{aligned} \text{Probability } (X|Y) \\ = \frac{\text{probability } (Y|X) \times \text{probability } (X)}{\text{probability } (Y)} \end{aligned}$$

To illustrate the incorporation of Bayesian methods in archaeology, more specifically, the determination of archaeological radiocarbon chronologies, the example, below, from Steier and Rom (2000) will serve. Fundamentally, Bayes’ theorem allows the combination of measured data from a sample, such as the radiocarbon ages for a set of Iron Age (Hallstatt) samples, with a knowledge of corresponding samples before (*prior* to) the measurement. Both the measured data and the prior information must be formulated mathematically as probability distributions. In the program OxCal the “BOUND” condition is usually used to estimate the boundary (i.e., start and end time) of the chronological sequence (Bronk 1995).

In a similar calibration program called “BCal,” the “group boundary ages” of a sequence can be elicited from (1) no absolute chronological information; (2) exact known age(s); the ages are normally distributed or (4) the ages have a uniform distribution (Dye 2004). In the Hallstatt group of ages, both “early” and “late” boundaries—750–400 BC—are known (Fig. 10.8). This, however, is the presumed range of the late Hallstatt period. The latest dates—2446 BP, 2386 BP, and 2491 BP—are closer to the succeeding Iron Age period, La Tene, than that of Hallstatt. From additional material information, the archaeologists “know” the ages should be “Hallsatt” rather than “La Tene” (the 2nd European Iron Age, ca. 450–50 BC).

Bayesian calculations done in OxCal and BCal seek to move ages outside the anticipated age range to that of an area of “higher probability,” e.g., to *within* the anticipated age range. A combination of a well-defined distribution of ^{14}C measurements for archaeological samples with additional information on their chronological order allows the Bayesian sequence algorithm to reduce uncertainties. However, in doing so, the improvement in precision will oftentimes reduce the accuracy of the ages (Steier and Rom 2000).

The one downside of the Bayesian approach as opposed to that of a “frequentist” methodology is the requirement of *prior* information. One can use

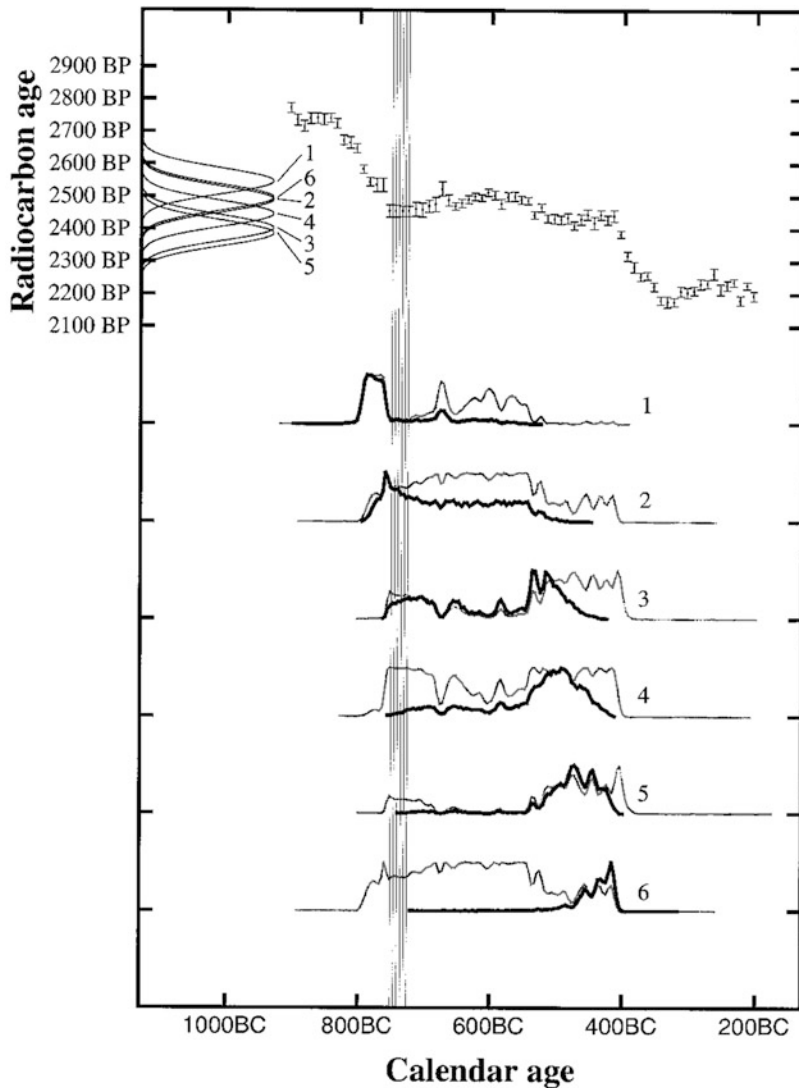


Fig. 10.8 For an assumed set of 6 samples #1 to #6 from the Hallstatt period (750–400 BC) with ages of 750 BC (#1), 745 BC (#2), 740 BC (#3), 735 BC (#4), 730 BC (#5), and 725 BC (#6) indicated by vertical thin lines, the corresponding 14C ages were looked up in the calibration curve. Due to the flatness of the calibration curve, we get the same 14C age of 2455 BP for all six samples. After adding a random scatter of ± 40 year, we obtain the following 14C ages: 2546 BP, 2490 BP, 2402 BP, 2446 BP, 2386 BP, and 2491 BP. By individual calibration, the samples can no more be assigned to distinct regions. The resulting probability distributions (gray curves) rather cover the whole Hallstatt period. These probability distributions correspond to our simulated 14C measurement data. After the Bayesian sequence algorithm is

applied, one can see its tendency to divide the period into six parts of equal size (black curves). Due to the flatness of the calibration curve, the general shape of the individually calibrated and of the “sequenced” probability distributions is the same which true ages ever are assumed. In our example, the posterior 95 % confidence intervals of samples #4, #5, and #6 are not in agreement with their assumed true ages. All the calculations (single calibration and sequencing) were performed with OxCal v2.18 (Ramsey 1995) using the INTCAL98 14C calibration curve (Stuiver et al. 1998). The program normalizes the individual and the “sequenced” probability distributions to the same maximum (*probability*) value (Italics added for emphasis)

a reasonable guess or estimate, but the assigning numbers to subjective judgments can produce results that may not measure up to estimates made from observations, after the fact, such as

those derived using traditional statistical methods. As in all things, the more information available generally improves the result—whether using frequentist or Bayesian methods.

Theory and Practice in Geoarchaeology: 11

A Brief Discussion with Examples

11.1 Introduction

As previously noted, the first edition of this book did not contain any discussion of theory nor for that matter practice in geoarchaeology. In many regards, the present chapter reprises much of that banished discussion, hence the seemingly heavy reliance on articles that date from that earlier time period. Those discussions are still germane and have been largely retained from those preceding edits as well as updated. Henry Frankel (2012) in his four-volume treatise on the controversy of continental drift and the rise of plate tectonics theory makes it clear that plate tectonics theory is just that—a theory. There is no agreed upon explanation for the origin nor the mechanism for movement of the Earth’s continental plates. Plates move; that is proven, but that is the mechanism, not the reason nor the explanation. That said, continental drift-plate tectonics theory is the greatest theoretical accomplishment of the twentieth century by earth science. Before that time, geology made, perhaps, two salient contributions to the general knowledge of the Earth system. The first was the principle of uniformitarianism, as proposed by James Hutton, and established in geology by Lyell, as more than just a “method” for describing the Earth. Likewise, geology’s recognition of the antiquity of the Earth expanded our understanding of the natural world. Arthur Holmes published *The Age of the Earth: An Introduction to Geological Ideas*

(Holmes 1913/1927) in which he presented a range of 1.6–3.0 billion years.

In many ways, geoarchaeological theory development recalls the development of the theory of a “Paleolithic” as mentioned in the introduction of this work. As noted, Edouard Lartet (1801–1871) developed the first useful chronology for the Paleolithic, using paleontology as a guide. Henri Breuil and Gabriel de Mortillet produced subsequent chronologies that quickly replaced Lartet’s “faunal chronology,” at least in France. Gabriel de Mortillet recognized the great temporal length encompassed by the Paleolithic, but he did not know exactly how much time was involved, but geology clearly inferred that it was significant. As noted above, any real estimation of the great age of the Earth would have to wait for Holmes’ study of radioactivity and the antiquity of the Earth.

Geoarchaeology is more than just a method in support of archaeological explanation. One only has to recall Butzer’s description of geoarchaeology as a disciplinary intersection between its parent disciplines to grasp this fact (Butzer 2008; Wilson 2011). In Butzer’s view, “The goal of contextual archaeology should be the study of archaeological sites as part of a human ecosystem, within which past communities interacted spatially, economically, and socially with the environmental subsystem into which they were adaptively networked” (Butzer 1982). Butzer, however, was criticized

by reviewers of his 1982 work for promoting the topics of site formation, modification, and destruction as human ecology which, strictly speaking, they are not (Pope 1986). Cultural adaptation is a central theme in ecological anthropology and should be utilized for understanding archaeology as human ecology. Human behavioral ecology specifically examines how human behaviors can maximize fitness within given environmental parameters (MacArthur and Pianka 1966; Thomas et al. 2008), without attempting to determine the mechanism by which a behavior is transmitted. These analyses are most effective at the population level where adaptation operates, instead of attempting to address changes in individuals' behaviors (Bamforth 2002). This allows for an integrated bio-cultural analysis that avoids the environmental determinism of earlier evolutionary-based anthropological theory. Instead, hypotheses are crafted to operationalize the range of what is possible, as well as what is optimal, within a given landscape (Bird and O'Connell 2006:146; Kelly 1995:109). Human behaviors that do not follow optimal models are usually interpreted as cultural and/or as suboptimal responses to periods of environmental instability and lack of perfect knowledge of the environment or as missing critical variable(s) in the model (e.g., Broughton 2002; Matsumura et al. 2010). This approach builds on Binford's (1980) basic model for foraging versus collection/logistical activities and patterns of mobility, allowing insights not only into the types of occupations seen in the archaeological record but also the potential resource bases that both allow and constrain those occupations.

By 2008, Butzer had identified archaeotaphonomy as the intersection between the human past and the processes of geomorphology. He argued that "The logical charge for geoarchaeology is to identify and assess the role of the filters (cultural and physical) and processes that impact the 'coming together' of those material residues and their transformation into an archaeological record" (*supra*). Butzer no longer saw geoarchaeology as human ecology per se but as a powerful way to discern the role of that

ecology in the production of an archaeological record of that ecology and its attendant behavior.

The Society for American Archaeology (SAA) defines context as follows: "Context in archaeology refers to the relationship that artifacts have to each other and the situation in which they are found. Every artifact found on an archaeological site has a precisely defined location. The exact spot where an artifact is found is recorded before it is removed from that location. Context is what allows archaeologists to understand the relationship between artifacts on the same site and how different archaeological sites are related to each other (http://www.saa.org/public/educators/03_whatis.html#06)."

11.2 Geoarchaeology and Landscapes

One current use of theory in geoarchaeology is the study of "landscapes." The retrodiction of these landscapes from geological/geomorphological data reifies landscape as a viable concept for describing past environments and the cultures that interacted and modified them. Landscapes per se are theoretical constructs just as "types" which are commonly used in the description of archaeological materials. Like artifactual types, such as ceramic types, landscapes are arbitrary constructions aimed at facilitating research (Lohse 1995; Chap. 8). Landscapes are not synonymous with natural environments. Landscapes are synthetic (Jackson 1984). Landscapes allow the description and categorization of a multitude of disparate variables—climate, soils, fauna, flora, etc.—that otherwise would be evaluated singularly. The construction of landscapes allows for the conjunction of those variables into a logical theoretical system for use in comparison across space and time. Archaeological contexts can and should be interpreted with an eye toward landscape transformation. Emphasis is placed on documenting the passage from stable (soil forming) to depositional (dynamic) environments and linking these transitions to an archaeological record at the local to regional scales (Stein 1993). Geoarchaeological investigations provide the key

to recognizing landscape and environmental change within a region, as well as reconstructing ancient landscapes and paleoclimatic regimes (Wilson 2011).

Productivity and soils have been recognized as a key component of human landscapes as well as environments (Jackson 1984; Eidl 1985). Eugene Odum, often characterized as the “father of modern ecology,” recognized the relationship of soils to the net primary production of an ecosystem (Odum 1960). Net primary production (i.e., apparent photosynthesis or total photosynthesis minus plant respiration), and secondarily with the overall heterotrophic utilization of the annual net productivity, was dependent, directly, on the attributes of soils. Texture of the soil, and especially the texture of the subsoil, has proved to be a key factor in the ecology of the communities which have developed on former agricultural land. The amount of clay and silt in the subsoil largely controlled the water- and nutrient-holding capacities of the soil as a whole and thereby the availability of water and nutrients to the plants. Soil type, thereby, greatly influenced the pattern of ecological succession (*supra*). A thorough understanding of culture and culture change is not possible without an appreciation of the environmental context. The genesis and geomorphosis of landscapes, with specific reference to anthropogenic inputs, are therefore a key aspect of the theoretical focus in today’s geoarchaeology.

11.3 Geoarchaeology at the Scale of Sites and Artifacts

Beyond landscapes, many geoarchaeologists have developed a micromorphic-based theory of “living surfaces.” In the example of the rock shelter of Riparo Dalmeri in Trentino, in Chap. 2, the “Epigravettian surface” is defined and described using both archaeologically theoretically constructed tool “types” that are “Epigravettian” and geoarchaeologically constructed “micromorphic” indices for past anthropogenic modification of sediments and inclusions within those sediments. Goldberg

and Macphail (2006) discussion of experimental geoarchaeology affords insights into the utility of geochemical analyses of residues as proxies for the magnitude and pattern of human and animal activity in sites when linked to the microstratigraphy. In Goldberg and Macphail’s view, as that of this textbook, the systematic study of sediments, soils, and stratigraphy is a prelude to the treatment of the possible range of depositional and weathering environments. To these researchers, micromorphology is an indispensable and robust tool for not only documenting the contextual position of archaeological objects and features within the matrix of the site but also for making accurate interpretations of the archaeological record (Goldberg and Berna 2010). Their detailed micromorphic and microstratigraphic approaches display the context of the all the material in its true space. Their analysis and exhibition of objects within the thin-section or impregnated block provide information about the integrity of these objects, how they got there, and what were the human activities associated with their initial production (i.e., burning) but also human activity associated with their modification (e.g., displacement by trampling or other taphonomic processes) or activities associated with hearth management (e.g., charging, rake out) (*supra*).

At the level of the artifact, Fladmark’s (1982) landmark paper on microdebitage effectively refocused the study of anthropogenic sediments beyond minerals and organic inclusions. Significantly, Fladmark’s investigation was not an analysis of small artifacts generally but specifically focused on lithic technology *per se*. Even so, Fladmark recognized a larger potential for the identification and study of microdebitage (*supra*; Stein and Teltser 1989; Dunnell and Stein 1989). From a theoretical perspective, an artifact is anything that displays one or more attributes as a consequence of human activity (Dunnell 1971; Dunnell and Stein 1989). The artifact, like landscape, is a theoretical construct. Through logical analogy and association, archaeologists, beginning with inquiries into the Paleolithic, have expanded the range of things that we come to regard as artifacts. Prehistorians

began to recognize more primitive tools such as stone choppers and, then, more elaborate structures, such as Stonehenges and earthen mounds, as the creations of prehistoric people.

The question of scale has direct relevance to the definition of what is or is not an artifact. Artifacts too large to be transported become “site features” or “site structures.” Very large artifacts, like stelae or menhirs, remain vaguely and arbitrarily delineated between the portable object and the stationary “site” (Dunnell 1988). Before workers like Fladmark, artifacts too small to be recovered individually had been regularly ignored, and their recovery limited to “samples” of the matrix (often called “soil samples” (Stein and Farrand 1985; Stein 1987; Dunnell and Stein *supra*)). Along the dimension of size, artifact became, largely by default, synonymous with objects that can be picked up with the hand and identified without magnification. Microartifacts denote all objects smaller than a given size that otherwise qualify as artifacts (*supra*). So classified, the microartifact thus becomes a concern of the geoarchaeologist because, in the course of their sedimentological and micromorphic studies, these materials are seen and identified.

All artifacts, features/structures, living surfaces, and landscapes are equal in their identification as constructs—heuristic or otherwise—within a theoretical utility for a study of prehistoric humanity.

Before we move to other considerations of theory in geoarchaeology, one should consider some aspects of classification with regard to artifacts. Artifacts have both size and shape or morphology. Archaeologists have used both of these parameters to make the logical leap to “function.” A bifacially flaked stone object is an “artifact” and a “tool.” The latter category refers to function. As Lohse has noted (1905), researchers cannot assume the happy coincidence between morphology and postulated use. Many times the artifact “type” such as projectile point style is a point along a continuum of shapes and sizes that are classified within that specific type. Likewise, its function may lie along another spectrum of possible uses—hide preparation, cutting, abrading, etc. Binford (1964) and others

(Clarke 1968) held that, at best, artifact types are theoretical generalizations of patterns of size, shape, and inferred use. Classification does not denote function nor does repetition infer proof or verification (Lohse 1995). Archaeological theory holds that all cultures consist of patterned production and interactions of their constituent individual members and that the patterns of (artifactual) debris result from the action of those individuals (Schiffer 1972, 1976). It is in this domain that geoarchaeology can contribute to the difficult task of elucidating past human behavior. Without entering into too much discussion of epistemology and archaeological methodologies, it is suffice to say that geoarchaeology must, perforce, utilize theory in its approach to anthropogenically created phenomena, be it artifacts, features, or landscapes. The level of abstraction required is a function of the specific inquiry’s aims or goals.

11.4 Geoarchaeology and the Origins of the Deliberate Human Use of Fire

Examples of current geoarchaeological inquiry are those examining the presence and origin of fire in early archaeological settings (Karkanas et al. 2007; Berna et al. 2012). Fire was one of the first major ways that humans started affecting the natural environment. There is considerable debate about when the earliest deliberate use of fire was, but it is clear that hominids controlled fire at least several hundred thousand years ago (Goudie 2013). The earliest evidence for hominin use of fire dates to more than a million years ago. However, only when fire use became a regular part of human behavioral adaptations could its benefits be fully realized and its evolutionary consequences fully expressed. It remains an open question when the use of fire shifted from occasional and opportunistic to habitual and planned (Shimelmitz et al. 2014). Fire provided humans with tremendous advantages: cooking fires provided heat and light as well as more digestible food; vegetation could be burned to open up the landscape, making hunting easier,

and to direct herds of animals to slaughter. Fire could be used for protection from predators, for eliminating vermin and noxious insects, for improving the quality of some lithic raw materials (Wilson 2011). Fire has been cited as a key factor in the development of early social behavior by serving a focal point for human groups (Wrangham 2009). Shimelmitz et al. (2014) stress that identifying when habitual fire use emerged is of major importance for understanding human evolutionary history. Fire offered many potential advantages to hominins (e.g., de Lumley 2006; Stiner et al. 2011), and its full impact on biological and behavioral evolution would have been felt only when fire became a routine component of hominin lifeways (Rolland 2004). Based on experience with deposits at Zhoukoudian and Qesem Caves, Israel (Karkanas et al. 2007), micromorphology has proven key for studying the evidence for burning and other activities related to the use of fire in Layer 8 at the Middle French Paleolithic site of Pech de l’Azé IV (Goldberg and Sherwood 2006; Goldberg et al. 2001; Dibble et al. 2009a, b).

11.5 Geoarchaeology and the Study of Natural Disaster

As illustrated in Chap. 3, the role of catastrophe in historic explanation requires more than textural evidence. Geoarchaeology has proven to be the arbiter for both examples presented in this textbook of tsunamic natural disasters, one in the Lake Geneva and an earlier Bronze Age disaster in the Aegean. The geoarchaeological evidence for the Medieval disaster of 563 AD fell to Katrina Kremer to demonstrate conclusively (Kremer et al. 2015). At Crete the evidence for tsunamic destruction of coastal Minoan harbors and towns has only been recently proven by geoarchaeological studies by Bruins and his coworkers (Bruins et al. 2008). These examples, along with Yenikapi harbor, Istanbul, point out the utility of identifying the very real role of natural system processes into that of prehistoric and early historic cultural systems, however dramatic. The Yenikapi harbor/Harbor of

Theodosius Project in Istanbul, Turkey, is an example of geoarchaeology integrating the stratigraphic sequence into the context of the harbor’s history as a whole (Bony et al. 2012; Perinçek 2010). A key finding of those studies was a high-energy deposit interpreted as being of tsunami origin and related to an earthquake of 557 AD. A bio-sedimentological analysis of this facies measured coarse sands and gravels, created by two tsunami wave trains, containing reworked material such as woods, bones, marble blocks, amphora fragments, ceramics, coins, shells, and plant remains. Since Kremer’s findings regarding the tsunami of 563 AD, subsequent research in the Lake Geneva and elsewhere in the Alpine region (Schnellmann et al. 2006; Kremer et al. 2015) has demonstrated that tectonics and debris flows had common and important roles in lives of lacustrine cultures just as earthquakes have today in other landform contexts.

11.6 Geoarchaeology and a Brief History of Archaeological Theory

Schuldenrein (2007) makes the plea, in the strongest terms, that geoarchaeologists must be formally trained in archaeology, and its theory, as well as earth science, since the modern practitioner is invariably asked to answer archaeological questions. Many contemporary geoarchaeological projects in alluvial landscapes place increased focus on the synthesis of drainage-wide chronologies and stratigraphies that have implications for linked human settlement and climatic models (*supra*). He is also correct, at least from the point of view of the USA, that geoarchaeology is practiced primarily within cultural resource management (CRM) contexts. Geoarchaeology has come into its own as part and parcel of both research and CRM archaeology in North America since the 1970s, but was almost always a component of Paleo-Indian archaeology since at least the 1930s (Holliday 2009). The USA is not alone in requiring specialists of all types—historical, zoological, botanical, malacological,

geoarchaeological, etc.—on publicly funded archaeological projects.

In many respects to the discussions among archaeologists in the 1980s and 1990s mirror those among present-day geoarchaeologists. Subdisciplines such as zooarchaeology, likewise, addressed the place of theory within its methodology (Gifford-Gonzalez 1991). Schuldenrein's concern for geoarchaeologists being well versed in archaeological theory and practice is well placed and surely contextualized within these earlier debates in archaeology itself. In this author's experience, this does not always happen even in academic programs such the University of Georgia's Archaeological Geology Program. Students do graduate with significant technical proficiency in earth science but remain naïve regarding any in-depth knowledge of the archaeological context of their particular research. It is one thing to be expert in EMPA material analysis and yet quite another to be equally expert in the material under analysis.

Epistemology and methodology are part of a wider set of discussions about analogy and uniformitarian assumptions in English-speaking archaeology (e.g., Salmon 1967, 1982; Wylie 1982, 1985, 1988, 1989). The relationship of patterning in archaeological assemblages to its causal agencies is often ambiguous. Assemblages—frequencies of different elements or traces—may be produced by various combinations of processes. Geologists, paleontologists, and archaeologists feel warranted in taking the stand that prehistoric entities can be accounted for by invoking the past operation of presently observable processes because of a multitude of examples in which the past-present analogical relationship appears to be very strong. Lyell's (1831, 1833) original arguments for a uniformitarian position were induced from such a multitude of exemplary cases, one of which involved his visit to Pompeii. Methodological uniformitarianism thus conforms to one of Carloye's (1971) descriptions of the role analogy plays in building general theory. He asserts that, in the development of theory through the use of analogue models, more formal statements of abstract relations are first suggested

by commonalities of several analogue models (Gifford-Gonzalez 1991).

Among the bodies of knowledge most widely used to better understand patterning in archaeology is geological “context.” The environmental and depositional information offered by sedimentary context has been emphasized in so many analyses of prehistoric faunal assemblages that it may be ascribed a privileged status, seemingly more “real” than other types of prehistoric evidence. It is an archaeological and paleontological truism that meticulous comparison of the geological contexts and the preserved remains of actual fossil assemblages is a secure and productive analytic method. However, relying on the “reality” of geological context to lessen the ambiguities of faunal assemblages may obscure the fact that inference of geological processes depends on relational analogies assembled and systematized by many geologists over the past 200 years (*supra*). Sedimentologists use the same strategy of establishing causation through contemporary observations, assess the range of possible effects of the same cause (e.g., Walker 1980), and face the same problems of equifinality in their analogues (e.g., Reineck and Singh 1975; Selley 1978:272–277; Farrand and Stein 1988). Like uniformitarian assumptions, the “facts” of geological context are based in analogical reasoning and must be understood as such.

The pitfalls of misapplication of uniformitarian assumptions and faulty analogies include what Lawrence (1971) called “transferred ecology,” which attributes most of a modern ecosystem's features to an ancient one on the basis of a few points of physical similarity between prehistoric and contemporary cases. Another exemplar from ecology is the notion of “no-analog” communities (Williams and Jackson 2007). No-analog communities are those that are compositionally unlike any found today. They occurred frequently in the past and will likely reoccur in a future greenhouse world. Well-documented no-analog plant communities existed in late-glacial North America (Overpeck, 1987) are closely linked to “novel” climates also lacking modern analogues, characterized by

high seasonality of temperature. Future novel climates will be warmer than any present climates globally, with spatially variable shifts in precipitation, and increase the risk of species reshuffling into no-analog communities and other ecological surprises (Williams and Jackson *supra*). Most paleoecological studies that at least partially parameterized from modern observations—actualistic—such as those that are geoarchaeologically based, may fail to accurately identify ecological responses to those novel climates. One such example cited in this chapter involves identifying the ecological response of the Norse Greenland colonies to the onset of the Little Ice Age.

A strategy of deduction from uniformitarian “laws” (e.g., Binford 1962, 1964; Freeman 1968) was a position reasserted in the debates of the 1980s by Richard Gould and others (1980; Gould and Watson 1982). In her critiques of this position, Wylie (1982, 1985) argued these writers had not considered that by using this form of an argument about the unobservable past constitutes a special type of very strongly warranted analogy. She notes, further, that the “escape” from analogy offered by scientific laws is really a refinement and elaboration of the analogical model of inference. Inference has implications for any research building or use in “middle-range theory.” More and/or better ampliative inferences can be based on patterning in the observed frequencies of various indices. Archaeological epistemology, hypothesis formation and selection, and methods of inference are unavoidably analogical (Gifford-Gonzalez 1989, 1991). Analogical reasoning based on well-controlled actualistic research is a preferred strategy in modern paleontological research. The uniformitarian theoretical perspective and the actualistic research strategy that follows from it have been basic to the generation of knowledge in the historical sciences since modern geology began (Lyell 1830; Hooykaas 1970).

The late Lewis Binford (1962, 1964, 1978, 1981) argued that archaeologists should name their materials, create relevant analytic categories, and assign meaning to patterning in their materials by analogy with modern cases.

This assertion was the basis for his program of building “middle range of theory.” The first aspect of the problem centers on the meanings which can be assigned to patterning in artifact assemblages. It is the epistemological problem of reliably establishing what we think such patterning means, in terms of the behaviors and contexts we ultimately want to study. This problem may be broken down into three related parts, each of which has a different, discipline-specific “remedy”: (1) unclear analytic concepts, (2) equifinality of causes in patterning of assemblages, and (3) lack of information on faunal remains in behavioral or ecological contexts. Returning to context as a construct, it is useful to distinguish two levels of “context”: behavioral context and ecological context or the systemic and archaeological contexts (cf. Schiffer 1972, 1986, 1987). Each is linked to the other by empirically evaluable bridging statements (again, middle-range theory). Any specific linkage between levels of a system is strengthened by additional, multiple, independent lines of information.

That a particular attribute or “cause” may not inevitably signify a closely specifiable natural, behavioral, or ecological context or process is the problem of equifinality—(2) in the three-part epistemological problem outlined above (Lyman 1985). In terms of equifinality, different processes can create the same pattern: the immediate conditions of production (e.g., stone, bone, and certain physical attributes of force in their encounter) are specifiable, but the circumstances—what most of us might call the agent-causing factors (e.g., a hammer stone versus a rockfall or flooding as causes for a cave’s bone deposits)—are, indeed, separable from the patterns themselves. The looming question is whether the proximate causes are what we infer or even the idea of “trampling,” itself, is theoretical construct itself and merits its own inquiry. Perhaps, this is overly negative because recent geoarchaeological studies, carefully framed and executed, have made significant contributions in improving our understanding of the Middle Paleolithic in France.

In the case of the French rock shelter, Fontéchevade taphonomic processes were found to be ultimately responsible for the distribution

as well as the overall nature of the artifactual and biological remains found there (Chase et al. 2009; Dibble et al. 2006). As sedimentological studies ascertained, the cave sediments were formed due to the action of very differing processes, with most of the materials coming from the overlaying plateau (through chimneys) and from the cave walls and ceiling as *eboulis*. Restudy also indicated that only a few of the archaeological finds were produced and/or introduced into the cave by humans during only occasional intermittent and short occupations of the cave. Harking back our discussion of human agency for fire, the existence of hearths and activity zones suggested by earlier excavators found no support in the micromorphic and mineralogic data. Lastly, the Tayacian assemblage of Fontéchevade was mainly produced by natural (formation) processes as were any similar, if not all, assemblages of this kind elsewhere (*supra*). Fontéchevade illustrates the value of restudy of archaeological materials and their geologic context. Clearer lines of evidence weighed against better theoretical/conceptual analogues eliminated much of the equifinality, leading to a set of more parsimonious explanations and refutation of earlier incorrect ones.

11.7 Enter Probability

Outcomes of the interaction of multiple variables in ecosystems may be regular, but the observed regularities are often better described in probabilistic terms. In terms of archaeology, no matter how deterministic the relationship between the immediate causes of certain archaeological assemblages, and even their links to specific causes, when archaeologists seek to set these causes in behavioral and ecological systems, the probabilistic nature of the operations of these systems precludes extending the “if-then” logic of deterministic statements. Instead, if X, then there is, say, an XX probability of Y. Explanation becomes a probabilistic statement to reduce uncertainty. The recent interest in Bayesian calculations particularly in regard to radiocarbon dating (cf. preceding chapter) illustrates the

recognition, as Thomas Bayes had postulated, that outcomes are not equiprobable nor all significant. The most important aspect of Bayesian approaches involves the recognition that the probability of a given result or outcome can rely on newer, but not necessarily “better,” data from other sources in any given inquiry.

In the use of relational analogies that are probabilistic in their predictions, there lays another methodological question: how do we discern and account for these relationships? To establish whether strong linkages (necessary and sufficient conditions, determining structures, etc.) exist between archaeological deposits and their production, we need enough contemporary (Bayesian?) cases to assess the supposed regularities of the relationships. To evaluate inductive generalizations drawn from such observations, we need confirmatory research which helps isolate the functional linkages in any regularities and assess whether these supposed linkages, indeed, operate in an uniformitarian fashion.

Prior to hypothesis testing, archaeologists typically employ analogy to evaluate the plausibility of bridging arguments which give objects and features a functional meaning. Archaeologists, as should geoarchaeologists, select the more plausible of alternative hypotheses about the functioning of prehistoric systems through analogy with contemporary cases (Binford 1978). Such uses of analogy are not unique to archaeological reasoning and have been analyzed in other sciences (e.g., Salmon 1967, 1982). Wylie (1989: 15) notes that they regularly marshal “independently constituted lines of evidence” which “converge either in supporting or refuting” their proposed linkages between past practices and the materials studied. This, she argues, is a means of coping with a lack of strongly deterministic epistemic foundations for their inferences. Again, multiple, independent sources of knowledge about analogues for archaeological entities are required both to generate and to evaluate “reconstructive hypotheses” drawn from archaeological data.

Accepting the analogical nature of most archaeological reasoning requires that we face

fundamental epistemological and methodological questions. How do we know what we purport to know, and how do we evaluate the reliability of our knowledge? We have discerned the best routes to inferential confidence: establishing strong relational analogies. “The archaeological record emphasizes that adaptation has in the past been associated with great social upheavals that could not have been foreseen by those who were undertaking the adaptation” (Brooks 2006). A society interacts with its environment according to its worldview that it will rely upon, and impact on, certain aspects of that environment (Leeuw et al. 2005). There is, perhaps, no better example of the latter statement than the demise of the Norse Greenland settlements (McGovern 1980, 1990; Buckland et al. 1996, 2004). Iceland, another more successful story in the North Atlantic expansion of the Medieval Norse, still bears evidence of the recurrence of natural disaster in those cultures.

11.8 Geoarchaeology, Theory, and Practice: Examples

11.8.1 The Medieval Norse Colonies of Greenland: What Were They Thinking?

The end of the Norse farms in Greenland never ceases to fascinate (Seaver 1996; Lynnerup 1998; Stockinger 2013). Explanations have ranged from abduction by pirates to “it got cold so they died” (with apologies to Tom McGovern) (Buckland et al. 2004; Buckland et al. 2009). With further apologies to McGovern, he has suggested, in somewhat mock seriousness, that the residents of Norse Greenland, after almost 400 years of settlement, had three choices when the Medieval Warm Period (MWP) ended and the Little Ice Age began in earnest. These choices included (1) build a bigger church (by that time Greenland had its own bishop), (2) burn a witch (blaming witchcraft in the Middle Ages, or in some societies even today, had credence), and (3) adapt (culturally). McGovern, again, noted, somewhat in jest, that the Norse seem to have

opted for 1 or 2. In relation to our discussion regarding theory and practice in geoarchaeology, McGovern’s “options” are testable hypotheses.

Recent studies of nitrogen and carbon isotope ratios in the bone from Norse Greenlandic cemeteries (Arneborg et al. 1999) have confirmed a significant and increasing marine component in the human diet. The most likely pathway for this is via seal meat, but there remains the possibility that fish were taken from outer fiord stations, gutted and beheaded there, and returned as fillets. The absence of fishing gear in the artifact assemblages is curious but real. In part, the increased use of marine resources suggests that Norse Greenland did attempt to adapt to the changing conditions and militates against McGovern’s suggestions of outright cultural intransigency.

Having refined their models of landscape exploitation, from stocking models to input from wild plant and animal sources (Barlow et al. 1998), the paleoecological record might be expected to provide the answers, but that evidence is enigmatic (Buckland *supra*). Today’s permafrost in the Western Settlement of Norse Greenland provides for the preservation of a paleoecological record (Buckland et al. 1983, 2004; McGovern et al. 1983). That evidence has been used in parallel with the climate data derived from the ice cores to examine the abandonment of the settlement ca. AD 1350 (Buckland et al. 1996; Barlow et al. 1998). As on the other sites examined in the Western Settlement, house floors for rooms occupied by both humans and animals were equally foul, with animal feces and the protein-feeding flies, *Heleomyza borealis* and *Teleomarina flavipes*, often occurring by the hundred in samples of the flooring material, a mix of beech twigs, moss, and hay debris. Such floors have a long history for animal bedding in Scandinavia (Göransson 2002), but their use for humans reflects an apparent need to provide insulation from an increasingly permanently frozen ground (Buckland et al. 1994).

Fresh lines of research have led to a productive shift from debates over one or another monocausal explanation for the extinction of the Norse colony to more interesting controversies over the nature

and organization of Norse society in Greenland (Berglund 1986; McGovern 1990; Buckland and Panagiotakopulu 2001). Dugmore et al. (2007) have argued for a sharply hierarchical later-Medieval society managed by partly foreign elites and dominated by the episcopal manor at Gardar in the Eastern Settlement and downplayed the role of the Latin church in Greenland, modeling a much more autonomous set of complex chiefdomships rather than a peripheralized colony of a Medieval European core. Most current authors agree on the vital role of Norse decision-making in response to the challenges of Inuit contact, climate change, and the increasing isolation from European markets (Dugmore *supra*). Changing Medieval economies and patterns of trade, rather than simple climatic deterioration, could have marginalized the Norse Greenland settlements and effectively sealed their fate. In the scholarship, there seems to be a decisive shift away from simplistic explanations for the settlements' extinction that treat human adaptive (or a maladaptive) strategies as a dependent variable, but, nonetheless, Lynnerup's (1998) model of gradual attrition of the communities and a final abandonment by the last families, moving first to the Eastern Settlement, and perhaps finally to Iceland, gains some support from the paleoecological research.

11.8.2 Medieval Iceland to AD 1783–1784: Tephra and Time

Frankel (2012) on the third volume of his treatise on continental drift theory and plate tectonics uses an aerial view of the Laki fissure of Iceland. The Laki eruption of 1783–1784 was the greatest human disaster in Icelandic history (Jackson 1982). Three hundred years after the human settlement of Greenland failed, the same fate almost befell its parent. As an Earth system generated cataclysm, the Laki eruption, in its scope, killed proportionately as much of the Icelandic population as the Black Death did in Europe three to four centuries earlier—almost one-third of the inhabitants died of disease and famine (*supra*; Grattan and Charman 1994). One cannot wonder

about this island of fire and ice, and the role of volcanism, on a scale unique to Iceland, might have in regard to regional if not global climate changes. Greenland's fate may have been more closely the result of Iceland's "monsters"—Laki, Hekla, and Katla—and their possible exacerbation of an orbitally induced climate shift.

The earliest tephra associated with the Norse colonization is called the "Settlement Ash" of 870 AD (Thorarinsson 1944; Haflidason et al. 2000). Tephra layers deposited in Iceland in historical time (~1100 cal. year BP) have often been identified and dated with relative accuracy by reasons of written records, in many cases even to the exact day of the tephra fall. Iceland's high-resolution tephrochronologic sequence has been facilitated by the rapid formation of both peat and loessic, and as a consequence, tephra layers of only a few years difference in age can be resolved in soil profiles. This provides a chronological context rivaling dendrochronology in temporal resolution. Iceland is not alone in the use of tephrochronology for archaeological purposes. Germany has the Laacher See ash, created by a massive explosive eruption at the beginning of the Holocene and a useful marker for this period where present (Boggard and Schmincke 1985; Moscariello and Costa 1997).

Outside of tephra, the geoarchaeology and sedimentological studies of early Norse settlements can be difficult. Sediment deposits at the Icelandic settlement of Reykholt in Borgarfjörður have produced only the biased sample provided by charred plant remains and no insects similar to those observed in Greenland deposits (Sveinbjarnardóttir 1992; Buckland et al. 2005). In Mývatnssveit, the important re-excavation of Hofstair has similarly produced no anaerobic sediments, essential for the overall preservation of organic materials, although application of soil thin-section micromorphology and biochemical techniques has provided important new data (Simpson et al. 1999). Molluscan and fish remains from the same deposit showed a surprising marine connection (McGovern 1990) for a site next to Icelandic best known Salmon River (Laxá), and this serves to drive home the overextended network of an early Medieval

Icelandic economy, a point which the paleo-ecological record is also capable of adding to the Greenland story of demise.

11.9 Example 2: The Scull Shoals Mill Village Site, Oconee River, Georgia, USA

The now-abandoned historic Scull Shoals Mill Village site is located in the Inner Piedmont of Georgia, USA. As Reusser et al. (YEAR) describe, it along with other historic sites with containment structures (dams; diversion structures such as flumes) trapped eroded sediments even before larger reservoirs were built in the twentieth century (Ferguson 1997, 1999). In the nineteenth century, the Scull Shoals village was the site of one of the first and largest mills in this region with a four-story brick main building containing 2000 spindles manned by 500 workers (*supra*). Nothing remains of this large complex, today, except a few ruins and piles of masonry and bricks (Fig. 11.1). It, like the Norse Greenland colonial failure, is allegorical for environmental change and the human inability to adapt—or so it would appear in the simplest explanations. Archaeology and history rarely unearth the simplest explanations. Rather, those findings—including more and more

geoarchaeological evidence—support nuanced and complex causation for these “failures.”

At Scull Shoals, the demands of the large mill for cotton required the clearance of over 4000 acres (2400 ha) of what was originally oak-hickory forest. Exposed to rainfall, the upland soils were rapidly eroded. Ferguson describes “topsoil being peeled off in a sheet, taking with it the entire seedbed and rooting zone... while leaving the exposed subsoil (B-horizon) tofurther erosion” (*supra*). He describes this erosion as “catastrophic.” Ferguson is a geohydrologist who made a quantitative study of the hydrology and sediment loss at this location. Sediment loads in rivers like the Oconee declined after cotton agriculture ended in the early twentieth century. The cumulative erosion cited by both Ferguson and Reusser et al. (*supra*) was first described by Trimble (1974). Trimble tracked erosion (inches) from just prior to 1800 to just past 1950, with steady, synoptic rise from zero to 8+ inches (*supra*).

At Scull Shoals that sediment largely remains either in the river, aggraded behind old containment structures, or in the valley itself. Ferguson measured 10 feet (3 m) of sediment at the Scull Shoals location while he estimates a total sediment depth of 14 feet (4 m). Ferguson cites the geophysical work of the author and students at the mill site where metal and material remains were detected, buried in over 6 feet (1.6 m) depths

Fig. 11.1 Painting of the Scull Shoals mill, in the nineteenth century; at its peak





Fig. 11.2 A 1.5 m sediment core, using a cryoprobe at the Scull Shoals site, *right* (Photographs by the author)

using ground-penetrating radar (GPR), magnetometry, and sediment coring (*supra*; Garrison et al. 2002) (Fig. 11.2). Ferguson charted a long-term alluvial cycle of the Oconee watershed that has the peak of valley filling between 1800 and 1930 with a steady headwater erosion/incision, driven by natural factors, but with lateral meandering and downstream (sediment) transfer below Scull Shoals (*supra*). It must be noted that a large storage reservoir exists just below Scull Shoals today and that any legacy sediments, that have been remobilized, reside there.

The storage of sediment is a common feature of almost all alluvial systems. If not bed storage, then it is floodplain storage (cf. Chap. 2). John Wesley Powell defined the concept of base level and the base level in the late nineteenth- and early twentieth-century Oconee River raised to point that, what had been floods contained within the natural levees, became devastating floodplain inundations which occurred more and more frequently (Hunt 1980). The sedimentological evidence of these floods is clearly seen in Fig. 11.2. One reason the cryoprobe core extends only 1.5 m is that it “bottomed” into the oak flooring of the now-buried mill’s lower level.

There may even be a volcanological dimension to the demise of Scull Shoals. After the well-known 1883 eruption of Krakatoa, average global temperatures were up to 1.2° cooler for

the next 5 years (Winchester 2003). It is subsequent to this period that the more devastating floods (1884) occurred, leading to the closure of the mill and loss of the highway bridge at the town (*supra*; Skarda 2007). No direct meteorological link, however, has been made between the eruption and increased precipitation in the American Southeast. It remains an open question but one that could be investigated using a geoarchaeological paradigm.

If we would accept simple explanations, then the demise of Scull Shoals is a cautionary tale of habitat destruction—land clearance, erosion, and increased flooding—such that livability of the mill town became untenable, resulting in its ultimate abandonment. Much like the original explanation for Greenland, environmental change and increased hardship led to the ultimate abandonment of the Western and Eastern Settlements. In light of more recent scholarship based on a broader inspection of data sets—glacial, sedimentological, hydrological (in the case of Scull Shoals and even Greenland (Larsen and Brock 2014)), economics, transportation, geomorphological, etc.—the explanations become more complicated. In both Greenland and the Georgia Piedmont, landscapes were altered to the point that economic practices that were sustainable in the past became less so. Add to this picture of

“natural” system change unfavorable changes in the markets and economies of both the late-Medieval and postcolonial milieus, then “failure” becomes a more predictable result.

11.10 Concluding Thoughts

Geoarchaeology or archaeological geology by whatever name has developed a need and application for theory within its modern practice. Most, if not all, practitioners are cognizant of this and design their research accordingly. The strength of support for an analytical result and subsequent conclusion or conclusions increases with strong analogues as well as multiple lines of evidence. Hesse et al. (1986) in a discussion of

archaeogeophysical methodology called for the use of “multiple sensors” as way to enhance and support the interpretation of that form of data. One sensor—GPR—is good, GPR *plus* resistivity is better, etc. Hesse was calling for multiple lines of independent evidence to increase confidence in the analytical results. Even at that, the accuracy of the findings may not increase nor the epistemic certainty of a result, because the method or methods used actually may not answer the question at hand (Foulger et al. 2015). Those answers may lie elsewhere in the search for agency and causation. As scientists, geoarchaeologists must gauge their choice of methods by their adequacy in explanation. Parsimony and William of Ockham’s razor remains more than just useful tools.

References

Abbe MB (2011) A roman marble replica of the “South Slope Head”: polychromy and identification. *Source Notes Hist Art* 30:18–24

Abbe MB (2013) An Archaeological description of the Richmond Caligula. In: Frischer B, Schertz P (eds) *Caligula 3-D: Man, Myth, Emperor*. Proceedings of the international symposium on the Richmond Caligula. Virtual World Heritage Sculpture Laboratory; Brill Press, Leiden

Adams AE, MacKenzie WS, Guilford C (1997) *Atlas of sedimentary rocks under the microscope*. Addison Wesley Longman, Harlow

Adams AE, MacKenzie WS, Guilford C (1984) *Atlas of sedimentary rocks under the microscope*. Longman/Wiley, London

Adderley WP, Simpson IA, Vésteinsson O (2008) Local-scale adaptations: a modeled assessment of soil, landscape, microclimatic, and management factors in Norse home-field productivities. *Geoarchaeology* 23 (4):500–527

Agassiz L (1840) *Etudes des glaciers*, vol 3, Proceedings of the Geological Society of London. Geological Society, London

Agassiz L (1967) *Studies on glaciers*; preceded by the discourse of Neuchâtel. Hafner, New York

Aitken MJ (1974) *Physics and archaeology*, 2nd edn. Clarendon Press, Oxford

Akrige DG, Benoit PH (2001) Luminescence properties of chert and some archaeological applications. *J Archaeol Sci* 28:143–151

Albert RM, Berna F, Goldberg P (2012) Insights on Neanderthal fire use at Kebara Cave (Israel) through high resolution study of prehistoric combustion features: evidence from phytoliths and thin sections. *Quat Int* 247:278–293

Aldenderfer M, Craig NM, Speakman RJ, Popelka-Filcoff R (2008) Four-thousand-year-old gold artifacts from the Lake Titicaca basin, southern Peru. *Proc Natl Acad Sci* 105(13):5002–5005

Allard GO, Whitney JA (1994) *Environmental geology lab manual*. Wm. C. Brown, Dubuque

Allen DF (ed) (1980) *The coins of the ancient celts*. Edinburgh University Press, Edinburgh

Al-Suwaidi M, Ward BC, Wilson MC, Hebda RJ, Nagorsen DW, Marshall D, Ghaleb B, Wigen RJ, Enkin RJ (2006) Late Wisconsinan port Eliza cave deposits and their implications for human coastal migration, Vancouver Island, Canada. *Geoarchaeology* 21(4):307–332

Ambrose SH, Lorenz KG (1990) Social and ecological models for the Middle Stone Age in southern Africa. In: Mellars P (ed) *The emergence of modern humans: an archaeological perspective*. Cornell University Press, Ithaca, pp 3–33

Ambroz JA, Glasscock MD, Skinner CE (2001) Chemical differentiation of obsidian within the Glass Buttes complex. *J Archaeol Sci* 28:741–746

Andersen ST (1986) Paleoecological studies in terrestrial soils. In: Berglund BE (ed) *Handbook of holocene paleoecology and paleohydrology*. Wiley, New York

Anderson TJ (2003) Des artisans à la campagne: carrière de meules, forge et voie gallo-romaines à Châbles (FR), vol 19. Academic Press Fribourg, Saint-Paul

Anderson DG, Gillam C (2000) Paleoindian colonization of the Americas: implications from an examination of physiography, demography, and artifact distribution. *Am Antiq* 65(1):43–66

Anderson DG, Sassaman K (1996) Modeling paleoindian and early archaic settlement in the southeast: a historical perspective. In: Anderson DG, Sassaman KE (eds) *The paleoindian and early archaic southeast*. University of Alabama Press, Tuscaloosa, pp 16–28

Anderson DG, Schulderein J (1985) Prehistoric human ecology along the Upper Savannah River: excavations at Rucker's bottom, Abbeville and Bullard Site Groups. Report prepared for the National Park Service by Commonwealth Associates, Jackson

Anderson T, Villet D, Serneels V (1999) La fabrication des meules en grès coquillier sur le site gallo-romain de Châbles-Les Saux (FR). *Archéologie Suisse* 22 (4):182–189

Andrews HE, Besancon JR, Bolze CE, Dolan M, Kempfer K, Reed RM, Riley CM, Thompson MD (1997a) Igneous rocks and volcanic hazards. In: Busch RM (ed) *Laboratory manual in physical geology*. Prentice Hall, Upper Saddle, pp 50–68

Andrews HE, Besancon JR, Gore PJW, Thompson MD (1997b) Sedimentary rocks, processes and environments. In: Busch RM (ed) Laboratory manual in physical geology. Prentice Hall, Upper Saddle River, pp 69–92

Andrews TD, MacKay G, Andrew L (2009) Hunters of the alpine ice: the NWT ice patch study. Prince of Wales Northern Heritage Centre, Yellowknife

Andrews TD, MacKay G, Andrew L (2012) Archaeological investigations of alpine ice patches in the Selwyn Mountains, Northwest Territories, Canada. *Arctic* 65 (1):1–21

Angelucci DE (2010) The recognition and description of lithic artifacts in thin section. *Geoarchaeology* 25 (2):220–232

Angelucci DE, Bassetti M (2009) Humans and their landscape from the Alpine Last Glacial Maximum to the Middle Holocene in Trentino: geoarchaeological considerations. *Preistoria Alpina* 44(5):59–78

Anuskiewicz RJ, Dunbar JS (1993) Of Prehistoric man at ray hole springs: a drowned sinkhole located 32 KM offshore on the continental shelf in 12 M seawater. In: Diving for science 1993: Proceedings of the American Academy of Underwater Sciences Thirteenth Annual Scientific Diving Symposium, Pacific Grove, pp 1–22

Arakawa F, Miskell-Gerhardt K (2009) Geoarchaeological investigation of the lithic resources in the central Mesa Verde region, Colorado, U.S.A. *Geoarchaeology* 24(2):204–223

Arias M, Barral MT, Diaz-Fierros F (1995) Effects of iron and aluminium oxides on the colloidal and surface properties of kaolin. *Clays Clay Miner* 43:406–416

Arneborg J, Heinemeier J, Lynnerup N, Nielsen HL, Rud N, Sveinbjörnsdóttir AE (1999) Change of diet of the Greenland Vikings determined from stable isotope analysis and ¹⁴C dating of their bones. *Radiocarbon* 41(2):157–168

Arnold B, Money C (1978) Les amas des galets un village littoral d'Auvernier-Nord (Bronze final; lac de Neuchâtel): études géologique et archéologique. *Bull Société neuchâteloise Sci Nat* 101:153–166

Arnold DE, Neff H, Bishop RL, Glascock MD (1999) Testing interpretive assumptions of neutron activation analysis. In: Chilton ES (ed) Material meanings. The University of Utah Press, Salt Lake City

Artioli G, Angelini I (2011) Mineralogy and archaeometry: fatal attraction. *Eur J Mineral* 23 (6):849–855

Arrhenius O (1931) Die Bodenanalyse im dienst der Archäologie. *Zeitschrift für Pflanzernährung, Düngung, Bodenkunde* 10(27–29):427–439

Ashley GM, Driese SG (2000) Paleopedology and paleohydrology of a volcaniclastic paleosol interval: Implications for early Pleistocene stratigraphy and paleoclimatic record, Olduvai Gorge, Tanzania. *J Sediment Res* 70(5):1065–1080

Aspinall A, Lyman JT (1970) An induced polarization instrument for the detection of near surface features. *Prozepzioni Archaeologiche* 5:67–75

Aspinall A, Crummett JG (1997) The electrical pseudosection. *Archaeol Prospect* 4:37–47

Aspinall A, Gaffney C, Conyers L (2008) Archaeological prospection—the first fifteen years. *Archaeol Prospect* 15(4):241–245

Aspinall A, Gaffney C, Schmidt A (2009) Magnetometry for archaeologists, vol 2. Rowman Altamira, Lanham

Astrup EE, Martens I (2011) Studies of Viking age swords: metallography and archaeology. *Gladius* XXXI:203–206

Backwell L, d'Errico F, Wadley L (2008) Middle stone age bone tools from the Howiesons Poort layers, Sibudu Cave, South Africa. *J Archaeol Sci* 35 (6):1566–1580

Bahn P, Renfrew C (1999) Archaeology: a brief introduction, 7th edn. Prentice-Hall, London

Baietto V, Villeneuve G, Schvoerer M, Bechtel F, Herz N (1999) Investigation of electron paramagnetic resonance peaks in some powdered white marble. *Archaeometry* 41(2):253–265

Bailey G, Flemming N (2008) Archaeology of the continental shelf: marine resources, submerged landscapes and underwater archaeology. *Quat Sci Rev* 27 (23–24):2153–2165

Baker CM (1978) The size effect: an explanation of variability in surface artifact assemblage. *Am Antiq* 43(2):288–293

Balco G, Rovey CW II (2010) Absolute chronology for major Pleistocene advances of the Laurentide Ice sheet. *Geology* 38:795–798

Baldwin WE, Morton RA, Putney TR, Katuna MP, Harris MS, Gayes PT, Driscoll NW, Denny JF, Schwab WC (2006) Migration of the Pee Dee River system inferred from ancestral paleochannels underlying the South Carolina Grand Strand and Long Bay inner shelf. *Geol Soc Am Bull* 118(5/6):533–549

Ball T, Gardner JS, Brotherton JD (1996) Identifying phytoliths produced by the inflorescence bracts of three species of wheat (*Triticum monococcum* L., *T. dicoccum* and *T. aestivum* L.) using computer-assisted image and statistical analysis. *J Archaeol Sci* 23(4):619–632

Bamforth DB (2002) Evidence and metaphor in evolutionary archaeology. *Am Antiq* 67(3):435–452

Banning EB (2000) Soils, sediments, and geomorphology. The archaeologist's laboratory: the analysis of archaeological data. *Interdisciplinary Contributions to Archaeology*, Springer U.S., New York, pp 235–247

Barba L (2007) Chemical residues in lime-plaster archaeological floors. *Geoarchaeology* 22(4):439–452

Barba L, Lazos L (2000) Chemical analysis of floors for the identification of activity areas: a review. *Antropología y Técnica* 6:59–70

Barbin V, Ramseyer K, Burns SJ, Decroze D, Maier JL, Chamay J (1991) Cathodoluminescence signature of white marble artefacts. *Mat Res Soc Symp Proc* 185:299–308

Barbin V, Ramseyer K, Decroze D, Burns SJ, Chambay J, Maier JL (1992) Cathodoluminescence of

white marbles: an overview. *Archaeometry* 34(2):175–183

Bartolomei G, Broglia A, Cattani L, Cremaschi M, Lanzinger M, Leonard P (1985) Risultati preliminari dalle nuove ricerche nella Grotta di Paina. *Jagen und Sammeln. Jahrbuch des Bernischen Historischen Museum*, Bern, pp 63–64, 43–54

Barker RD (1992) A simple algorithm for electrical imaging of the subsurface. *First Break* 10(2):53–62

Barlow LK, Sadler JP, Ogilvie A, Buckland PC, Amorosi T, Ingimundarsson JH, Skidmore P, Dugmore AJ, McGovern TH (1998) Ice core and environmental evidence for the end of Norse Greenland. *The Holocene* 7:489–499

Basso K (1996) *Wisdom sits in places*. University of New Mexico Press, Albuquerque

Bateman AM (1950) *Economic mineral deposits*, 2nd edn. Wiley, New York

Baxter MJ, Jackson CM (2001) Variable selection in artefact compositional studies. *Archaeometry* 43:253–268

Bayes T (1763) An essay towards solving a problem in the doctrine of chances. *Philos Trans R Soc Lond* 53:370–418, A postscript and a LaTec source file version of this paper are available at URL: <http://www.york.ac.uk/depts/maths/histstat/essay.ps> and <http://www.york.ac.uk/depts/maths/histstat/essay.htm> respectively

BCal can be found at: <http://bcal.sheffield.ac.uk>

Beach T, Dunning N, Doyle M (2008) Geoarchaeology and geomorphology: soils, sediments and societies. *Geomorphology* (Special Issue) 101:413–415

Bearrs EC (1966) *Hard luck ironclad*. Louisiana State University Press, Baton Rouge

Bender SJ (1983) Hunter-gatherer subsistence and settlement in a mountainous environment: the prehistory of the Northern Tetons. State University of New York at Albany

Bender SJ, Wright GA (1988) High-altitude occupations, cultural process, and high plains prehistory: retrospect and prospect. *Am Anthropol* 90(3):619–639

Benedict JB (1985) Arapaho Pass: glacial geology and archeology at the crest of the Colorado Front Range. Center for Mountain Archeology Research Report, no. 3. Ward, Colorado

Benedetti MM, Cordova CE, Beach T (2011) Soils, sediments, and geoarchaeology: introduction. *Catena* 85:83–86

Benjamin J (2010) Submerged prehistoric landscapes and underwater site discovery: reevaluating the ‘Danish Model’ for international practice. *J Island Coast Archaeol* 5:253–270

Benjamin J, Hale A (2012) Marine, maritime, or submerged prehistory? Contextualizing the prehistoric underwater archaeologies of inland, coastal and offshore environments. *Eur J Archaeol* 15(2):237–256

Bentsen SE (2014) Using pyrotechnology: fire-related features and activities with a focus on the African middle stone age. *J Archaeol Res* 22(2):141–175

Bergadà MM (1998) Estudio geoarqueológico de los asentamientos prehistóricos del Pleistoceno Superior y el Holoceno inicial en Catalunya. *BAR International Series* 742, Oxford

Berglund J (1986) Decline of the Norse settlements in Greenland. *Arct Anthropol* 23:109–135

Berglund J (1986) The decline of the Norse settlements in Greenland. *Arctic Anthropol* 23(1/2):109–137

Berna F, Goldberg P (2007) Assessing Paleolithic pyrotechnology and associated hominin behavior in Israel. *Israel J Earth Sci* 56:107–121

Berna F, Goldberg P, Kolska Horwitz L, Brink J, Holt S, Bamford M, Chaza M (2012) Microstratigraphic evidence of in situ fire in the Acheulean strata of Wonderwerk Cave, Northern Cape province, South Africa. *Proc Natl Acad Sci* 109:1215–1220

Berner EK, Berner RA (2012) *Global environment: water, air, and geochemical cycles*. Princeton University Press, Princeton

Bertsch PM, Seaman JC (1999) Characterization of complex mineral assemblages: implications for contaminant transport and environmental remediation. *Proc Natl Acad Sci* 96(7):3350–3357

Besse M (ed) (2014) *Around the Petit-Chasseur site in Sion (Valais, Switzerland) and new approaches to the bell beaker culture*. Proceedings of the International Conference (Sion, Switzerland – October 27th–30th 2011). Archaeopress, Oxford

Bettis EA III (1995) Archaeological geology of the archaic period in north America, vol 297, Geological Society of America Special Paper. Geological Society of America, Boulder

Bettis EA III, Muhs DR, Roberts HM, Wintle AG (2003) Last glacial loess in the conterminous USA. *Quat Sci Rev* 22(18):907–1946

Bevins RE, Pearce NJ, Ixer RA (2011) Stonehenge rhyolitic bluestone sources and the application of zircon chemistry as a new tool for provenancing rhyolitic lithics. *J Archaeol Sci* 38(3):605–622

Binford LR (1962) Archaeology as anthropology. *Am Antiq* 28:217–225

Binford LR (1964) A consideration of archaeological research design. *Am Antiq* 29(4):425–441

Binford LR (1978) *Nunamiut ethnoarchaeology*. Academic, New York

Binford LR (1980) Willow smoke and dogs’ tails: hunter-gatherer settlement systems and archaeological site formation. *Am Antiq* 45:4–20

Binford LR (1981) *Bones: ancient men and modern myths*. Academic, New York

Bird DW, O’Connell JF (2006) Behavioral ecology and archaeology. *J Archaeol Res* 14(2):143–188

Birkeland PW (1984) *Soils and geomorphology*. Oxford University Press, New York

Bishop RL (1992) Comments on section II: variation, characterization of ceramic pastes in archaeology. In: Neff H (ed) *Monographs in world archaeology*, vol 7. Prehistory Press, Madison, pp 167–170

Bishop RL, Rands RL, Holley GR (1982) Ceramic compositional analysis in archaeological perspective. In: Schiffer MB (ed) *Advances in archaeological method and theory*, vol 5. Academic, pp 275–330

Bishop RL (1994) Pre-Columbian pottery: research in the Maya region. In: *Archaeometry of pre-Columbian sites and artifacts: proceedings of a symposium organized by the UCLA Institute of Archaeology and the Getty Conservation Institute*, Los Angeles, 23–27 March 1992, pp 15–65. Getty Conservation Institute

Bisi F, Broglio A, Guerreschi A, Radmilli A (1983) L'Epigravettien Evolue et final dans la zone haute et moyenne adriatique. *Rivista di scienze preistoriche* 32 (1):229–265

Blackman MJ (1992) The effect of human size sorting on the mineralogy and chemistry of ceramic clays. In: Neff H (ed) *Chemical characterization of ceramic pastes in archaeology*. Prehistory Press, Madison, pp 113–124

Blackwell B, Schwarz H (1993) Archaeochronology and scale. In: Stein JK, Linse AR (eds) *Effects of scale on archaeological and geoscientific perspectives*, vol 283, Geological Society of America, Special Paper. Geological Society of America, Boulder, Godfrey-Smith DI, Blanchard RW, Rehm G, and

Blair TC, McPherson JG (1999) Grain-size and textural classification of coarse sedimentary particles. *J Sediment Res* 69:6–19

Blatt H (1982) *Sedimentary petrology*. W. H Freeman, San Francisco

Blumenshine RJ, Masao FT (1991) Living sites at Olduvai Gorge, Tanzania? Preliminary landscape archaeology results in the basal Bed II lake margin zone. *J Hum Evol* 21:451–462

Blumenshine RJ, Peters CR (1998) Archaeological predictions for hominid land use in the paleo-Olduvai Basin, Tanzania, during lowermost Bed II times. *J Hum Evol* 34:565–607. doi:10.1006/jhev.1998.0216

Blyth PH (1977) The effectiveness of Greek armour against arrows in the Persian war (490–479 BC): an interdisciplinary enquiry. Doctoral dissertation. University of Reading

Boaretto E, Wu X, Yuan J, Bar-Yosef O, Chu V, Pan Y, Weiner S, Liu K, Cohen D, Jiao T, Li S, Gu H, Goldberg P, Weiner S (2009) Radiocarbon dating of charcoal and bone collagen associated with early pottery at Yuchanyan Cave, Hunan Province, China. *Proc Natl Acad Sci U S A* 106(24):9595–9600

Bond G, Broecker W, Johnson S, McMamus J, Labeyrie L, Jouzel L, Bonani G (1993) Correlation between climate records from North Atlantic sediments and Greenland ice. *Nature* 365:143–147

Bond GC, Showers W, Elliot M, Evans M, Lotti R, Hajdas I, Bonani G, Johnson S (1999) The North Atlantic's 1–2 kyr climate rhythm: relation to Heinrich events, Dansgaard/Oeschger cycles and the little ice age. In: Clark PU, Webb RS, Keigwin LD (eds) *Mechanisms of global change at millennial time scales*, vol 112, *Geophysical Monograph*. American Geophysical Union, Washington, DC, pp 59–76

Bonnefille R (1984) Palynological research at Olduvai Gorge. *Nat Geog Soc Res Rep* 17:227–243

Bony G, Mariner N, Morhange C, Kaniewski D, Perinçek D (2012) A high-energy deposit in the Byzantine harbour of Yenikapı, Istanbul (Turkey). *Quat Int* 266:117–130

Bordes F (1954) The Deposits in Pech-De-Laze (Dordogne), vol 1, Mousterien in the Acheulian Tradition. *Anthropologie* 58(5–6):401–432

Bordes F (1968) *The old stone age*, vol 30. McGraw-Hill, New York

Bordes F (1972) *A tale of two caves*. Harper and Row, London

Bosinski G (1992) Eiszeitjäger im Neuwieder Becken. *Archäologie an Mittelrhein und Mosel*. Band 1. Gesellschaft für Archäologie Am Mittelrhein und Mosel E.V. Archäologische Denkmalpflege Amt, Koblenz

Bourgarit D (2007) Chalcolithic copper smelting. In: La Niece S, Hook D, Craddock PT (eds) *Metals and mines: studies in archaeometallurgy*. Archetype Publications, London, pp 3–14

Bozart S (1993) Maize (*Zea Mays*) cob phytoliths from a central Kansas Great Bend Aspect archaeological site. *Plains Anthropol* 38:279–286

Bozarth SR (1986) Morphologically distinctive *Phaseolus*, *Cucurbita* and *Helianthus annuus* phytoliths. Plant opal phytolith analysis in archaeology and paleoecology. In: Rovner I (ed) *Occasional papers of the Phytolitharian*. North Carolina State University, Raleigh, pp 56–66

Brady N (1990) *The nature and properties of soils*. MacMillan, New York

Braidwood RJ, Çambel H, Schirmer W (1981) Beginnings of village-farming communities in South-eastern Turkey: Çayönü Tepesi, 1978 and 1979. *J Field Archaeol* 8(1):249–258

Braun DP (1982) Radiographic analysis of temper in ceramic vessels: goals and initial methods. *J Field Archaeol* 9(2):183–192

Braun DP (1983) Pots as tools. In: Moore J, Keene AS (eds) *Archaeological hammers and theories*. Academic, New York, pp 107–134

Bray ISJ (1994) Geochemical methods for provenance studies of steatite. Scottish Universities Research and Reactor Centre, University of Glasgow, Glasgow, Scotland

Briard J (1979) *The Bronze Age in Barbarian Europe: from the Megaliths to the Celts*. Routledge & Kegan Paul Books, London/Boston

Briggs K, Thomson K, Gaffney V (2007) A geomorphological investigation of submerged depositional features within the outer silver pit, southern north sea. In: Gaffney V, Thomson K, Fitch J (eds) *Mapping Doggerland: the Mesolithic landscapes of the southern North sea*. Archaeopress, Oxford, pp 43–60

Brongniart A (1813) *Essai de classification minéralogique des roches mélangées*. *J Min* XXXIV:190–199

Bronitsky G (ed) (1989) *Pottery technology: ideas and approaches*. Westview Press, Boulder

Bronk RC (1995) Radiocarbon calibration and analysis of stratigraphy: the OxCal program. *Radiocarbon* 37 (2):425–430

Bronson B (1986) The making and selling of wootz, a crucible steel of India. *Archeomaterials* 1(1):13–51

Brook GA, Coward JB, Marais E (1996) Wet and dry periods in the southern African summer rainfall zone during the last 300kyr from speleothem, tufa and sand dune age data. In: Heine K (ed) *Paleoecology of Africa and the surrounding islands*, vol 24. Balkema, Rotterdam, pp 147–158

Brooks N (2006) Cultural responses to aridity in the middle Holocene and increased social complexity. *Quat Int* 151:29–49

Broughton JM (2002) Prey spatial structure and behavior affect archaeological tests of optimal foraging models: examples from the Emeryville Shellmound vertebrate fauna. *World Archaeol* 34:60–83

Brower JV, Hill AJ, Lewis TH, Winchell NH (1911) *The aborigines of Minnesota: a report based on the collections of Jacob V. Brower, and on the field surveys and notes of Alfred J. Hill and Theodore H. Lewis*. The Pioneer Company, St Paul

Brown DA (1984) Prospects and limits of a phytolith key for grasses in the central United States. *J Archaeol Sci* 11(4):345–368

Brown JA (1989) The beginnings of pottery as an economic process. In: van der Leeuw SE, Torrence R (eds) *What's new? A closer look at the process of innovation*. Unwin Hyman, London, pp 203–224

Brown RM (2000) *The ceramics of Southeast Asia: their dating and identification*. Art Media Resources, Chicago

Brown KS, Marean CW, Herries AJR, Jacobs Z, Tribolo C, Braun D, Roberts DL, Meyer MC, Bernatchez J (2009) Fires as an engineering tool of early humans. *Science* 325:859–862

Brunet M, Guy F, Pilbeam D, Mackaye HT, Likius A, Ahounta D, Beauvilain A, Blondel C, Bocherens H, Boissier J-R, De Bonis L, Coppens Y, Dejax J, Denys C, Düringer P, Eisenmann V, Fanone G, Fronty P, Geraads D, Lehmann T, Lihoreau F, Louchart A, Mahamat A, Merceron G, Mouchelin G, Otero O, Campomanes PP, Ponce De Leon M, Rage J-C, Sapanet M, Schuster M, Sudre J, Tassy P, Valentini X, Vignaud P, Viriot L, Zazzo A, Zollikofer C (2002) A new hominid from the Upper Miocene of Chad, Central Africa. *Nature* 418:145–151

Bruno M, Lazzarini L (1995) Discovery of the sienese provenance of brecci dorata and breccia giallo fibrosa, and the origin of breccia rossa appennica. *Archeomateriaux: Mabres et autres roches. Actes de la IV^e Conference internationale, ASMOSIA IV. CRPAA. Pub. Press Univeritaires Bordeaux*

Bruins HJ, MacGillivray JA, Synolakis CE, Benjamini C, Keller J, Kisch HJ, Klügel A, Van Der Plicht J (2008) Geoarchaeological tsunami deposits at Palaikastro (Crete) and the Late Minoan IA eruption of Santorini. *J Archaeol Sci* 35(1):191–212

Bruins HJ, MacGillivray JA, Synolakis CE, Benjamini C, Keller J, Kisch HJ, Klügel A, Van Der Plicht J (2008) Geoarchaeological tsunami deposits at Palaikastro (Crete) and the Late Minoan IA eruption of Santorini. *J Archaeol Sci* 35(1):191–212

Bryant VM Jr (1974) The role of coprolyte analysis in archaeology. *Bull Tex Archaeol Soc* 45:1–28

Bryant VM Jr (1978) Palynology: a useful method for determining paleoenvironmental. *Tex J Sci* 30:25–42

Bryant VM Jr (1989) Pollen: nature's fingerprints of plants. In: 1990 yearbook of science and the future. *Encyclopedia Britannica*, Chicago

Bryant VM Jr, Holloway RG (1983) The role of palynology in archaeology. In: Schiffer MB (ed) *Advances in archaeological method and theory*. Academic, New York, pp 191–223

Bryson RA (1988) What the climatic past tells us about the environmental future. *Earth* 88:230–247

Buckland PC, Panagiotakopulu E (2001) Archaeology and the palaeoecology of the Norse Atlantic Islands: A review. In: *Viking and Norse in the North Atlantic, Annales Societatis Scientiarum Feroensis, Supplementum 44: proceedings of the 14th Viking Congress*, Tórshavn, pp 167–181

Bunn RA, Magelky RD, Ryan JN, Elimelech M (2002) Mobilization of natural colloids from an iron oxide-coated sand aquifer: effect of pH and ionic strength. *Environ Sci Technol* 36(3):314–322

Buchdahl G (1951) Induction and scientific method. *Mind N Series* 60(237):16–34

Buck CE, Millard AR (eds) (2004) *Tools for constructing chronologies: crossing disciplinary boundaries*, vol 177, *Lecture Notes in Statistics*. Springer, London

Buckland PC, Perry DW (1989) Ectoparasites of sheep from Storaborg, Iceland and their interpretation piss, parasites and people, a pateoecological perspective. *Hikuin* 15:37–46

Buckland PC, Panagiotakopulu E (2005) Archaeology and the palaeoecology of the North Atlantic islands: a review. In: Mortensen A, Arge S (eds) *Viking and Norse in the North Atlantic: selected papers from the Proceedings of the 14th Viking Congress, Tórshavn, 19–30 July 2001*. The Faroese Academy of Sciences in collaboration with the Historical Museum of the Faroe Islands, Tórshavn, pp 1

Buckland PC, Sveinbjarnardóttir G, Savory D, McGovern TH, Skidmore P, Andreassen C (1983) Norsemen at Nipaitsqoq, Greenland. A palaeoecological investigation. *Nor Archaeol Rev* 16:86–98

Buckland PC, McGovern TH, Sadler JP, Skidmore P (1994) Twig layers, floors and middens. Recent palaeoecological research in the Western Settlement, Greenland. In: Ambrosiani B, Clarke H (eds) *Developments around the Baltic and the North Sea in the viking age (twelfth viking congress)*. Stockholm, 3:132–143

Buckland PC, Amorosi T, Barlow LK, Dugmore AJ, Mayewski PA, McGovern TH, Ogilvie AEJ, Sadler JP, Skidmore P (1996) Bioarchaeological and climatological evidence for the fate of Norse farmers in medieval Greenland. *Antiquity* 70(267):88–96

Buckland PC, Panagiotakopulu E, Buckland PI (2004) What's eating Halvdan the Black? Fossil insects and the study of a burial mound in its landscape context. In: Larsen JH, Rolsen P (eds) *Halvdanshaugen – Arkeologi, historie og naturvitenskap*. University Museum of Cultural Heritage 3, University of Oslo, pp 353–376

Buckland PC, Edwards KJ, Panagiotakopulu E, Schofield JE (2009) Palaeoecological and historical evidence for manuring and irrigation at Garðar (Igaliku), Norse Eastern Settlement, Greenland. *Holocene* 19 (1):105–116

Buckley DE, Mackinnon WG, Cranston RE, Christian HA (1994) Marine. *Geology* 117(1–4):95–106

Budd P, Gale D, Pollard AM, Thomas RG, Williams PA (1993) Evaluating lead isotope data: further observations. *Archaeometry* 35:241–263

Bukry D (1979) Comments on opal phytoliths and stratigraphy of Neogene silica-flagellates and coccoliths at Deep Sea Drilling Project Site 397 off northwest Africa. In: Shambach JD (ed) *Initial reports of the deep sea drilling project*, vol 49. U.S. Government Printing Office, Washington, DC, pp 977–1009

Buol SW, Hole FD (1961) Clay skin genesis in Wisconsin soils. *Soil Sci Soc Am J* 25(5):377–379

Burger HR (1992) *Exploration geophysics of the shallow subsurface*. Prentice Hall, Englewood Cliffs

Brunet M, Guy F, Pilbeam D, Mackaye HT, Likius A, Ahounta D, Beauvilain A, Blondel C, Bocherens H, Boissarie J-R, De Bonis L, Cottens Y, Dejax J, Denys C, Duringer P, Eisenmann V, Fanone G, Fronto P, Geraads D, Lehmann T, Lihoreau F, Louchart A, Mahamat A, Merceron G, Mouchelin G, Otero O, Pelaez Campomanes P, Ponce De Leon M, Rage J-C, Sapanet M, Schuster M, Sudre J, Tassy P, Valentin X, Vignaud P, Viriot L, Zazzo A, Zollikofer C (2002) A new hominid from the Upper Miocene of Chad, Central Africa. *Nature* 418:145–151

Busch RM (ed) (1996) *Laboratory manual in physical geology*, 4th edn. Prentice-Hall, Upper Saddle River

Bushnell TM (1943) Some aspects of the soil catena concept. *Soil Sci Soc Am J* 7:466–476

Butzer KW (1971) *Environment and archaeology*, 2nd edn. Aldine, Chicago

Butzer KW (1982) *Archaeology as human ecology*. Cambridge University Press, Cambridge

Butzer K (2008) Challenges for a cross-disciplinary geoarchaeology: the intersection between environmental history and geomorphology. *Geomorphology* 101(1–2):402–411

Caldwell AC (1965) Sulfur in plant materials by digestion with nitric and perchloric acid. *Soil Sci Soc Am Proc* 29:71–72

Camuto C (2004a) Air. In: Dallmeyer D (ed) *Elemental south*. The University of Georgia Press, Athens

Camuto C (2004b) Fire in the path. In: Dallmeyer D (ed) *Elemental south*. The University of Georgia Press, Athens

Cannon MD (2001) Archaeological relative abundance, sample size and statistical methods. *J Archaeol Sci* 28:185–195

Carey C (1999) Secrets of the sacrificed. *Discov Archaeol* 1(4):46–53

Carlooy JC (1971) An interpretation of scientific models involving analogies. *Philos Sci* 38:562–569

Carlson RL, Miller DJA (2005) Unraveling the structure and composition of the oceanic crust. *Sea Technol* 46 (10):10–13

Carr C (1984) The nature of organization of intrasite archaeological records and spatial analytic approaches to their investigation. *Adv Archaeol Method Theory* 7:103–222

Carr C (1990) Advances in ceramic radiography and analysis: applications and potentials. *J Archaeol Sci* 17(1):13–34

Carr Donald D, Herz N (1989) *Concise encyclopedia of mineral resources*, *Advances in materials science and engineering*. MIT Press, Cambridge, MA

Carr TL, Turner MD (1996) Investigating regional lithic procurement using multi-spectral imagery and geophysical prospection. *Archaeol Prospect* 3:109–127

Carter DL, Berg RD, Sanders BJ (1985) The effect of furrow irrigation erosion on crop productivity. *Soil Sci Soc Am J* 49(1):207–211

Carver RE (ed) (1971) *Procedures in sedimentary geology*. Wiley-Interscience, New York

Casali F (2006) X-ray and neutron digital radiography and computed tomography for cultural heritage. *Phys Tech Study Art Archaeol Cult Herit* 1:41–123

Castella D (1998) Aux Portes d'Aventicum: Dix ans d'archéologie autoroute à Avenches. *Documents du Musée d'Avenches*, 4

Caton-Thompson G, Gardner EW (1931) *The desert Fayum*. The Royal Anthropological Institute of Great Britain and Ireland, London

Caton-Thompson G, Gardner EW (1934) *The desert Fayum*, vol 1. Royal Anthropological Institute of Great Britain and Ireland, London

Catt JA, Weir AH (1976) The study of archaeologically important sediments by petrographic techniques. In: Davidson DA, Shackley MC (eds) *Geoarchaeology*. Westview Press, Boulder

Cavanagh WG, Hirst S, Litton CD (1988) Soil phosphate, site boundaries and change point analysis. *J Field Archaeol* 15:67–83

Cerling TE, Hay RL (1986) An isotopic study of paleosol carbonates from Olduvai Gorge. *Quatern Res* 25:63–78

Chad S (2014) Sahara, last lakes of green. *Saudi Aramco World* 65(3):12–27

Champion T, Gamble C, Shennan S, Whittle A (1984) *Prehistoric Europe*. Academic, London

Charters S, Evershed RP, Goad LJ, Leyden A, Blinkhorn PW, Denham V (1993) Quantification and distribution of lipid in archaeological ceramics: implications for sampling potsherds for organic residue analysis and the classification of vessel use. *Archaeometry* 35 (2):211–223

Chase AF, Chase DZ, Weishampel JF, Drake JB, Shrestha RL, Slatton KC, Awe JJ, Carter WE (2011) Airborne LiDAR, archaeology, and the ancient Maya landscape at Caracol, Belize. *J Archaeol Sci* 38(2):387–398

Chase PG, Debénath A, Dibble HL, McPherron SP (2009) The cave of Fontéchevade: recent excavations and their paleoanthropological implications. Cambridge University Press, New York

Chayes F (1954) The theory of thin-section analysis. *J Geol* 62:92–101

Chayes F (1956) Petrographic modal analysis. Wiley, New York

Chase PG, Debénath A, Dibble HL, McPherron SP (2009) The cave of Fontéchevade: recent excavations and their paleoanthropological implications. Cambridge University Press, New York, 270 pp

Cherry J (1988) Island origins. In: Cunliffe B (ed) *Origins*. The Dorsey Press, Chicago

Chevallier P, Legrand F, Gruel K, Brissaud I, Tarrats-Saunac A (1993) Étude par rayonnement synchrotron de moules à alvéoles de la Tène finale trouvés à Villeneuve-St-Germain et au Mont-Beuvray. *Revue d'archéométrie* 17:75–88

Childe VG (1951) *Man makes himself*. New American Library, New York

Childe VG (1948) *Man makes himself*. Watts & Co, London

Childs ST (1991) Transformations: iron and copper production in Central Africa. In: Recent trends in archaeometallurgical research. Smithsonian, pp 33–46

Chowns TM, Schultz BS, Griffin JR, Crook MR Jr (2008) Relocation of Brunswick river and other estuaries on the Georgia, USA coast as a consequence of Holocene transgression. *Southeast Geol* 45(3):143–159

Ciliberto E, Spoto G (2000) *Modern analytical methods in art and archaeology*. Wiley, New York

Clark AJ (1990) *Seeing beneath the soil*. B.T. Batsford Ltd, London

Clark OA (2003) *Seeing beneath the soil: prospecting methods in archaeology*. Routledge, London

Clarke DL (1968) *Analytical archaeology*. Methuen, London

Clarke GR, Beckett P (1971) *The study of soil in the field*. Oxford University Press, Oxford

Clottes J (2001) *La Grotte Chauvet – L'Art des Origines*. Editions de Sevil, Paris

Clottes J, Courtin J (1996) The cave beneath the sea: paleolithic images at cosquer. H. N. Abrams, New York

Coles BJ (1998) Doggerland: a speculative survey. *Proc Prehist Soc* 64:45–81

Coles BJ (2000) Doggerland: the cultural dynamics of a shifting coastline. In: Pye K, Allen JRL (eds) *Coastal and estuarine environments: sedimentology, geomorphology and geoarchaeology*, vol 175, Geological Society, London, Special Publications. The Geological Society of London, London, pp 393–401

Collinson JD (1996) Alluvial sediment. In: Reading HG (ed) *Sedimentary environments: processes, facies and stratigraphy*, 3rd edn. Blackwell Science, Oxford, pp 37–82

Collon P, Wiescher M (2012) Accelerated ion beams for art forensics. *Phys Today* 65(1):58–59

Colomban P, Sagon G, Huy LQ, Liem NQ, Mazerolles L (2004) Vietnamese (15th century) blue-and-white, *Tam Thai* lustre porcelain/stonewares: glaze composition and decoration techniques. *Archaeometry* 46 (1):125–136

Comer DC (1998) Discovering archeological sites from space. *CRM* 5:9–11

Comer DC (1998) CRM discovering archeological sites from space. *CRM Bulletin* 5:9–11

Comer DC, Harrower MJ (2013) *Mapping archaeological landscapes from space*, vol 5. Springer, New York

Compton RR (1962) Manual of field geology. *Soil Sci* 93 (4):295

Conklin AR (2013) *Introduction to soil chemistry: analysis and instrumentation*. Wiley, New York

Conroy GC, Pontzer H (2012) Reconstructing human origins: a modern synthesis, 3rd edn. Norton, New York

Conte DJ, Thompson DJ, Moses LL (1997) *Earth science: an integrated perspective*, 2nd edn. Wm. C. Brown, Dubuque

Conyers LB, Goodman D (1997) *Ground-penetrating radar. An introduction for archaeologist*. AltaMira Press, Walnut Creek

Conyers LB (2012) *Interpreting ground-penetrating radar for archaeology*. Left Coast Press, Walnut Creek

Conyers LB (2013) *Ground-penetrating radar for archaeology*, 3rd edn. Altamira Press, Lanham

Corboud P (2004) Une plongée dans l'histoire la recherché: la découverte des sites littoraux préhistoriques lémaniques. *Archéologie Suisse* 27 (4):22–29

Corti ECC (1951) *The destruction of Pompeii and Herculaneum*. Routledge and Kegan, London

Cortegoso V (2005) Mid-Holocene hunters in the Andes Mountains: environment, resources and technological strategies. *Quat Int* 132(1):71–80

Courty M-A (1992) Soil micromorphology in archaeology. *Proc Br Acad* 77:39–59, Oxford University Press. London

Courty MA, Roux V (1995) Identification of wheel throwing on the basis of ceramic surface features and microfabrics. *J Archaeol Sci* 22:17–50

Courty MA, Roux V (1995) Identification of wheel throwing on the basis of ceramic surface features and microfabrics. *J Archaeol Sci* 22(1):17–50

Courty M-A, Goldberg PA, Macphail RI (1989) *Soil and micromorphology in archaeology*. Cambridge University Press, Cambridge

Courty MA, Goldberg P, Macphail R (1990) Soils and micromorphology in archaeology. *Soil Sci* 150(6):904

Cowgill GL (1964) The selection of samples from large sherd collections. *Am Antiq* 29(4):467–473

Craddock PT (1980) The composition of copper produced at the ancient smelting camps in the Wadi Timna, Israel.

In: Craddock PT (ed.) *Scientific studies in early mining and extractive metallurgy*. British Museum Research Laboratory, British Museum Press. London, 165 ff

Craddock PT (2001) From hearth to furnace: evidences for the earliest smelting technologies in the eastern Mediterranean. *Paléorient* 26:151–165

Craddock PT, Cowell MR, Leese MN, Houghes MJ (1983) The trace element composition of polished flint axes as an indicator of source. *Archaeometry* 25:135–163

Craddock P, Gurney D, Pryor F, Hughes M (1985) The application of phosphate analysis to the location and interpretation of archaeological sites. *Archaeol J* 142:361–376

Craig OE, Saul H, Lucquin A, Nishida Y, Taché K, Clarke L, Thompson A, Altoft DT, Uchiyama J, Ajimoto M, Gibbs K, Isaksson S, Heron CP, Jordan P (2013) Earliest evidence for the use of pottery. *Nature* 496:351–354

Cremeens DL, Hart JP (1995) On chronostratigraphy, pedostratigraphy, and archaeological context. Pedological perspectives in archaeological research, vol 44, SSSA Special Publication. Soil Science Society of America, Madison

Cunliffe B (1988) Aegean civilization and barbarian Europe. In: Cunliffe B (ed) *Origins*. The Dorsey Press, Chicago

d'Entrecolles FX (1743) Letters to Pere Orry. In: *Lettres edifiantes et curieuses écrites des missions étrangères par quelques missionnaires de la compagnie de Jésus*, Paris. [English translation by and in Tichane, 1983]

Dalan RA, Musser JM Jr, Stein JK (1992) Geophysical exploration of the shell midden. In: Stein JK (ed) *Deciphering a shell midden*. Academic, San Diego

Dalmeri G, Bassetti M, Cusinato A, Kompatscher K, Kompatscher MH (2005) The discovery of a painted anthropomorphic figure at Riparo Dalmeri and new insights into alpine Epigravettian art. *Preistoria Alpina* 41:163–169

Daniel G (1967) *The origins and growth of archaeology*. Penguin Books, Baltimore

Dart R (1957) The osteodontokeratic culture of *Australopithecus prometheus*. *Transvaal Museum Memoirs*, no. 10. Pretoria

Darwin C (1881) *The formation of vegetable mould. Through the action of worms, with observation on their habits*. J. Murray, London, 326 pp. (facsimiles republished in 1982 and 1985 by U. of Chicago Press, Chicago)

Davidson DA, Shackley ML (eds) (1976) *Geoarchaeology*. Westview Press, Boulder

Davis WM (1899) The geographical cycle. *Geogr J* 14:481–504

Davis M (1969) Palynology and environmental history during the quaternary period. *Am Sci* 57(3):317–322

Davis JC (1986) *Statistics and data analysis in geology*. Wiley, New York

Davis LG (2006) Geoarchaeological insights from Indian Sands, a Late Pleistocene Site on the Southern Northwest Coast, USA. *Geoarchaeology* 21(4):351–361

Day PR (1965) Particle fractionation and particle size analysis. In: Black CA et al (eds) *Methods of soils analysis, part I. Agronomy* 9:545–567

Day PM, Quinn PS, Rutter JB, Kilikoglou V (2011) A world of goods: transport jars and commodity exchange at the late bronze age harbor of Kommos, Crete. *Hesperia* 80(4):511–558

de Boris L, Melentis J (1991) *Age et position phyletique du Crâne de Petralona (Grèce)*. Les Premiers Européens. Editions du C.T.H.S, Paris

de Bruin M, Korthoven TJM, van der Steen AJ, Huitman JPW, Duin RPW (1976) The use of trace element concentrations in the identification of objects. *Archaeometry* 18:75–83

de Lumley H (1969) A paleolithic camp at Nice. *Sci Am* 220(5):42–50

de Lumley H (2006) Il y a 400,000 ans: la domestication du feu, un formidable moteur d'hominisation. *Comptes Rendus Palévol* 5(1–2):149–154. doi:10.1016/j.crpv.2005.11.014

Del Monte M, Ausset P, Lefevre RA (1998) Traces of ancient colors on Trajan's Column. *Archaeometry* 40 (2):403–412

DeMenocal PB (1995) Plio-Pleistocene African climate. *Science* 270(5233):53–59

DeMenocal P, Ortiz J, Guilderson T, Adkins J, Sarnthein M, Baker L, Yarusinsky M (2000) Abrupt onset and termination of the African humid period: rapid climate responses to gradual insolation forcing. *Quat Sci Rev* 19:347–361

Deocampo DM, Ashley GM (1999) Siliceous islands in a carbonate sea: modern and Pleistocene spring-fed wetlands in Ngorongoro Crater and Olduvai Gorge, Tanzania. *J Sediment Res* 69:1147–1151

Deocampo DM, Blumenshine RJ, Ashley GM (2002) Wetland diagenesis and traces of early hominids, Olduvai Gorge, Tanzania. *Quatern Res* 57(2):271–281

Descantes C, Neff H, Glasscock MD, Dickinson WR (2001) Chemical characterization of Micronesian ceramics through instrumental neutron activation analysis. A preliminary provenance study. *J Archaeol Sci* 28:1185–1190

Desor M (1873) Sur les haches en néphrite et en jadeite. In: Muquardt C (ed) *Congrès International d' Anthropologie et d' Archéologie Préhistoriques*, 6e session, Bruxelles, 1872, pp 351–359

Dibble HL, McPherron SJ, Chase P, Farrand WR, Debénath A (2006) Taphonomy and the concept of Paleolithic cultures: the case of the Tayacian from Fontéchevade. *PaleoAnthropology*:1–21

Dibble HL, McPherron SP, Sandgathe D, Goldberg P, Turq A, Lenoir M (2009a) Context, curation, and bias: an evaluation of the Middle Paleolithic collections of Combe-Grenal (France). *J Archaeol Sci* 36(11):2540–2550

Dibble HL, Berna F, Goldberg P, McPherron SP, Mentzer S, Niven L, Turq A (2009b) A preliminary report on Pech de l'Azé IV, layer 8 (Middle Paleolithic, France). *PaleoAnthropology* 2009:182–219

Dibner B (1958) *Agricola on metals*. Burndy Library, Norwalk

Diederichs S, Ortman SG, Schleher KL, Varien MD (2013) The neolithic revolution in the pueblo world: new evidence from the basketmaker III period in Southwestern Colorado. Presented at the 78th Annual Meeting of the Society for American Archaeology, Honolulu

Digby A (1948) Radiographic examination of Peruvian pottery techniques. *Actes du XXVIII Congrès International des Américainistes*, Paris

Dixon TN (2004) The crannogs of Scotland: an underwater archaeology. Tempus Publications Limited, Stroud

Dixon EJ (1979) A predictive model for the distribution of archaeological sites on the Bering continental shelf. Unpublished PhD dissertation, Department of Anthropology, Brown University

Dixon EJ (1983) Pleistocene proboscidean fossils from the Alaskan continental shelf. *Quatern Res* 20(1):113–119

Dixon EJ (2013) Late Pleistocene colonization of north America from northeast Asia: new insights from large-scale paleogeographic reconstructions. *Quat Int* 285:57–67

Dokuchaev VV (1899) On the theory of natural zones, vol 6, *Sochineniya* (Collected Works). Academy Sciences of the USSR, Moscow

Dort W Jr (1978) Geologic basis for assignment of >18,000 year age to cultural material at the Shriner site, Daviss County, Northwestern Missouri. Abstracts. Geological Society of America Annual Meeting

Douglas MC (2000) An electron microprobe study of 19th century staffordshire glazes and pigments including those of the spode pottery works. Unpublished Masters thesis. University of Georgia, Athens

Drennan RD (1996) Statistics for archaeologists. Plenum, New York

Driese SG, Schultz BS, McKay LD (2011) Genesis of clay-rich soils from carbonate bedrock on upland surfaces in the valley and ridge province, eastern Tennessee, USA. *Southeast Geol* 48(1):1–22

Dubessy J, Caumon M-C, Rull F (2012) Raman spectroscopy applied to earth sciences and cultural heritage. EMU notes in mineralogy, vol 12. European Mineralogical Union, Jena

Dugmore AJ, Keller C, McGovern TH (2007) Norse Greenland settlement: reflections on climate change, trade, and the contrasting fates of human settlements in the North Atlantic islands. *Arctic Anthropol* 44 (1):12–36

Dunbar JS, Webb SD, Faught M, Anuskiewicz RJ, Stright MJ (1989) Archaeological sites in the drowned tertiary karst region of the Eastern Gulf of Mexico. In: Underwater Archaeology Proceedings from the Society for Historical Archaeology Conference, Baltimore

Dunnell RC (1971) Systematics in prehistory. Free Press, New York, 214 pp

Dunnell RC (1988) Formation of the archaeological record and the notion site. Paper presented at the 53rd Annual Meeting of the Society for American Archaeology, Phoenix

Dunnell RC, Stein JK (1988) Theoretical issues in the interpretations of microartifact. *Geoarchaeology* 4 (1):31–42

Dunnell RC, Stein JK (1989) Theroretical issues in the interpretation of microartifacts. *Geoarchaeology* 4 (4):31–42

Dunnell RC, McCutcheon PT, Ikeya M, Toyoda S (1994) Heat treatment of Mill Creek and Dover cherts on the Malden Plain, southeast Missouri. *J Archaeol Sci* 21 (1):79–89

Durman A (1988) The Vučedol culture. In: Durman A (ed) *Vučedol -three thousand years B.C.* Muzejski pros-tor, Zagreb, pp 45–48

Durman A (1997) Tin in Southeastern Europe? *Opuscula Archaeologica Radovi Arheološkog zavoda* 21(1):7–14

Durman A (2004) Vučedolski hromi bog: zašto svi metalurški bogovi šepaju? (The lame God of Vučedol: why do all gods of metallurgy limp?). *Gradski muzej Vukovar*

Durman A (ed) (2007) One hundred Croatian archeological sites. (Zagreb: Leksikografski Zavod Miroslav Krleža, in collaboration with the Croatian Archaeological Society, 367 pp

Dye TD (2004) Bayesian statistics for archaeologists. T. S. Dye & Colleagues, Archaeologists, Honolulu

Earth Observing System (EOS) (1987) HIRIS, high resolution imaging spectrometer: science opportunities in the 1990s, vol IIC. National Aeronautical and Space Administration, Washington, DC

Easterbrook DS (1998) Surface processes and landforms. Macmillan, New York

Easterbrook DJ, Kovanen DJ (1999) Early holocene glaciation of the North Cascades near Mt. Baker, Washington. *Geol Soc Am Abstr Prog* 31(7):367

Edgerton FN (1962) The scientific contributions of François Alphonse Forel, the founder of limnology. *Schweizerische Zeitschrift für Hydrologie* 24(2): 181–199

Edgerton H (1986) Sonar images. Prentice Hall, Englewood Cliffs

Edginton DN, Robbins JA (1991) Standard operating procedure for collection of sediment samples. Great Lakes Water Institute. University of Wisconsin, Milwaukee

Ehrenberg CG (1854) *Mikrogeologie*. Leopold Voss, Leipzig

Ehrenreich RM (ed) (1991) Metals in society: theory beyond analysis. MASCA Research Papers in Science and Archaeology, 8(II). 92 pp

Edit RC (1973) A rapid chemical test for archaeological site surveying. *Am Antiq* 38:206–210

Edit RC (1977) Detection and examination of anthrosols by phosphate analysis. *Science* 197:1327–1333

Edit RC (1985) Theoretical and practical considerations in the analysis of anthrosols. In: Rapp G Jr, Gifford JA

(eds) Archaeological geology. Yale University Press, New Haven, pp 155–190

Eidt RC, Woods WI (1974) Abandoned settlement analysis: theory and practice. Field Test Associates, Shorewood

Eighmy JL, Sternberg RS (eds) (1990) Archaeomagnetic dating. University of Arizona Press, Tucson

El-Gammil MM, El-Mahmondi AS, Osman SS, Hassareem AG, Metwaly MA (1999) Geoelectric resistance scanning on parts of Abydos cemetery region, Sohag Governorate, Upper Egypt. *Archaeol Prospect* 6:225–239

Ellwood BB, Harrold FB, Marks AE (1994) Site identification and correlation using geoarchaeological methods at the CabeHo do Porto Marinlo (CPM) locality Rio Maior. Portugal. *J Archaeol Sci* 21(6):779–784

Ellwood BB, Peter DE, Balsam W, Schieber J (1995) Magnetic and geochemical variations as indicators of paleoclimate and archaeological site evolution: examples from 41 TR68, Fort Worth, Texas. *J Archaeol Sci* 22(3):409–415

Emerson T, Farnsworth K, Wisseman S, Hughes R (2013) The allure of the exotic: reexamining the use of local and distant pipestone quarries in Ohio Hopewell Pipe Caches. *Am Antiqu* 78(1):48–67

Emery D (1996) Carbonate systems. In: Emery D, Myers K (eds) Sequence stratigraphy. Blackwell Science Ltd, Victoria, pp 211–237

Emery WB (1961) Archaic Egypt. Pelican Books, Baltimore

Emery D, Myers K (eds) (2009) Sequence stratigraphy. Wiley, Malden

Engel BA (1996) Methodologies for development of hydrologic response units based on terrain, land cover and soils data. GIS and environmental modeling, pp 123–128

Epstein SM (1993) Cultural choice and technological consequences: constraint of innovation in the late prehistoric copper smelting industry of Cerro Huarina, Peru. Ph.D. Thesis. University of Pennsylvania

Erlanson JM, Tveskov MA, Byram RS (1998) The development of maritime adaptations on the southern northwest coast of north America. *Arctic Archaeol* 35 (1):6–22

Erlanson JM, Torben CR, Todd JB, Casperson M, Culleton B, Fulfrost B, Garcia T, Guthrie DA, Jew N, Kennett DJ, Moss ML, Reeder L, Skinner C, Watts J, Willis L (2011) Paleoindian seafaring, maritime technologies, and coastal foraging on California's channel islands. *Science* 331 (6021):1181–1185

Evans IS (1972) General geomorphometry, derivatives of altitudes and descriptive statistics. In: Chorley RJ (ed) Spatial analysis in geomorphology. Harper and row, New York, pp 17–90

Evidence for coastal adaptations in Georgia and South Carolina (1988) *Archaeol Eastern N Am* 16:137–158

Evershed RP (1990) Preliminary report of the analysis of lipids from samples of skin from seven Dutch bog bodies. *Archaeometry* 32(2):139–153

Evershed RP (2008) Organic residue analysis in archaeology: the archaeological biomarker revolution. *Archaeometry* 50:895–924

Evershed RP, Heron C, Charters S, Goad LJ (1992) The survival of food residues: new methods of analysis, interpretation and application. In: Pollard AM (ed) New developments in archaeological science: a joint symposium of the Royal Society and the British Academy, February 1991, pp 187–208. Proceedings of the British Academy 77. Oxford University Press, Oxford. *Archaeometry* 34(2): 253–265

Evershed RP, Mottram HR, Dudd SN, Charters S, Stott AW, Lawrence GJ, Gibson AM, Conner A, Blinkhorn PW, Reeves V (1997) New criteria for the identification of animal fats preserved in archaeological pottery. *Naturwissenschaften* 84(9):402–406

Fadem CM, Perryman CR, Hauser EM, Birkel JF (2014) Geoarchaeology and the basketmaker communities project: preliminary results. Geological Society of America Annual Meeting, Vancouver, British Columbia (19–22 Oct 2014)

Faegri K, Iverson J (1975) Textbook of pollen analysis, 3rd edn. Hafner Publishing, New York

Fagan BM (1994) Quest for the past, 2nd edn. Waveland Press, Prospect Heights

Fagan BM (1999) Archaeology: theories, methods and practice. Thames and Hudson, London

FAO (1988) FAG/Unesco soil map of the world, revised legend, with corrections and updates. World Soil Resources Report 60, FAO, Rome. Reprinted with updates as Technical Paper 20, ISRIC, Wageningen

Farrand WR (1975) The analysis of quaternary cave sediments. *World Archaeol* 10:290–301

Faught MK (2004a) Submerged Paleoindian and Archaic Sites of the Big Bend, Florida. *J Field Archaeol* 29 (3/4):273–290

Faught MK (2004b) The underwater archaeology of paleolandscapes, Apalachee Bay, Florida. *Am Antiq* 69(2):275–289

Faught MK (2008) Archaeological roots of human diversity in the new world: a compilation of accurate and precise radiocarbon ages from earliest sites. *Am Antiq* 73(4):670–698

Faught MK, Donoghue JF (1997) Marine inundated archaeological sites and paleofluvial systems: examples from a karst-controlled continental shelf setting in Apalachee Bay. *Geoarchaeology* 12 (5):417–458

Faught MK, Gusick AE (2011) Submerged prehistory in the Americas. In: Benjamin J, Bonsall C, Pickard C, Fischer A (eds) Submerged prehistory. Oxbow, Oxford, pp 145–157

Faure G (1986) Principles of isotope geology. Wiley, New York

Feathers JF (1989) Effects of temper on strength of ceramics: response to Broniksky and Hamer. *Am Antiq* 54:579–588

Fedje DW, Josenhans H (2000) Drowned forests and archaeology on the continental shelf of British Columbia, Canada. *Geology* 28(2):99–102

Ferguson BK (1997) Flood and sediment interpretation at the historic Scull Shoals Mill. In: Proceedings of the 1997 Georgia Water Resources Conference, March, pp 20–22

Ferguson BK (1999) The alluvial history and environmental legacy of the abandoned Scull Shoals mill. *Landsc J* 18(2):147–156

Ferguson J (2014) Munsell notations and color names: recommendations for archaeological practice. *J Field Archaeol* 39(4):327–335, <http://dx.doi.org.proxy-remote.galib.uga.edu/10.1179/0093469014Z.00000000097>

Fernández-Hernandez J, González-Aguilera D, Rodríguez-Gonzálvez P, Mancera-Taboada J (2015) Image based modelling from Unmanned Aerial Vehicle (UAV) photogrammetry: an effective, low-cost tool for archaeological applications. *Archaeometry* 57(1):128–145

Ferring CR, Perttula TK (1987) Defining the provenience of red-slipped pottery from Texas and Oklahoma by petrographic methods. *J Archaeol Sci* 14:437–456

Fiedel SJ, Sounthor JR, Brown TA (1995) The GISP ice core record of volcanism since 7000 B.C. *Science* 267:256–258

Finley JB, Kornfeld M, Andrews BN, Frison GC, Finley CC, Bies MT (2005) Rockshelter archaeology and geoarchaeology in the Bighorn Mountains, Wyoming. *Plains Anthropol* 50(195):227–248

Fischer A (2011) Stone age on the continental shelf: an eroding resource. In: Benjamin J, Bonsall C, Pickard C, Fischer A (eds) *Submerged prehistory*. Oxbox Books, Oxford, pp 298–310

Fitch S, Thomson K, Gaffney V (2005) Late Pleistocene and Holocene depositional systems and the palaeogeography of the Dogger Bank, North Sea. *Quatern Res* 64(2):185–196

Fitch S, Gaffney V, Thomson K (2007) In sight of Doggerland: from speculative survey to landscape exploration. *Internet Archaeol* 22:1–20

Fladmark KR (1970) Preliminary report on the archaeology of the Queen Charlotte Islands. *BC Stud Br C Q* 6 (7):18–45

Fladmark KR (1979) Routes: alternative migration corridors for early man in North America. *Am Antiq* 44:183–194

Fladmark KR (1982) Microdebitage analysis: initial considerations. *J Archaeol Sci* 9(2):205–222

Flam FD (2014) The odds, continually updated. *The New York Times, Science Times*, 9-30-2014: D1–D2

Flatman JC, Evans AM (2014) Prehistoric archaeology of the continental shelf: the state of the science in 2013. In: Evans AM, Flatman JC, Flemming NC (eds) *Prehistoric archaeology of the continental shelf: a global review*. Springer, New York, pp 1–12

Flenniken JJ, Garrison EG (1975) Thermally altered novaculite and stone tool manufacturing techniques. *J Field Archaeol* 2:125–131

Florsch N, Llubes M, Téreygeol F, Ghorbani A, Roblet P (2011) Quantification of slag heap volumes and masses through the use of induced polarization: application to the Castel-Minier site. *J Archaeol Sci* 38:438–451

Flygel E (1982) Microfacies analysis of limestones. Springer, Berlin

Folk RL (1948) The distinction between grain size and mineral composition in sedimentary-rock nomenclature. *J Geol* 62(4):344–359

Folk RL (1968) Petrology of sedimentary rocks. Hemphill, Austin

Folk RL (1980) Petrology of sedimentary rocks. Hemphill Publishing Company Forenbaher, Stašo. 1993. The late copper age architecture at Vučedol, Croatia. *J Field Archaeol* 21(3):307–323

Follmer LR (1982) The geomorphology of the Sangamon surface: its spatial and temporal attributes. In: Thorn CE (ed) *Space and time in geomorphology*. Allen and Unwin, London, pp 117–146

Follmer LR (1985) Surficial geology and soils of the Rhoads archaeological site near Lincoln, Illinois. *Am Archaeol* 5(2):150–160

Fontana, F, Guerreschi A, Liagre J (2002) RiparoTagliente. La serie epigravettiana. In: Aspes A (ed) *La Preistoria Veronese. Contributi aggiornamenti. Memorie del Museo Civico di Storia Naturale di Verona*, 5, pp 42–47

Forbes RJ (1964) Metallurgy in antiquity: a notebook for archaeologists and technologists, vol 8. Brill Archive, Leiden

Ford WE (1918) The growth of mineralogy from 1818–1918. *Am J Sci* 46:240–254

Foulger GR, Panza GP, Artemieva IM, Bastow ID, Cammarano F, Doglioni C, Evans JR, Hamilton WB, Julian BR, Lustrino M, Thybo H, Yanovskaya TB (2015) What lies deep? *Eos* 96(17):10–15

Foust RD Jr, Ambler JR, Turner LD (1989) Trace element analysis of Pueblo II Kayenta Anasazi sherds. In: Allen RO (ed) *Archaeological chemistry*, vol IV. American Ceramic Society, Washington, DC, pp 125–144

Fowlkes EB, Gnanadesikan R, Kettenring JR (1988) Variable selection in clustering. *J Classif* 5:205–288

Frame LD (2009) Technological change in southwestern Asia: metallurgical production styles and social values during the chalcolithic and early bronze age. Ph.D. dissertation, University of Arizona

Frankel HR (2012) *The continental drift controversy*, vol I–IV. Cambridge University Press, Cambridge

Fredengren C (2002) *Crannogs: a study of people's interaction with lakes, with particular reference to Lough Gara in the north-west of Ireland*. Wordwell, Dublin

Freeman L (1968) A theoretical framework for interpreting archaeological materials. In: Lee RB, DeVore I (eds) *Man the hunter*. Aldine, Chicago, pp 262–267

Freestone IC, Middleton AP (1987) Mineralogical applications of the analytical SEM in archaeology. *Mineral Mag* 51:21–31

Fry WH (1933) Petrographic methods for soil laboratories. US Department of Agriculture, Washington, DC

Gaffney C (2008) Detecting trends in the prediction of the buried past: a review of geophysical techniques in archaeology. *Archaeometry* 50(2):313–336

Gaffney VL, Thomson K, Fitch S (2007) Mapping Doggerland: the Mesolithic landscapes of the southern North Sea. Archaeopress, Oxford

Gagliano SM, Pearson CE, Weinstein RA, Wiseman DE, McClendon CE (1982) Sedimentary studies of prehistoric archaeological sites. Coastal Environments, Baton Rouge

Galehouse JS (1971) Point counting. In: Carver R (ed) Procedures in sedimentary petrology. Wiley Interscience, New York

Gall J-C (1983) Ancient sedimentary environments and the habitats of the living organisms: introduction to paleoecology. Springer, New York

Gall JC (2012) Ancient sedimentary environments and the habitats of living organisms: introduction to palaeoecology. Springer Science & Business Media

Garrels RM, Mackenzie FT (1971) Evolution of sedimentary rocks. W. W. Norton, New York

Garret EM (1986) A petrographic analysis of Black Mesa ceramics. In: Plog S (ed) Spatial organization and trade. Southern Illinois Press, Carbondale, pp 114–142

Garrison EG (1973) Alpha-recoils tracks for archaeological dating. Unpublished Master's Thesis. The University of Arkansas, Fayetteville

Garrison EG (1998) Radar prospection and cryoprobes – early results from Georgia. *Archaeol Prospect* 5:57–65

Garrison EG (1999) A history of engineering and technology, 2nd edn. CRC Press, Boca Raton

Garrison EG (2001) Physics and archaeology. *Phys Today* 54:32–36

Garrison EG, Rowlett R, McKown D (1977) Neutron activation analysis of coins and coin-molds of the Titelberg. Paper presented at the 1977 Archaeometry Symposium. University of Pennsylvania, Philadelphia

Garrison EG, McGimsey CR, Zinke OH (1978) Alpha-recoil tracks in archaeological ceramic dating. *Archaeometry* 20(1):39–46

Garrison EG, Cook Hale J, Holland JL, Kelley AR, Kelley JT, Lowery D, Merwin DE, Robinson DS, Schaefer CA, Thomas BW, Thomas LA, Watts GP (2012c) Prehistoric Site Potential and Historic Shipwrecks on the Atlantic Outer Continental Shelf. OCS Study, BOEM 2012-008. U.S. Department of the Interior, Bureau of Ocean Energy Management, Regulation and Enforcement, Atlantic OCS Region

Garrison E, Šerman N, Schneider K (2002) Geoarchaeological coring, using cryoprobe techniques: an example from the American Southeast. In: *Archaeometry* 98: Proceedings of the 31st Symposium, Budapest, April 26–May 3, 1998, vol 2. Archaeopress, p 119

Garrison EG, Reppert PA, Schneider KA (2005) Geoprospection of Mound A, Etowah Mounds State Park, Georgia. *EOS Trans Am Geophys Union* 86(1)

Garrison EG, McFall G, Noakes SE (2008) Shallow marine margin sediments, modern marine erosion and the fate of sequence boundaries Georgia Bight (USA). *Southeast Geol* 45(3):143–159

Garrison EG, Weaver W, Littman SL, Cook Hale J, Srivastava P (2012a) Late quaternary paleoecology and Heinrich events at Gray's reef national marine sanctuary, South Atlantic Bight, Georgia. *Southeast Geol* 48(4):165–184

Garrison EG, Cook Hale J, Holland JL, Kelley AR, Kelley JT, Lowery D, Merwin DE, Robinson DS, Schaefer CA, Thomas BW, Thomas LA, Watts GP (2012b) Prehistoric site potential and historic shipwrecks on the Atlantic outer continental shelf. OCS study, BOEM 2012-008. U.S. Department of the Interior, Bureau of Ocean Energy Management, Regulation and Enforcement, Atlantic OCS Region

Garrison EG, Anderson TA, Schneider KA (2013a) Shallow geophysical prospection in Fribourg, Switzerland: a ground radar survey of medieval and roman sites. In: Vermeulen F, Corsi C (eds) Non-destructive approaches to complex archaeological sites in Europe: a round-up. Radio-Past Colloquium, Ghent, pp 15–17

Garrison EG, Cook Hale J, Faught MK (2013b) Scientific diving in Coastal Georgia: 8000 year-old trees, prehistoric shell middens and sea level change. In: Proceedings of the 2013 AAUS/ESDP Curaçao Joint International Scientific Diving Symposium, 24–27 Oct 2013, Curaçao

Garrison EG, Anderson TA, Schneider KA (2014) Architectural inference from ground penetrating radar (GPR) surveys of an unexcavated Roman Country Villa, Châtillon-La Vuarda, Switzerland. Paper presented at the 79th Annual Meeting of the Society for American Archaeology, 23–27 Apr 2014, Austin

Gass IG (1968) Is the troodos massif of Cyprus a fragment of Mesozoic ocean floor? *Nature* 220:39–42

Gater J, Gaffney VL (2003) Revealing the buried past: geophysics for archaeologists. Tempus, Stroud

Gè T, Courty M-A, Matthews W, Wattez J (1993) Sedimentation foramtion processes of occupation surfaces. In: Goldberg P, Nash PT, Petraglia MD (eds) Formation processes in archaeological contexts, vol 17, Monographs in World Archaeology. Prehistory Press, Madison, pp 143–163

Gee GW, Bauder JW (1986) In: Klute A (ed) Methods of soil analysis, part I. Physical and mineralogical methods, 2nd edn. Soil Science Society of America, Madison

Gendron F, Smith DC, Gendron-Badou A (2002) Discovery of jadeite-jade in Guatemala confirmed by non-destructive Raman microscopy. *J Archaeol Sci* 29:837–851

Gerrard MC (1991) Sedimentary petrology and the archaeologist: the study of ancient ceramics. In: Developments in sedimentary provenance studies. In: Morton AC, Todd SP, Haughton DW (eds) Geological Society Special Publication 57, pp 189–197

Gibbard PL, Head MJ (2009) IUGS ratification of the quaternary system/period and the Pleistocene series/epoch with a base at 2.588 MA. *Quaternaire* 20 (4):411–412

Gibbons A (1991) A new look@ for archaeology. *Science* 252:918–920

Gifford-Gonzalez D (1989) Ethnographic analogues for interpreting modified bones: some cases from East Africa. In: Bone modification. Center for the Study of the First Americans, University of Marine, Orono, pp 179–246

Gifford-Gonzalez D (1991) Bones are not enough: analogues, knowledge, and interpretive strategies in zooarchaeology. *J Anthropol Archaeol* L:215–254

Gladfelter BG (1977) Geoarchaeology: the geomorphologist and archaeology. *Am Antiq* 42:512–538

Glasscock MD (1992) Characterization of archaeological ceramics by neutron activation analysis and multivariate statistics. In: Neff H (ed) Chemical characterization of ceramic pastes in archaeology, vol 7, Monographs in World Archaeology. Prehistory Press, Madison, pp 11–26

Glasscock MD, Neff H, Cogswell J, Herrera RS (1996) Neutron activation analysis for archaeological applications. Unpublished ms. Missouri University Research Reactor Archaeometry laboratory, Columbia

Glasscock MD, Speakman RJ, Popelka-Filcoff RS (eds) (2007a) Archaeological chemistry: analytical approaches and archaeological interpretation, ACS Symposium Series 969. American Chemical Society, Washington, DC

Glasscock M, Speakman RJ, Popelka-Filcoff RS (2007b) Archaeological chemistry: analytical techniques and archaeological interpretation, ACS Symposium Series 969. American Chemical Society, Washington, DC

Glasscock MD, Neff H, Stryker KS, Johnson TN (1994) Sourcing archaeological obsidian by abbreviated NAA procedure. *J Radioanal Nucl Chem Artic* 180:29–35

Glumac PD (1991) Recent trends in archaeometallurgical research. MASCA research papers in science and archaeology, vol 8(I). The University Museum, University of Pennsylvania, Philadelphia, p 92

Godfrey-Smith DI, Huntley DJ, Chen WH (1988) Optical dating of quartz and feldspar sediment extracts. *Quart Sci Rev* 7:373–380

Goffer Z (2006) Archaeological chemistry, 2nd edn, vol 170. Wiley

Goldberg PA (1995) Microstratigraphy, micromorphology site formation processes, soils. In: The practical impact of science on field archaeology: maintaining long-term analytical options. a workshop on cyprus, 22–23 July 1995. The Weiner Laboratory of the American School of Classical Studies, Athens

Goldberg P (1999) Late-terminal classic Maya pottery in northern Belize: a petrographic analysis of sherd samples from Colha and Kichpanha. *Iceland, HB. J Archaeol Sci* 26(8):951–966

Goldberg P, Bar-Yosef O (1998) Site formation processes in Kebara and Hayonim Caves and their significance in Levantine prehistoric caves. In: Akazawa T, Aoki K, Bar-Yosef O (eds) Neandertals and modern humans in Western Asia. Plenum, New York, pp 107–125

Goldberg P, Berna F (2010) Micromorphology and context. *Quat Int* 214(1):56–62

Goldberg P, MacPhail RI (2006) Practical and theoretical geoarchaeology. Blackwell Publishing, Malden

Goldberg P, Miller CE, Schiegl S, Ligouis B, Berna F, Conard NJ, Wadley L (2009) Bedding, hearths, and site maintenance in the Middle Stone age of Sibudu cave, KwaZulu-Natal, South Africa. *Archaeol Anthropol Sci* 1(2):95–122

Goldberg P, Sherwood SC (2006) Deciphering human prehistory through the geoarchaeological study of cave sediments. *Evol Anthropol* 15:20–36

Goldberg P, Weiner S, Bar-Yosef O, Xu Q, Liu J (2001) Site formation processes at Zhoukoudian, China. *J Hum Evol* 41(5):483–530

Goldschmidt VM (1912) Die kontaktmetamorphose im Kristianagebiet. *Geologiska Föreningen i Stockholm Förhandlingar* 34(7):812–819

González LR (2004) Bronces sin nombre: La metalurgia prehispánica en el Noroeste Argentino. TusQuets

Goodman D, Conyers LA (1998) Ground penetrating radar: an introduction for archaeologists. Altamira Publishing, Walnut Creek

Goodman D, Piro S (2013) GPR remote sensing in archaeology. Geotechnologies and the environment, no. 9. Springer Science, New York

Goodey AC, Steffy K (2003) Evidence of a Clovis occupation at the Topper site, 38AL23, Allendale County, South Carolina. *Curr Res Pleistocene* 20:23–25

Goffer Z (1980) Archaeological chemistry: a sourcebook on the applications of chemistry to archaeological. Wiley, New York

Goffer Z (2006) Archaeological chemistry, vol 170, 2nd edn. Wiley/Wiley-Interscience, New York

Goren Y (2014) The operation of a portable petrographic thin-section laboratory for field studies. New York Microscopical Society Newsletter

Goren Y, Bunimovitz S, Finkelstein I, Na'aman N (2003) The location of Alashiya: new evidence from petrographic investigation El-Amarna and Ugarit. *Am J Archaeol* 107:233–255

Göransson H (2002) Alvastra pile dwelling – a 5000-year-old byre? In: Viklund K (ed) Nordic Archaeobotany – NAG 2000 in Umeå Umeå, University of Umeå Environmental Archaeology Laboratory, Department of Archaeology & Sami Studies, 15, pp 67–84

Gorsuch R (1984) Factor analysis. L. Erlbaum Associates, Hillsdale

Gosselain OP (1992) The bonfire of enquiries? Pottery firing temperature in archaeology: what for? *J Archaeol Sci* 19:243–259

Goudie AS (2013) The human impact on the natural environment: past, present, and future. Wiley, Hoboken

Gould RA (1980) Living archaeology. Cambridge Univ Press, Cambridge

Gould RA, Watson PJ (1982) A dialogue on the meaning and use of analogy in ethnoarchaeological reasoning. *J Anthropol Archaeol* 1:335–381

Grattan J, Charman DJ (1994) Non-climatic factors and the environmental impact of volcanic volatiles: implications of the Laki Fissure eruption of AD 1783. *The Holocene* 4(1):101–106

Gratuze B, Goivagnoli A, Banadon JN, Telouk P, Imbert JL (1993) Aport de la méthode ICP-MS couplée à l’ablation laser pour la caractérisation des archéomatériaux. *Revue d’archéométrie* 17:89–104

Grebothé D, Lassau G, Ruckstuhl, Seifert M (1990) Thayngen SH-Weier: Trockeneisondierung 1989. *Jahrb Schweizerischen Ges Ur-und Frühgeschichte* 73:167–175

Green AJ (1981) Particle-size analysis. In: McKeague JA (ed) Manual on soil sampling and methods of analysis. Canadian Society of Soil Science, Ottawa, pp 4–29

Green RE, Krause J, Briggs AW, Maricic T, Stenzel U, Kircher M, Patterson N, Li H, Zhai W, Fritz MHY, Hansen NF (2010) A draft sequence of the Neandertal genome. *Science* 328(5979):710–722

Greenough JD, Dobosi G, Owen JV (1999) Fingerprinting ancient Egyptian quarries: preliminary results using laser ablation microprobe-inductively coupled plasma-mass spectroscopy. *Archaeometry* 41 (2):227–238

Griffiths GH, Barker RD (1994) Electrical imaging in archaeology. *J Archaeol Sci* 21:153–158

Grine FE, Klein RG, Volman TP (1991) Dating, archaeology, and human fossils from the Middle Stone Age Levels of Die Kelders, South Africa. *J Hum Evol* 21:363–395

Grob A (1896) Beiträge zur Anatomie der Epidermis der Gramineenblätter. *Biblioteca Bot* 36:1–63

Grøn O (2006) Does the future of investigations in Mesolithic and Neolithic peat bog settlements lie under water? *Notae Praehistoricae* 26:1–8

Grøn O (2007) The investigation of submerged stone age landscapes using diving as a research tool: an example from Denmark. *Underw Technol* 27(3):109–114

Grøn O, Skaarup J (2004) Submerged stone age coastal zones in Denmark: investigation strategies and results. *CBA Res Rep* 141:53–56, English Heritage/Council for British Archaeology. York

Gruhn R (1994) The pacific coast route of initial entry: an overview. In: Bonnichsen R, Steele DG (eds) Method and theory for investigating the peopling of the Americas. Centerfor the Study of the First Americans, Oregon State University, Corvallis, pp 249–256

Gruhn R (1998) Linguistic evidence in support of the coastal route of earliest entry in the New World. *Man* 23:77–100

GSA Today (2002) 2001 medals and awards. *Geol Soc Am* 12:21–22

Guilbert JM, Park CF (1986) The geology of ore deposits. W. H. Freeman, San Francisco

Guineau B, Lorblanchet M, Gratuze B, Dulin L, Roger P, Akrich R, Muller F (2001) Manganese black pigments in prehistoric paintings: the case of the black frieze of Pech Merle (France). *Archaeometry* 43:211–225

Gunderson JH (1987) Archeology of the high plains. Cultural resource series no. 19. Bureau of Land Management, Colorado State Office, Denver

Gvirtzman G, Weider M (2001) Climate of the last 53,000 years in the eastern Mediterranean, based on soil-sequence stratigraphy in the coastal plain of Isreal. *Quat Sci Rev* 20:1827–1849

Hach Company (1992) Hach water analysis handbook, 2nd edn. Hach Co., Loveland

Hadorn Ph (1994) Saint-Blaise/Bains des Dames, 1. Palynologie d’ un site néolithique et historic de la végétation der derniers 16,000 ans. Neuchâtel, Musé cantonal d’archéologie. Archeologie Neuchateloise, 18

Haflidason H, Eiriksson J, van Kreveld S (2000) The tephrochronology of Iceland and the north Atlantic region during the middle and late quaternary: a review. *J Quat Sci* 15:3–22

Hafner A (2012) Archaeological discoveries on Schnidejoch and at other ice sites in the European alps. *Arctic* 65(Suppl 1):189–202

Hampton RE (1994) Introductory biological statistics. Wm. C. Brown Publishers, Dubuque

Hancock R, Betancourt PP (1987) INAA of Minoan ceramics from Kommos, Crete. *J Radioanal Nucl Chem* 114:393–401

Hancock RGV, Millet NB, Mills AJ (1986) A rapid INAA method to characterize Egyptian ceramics. *J Archaeol Sci* 13(2):107–117

Hannibal JT, Evans KR (2010) Civil War and cultural geology of southwestern Missouri, part 1: the geology of Wilson’s creek battlefield and the history of stone quarrying and stone use. *Field Guides* 17:39–68, The Geological Society of America. Boulder, CO

Harbottle G (1976) Activation analysis in archaeology. *Radiochemistry* 3:33–72, The Chemical Society. London

Harris MS, Gayes PT, Kindinger JL, Flocks JG, Krantz DE, Donovan P (2005) Quaternary geomorphology and modern coastal development in response to an inherent geologic framework: an example from Charleston, South Carolina. *J Coastal Res* 21:49–64

Harris MS, Sautter LR, Johnson KL, Luciano KE, Sedberry GR, Wright EE, Siuda AN (2013) Continental shelf landscapes of the southeastern United States since the last interglacial. *Geomorphology* 203:6–24

Hart CJR, Mair JL, Goldfarb RJ, Groves DI (2005) Source and redox controls on metallogenetic variations in intrusion-related ore systems, Tombstone-Tungsten Belt, Yukon Territory. In: Ishihara S, Stephens WE, Harley SL, Arima M, Nakajima T (eds) Fifth Hutton symposium; the origin of granites and related rocks, vol 389, Special paper. Geological Society of America, Boulder, pp 339–356

Harvig L, Lynnerup N, Amsgaard Ebsen J (2011) Computed tomography and computed radiography of late bronze age cremation urns from Denmark: an interdisciplinary attempt to develop methods applied in bioarchaeological cremation research. *Archaeometry* 54(2):369–387

Hassan FA (1977) Field manual to Geoarchaeology. Manuscript

Hassan FA (1979) Geoarchaeology: the geologist and archaeology. *Am Antiqu* 2:267–270

Hassan FA (1988) Fluvial systems and geoarchaeology in arid lands with examples from north Africa, the Near East and the American Southwest. In: Stein JK, Farrand WR (eds) *Archaeological sediments in context*. Center for the Study of Man, Orono

Hassett MJ, Weiss M (1991) *Introductory statistics*. Addison-Wesley, New York

Hassett MJ, Weiss M (1993) *Introductory statistics*, 3rd edn. Addison-Wesley, New York

Hauptmann A, Weisgerber G, Bachmann H-G (1989) Ancient copper production in the area of Feinan, Khirbet En-Nahas and Wadi El-Jariye, Wadi Arabah, Jordan. In: Fleming S (ed) *History of technology: the role of metals*. University Museum, University of Pennsylvania, Philadelphia, pp 6–16

Hauptmann A, Weisgerber G, Knauf EA (1985) Archäolometallurgische Untersuchungen zur Kupferverhüttung der frühen Bronzezeit in Feinan, Wadi Arabah, Jordanien. *Jahrb Römisches-Germanisches Zentralmuseums* 35:510–516

Hauptmann A, Weisgerber G, Bachmann H-G (1989) Ancient copper production in the area of Feinan, Khirbet En-Nahas and Wadi El-Jariye, Wadi Arabah, Jordan. In: Fleming, Schenck (eds) *History of technology: the role of metals*, pp 6–16

Hawkes J (1995) *Discovering statistics*. Quant Publishing, Charleston

Hay RL (1976) *Geology of Olduvai Gorge: a study of sedimentation in a Semiarid basin*. University of California Press, Berkeley

Hay RL (1990) Olduvai Gorge; a case history in the interpretation of hominid Paleoenvironments in East Africa. In: Laporte LF (ed) *Establishment of a Geologic Framework for Paleoanthropology*. Geological Society of America Special Papers 242, Boulder, CO, pp 23–37

Hay RL, Kyser TK (2001) Chemical sedimentology and paleoenvironmental history of Lake Olduvai, a Pliocene lake in northern Tanzania. *Geol Soc Am Bull* 113 (12):1505–1521

Hayden B (1995) The emergence of prestige technologies and pottery. In: Barnett WK, Hoopes JW (eds) *The emergence of pottery*. Smithsonian Institution, Washington, DC, pp 257–266

Hayden B (1998) Practical and prestige technologies: the evolution of material systems. *J Archaeol Method Theory* 5(1):1–55

Haynes CV Jr (1995) Geochronology of paleoenvironmental change, Clovis type site, Blackwater Draw, New Mexico. *Geoarchaeology* 10:317–388

Heaney PJ (1995) Moganite as an indicator for vanished evaporites: a testament reborn? *J Sediment Res* A65:633–638

Heard P (1996) Cathodoluminescence-interesting phenomenon on useful technique? *Microsc Anal* 16:25–27

Hedges REM, Housley RA, Bronk CR, Van Klinken GJ (1990) Radiocarbon dates from the Oxford AMS system: *Archaeometry Dateiist* 11. *Archaeometry* 32 (2):211–237

Henderson J (2000) *The science and archaeology of materials*. Routledge, London

Henri-Martin G (1957) *La Grotte de Fontechevade. Première Partie: Historique, Fouilles, Stratigraphie, Archéologie*. Archives de l’Institut de Paléontologie Humaine 28. Masson et Compagnie, Paris

Hendy CH (1971) The isotopic geochemistry of speleothems, 1. The calculation of the effects of different modes of formation on the isotopic composition of speleothems and their applicability as paleolimatic indicators. *Geochim Cosmochim Acta* 35:801–824

Henshilwood CS, Sealy JC, Yates R, Cruz-Uribe K, Goldberg P, Grine FE, Klein RG, Poggenpoel C, Van Niekerk K, Watts I (2001) Blombos Cave, southern Cape, South Africa: preliminary report on the 1992–1999 excavations of the Middle Stone Age levels. *J Archaeol Sci* 28(4):421–448

Herbert JM, McReynolds TE (eds) (2008) *Woodland pottery sourcing in the Carolina sandhills*. University of North Carolina, Chapel Hill

Herbich T (1993) The variations of shaft fills as the basis of the estimation of flint mine extent: a Wierzica study. *Archaeologia Polona* 31:71–82

Hermes OD, Luedtke BE, Ritchie D (2001) Melrose green rhyolite: its geologic setting and petrographic and geo-chemical characteristics. *J Archaeol Sci* 28:913–928

Heron C, Evershed RP (1993) The analysis of organic residues and the study of pottery use. *Archaeol Method Theory* 5:247–284

Heron C (1989) The analysis of organic residues in archaeological ceramics. Ph.D. dissertation, University of Wales College of Cardiff

Herz N (1987) Carbon and oxygen isotopic ratios: a data base for classical Greek and Roman marble. *Archaeometry* 29(1):35–43

Herz N, Garrison EG (1998) *Geological methods for archaeology*. Oxford University Press, New York

Herz N, Pike S (2005) Isotopic signatures and marble consanguinity: hellenistic aphrodites and Philadelphia franklins. *Archaeological Institute of America Annual Meeting*, 6–9 Jan 2005, Boston

Hesse A (1999) Multi-parametric survey for archaeology. How and why, or how and why not? *J Appl Geophys* 41(2–3):157–168

Hesse A, Jolivet A, Tabbagh A (1986) New prospects in shallow depth electrical surveying for archeological and pedological applications. *Geophysics* 51:585–594

Higgins MD, Higgins R (1996) A geological companion to Greece and the Aegean. Cornell University Press, Ithaca

Hill CL (1999) Radiocarbon geochronology of strata containing *Mammuthus* (mammoth), Red Rock River, Montana. *Curr Res Pleistocene* 16:118–120

Hill CL (2006) Stratigraphic and geochronologic contexts of mammoth (*Mammuthus*) and other Pleistocene fauna, Upper Missouri Basin (northern Great Plains and Rocky Mountains), USA. *Quat Int* 142:87–106

Hill RS (2012) Final report: artist and community collaboration initiative. Lifelong education, administration and policy, College of Education and the Institute of Native American Studies. The University of Georgia, Athens

Hoard RJ, Holen SR, Glasscock MD, Neff H, Elam JM (1992) Neutron activation analysis of stone from the Chadron formation and a Clovis site on The Great Plains. *J Archaeol Sci* 19:655–665

Hochuli S (1994) Unter den ABahn 2000; Gefrierkern Bohrung in Kanton Zug. *Archäologie der Schweiz* 17(1):25–30

Hodder I (1982) Theoretical archaeology: a reactionary view. In: Hodder I (ed) *Symbolic and structural archaeology*. Cambridge Univ. Press, Cambridge, pp 1–16

Hodgson JM (1978) Soil sampling and soil description. Oxford University Press, London

Holcomb DW (1996) Shuttle imaging radar and archaeological survey in the China Taklamakan desert. *J Field Archaeol* 19(1):129–138

Holland HD, Zbinden EA (1988) Paleosols and the evolution of the atmosphere: part I. In: Lerman A, Meybeck M (eds) *Physical and chemical weathering in geochemical cycles*. Kluwer Academic Publishers, Dordrecht, pp 61–82

Holley GR, Dalan RA, Smith PA (1993) Investigations in the Cahokia Site Grand Plaza. *Am Antiq* 58(2):306–319

Holliday VT (2009) Geoarchaeology and the search for the first Americans. *Catena* 78:310–322

Holmes A (1930) Petrographic methods and calculations. Van Nostrand, New York

Holmes WH (1892) Modern quarry refuse and the Palaeolithic theory. *Science* 20:295–297

Holmes WH (1893) Are there traces of glacial man in the Trenton gravels? *J Geol* 1(1):15–37

Holmes WH (1894) Natural history of flaked stone implements. Schulte Publishing Company, Chicago

Holmes A (1913/1927) The age of the earth. Harper & Brothers, London

Holton I (2012) Is energy-dispersive spectroscopy in SEM a substitute for electron probe microanalysis? *Microsc Anal* 26(4):S4–S7

Hong Z, Xiao-Nian Z (1992) Electrokinetic properties of Ferralsols in China in relation to pedogenic development. *Geoderma* 54(1):173–188

Hoover H (1912) De re Metallica. The Mining Magazine, London

Hooykaas R (1970) Catastrophism in geology, its scientific character in relation to actualism and uniformitarianism. *Koninklijke Nederlandse Akademie van Wetenschappen, afd Letterkunde, Med (nr) 33:271–316*

Hošek J, Košta J, Bártá P (2012) The metallographic examination of sword no. 438 as part of a systematic survey of swords from the early medieval stronghold of Mikulčice, Czech Republic. *Gladius* XXXII:87–102

Hosler D (1988a) The metallurgy of ancient west Mexico. In: Maddin R (ed) *The beginning of the use of metals and alloys*. MIT Press, London, pp 340–341

Hosler D (1988b) Ancient west Mexican metallurgy: South and Central American origins and west Mexican transformations. *Am Anthropol* 90(4):832–855

Hosler D (2014) Mesoamerican metallurgy: the perspective from the west. In: Roberts BW, Thornton CP (eds) *Archaeometallurgy in global perspective*. Springer, New York, pp 329–360

Howell JM (1987) Early farming in northwestern Europe. *Sci Am* 237:118–126

Hsu KJ (1994) The geology of Switzerland: an introduction to tectonic facies. Princeton University Press, Princeton

Hsű K (1995) The geology of Switzerland. Princeton University Press, Princeton

Hunt CC (1980) The settlement, development, and decline of the scull shoals community in Greene and Oconee Counties, 1784–1920. In: Historical survey report, scull shoals community, Greene County, Georgia. Archaeological survey of Cobb-Fulton Counties: performed for U. S. Department of Agriculture, Forest Service, Contract, pp 38–3231

Hunt JL Jr (1974) The geology and origin of Gray's Reef, Georgia continental shelf. Unpublished Masters Thesis. The University of Georgia, Athens, 83 pp

Hunt AM, Speakman RJ (2015) Portable XRF analysis of archaeological sediments and ceramics. *J Archaeol Sci* 53:626–638

Hutchinson RW (1965) Genesis of Canadian massive sulphides by comparison to Cyprus deposits. *Transactions LXVIII:286–300, The Canadian Mining and Metallurgical Bulletin*. Montreal

Hutton J (1788) The theory of the earth; or an investigation of laws observable on the composition, dissolution and restoration of land upon the globe. *Trans R Soc Edinb* 1(2):209–304

Ikawa-Smith F (1976) On ceramic technology in East Asia. *Curr Anthropol* 17:513–515

Ikeya M (1985) Electron spin resonance. In: Rutter NW (ed) *Dating methods of pleistocene deposits and their problems*. Geoscience Canada reprint series, vol 2, pp 73–87

Inbar M, Hubp JL, Villers Riuz L (1994) The geomorphological evolution of the Paricutin cone and lava flow, Mexico, 1943–1990. *Geomorphology* 9:57–76

Indurante SJ, Follmer LR, Hammer RD, Koenig PG (1990) Particle-size analysis by a modified pipette procedure. *Soil Sci Soc Am J* 54:560–563

Ismail-Meyer K, Rentzel P, Wiemann P (2013) Neolithic lakeshore settlements in Switzerland: new insights on site formation processes from micromorphology. *Geoarchaeology* 28(4):317–339

Ionescu C, Hoeck V (2011) Firing-induced transformations in Copper Age ceramics from NE Romania. *Eur J Mineral* 23:937–958

Ivester AH, Leigh DS, Godfrey-Smith DI (2001) Chronology of Inland Eolian Dunes on the Coastal Plain of Georgia, USA. *Quat Res* 55:293–302

Ixer RA, Bevins R (2010) The petrography, affinity and provenance of lithics from the Cursus field, Stonehenge. *Wiltshire Archaeol Nat Hist Mag* 103:1–15

Ixer RA, Patrix RAD (2003) Copper-arsenic ores and Bronze Age mining and metallurgy with special reference to the British Isles. In: Craddock P, Lang J (eds) *Mining and metal production through the ages*. British Museum Press, London, pp 9–20

Jackson EL (1982) The Laki eruption of 1783: impacts on population and settlement in Iceland. *Geography* 67:42–50

Jackson JB (1984) *Discovering the vernacular landscape*. Yale University Press, New Haven

Jarvis KE, Gray AL, Houk RS (1992) *Handbook of inductively coupled plasma mass spectrometry*. Blackie, Glasgow

Jelinek A, Farrand WR, Haas G, Horowitz A, Goldberg PA (1973) New excavations at Tabun Cave, Mount Carmel, Israel: preliminary report. *Paléorient* I:151–183

Jenny H (1941) *Factors of soil formation: a system of quantitative pedology*. McGraw-Hill, New York

Jercher M, Pring A, Jones PG, Raven MD (1998) Rietveld x-ray diffraction and x-ray fluorescence analysis of Australian aboriginal ochres. *Archaeometry* 40:383–401

Jiazh L (1984) The evolution of Chinese pottery and porcelain technology. In: Kingery WD (ed) *The development of Chinese white porcelain, technology and style, ceramics and civilization*, vol I. The American Ceramic Society, Columbus, pp 135–162

Johanssen A (1938) *A descriptive petrography of the igneous rocks*. University of Chicago Press, Chicago

Johnson DL (1990) Biomantle evolution and redistribution of earth materials and artifacts. *Soil Sci* 149:84–102

Johnson IS (1994) Geochemical methods for provenance studies of steatite. PhD thesis. University of Glasgow. <http://theses.gla.ac.uk/2735/> ADD

Johnson DL (1998) Paleosols are buried soils. In: Follmer LR, Johnson DL, Catt JA (eds) *Quaternary international: revisit of concepts in paleopedology*, vol 51–52, p 7

Johnson DR (1999) Darwin the archaeologist. *Discov Archaeol* 1(1):6–7

Johnson NL, Leone FC (1964) *Statistics and experimental design in engineering and the physical sciences*, vol I. Wiley, New York

Johnson DL, Watson-Stegner D (1990) The soil evolution model as a framework for evaluating pedoturbation in archaeological site formation. In: Lasca NP, Donoghue J (eds) *Archaeological geology of North America*, vol 4. Geological Society of America Centennial Special, Boulder, pp 541–558

Johnson DL (2002) Darwin would be proud: bioturbation, dynamic denudation, and the power of theory in science. *Geoarchaeology* 17(1):7–40

Jones JE (1982) The Laurion silver mines: a review of recent researches and results. *Greece and Rome (Second Series)* 29(02):169–183

Jones RL (1964) Note on occurrence of opal phytoliths in some Cenozoic sedimentary rocks. *J Paleontol* 38:773–775

Jones AA (1991) X-ray fluorescence analysis. In: Smith KA (ed) *Soil analysis: modern instrumental techniques*, 2nd edn. Marcel Dekker, New York, pp 287–324

Jones DM (ed) (2007) *Geoarchaeology: using earth sciences to understand the archaeological record*. English Heritage Publishing, Hawthornes

Josephs R (2005) A petrographic analysis of extended Middle Missouri ceramics from North Dakota. *Plains Anthropol* 50(194):111–119

Jovanovic B (1988) Early metallurgy in Yugoslavia. In: *The beginning of the use of metals and alloys*. pp 69–79

Jugo PJ (2009) Sulfur content at sulfide saturation in oxidized magmas. *Geology* 37:415–418. doi:10.1130/G25527A.1

Jurmain R, Nelson H, Kilgore L, Trevathan W (2000) *Introduction to physical anthropology*. Wadsworth, Belmont

Kafafi ZA (2014) New insights on the copper mines of Wadi Faynan/Jordan. *Palest Explor Q* 146 (4):263–280

Kallithrakas-Kontos N, Katsamos AA, Aravantinos A (1993) Study of ancient Greek copper coins from Nikopolis (Epirus) and Thessaloniki (Macedonia). *Archaeometry* 35:265–278

Kamei H, Nishimura Y, Komatsu M, Saito M (1992) A new instrument: a three-component Fluxgate gradiometer. *Abstracts of the International Archaeometry Symposium*, Los Angeles, p 71

Kamilli D, Lamborg-Karlovsky CC (1979) Petrographic and electron microprobe analysis of ceramics from Tepe Yalya. *Archaeometry* 21:47–60

Kamilli D, Sternberg A (1985) New approaches to mineral analysis in ancient ceramics. In: Rapp G Jr, Gifford JA (eds) *Archaeological geology*. Yale University Press, New Haven, pp 313–330

Karkanas P, Shahack-Gross R, Ayalon A, Bar-Matthews M, Barkai R, Frumkin A, Gopher A, Stiner MC (2007) Evidence for habitual use of fire at the end of the Lower Paleolithic: site-formation processes at Qesem Cave, Israel. *J Hum Evol* 53 (2):197–212

Keally CT, Taniguchi Y, Kuzmin YV, Shewkomud IY (2004) Chronology of the beginning of pottery manufacture in East Asia. *Radiocarbon* 46(1):345–352

Kearey P, Brooks M (1991) An introduction to geological exploration. Blackwell Science, Oxford

Keene DA (2004) Reevaluating late prehistoric coastal subsistence and settlement strategies: new data from Grove's Creek Site, Skidaway Island, Georgia. *Am Antiq* 69(40):671–688

Keene DA, Garrison EG (2013) A survey of Irene phase architecture on the Georgia coast. Life among the tides: recent archaeology on the Georgia Bight: Proceedings of the Sixth Caldwell Conference, St. Catherines Island, Georgia, 20–22 May 2011. In: Thompson VD, Thomas DH (eds) Anthropological papers of the American Museum of natural history, no. 98, pp 289–315

Keith M, Haase KM, Schwarz-Schampera U, Klemd R (2014) Effects of temperature, sulfur and oxygen fugacity on the composition of sphalerite from submarine hydrothermal vents. *Geology* 42:699–702

Klein RG (2000) Archaeology and the evolution of human behavior. *Evol Anthropol* 9:17–36

Keller EA, Pinter N (2002) Active tectonics: earthquakes, uplift and landscape, 2nd edn. Prentice Hall, Upper Saddle River

Kelley JT, Belknap DF, Kelley AR, Claesson SH (2013) A model for drowned terrestrial habitats with associated archaeological remains in the northwestern gulf of Maine, USA. *Mar Geol* 338:1–16

Kelly RL (1995) The foraging spectrum: diversity in hunter-gatherer lifeways. Smithsonian Institution Press, Washington, DC

Kelly KL, Judd DB (1976) Color: universal language and dictionary of names. U.S. National Bureau of Standards Special Publication 440. U.S. Department of Commerce, Washington, DC

Kempe DRC, Harvey AP (eds) (1983) The petrology of archaeological artifacts. Clarendon Press, Oxford

Kempthorne O, Allamaras RR (1986) Errors and variability of observations. Methods of soil analysis. Part I. Agronomy-Soil Science Society of America, Madison, pp 1–31

Kennett JP, Baldauf JG et al (1994) Proc. ODP, International Reports, 146 (Part 2): College Station, Texas (Ocean Drilling Program)

Kennett DJ, Neff H, Glasscock MD, Mason AZ (2001) Interface – archaeology and technology. A geochemical revolution: inductively coupled plasma mass spectroscopy. *SAA Archeol Rec* 1:22–26

Kesler SE (1973) Copper, molybdenum and gold abundances in porphyry copper deposits. *Econ Geol* 68:106–112

Khakimov Akh R (1957) Artificial freezing of soils. Theory and practice. Academy of Sciences of the U.S.S.R. Permafrost Institute in V.A. Obruch. Translation by Israel Program in Scientific Translations (1966)

Kilikoglou V, Maniatis Y, Grimanis AP (1988) The effect of purification and firing of clays on trace element provenance studies. *Archaeometry* 30(1):37–46

Kilikoglou V, Vekinis G, Maniatis Y (1995) Toughening of ceramic earthenwares by quartz inclusions: an ancient art revisited. *Ada Metall Mater* 43:2959–2965

Kilikoglou V, Vekinis G, Maniatis Y, Day PM (1998) Mechanical performance of quartz tempered ceramics. Part 1: strength and toughness. *Archaeometry* 40:261–279

Killick D (1991) The relevance of recent African iron-smelting practice to reconstructions of prehistoric smelting technology. In: Recent trends in archaeometallurgical research. pp 47–54

Killick D (2009) Cairo to Cape: the spread of metallurgy through eastern and southern Africa. *J World Prehistory* 22:399–414

Killick D (2014) From ores to metals. In: Roberts BW, Thornton CP (eds) Archaeometallurgy in global perspective. Springer, New York, pp 11–45

Kim J, Liaw PK (1998) The nondestructive evaluation of advanced ceramics and ceramic-matrix composites. *Nondestruct Eval Overview* 50(11):1–15

Kingery WD (1984) Interactions of ceramic technology with society. In: Rice PM (ed) Pots and potters: current approaches in ceramic archaeology, vol 24, Monograph. Institute of Archaeology, University of California, Los Angeles, pp 171–178

Kingery WD (1990) The changing roles of ceramics in society: 26,000 BP to the present. American Ceramic Society, Westerville

Kingery WD (1992a) Sintering from prehistoric times to the present. *Solid State Phenom* 25:1–10

Kingery WD (1992b) Attic pottery gloss technology. *Archaeomaterials* 5:47–54

Kingery WD (1993) A role for materials science. In: Kingery WD (ed) Learning from things. Smithsonian Institution Press, Washington, DC, pp 175–180

Kingery WD, Friermann JD (1974) The firing temperature of a karanova sherd and inferences about southeast European chalcolithic refractory technology. *Proc Prehist Soc* 40:204–205

Kingery WD, Vandiver PB (1988) Ceramic masterpieces—art structure and technology. Free Press (Macmillan), New York

Kish L (1965) Survey sampling. Wiley, New York

Klecka WR (1975) Discriminate analysis. In: Nie NH et al (eds) Statistical package for the social sciences (SPSS). McGraw-Hill, Englewood Cliffs, pp 434–467

Klockenkemper R, Bubert H, Hasler K (1999) Detection of near-surface silver enrichment on Roman coins. *Archaeometry* 41(2):311–320

Kooistra MJ, Kooistra LI (2003) Integrated research in archaeology using soil micromorphology and palynology. *Catena* 54:603–617

Kovarovic K, Aiello LC, Cardini A, Lockwood CA (2011) Discriminant function analyses in archaeology:

are classification rates too good to be true? *J Archaeol Sci* 38:3006–3018

Kraft JC (1994) Archaeological geology. *Geotimes* 39:12–13

Kraft JC, Belknap DF, Kayan I (1983) Potentials of discovery of human occupation sites on the continental shelves and nearshore coastal zone. In: Masters PM, Flemming NC (eds) Quaternary coastlines and marine archaeology: towards the prehistory of land bridges and continental shelves. Academic, London, pp 87–120

Kramer C (1985) Ceramic ethnoarchaeology. *Annu Rev Anthropol* 14:77–102

Kremer K, Simpson G, Girardclos S (2012) Giant Lake Geneva tsunami in AD 563. *Nat Geosci* 5:756–757

Kremer K, Marillier F, Hilbe M, Simpson G, Dupuy D, Yrro BJF, Rachoud-Schneider A-M, Corboud P, Bellwald B, Wildi W, Girardclos S (2014) Lake dwellers occupation gap in Lake Geneva (France–Switzerland) possibly explained by an earthquake–mass movement–tsunami event during Early Bronze Age. *Earth Planet Sci Lett* 385:28–39

Kremer K, Hilbe M, Simpson G, Decrouy L, Wildi W, Girardclos S (2015) Reconstructing 4000 years of mass movement and tsunami history in a deep peri-Alpine lake (Lake Geneva, France–Switzerland). *Sedimentology* 62(5):1305–1327

Krings M, Stone A, Schmitz RW, Krainitzi H, Stoneking M, Pääbo S (1997) Neanderthal DNA sequences and the origin of modern humans. *Cell* 90:19–30

Kröpelin S, Verschuren D, Lézine A-M, Eggermont H, Cocquyt C, Francus P, Cazet J-P, Fagot M, Rumes B, Russel JM, Darius F, Conley DJ, Schuster M, von Suchodolitz H, Dr. Engstrom R (2008) Climate-driven ecosystem succession in the Sahara: the past 6000 years. *Science* 320:765–768

Krumbein WC, Pettijohn FJ (1938) Manual of sedimentary petrography. Appleton and Century, New York

Kubiena WL (1938) Micropedology. Collegiate Press Inc., Ames

Kubiena ML (1953) The soils of Europe. Murby, London

Kuhn RD, Sempowski ML (2001) A new approach to dating the league of the Iroquois. *Am Antiq* 66:301–314

Kukla G, Heller F, Liu X, Xu M, Liu TS, An ZS (1988) Pleistocene climates in China dated by magnetic susceptibility. *Geology* 16:811–814

Kuper R, Lohr H, Lyning J, Stehli P, Zimmerman A (1977) Der Band Keramische Siedlungplatz Langweiler, 9, Gem. Aldenhoven, Kr. Dyren. *Rheinische Ausgrabungen* 18. Rheinland – Verlag, Bonn

Kvamme KL (2001) Current practices in archaeogeophysics. In: Goldberg P, Holliday VT, Ferring CR (eds) Earth sciences and archaeology. Springer, New York, pp 353–384

Kzanowski WJ (1988) Principles of multivariate analysis. Clarendon Press, Oxford

Lacroix D, Bell T, Shaw J, Westley K (2014) Submerged archaeological landscapes and the recording of pre-contact history: examples from Atlantic Canada. In: Evans AM, Flatman JC, Flemming NC (eds) Prehistoric archaeology on the continental shelf. Springer, New York, pp 13–35

Lamberg-Karlovsky CC (1974) Excavations at Tepe Yalya. In: Willey GR (ed) Archaeological researches in retrospect. Winthrop, Cambridge, pp 269–292

Larsen D, Brock CF (2014) Sedimentology and petrology of the eocene memphis sand and younger terrace deposits in surface exposures of Western Tennessee. *Southeast Geol* 50(4):193–214

Larsen NK, Kjær KH, Lecavalier B, Bjørk AA, Colding S, Huybrechts P, Jakobsen KE, Kjeldsen KK, Knudsen KL, Odgaard BV, Olsen J (2015) The response of the southern Greenland ice sheet to the Holocene thermal maximum. *Geology* 43(4):291–294

Lassau G, Riethmann P (1988) Trockeneisondierung, ein Prospektionsverfahren im Seeuferbereich. *Jahrb Schweizerischen Ges Ur- und Frühgeschichte* 71:241–247

Lavin L (1988) Coastal adaptations in southern New England and southern New York. In: Archaeology of Eastern North America. pp 101–120

Lawrence D (1971) The nature and structure of paleoecology. *J Paleontol* 45:59347

Layzell AL, Eppes MC, Lewis RQ (2012) Soil chronosequence study of the terraces of the Catawba river near Charlotte, NC: insights into the long-term evolution of a major piedmont drainage basin. *Southeast Geol* 49(10):13–24

Lazerwitz B (1968) Sampling theory and procedures in methodology in social research. McGraw-Hill, New York

Leach F, Manley B (1982) Minimum Mahalanobis distance functions and lithic source characterization by multi-element analysis. *N Z J Archaeol* 4:77–109

Leakey MD (1971) Olduvai Gorge, Volume 3, Excavations in Beds I and II, 1960–1963. Cambridge University Press, Cambridge, UK

LeBlanc G (2001) A review of EPA sample preparation techniques for organic compounds of liquid and solid samples. *LC-GC* 19:1120–1121

LeBorgne P (1960) Influence du fer sur les propriétés magnétiques du sol et sur celles du schiste et du granite. *Ann Geophys* 6(2):159–195

Lechtman H (2014) Andean metallurgy in prehistory. In: Roberts BW, Thornton CP (eds) Archaeometallurgy in global perspective. Springer, New York, pp 361–422

Lechtman H, Klein S (1999) The production of copper-arsenic alloys (arsenic bronze) by cosmelting: modern experiment and ancient practice. *J Archaeol Sci* 26 (5):497–526

Leigh DS (1998) Evaluating artifact burial by eolian versus bioturbation processes, South Carolina sandhills, USA. *Geoarchaeology* 13:309–330

Leigh DS (2001) Buried artifacts in sandy soils: techniques for evaluation pedoturbation versus

sedimentation. In: Goldberg P, Holliday VT, Ferring CR (eds) *Earth sciences and archaeology*. Kluwe, New York, pp 269–293

Leigh DS, Knox JC (1994) Loess of the Upper Mississippi Valley driftless area. *Quat Res* 42(1):30–40

Lencolais G, Auffret J-P, Bourillet J-F (2003) The quaternary channel river: seismic stratigraphy of its palaeovalleys and deeps. *J Quat Sci* 18(3-4):245–260

Leopold LB, Bull WB (1979) Base level, aggradation, and grade. *Proc Am Philos Soc* 123(3):168–202

Leroi-Gourhan L (1943–1945) *Evolution et techniques*, vol 1–2. Michel, Paris

Leroi-Gourhan A (1993) *Gesture and speech (Le geste et la parole)*. Bostock Berger A translater. MIT Press, Cambridge, MA

Lespez L, Papadopolous S (2008) Etude geoarchaeologique du site d'Aghios Ioannis a Thasos. *BCH* 132:667–692

Leudtke BE (1992) *An archaeologist's guide to chert and flint*. University of California Press, Los Angeles

Leute U (1987) *Archaeometry*. VCH Verlag, Weinheim

Levin HL (1988) *The earth through time*, 3rd edn. Saunders College Publishing, Philadelphia

Levin SA (1992) The problem of pattern and scale in ecology. *Ecology* 73:1943–1967

Levine MA (2007) Overcoming disciplinary solitude: the archaeology and geology of native copper in eastern north America. *Geoarchaeology* 22:49–66

Levy TE, Najjar M, Ben-Josef E (2014) New insights into the iron age archaeology of Edom, Southern Jordan, vol 35, *Monumenta Archaeologica*. University of New Mexico Press, Albuquerque

Lichtenstein KP (2003) Historic sedimentation and allostratigraphy of the South Fork Broad River, Northeast Georgia. M.S. Thesis. The University of Georgia, Athens. 87 p

Liritzis I, Zacharias N (2011) Portable XRF of archaeological artifacts: current research, potentials and limitations. In: *X-ray fluorescence spectrometry (XRF) in geoarchaeology*. Springer, New York, pp 109–142

Lincoln FC, Rietz HL (1913) The determination of the relative volumes of the components of rocks by mensuration methods. *Econ Geol* 8(2):120–139

Linderholm J, Lundberg E (1994) Chemical characterization of various archaeological soil samples using main and trace elements determined by inductively coupled plasma atomic emission spectrometry. *J Archaeol Sci* 21:303–314

Linderholm J (2007) Soil chemical surveying: a path to a deeper understanding of prehistoric sites and societies in Sweden. *Geoarchaeology* 22(4):417–438

Linford N (2006) The application of geophysical methods to archaeological prospection. *Rep Prog Phys* 69(7):2205

Littman SL (2000) Pleistocene/Holocene sea level change in the Georgia Bight: a paleoenvironmental reconstruction of Gray's Reef National Marine Sanctuary and J. Reef. Unpublished Masters Thesis. The University of Georgia, Athens

Lohse ES (1995) Northern intermountain west projectile point chronology. *Tebiwa* 25(1):3–51

Lombard JP (1987) Provenance of sand temper in Hohokam ceramics. *Geoarchaeology* 2:91–119

Longacre WA (ed) (1991) *Ceramic ethnoarchaeology*. University of Arizona Press, Tucson

López-Buendía AM, Romero-Sánchez MD, Rodes JM, Cuevas JM, Guillem C (2010) Energy efficiency contribution of the natural stone approach in processing and application. *Global Stone Congress*, 2010. Alicante, Spain

Lotter AF, Renberg I, Hansson H, Stockli R, Sturm M (1997) A remote controlled freeze corer for sampling unconsolidated surface sediments. *Aquat Sci* 59(4):295–303

Loy TH, Hardy BL (1992) Blood residue analysis of 90,000-year-old stone tools from Tabun Cave, Israel. *Antiquity* 66(250):24–35

Lubbock J (1865) *Pre-historic times*. Williams and Norgate, London

Lübke H (2002) Submarine stone age settlements as indicators of sea-level changes and the coastal evolution of the Wismar Bay area. *Greifswalder Geographische Arbeiten* 27:202–210

Lucas G (2008) Pálstóftir: a viking age shieling in Iceland. *Nor Archaeol Rev* 41(1):85–100

Lucas A, Harris JR (1962) *Ancient Egyptian materials and industries*. Edward Arnold Publishers Ltd, London

Luhmann L, Robson S, Kyle S, Boehm J (2013) Close-range photogrammetry and 3D imaging. Walter de Gruyter, Germany

Lutz J, Pernicka E (2013) Prehistoric copper from the Eastern Alps. In: Tykot RH (ed) *Proceedings of the 38th International Symposium on Archaeometry – May 10th–14th 2010, Tampa*. Open J Archaeometry 1:e25

Lyell C (1830) *Principles of geology*, being an attempt to explain former changes of the Earth's surface by reference to causes now in operation, vol I. John Murray, London

Lyell C (1830–1833) *Principles of geology*, 3 vols. John Murray, London

Lyell C (1863) *The geological evidences of the antiquity of man, with remarks on theories of the origin of species by variation*. John Murray, London

Lyell's principles of geology, 1st edition was 1831; 1833 – 2nd printing

Lyman RL (1985) Bone frequencies: differential transport, in situ destruction, and the MGU. *J Archaeol Sci* 12:221–236

Lynnerup N (1998) The Greenland Norse. A biological-anthropological study. *Meddelelser om Grönland. Man Soc* 24:1–149

MacArthur RH, Pianka ER (1966) On optimal use of a patchy environment. *Am Nat* 100:603–609

Mack GH, James WC, Monger HC (1993) Classification of paleosols. *Geol Soc Am Bull* 105:129–136

Mackensie WS, Donaldson CH, Guilford C (1982) *Atlas of igneous rocks and their textures*. Addison Wesley Longman Ltd, Harlow

MacKenzie WS, Adams AE (1994) *The color atlas of rocks and minerals in thin section*. Wiley, New York

MacKenzie WS, Donaldson CH, Guilford C (1982) *Atlas of igneous rocks and their textures*. Pearson, Essex

Maggetti M (1982) Phase analysis and its significance for technology and origin. In: Olin JS, Franklin AD (eds) *Archaeological ceramics*. Smithsonian Institution, Washington, DC, pp 121–133

Maggetti M (2011) Paul-Louis Cyfflé's (1724–1806) search for porcelain. *Eur J Mineral* 23:993–1006

Maggetti M, Galetti G, Schwandler G, Picon M, Wessicken R (1981) Campanian pottery: the nature of the black coating. *Archaeometry* 23:199–207

Maher LJ (1981) Statistics for microfossil concentration measurements employing samples spiked with marker grains. *Rev Paleobotany Palynol* 32:153–191

Majewski T, O'Brien MJ (1987) The use and misuse of nineteenth-century English and American ceramics in archaeological analysis. *Adv Archaeol Method Theory* 11:97–209

Malainey ME, Przybylski R, Sheriff BL (1999) Identifying the former contacts of late Precontact period pottery vessels from Western Canada using gas chromatography. *J Archaeol Sci* 26(4):425–438

Mallol C, Hernández CM, Cabanes D, Machado J, Sistiaga A, Pérez L, Galván B (2013) Human actions performed on simple combustion structures: an experimental approach to the study of middle palaeolithic fire. *Quat Int* 315:3–15

Mallory-Greenough LM, Greenough JD, Owen JV (1998a) Provenance of temper in a New Kingdom Egyptian pottery sherd: evidence from the petrology and mineralogy of basalt fragments. *Geoarchaeology* 13(4):391–410

Mallory-Greenough LM, Greenough JD, Owen JV (1998b) New data for old pots: trace-element characterization of ancient Egyptian pottery using ICP-MS. *J Archaeol Sci* 25(1):85–97

Mannoni T (1984) Metodi di datazione dell'edilizia storica. *Archeologia Medievale* 11:396

Mannoni L, Mannoni T (1984) *Marble. Facts on File Publications*, New York

Manzanilla LR (2007) Las 'casas' nobles de los barrios de Teotihuacan: estructuras exclusionistas en un entorno corporativo. *Memoria del El Colegio Nacional*, pp 453–470

Margolis SV (1989) Authenticating ancient marble sculpture. *Sci Am* 260(6):104–110

Marin-Spiotta E, Chaopricha NT, Plante AF, Diefendorf AF, Mueller CW, Grandy AS, Mason JA (2014) Long-term stabilization of deep soil carbon by fire and burial during early Holocene climate change. *Nat Geosci* 7:428–432

Marmet E, Bina M, Fedoroffand N, Tabbagh A (1999) Relationships between human activity and the magnetic properties of soils: a case study in the medieval site of Roissy-en-France. *Archaeol Prospect* 6:161–170

Warrick AW, Meyers DE, Nielsen DR (1986) Geostatistical methods applied to soil science. *Methods of soil analysis, part I*. Agronomy monograph no. 9, 2nd edn. American Society of Agronomy - Soil Science Society of America, Madison

Marshall A (1999) Magnetic prospection at high resolution: survey of large silo-pits in iron age enclosures. *Archaeol Prospect* 6:11–29

Martin PD (1970) *The last 10,000 years*. University of Arizona Press, Tucson

Martin C (1993) Radiocarbon ages on late Pleistocene loess stratigraphy of Nebraska and Kansas, Central Great Plains, U.S.A. *Quat Sci Rev* 12:179–188

Maslin MA (2000) North Atlantic iceberg armadas. *Sci Spectra* 22:40–50

Matson FR (1960) The quantitative study of ceramic materials. In: Heizer RF, Cook SF (eds) *The application of quantitative methods in archaeology*, vol 28, Viking Fund Publications in Anthropology. Wenner-Gren Foundation, New York, pp 43–51

Matson FR (1961) *Ceramics and man*, vol 41, Viking Fund Publications in Anthropology. Methuen, London

Matsumura S, Arlinghaus R, Dieckmann U (2010) Foraging on spatially distributed resources with sub-optimal movement, imperfect information, and travelling costs: departures from the ideal free distribution. *Oikos* 119(9):1469–1483

Mazeran R (1995) Les brèches exploitées comme marbre dans le Sud-Est de la France à l'époque romaine. *Archéométrieaux: Marbres et autres roches. Actes de la IV^e Conference internationale, ASMOSIA IV. CRPA*. Pub. Presses Universitaires de Bordeaux

McCauley JF, Schaber GG, Breed CS, Grolier MJ, Haynes CU, Issawi B, Elachi C, Blom R (1982) Sub-surface valleys and geoarchaeology of the Eastern Sahara revealed by Shuttle Radar. *Science* 218:1004

McCown TD, Keith A (1939) *The fossil human remains from the Levalloiso-Mousterian*. Clarendon Press, Oxford

McGovern TH (1980) Cows, harp seals, and churchbells: adaptation and extinction in Norse Greenland. *Hum Ecol* 8(3):245–275

McGovern TH (1985) The arctic frontier of Norse Greenland. In: Green S, Peltman S (eds) *The archaeology of frontiers and boundaries*. Academic, New York, pp 275–323

McGovern TH (1990) The archaeology of the Norse north Atlantic. *Annu Rev Anthropol* 19:331–351

McGovern TH, Buckland PC, Savory D, Sveinbjarnardottir G, Andreason C, Skidmore P (1983) A study of the faunal and floral remains from two Norse farms in the Western Settlement, Greenland. *Arctic Anthropol* 20:93–120

McKay ED (1979) Stratigraphy of Wisconsin and older loesses in southwestern Illinois. *Ill Geol Surv Guideb* 14:37–67

McMorrow J (1995) Multispectral remote sensing of archaeological sites: NERC airborne thematic mapper images of the Oxford flood plain. In: Beavis J, Baker K (eds) *Science and the site*. Bournemouth University Occasional Papers 1, Bournemouth

McReynolds TE, Skaggs SA, Schroeder PA (2008) Feldspar and clay mineralogy. In: Herbert JM, McReynolds TE (eds) Woodland pottery sourcing in the Carolina Sandhills. Research report no. 29. Research Laboratories of Archaeology. The University of North Carolina at Chapel Hill, Chapel Hill

Meats C (1996) An appraisal of the problems involved in three-dimensional ground penetrating radar imaging of archaeological features. *Archaeometry* 38 (2):359–379

Meignen L, Bar-Yosef O, Mercier N, Valladas H, Goldberg P, Vandermeersch B (2001) Apport des datations au problème de l'origine des Hommes modernes au Proche-Orient. In: JN, Buibert P, Michel V (eds) XXIe rencontres internationales d'archéologie et d'histoire d'Antibes: Editions APDCA, pp 295–313

Meinert LD, Dipple GM, Nicolescu S (2005) World skarn deposits. In: Hedenquist JW, Thompson JFH, Goldfarb RJ, Richards JP (eds) Economic geology 100th anniversary volume. Society of Economic Geologists, Littleton, pp 299–336

Meixnar H, Paar W (1982) New observations on ore formation and weathering of the Kamariza Deposit, Laurion, SE Attica (Greece). In: Ore genesis. special publication of the society for geology applied to mineral deposits, vol 2. pp 760–776

Melas EM (1985) The islands of Karpathos, Saros and Kasos in the neolithic and bronze age. *Stud Mediterr Archaeol* LXVII:15–24

Mellaart J (1966) Excavations at Catal Hüyük, 1965: fourth preliminary report. *Anatol Stud* 16:165–191

Mentzer SM (2014) Microarchaeological approaches to the identification and interpretation of combustion features in prehistoric archaeological sites. *J Archaeol Method Theory* 21(3):616–668

Meriweather DA (1999) Freezer anthropology: new uses for old blood. *Philos Trans R Soc Lond B* 354:121–129

Merwin DE (2010) Submerged evidence of early human occupation in the New York Bight. Unpublished Doctoral Dissertation, Stony Brook University

Meschel SV (1980) Chemistry and archaeology: a synergism. *Chemtech* 10(7):404–410

Mikhail EH, Briner GP (1978) Routine particle size analysis using sodium hypochlorite and ultra-sonic dispersion. *Aust J Soc Res* 14:241–244

Milsom J, Eriksen A (2011) Field geophysics, 4th edn. Wiley, Oxford

Miskimmin BM, Curtis PJ, Schindler DW, Lafaut N (1996) A new hammer-driven freeze corer. *J Paleolimnol* 15(3):265–269

Momaday NS (1994) Values. In: Hill N Jr (ed) Words of power: voices from Indian America. Fulcrum, Golden

Monttana A, Grespi R, Liborio G (1977) Simon and Schuster's guide to rocks and minerals. Simon and Schuster, New York

Morrison I (1985) Landscape with lake dwellings: the crannogs of Scotland. University Press, Edinburgh

Morrison RB (1991) Quaternary stratigraphic, hydrologic, and climatic history of the great basin, with emphasis on lakes Lahontan, Bonneville and Tecopa. In: Morrison RB (ed) Quaternary nonglacial geology: coterminous U.S., vol K-2, The Geology of North America. Geological Society of America, Boulder, pp 293–320

Morrison RB, Davis JO (1984) Supplemental guidebook for field trip 13, quaternary stratigraphy and archaeology of the Lake Lahontan area. 1984 Annual Meeting of the Geological Society of America, Reno, Nevada, pp 252–281. Desert Research Institute, University of Nevada, Reno

MoscarIELLO A, Costa F (1997) The upper Laacher See Tephra in lake Geneva sediments: paleoenvironmental and paleoclimatological implications. *Schweiz Mineral Petrogr Mitt* 77(2):175–185

Muhly JD (1985) Sources of tin and the beginnings of bronze metallurgy. *Am J Archaeol* 89:275–291

Muhly JD (2006) Chrysokamino in the history of early metallurgy. *Hesperia Suppl* 36:155–177

Mulaik S (1972) The foundations of factor analysis. McGraw-Hill, New York

Mulholland SC, Rapp G Jr (eds) (1992) Phytolith systematics: emerging issues. Plenum Press, New York, pp 1–13

Mullins CE (1974) The magnetic properties of the soil and their application to archaeological prospecting. *Archaeo-Physica* 5:144–148

Munro R (1882) Ancient Scottish lake-dwellings or crannogs: with a supplementary chapter on remains of lake-dwellings in England. D. Douglas, Edinburgh

Murphy J, Riley JP (1962) A modified single solution for the determination of phosphorus in natural waters. *Anal Chim Acta* 27:21–26

NACSN (1983) North American Stratigraphic code. *Am Assoc Petr Geol Bull* 67(5):841–875

Neff H (1993) Archaeology theory, sampling, and analytical techniques in the archaeological study of prehistoric ceramics. *Am Antiquity* 58(1):23–44

Neff H, Glascock MD (1995) The state nuclear archaeology in North America. *J Radioact Nucl Chem* 196:275–286

Negrini RM (2002) Pluvial lake sizes in the northwestern great basin throughout the quaternary period. In: Hershler R, Madsen DB, Currey DR (eds) Great basin aquatic systems history. Smithsonian Contributions to the Earth Sciences, Washington, DC No. 33, pp 11–52

Nelson B (ed) (1984) Decoding prehistoric ceramics. Southern Illinois University Press, Carbondale

Nelson AR (1992) Lithofacies analysis of colluvial sediments; an aid in interpreting the Recent history of Quaternary normal faults in the Basin and Range Province, Western United States. *J Sediment Res* 62:607–621

Neogi S (2011) Scope of geoarchaeology in depicting the early hominin environments in the Gandheswari River Basin of Bankura district, West Bengal. eTraverse,

Indian J Spat Sci, I(2), Article 6— 4. The Geographical Institute

Nerantzis N, Papadopolous S (2013) Reassessment and new data on the diachronic relationship of Thasos Island with its indigenous metal resources; a review. *Archaeol Anthropol Sci* 5:183–196

Neubauer W, Eder-Hinterleitner A (1997) Resistivity and magnetics of the Roman town Carnuntum, Austria: an example of combined interpretation of prospection data. *Archaeol Prospect* 4(4):179–189

Neubauer W (1999) Geophysikalische Prospektion in der Archäologie. Institut für Ur- und Frühgeschichte, Wien

Nikischer T (1999) Modern mineral identification techniques, part I. WDS and EDS. *Mineral Rec* 30:297–300

Noel M, Xu B (1991) Archaeological investigation by electrical resistive tomography: a preliminary study. *Geophys J Int* 107:95–102

Notis MR (2014) Metals. In: Roberts BW, Thornton CP (eds) *Archaeometallurgy in global perspective*. Springer, New York, pp 47–66

Nur A, Ron H (1997) Earthquake-inspiration for Armageddon. *Biblic Archaeol Rev* 23(4):49–55

Odell GH (1975) Microwear in perspective: a sympathetic response to Lawrence A. Keeley. *World Archaeol* 7:226–240

Odell GH (2001) Stone tool research at the end of the millennium: classification, function, and behavior. *J Archaeol Res* 9(1):45–100

Odum EP (1960) Organic production and turnover in old field succession. *Ecology* 41(1):34–49

Odum EP (1995) *Ecology: science and society*. Sinauer, Sunderland

Olin JS, Blackman MJ (1989) Compositional classification of Mexican majolica ceramics of the Spanish colonial period. In: Allen RO (ed) *Archaeological chemistry*, vol IV. American Chemical Society, Washington, DC, pp 87–124

Olson GW (1981) *Soils and the environment*. Chapman and Hall, New York

Origlia F, Glizzotto E, Meccheri M, Spangenberg JE, Memmi IT, Papi E (2011) Mineralogical, petrographic and geochemical characterization of white and coloured Iberian marbles in the context of the provenancing of some artefacts from Thamusida (Kenitra, Morocco). *Eur J Mineral* 23:857–869

Orliac M (1975) Empreintes au latex des coupes du gisement magdalénien de Pincevent: technique et premier résultats. *Bull Soc Prehist Fr* 72:274–276

Osborn HF (1916) *Men of the old stone age*, 2nd edn. Chas. Scribner's Sons, New York

Osterwalder C, Andre R (1980) *La Suisse Préhistorique*, vol 1, 24th edn. Heures, Lausanne

Ostrooumov M (2009) Infrared reflection spectroscopic analysis as a non-destructive method of characterizing minerals and stone materials in geoarchaeological and archaeometric applications. *Geoarchaeology* 24 (5):619–637

Oviatt CG, Swinehart JB, Wilson JR (1997) Dryland landforms, hazards and risks. In: Busche RM (ed) *Laboratory manual for physical geology*, 4th edn. Prentice Hall, Upper Saddle River

Owen JV, Hansen D (1996) Compositional constraints on the identification of eighteenth-century porcelain sherds for Fort Beauséjour, New Brunswick, and Grassy Island, Nova Scotia, Canada. *Hist Archaeol* 30(4):88–100

Owens DL (1997) A feasibility study for phytolith research in the southeast from scull shoals in the Oconee National Forest and Skidaway Island, Georgia. Masters thesis. Department of Geology. University of Georgia, Athens

Oxburgh ER (1968) An outline of the geology of the central Eastern Alps. *Proc Geol Assoc* 79:1–4

OxCAL Program v2.18. URL: http://units.ox.ac.uk/departments/rhala/oxcal/oxcal_h.html

Palmer AN (1991) Original morphology of limestone caves. *GSA Bull* 103:1–21

Palmer JW, Hollander MG, Rodgers PSZ, Benjamin TM, Duffy CJ, Lambert JB, Brown JA (1998) Pre-Columbian metallurgy: technology, manufacture, and microprobe analyses of copper bells from the greater southwest. *Archaeometry* 40(2):361–382

Pandey RN (1987) Palaeo-environment and prehistory of Nepal. *Contrib Nepal Stud CNAS TU* 14(2):111–124

Pansu M, Gautheyrou J, Loyer J-Y (2001) Soil analysis: sampling, instrumentation and quality control. (trans: Sarma VAK, Balkema AA). Lisse

Papadopolous S (2008) Silver and copper production practices in the prehistoric settlement of Limenaria, Thasos. In: Tzachili I (ed) *Aegean metallurgy in the bronze age*, proceedings of an international symposium held at the University of Crete. Ta Pragmata, Rethymnon, pp 59–67

Papageorgiou I, Baxter MJ, Cau MA (2001) Model-based cluster analysis of artefact compositional data. *Archaeometry* 43:571–588

Parker SP (ed) (1994) *McGraw-Hill dictionary of geology and mineralogy*. McGraw-Hill, New York

Patel SB, Hedges REM, Kilner JA (1998) Surface analysis of archaeological obsidian by SIMS. *J Archaeol Sci* 25(10):1047–1054

Patella D, Hesse A (eds) Special issue: electric, magnetic and electromagnetic methods applied to cultural heritage. *J Appl Geophys* 41(2–3)

Pavich MJ, Markewich HW, Litwin RJ, Smoot JP, Brook GA (2010) Significance of Marine oxygen isotope stage OIS5a and OIS3 OSL dates from estuarine sediments flanking Chesapeake Bay. In Annual meeting of the Geological Society of America, Baltimore, MD, Abstracts with Programs, 42(1), p 101

Peacock DPS (1970) The scientific analysis of ancient ceramics: a review. *World Archaeol* 1:375–389

Peacock DPS (1981) Archaeology, ethnology, and ceramic production. In: Howard H, Morris E (eds) *Production and distribution: a ceramic viewpoint*, vol 120, B.A.R. International series. British Archaeological Reports, Oxford, pp 187–194

Pearsall DM (1989) Phytolith analysis. *Paleoethnobotany: a handbook of procedures*. Academic, London, pp 311–438

Pearsall DM, Trimball M (1984) Identifying past agricultural activity through soil phytolith analysis: a case study from the Hawaiian islands. *J Archaeol Sci* 11:119–133

Pearson CE, Weinstein RA, Wiseman DE, McClendon CM (1982) Sedimentary studies of prehistoric archaeological sites: criteria for the identification of submerged archaeological sites of the northern gulf of Mexico continental shelf. *Coastal Environments*, Baton Rouge, 118 p

Pearson CE, Kelley DB, Weinstein RA, Gagliano SA (1986) Archaeological investigations of the outer continental shelf: a study within the Sabine River Valley, Offshore Louisiana and Texas. OCS Study, MMS 86-0119. U.S. Department of the Interior. Minerals Management Service, New Orleans

Pearson CE, Weinstein RA, Kelley DB (2008) Prehistoric site discovery on the outer continental shelf, United States of America. Paper presented at the 6th World Archaeological Conference, Dublin, Jun 28–Jul 4

Pearson CE, Weinstein RA, Gagliano SM, Kelley DB (2014) Prehistoric site discovery on the outer continental shelf, gulf of Mexico, United States of America. In: Evans A, Flatman J, Flemming N (eds) *Prehistoric archaeology of the continental shelf: a global review*. Springer, New York, pp 53–72

Pecci A (2000) Análisis químico de piso y áreas de actividad. Estudio de caso en Teopanzaczo, Teotihuacan. Tesis de maestría. Cuidad Universitaria. Universidad Nacional Autónoma de México, México

Penck A, Brückner E (1909) *Die Alpen im Eiszeitalter*, vol 2. Tauchnitz, Leipzig

Penita M (1998) Personal communication

Pennisi E (2013) Out of the Kenyan mud, an ancient climate record. *Science* 341:476–479

Pérez JM, Esteve-Tébar R (2004) Pigment identification in Greek pottery by Raman spectroscopy. *Archaeometry* 46(4):607–614

Perinçek D (2008) Geoarchaeology of the excavation site for the last 8000 years and traces of natural catastrophes in geological profiles, Istanbul Archaeological Museum. Proceeding of the 1st Symposium on Marmaray-Metro Salvage Excavations 5th-6th May 2008, Turkey, pp 191–217 (in English and in Turkish)

Perinçek D (2010) Yenikapı kazı alanının son 8000 yıllık jeoarkeolojisi ve doğal afetlerin jeolojik kesitteki izleri. The Geoarchaeology of the Yenikapı Excavation Site in the Last 8000 years and Geological Traces of Natural Disasters (Istanbul, Turkey), 141. General Directorate of Mineral Research and Exploration Journal (MTA Dergisi, Ankara, Turkey (in Turkish with English abstract), pp 73–95

Perkins D (2011) *Mineralogy*. Pearson, London

Perkins D, Henke KR (2000) Minerals in thin section. Prentice-Hall, New Jersey

Pernicka E, Begemann F, Schmitt-Strecker S, Wagner GA (1993) Eneolithic and Early Bronze Age copper artefacts from the Balkans and their relation to Serbian copper ores. *Praehistorische Zeitschrift* 68(1):1–54

Pernicka E, Begemann F, Schmitt-Strecker S, Todorova H, Kuleff I (1997) Prehistoric copper in Bulgaria. Its composition and provenance. *Eurasia Antiqua* 3:41–180

Perret and Serneels (2006) In: *Proceedings of the 18th Biennial meeting of the society of Africanist Archaeologists*. No volume #

Perret S, Serneels V (2006) Technological characterisation and quantification of a large-scale iron smelting site in Fiko (Dogon plateau, Mali). *Proceedings actes ISA*, pp 453–463

Peters CR, Blumenshine RJ (1995) Landscape perspectives on possible land use patterns for early hominids in the Olduvai Basin. *J Hum Evol* 29:321–362. doi:10.1006/jhev.1995.1062

Peters CR, Blumenshine RJ (1996) Landscape perspectives on possible land use patterns for early Pleistocene hominids in the Olduvai Basin, Tanzania: part II, expanding the landscape models. In: Magori C et al (eds) *Four million years of hominid evolution in Africa: papers in honour of Dr. Mary Douglas Leakey's outstanding contribution in paleoanthropology*. pp 175–221. Kaupia-Darmstädter Beiträge zur Naturgeschichte, 6, Darmstadt

Petrequin P, Errera M, Cassen S, Billard G, Colas C, Maréchal D, Prodé F (2005) Des Alpes italiennes à l'Atlantique au Ve millénaire. Les quatre grandes haches polies de Vendeuil et Maizy (Aisne), Brenouille (Oise). *Rev Archéol Picardie Numéro Spéc* 22(1):75–104

Petrie WMF (1899) Sequences in prehistoric remains. *J Anthropol Inst* 29:295–301

Petrie WMF (1904) *Methods & aims in archaeology*. Macmillan and Company, Limited, London

Pettijohn FJ (1975) *Sedimentary rocks*. Harper and Brothers, New York

Pettijohn FJ, Potter PE, Siever R (1973) *Sand and sandstone*. Springer, Berlin

Peyrony D (1938) La Micoque, les fouilles récentes, leurs significations. *Bull Soc Préhist Fr* 6:257–288

Peyrony D (1950) Qu'est-ce que le Tayacien? *Bull Soc Préhist Fr* 3–4:102

Philpotts AR (1989) *Petrography of igneous and metamorphic rocks*. Prentice Hall, Englewood Cliffs

Picon M, Carre C, Cordoliani ML, Vicky M, Hernandez JC, Mignard MG (1975) Composition of the La Granfensengue, Banassac and Moutans Terra Sigillata. *Archaeometry* 17:191–199

Picouet P, Magnetti M, Piponnier P, Schroer M (1999) Cathodoluminescence spectroscopy of quartz grains as a tool for ceramic provenance. *J Archaeol Sci* 23 (4):619–632

Pigott VC (1999). The archaeometallurgy of the Asian old world, vol 16. U. Penn Museum of Archaeology, Philadelphia, PA

Pike SH (2000) Archaeological geology and geochemistry of Pentelic Marble, Mount Pentelikon, Attica. Unpublished Ph.D. dissertation. University of Georgia

Piperno D (1988) Phytolith analysis: an archaeological and geological perspective. Academic, San Diego, pp 47–49

Pizzuto JE (2012) Predicting the accumulation of mercury-contaminated sediment on riverbanks—an analytical approach. *Water Resour Res* 48(7): W07518. doi:10.1029/2012WR011906

Plog S (1980) Stylistic variation in prehistoric ceramics. Cambridge University Press, Cambridge

Poldervaart A, Hess HH (1951) Pyroxenes in the crystallization of basaltic magma. *J Geol* 59(5):472–489

Pollard AM (ed) (1999) Geoarchaeology: exploration, environments and resources, vol 165, Geological Society Special Publication. Geological Society, Bath

Pollard AM, Heron C (1996) Archaeological chemistry. The Royal Chemical Society, Cambridge

Pollard AM, Wood ND (1986) Development of Chinese porcelain technology at Jingdezhen. In: Olin JS, Blackman MJ (eds) Proceedings of the 24th international archaeometry symposium. Smithsonian Institution Press, Washington, DC, pp 105–114

Pope KO (1986) Review of “Archeology as Human Ecology”. *Geoarchaeology* 1(2):212

Pope F (2014) Dragon sea: a true tale of treasure, archaeology, and greed off the Coast of Vietnam. Houghton Mifflin Harcourt, Boston

Potts R (1998) Variability selection in hominid evolution. *Evol Ecol* 7:81–96

Potts PJ, Webb PC, Watson JS (1985) Energy dispersive x-ray fluorescence analysis of silicate rocks; comparison with wavelength-dispersive performance. *Analyst* 110:507–513

Powell AJ, Mc Donnell JG, Batt CM, Vernon RW (2002) An assessment of the magnetic response of an iron-smelting site. *Archaeometry* 44(4):651–665

Powers MC (1953) A new roundness scale for sedimentary particles. *J Sediment Petrol* 23(2):117–119

Powers AH (1992) Great expectations: a short historical review of European phytolith systematics. In: Mulholland SC, Rapp G Jr (eds) Phytolith systematics: emerging issues. Plenum Press, New York, pp 15–35

Preston D (1997) The lost man. *The New Yorker*, 16 Jun, pp 70–81

Pretola JP (2001) A feasibility study using silica polymorph ratios for sourcing chert and chalcedony lithic materials. *J Archaeol Sci* 28:721–739

Preuschen E (1973) Estrazione minrarie dell'eta dal Bronzo nel Trentino. *Prehist Alpina* 9:113–150

Price TD (ed) (1989) The chemistry of prehistoric human bone. Cambridge University Press, Cambridge, UK

Quinn R (2006) The role of scour in shipwreck site formation processes and the preservation of wreck- associated scour signatures in the sedimentary record—evidence from seabed and sub-surface data. *J Archaeol Sci* 33(10):1419–1432

Quinn PS (2013) Ceramic petrography: the interpretation of archaeological pottery & related artefacts in thin section ceramic petrography. Archaeopress, Oxford, i +254 pp

Radivojevic M (2012) On the origins of metallurgy in Europe: metal production in the Vinca Culture. Doctoral thesis, UCL (University College London)

Ramiro B, Hajduk A, Gil AF, Neme GA, Durán V, Glascock MD, Giesso M, Borrazzo K, de la Paz Pompei M, Salgán ML, Cortegoso V, Villarosa G, Rughini AA (2011) Obsidian in the south-central Andes: geological, geochemical, and archaeological assessment of north Patagonian sources (Argentina). *Quat Int* 245(1):25–36

Ramsey CB (1995) Radiocarbon calibration and analysis of stratigraphy; the OxCal program. *Radiocarbon* 37 (2):425–430

Ramseyer D (1992) Cites lacustres. Editon Du Cedarc, Treignes

Ramseyer K, Fischer J, Matter T, Eberhardt P, Geiss J (1989) A cathodoluminescence microscope for low intensity luminescence. *J Sediment Petrol* 59:619–622

Ramuz CF (1983) Les âmes dans le glacier. La Semaine littéraire, 1^{er} et 8 février 1913, in Nouvelles, croquis et morceaux, vol III. Slatkine, Genève, pp 7–28

Rapp G, Hill CL (1998) Geoarchaeology: the earth-science approach to archaeological interpretation. Yale University Press, New Haven

Rapp G Jr, Hill CL (1998) Geoarchaeology. Yale University Press, New Haven

Rapp GR (2002) Archaeomineralogy (natural science in archaeology series). Springer, Berlin/New York

Rapp G, Hill CL (2006) Geoarchaeology: the Earth Science approach to archaeological interpretation, 2nd edn. Yale University Press, New Haven

Rapp G Jr, Gifford JA (1985) Archaeological geology. Yale University Press, New Haven

Rapp G Jr, Albns J, Henrickson E (1984) Trace element discrimination of discrete sources of copper. In: Lambert JB (ed) Archaeological chemistry III. Am. Chem. Soc., Washington, DC, pp 273–293

Reading HG, Levell BK (1996) Controls on the sedimentary rock record. In: Reading HG (ed) Sedimentary environments: processes, facies and stratigraphy, 3rd edn. Blackwell Science, London

Reagan MJ, Rowlett RM, Garrison EG, Dort W Jr, Bryant VM Jr, Johannsen CJ (1978) Flake tools stratified below Paleo-Indian artifacts. *Science* 200:1272–1275

Reber EA, Evershed RP (2004) How did Mississippians prepare maize? The application of compound-specific carbon isotope analysis to absorbed pottery residues

from several Mississippi valley sites. *Archaeometry* 46(1):19–34

Reckin R (2013) Ice patch archaeology in global perspective: archaeological discoveries from alpine ice patches worldwide and their relationship with paleoclimates. *J World Prehistory* 26(4):323–385

Redman C (1999) Human impact on ancient environments. University of Arizona Press, Tucson

Redmount CA, Morgenstern ME (1996) Major and trace element analysis of modern Egyptian pottery. *J Archaeol Sci*

Reed SJB (1996) Electron microprobe analysis and scanning electron microscopy in geology. Cambridge University Press, Cambridge

Reineck H-E, Singh IB (1975) Depositional sedimentary environments. Springer, New York

Reitz EJ (1982) Availability and use of fish along coastal Georgia and Florida. *Southeast Archaeol* 1(1):65–88

Renfrew C, Bahn PG (1996) Archaeology: theories, methods and practice. Thames & Hudson, London

Renfrew C, Bahn PG (2000) Archaeology: theories, methods and practice. Thames & Hudson, New York

Renfrew C, Gimbutas M, Elster ES (eds) (2003) Excavations at Sitagroi: a prehistoric village in Northeast Greece, vol 2. Cotsen Institute of Archaeology

Renfrew C, Gimbutas M, Elster ES (eds) (2003) Excavations at Sitagroi: a prehistoric village in Northeast Greece, vol 2. Cotsen Institute of Archaeology, Los Angeles

Renfrew C, Bahn PG (2004) Archaeology: theories, methods and practice. Thames & Hudson, London/ New York

Richards JP (2009) Post-subduction porphyry Cu–Au and epithermal Au deposits: products of remelting of subduction-modified lithosphere. *Geology* 37:247–250

Richards JP (2010) Magmatic to hydrothermal metal fluxes in convergent and collided margins. *Ore Geol Rev* 40(2011):1–26

Richards JP (2011) Magmatic to hydrothermal metal fluxes in convergent and collided margins. *Ore Geol Rev* 40(1):1–26

Rietveld HM (1969) A profile refinement method for nuclear and magnetic structures. *J Appl Crystallogr* 2:65–71

Rietz E, Reitz EJ (1988) Evidence for coastal adaptations in Georgia and South Carolina. *Archaeol East North Am* 16:137–158

Reusser I, Bierman P, Rood D (2015) Quantifying human impacts on rates of erosion and sediment transport at a landscape scale. *Geology* 43(2):171–174

Riccardi AC (2009) IUGS ratified ICS recommendation on redefinition of Pleistocene and formal definition of base of quaternary. International Union of Geological Sciences

Rice PM (1987) Pottery analysis: a sourcebook. University of Chicago Press, Chicago

Rice PM (1996a) Recent ceramic analysis 1. Function, style, and origins. *J Archaeol Res* 4:133–163

Rice PM (1996b) Recent ceramic analysis: 2. Composition, production, and theory. *J Archaeol Res* 4:165–202

Rice PM (1999) On the origins of pottery. *J Archaeol Method Theory* 6(1):1–54

Rice PM (1987/2001). *Pottery analysis: a sourcebook*. University of Chicago Press, Chicago

Richter DD, Yaalon D (2012) The changing model of soil revisited. *Soil Sci Soc Am J* 76:766–778

Rick TC, Erlandson JM (2009) Coastal exploitation. *Science* 325(5943):952–953

Rick TC, Erlandson JM, Jew NP, Reeder-Myers LA (2013) Archaeological survey, paleogeography, and the search for Late Pleistocene Paleocoastal peoples of Santa Rosa Island, California. *J Field Archaeol* 38 (4):324–331

Rich FJ (1999) A report on the palynological characteristics of the brown coal samples from the Ennis Mine. Southeastern Section, Geological Society of America Field Guide, pp 24–25

Rigler M, Longo W (1994) High voltage scanning electron microscopy theory and applications. *Microsc Today* 94(5):2

Rinaldo A, Dietrich WE, Rigon R, Vogel GK, Rodriguez-Iturbe I (1995) Geomorphological signatures of varying climate. *Nature* 374:632–635

Ritter DF, Kochel RC, Miller JR (1995) *Process geomorphology*, 3rd edn. Wm. C. Brown, Dubuque

Robbiola L, Fiaud C (1992) Apport de l'analyse statistique des produits de corrosion à la compréhension des processus de dégradation des bronzes archéologiques. *Rev d'Archéométrie* 16:109–119

Robinson JW (1995) *Undergraduate instrumental analysis*, 5th edn. Marcel Dekker, New York

Roberts BW, Thornton CP (2014) Archaeometallurgy in global perspective. Springer, New York

Robertson AH (2006) Contrasting modes of ophiolite emplacement in the Eastern Mediterranean region. *Geol Soc London Memoirs* 32(1):235–261

Roberts BW, Thornton CP (2014) Archaeometallurgy in global perspective. Springer Science+Business Media, New York

Rockwell TK (2000) Use of soil geomorphology in fault studies. In: *Quaternary geochronology: methods and applications*. American Geophysical Union, Washington, DC

Roebroeks W, Villa P (2011) On the earliest evidence for habitual use of fire in Europe. *Proc Natl Acad Sci* 108 (13):5209–5214

Rolland N (2004) Was the emergence of home bases and domestic fire a punctuated event? A review of the Middle Pleistocene record in Eurasia. *Asian Perspect* 43:248–280. doi:[10.1353/asi.2004.0027](https://doi.org/10.1353/asi.2004.0027)

Rono PA (1984) Hydrothermal mineralization at seafloor spreading centers. *Earth Sci Rev* 20:1–104

Roper DC (1990) Protohistoric Pawnee hunting in the Nebraska sand hills: archeological investigations at two sites in the Calamus Reservoir: a report to U.S. Department of the Interior, Bureau of Reclamation, Great Plains Region, Billings

Rostoker RW, Pigott VC, Dvorak J (1989) Direct reduction of copper metal by oxide-sulphide mineral interaction. *Archeomaterials* 3:69–87

Rothenberg B, Merkel J (1995) Late Neolithic copper smelting in the Arabah. *Inst Archaeo-Metall Stud News* 19:1–17

Rovey CW II, Forir M, Balco G, Gaunt D (2010) Geomorphology and paleontology of Riverbluff Cave, Springfield, Missouri. In: Evans KR, Albers JS (eds) *From precambrian rift volcanoes in the Mississippi shelf margin: geological field excursions in the Ozark mountains*. Geological society of america field guide, vol 17. pp 31–38

Rovner I (1983) Major advances in archaeobotany: archaeological uses of phytolith analysis. In: Schiffer MB (ed) *Advances in archaeological method and theory*, vol 6. Academic, New York

Rovner I (1988) Macro-and micro-ecological reconstruction using plant opal phytolith data from archaeological sediments. *Geoarchaeology* 3:155–163

Rovner I (1996a) Personal communication

Rovner I (1996b) Morphometric facts and typological fallacies in Maize Phytolith Taxonomy. Unpublished manuscript

Rowlett RM, Thomas HL, Rowlett ESJ, Stout SD (1982) Stratified iron age house floors on the Titelberg, Luxembourg. *J Field Archaeol* 9(3):301–312

Rowlett RA (1988) Titelberg, a Celtic hillfort in Luxembourg. *Expedition* 30(2):31–40

Russ JC, Rovner I (1989) Stereological identification of opal phytolith populations from wild and cultivated *Zeae*. *Am Antiq* 54(4):784–792

Russell DA, Rich FJ, Schneider V, Lynch-Stieglitz J (2009) A warm thermal enclave in the Late Pleistocene of the South-eastern United States. *Biol Rev* 84:173–202

Rychner V, Kläntschi N (1995) Arsenic, nickel et antimoine. *Cahiers d'Archéologie*. Romande No.63, Tome 1. Lausanne

Rye O (1977) Pottery manufacturing techniques: X-ray studies. *Archaeometry* 19(2):205–210

Rye R, Holland HD (1998) Paleosols and the evolution of the atmospheric atmosphere: a critical review. *Am J Sci* 298:621–672

Sackett J (2011) Francois Bordes and the old stone age. *Backdirt, the Annual Review of the Cotsen Institute of Archaeology*. UCLA

Sackett J (1999) The archaeology of Solvieux: an Upper Paleolithic open air site in France (No. 19). Cotsen Institute of Archaeology

Salmon WC (1967) The foundations of scientific inference. University of Pittsburgh Press, Pittsburgh

Salmon WC (1982) Causality in archaeological explanation. In: Renfrew C, Rowlands MJ, Seagraves BA (eds) *Theory and explanation in archaeology*. Academic, Orlando, pp 45–55

Salvador A (1994) International stratigraphic guide: a guide to stratigraphic classification, terminology and procedure. IGUS, Trondheim

Samford P (1997) Response to the market: dating English underglaze transfer printed wares. *Hist Archaeol* 31 (2):1–30

Sandweiss DH, Solís RS, Moseley ME, Keefer DK, Ortloff CR (2009) Environmental change and economic development in coastal Peru between 5,800 and 3,600 years ago. *Proc Natl Acad Sci* 106 (5):1359–1363

Sasaki Y (1989) Two-dimensional joint inversion of magnetotelluric and dipole-dipole resistivity data. *Geophysics* 54:254–262

Sassaman KE (1993) Early pottery in the southeast: tradition and innovation in cooking technology. University of Alabama Press, Tuscaloosa

Sassaman KE, Anderson DG (1996) *Archaeology of the mid-Holocene Southeast*. University of Florida Press, Gainesville

Sassaman KE (2004) Complex hunter-gatherers in evolution and history: a North American perspective. *J Archaeol Res* 12(3):227–280

Sauer C (1925) The morphology of landscape. In: University of California Publications in Geography, vol 22. pp 19–53

Saunders R, Russo M (2011) Coastal shell middens in Florida: a view from the archaic period. *Quat Int* 239 (1–2):38–50

Sauter MR (1976) Switzerland from earliest times to the roman conquest. Thames and Hudson, London

Sayre EV, Dodson RW (1957) Neutron activation study of Mediterranean potsherds. *Am J Archaeol* 61:135–141

Schiffer MB (1972) Archeological context and systemic context. *Am Antiq* 37:156–165

Schiffer MB (1982) Hohokam chronology: an essay on history and method. In *Hohokam and Patayan: Prehistory of Southwestern Arizona*. Academic Press, New York, pp 299–344

Schiffer MB (1983) Toward the identification of formation processes. *Am Antiq* 48:675–706

Schiffer MB (1986) *Behavioral archaeology*. Academic, New York

Schiffer MB (1987) Formation processes of the archaeological record. University of New Mexico Press, Albuquerque

Schiffer MB (1988) The effects of surface treatment on permeability and evaporative cooling effectiveness of pottery. In: Farquhar RM, Hancock RGV, Pavlish LA (eds) *Proceedings of the 26th International Archaeometry Symposium*. University of Toronto, Toronto, pp 23–29

Schiffer MB (1976) Behavioral archeology. Academic, New York

Schiffer MB (1999) Behavioral archaeology: some clarifications. *Am Antiq* 64:166–168

Schiffer MB (1990) Technological change in water-storage and cooking pots: some predictions from experiment. In: *The changing roles of ceramics in society: 26,000 BP to the present*, vol 5. The American Ceramic Society, Inc, Westerville, pp 119–136

Schmidt PD (1978) Historical archaeology: a structural approach in an African Culture. Greenwood Press, Westport

Schmidt PR (1981) The origins of iron smelting in Africa: a complex technology in Tanzania (No. 1). Department of Anthropology, Brown University, Providence, RI

Schmidt P, Praz G, Slodczyk A, Bellot-gurlet L, Archer W, Miller CE (2012) Heat treatment in the Middle Stone Age (MSA): temperature induced transformations of silcrete and their technological implications. *J Archaeol Sci* 39(1):135–144

Schnellmann M, Anselmetti FS, Giardini D, Mckenzie JA (2006) 15,000 years of mass-movement history in Lake Lucerne: implications for seismic and tsunami hazards. *Eclogae Geol Helv* 99(3):409–428

Schroeder WA (1967) Geography through maps. The eastern Ozarks: a geographic interpretation of the Rolla 1:250,000 topographic Map. Special publication No. 13. National Council for Geographic Education, Illinois State University, Normal

Schuldenrein J (1991) Coring and the identity of cultural-resource environments: a comment on Stein. *Am Antiq* 56:131–137

Schuldenrein J (1995) Geochemistry, phosphate fractionation, and the detection of activity areas at prehistoric North American sites. Pedological perspectives in archaeological research. *Soil Science Society of America Special Publication* 44

Schuldenrein J (2007) The emergence of geoarchaeology in research and cultural resource management: part II. *SAA Archaeol Rec* 7(1):16–24

Scollar I, Weidner B, Segeth K (1986) Display of archaeological magnetic data. *Geophysics* 51:623–634

Scollar IB (1990) Archaeological prospecting, image processing, and remote sensing. Cambridge University Press, New York

Scott DA (2001) The application of scanning X-ray fluorescence microanalysis in the examination of cultural materials. *Archaeometry* 43(4):475–482

Schwartz HP, Liritzis Y, Dixon A (1980) Absolute dating of travertines from the Petralona Cave, Khalkidiki Peninsula, Greece. *Anthropos* 7:152–173

Seaman JC, Bertsch PM, Strom RN (1997) Characterization of colloids mobilized from southeastern coastal plain sediments. *Environ Sci Technol* 31(10):2782–2790

Seaver KA (1996) The frozen echo. Greenland and the exploration of north America ca. AD 1000–1500. Stanford University Press, Stanford

Sealy JC, Van der Merwe NJ (1985) Isotopic assessment of human diets in the southwestern Cape, South Africa. *Nature* 315:138–140

Seidov D, Maslin MA (1999) Collapse of the north Atlantic deep water circulation during the Heinrich events. *Geology* 27:23–26

Selley RC (1978) Ancient sedimentary environments, 2nd edn. Cornell Univ. Press, Ithaca

Semenov SA (1964) Prehistoric technology. Cory. Adams and Mackay, London

Shackley ML (1975) Archaeological sediments: a survey of analytical methods. Wiley, New York

Shackley MS (1998) Gamma rays, x-rays and stone tools: some recent advances in archaeological geochemistry. *J Archaeol Sci* 25:259–270

Shackley MS (ed) (2011a) X-ray fluorescence spectrometry (XRF) in geoarchaeology. Springer, New York

Shackley MS (2011b) An introduction to X-ray fluorescence (XRF) analysis in archaeology. In: Shackley MS (ed) X-ray fluorescence spectrometry (XRF) in geoarchaeology. Springer, New York, pp 7–44

Shane LCK (1992) Palynological procedures (draft). University of Minnesota, Minneapolis

Sharma PV (1997) Environmental and engineering geophysics. Cambridge University Press, Cambridge

Shepard AO (1936) The technology of Pecos pottery. In: Kidder AV, Shepard AO (eds) Glaze-paint, culinary and other wares, vol II, The Pottery of Pecos. Yale University Press, New Haven, pp 389–588

Shepard AO (1942) Rio Grande glaze-paint ware. A study illustrating the place of ceramic technological analysis in archaeological research. Publication 528. Carnegie Institution of Washington, Washington, DC

Shepard AO (1954) Ceramics for the archaeologist, Carnegie Institution of Washington Publication 609. Carnegie Institution, Washington, DC

Shepard AO (1956) Ceramics for the archaeologist, vol 609. Carnegie Institution of Washington, Washington, DC, p 1971

Shepard AO (1966) Rio Grande glaze-paint pottery: a test for petrographic analysis. In: Matson FR (ed) Ceramics and man, vol 41, Viking Fund Publications in Anthropology. Wenner-Gren Foundation, New York, pp 62–87

Sherwood SC (2001) Microartifacts. In: Goldberg P, Holliday VT, Ferring CR (eds) Earth sciences and archaeology. Kluwer Academic/Plenum Publishers, New York, pp 327–351

Sherratt S (2000) Catalogue of Cycladic antiquities in the Ashmolean Museum: the captive spirit, vol 1. Oxford University Press, Oxford

Shimada I (2000) The late Prehispanic coastal states. In: Minelli LL (ed) The Inca world. University of Oklahoma Press, Norman, pp 49–64, 97–110

Shimada I, Merkel J (1991) Copper-alloy metallurgy in ancient Peru. *Sci Am* 265:80–86

Shimelmitz R, Kuhn SL, Jelinek AJ, Ronen A, Clark AE, Weinstein-Evron M (2014) ‘Fire at will’: the emergence of habitual fire use 350,000 years ago. *J Hum Evol* 77:196–203

Shopov YY, Ford DC, Schwarz HP (1994) Luminescent microbanding in speleothems: high resolution chronology and paleoclimate. *Geology* 22:407–410

Shott MJ (2010) Size dependence in assemblage analysis measure: essentialism, materialism and “SHE” analysis in archaeology. *Am Antiq* 75(4):886–906

Shoval S, Beck P (2005) Thermo-FTIR spectroscopy analysis as a method of characterizing ancient ceramic technology. *J Therm Anal Calorim* 82:609–616

Shuter E, Teasdale WE (1989) Techniques of water-resources investigations of the United States geological survey, chapter F1: application of drilling, coring, and sampling to test holes and wells. U.S. Geological Survey, Washington, DC

Simpson IA, Milek KB, Gudmundsson G (1999) A reinterpretation of the great pit at Hofstadir, Iceland, using sediment thin section micromorphology. *Geoarchaeology* 14:511–530

Sinclair PJJ, Pikirayi I, Pwiti G, Soper R (1993) Urban trajectories on the Zimbabwean plateau. In: Shaw T, Sinclair P, Andah B, Okpoko A (eds) *The archaeology of Africa: food, metals and towns*. Routledge, London and New York, pp 705–731

Skaggs S (2007) Lead isotope analysis of Roman curse tablets. In: Glasscock M, Speakman RJ, Popelka-Filcoff RS (eds) *Archaeological chemistry: analytical techniques and archaeological interpretation*, vol 969, ACS Symposium Series. American Chemical Society, Washington, DC, pp 311–335

Skaggs S, Norman N, Garrison E, Coleman D, Bouhlel S (2012) Local mining or lead importation the Roman province of Africa Proconsularis? Lead isotope analysis of curse tablets from Roman Carthage, Tunisia. *J Archaeol Sci* 39(4):970–983

Skarda R (2007) Scull shoals: the mill village that vanished in Old Georgia. Old Oconee Books, Buckhead

Skibo JM, Schiffer MB, Reid KC (1989) Organic-tempered pottery: an experimental study. *Am Antiq* 54:122–146

Skibo JM, Schiffer MB (1995) The clay cooking pot: an exploration of women's technology. In: Skibo JM, Walker WH, Nielsen AE (eds) *Expanding archaeology*. University of Utah Press, Salt Lake City, pp 80–91

Skibo JM, Feinman GM (1999) *Pottery and people: a dynamic interaction*. University of Utah Press, Salt Lake City

de Sieveking G, Bush P, Ferguson J, Craddock PT, Hughes MJ, Cowell MR (1972) Prehistoric flint mines and their identification as sources as raw materials. *Archaeometry* 14:151–176

Sigurdsson H (1999) *Melting the earth: the history of ideas on volcanic eruptions*. New York, Oxford

Sinclair PJJ (1991) Archaeology in eastern Africa: an overview of current chronological issues. *J Afr Prehist* 32:179–219

Sinclair PJJ, Petré M (nd) Exploring the interface between modern and traditional information systems: the case of Great Zimbabwe. Unpublished ms. Sub Department of African and Comparative Anthropology. Uppsala University, Sweden

Singer MJ, Janitsky P (eds) (1986) Field and laboratory procedures used in a soil chronosequence study. U.S. Geological Survey Bulletin 1648. Geological Survey, Washington, DC

Singleton KL, Odell GH, Harris TM (1994) Atomic absorption spectrometry analysis of ceramic artefacts from a protohistoric site in Oklahoma. *J Archaeol Sci* 21:343–358

Sinopoli C (1991) *Approaches to archaeological ceramics*. Plenum, New York

Sikes NE (1994) Early hominid habitat preferences in East Africa: paleosol carbon isotopic evidence. *J Hum Evol* 27(1):25–45

Sjöberg A (1976) Phosphate analysis of anthropic soils. *J Field Archaeol* 3:447–454

Smith GA, Pun A (2006) *How does earth work?: physical geology and the process of science*. Pearson-Prentice Hall, Upper Saddle River

Smith MP (1964) Georgia petroglyphs. *Archaeology* 17 (1):54–56

Smith GD, Clark RJ (2004) Raman microscopy in archaeological science. *J Archaeol Sci* 31(8):1137–1160

Smith GD, Clark RJH (2004) Raman spectroscopy in archaeological science. *J Archaeol Sci* 31:1137–1160

Sneath PHA, Sokal RR (1973) *Numerical taxonomy: the principles and practice of numerical classification*. W.F. Freeman, San Francisco

Sohl NF, Owens JP (1991) *Cretaceous stratigraphy of the Carolina coastal plain. The geology of the Carolinas*. The University of Tennessee Press, Knoxville, pp 191–220

Soil and Plant Analysis Council, Inc (2000) *Soil analysis: handbook of reference methods*. CRC Press, Boca Raton

Soil Survey Division Staff (1993) *Soil survey manual. USDA Handbook*, vol 18. Washington, DC, p 138

Sojka RE, Carter DL, Brown MJ (1992) Imhoff cone determination of sediment in irrigation runoff. *Soil Sci Soc Am J* 56(3):884–890

Sokal RR, Rohlf FJ (eds) (1981) *Biometry*, 2nd edn. W.H. Freeman, New York. Spectroscopy of quartz grains as a tool for ceramic provenance. *J Archaeol Sci* 26(8):943–949

Soukup DA, Buck BJ, Harris W (2008) Preparing soils for mineralogical analyses. In: Ulery AL, Drees LR (eds) *Methods of soil analysis part 5—mineralogical methods*, SSSA book series 5.5. Soil Science Society of America, Madison/Aukeny

Souckova-Sigelová J (2001) Treatment and usage of iron in the Hittite Empire in the 2nd millennium BC. *Mediterranean Archaeol* 1:189–193

Speakman, Hunt (2014)

Speakman RJ, Neff H (eds) (2005) *Laser ablation-ICP-MS in archaeological research*. University of New Mexico Press, Albuquerque

Speakman RJ, Little NC, Creel D, Miller MR, Iñáñez JG (2011) Sourcing ceramics with portable XRF spectrometers? A comparison with INAA using Mimbres pottery from the American Southwest. *J Archaeol Sci* 38(12):3483–3496

Spindler K (1994) The man in the ice. Harmony, New York

Stahlschmidt MC, Miller CE, Ligouis B, Hambach U, Goldberg P, Berna F, Richter D, Urban B, Serangeli J, Conard NJ (2015) On the evidence for human use and control of fire at Schöningen. *J Hum Evol* 89:181–201, <http://dx.doi.org/10.1016/j.jhevol.2015.04.040>

Stanjek H, Häusler W (2004) Basics of x-ray diffraction. *Hyperfine Interact* 154(1–4):107–119

Starr JL, Parkin TB, Meisinger JJ (1995) Influence of sample-size on chemical and physical soil measurements. *Soil Sci Soc Am J* 59(3):713–719

Steier P, Rom W (2000) The use of Bayesian statistics for ¹⁴C dates of chronologically ordered samples: a critical analysis. *Radiocarbon* 42(2):183–198

Stein JK, Teltscher PA (1989) Size distributions of artifact classes: combining macro- and micro-fractions. *Geoarchaeology* 4:1–30

Stein JK (1993) Scale in archaeology, geosciences, and geoarchaeology. In: Stein JK, Linse AR (eds) Effects of scale on archaeological and geoscientific perspectives, Geological Society of America Special Paper 283. Geological Society of America, Boulder

Stein JK (1986) Coring archaeological sites. *Am Antiquity* 51:505–527

Stein JK (1987) Deposits for archaeologists. *Adv Archaeol Meth Theory* 11:337–395

Stein JK (1988) Interpreting sediments in cultural settings. In: Stein JK, Farrand WR (eds) Archaeological sediments in context. Center for the Study of Man, Orono, pp 5–19

Stein JK (1991) Coring in CRM and archaeology: a reminder. *Am Antiquity* 56:131–137

Stein JK, Farrand WR (eds) (1998) Archaeological sediments in context. Center for the Study of Early Man, Orono

Stein JK, Farrand WR (1985) Context and geoarchaeology: an introduction. In: Archaeological sediments in context. Orono, Center for the Study of Early Man, pp 1–4

Stein JK, Farrand WR (2001) Sediments in archaeological context. The University of Utah Press, Salt Lake City

Stein JK, Linse AR (eds) (1993) Effects of scale on archaeological and geoscientific perspectives, Geological Society of America Special Paper, 283. Geological Society of America, Boulder

Steinmann G (1927) Die ophiolitischen Zonen in den mediterranen Kettengebirgen, translated and reprinted by Bernoulli and Friedman. In: Dilek, Newcomb (eds) Ophiolite concept and the evolution of geologic thought. Geological Society of America Special Publication 373, 77–91

Stevens PR, Walker TW (1970) The chronosequence concept and soil formation. *Q Rev Biol* 45 (4):333–350

Stewart JD, Fralick P, Hancock RGV, Kelley JH, Garrett EM (1990) Petrographic analysis and INAA geochemistry of prehistoric ceramics from Robinson Pueblo, New Mexico. *J Archaeol Sci* 17:601–625

Stiner MC, Goldberg P (2000) Long gone or never was? Infrared and macroscopic data on bone diagenesis in Hayonim Cave (Israel). *J Hum Evol* 38(3):A29–A30

Stiner MC, Gopher A, Barkai R (2011) Hearth-side socioeconomics, hunting and paleoecology during the late Lower Paleolithic at Qesem Cave, Israel. *J Hum Evol* 60(2):213–233

Stockinger G (2013) Abandoned colony in Greenland: archaeologists find clues to Viking mystery. *Der Spiegel International*, 2

Stoltman JB (1989) A quantitative approach to the petrographic analysis of ceramic thin sections. *Am Antiquity* 54:147–160

Stoltman JB (1991) Ceramic petrography as a technique for documenting cultural interaction: an example from the upper Mississippi Valley. *Am Antiquity* 56 (1):103–120

Stoltman JB (2001) The role of petrography in the study of archaeological ceramics. In: Goldberg P, Holliday VT, Ferring CR (eds) Earth sciences and archaeology. Springer, New York, pp 297–326

Stone JFS (1948) The Stonehenge cursus and its affinities. *Archaeol J* 104:7–19

Stos-Gale ZA (1995) Isotope archaeology—a review. In: Beavis J, Barker K (eds) Science and Site. Bournemouth University. Occasional Paper 1

Streckeisen A (1979) Classification and nomenclature of volcanic rocks, lampropyres, carbonatites, melilitic rocks: recommendations and suggestions of the IUGS subcommission or the systematics of igneous rocks. *Geology* 7:331–335

Straight MJ (1986a) Evaluation of archaeological site potential on the Gulf of Mexico continental shelf using high-resolution seismic data. *Geophysics* 51 (3):605

Straight MJ (1986b) Human occupation of the continental shelf during the Late Pleistocene/early Holocene: methods for site location. *Geoarchaeology* 1 (4):347–363

Straight MJ (1990) Archaeological sites on the North American continental shelf. *Archaeol Geol N Am* 439–465

Straight MJ (1995) Archaic period sites on the continental shelf of north America: the effect of relative sea-level changes on archaeological site locations and preservation. In: Bettis EA III (ed) Archaeological geology of the archaic period in North America, Geological Society of America Special Paper 297. Geological Society of America, Boulder, pp 131–148

Stubbs CCA, Sautter L, Scott HM (2007) The transect river channel: sonar and scuba exploration of an ancient river. Poster presentation, Southeastern Section Meeting of the Geological Society of America, Savannah, Georgia, March 29th

Struve GA (1835) De silica in *plantis nonnullis*. PhD dissertation. University of Berlin

Stuiver M, Reimer PJ, Braziunas TF (1998) High precision radiocarbon age calibration for terrestrial and marine samples. *Radiocarbon* 40(3):1041–1083

Sullivan AP (1984) Design styles and Cibola whiteware: examples from the grasshopper area, east-central Arizona. In: Sullivan AP, Hantman JL (eds) *Regional analysis of prehistoric ceramic variation: contemporary studies of the Cibola whitewares*, Anthropological Research Papers No. 31. Arizona State University, Tempe, pp 74–93

Sullivan AP (1988) Prehistoric southwestern ceramic manufacture: the limitations of current evidence. *Am Antiq* 53:23–35

Susino GJ (2010) Optical dating and lithic microwaste—archaeological applications. *Quat Geochronol* 5 (2–3):306–310

Sveinbjarnardóttir G (1992) Farm abandonment in medieval and post-medieval Iceland: an interdisciplinary study. *Oxbow Monograph*, Oxford

Swartz CH, Ulery AL, Gschwend PM (1997) An AEM-TEM study of nanometer-scale mineral associations in an aquifer sand: implications for colloid mobilization. *Geochim Cosmochim Acta* 61(4):707–718

Szymański JE, Tsourlos P (1993) The resistive tomography technique for archaeology: an introduction and review. *Archaeologia Polona* 31:5–32

Takahashi H, McSwiggen P, Nielsen C (2014) A unique wave-length dispersive soft x-ray emission spectrometer for electron probe x-ray microanalyzers. *Microsc Anal* 28(7):S5–S8

Tarbuck EJ, Lutgens FT (1987) *The earth*, 2nd edn. Merrill Publishing, Columbus

Tarbuck EJ, Lutgens FK (1984) *Earth: an introduction to physical geology*. Prentice Hall, Upper Saddle River

Tarbuck EJ, Lutgens FK (1996) *Earth: an introduction to physical geology*. Prentice Hall, Upper Saddle River

Terauchi M, Yamamoto H, Tanaka M (2001) Development of a sub-eV resolution soft x-ray spectrometer for a transmission electron microscope. *J Electron Microsc (Tokyo)* 50(2):101–1054

Thieme H (1997) Palaeolithic hunting spears from Germany. *Nature* 385:807–810

Thieme H (2003) Lower Palaeolithic sites at Schoningen, Lower Saxony, Germany. *BAR Int Ser* 1115:9–28

Thieme DM, Schuldenrein J (1998) Wyoming valley landscape evolution and the emergence of the Wyoming valley culture. *Pennsylvania Archaeol* 68 (2):1–17

Thieme DM (2006) Bounding discontinuities in Susquehanna Valley Alluvium using stratigraphy to reconstruct prehistoric landscapes and archaeological site formation. *Geol Soc Am Abstr Prog* 38(7):453

Thomas DH (1976) *Figuring anthropology*. Holt, Rinehart and Winston, New York

Thomas DH (1998a) St. Catherines: an island in time. Georgia Endowment for the Humanities, Atlanta

Thomas DH (1998b) *Archaeology*, 3rd edn. Harcourt Brace, Fort Worth

Thomas DH, Andrus CFT, Bishop GA, Blair E, Blanton DB, Crowe DE, DePratter CB, Dukes J, Francis P Jr, Guerrero D, Hayes RH, Kick M, Larsen CS, Licate C, Linsley DM, May JA, Sanger MC, Saunders R, Semon A (2008) Native American landscapes of St. Catherines Island, Georgia. Part 3; *Anthropological papers of the American Museum of Natural History*, no. 88, pt. 3, New York

Thomas DH, Sanger M, Anderson DG (2010) Trend, tradition, and turmoil: what happened to the southeastern archaic? In: Thomas DH, Sanger M (eds) *Proceedings of the Third Caldwell Conference, St. Catherines Island, Georgia, 9–11 May 2008. Anthropological Papers of the American Museum of Natural History*, no. 93, New York

Thompson VD, Worth JE (2011) Dwellers by the sea: native American adaptations along the southern coasts of eastern North America. *J Archaeol Res* 19(1):51–101

Thoms AV (1995) Sediments and natural site formation processes at 41JT5. In: Carlson SB (ed) *The Anson Jones plantation archaeological and historical investigations at 41JT5 and 41JT6, Washington County, Texas, Reports of Investigations No. 2*. Center for Environmental Archaeology, Texas A&M University, College Station

Thoms AV (2007) Fire-cracked rock feature on sandy landforms in the Northern Rocky Mountains: toward establishing reliable frames of reference for assessing site integrity. *Geoarchaeol Int J* 22(5):47–510

Thomson CW (1877) *The voyage of the 'Challenger'. The Atlantic. A preliminary account of the general results of the exploring voyage of H.M.S. Challenger during the year 1873 and the early part of the year 1876. Volume 2*. MacMillan and Co. Digital Edition published in 2014. Cambridge University Press

Thorarinsson S (1944) *Tefrokronologiska studier på Island*. *Geogr Ann* 26:1–217

Till JL, Guyodo Y, Lagroix F, Morin G, Ona-Nguema G (2015) Goethite as a potential source of magnetic nanoparticles in sediments. *Geology* 43(1):75–78

Tilston M, Arnott RW, Rennie CD, Long B (2015) The influence of grain size on the velocity and sediment concentration profiles and depositional record of turbidity currents. *Geology* 43(9):839–842

Tite M, Mullins C (1969) Electromagnetic surveying: a preliminary investigation. *Prospezioni Archeol* 4:95–124

Tite MS (1972) *Methods of physical examination in archaeology*. Seminar Press, London

Tite MS (1992) The impact of electron microscopy on ceramic studies. In: Pollard AM (ed) *New developments in archaeological science*. Oxford University Press, London, pp 111–131

Tite MS, Linington RE (1975) Effects of climate on the magnetic susceptibility of soils. *Nature* 256:565–566

Tite MS, Maniatis Y (1975) Examination of ancient pottery using the scanning electron microscope. *Nature* 257:122–123

Tite MS (1995) Firing temperature determinations—how and why? In: Lindahl A, Stilborg O (eds) *The aim of laboratory analyses of ceramics in archaeology*, Kungl. Vitterhets Historie och Antikvitets Akademien Konferenser 34, Stockholm, pp 37–42

Tite M (1999) Pottery production, distribution, and consumption: the contribution of the physical sciences. *J Archaeol Method Theory* 6(3):181–233

Tite MS, Maniatis Y, Meeks ND, Bimson M, Hughes MJ, Leppard SC (1982) 3. Technological studies of ancient ceramics from the Near East, Aegean, and southeast Europe. In: Early pyrotechnology: the evolution of the first fire-using industries. Papers presented at a seminar on early pyrotechnology held at the Smithsonian Institution, Washington, DC, and the National Bureau of Standards, Gaithersburg, Maryland, 19–20 April 1979. One of the Smithsonian Institution-National Bureau of Standards seminars on the application of the Materials and Measurement Sciences to Archeology and Museum Conservation, organized by Franklin D. Alan and Jacqueline S. Olin, pp 61–71. Smithsonian Institution Press

Titterington PF (1935) Certain, bluff mounds of western Jersey County, Illinois. *Am Antiqu* 1(1):646

Tobias PV (1991) Olduvai Gorge, vol. 4a and 4b: the skulls, endocasts and teeth of homo habilis. Cambridge University Press, Cambridge, UK

Toom DL, Kvamme KL (2002) The “big house” at Whistling Elk Village (39HU242): geophysical findings and archaeological truths. *Plains Anthropol* 47:5–16

Topographic Science Working Group (1988) Topographic science working group report to the land processes branch. Earth Science and Applications Division, NASA Headquarters

Tourloukis V, Karkanas P (2012) Geoarchaeology in Greece: a review. *J Virtual Explorer* 42:4

Trimble S (1974) Man-induced soil erosion on the southern piedmont 1700–1970. Soil Conservation Society of America, Aukeny

Tringham R, Cooper G, Odell G, Voytek B, Whitman A (1974) Experimentation in the formation of edge damage: a new approach to lithic analysis. *J Field Archaeol* 1(1–2):171–196

Tripp AC, Hohmann GW, Swift CM Jr (1984) Two-dimensional resistivity inversion. *Geophysics* 49:1708–1717

Tri BM, Nguyen-Long K (2001) Vietnamese blue and white ceramics. The Social Sciences Publishing House, Hanoi

Truncer J (2004) Steatite vessel age and occurrence in temperate eastern North America. *Am Antiqu* 69:487–513

Tukey JW (1977) Exploratory data analysis. Addison-Wesley, Reading

Turner G, Siggins AF, Hunt LD (1993) Ground penetrating radar—will it clear the haze at your site? *Explor Geophys* 24:819–832

Twiss PC, Suess E, Smith RM (1969) Morphological classification of grass phytoliths. *Proc Soil Sci Soc Am* 33:109–115

Twiss PC (2001) A curmudgeon’s view of grass phytolithology. In: Meunier JD, Colin F (eds) Phytoliths: applications in earth sciences and human history. A.A. Balkema Pub, Lisse

Tykot RH (1996) Mediterranean islands and multiple flows: the sources and exploitation of Sardinian obsidian. In: Shackley MS (ed) Methods and theory in archaeological obsidian studies. Plenum, New York

Ure AM (1991) Atomic absorption and flame emissin spectrometry. In: Smith KA (ed) Soil analysis: modern instrumental techniques, vol 2, 2nd edn. Marcel Dekker, New York, pp 1–62

Valentine KWG, Dalrymple JB (1976) Quaternary buried paleosols: a critical review. *Quat Res* 6:209–222

Vance ED (1985) Potential of microartifacts other than microdebitage. Paper presented at the 50th Annual Meeting of the Society for American Archaeology, Denver

Vance ED (1986) Microdebitage analysis in activity analysis: an application. *Northwest Anthropol Res Notes* 20:179–189

Vance ED (1987) Microdebitage and archaeological activity analysis. *Archaeology* 40:58–59

Van der Leeuw SE, the Archaeomedes Research Team (2005) Climate, hydrology, land use, and environmental degradation in the lower Rhone Valley during the Roman period. *Compt Rendus Geosci* 337:9–27

Van der Boggard P, Schmincke HU (1985) Laacher See Tephra: a widespread isochronous late Quaternary tephra layer in central and northern Europe. *Geol Soc Am Bull* 96(12):1554–1571

Van der Plas L, Tobi AC (1965) A chart for judging the reliability of point counting results. *Am J Sci* 263:87–90

van der Merwe NJ, Avery DH (1982) Pathways to steel. *Am Sci* 70:146–155

van der Merwe NJ, Avery DH (1987) Science and magic in African technology: traditional iron smelting in Malawi. *Africa* 57(2):143–172

Van der Merwe NJ (1992) Light stable isotopes and the reconstruction of prehistoric diets. New developments in archaeological science. Oxford University Press, pp 247–264

Vanderford CF (1897) The soils of Tennessee. *Bull Tenn Agric Ext Station* 10:31–139

Vandiver P (2001) The role of materials research in ceramics and archaeology. *Ann Rev Mater Res* 31 (1):373–385

Vandiver P (1988) The implications of variation in ceramic technology: the forming of Neolithic storage vessels in China and the Near East. *Archaeomaterials* 2:139–174

Vandiver PB, Soffer O, Klima B, Svoboda J (1989) The origins of ceramic technology at Dolni Věstonice, Czechoslovakia. *Science* 246(4933):1002–1008

Vaughn SJ (1990) Petrographic analysis of the early Cycladic wares from Akrotiri, Thera. In: Hardy DA (ed) Thera and the Aegean World III, Vol. 1: archaeology. Thera Foundation, London, pp 470–487

Vaughn SJ (1991) Material and technical characterization of Base Ring Ware: a new fabric technology. In: Barlow JA, Bolger DL, Kling B (eds) Cypriot ceramics: reading the prehistoric record, University Museum Monograph 74. University of Pennsylvania, Philadelphia, pp 199–130

Velde B, Druc IC (1998) Archaeological ceramic materials. Springer, Berlin

Verhoogen J (1969) Magnetic properties of rocks. *Geophys Monogr* 13:627–633

Vincent WF, Bertola C (2012) François Alphonse FOREL. *Archives des Sciences* 65:51–64

Vineyard JD, Feder GL (1982) Springs of Missouri, revised edn. WR29. Missouri Geological Survey and Water Resources, Jefferson City, MO

Vitali W, Franklin UM (1986) New approaches to the characterization and classification of ceramics on the basis of their elemental composition. *J Archaeol Sci* 13:161–170

Vitousek PM, Chadwick OA, Crews TE, Fownes JA, Hendricks DM, Herbert D (1997) Soil and ecosystem development across the Hawaiian Islands. *GSA Today* 7:1–8

Vineyard JD, Feder GL (1988) Springs of Missouri. Missouri Geological Survey and Water Resources, Rolla

Vita-Finzi C, Stringer C (2007) The setting of the Mt. Carmel caves reassessed. *Quat Sci Rev* 26 (3):436–440

Vogt G (1900) Studies on Chinese porcelain. *Bull Soc d'Encouragement pour l'Industrie Nat Paris* 99:530–612 [In French; English translation by and in Tichane, 1983]

Weber-Tièche I, Sordolillet D (2008) Plateau de Bevaix, 4. Etude géologique en contexte archéologique. Neuchâtel

Wagner GA (1998) Age determination of young rocks and artifacts. Springer, Berlin

Wagner U, Wagner FE, Riederer J (1986) The use of Mossbauer spectroscopy in archaeometric studies. In: Olin JS, Blackmann MJ (eds) Proceedings of the 1984 International Symposium on Archaeometry. Smithsonian Institution Press, Washington, DC, pp 129–142

Walderhaug O, Rykkje J (2000) Some examples of the effect of crystallographic orientation on cathodoluminescence colors of quartz. *J Sediment Res* 70:545–548

Walker RG (ed) (1980) Facies models: geoscience Canada, reprint series 1. Geological Society of Canada, Toronto

Wall H, Polyakova E, Jacobberger R, Arnold M (2014) Uncovering the characteristics of the chemical vapor deposition of graphene with rapid Raman imaging. *Microsc Anal* 28(96):18–20

Wallace WA (1981) The philosophical setting of medieval science. In: Prelude to Galileo. Springer Netherlands, pp 3–28

Waltham D (1994) Mathematics: a simple tool for geologists. Chapman and Hall, London

Ward G (1974) A systematic approach to the definition of sources of raw material. *Archaeometry* 16:55–63

Warren P (1988) Crete: the Minoans and their gods. In: Cunliffe B (ed) Origins. The Dorsey Press, Chicago

Warrick AW, Meyers DE, Nielsen DR (1986) Geostatistical methods applied to soil science. Methods of soil analysis, part I. *Agronomy Monograph* no. 9, 2nd edn. Washington, DC

Warwick FV, Bertola C (2012) François Alphonse Forel and the oceanography of lakes. *Arch Sci* 65:51–64

Wascher HL, Alexander JD, Ray BW, Beavers AH, Odell RT (1960) Characteristics of soils associated with glacial tills in northeastern Illinois. University of Illinois, Agricultural Station, Bulletin No. 665. Champaign-Urbana

Waters MR (1992) Principles of geoarchaeology: a north American perspective. University of Arizona Press, Tucson

Weaver W (2002) Paleoecology and prehistory: fossil pollen at Gray's Reef National Marine Sanctuary, Georgia. Unpublished Masters Thesis. The University of Georgia, Athens

Weems RE, Edwards LE (2001) Geology of oligocene, miocene and younger deposits in Coastal Georgia. Georgia Geologic Survey Bulletin 131. Department of Natural Resources, Environmental Protection Division. 124 p

Weems RE, Lewis WA (2002) Structural and tectonic setting of the Charleston, South Carolina, region: evidence from the tertiary stratigraphic record. *Geol Soc Am Bull* 114(1):24–42

Weiner S, Goldberg P, Bar-Yosef O (1993) Bone preservation in Kebara Cave, Israel using on-site Fourier transform infrared spectroscopy. *J Archaeol Sci* 20 (6):613–627

Weiner S, Xu Q, Goldberg P, Liu J, Bar-Yosef O (1998) Evidence for the use of fire at Zhoukoudian, China. *Science* 281(5374):251–253

Wenner D, van der Merwe N (1987) Mining for the lowest grade ore: traditional iron production in northern Malawi. *Geoarchaeology* 2(3):199–216

Wells EW III, Sherwood SC, Hollenbach KD (2015) Soapstone vessel chronology and function in the soutehr Appalachians of eastern Tennessee: the Apple Barn site (40BT90) assemblage. *Southeast Archaeol* 33:153–167

Wendorf F (nd) From under desert sands. In: Parry JT (ed) Manual of remote sensing. The American Society of Photogrammetry and Remote Sensing, Bethesda

Wendorf F, Krieger AD, Albritton CC, Stewart TD (1955) The midland discovery. University of Texas Press, Austin

Wendorf F, Close AE, Schild R (1987) A survey of the Egyptian radar channels: example of applied archaeology. *J Field Archaeol* 14:43–63

Wertime TA (1978) The search for ancient tin: the geographic and historic boundaries. In: Franklin A, Odin JS, Wertime TA (eds) The search for ancient tin. U.S. Government Printing Office, Washington, DC, pp 1–6

Werz BEJS, Flemming N (2001) Discovery in Table Bay of the oldest hand axes yet found underwater demonstrates preservation of hominid artifacts on the continental shelf. *S Afr J Sci* 97(5):183–185

Werz B, Cawthra H, Compton J (2014) Recent developments in Africam offshore prehistoric research, with an emphasis on South Africa. In: Evans AM, Flatman JC, Flemming NC (eds) *Prehistoric archaeology of the continental shelf: a global review*. Springer, New York, pp 233–253

West SM (1992) Temper, thermal shock and cooking pots: a study of tempering materials and their physical significance in prehistoric and traditional cooking pottery. Unpublished M.Sc. thesis. University of Arizona, Tucson

West LT, Dubos RB (2013) Soils of the blue ridge mountains in Georgia properties, diversity and suitability for wine grape production. In: Schroeder PA, Forrest JT, German JM (eds) *The Dahlonega wine and gold district: geology and terroir of viticulture in Northeastern Georgia*. Georgia Geological Society Guidebook 33(1):69–82

Weymouth JW (1996) Digs without digging, exploring archaeological sites with geophysical techniques. *Geotimes* 41:16–19

Whitbread IK (1989) A proposal for the systematic description of thin sections towards the study of ancient ceramic technology. In: Maniatis Y (ed) *Archaeometry, proceedings of the 25th International Symposium*. Elsevier, Amsterdam, pp 127–138

Whittig LD, Allardice WR (1986) X-ray diffraction techniques. In: Klute A (ed) *Methods of soil analysis, part I*, 2nd edn. American Society of Agronomy, Madison, pp 331–362

Wickham-Jones CR (2005) Summer walkers? – mobility and the Mesolithic. In: Milner N, Woodman P (eds) *Mesolithic studies at the beginning of the 21st century*. Oxbow Books, Oxford

Wickham-Jones CR (2010) Fear of farming. Oxbow Books, Oxford

Willey GR, Phillips P (1958) *Method and theory in American archaeology*. University of Chicago Press, Chicago, 280 p

Williams M (1998) *A world engraved: archaeology of the Swift Creek Culture*. University of Alabama Press

Williams A (2009) A metallurgical study of some Viking swords. *Gladius* XXIX:121–184

Williams AN (2012) The use of summed radiocarbon probability distributions in archaeology: a review of methods. *J Archaeol Sci* 39(3):578–589

Williams DF (1983) Petrology of ceramics. In: Kempe DRC, Harvey AP (eds) *The petrology of artefacts*. Clarendon Press, Oxford, pp 301–329

Williams H, Turner FJ, Gilbert CM (1955) *Petrography*. W.H. Freeman, San Francisco

Williams JM (1984a) A new resistivity device. *J Field Archaeol* 11:110–114

Williams MAJ (1984b) Late quaternary prehistoric environments in the Sahara. In: Clark JD, Brandt SA (eds) *From hunters to farmers*. University of California Press, Berkeley, pp 74–83

Williams JM, Shapiro G (1982) A search for the eighteenth century village at michlimackinac: a soil resistivity survey. *Archaeological Completion Report Series*. No. 4. Mackinac Island State Park Commission, Michigan

Williams JW, Jackson ST (2007) Novel climates, no-analog communities, and ecological surprises. *Front Ecol Environ* 5:475–482, <http://dx.doi.org/10.1890/070037>

Williams-Thorpe O, Potts PJ, Webb PC (1999) Field-portable non-destructive analysis of lithic archaeological samples by x-ray fluorescence instrumentation using a mercury iodide detector: comparison with wavelength-dispersive XRF and a case study in British stone axe provenancing. *J Archaeol Sci* 26 (2):215–237

Wilson JT (1966) Did the Atlantic close and then re-open? *Nature* 211:676–681

Wilson L (ed) (2011)

Wilson L (ed) (2011) *Human interactions with the geosphere: the geoarchaeological perspective*, vol 352. Geological Society, London, pp 1–9, Special Publications

Winchester S (2003) *Krakatoa: the day the world exploded, August 27, 1883*. Harper-Collins, New York

Winiger J (1981) *Spielzug und Seeufersiedlungen*. *Helv Archeol* 45(48):209–217

Winkler EM (1994) *Stone in architecture*. Springer, Berlin

Wisseman SU, Emerson TE, Hughes RE, Farnsworth KB (2012) Refining the identification of native American pipestone quarries in the midcontinental United States. *J Archaeol Sci* 39:2496–2505

Wiseman J (1996) Wonders of radar imagery: glimpses of the ancient world from space. *Archaeology* 49:14–18

Witten AJ (2006) *Handbook of geophysics and archaeology*. Equinox, London

Wood WR, McMillan RB (eds) (1975) *Prehistoric man and his environments: a case study in the Ozark highlands*. Academic, New York

Woods WI (1977) The quantitative analysis of soil phosphate. *Am Antiq* 42:248–252

Woolsey JR, Henry VJ (1974) Shallow, high resolution seismic investigations of the Georgia coast and inner continental shelf. *Georgia Geol Surv Bull* 87:167–187

Wrangham R (2009) *Catching fire: how cooking made us human*. Basic Books, New York

Wright GF, Haynes HW (1892) *Man and the glacial period*, vol 69. Kegan Paul, London

Wright GA, Bender S, Reeve S (1980) High country adaptions. *Plains Anthropol* 25(89):181–197

Wilson L (ed) (2011) *Human interactions with the geosphere: the geoarchaeological perspective*, vol 352. Geological Society, London, pp 1–9, Special Publications

Wylie A (1982) Epistemological issues raised by structuralist archaeology. In: Hodder I (ed) *Symbolic and structural archaeology*. Cambridge University Press, Cambridge, pp 39–46

Wylie A (1985) The reaction against analogy. *Adv Archaeol Method Theory* 8:63–111

Wylie A (1988) Simple analogy and the role of relevance assumptions: implications from archaeological practice. *Int Stud Philos* 2:134–150

Wylie A (1989) Archaeological cables and tacking: the implications for practice for Bernstein's, "Options beyond objectivism and relativism". *Philos Soc Sci* 19:1–18

Wynn JC (1987) Penrose conference report on archaeology and geology, 7–11 Dec 1986, St. Simon=s Island. U.S. Geological Survey Administrative Report, 35 pages

Wynn JC (1990) Applications of high-resolution geo-physical methods to archaeology. In: Lasca NP, Donahue J (eds) Archaeological geology of North America, vol 4, Centennial Special. Geological Society of America, Boulder

Wu X, Zhang C, Goldberg P, Cohen D, Pan Y, Arpin T, Bar-Yosef O (2012) Early pottery at 20,000 years ago in Xianrendong Cave, China. *Science* 336 (6089):1696–1700

Wu X, Zhang C, Goldberg P, Cohen D, Pan Y, Arpin T, Bar-Yosef O (2012) Early pottery at 20,000 years ago in Xianrendong Cave, China. *Science* 336 (6089):1696–1700

Yaalon DH (1976) "Calgon" no longer suitable. *Soil Sci Soc Am J* 40(2):333–333

Yacobi BG (1994) In: Yacobi BG, Holt DB, Kazmerski LL (eds) *Cathodoluminescence in microanalysis of solids*. Plenum, New York

Yardley BWD (1989) An introduction to metamorphic petrology. Longman Scientific & Technical, Essex

Yardley BWD, Mackensie WS, Guilford C (1990) *Atlas of metamorphic rocks and their textures*. Longman, Harlow

Zahid KM, Barbeau DL Jr (2011) Constructing sandstone provenance and classification ternary diagrams using an electronic spreadsheet. *J Sediment Res* 81(9):702–707

Zhang WC, Goldberg P, Cohen D, Pan Y, Arpin T, Bar-Yosef O (2012) Early pottery at 20,000 years ago in Xianrendong Cave, China. *Science* 336:1696–1700

Zuffardi P (1977) Ore/mineral deposits related to the Mesozoic ophiolites in Italy. In: Ridge JD (ed) IAGOD 5th symposium, proc. E. Schweizerbart'sche Verlagsbuchhandlung, Stuttgart, pp 314–323